

**PETROLOGY AND GEOCHEMISTRY OF CAMBRIAN  
VOLCANIC ROCKS FROM THE AVALON ZONE IN  
NEWFOUNDLAND AND NEW BRUNSWICK**

**CENTRE FOR NEWFOUNDLAND STUDIES**

**TOTAL OF 10 PAGES ONLY  
MAY BE XEROXED**

**(Without Author's Permission)**

**JOHN DAVID GREENOUGH**



## CANADIAN THESES ON MICROFICHE

I.S.B.N.

## THESES CANADIENNES SUR MICROFICHE



National Library of Canada  
Collections Development Branch

Canadian Theses on  
Microfiche Service

Ottawa, Canada  
K1A 0N4

Bibliothèque nationale du Canada  
Direction du développement des collections

Service des thèses canadiennes  
sur microfiche

### NOTICE

The quality of this microfiche is heavily dependent upon the quality of the original thesis submitted for microfilming. Every effort has been made to ensure the highest quality of reproduction possible.

If pages are missing, contact the university which granted the degree.

Some pages may have indistinct print especially if the original pages were typed with a poor typewriter ribbon or if the university sent us a poor photocopy.

Previously copyrighted materials (journal articles, published tests, etc.) are not filmed.

Reproduction in full or in part of this film is governed by the Canadian Copyright Act, R.S.C. 1970, c. C-30. Please read the authorization forms which accompany this thesis.

THIS DISSERTATION  
HAS BEEN MICROFILMED  
EXACTLY AS RECEIVED

### AVIS

La qualité de cette microfiche dépend grandement de la qualité de la thèse soumise au microfilmage. Nous avons tout fait pour assurer une qualité supérieure de reproduction.

S'il manque des pages, veuillez communiquer avec l'université qui a conféré le grade.

La qualité d'impression de certaines pages peut laisser à désirer, surtout si les pages originales ont été dactylographiées à l'aide d'un ruban usé ou si l'université nous a fait parvenir une photocopie de mauvaise qualité.

Les documents qui font déjà l'objet d'un droit d'auteur (articles de revue, examens publiés, etc.) ne sont pas microfilmés.

La reproduction, même partielle, de ce microfilm est soumise à la Loi canadienne sur le droit d'auteur, SRC 1970, c. C-30. Veuillez prendre connaissance des formules d'autorisation qui accompagnent cette thèse.

LA THÈSE A ÉTÉ  
MICROFILMÉE TELLE QUE  
NOUS L'AVONS REÇUE

PETROLOGY AND GEOCHEMISTRY OF CAMBRIAN VOLCANIC ROCKS  
FROM THE AVALON ZONE IN NEWFOUNDLAND AND NEW BRUNSWICK

By



John David Greenough, B.Sc., M.Sc.

A thesis submitted to the School of Graduate  
Studies in partial fulfillment of the  
requirements for the degree of  
Doctor of Philosophy

Department of Earth Sciences  
Memorial University of Newfoundland

May 1984

St. John's

Newfoundland



# ABSTRACT

11

This thesis examines the petrology and geochemistry of Cambrian volcanic rocks from the Avalon Peninsula (Newfoundland) and southern New Brunswick as well as Silurian sills and Devonian (?) dikes from the Avalon Peninsula. The geochemistry of these rocks provides new information on Early Paleozoic tectonism affecting Avalonian terrane in eastern North America. The effects of low grade metamorphism on the primary geochemistry of each rock group are also discussed.

Middle Cambrian basalts on Cape St. Mary's (Avalon Peninsula) were affected by two phases of alteration that resulted in the formation of chlorite and carbonate. The effects of the chlorite formation on element concentrations resemble those observed for basalt/seawater interaction, whereas the effects of carbonate addition are similar to those produced in high CO<sub>2</sub> systems. Basalts in the Beaver Harbour area of New Brunswick show similar two-phase alteration, but phosphorous and yttrium were added during the carbonate addition phase suggesting that there were differences in the metasomatic solutions between the two areas.

Silurian sills on Cape St. Mary's show primary textural, mineralogical and bulk-rock geochemical characteristics indicative of high volatile contents. Thermogravitative processes probably involving volatile

complexing of some elements caused enrichment of these elements in the upper portions of the sills, or removal from the sill system as a whole. The parental sill magma was geochemically somewhat evolved, tholeiitic, and closely resembled compositions observed in flood basalt and rift provinces.

Dikes in the Cape St. Mary's study area show a range of bulk rock compositions representative of at least two batches of magma that underwent varying degrees of evolution. Some of the rocks appear to have alkaline characteristics whereas others have tholeiitic attributes, but all were probably produced in a tensional environment. These rocks resemble Devonian dikes around Bonavista Bay and could be time equivalent.

The Cape St. Mary's Cambrian basalts and their feeder pipes display (primary) whole-rock and mineralogical compositions representative of evolved alkali basalts. Lower to Middle Cambrian volcanic rocks in New Brunswick form a bimodal suite, the basaltic portion of which shows compositions ranging from relatively unevolved to highly evolved tholeiites.

A review of information on the Precambrian stratigraphy, Cambrian lithologies, fauna, stratigraphy, and paleomagnetism in the Acado-Baltic province shows that most of western Europe and eastern North America probably formed a large continental block that remained at lower latitudes

iv

throughout the Cambrian. The bimodal nature of the volcanic rocks over this terrane along with their relatively small volume indicates they formed in a continental rifting environment. Basaltic rocks in southern New Brunswick, Cape Breton, Norway, Poland, and on the Avalon Peninsula show compositions consistent with this interpretation. The small volume of the volcanic rocks and platformal character of the associated sedimentary rocks suggest that the area experienced relatively stable tectonic conditions during the Cambrian with small amounts of extension causing the rift-type volcanism. The tension affected a broad area and resulted in a number of narrow basins but few rift valleys. Volcanism was much more common during the Early and Middle Cambrian than during the Late Cambrian suggesting that the tensional tectonic regime may have waned in the Late Cambrian in direct or indirect response to processes which led to (Ordovician) closing of the Iapetus Ocean. Sills and dikes on Cape St. Mary's provide local evidence that the stable tectonic conditions with small-scale tension persisted throughout the Early Paleozoic.

To my parents  
for support and encouragement



ACKNOWLEDGMENTS

The writer wishes to express appreciation to Mr. D. Osmond, Mr. H. Butler, Mrs. D. Strange, Mr. W. Marsh, and Mr. W. Howell for assistance in the preparation of figures, plates and tables in the thesis. Mrs. G. Andrews is thanked for her role in acquiring the major element data. Help and guidance received from Dr. H. Longrich in the operation of the electron microprobe as well as on computer related problems is gratefully acknowledged. The technical expertise of Mr. D. Press made possible the efficient acquisition and processing of most of the geochemical data and the author is very thankful for his "24 hour" help.

The author thanks Mr. S. McCutcheon for aiding in the collection of the New Brunswick rocks and for providing critical information on the local geology. Appreciation is also expressed to Mr. K. Cameron for providing polished thin sections of the Bourinot rocks from Nova Scotia. Doctor T. Krogh is thanked for his help in acquiring a radiometric age date on the sill rocks. The author was assisted in the field by Mr. G. Whelan, and his enthusiastic contribution to the project is greatly appreciated. Dr. J. Hodych furnished valuable information on sampling localities for the sill rocks as well as paleomagnetic data which helped the author determine if these rocks should be included in the thesis. Mr. D. Wilton and Mr. J. V. Owen provided many hours of helpful conversation, as well as criticism and advice on the

manuscript.

vi

Doctor D. Strong and Dr. B. Fryer are thanked for their supervision, and advice, as well as their thorough review and criticism of early versions of the manuscript. Dr. J. Malpas kindly provided guidance and assistance in preparing the final copy of the thesis. Most of all the author wishes to thank Dr. V. S. Papezik for his constructive criticism, guidance, encouragement, financial support, and for making the whole project possible.

Personal financial support during the course of study came from The Memorial University of Newfoundland as well as from my parents. This support is gratefully acknowledged. Financial support for the research came from a NSERC grant held by Dr. V. S. Papezik.

TABLE OF CONTENTS

|  | PAGE  |
|--|-------|
| TITLE PAGE   | 1     |
| ABSTRACT   | 11    |
| ACKNOWLEDGEMENTS   | vi    |
| TABLE OF CONTENTS  | viii  |
| LIST OF TABLES   | xii   |
| TABLE OF FIGURES   | xv    |
| TABLE OF PLATES  | xviii |
| CHAPTER 1 INTRODUCTION   | 1     |
| 1.1 GENERAL STATEMENT  | 1     |
| 1.2 PROBLEM AND SCOPE  | 2     |
| 1.3 PALEOGEOGRAPHY   | 4     |
| 1.4 DISTRIBUTION OF CAMBRIAN VOLCANIC ROCKS                                  | 16    |
| CHAPTER 2 GEOLOGY OF THE VOLCANIC ROCKS IN<br>NEWFOUNDLAND AND NEW BRUNSWICK | 23    |
| 2.1 INTRODUCTION   | 23    |
| 2.2 CAPE ST. MARY'S STUDY AREA   | 26    |
| 2.2.1 General Geology of Cape St. Mary's                                     | 26    |
| 2.2.2 Cambrian Extrusive rocks   | 36    |
| 2.2.3 Feeder Pipes   | 45    |
| 2.2.4 Sills  | 49    |
| 2.2.5 Dikes  | 52    |
| 2.3 SOUTHERN NEW BRUNSWICK   | 55    |
| 2.3.1 Beaver Harbour Area  | 58    |
| 2.3.2 Long Reach Area  | 59    |

|   |      |
|---|------|
|   | ix   |
|   | PAGE |
| CHAPTER 3 PETROGRAPHY OF THE VOLCANIC ROCKS                             | 62   |
| 3.1 INTRODUCTION  | 62   |
| 3.2 CAPE ST. MARY'S VOLCANIC ROCKS                                      | 62   |
| 3.2.1 Middle Cambrian Lapilli Tuffs                                     | 62   |
| 3.2.2 Pillow Basalts  | 72   |
| 3.2.3 Feeder Pipes  | 76   |
| 3.2.4 Sills   | 82   |
| 3.2.5 Dikes   | 94   |
| 3.3 NEW BRUNSWICK   | 97   |
| 3.3.1 Beaver Harbour Area   | 97   |
| 3.3.2 Long Reach Area   | 102  |
| Felsic Pyroclastic Rocks  | 102  |
| Mafic Rocks   | 103  |
| 3.4 CAPE BRETON, NOVA SCOTIA  | 107  |
| CHAPTER 4 GEOCHEMISTRY OF LOWER PALEOZOIC<br>AVALON ZONE VOLCANIC ROCKS | 108  |
| 4.1 INTRODUCTION  | 108  |
| 4.2 CAMBRIAN FLOWS AND FEEDER PIPES                                     | 109  |
| 4.2.1 Alteration Of The Flows   | 109  |
| Presentation Of Data  | 110  |
| Discussion  | 127  |
| 4.2.2 Alteration Of The Feeder Pipes                                    | 134  |
| 4.2.3 Primary Whole-Rock Geochemistry                                   | 134  |
| 4.2.4 Pyroxene Compositions   | 151  |
| Flows   | 151  |
| Feeder Pipes  | 155  |
| 4.2.5 Discussion - Flows and Feeder Pipes                               | 160  |



|  |      |
|--|------|
|  | x    |
|  | PAGE |
| 4.3 CAPE ST. MARY'S SILLS                      | 165  |
| 4.3.1 Whole-Rock Geochemistry                  | 165  |
| 4.3.2 Mineral Chemistry                        | 173  |
| Plagioclase                                    | 173  |
| Olivine  | 181  |
| Pyroxene                                       | 185  |
| Amphiboles                                     | 194  |
| Biotite  | 197  |
| Baddeleyite ZrO <sub>2</sub>                   | 198  |
| 4.3.3 Differentiation of the Sills             | 204  |
| End-Member Rock Types                          | 204  |
| Models For Differentiation                     | 206  |
| 4.3.4 Discussion of Sills                      | 225  |
| 4.4 CAPE ST. MARY'S DIKES                      | 233  |
| 4.4.1 Bulk-Rock Chemistry                      | 233  |
| 4.4.2 Mineral Chemistry                        | 238  |
| 4.4.3 Discussion of Dikes                      | 241  |
| 4.5 NEW BRUNSWICK VOLCANIC ROCKS               | 247  |
| 4.5.1 Alteration Geochemistry - Beaver Harbour | 247  |
| Presentation of Data                           | 250  |
| Discussion                                     | 259  |
| 4.5.2 Alteration Geochemistry - Long Reach     | 267  |
| 4.5.3 Primary Whole-Rock Geochemistry          | 268  |
| Beaver Harbour Basalts                         | 268  |
| Long Reach Phyric Basalts                      | 280  |
| Long Reach Aphyric Basalts                     | 283  |

|   | PAGE |
|---|------|
| Long Reach Felsic Rocks                             | 286  |
| 4.5.4 Pyroxenes in Long Reach Basalts               | 289  |
| 4.5.5 Discussion                                    | 293  |
| 4.6 CAPE BRETON VOLCANIC ROCKS                      | 297  |
| 4.6.1 Whole-Rock Geochemistry                       | 297  |
| 4.6.2 Pyroxene Compositions                         | 299  |
| 4.7 NORWEGIAN BASALTS                               | 301  |
| 4.8 POLISH VOLCANIC ROCKS                           | 302  |
| CHAPTER 5 TECTONICS AND PETROGENETIC CONSIDERATIONS | 304  |
| 5.1 INTRODUCTION                                    | 304  |
| 5.2 SIMILARITIES TO PLATFORMS                       | 304  |
| 5.3 EVIDENCE FOR TENSION                            | 306  |
| 5.3.1 Style of Volcanism                            | 306  |
| 5.3.2 Chemical Characteristics<br>Of Volcanic Rocks | 308  |
| 5.3.3 Relationship To Underlying Stratigraphy       | 321  |
| 5.3.4 Taphrogenic Features                          | 322  |
| 5.4 SUMMARY AND DISCUSSION                          | 332  |
| CHAPTER 6 CONCLUSIONS                               | 336  |
| REFERENCES CITED                                    | 344  |
| APPENDIX A EXPERIMENTAL METHODS                     | 374  |
| APPENDIX B WHOLE-ROCK ANALYSES                      | 379  |
| APPENDIX C MINERAL ANALYSES                         | 423  |

# LIST OF TABLES

xii

|  | PAGE |
|--|------|
| Table 1.1 Summary of the characteristics of Cambrian volcanic rocks.                       | 17   |
| Table 2.1 List of Avalon unit names.   | 32   |
| Table 2.2 Table of unit names - southern New Brunswick.                                    | 56   |
| Table 3.1 Classification and textural characteristics of fragmental rocks.                 | 70   |
| Table 3.2 Feeder pipe textures and mineralogy.   | 79   |
| Table 3.3 Summary of alteration minerals in the feeder pipes.                              | 81   |
| Table 3.4 Gull Cove sill mineralogy and textures.  | 85   |
| Table 4.1 Major and trace element concentrations in Cape St. Mary's Cambrian meta-basalts. | 113  |
| Table 4.2 Alteration equations - Cape St. Mary's metabasalts.                              | 117  |
| Table 4.3 Rare earth element concentrations in Cape St. Mary's Cambrian basalts.           | 128  |
| Table 4.4 Major element analyses of least altered Cape St. Mary's extrusive rocks.         | 137  |
| Table 4.5 Major element and normative composition of selected feeder pipe samples.         | 138  |
| Table 4.6 Trace element analyses of least altered basalt samples and feeder pipe samples.  | 139  |
| Table 4.7 Rare earth element concentrations in representative feeder pipe samples.         | 154  |
| Table 4.8 Representative analyses of pyroxenes from the extrusive rocks.                   | 156  |
| Table 4.9 Representative feeder pipe pyroxene analyses.                                    | 159  |
| Table 4.10 Results of petrogenetic modelling of lava - feeder pipe compositions.           | 163  |

|  |      |
|--|------|
|  | xiii |
|  | PAGE |
| Table 4.11 Major element and normative composition of representative sill samples.     | 171  |
| Table 4.12 Representative trace element analyses of sill rocks.                        | 172  |
| Table 4.13 Rare earth element concentrations in representative sill rocks.             | 176  |
| Table 4.14 Representative analyses of sill plagioclases.                               | 177  |
| Table 4.15 Representative analyses of sill olivine.                                    | 182  |
| Table 4.16 Representative analyses of sill pyroxenes.                                  | 186  |
| Table 4.17 Amphibole pleochroism and composition.                                      | 195  |
| Table 4.18 Representative analyses of sill biotites.                                   | 199  |
| Table 4.19 Baddeleyite analyses.   | 203  |
| Table 4.20 Endmember rock types in Gull Cove sill.                                     | 205  |
| Table 4.21 Modelling of sill trace element concentrations.                             | 209  |
| Table 4.22 Major element and normative composition of least altered dike samples.      | 234  |
| Table 4.23 Trace element composition of least altered dike samples.                    | 235  |
| Table 4.24 REE concentrations in four dike samples.                                    | 235  |
| Table 4.25 Representative analyses of dike pyroxenes.                                  | 242  |
| Table 4.26 Representative analyses of Beaver Harbour meta-volcanic rocks.              | 248  |
| Table 4.27 Equations relating element removal and addition during alteration.          | 254  |
| Table 4.28 REE concentrations in four Beaver Harbour meta-basalt samples.              | 262  |
| Table 4.29 Major element composition of least altered New Brunswick volcanic rocks.    | 269  |
| Table 4.30 Trace element concentrations in least altered New Brunswick volcanic rocks. | 271  |



|            |   |     |
|------------|---|-----|
| Table 4.31 | REE concentrations in Long Reach<br>basalt samples.   | 271 |
| Table 4.32 | Representative analyses of Long Reach<br>pyroxenes.   | 290 |
| Table 4.34 | Composition of representative Cambrian<br>basalts from Poland , Norway, and<br>Nova Scotia. | 298 |
| Table 4.34 | Representative analyses of Cape Breton<br>pyroxenes.  | 300 |

TABLE OF FIGURES

|  | PAGE |
|--|------|
| Figure 1.1 Distribution of terrane bearing Acado-Baltic sedimentary rocks.               | 6    |
| Figure 1.2 Generalized Cambrian stratigraphic sections.                                  | 8    |
| Figure 1.3 Paleogeographic reconstruction of the Acado-Baltic Cambrian.                  | 15   |
| Figure 2.1 Geological sketch map of the Cape St. Mary's study area.                      | 25   |
| Figure 2.2 Geological sketch map of the Beaver Harbour area, New Brunswick.              | 28   |
| Figure 2.3 Geological sketch map of the Long Reach area, New Brunswick.                  | 30   |
| Figure 2.4 Stratigraphic position of Cambrian volcanic rocks - Cape St. Mary's.          | 34   |
| Figure 3.1 Section of pyroclastic fall deposit Hopeall Head.                             | 65   |
| Figure 3.2 Vertical section through the Gull Cove sill.                                  | 84   |
| Figure 4.1 Volume factor diagram for three Cambrian basalts from Cape St. Mary's.        | 115  |
| Figure 4.2 The effect of metasomatism on element concentrations - Chapel Arm lavas.      | 120  |
| Figure 4.3 The effect of metasomatism on element concentrations - Cape Dog lavas.        | 122  |
| Figure 4.4 Possible alteration effects in Placentia Junction and Hopeall Head samples.   | 125  |
| Figure 4.5 Chondrite-normalized REE patterns for the Cambrian basalts, and feeder pipes. | 130  |
| Figure 4.6 Plot of SiO <sub>2</sub> and MgO against LOI - feeder pipe samples.           | 136  |
| Figure 4.7 Major element variation diagrams - Cape St. Mary's feeder pipe rocks.         | 142  |

|  | PAGE |
|--|------|
| Figure 4.8 Trace element variation diagrams - Cape St. Mary's feeder pipe rocks.                             | 144  |
| Figure 4.9 Plot of Mg' versus Al <sub>2</sub> O <sub>3</sub> in the feeder pipes, sills, dikes.              | 146  |
| Figure 4.10 Plot of Mg' versus TiO <sub>2</sub> in the feeder pipes, sills, and dikes.                       | 148  |
| Figure 4.11 AFM diagram - Cape St. Mary's feeder pipe, and sill rocks.                                       | 150  |
| Figure 4.12 Zirconium versus Nb diagrams.  | 153  |
| Figure 4.13 Pyroxene quadrilateral - Cape St. Mary's extrusive rocks and feeder pipes                        | 158  |
| Figure 4.14 TiO <sub>2</sub> -MnO-Na <sub>2</sub> O diagram - Cape St. Mary's Cambrian pyroxene data.        | 162  |
| Figure 4.15 Major element variation diagrams - Gull Cove sill.   | 167  |
| Figure 4.16 Trace element variation diagrams showing sill data.  | 169  |
| Figure 4.17 REE patterns in sill and dike rocks.   | 175  |
| Figure 4.18 An content of sill plagioclases.   | 179  |
| Figure 4.19 Fo content of sill olivines.   | 184  |
| Figure 4.20 Pyroxene quadrilateral showing Cape St. Mary's sill data.  | 188  |
| Figure 4.21 Wo, En, and Ti (atomic) content of Cape St. Mary's sill pyroxenes.                               | 190  |
| Figure 4.22 TiO <sub>2</sub> -MnO-Na <sub>2</sub> O discrimination diagram - Cape St. Mary's sill pyroxenes. | 193  |
| Figure 4.23 FeO/MgO ratios in biotites from the Cape St. Mary's sills.                                       | 201  |
| Figure 4.24 Bar-graphs showing the movement of elements within the Gull Cove sill.                           | 219  |
| Figure 4.25 Schematic diagram illustrating element movement within the Gull Cove sill.                       | 224  |
| Figure 4.26 Ternary diagrams showing the effect of water pressure on silica activity.                        | 229  |

|   | PAGE |
|---|------|
| Figure 4.27 Solubility of water in various magma types at varying pressures.                                    | 232  |
| Figure 4.28 Variation diagrams for selected major elements - Cape St. Mary's dike samples.                      | 237  |
| Figure 4.29 Variation diagrams for selected trace elements - Cape St. Mary's dike samples.                      | 240  |
| Figure 4.30 Pyroxene quadrilateral showing pyroxenes from the Cape St. Mary's dike rocks.                       | 244  |
| Figure 4.31 TiO <sub>2</sub> -MnO-Na <sub>2</sub> O discrimination diagram - Cape St. Mary's dike pyroxenes.    | 246  |
| Figure 4.32 Volume factor diagram for three Cambrian basalt samples from Beaver Harbour.                        | 252  |
| Figure 4.33 Diagram showing the effects of metamorphism on Beaver Harbour samples.                              | 256  |
| Figure 4.34 Chondrite-normalized REE patterns for Beaver Harbour meta-basalts.                                  | 261  |
| Figure 4.35 Major element variation diagram - New Brunswick volcanic rocks.                                     | 273  |
| Figure 4.36 Trace element variation diagram - New Brunswick volcanic rocks.                                     | 275  |
| Figure 4.37 Mg' versus Al <sub>2</sub> O <sub>3</sub> diagrams.   | 277  |
| Figure 4.38 Mg' versus TiO <sub>2</sub> diagrams.   | 279  |
| Figure 4.39 Zr versus Nb diagrams.  | 282  |
| Figure 4.40 REE diagram comparing Cambrian basalts from various localities.                                     | 285  |
| Figure 4.41 Enrichment/depletion diagram for the Long Reach felsic rocks.                                       | 288  |
| Figure 4.42 Pyroxene quadrilateral showing pyroxenes from Long Reach and Bourinot basalts.                      | 292  |
| Figure 4.43 TiO <sub>2</sub> -MnO-Na <sub>2</sub> O discrimination diagram - Long Reach and Bourinot pyroxenes. | 295  |
| Figure 5.1 Isopach map of the Random Formation.   | 324  |
| Figure 5.2 Isopach map of the Brigus Formation.   | 327  |

# TABLE OF PLATES

xviii

|  | PAGE |
|--|------|
| Plate 2.1 Pillow basalts along the shores of Chapel Arm.   | 39   |
| Plate 2.2 Bedded volcanoclastics in the road cut at Placentia Junction.                                  | 42   |
| Plate 2.3 Photo of feeder pipe - Spread Eagle Peak.  | 47   |
| Plate 2.4 Cape St. Mary's sills.   | 51   |
| Plate 2.5 Cape St. Mary's dikes.   | 54   |
| Plate 3.1 Photomicrographs of volcanoclastic rocks.  | 67   |
| Plate 3.2 Photomicrographs of meta-basalts from Chapel Arm.  | 75   |
| Plate 3.3 Photomicrographs of highly altered basalt sample and cumulus feeder pipe sample.               | 78   |
| Plate 3.4 Olivine layers in weathered sill boulders and photomicrograph of poikilitic sill augite grain. | 89   |
| Plate 3.5 Photomicrographs of sill olivine bearing gabbro and sill granophyre.                           | 93   |
| Plate 3.6 Large plagioclase phenocryst in a dike at Patricks Cove.                                       | 96   |
| Plate 3.7 Photomicrographs of hematite rich volcanoclastic rocks - Beaver Harbour.                       | 100  |
| Plate 3.8 Photomicrograph of chlorite rich Beaver Harbour sample.  | 101  |
| Plate 3.9 Photomicrographs of aphyric and phyrlic basalt samples - Long Reach area.                      | 106  |

## CHAPTER 1. INTRODUCTION

### 1.1 GENERAL STATEMENT

Perhaps some indication of the importance of the Cambrian to the development of the science of geology is given by the observation that earlier time periods, representing 90 percent of earth history, are summarily referred to as pre-Cambrian. Why is the Cambrian period looked on as being so important? There was a proliferation of life forms, such that nearly all of the phyla representing present day life appeared during this time. The reason (reasons) for this diversification remains one of the greatest enigmas of modern science.

The Cambrian System was named by Sedgewick in 1835, after the Principality in Wales, and applied to rocks in this area (Rushton, 1974). Correlatives of these rocks in eastern North America and western Europe have played an important role in the formulation of plate tectonic theory, which has revolutionized the science. Wilson (1966) in his classic paper "Did the Atlantic Close and Then Re-Open?" used the differences between the Acado-Baltic fauna of rocks in eastern-most North America (and western Europe), and the fauna of Cambrian rocks on the North American craton to argue for the geographic separation of these areas by a major ocean during the Cambrian. It is rather ironic that the Lower aleozoic rocks of easternmost North America, which were so important to changing the way we think about

orogenesis, remain among the least understood rocks in the Appalachian Orogen (Williams and Hatcher, 1982).

## 1.2 PROBLEM AND SCOPE

There are several aspects to the study which are outlined in this section. In its initial stages the project called for a detailed examination of Lower Paleozoic rocks of the Avalon Zone (as defined by Williams, 1978a, 1978b) in Newfoundland, with emphasis to be placed on the igneous rocks. As the project developed, Cambrian volcanic rocks from the Avalon Zone in southern New Brunswick were also studied and they allow comparison with the Avalon Peninsula rocks and give the project more regional significance.

Cambrian shales and siltstones together with coarser grained Lower Ordovician siliciclastics are volumetrically the most important Lower Paleozoic rocks on the Avalon Peninsula. Igneous rocks consist of minor Cambrian basaltic flows and volcanoclastic rocks (lapilli and ash fall tuffs) as well as "plugs", sills, and dikes which at the time of project initiation were of uncertain age. Apart from regional mapping, these igneous rocks had never been studied, and this project was undertaken to rectify this situation. As on the Avalon Peninsula in Newfoundland, Lower to Middle Cambrian mafic flows and pyroclastic rocks as well as silicic pyroclastic rocks make up only a small proportion of the shale and siltstone dominated Cambrian stratigraphy in southern New Brunswick. These rocks are also examined in

detail in this thesis.

By studying the petrology and geochemistry of the Avalon Zone volcanic rocks, and giving the stratigraphy a fresh examination in the light of recent tectonic ideas, this report casts new light on the tectonics of this area particularly during the Cambrian. Regional models for Cambrian volcanism and tectonism are developed by reviewing the distribution and characteristics of Cambrian volcanic rocks from other areas in western Europe and eastern North America which probably formed part of the same continental block during the Cambrian.

An important problem encountered in trying to evaluate the primary geochemical characteristics of the volcanic rocks is that they are all mineralogically altered to varying degrees. In cases where this alteration had an important effect on the primary geochemical characteristics of the rocks a detailed analysis of the resulting geochemical patterns is presented.

The following paragraph gives an outline of the thesis format. Sections 1.3 and 1.4 of this chapter review Cambrian paleogeography and volcanism and help establish the (Cambrian) geographic relationship between the southern New Brunswick and Avalon Peninsula rocks and their time equivalents in western Europe and eastern North America. The review of Cambrian volcanism is not exhaustive but comprehensive enough to establish the general



4

characteristics of the volcanism. In Chapter 2 the general geology and geologic setting of the volcanic rocks in the two primary study areas (ie. Avalon Peninsula and southern New Brunswick) are discussed. Chapter 3 provides details on the petrography of these volcanic rocks and also briefly reviews the petrography of Cambrian volcanic rocks from Cape Breton Island, Nova Scotia, which were geochemically examined by Cameron (1980). The latter rocks are discussed because new data are presented, in the following chapter, on their pyroxene compositions. Mineral and whole-rock geochemical data (major, trace, and rare earth element analyses) for the volcanic rocks from the Avalon Peninsula and southern New Brunswick are discussed in Chapter 4. For comparative purposes, published geochemical information on the composition of Cambrian basalts from Poland, Norway, and Cape Breton (Nova Scotia) are reviewed at the end of Chapter 4. The data presented in Chapters 1 through 4 are integrated and analyzed in Chapter 5 so as to develop models for volcanism and tectonism in the Acado-Baltic province during the Cambrian.

### 1.3 PALEOGEOGRAPHY

Scattered remnants of Cambrian stratigraphy around the North Atlantic (Figure 1.1) show similar lithologies, sequences of lithologies, underlying Precambrian stratigraphy, and faunas belonging to the Acado-Baltic faunal province. The similarities support the idea that all

Figure 1.1 Distribution of terrane bearing Acado-Baltic sedimentary rocks. Localities examined in the thesis are numbered as follows: 1 southern Appalachians, 2 New England, 3 southern New Brunswick, 4 Antigonish Highlands, Nova Scotia, 5 Cape Breton, Nova Scotia, 6 Avalon Peninsula, Newfoundland, 7 southern British Isles, 8 central Norway, 9 Poland, 10 Czechoslovakia, 11 central France, 12 southern France, 13 northern Spain, 14 Portugal, 15 southern Spain, 16 Haut Atlas, Morocco, 17 Anti Atlas, Morocco. Cambrian volcanic rocks can be found within all of the above areas except New England. Note that Morocco and the southern Appalachians are given only cursory treatment in the thesis for reasons given in the text. For illustrative purposes the map uses the Triassic paleogeographic reconstruction of Bullard et al. (1965).

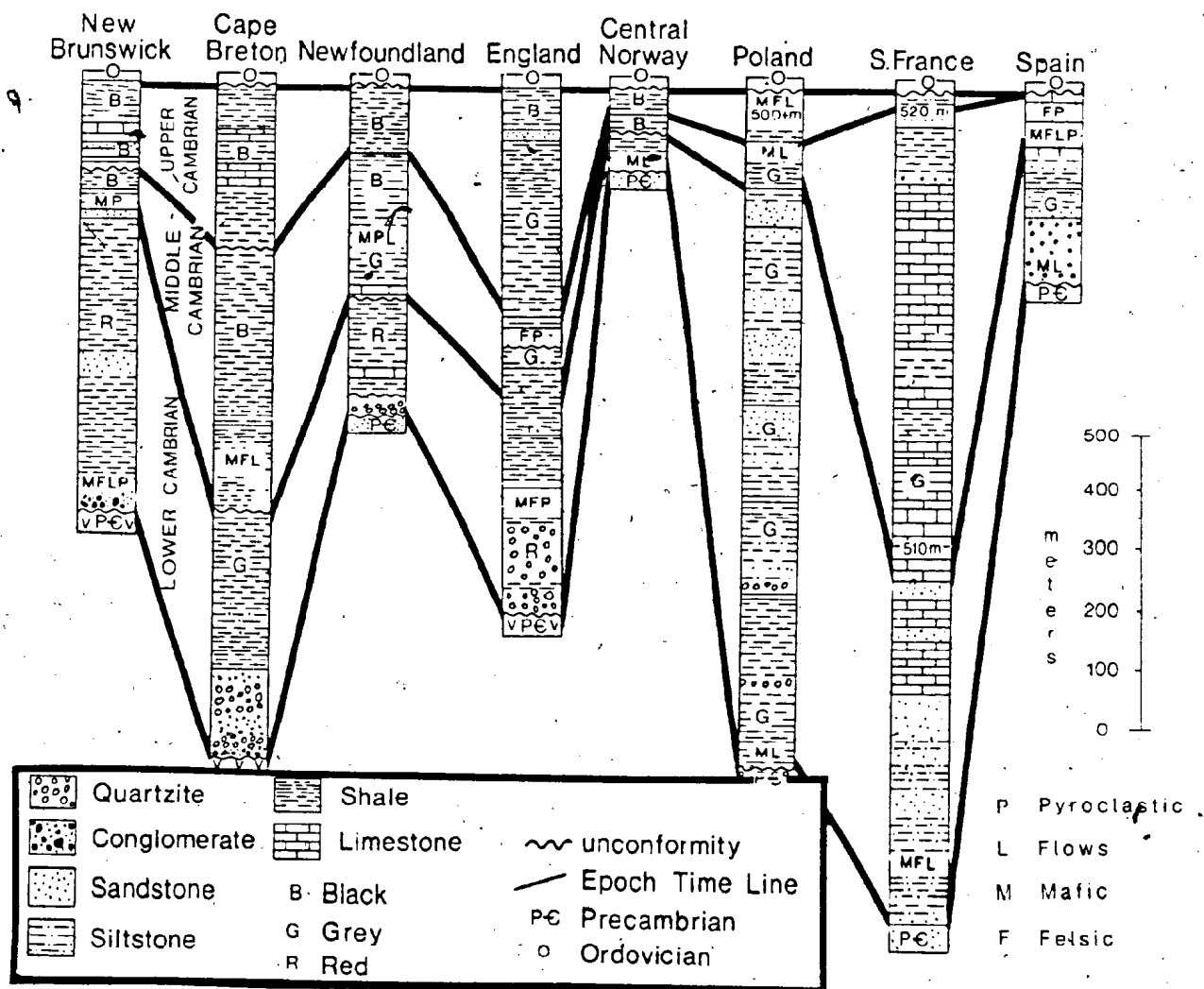


of these areas formed parts of a single continental block during the Cambrian. The following discussion reviews the information supporting this hypothesis.

Various papers have shown that the stratigraphy underlying the Acado-Baltic sequences is in most cases similar, implying that they were together prior to the Cambrian. For example, Schenk (1971) reviewed the Proterozoic rocks of eastern Canada and northwestern Africa, Rast et al. (1976) compared those of eastern Canada, Britain, and France, Strong (1979) integrated information from the Iberian Peninsula, Zoubek (1977) correlated the Bohemian Massif with the Armorican Massif, and various authors have correlated eastern Newfoundland (Avalon Zone) with the eastern United States (eg. Williams, 1978a; Kaye and Zartman, 1980; O'Brien and King, 1982). The only area which seems to show a substantially different Precambrian history is Norway, where Grenville age basement is overlain by a thick clastic succession (Berthelsen, 1980). In summary it appears all of the areas studied here, with the exception of the Baltic Shield, had common Late Precambrian histories.

Generalized sections portraying the typical characteristics of Cambrian stratigraphy at various localities are portrayed in Figure 1.2. These sections show that the Acado-Baltic province can be divided into two portions: north and south. Sections from the north (New Brunswick, Cape Breton, Newfoundland, Norway, England and

Figure 1.2 Generalized Cambrian stratigraphic sections for areas with Acado-Baltic stratigraphy in eastern North America and western Europe. The sections illustrate some of the more important characteristics of the Cambrian stratigraphy in each area. The location of volcanic rocks in the stratigraphy is diagramatic in that their thicknesses are not shown and the volcanic rocks need not (and in most cases do not) occur at all localities (ie. outcrops) within a particular area. Sources for the sections are as follows: New Brunswick (southern), Hayes and Howell (1937); Cape Breton, Hutchinson (1952); Newfoundland (Avalon Peninsula), McCartney (1967), and Fletcher (1972); Norway, Henningsmoen (1956), and Banks et al. (1971), Dypvik (1977); Poland, Samsonowicz (1956); England, Rushton (1974); France, Geze (1956); S. Spain, Teixeira (1978), Dupont and Vegas (1978). Sources for information on the volcanic rocks are given in Table 1.1.



Poland) are characterized by a basal conglomerate or quartzite which unconformably overlies the Late Precambrian. The Lower Cambrian usually consists of red or grey shales, and the Middle and Upper Cambrian of monotonous grey and black shales. With the exception of the Polish section, sandstones are of minor importance, as are carbonates. The total thickness of the sections is usually less than 1000 meters. These localities usually show unconformities in the stratigraphy, or faunal breaks (abrupt changes in the fauna), at the end of the Lower, Middle and Upper Cambrian (Henningsmoen, 1969).

Some lithologies such as the distinctive pink algal limestone referred to in Newfoundland as the Smith Point Formation are wide spread. Chemically precipitated manganese beds requiring unusual and specific physical - chemical conditions of formation occur in Newfoundland and Wales (Douglas, 1981) and were identified during the course of this study in New Brunswick. Nodules of black, bituminous limestone occur within the Upper Cambrian shales at nearly all of the Cambrian localities in the North Atlantic (Henningsmoen, 1969). In summary, these similarities necessitate very similar depositional, climatic, and tectonic environments controlling their formation and strongly suggest close geographic ties between these areas during the Cambrian.

Stratigraphic sections from the southern portion of the

Acado-Baltic province (France and Spain, Figure 1.2), usually show relatively thick carbonate sequences. The Lower Cambrian is in some cases conformable with the Late Precambrian, commonly arenaceous at the base, and carbonate rich above. Unlike in the northern areas, where red coloration of the Lower Cambrian rocks is the norm, these rocks tend to be green or grey in color. The Middle Cambrian is also typified by an abundance of carbonates and the Upper Cambrian is either missing or poorly developed at most localities. Despite the poor development of the Upper Cambrian, these areas tend to display total stratigraphic thicknesses of at least a thousand meters, though there are exceptions such as in southern Spain.

The lithologic and stratigraphic differences between the northern and southern portions of the Acado-Baltic province could have important paleogeographic implications; that is they could indicate the presence of separate continental blocks during the Cambrian. Brasier (1980) outlined facies models and successions for the Avalon, Baltic, Armorican, and southern Europe platforms and suggested that most of the sedimentation in these sequences took place on ocean-facing shelves with carbonate barriers (also see Dore 1977) present on the southern Europe platform. He suggested the presence of phosphatic sediments, "glauconite, pyrite, hematite, Mn oxides and carbonates, red shales, bituminous shales, and nodular wackestone biomicrites", especially in the Avalon and Baltic areas, indicates very low or negative



sedimentation rates. These rocks apparently resemble sediments on the shelves of SW Africa, Peru, and Chile, which are close to the oxygen minimum, and associated with intense upwelling of cold water and phytoplankton blooms. Brasier (1980) proposed that rifting during the early Cambrian may have created a narrow sea way which enhanced the upwelling of water. Onshore flow of these currents, especially in the Avalon and Baltic areas, may have checked the formation of carbonates and impeded sedimentation. In summary the differences between the northern and southern portions of the Acado-Baltic province may be related to differences in paleoenvironmental conditions as opposed to the presence of separate continental blocks.

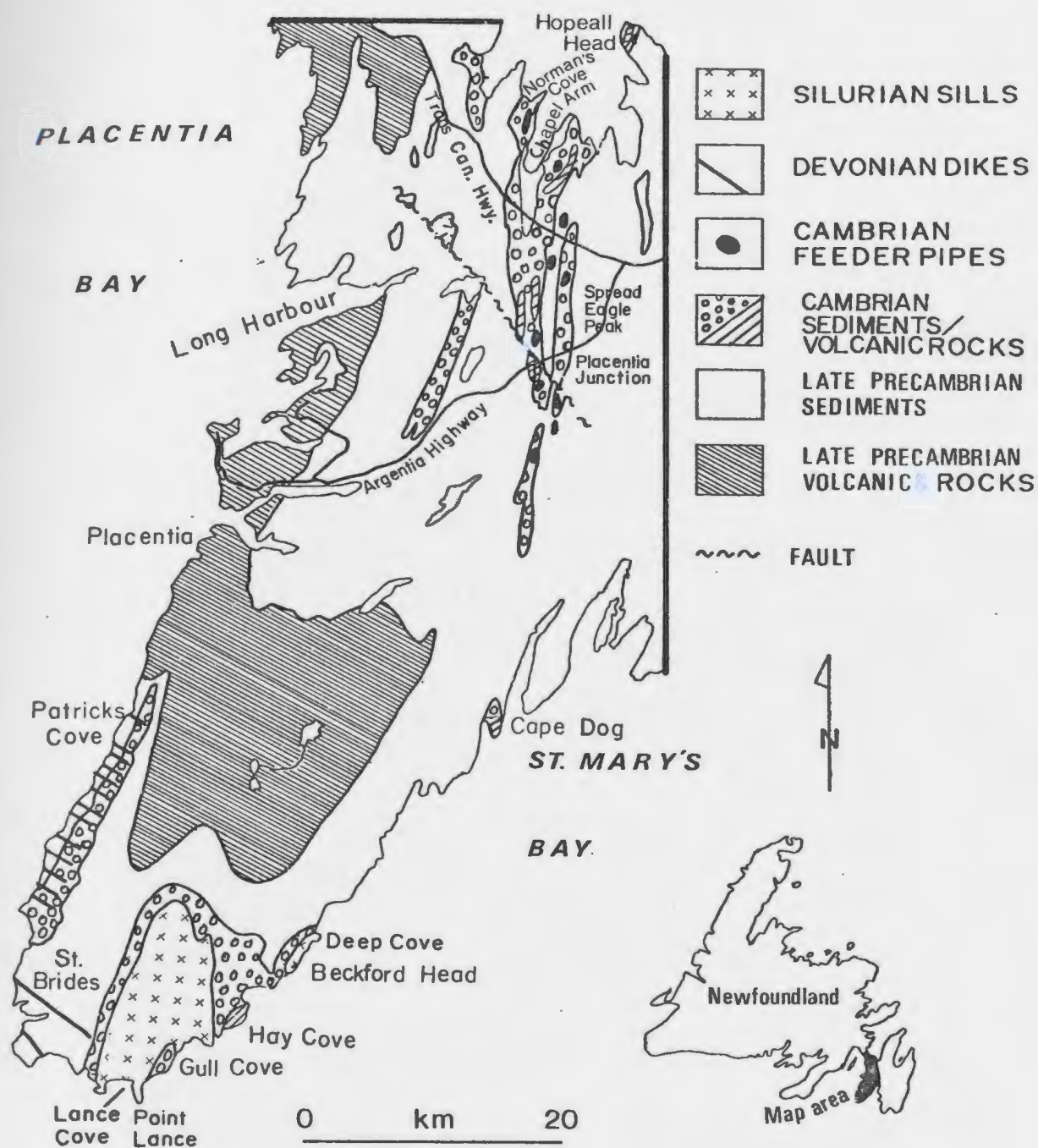
Comparison of Cambrian trilobite faunas at the generic level from around the globe reveals that there are four main faunal provinces; European (Acado-Baltic), American, Siberian, and Chinese (eg. Palmer, 1972; Burrett and Richardson, 1980). These studies assume that, for benthonic faunas, similarity between faunas indicates the lack of any ocean barrier between them (Hughes, 1981). All of the localities studied here, on both sides of the Atlantic, show a fauna belonging to the Acado-Baltic province (cf. Palmer, 1971, 1972, 1977; Henningsmoen, 1969; Hallam, 1972; Burrett and Richardson, 1980).

The European faunal province has been divided into northern and southern portions (eg. Palmer, 1977; Burrett

and Richardson, 1980) which correspond with the lithological subdivision discussed above. Recent work by Skehan et al. (1977, 1978, 1981) shows that this division is also applicable to the Appalachian orogen. Burrett and Richardson (1980), proposed that the lower diversity of faunas and rarity of carbonates in the northern area, compared with the southern area, indicates formation of the former at higher latitudes and under cooler conditions. If so the faunal and lithological differences may be due to climatic (water temperature) and sedimentary facies variations. However, they proposed the existence of a small, mid-European ocean, that somewhat restricted faunal exchange within the province. Because of the complex interplay of environmental factors, it is difficult to determine how different two areas must be (faunally) in order to justify the assumption of isolation (Hughes, 1981).

The numerous world paleogeographic reconstructions based on paleomagnetism (eg. Ziegler et al., 1977, 1979; Kanasewich, 1978; Scotese et al., 1979; Morel and Irving, 1978; Smith et al., 1980 and reviewed by Ziegler, 1981; also see Johnson and Van der Voo, 1983) suggest that both the northern and southern portions of the Acado-Baltic province occupied low to middle latitudes during the Cambrian (Figure 1.3). Apparent polar wander curves indicate the northern and southern portions of the province moved together during the Cambrian (Van der Voo et al., 1980) This information favours a climatic origin for the differences in lithology and fauna

Figure 1.3 Paleogeographic reconstruction of the Acado-Baltic province during the Early Cambrian also showing the types and distribution of volcanic rocks. The latitude lines are those suggested by Smith et al. (1980, p. 94) for the Early Cambrian of Europe and are based on a review of paleomagnetic data. The rocks in eastern North America have been moved north relative to the Smith et al. (1980) reconstruction in order to bring the Avalon Peninsula, Nova Scotia and New Brunswick closer to the British Isles which they resemble lithologically. The reconstruction leaves more southerly localities in the Appalachians (eg. Rhode Island), which appear to belong to the southern portion of the Acado-Baltic province (Skehan et al., 1977, 1978), adjacent to Spain and France. The Acado-Baltic area may have been subjected to considerable internal deformation during the Early Paleozoic, such that the present relationship of various localities is now contorted (Van der Voo et al., 1980).



rather than a mid-European ocean. For example, the southern portion of the Acado-Baltic province may have been ocean facing, and exposed to ocean currents whereas the northern areas may represent restricted, euxinic inland basins or areas which experienced upwelling of cold  $O_2$ -depleted currents as proposed by Brasier (1980). This hypothesis seems preferable to suggesting the presence of a small sea as vestiges of such an ocean have not been found.

#### 1.4 DISTRIBUTION OF CAMBRIAN VOLCANIC ROCKS

As a generalization, volcanic rocks are not very common within Acado-Baltic Cambrian stratigraphy. Using the southern New Brunswick area as an example, most outcrops of Cambrian rocks occur in the St. John area but only in the the areal smaller Long Reach and Beaver Harbour areas are volcanic rocks found as thin units at particular outcrops (see southern New Brunswick volcanic rocks, Chapter 2). Despite the fact that volcanic rocks are volumetrically unimportant within the Cambrian stratigraphy, they can be found at particular outcrops within just about all of the broad areas studied in this report (Table 1.1).

Most areas show a bimodal distribution of rock types. In the northern portion of the Acado-Baltic province basalts tend to predominate over felsic rocks, where a bimodal distribution is shown, whereas in the southern portion the felsic rocks tend to be more important. The available information (ie. New Brunswick, Nova Scotia, Czechoslovakia,

Table 1.1. Summary of the characteristics of Cambrian volcanic rocks.

| Location                | Distrib.<br>of Rock<br>Types | Dominant<br>Rock<br>Types | Chem.<br>Affinities        | Proport.<br>of Flows to<br>Volcanic-<br>clastic<br>Rocks | Thick-<br>ness    | Geographic<br>Distribution | Assoc.<br>Tecton-<br>ism | Age   |
|-------------------------|------------------------------|---------------------------|----------------------------|--|-------------------|----------------------------|--------------------------|---|
| Beaver<br>Harbour, N.B. | Unimodal                     | Evolved<br>Basalt         | Tholeiitic                 | Equal  | <<br>100 M        | Local                      | ?                        | Middle<br>Cambrian                                |
| Long<br>Reach, N.B.     | Bimodal                      | Basalt                    | Tholeiitic                 | Flows<br>Predominate                                     | <<br>50 M         | Local                      | Basins<br>Formed         | Eocambrian<br>to Lower<br>Cambrian                |
| Cape<br>Breton, N.S.    | Bimodal                      | Basalt                    | Tholeiitic                 | Flows<br>Predominate                                     | 600 M             | Local                      | Basins<br>Formed         | Middle<br>Cambrian                                |
| Avalon<br>Pen.          | Unimodal                     | Basalt                    | Alkalic                    | Equal  | <<br>200 M        | Local                      | Basins<br>Formed         | Middle<br>Cambrian                                |
| Britain                 | Bimodal                      | Basalts                   | ?                          | Mostly<br>Volcanic-<br>clastic Rks.                      | 1200 M            | Local                      | ?                        | Lower and<br>Middle<br>Cambrian                   |
| Norway                  | Unimodal                     | Basalts                   | Alkalic and<br>Tholeiitic  | Mostly<br>Flows  | <<br>50 M         | Local                      | Faulting                 | Eocambrian<br>Lr. Cambrian                        |
| N & NE<br>Poland        | Bimodal                      | Basalts                   | ?                          | Flows<br>Predominate                                     | 100 M             | Local                      | ?                        | Eocambrian<br>Lr. Cambrian<br>& Upper<br>Cambrian |
| SW<br>Poland            | Bimodal                      | Basalts                   | Alkalic and<br>Subalkaline | Flows<br>Predominate                                     | 1000 to<br>2000 M | Wide                       | Late stage<br>folding    | Upper<br>Cambrian                                 |

Table 1.1 (Cont'd.)

| Location                       | Distrib.<br>of Rock<br>Types | Domin-<br>ant<br>Rock<br>Types | Chem.<br>Affinit-<br>ies | Proport.<br>of Flows to<br>Volcani-<br>clastic<br>rocks | Thick-<br>ness     | Geog-<br>raphic<br>Distri-<br>bution <sup>2</sup> | Assoc.<br>Tecton-<br>ism                        | Age                                   |
|--------------------------------|------------------------------|--------------------------------|--------------------------|---|--------------------|---|---|---------------------------------------|
| Czecho-<br>slovakia            | Unimodal                     | Felsic<br>Rocks                | Sub-<br>alkaline         | Mostly<br>Flows   | 1000 M             | Wide  | Emplaced<br>along<br>faults,<br>late<br>folding | Middle to<br>Upper<br>Cambrian        |
| N. France                      | Bimodal                      | Felsic<br>Rocks                | Sub-<br>alkaline         | Volcani-<br>clastic Rks.<br>Predominate                 | Approx.<br>500 M   | Wide  |   | Lower to<br>Middle<br>Cambrian        |
| S. France                      | Bimodal                      | Basalts                        | Sub-<br>alkaline         | Flows   | Less than<br>100 M | Local   |   | Lower<br>Cambrian                     |
| Portugal &<br>NW Spain         | Unimodal                     | Basalts                        | Alkaline                 | Mostly<br>Flows   | <<br>50 M          | Local   | Faulting<br>and<br>Basin                        | Lower Middle<br>and Upper<br>Cambrian |
| Southern &<br>Central<br>Spain | Bimodal                      | Felsic<br>Rocks                | Sub-<br>alkaline         | Mostly<br>Flows   | <<br>50 M          | Local   | Sub-<br>sidence                                 | Lower to<br>Middle<br>Cambrian        |

Table 1.1 (Cont'd)

- 
1. Mostly  $>80$ , Predominate  $>50$  to  $<80$ , Equal 50.
  2. Local means present only locally, wide implies present in most sections in the area.

## Sources:

Beaver Harbour, N.B., Helmstaedt (1968), and this study.

Long Reach, N.B., Hayes and Howell (1937), McCutcheon (1981), and this study.

Cape Breton, N.S., Hutchinson (1952), Helmstaedt and Tella (1973), Cameron (1980), Keppie and Dostal (1980), and this study.

Avalon Peninsula, Nfld., Hutchinson (1962), McCartney (1967), Fletcher (1972) and this study.

Britain, Rushton (1974, p. 62, 67, 71, 78, 99) and Greenly (1944, 1945).

Norway, Henningsmoen (1956), Ramberg and Barth (1966), Bjorlykke (1978), Ramberg and Larsen (1978), Nystuen (1981, 1982), Furnes et al. (1983).

N and NE Poland, Znosko (1965), Juskołiak and Ryka (1967), and Chlebowski (1978).

SW Poland, Teisseyre (1968) and Baranowski et al. (1984).

Czechoslovakia, Svoboda et al. (1966), Waldhausrova (1966, 1971), Palicova and Stovickova (1968), Vidal et al. (1975) and Fiala (1978a, b).

N and central France, Boyer (1966, 1974), Dore et al. (1972), Le Gall et al. (1975), Le Gall (1978), Boyer et al. (1979) and Chauvel (1979).

S France, Boyer (1974), Dore (1977) and Boyer et al. (1979).

N Spain and Portugal, Teixeira (1956) and Parga (1969).

S Spain, Dupont and Vegas (1978) and Guillou (1971).

---



France, Spain) shows that the felsic rocks are usually peraluminous. Czechoslovakia is unique in that the rocks show a unimodal distribution with felsic rocks dominant.

Data elucidating the chemical affinities of Cambrian basalts on the Avalon Peninsula in Newfoundland, and southern New Brunswick are presented in Chapter 4. The Avalon Peninsula basalts show alkaline chemical characteristics closely resembling rift basalts as is probably the case with basalts from Poland (Baranowski et al., 1984). Those from New Brunswick, Nova Scotia (Cameron, 1980), and Norway (actually Eocambrian, see Chapter 4 and Furnes et al., 1983) are continental tholeiites that show geochemical characteristics most commonly associated with continental rupture. As yet, detailed geochemical studies have not been carried out on the basalts from other areas in the Acado-baltic province.

The Cambrian volcanic rocks at most localities consist of only a few flows or tuffaceous beds representing single eruptive episodes with limited areal extent (Table 1.1). The thickest Cambrian volcanic sequences are developed in Poland and Czechoslovakia where the volcanism is predominantly Late Cambrian. Volcanism in the Acado-Baltic province was apparently most common in the Middle Cambrian (most number of localities), and least common in the Upper Cambrian (Table 1.1).

The characteristics of the volcanic rocks from several of the areas

shown in Figure 1.1 are not presented in Table 1.1 because some critical information was unavailable. These areas are briefly discussed below.

Volcanic rocks giving Rb-Sr and Pb-Pb age dates between 580 and 520 million years (Bland and Blackburn, 1980; Black, 1980) have been reported, in association with Cambrian sedimentary rocks (mostly shales) bearing Acado-Baltic fauna (eg. St. Jean, 1973; Maher et al., 1981; Samson et al., 1982), from the Carolina Slate Belt in the Southern Appalachians. However, due to complex folding, a paucity of fossils, poor resolution of age dates, and lack of detailed mapping, the importance and stratigraphic relationships of these rocks remain poorly understood. The available information suggests that volcanic rocks showing a basalt-rhyolite bimodal distribution make up a large proportion of the relatively thick (8 km), volcano-sedimentary sequences (Costello et al., 1981; Stromquist and Sundelius, 1969). Geochemical data on the volcanic rocks together with facies relationships have been interpreted by various authors as indicative of an island arc tectonic setting for the slate belt (eg. Butler and Ragland, 1969; Black, 1980; Bland and Blackburn, 1980). If this early work is accurate, the thick volcano-sedimentary sequences of the slate belt contrast sharply with the stratigraphy and style of volcanism in other areas of the Acado-Baltic province (compare with Figure 1.2 and Table 1.1).

Reviews of the stratigraphy of Acado-Baltic Cambrian rocks in New England make no mention of any Cambrian volcanism (eg. Theokritoff, 1968; Palmer, 1971). Kaye and Zartman (1980) suggested that a rhyolite flow or dome (along with minor andesite and felsite) in the Boston Basin, giving a Pb-Pb age of about 600 million years, may represent very early Cambrian volcanism at this locality. However, Lenk et al. (1982) used microfossils to show that these rocks are probably Late Precambrian (Vendian). Cambrian stratigraphy in southern Rhode Island apparently differs substantially from that in the rest of New England but volcanic rocks have not been reported from the area (Skehan et al. 1977, 1978, 1981, and written comm. 1981).

Moroccan rocks are not examined here in detail however, a superficial review of the Moroccan Cambrian shows that volcanic rocks are common in both the Haut Atlas and Anti-Atlas areas. Andesites, trachyandesites, trachytes and acid lavas and pyroclastic rocks, make up thin units in the Lower Cambrian of the Haut Atlas area in Morocco (Termier and Termier, 1966; Michard, 1976, pages 58 and 157; Daly and Pozzi, 1977; Benziane et al., 1983). Thick sections of basaltic lavas and pyroclastic rocks in the Anti Atlas area accompanied Cadomian movements during the late Middle Cambrian (Furon, 1956; Furon, 1963; Michard, 1976, page 59).

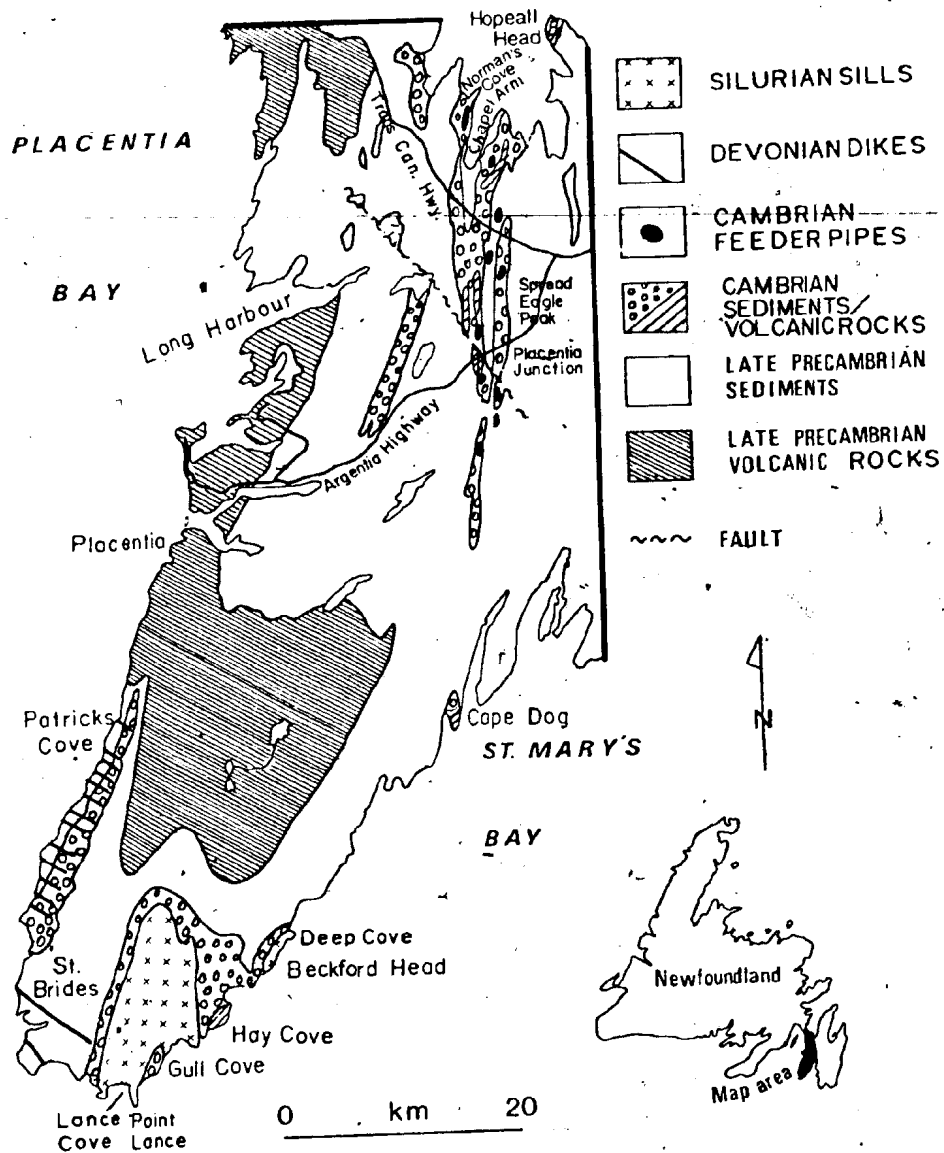
CHAPTER 2 GEOLOGY OF THE VOLCANIC ROCKS IN  
NEWFOUNDLAND AND NEW BRUNSWICK

2.1 INTRODUCTION

At the time this project was started, Cambrian volcanic rocks were known from "Avalonian" terrane in Newfoundland and New Brunswick. Work by Hutchinson (1962), McCartney (1967) and Fletcher (1972) demonstrated the presence of Middle Cambrian pillow basalts and tuffaceous rocks between Trinity Bay and Placentia Bay on Cape St. Mary's (Figure 2.1, pocket Maps A and B) but only Fletcher's map showed the distribution of the rocks in the southern portion of the study area (pocket Map B). Along with the extrusive rocks there are three groups of shallow level intrusive rocks (the feeder pipes, sills, and dikes) which earlier mapping efforts (Fletcher, 1972; McCartney, 1967) revealed could be Cambrian. In this chapter new information regarding the field relationships of the extrusive and intrusive rocks is discussed.

The classical work of Hayes and Howell (1937) established that a relatively complete, Cambrian stratigraphic section, with Acado-Baltic fauna, is present in the Saint John area of southern New Brunswick. However, they found no evidence for any Cambrian volcanism. Helmstaedt (1968) first found Middle Cambrian mafic volcanoclastic rocks in a previously unreported Cambrian section at Beaver Harbour about 50 km west of Saint John

Figure 2.1 Geological sketch map of the Cape St. Mary's study area. The map is a compilation of work done by the author, Fletcher (1972), and McCartney (1967).



(Figure 2.2). A field trip to sample these rocks revealed that there were problems with the geological relationships reported by Helmstaedt (1968). McCutcheon (personal communication) reexamined the section and his analysis is given in this chapter. Lower Cambrian basaltic flows and felsic pyroclastic rocks were reported from the Long Reach area (Figure 2.3) by McCutcheon (1981). Their field relationships and distribution are described here on the basis of information provided by McCutcheon.

The only other volcanic rocks in the southern New Brunswick area, which may be Cambrian, are flows, pillow lavas, and volcanoclastic rocks at Grand Manan (Stringer and Pajari, 1981), and massive mafic flows and pillow lavas across the New Brunswick-Maine border near Calais (Ruitenberg and Ludman, 1978). The age and stratigraphic relationships of both these groups of rocks remain uncertain so they are given no further discussion here.

## 2.2 CAPE ST. MARY'S STUDY AREA

### 2.2.1 General Geology of Cape St. Mary's

All of the known Cambrian volcanic rocks on the Avalon Peninsula occur in a narrow belt on Cape St. Mary's (Figure 2.1, see Maps A and B in pocket for details). The stratigraphy of Cape St. Mary's is fairly well known as a result of studies by Hutchinson (1962), McCartney (1967), and Fletcher (1972) and is summarized below and in Table 2.1.

Figure 2.2 Geological sketch map of the Beaver Harbour area in New Brunswick. The geology is modified after Helmstaedt (1968) by McCutcheon (1982; personal communication) and used here by permission.



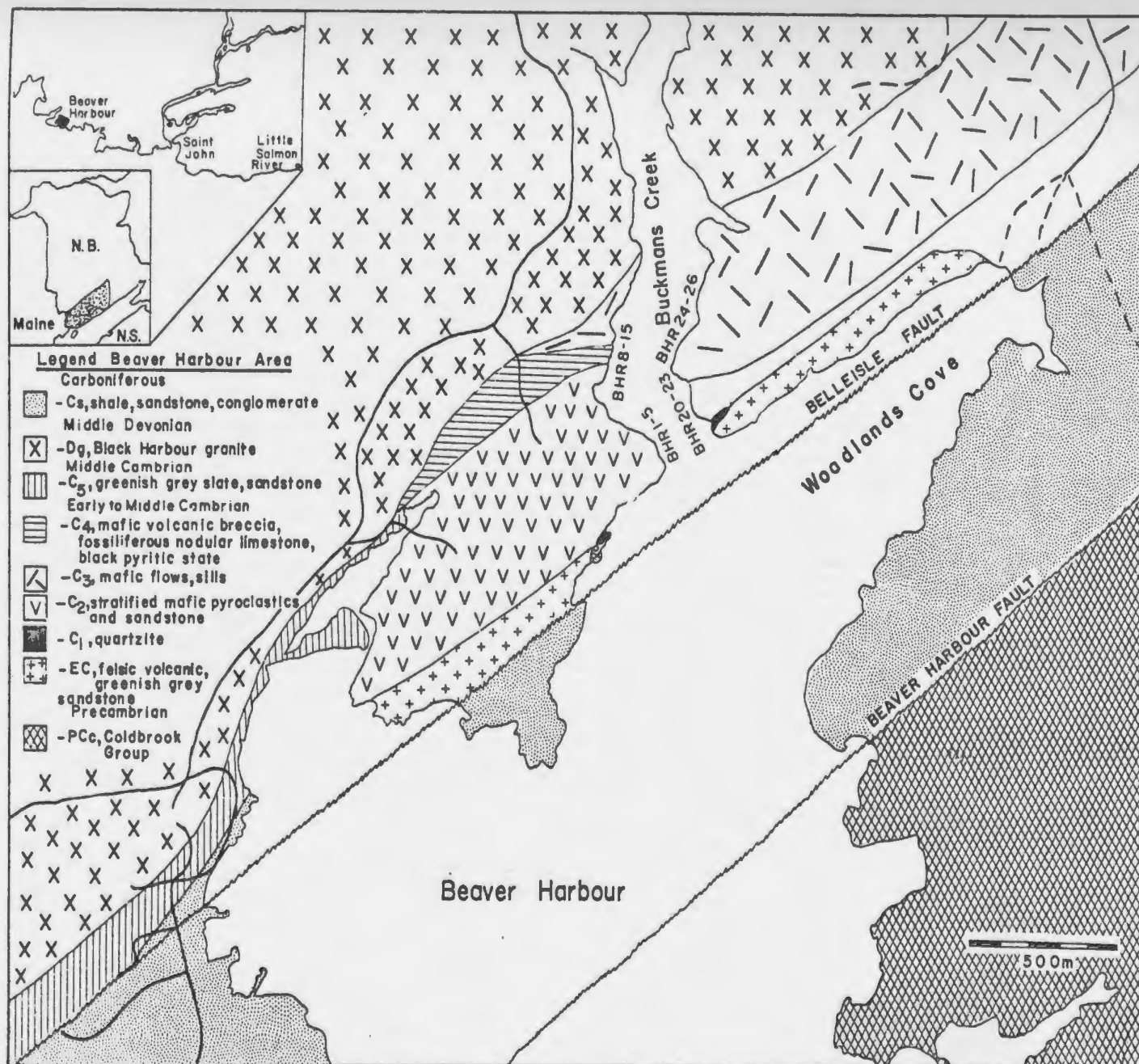
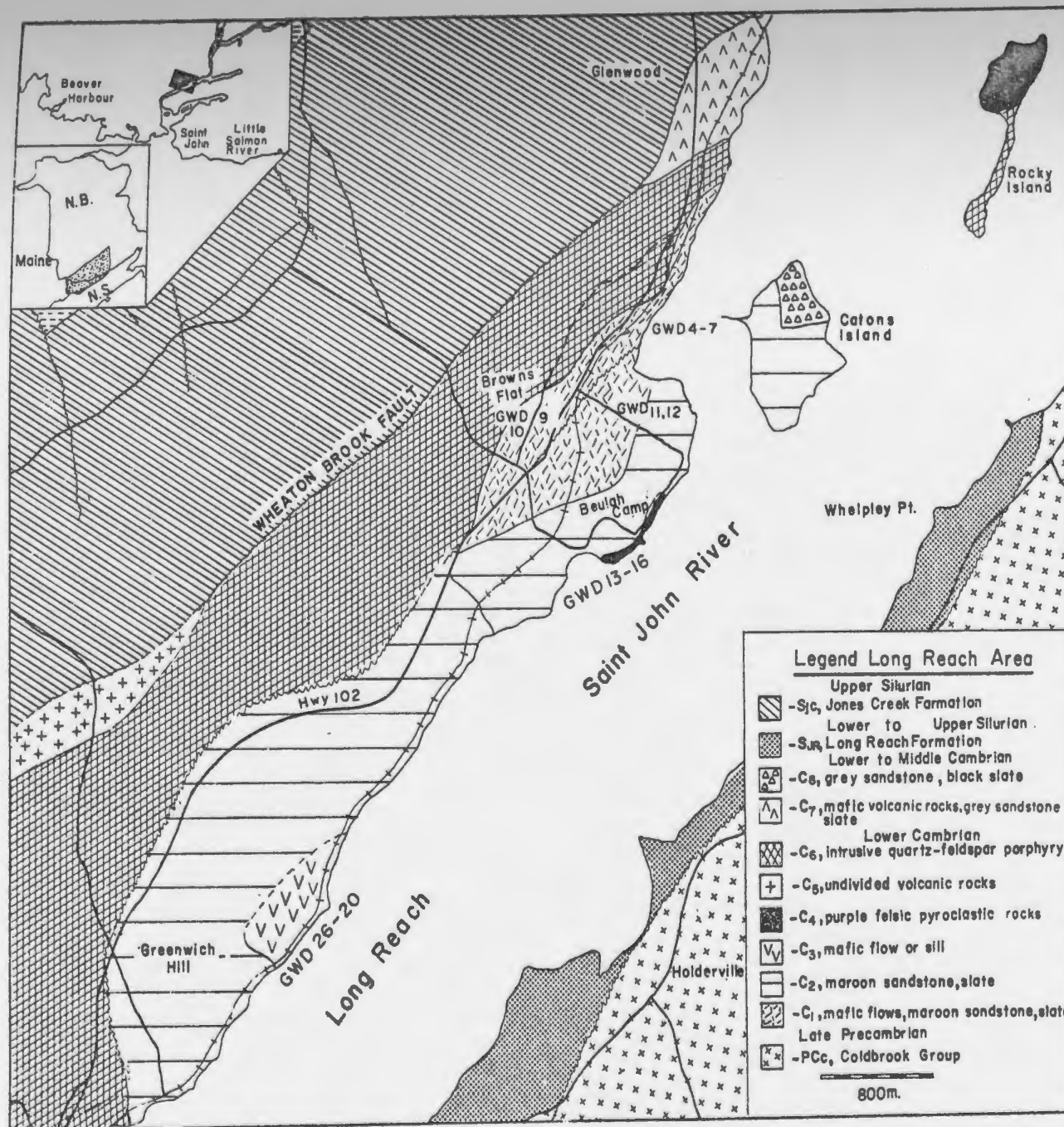


Figure 2.3. Geological sketch map of the Long Reach area in New Brunswick. The geology is by McCutcheon (1982, personal communication) and used here by permission.



The oldest rocks in the Cape St. Mary's study area, belong to the Late Precambrian Musgravetown Group. They consist of mafic flows and tuffs with minor rhyolitic flows and tuffs (Bull Arm Formation) and an overlying sequence of mostly red siltstones and coarser clastic sedimentary rocks. Unconformably above these rocks are the Random, Chapel Island and Rencontre Formations, which consist of varying amounts of white quartzites, quartz pebble conglomerates, arkoses, and siltstones. For the most part, these sedimentary rocks are Lower Cambrian (Anderson, 1981). Unconformably above the arenaceous rocks are bright red shales and siltstones of the Bonavista Formation, lithologically distinctive limestones of the Smith Point Formation, and more red shales assigned to the Brigus Formation, all of which are Lower Cambrian (Table 2.1).

A minor unconformity at the top of the Brigus Formation separates it from a distinctive manganese carbonate bed at the base of the Chamberlain's Brook Formation (Table 2.1). The shales of the Chamberlain's Brook Formation are dull grey-green. Those of the Manuel's River Formation appear darker or black, but away from the shoreline it is impossible to tell them from the underlying Chamberlain's Brook rocks. Both formations are Middle Cambrian and both contain extrusive volcanic rocks which are the subject of this study (Figure 2.1, Figure 2.4 and pocket Maps A and B).

Table 2.1. Rock units of the Avalon Peninsula showing corresponding ages, divisions, and lithologies.

| Age              | Unit  | Lithology   |
|------------------|---|---|
| Lower Ordovician | Wabana Group<br>Bell Island Group<br>Clarenville Formation  | Shales, sandstones, and oolitic hematite beds.  |
| Upper Cambrian   | Gull Cove<br>Beckford Head<br>Elliot Cove Formations  | Grey to black siltstones and shales.  |
| Middle Cambrian  | Manuels River Formation<br><br>Chamberlains Brook Formation   | Dark grey to black shales, volcanic rocks.<br>Grey green shales, volcanic rocks, Mn bed at base.  |
| Lower Cambrian   | Brigus Formation<br>Smith Point Formation<br>Bonavista Formation<br>Random<br>Chapel Island, and<br>Rencontre Formations  | Red shales.<br>Pink algal limestones.<br>Red shales and siltstones.<br>Fine to coarse grained siliciclastics.   |
| Late Proterozoic | Signal Hill,<br>Musgravetown, and<br>Hodgewater Groups<br>Bell Bay and Bull<br>Arm Formations<br>Conception and Connecting Point Groups<br><br>Love Cove and Harbour<br>Main Groups | Red, coarse grained molasse sediments.<br><br>Basalt-rhyolite suite of volcanic rocks.<br>Fine grained, flysch-like marine volcanoclastic and sedimentary rocks.<br>Marine and terrestrial mafic and acidic, alkaline volcanic rocks. |

Figure 2.4. Sections showing the stratigraphic positioning of Cambrian volcanic rocks in the Cape St. Mary's study area. Volcanic rocks occur within the Chamberlains Brook Formation at Hopeall Head and Cape Dog and within the Manuels River Formation at Chapel Arm and Hay Cove. Note that the pillow lavas at Hopeall Head and tuffaceous rocks at Placentia Junction are shown within the Manuels River Formation but their position in the stratigraphy is uncertain. The localized nature of the volcanic eruptions is illustrated by the absence of volcanic rocks in the Chamberlains Brook Formation at Chapel Arm, though they occur at Hopeall Head just 10 km away. Similarly Fletcher (1972) found that the Hay Cove volcanic rocks disappear only 10 km north of Hay Cove and the Cape Dog volcanic member is absent in sections of the Chamberlains Brook Formation 15 km to the south of Cape Dog. The stratigraphic sections for Hopeall Head, Chapel Arm, and Cape Dog are from Hutchinson (1962) and the section for Hay Cove is from Fletcher (1972).

# Symbols

P Pillow lava

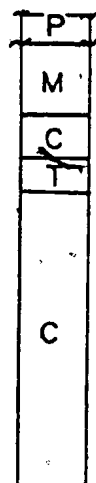
T Lapilli tuff

M Manuels River Formation (shale)

C Chamberlains Brook Formation (shale)

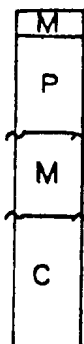
~ Indicates portion of section not observed

Hopeall Head

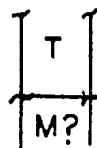


N

Chapel Arm



Placentia Junction



Cape Dog



Hay Cove



S

km.

0 10 20

325

300

200

100

0

Meters

In the southern portion of the study area, grey and green siltstones of the Gull Cove and Beckford Head Formations, which are Upper Cambrian, conformably overlie the Manuels River Formation.

McCartney (1967) mapped a series of gabbroic "plugs" which, together with the Middle Cambrian extrusive rocks, form a belt of volcanic rocks stretching from Chapel Arm to Cape Dog (Figure 2.1). Because of their proximity to the extrusive rocks, and because the youngest rocks they intrude are in the lower portions of the Chamberlain's Brook Formation, McCartney suggested that the intrusions may be Middle Cambrian, and the feeders to the extrusive rocks.

Fletcher (1972) first noted the occurrence of layered gabbroic sills near the end of Cape St. Mary's (Figure 2.1 and pocket Map A). He pointed out that the sills intrude Upper Cambrian shales; the youngest rocks on Cape St. Mary's, (Table 2.1) and that they were folded by Devonian deformation. He believed the rocks are probably Upper Cambrian or Lower Ordovician and for this reason the decision was made to include them in this study.

Fletcher (1972) also reported the presence of numerous diabase dikes on the eastern shores of Placentia Bay, (Figure 2.1 and pocket Map A). He suggested they may be Devonian because they resemble dikes of that age mapped by Jenness (1963), in the Terra Nova map area. However, Fletcher's work did not rule out the possibility that the



dikes and sills (mentioned above) are comagmatic.

### 2.2.2 Cambrian Extrusive rocks

Basaltic flows, and/or tuffs occur at a number of localities on Cape St. Mary's (Figure 2.1, see maps A and B in pocket for details). The most northerly of these is Hopeall Head, which forms a small peninsula along the southeastern shore of Trinity Bay. Lapilli tuffs occur on the western limb of a northerly trending syncline, and are exposed on the northern and southern shores of the peninsula. A major north-south trending fault separates the volcanoclastic rocks (sampling localities PL53, PL129 and PL132, pocket Map A) from pillow basalts (PL54) and breccia (PL128), on the western extremity of the peninsula.

The tuffs occur in the upper portion of the Chamberlains Brook Formation (Table 2.1, Figure 2.4), and according to McCartney (1967) and Hutchinson (1962) are about 5 meters thick. A tuff section 5.3 meters thick occurs at the northern end of Hopeall Head (sampling locality PL129, pocket Map A) and the unit is approximately the same thickness at the most southeasterly exposure (0.2 km SE of PL53) but it is nearly 12 meters thick at the southwest corner of Hopeall Head (locality PL 53).

Fletcher (1972) assumed that the pillow basalts were produced at the same time as the tuffs and assigned them to the upper portion of the Chamberlains Brook Formation.

However, the stratigraphic position of the pillow basalts cannot be determined because they are everywhere in fault contact with the surrounding sedimentary and volcanoclastic rocks. The pillow lavas are probably Middle Cambrian because they are associated, and probably contemporaneous, with minor grey shales which are almost certainly of this age. The fact that pillow lavas are not found with the tuffs and vice versa, yet the two are juxtaposed along a normal fault, suggests that they were not produced by the same event. The pillow lavas may overlie the volcanoclastic rocks because no evidence has been found in the stratigraphic column for any volcanism below the volcanoclastic rocks, despite excellent exposures on both the north and south shores of Hopeall Head. The thickness of the pillow basalts cannot be determined due to incomplete exposure and structural complications, but they are at least 5 meters thick.

Middle Cambrian pillow basalts and minor volcanoclastic rocks also occur around the shores of Chapel Arm, at the southern tip of Trinity Bay (Plate 2.1, Figure 2.1 and pocket Map A). The pillow lavas vary from a few meters to approximately forty meters in thickness. A pillow breccia, three meters thick, occurs along the shoreline about one kilometer south of Normans Cove (between sampling localities LC18 and LC19, pocket Map A). Inland from the shore the lavas form resistant ridges which can be traced as far south as Placentia Junction (Figure 2.1 and pocket Map A).

Plate 2.1 Pillow basalts along the shores of Qhapel Arm. Inspection of the pillows in the field shows that the concentric zoning evident in cross sections of the pillows is due to variations in the size and percentages of vesicles in the pillows. Photos were taken at sampling locality LC17, (pocket Map A).



McCartney (1967) found that two volcanic events were represented at Chapel Arm, both occurring within the "Paradoxides davidis" zone of the Manuels River Formation, but they are separated by several meters of shale. It is difficult to determine with certainty if the extrusive rocks, which occur inland, are exactly time correlative with those along the shores, because fossil bearing exposures are practically impossible to find.

McCartney (1967) makes no mention of the sill exposures associated with the pillow basalts, and probably thought they are massive flows. There are usually two sills found together, each about 7 meters thick and separated by about 6 meters of shale. The steep sea cliff approximately 2 kilometers long on the east shore of Chapel Arm (eg. localities CA40 to CA42 pocket Map A) is actually made up of two sills, each dipping at approximately 75 degrees west. The two sills become dikes and cut across shales to form pillow basalts near the northern end of Chapel Arm at Mcleod Point (locality CA64). These exposures show conclusively that the sills are related to the events which produced the pillow lavas.

Basaltic lapilli tuffs are exposed in a road cut some 250 meters long, along the Argentinia access highway, near Placentia Junction, (Plate 2.2, Figure 2.1 and pocket Map A localities PL60 to PL80 and PL140 to PL172). The volcanoclastic unit is fault bounded on both the east and

Plate 2.2 Bedded pyroclastic rocks in the road cut at Piacentia Junction. In the upper photograph the hammer head is resting on fine grained tuff. Above and below the hammer head are coarser grained lapilli tuffs. A large sedimentary clast is partly obscured by the shadow of the hammer handle. The lower photograph gives a closer view of the lapilli tuffs. Note the spindle shaped clast below the penny. Both photographs were taken at sampling locality PL84 (pocket Map A).





west sides, and a lack of exposures to the north and south of the road cut prevents the observation of contact relations. The west end of the outcrop is entirely mylonitized, and the adjacent rocks are not exposed. Black Middle Cambrian shales probably belonging to the Manuela River Formation are in fault contact with the outcrop to the east. The actual age of the tuffs cannot be determined, but their similarity to the Cambrian volcanoclastic rocks at Hopeall Head and other Cambrian rocks at Cape Dog and Hay Cove suggests they are probably Middle Cambrian (Figure 2.4). This locality was recorded by McCartney (1967) as one of the "plugs" or feeder pipes in the area. However, the blasted road cut was not present when McCartney did his work.

Approximately 30 kilometers south of Placentia Junction, basaltic lapilli tuffs and pillow basalts occur along the sea cliffs of St. Mary's Bay, at Cape Dog. These rocks resemble those at Hopeall Head, Chapel Arm and Placentia Junction, and represent a southerly extension of the volcanic belt (Figure 2.1 and pocket Map B). The tuffs make up most of what is known as Cape Dog, and occur in the axis of a syncline plunging gently to the south and with low dips on the limbs. Small faults with, at most, several meters of displacement and variable orientation complicate the geology. To the northeast (sampling localities PL30 to PL37 pocket Map B) the tuffs rest directly on shales but on the southwest side of Cape Dog they occur above pillow lavas



(lavas at localities PL38 to PL40) underlain by Cambrian shales. Fletcher (1972) estimated that the section is about 60 meters thick. This seems reasonable as the syncline plunges gently, and the point of maximum relief (75 meters) is slightly north of where the volcanic unit meets the water line.

McCartney (1967) assigned the Cape Dog volcanic rocks to the Manuels River Formation because they resemble the volcanic rocks of this formation at Chapel Arm. Fletcher (1972) argued that the volcanic rocks are stratigraphically equivalent to those near the top of the Chamberlains Brook Formation at Hopeall Head (see Table 2.1 and Figure 2.4). His conclusions are supported by the observation that Mn-bearing sedimentary rocks, which are characteristic of the base of this formation, occur a few meters below the pillow lavas. In either case they are Middle Cambrian.

The thickest section of Cambrian lapilli tuffs occurs at Hay Cove, along the west shore of St. Mary's Bay (Figure 2.1 also see pocket Map B). The actual thickness of the unit is difficult to determine because most exposures form steep sea-cliffs, which are hazardous to examine. The rocks are accessible at their most southerly exposure (localities SB38 to SB40 pocket Map B) where an incomplete section 125 meters thick was measured; however the total thickness may exceed 200 meters. The southern sea-cliff exposures show that the unit is folded and forms a large syncline to the

west, and an anticline to the east. Several thin mafic sills at the base of the tuff section at Hay Cove may have been mistaken by Fletcher (1972) for thin flows as pillow lavas were never observed during the course of this study. The tuffs also occur at Beckford Head (Figure 2.1 and Map B), only three km to the northeast, as a thin bed 0.7 meters thick. The unit cannot be found north of Deep Cove (4 km northeast of Hay Cove) where it is a mere 0.3 meters thick (Fletcher, 1972). According to Fletcher (1972) these volcanic rocks occur within the "Paradoxides davidis" zone and are therefore contemporaneous with the flows at Chapel Arm (Figure 2.4).

#### 2.2.3 Feeder Pipes

At least 10 small pipe-like intrusive bodies, probably of sub-volcanic origin, occur in a narrow belt extending south from Chapel Arm to St. Mary's Bay (Figure 2.1). These shallow-level intrusive rocks (hereafter referred to as feeder pipes) form ovoid, erosion resistant, knobs on the countryside (Plate 2.3). They range in length from 0.5 to 2.0 kilometers and are usually less than 0.5 kilometers in width. McCartney (1967) proposed that these rocks were the feeder pipes for the Middle Cambrian tuffaceous rocks and pillow basalts because they occur adjacent to, but never cut sedimentary rocks stratigraphically overlying, the extrusive rocks.

Plate 2.3 Erosion resistant feeder pipe making up Spread Eagle Peak forms a topographic high point. Columnar jointing is evident in the lower photograph. Both photographs were taken looking west on Spread Eagle Peak (Figure 2.1 and sampling localities CA162 to CA165 pocket Map A).



Despite detailed mapping, outcrops which would conclusively establish the relationship between the feeder pipes and extrusive rocks were not observed. Dating the feeder pipes by radiometric methods proved impossible because of problems with alteration (Rb-Sr whole rock and mineral methods), and a lack of zircons (U-Pb techniques). However, some new indirect evidence suggests that the feeder pipes were the sources of the extrusive rocks. Pillow basalts east of the pipe at Normans Cove (eg. pipe sampling localities CA33 and CA142) seem to increase in thickness toward the west (basalts thicker at locality LC15 than LC18) as might be expected if the pipe was the source for the lavas. It also appears that feeder pipes cutting sedimentary rocks highest in the local stratigraphic column show the best development of columnar jointing, (eg. Spread Eagle Peak, sampling localities CA162 to CA164; also see Plate 2.3) and may be slightly finer grained than those more deeply eroded (eg. feeder pipe 3 km NW of Spread Eagle sampling localities CA177 to CA180). These observations suggest the former were closer to the surface and cooled more quickly. According to Dr. J. Hodych (personal communication), preliminary paleomagnetic data on a sample from Spread Eagle Peak indicates a pole position consistent with a Cambrian age for the pipe. In summary, the available circumstantial evidence indicates that the pipes were the feeders to the Cambrian extrusive rocks.

All known occurrences of the gabbroic sills are at the southern tip of Cape St. Mary's (Figure 2.1 and pocket Map B) where they form a swarm as shown by excellent exposures in sea-cliffs on Placentia and St. Mary's Bays. These rocks form small tabular intrusive bodies ranging in thickness from a few tens of centimeters to 60 meters. In outcrop the most striking features of the thicker sills, such as at Lance Cove (sampling localities SB60 and SB61 pocket Map B) and Gull Cove (localities SB6 and SB7), are their layering and coarse grained nature. Light colored granophyric layers in the thicker sills contrast sharply with the dark gabbroic rocks (Plate 2.4) but make up only small portions of the sills. At other localities, such as at Point Lance (sampling locality SB21), the sills occur as multiple injections commonly about one meter in thickness (Plate 2.4).

Fletcher (1972) found that the sills intrude Upper Cambrian shales, the youngest rocks on Cape St. Mary's (Table 2.1) and that they have been folded by Devonian deformation. He believed the rocks were probably Upper Cambrian or Lower Ordovician. Hodych and coworkers (personal communication) attempted to date the rocks by K - Ar methods but obtained reset Devonian ages. An age of  $516 \pm 31$  Ma. was obtained using Rb - Sr methods as part of this study, but the large error on this date, plus the fact that the sample with highest Rb (when included) gave an unrealistic Jurassic

Plate 2.4 A. Photograph showing a sill swarm at Point Lance. Most of the cliff consists of thin sills which are separated by thinner and lighter colored shale that erodes more easily than the sill rocks. The rocks shown in the photograph occur at sampling locality SB24 (pocket Map B).

B. A granophyric layer in the thick sill at Lance Cove. The lens cap is resting on the granophyre and approximately 10 cm above it are gabbroic rocks. The photograph was taken at sampling locality SB59 (pocket Map B).







age, make the number unacceptable. In a final attempt to determine the age of the rocks U - Pb methods were used to date zircon and baddeleyite grains concentrated from the sill at Lance Cove. These methods gave a reasonable and acceptable age for the sills of  $425 \pm 5$  Ma (T. Krogh, personal communication).

#### 2.2.5 Dikes

Most exposures of the diabase dikes occur on the eastern shores of Placentia Bay, though they are found at scattered localities over most the southern portion of the Cape St. Mary's study area (Figure 2.1 and pocket Map B). They take the form of multiple injections, ranging in width from 0.3 meters to 4.5 meters and averaging about 1.3 meters (Plate 2.5). Despite folding they are mostly vertical because their strikes, which average 120 degrees (range = 90 to 140 degrees), are at approximately right angles to fold axes in the area.

The dikes were first mapped by Fletcher (1972), who suggested they may be Devonian because they resemble dikes of that age mapped by Jenness (1963) 150 km to the NNW. The dikes cut Late Precambrian as well as Lower, Middle, and Upper Cambrian sedimentary rocks, and Fletcher (1972) noted at least one locality where a dike cuts one of the sills. The latter observation suggests the dikes postdate the sills. During the course of this study, a dike was found cutting a thin sill at Hay Cove (sampling locality SB38 pocket Map B). The small number of cross-cutting

Plate 2.5 A. Photograph showing three mafic dikes cutting limestones belonging to the Smith Point Formation at St. Brides (sampling locality SB26 pocket Map B).

B. Photograph illustrating the intense deformation suffered by some of the dikes. Fractures in the dike are filled with calcite. Photograph was taken at Patrick's Cove, sampling locality SB56 (pocket Map B).



relationships does not rule out the possibility that the sills and dikes are comagmatic - a hypothesis tested with the geochemistry. The age of these rocks remains problematical, but the petrological and chemical information shows that the dikes are similar to rocks described by Jayasinghe (1978) from the Bonavista Bay area which are between 340 and 400 Ma.

### 2.3 SOUTHERN NEW BRUNSWICK

#### 2.3.1 Geology of Southern New Brunswick

The geology of the Avalon Zone in southern New Brunswick has been reviewed by Rast et al. (1976), Ruitenberg et al. (1977), and Rast et al. (1978) and is summarized in Table 2.2. The following discussion summarizes information from these papers and draws on some more recent information for completeness. The oldest rocks in southern New Brunswick consist of marbles, calcareous siltstones, semipelitic rocks and quartzites of the Green Head Group which tend to show a gneissic fabric (Olszewski and Gaudette, 1982). These metasedimentary rocks are believed to be Neohelikian on the basis of stromatolites (Hoffman, 1974).

The Green Head rocks are in fault contact with, but almost certainly unconformably overlain by, the Coldbrook Group. The Coldbrook volcanic sequence can be divided into three belts termed the Eastern, Central, and Western

Table 2.2. Rock units of southern New Brunswick showing corresponding ages, divisions and lithologies.

| Period          | Unit                        | Lithology  |
|-----------------|-----------------------------|--|
| Ordovician      | Navy Island Formation       | Thin bedded black shale.   |
|                 | Narrows Formation           | Dark grey and black shale with a few limestone concretions and sandstone beds. |
| Upper Cambrian  | Black Shale Brook Formation | Thin bedded black shale.   |
|                 | Agnostus cove Formation     | Black and grey shale and sandstones with lenses of grey limestone.             |
| Middle Cambrian | Hastings Cove Formation     | Thin bedded black shale with thin sandstone beds, and limestone nodules.       |
|                 | Porter Road Formation       | Black shale.   |
|                 | Fossil Brook Formation      | Black limestone and shale.   |
| Lower Cambrian  | Hanford Brook Formation     | Micaceous red shale and fine grained grey sandstone.                           |
|                 | Glen Falls Formation        | White sandstone.   |
|                 | Ratcliff Brook Formation    | Purple sandstone and shale with conglomerate at the base.                      |
| Madrynian       | Coldbrook Group             | Terrestrial mafic and felsic volcanics, minor limestones and siliciclastics.   |
| Helikian        | Green Head Group            | Marble, calcareous quartz siltstone, semipelites, quartzite, gneisses.         |

Volcanic Belts (Giles and Ruitenberg, 1977). The Eastern Belt consists of a shallow marine sequence of pillow lavas and tuff, interbedded with siliciclastics and limestones. The Central and Western Belts are made up almost entirely of terrestrial, mafic and felsic volcanic rocks.

The Cambrian Saint John Group unconformably overlies the Coldbrook rocks. The type section was divided into eleven "formations" by Hayes and Howell (1937), but many of these are biostratigraphic, rather than lithostratigraphic units (Table 2.2). At the base, fine grained red sandstones and shales, of Eocambrian or Lower Cambrian age make up the Ratcliff Brook Formation. The variable thickness of this unit (60 to 600 meters) suggests it may be separated from the overlying white, medium to coarse grained, and cross-bedded sandstone of the Glen Falls Formation, by a major unconformity (McCutcheon, personal communication). Above the Glen Falls beds, the late Lower Cambrian Hanford Brook Formation, is the first trilobite bearing unit and therefore the first with a firmly established age. The Black Limestone separates gray shales and sandstones of the Hanford Brook Formation, from several biostratigraphic units with gray and black shales, and forms the base of the Middle Cambrian. The Upper Cambrian Agnostus Cove Formation is distinguished from the Middle Cambrian rocks by fine to medium grained arenite beds, and is overlain by black, Upper Cambrian to Lower Ordovician shales. The trilobite fauna associated with these rocks belongs to the Acado-Baltic

province" and has been correlated with that of Cape Breton and eastern Newfoundland, as well as most of northern Europe (Henningsmoen, 1969; Palmer, 1972, 1977; Hallam, 1972; Burrett and Richardson, 1980).

The Cambrian sedimentary rocks in the Long Reach area are similar to those in the type section (McCutcheon, 1981) but primarily Lower Cambrian rocks are preserved in the Long Reach area, and volcanic rocks are found in the section. At Beaver Harbour, where volcanic rocks also occur, the section is highly faulted and only a small portion is exposed so that detailed comparison with the type section is impossible.

#### 2.3.2 Beaver Harbour Area

Helmstaedt (1968) reported "greenish and purple pyroclastic rocks" associated with Middle Cambrian limestone on Buckmans Creek, at the head of Beaver Harbour (Figure 2.2). The faulted nature of the section prevented him from stating with confidence that all of the rocks along the creek are Middle Cambrian in age. McCutcheon (personal communication) has reexamined the section, and according to him it is divisible into five parts - units EC and C1 to C4 in Figure 2.2. On both sides of Buckmans Creek, a 20 to 30 meter thick unit (C1) comprised of quartzite and redbeds, disconformably (?) overlies felsic volcanic rocks (EC) that were considered Silurian in age by Helmstaedt (1968). Above this unit, and facing north are predominantly purple colored

pyroclastic rocks (C2) approximately 60 m thick, which on the west side of the creek form a discontinuous outcrop that is entirely green at the top. On the east side of the creek these rocks are in fault contact with a dark green flow (C3) that Helmstaedt (1968) assigned a Silurian age.

On the west side of Buckmans Creek the pyroclastic rocks are in fault contact with a unit (C4) that contains the Middle Cambrian fossil locality of Helmstaedt (1968). This unit dips north, but bedding - cleavage relationships indicate that it is overturned. It contains, from apparent bottom to top, 20 m of volcanic breccia, 7 m of gray clastics with volcanic detritus, 2 m of fossiliferous nodular limestone, and 1.5 m of black shale. To the north, it is in fault contact with the same flow (C3) as observed on the east side of the creek.

McCutcheon (personal communication) suggested that the volcanic rocks on Buckmans Creek are most likely late Lower to early Middle Cambrian if the quartzite at the base of the section is correlative to the Glen Falls Formation near St. John (Table 2.2).

### 2.3.3 Long Reach Area

Both felsic and mafic volcanic rocks occur in the Long Reach area in association with red beds of Early Cambrian or perhaps Eocambrian age (McCutcheon, 1981). The felsic pyroclastic rocks occur at Beulah Camp and on Rocky Island



(unit C4 Figure 2.3) in a unit probably less than 30 meters thick. They are red in color, and form beds tens of centimeters thick, defined by variations in clast size and hue.

Mafic rocks occur in the Long Reach area at road cuts along Highway 102 at Browns Flat (unit C1, sampling localities GWD3 to GWD10 Figure 2.3), in the gravel road that leads to the Saint John River at Beulah Camp (sampling localities GWD11 and GWD12), and at an exposure along the railway tracks at Greenwich Hill (unit C3, Figure 2.3). Basalts flows from the former two localities are interbedded with red beds (unit C2) which are probably Lower Cambrian (McCutcheon, 1981). The poor exposure of these flows makes it difficult to determine their thickness, but the outcrops in the road to Beulah Camp suggest they are less than 10 meters thick.

The mafic rocks at Greenwich Hill are troublesome in terms of their contact relations, and therefore their age. Although the actual contact with the underlying red beds is not exposed it is evident in the field that it must run parallel to, and is probably conformable with, bedding apparent in the sedimentary rocks. Because the nature of the upper contact is not apparent either, it is not certain whether the outcrop represents a sill or a thick (greater than 10 m) flow. Vesicles were never observed in the unit and it appears massive in the field, so textural evidence

indicating whether it is a flow or a sill is lacking. Field relationships suggest that a dike cutting red beds below the unit may have been a feeder to the latter.

### CHAPTER 3 PETROGRAPHY OF THE VOLCANIC ROCKS

#### 3.1 INTRODUCTION

This chapter of the thesis discusses the primary and secondary mineralogical and textural characteristics of the volcanic rocks geochemically examined in the next chapter. Because new data on pyroxene compositions in Middle Cambrian volcanic rocks from Cape Breton Island are examined in Chapter 5, Cameron's work on the petrography of these rocks is also reviewed.

#### 3.2 CAPE ST. MARY'S

##### 3.2.1 Middle Cambrian Lapilli Tuffs

Middle Cambrian lapilli tuffs, as discussed in Chapter 2, occur at Hopeall Head, Placentia Junction, Cape Dog and Hay Cove (Figure 2.1, see pocket Maps A and B for details). Although there are some differences in the rocks between localities, they are in general texturally and mineralogically very similar. Outcrops are usually grey to dark grey in color and, with the exception of Cape Dog, bedding is well defined by rapid changes in clast size, the percentage of calcite in the matrix, and small changes in the color of the matrix material (Plate 2.2). Cross bedding was noted in a couple of the beds at Hay Cove (sampling locality SB42 pocket Map B) but this feature is generally absent. Bed thicknesses range from a few centimeters to

several meters at Hay Cove (sampling locality SB42). A typical tuff section (Hopeall Head, sampling locality PL53 pocket Map A) showing bed thicknesses and clast sizes is shown in Figure 3.1.

The clasts are monolithologic, and within beds, fairly well sorted. The volcanic material ranges in size from over one centimeter to less than 0.3 millimeters (ash size) but most is between 0.1 and 0.5 centimeters. Elliptical bombs 10 to 20 centimeters long were observed at Hay Cove (sampling locality SB37 pocket Map B). Primary textures of the clasts are usually very well preserved. They tend to have elliptical shapes, and contain about 60 percent vesicles. These vesicles are round in the center of the clasts, and somewhat oval at the edges. They typically measure 0.2 millimeters across, and are filled with either chlorite or calcite. The clasts, which were once tachylitic pumice fragments, are now composed of chlorite with minor albite and sphene. At Placentia Junction, some of the clasts are composed of a colorless chlorite which appears isotropic under crossed nicols. These clasts give the rock an amazingly fresh appearance (Plate 3.1).

Individual clasts show a limited amount of contact and "float" in a secondary calcite matrix which makes up between two and twenty percent of the rock (Plate 3.1). At Hopeall Head (sampling locality PL132 Map A) and Hay Cove (locality SB42, Map B) small amounts of hematite in the calcite matrix




Figure 3.1 Section of pyroclastic fall deposit at Hopeall Head. The section was measured at locality PL53 (pocket Map A). Clast sizes and bed thicknesses are representative of most of the other volcanoclastic sections in the Cape St. Mary's study area (Figure 2.1). The absence of sedimentary breaks or evidence for reworking within the section suggests that it represents the product of one volcanic eruption.

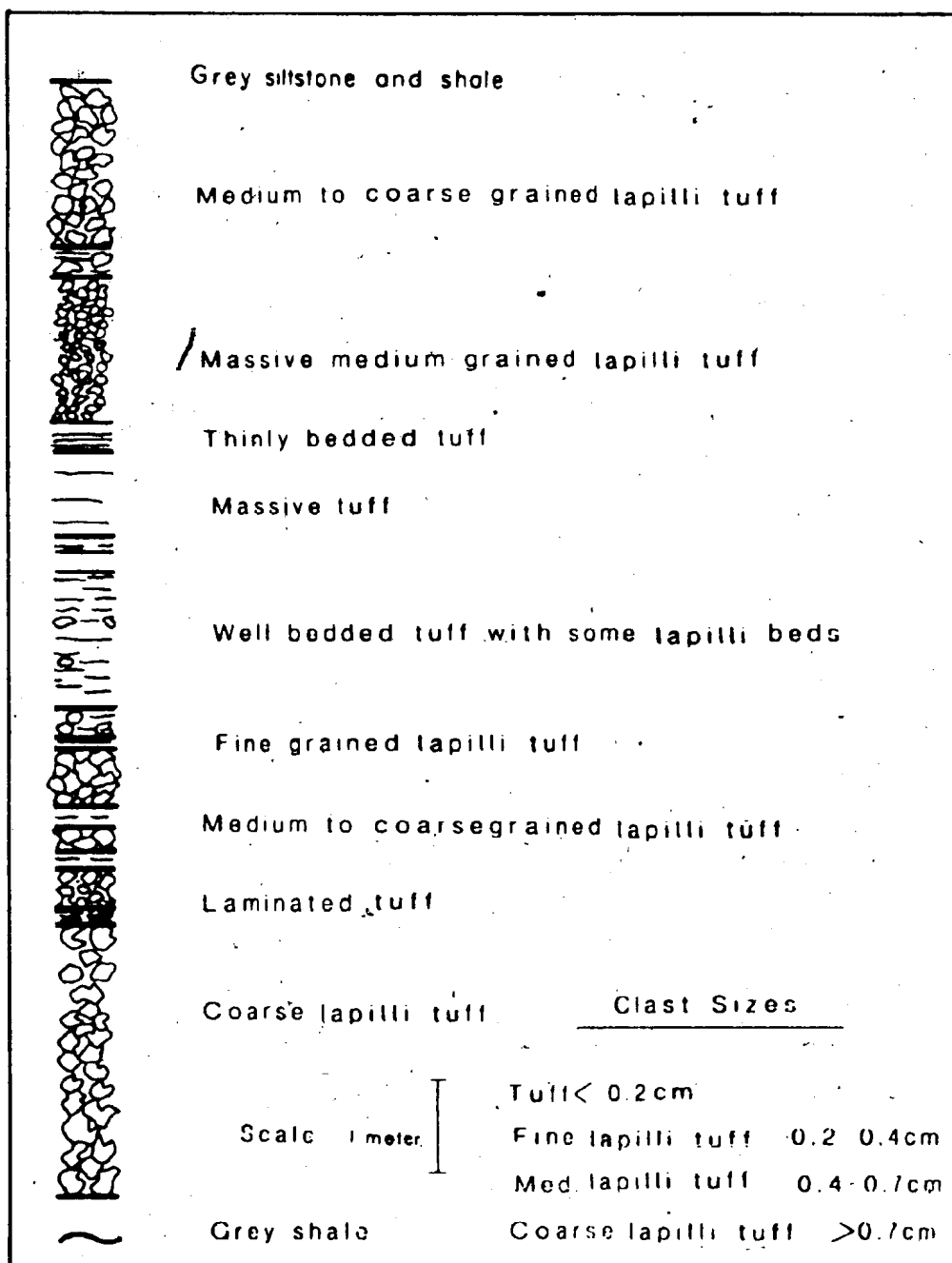
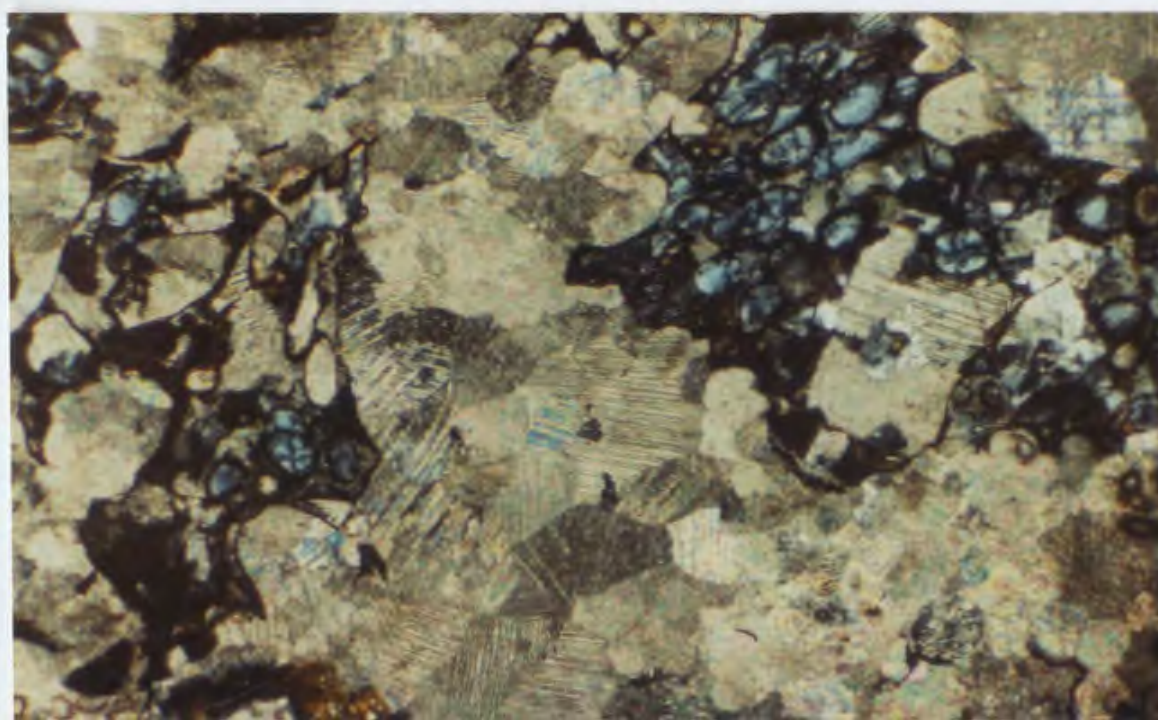
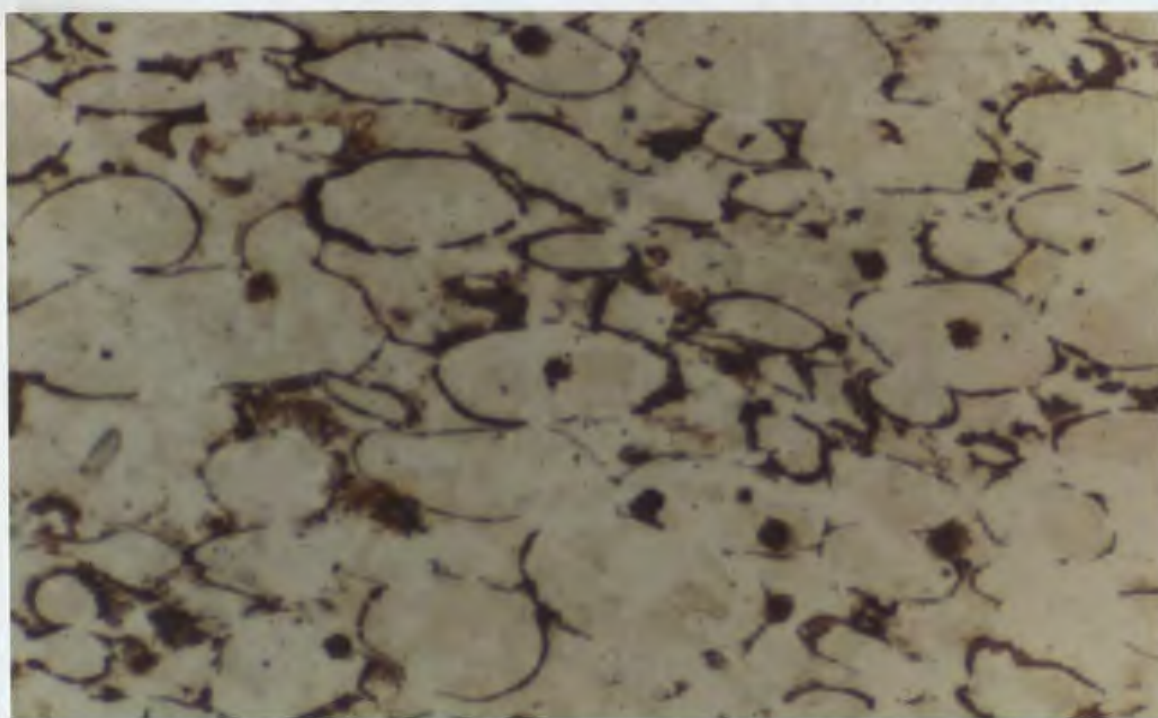


Plate 3.1 A. Center of a clast which consists mostly of relatively colorless chlorite and deep brown sphene. Oval areas represent outlines of vesicles which are filled with colorless chlorite. The clast goes entirely extinct under crossed nicols. Photograph taken under plane light, with longest dimension equal to 2.8 mm. The sample is PL83 from the road cut at Placentia Junction (pocket Map A).

B. A highly altered volcaniclastic sample from Hopeall Head (PL132J pocket Map A) showing an equigranular carbonate texture between relict "ghosts" of chlorite-rich clasts. The oval blue patches are vesicles filled with chlorite (anomalous blue) whereas the striated mineral with high-order white coloration is calcite. The clast on the right has largely been removed by the carbonate solutions and only the rims of some vesicles remain. Photomicrograph taken under crossed nicols with the longest dimension of the photograph equal to 11.6 mm.





give the rocks a pink color. The calcite tends to form large crystal grains, and in samples where its percentage is high the rock resembles a recrystallized limestone (Plate 3.1). In the tuff beds the grain size of the calcite tends to be much smaller, and cryptocrystalline in appearance. In some samples, "ghosts" of the original clasts remain in the calcite "matrix", making it difficult to ascertain the original sizes and shapes of the clasts.

Cherty clasts, generally less than 10 centimeters across are found in the Hopeall Head, Placentia Junction, and Cape Dog sections. Locally they form distinct beds, usually less than 15 centimeters thick. Thin bedding laminae, and soft sediment structures within the cherty clasts suggest they are pieces of the basin floor ripped up during the eruptions. These clasts are usually volumetrically unimportant, but at Cape Dog they comprise up to 2 percent of the volcanoclastic rocks and can measure 50 centimeters across. In addition, the matrix of the Cape Dog volcanoclastic rocks appears to contain 2 or 3 percent mud. These observations, plus the fact that the Cape Dog rocks show very little bedding, suggest that they may have formed very close to the vent.

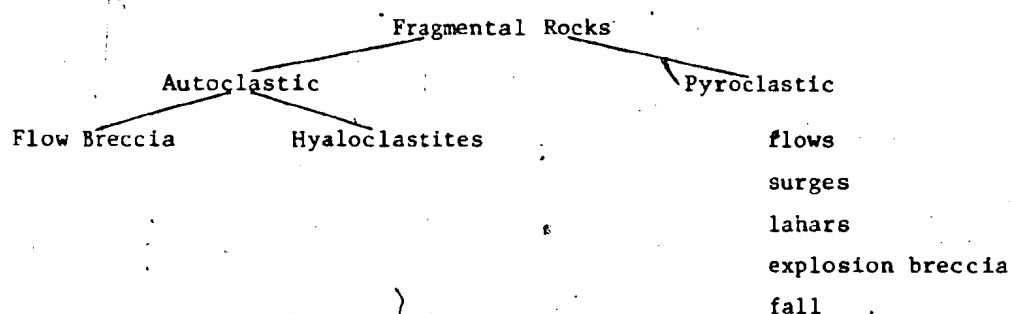
Augite appears to be the only primary mineral preserved in the volcanoclastic rocks, and it was observed in very few samples. One sample from Cape Dog contained less than one percent of the mineral, as did several of the bombs from Hay

Cove. The compositions of these pyroxenes are discussed in detail in the geochemistry section. Secondary minerals useful in establishing the temperatures and pressures of metamorphism are absent. The formation of many minerals characteristic of low grade metamorphism (eg. prehnite, pumpellyite) is inhibited if the  $\text{CO}_2$  partial pressure is high (Winkler, 1976). Large amounts of calcite in nearly all samples suggest that this was the case in most of the rocks examined in this study.

Textural characteristics of the tuffs, such as the rapid grain-size changes between beds, and the well sorted, monolithologic nature of the ash to coarse lapilli sized clasts show that the rocks are pyroclastic fall deposits (cf. Walker, 1971; Sheridan, 1971; Sparks et al., 1973; summary in Table 3.1). Pyroclastic flows, lahars and explosion breccias are usually poorly sorted and stratified (Nairn and Self, 1978; Crandell, 1971; Self, 1982), and surge deposits are generally cross-bedded (Sparks, 1976; Lajoie, 1979). Although cross-bedding may occasionally be present it is not common. Flows, surges, and lahars usually require relief, that is a substantial volcanic edifice, as a prerequisite to their formation (Self, 1982). Apparently the eruptions produced such small amounts of volcanic material that a high volcanic edifice never formed.

Early work suggested the size and percentage of vesicles in pillow basalts could be used as water depth

Table 3.1 Classification and textural characteristics of fragmental rocks.



#### Type Characteristics

**Flow Breccia:** Coarse grained, highly angular, very poorly sorted, monolithologic, may contain complete pillows or pillow fragments, localized due to mechanical disruption of partially solidified flow.

**Hyaloclastites:** Fine grained, monolithologic, localized, due to thermal disintegration of magma on contact with cool water.

**Pyroclastic flows:** Poorly sorted, may contain foreign clasts, fill valleys and depressions, may show grading, may be poorly stratified but are usually homogeneous. Produced by gravity induced movement of hot pyroclastic material with high ratio of gas to solid.

**Pyroclastic surge:** Cross bedded, individual laminae well sorted, thickest in depressions, show unidirectional bed form, may contain foreign clasts, produced by turbulent gravity induced movement of material with low gas/solid ratio.

**Lahars:** Very similar to flow deposits, poorly sorted, may be polyolithologic, produced by water mobilization of fresh pyroclastics or remobilization of flow or fall deposits.

**Explosion breccia:** Form essentially in place or close to vent, unstratified, poorly sorted, commonly decrease in thickness away from vent, may be polyolithologic. Due to vent explosions which fragment lava, or country rocks.

**Pyroclastic fall:** Well sorted, well bedded, no cross bedding, may show graded bedding, equally thick over all but steepest topography, thickness decreases away from vent.

Sources: Lajoie (1979); Self (1982).

indicators (Moore, 1965; Jones, 1969), but Moore (1979), and Moore et al. (1982) questioned this by showing the variables are also composition-dependent. Some indication of the water depths may be garnered from the volcanoclastic rocks. Various workers (eg. Moore and Fiske, 1969; Ayres, 1982) have shown that fragmental rocks will only be common when eruptions take place at water depths less than 500 meters.

Walker and Croasdale (1971) showed that pyroclastics produced where water does not have access to the vent (Strombolian) are coarser-grained (greater than 1 to 2 millimeters) and better sorted, than those where water has access to the vent (Surtseyan). Strombolian eruptions usually produce beds greater than 5 centimeters in thickness but those from Surtseyan eruptions are commonly less than 1 centimeter in thickness. Strombolian pyroclastic fragments show droplet shaped forms which result from surface tension (see Heiken, 1972), but Surtseyan fragments are blocky and broken. It would appear that water did not have access to the Cape St. Mary's vents because beds are tens of centimeters thick and usually contain well sorted lapilli sized clasts with spindle (tear-drop) shapes. Although the vents were probably subaerial, pillow lavas below the volcanoclastic rocks at Cape Dog show that the volcanism started below water.

The volcanoclastic sections at each locality appear to represent single eruptive episodes (Figure 3.1) as

sedimentary breaks or evidence of reworking were never observed. They tend to show large thickness variations over short distances (Chapter 2 and Figure 2.4), suggesting that the eruptions were small, localized and unexplosive as is common for continental basaltic eruptions.

### 3.2.2 Pillow Basalts

Pillow basalts occurring at Hopeall Head, Chapel Arm and Cape Dog show excellent preservation of large scale primary features (Plate 2.1). The lavas at most localities around Chapel Arm (eg. sampling localities LC17, CA18 and PL55 Map A) and Hopeall Head (locality PL54) form normal to large bun pillows (terminology after Dimroth et al., 1978) less than 1 meter across (Plate 2.1, sampling localities LC17, PL55, and PL54), but some larger mattress-shaped megapillows are also present. Megapillows as much as 4 meters across occur at Cape Dog (locality PL40 Map B). According to Dimroth et al. (1978), such large pillows probably formed close to the vent, an analysis consistent with the volcaniclastic rocks (discussed above). Pillow breccias at Hopeall Head (sampling locality PL128 Map A) and near Normans Cove (between localities LC18 and LC19 Map A), are composed of clasts about 8 centimeters across and occur below bun pillows generally less than one meter across. Texturally similar breccias have been reported by Dimroth et al. (1978) from the Rouyn-Noranda area, but at that locality the breccia always overlies the pillow lavas.

The outer selvages of the pillows are extremely fine-grained, and were probably once glassy. Most of the pillows show well preserved concentric cooling cracks and changes in the density and size of vesicles between the center and edge. The centers of the pillows are usually devoid of any vesicles. Moving toward the edge of the pillows, the first vesicles encountered are large (5 mm across). Their size tends to decrease to about 0.2 mm as their number increases toward the edge of the pillows, but the outer edge (10 mm) is again free of vesicles. As much as 30 percent of the rock (by volume) consists of vesicles filled with calcite, quartz, or chlorite. Most of the amygdules are monomineralic, the most common mineral being calcite. An interesting characteristic of Cape Dog pillows (localities PL38 and PL39 Map B) is that their centers often contain a cavity, as much as 40 centimeters across, which is partially or totally filled with quartz and/or calcite. The minerals in the cavities commonly show good crystal forms between one and two centimeters in length.

Only about one percent of the pillow lava samples contain any primary silicate minerals. Secondary minerals commonly observed, in order of abundance, are chlorite, albite, calcite, sphene, and Fe oxides. Chlorite and albite form pseudomorphs of the original pyroxene and plagioclase grains and in this way the original quench, subophitic and rarely (pyroxene?) porphyritic textures appear to be preserved. The centers of the pillows tend to be


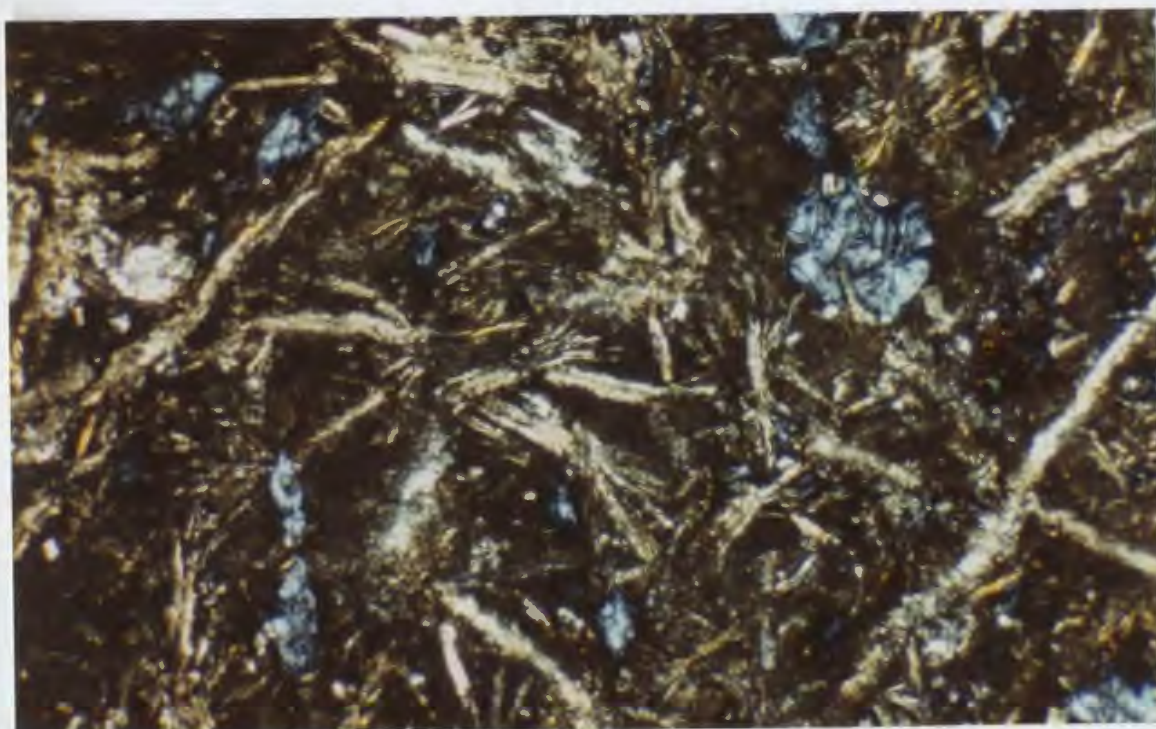
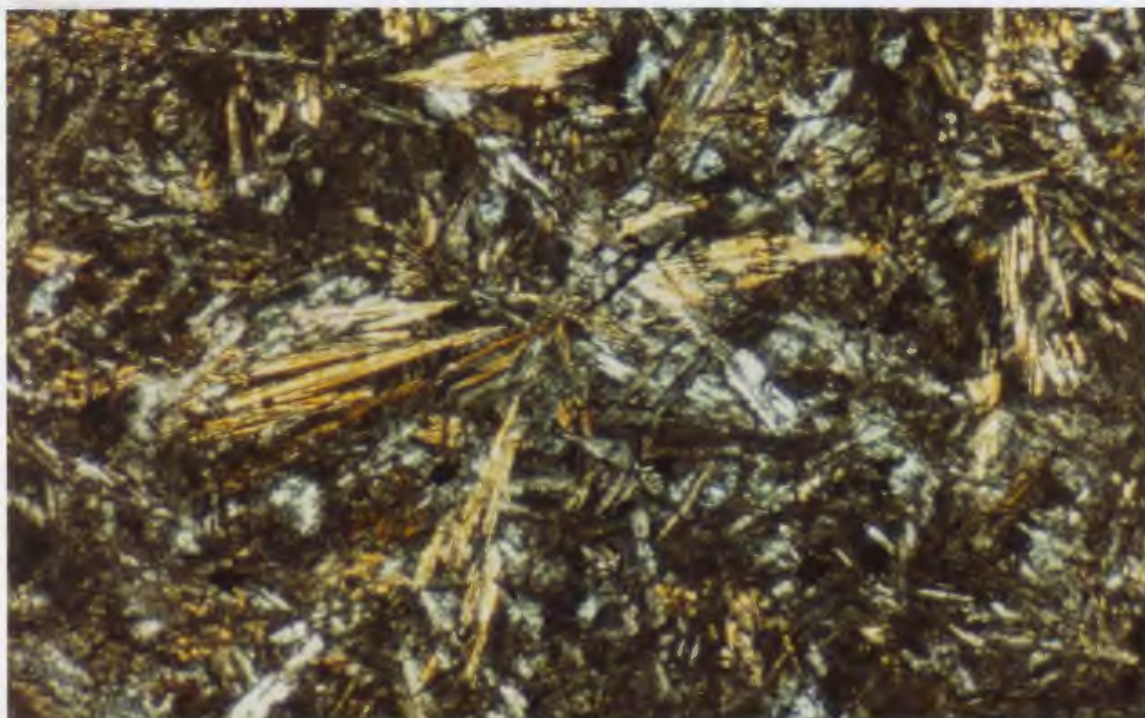


Plate 3.2 A. Photomicrograph of quenched basalt from Normans Cove. The yellow needles are clinopyroxene grains showing a variolitic texture. White areas are albitized plagioclase grains and darker areas represent small patches of chlorite and extinct clinopyroxene and albite grains. Photograph of LC15B (pocket Map A) was taken under crossed nicols with the longest dimension equal to 2.8 mm.

B. Chloritized and albitized basalt with minor secondary carbonate. Oval areas showing deep blue coloration are vesicles filled with chlorite. Light colored needles are mostly plagioclase together with some calcite. Chlorite together with some extinct plagioclase and clinopyroxene form the dark areas. Photograph of sample CA45 (east side of Chapel Arm pocket Map A) was taken under crossed nicols with the longest dimension equal to 11.6 mm.





coarser-grained than the outer portions, but the average size of albite grains is 0.2 mm. In the more altered samples, calcite forms irregularly shaped patches which indiscriminately cut across the chlorite and albite grains (Plate 3.3a).

A few samples of the pillow lavas collected from the ridge just east of the feeder pipe at Normans Cove (Figure 2.1, sampling locality LC15 Map A) and some of the samples from Cape Dog (localities PL38 and PL44 Map B) contain relict primary mineralogy (Plate 3.2). The Normans Cove samples show purplish-brown augitic pyroxenes, as well as magnetite; but other minerals, such as plagioclase are altered. Pyroxene and magnetite locally form a variolitic texture, probably caused by quenching of the lava (Lofgren, 1971). These samples are also important because they tend to have low carbonate contents. The low grade metamorphic assemblage actinolite, chlorite, epidote, and albite was observed in one of the samples, and indicates lower CO<sub>2</sub> pressures during the metamorphism (Winkler, 1976).

### 3.2.3 Feeder Pipes

The feeder pipes show a variety of rock types which can be conveniently divided into four groups: gabbros, melanogabbros, pegmatitic leucogabbros, and aplitic leucogabbros. Typical primary mineral percentages, grain sizes and textural features of these rock types are summarized in Table 3.2. Primary plagioclase was never

Plate 3.3 A. Highly altered basalt with patches of calcite. The large white spots are calcite grains whereas the smaller white laths are plagioclase (albite) grains. Chlorite forms the black to deep blue areas. Photograph of sample CA18 from Chapel Arm (pocket Map A) was taken under crossed nicols with the longest dimension equal to 11.6 mm.

B. Photograph of feeder pipe melanogabbro showing serpentinized olivine (yellow patches in upper left portion of photograph) and relict augite (smaller patches with first to second order interference colors). Photograph was taken under crossed nicols with longest dimension equal to 11.6 mm. The sample is from the feeder pipe 1.5 km west of Spread Eagle Peak (sampling locality CA169 pocket Map A).

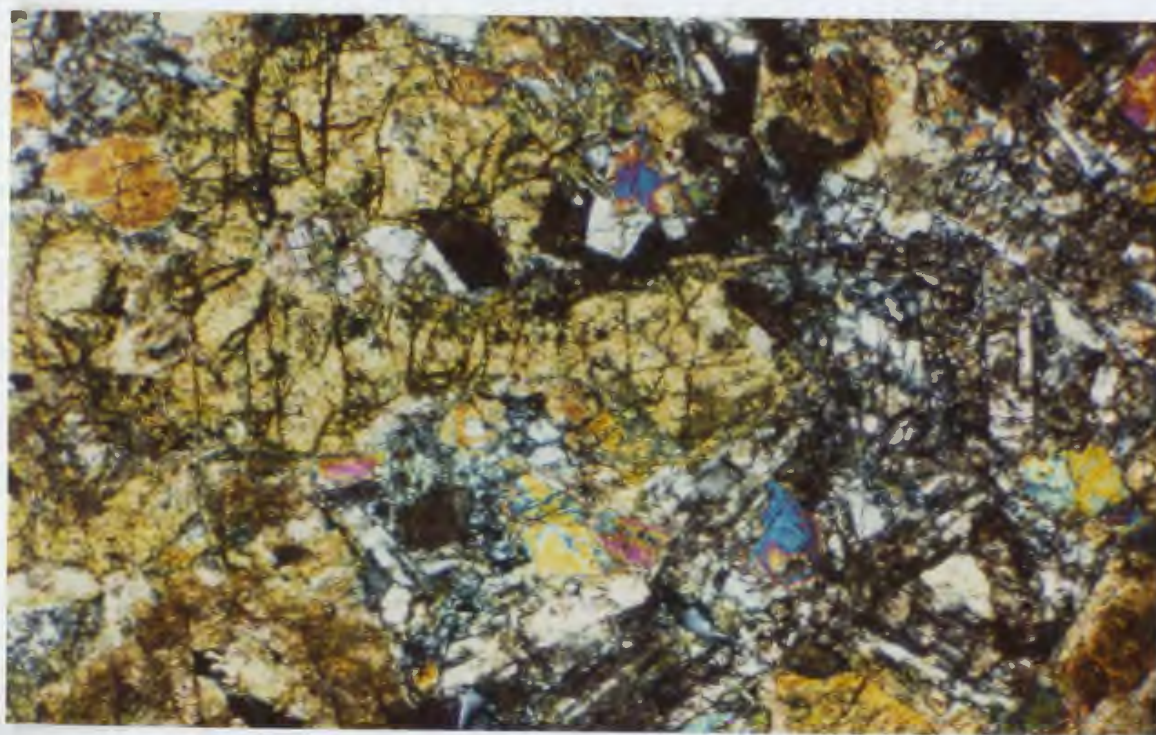
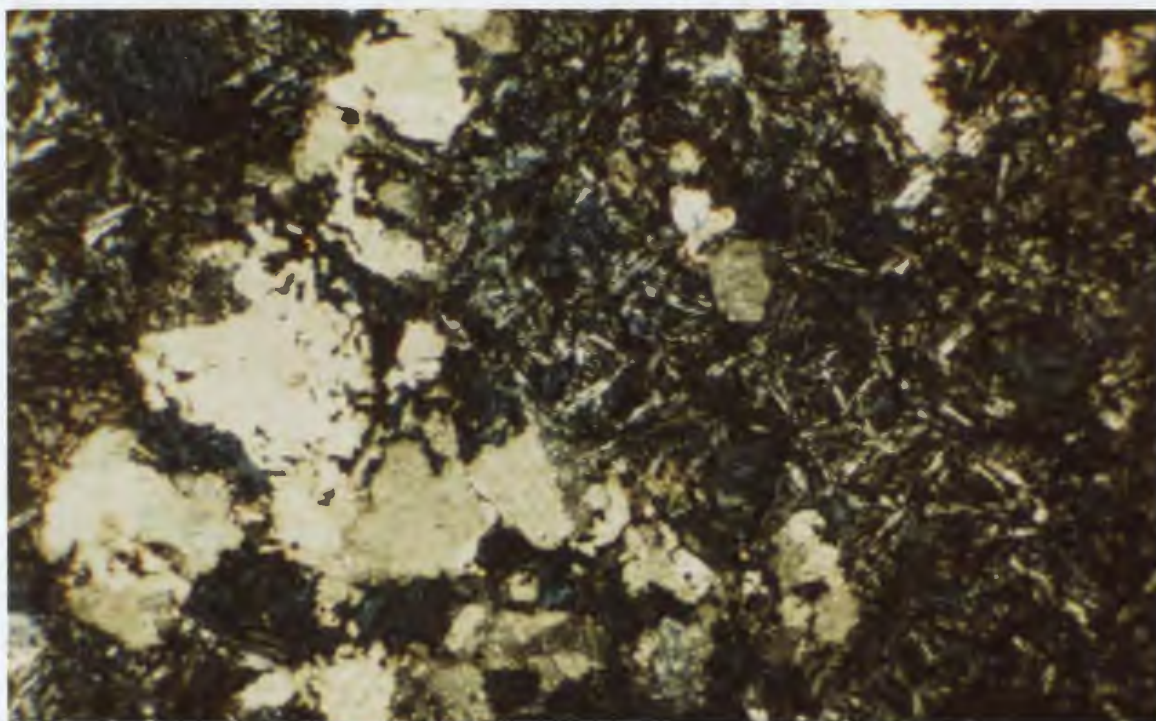


Table 3.2 Feeder pipe textures and mineralogy.

|                        | Minerals    | %  | Grain Size | Texture  |
|------------------------|-------------|----|------------|--|
| Gabbro                 | Augite      | 60 | 0.7 mm     | Euhedral to subhedral, sometimes glomeroporphyritic, zoned, twinned. |
|                        | Plagioclase | 38 | 1.0 mm     | Subhedral to Anhedral  |
|                        | Apatite     | <1 | 1.0 mm     | Euhedral   |
|                        | Opaques     | 2  | 0.5 mm     | Subhedral to Euhedral  |
| Melano-Gabbro          | Olivine     | 30 | 1.5 mm     | Euhedral   |
|                        | Augite      | 50 | 1.5 mm     | Euhedral, zoned slightly, sometimes adcumulus                        |
|                        | Plagioclase | 19 | 0.7 mm     | Anhedral   |
|                        | Apatite     | <1 | 0.7 mm     | Euhedral   |
|                        | Opaques     | 1  | 0.3 mm     | Subhedral to Euhedral, sometimes cumulus                             |
| Pegmatitic Leucogabbro | Augite      | 14 | 3.0 mm     | Poikilitic   |
|                        | Plagioclase | 82 | 3.5+0.6 mm | Some large and euhedral, matrix anhedral                             |
|                        | Apatite     | 2  | 0.8 mm     | Euhedral   |
|                        | Opaques     | 2  | 1.0 mm     | Subhedral  |
| Aplitic Leucogabbro    | Augite      | 20 | 0.2 mm     | Equigranular, Anhedral   |
|                        | Plagioclase | 71 | 0.2 mm     | Equigranular, Subhedral to Anhedral                                  |

Mineral percentages are estimates in "typical" samples.

Examples of "typical" samples from the Norman's Cove feeder pipe are: gabbro, CA28I, melanogabbro CA28E; pegmatitic leucogabbro, CA28C; aplitic leucogabbro, PL7, see pocket Map A.

observed in any of the feeder pipe samples but albite pseudomorphs usually preserve original textural features. Similarly, serpentine commonly forms pseudomorphs of a mineral whose shape resembles olivine, but unaltered grains were not observed. Although primary augite (see mineral chemistry, Chapter 4) is present in most samples (Plate 3.3b), a low Ca pyroxene was never observed. Apatite is easily identified in nearly all of the feeder pipe samples; however, pegmatitic pods within the pipe at Normans Cove contain as much as 2 percent apatite suggesting the magma was relatively rich in phosphorus.

With the exception of samples in close contact with the sedimentary rocks the alteration mineralogy of the feeder pipes is noticeably different from that of the pillow lavas. Calcite percentages are generally low, and a very low grade, low pressure mineral assemblage indicative of pumpellyite-prehnite facies metamorphism (prehnite, chlorite, actinolite, albite, and sometimes epidote) is present in most of the feeder pipes. This assemblage is not very common in most low grade metamorphic terrains (Winkler, 1976) suggesting that the prehnite either postdates or predates peak metamorphic conditions. The mineral assemblage albite, actinolite, chlorite, and epidote, present in the feeder pipe at Normans Cove is typical of low grade (greenschist facies) metamorphism. Table 3.3 gives a list of the alteration minerals and corresponding metamorphic zones (after Winkler, 1976) observed in six of the feeder pipes.

Table 3.3. Summary of alteration minerals in the feeder pipes.

| Mineral             | 1<br>Normans<br>Cove | 2<br>E.Chapel<br>Arm | 3<br>Spread<br>Eagle<br>Peak | 4<br>W.Spread<br>Eagle<br>Peak | 5<br>N. of<br>Trans-<br>Can.Hwy. | 6<br>Placentia<br>Jct. |
|---------------------|----------------------|----------------------|------------------------------|--------------------------------|----------------------------------|------------------------|
| Albite              | ✓                    | ✓                    | ✓                            | ✓                              | ✓                                | ✓                      |
| Chlorite            | ✓                    | ✓                    | ✓                            | ✓                              | ✓                                | ✓                      |
| Calcite             | ✓                    | ✓                    | ✓                            |                                |                                  | ✓                      |
| Actinolite          | ✓                    | ✓                    | ✓                            | ✓                              | ✓                                | ✓                      |
| Epidote             | ✓                    |                      |                              |                                | ✓                                |                        |
| Prehnite            |                      | ✓                    | ✓                            | ✓                              | ✓                                |                        |
| Sphene              | ✓                    | ✓                    | ✓                            |                                | ✓                                | ✓                      |
| Quartz              | ✓                    |                      | ✓                            | ✓                              | ✓                                |                        |
| Biotite             | ✓                    |                      | ✓                            |                                |                                  |                        |
| Hematite            | ✓                    |                      |                              |                                |                                  |                        |
| Sampling<br>Station | CA28C                | CA87                 | CA164                        | CA170                          | CA178                            | PL211                  |

1 = Ab + Act + Ch + Ep. Zone (low grade of greenschist facies)

2,3,4,5 = Pr + Ch + Act + Ab ± Ep. Zone (very low grade or  
prehnite facies)

6 = Ab + Act + Ch. Zone (low grade or greenschist facies)

See pocket Map A for sampling stations.

The presence of prehnite shows that pressures were low during metamorphism (Winkler, 1976). Pumpellyite was not identified in any of the specimens.

#### 3.2.4 Sills

A well exposed sill at Gull Cove (sampling localities SB6 and SB7 Map B), about 50 meters thick, displays most of the lithological, mineralogical and textural features found in the thicker sills in the area. These features are summarized in Figure 3.2 and Table 3.4. Gabbros make up over 90 percent of the sill, and granophyric dikes and layers within the gabbros constitute the remainder. The compositions of most primary mineral phases are examined in Chapter 4, whereas the discussion here concentrates on their distribution, percentages and textural attributes. Gabbros in the lower half of the Gull Cove sill show poikilitic augite grains (Plate 3.4) which tend to increase in size with increasing height in the sill, though local grain size variations produce the layering evident in the field (Table 3.4). Augite grain sizes and percentages tend to decrease slightly in gabbros from the middle portion of the sill. These middle gabbros are cut by thin granophyric sills and dikes extend up to a granophyric layer that is three meters thick. Above this upper granophyre, a five meter thick upper gabbro shows decreasing grain sizes toward the chilled margin.

Figure 3.2 Vertical section through the Gull Cove sill. The sizes (in mm) of augite grains in the gabbroic rocks and amphibole grains in the granophyric rocks are graphically illustrated.



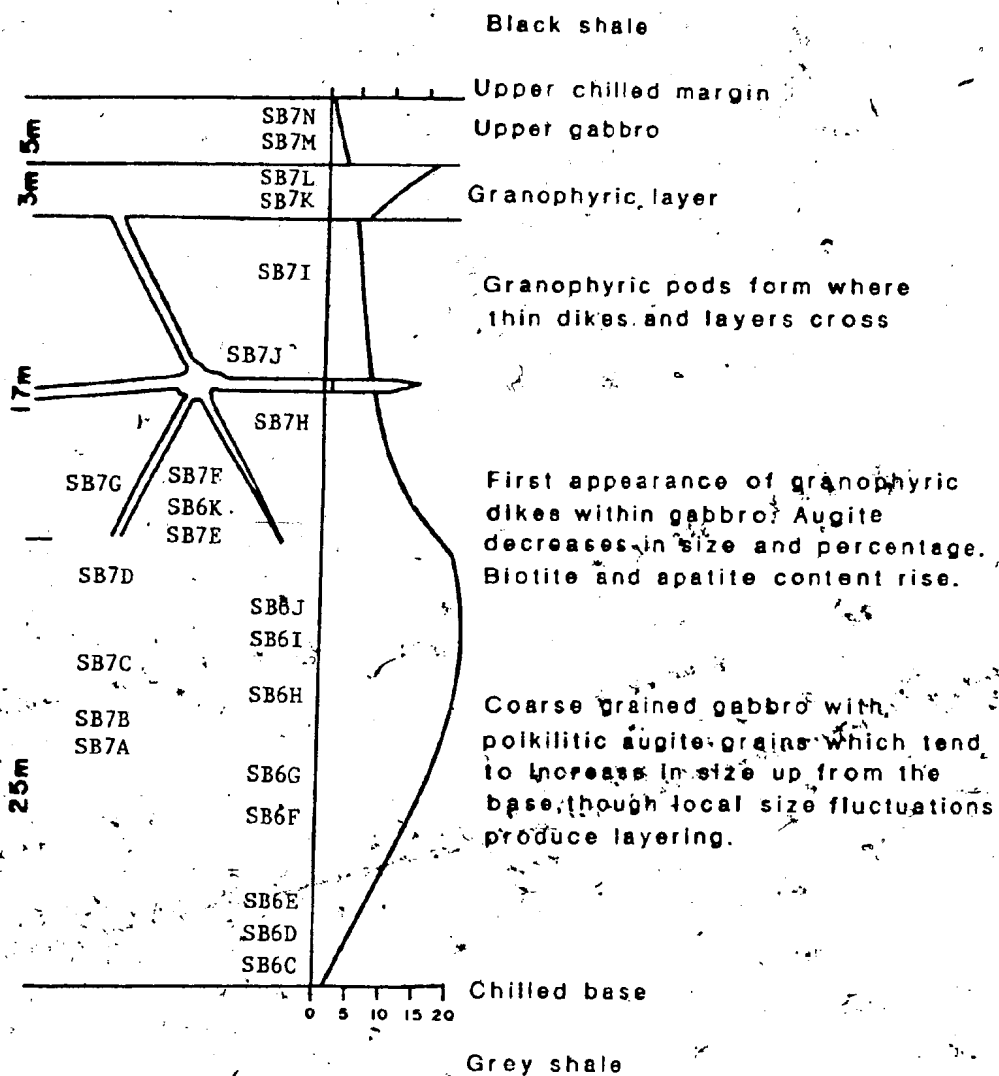


Table 3.4. Gull Cove Sill mineralogy and textures.

| Location   | Primary Minerals | Approximate Percentages <sup>1</sup> | Average Sizes(mm) | Textures                   |
|--|------------------|--------------------------------------|-------------------|----------------------------|
| <u>Mafic Rocks</u>                                   |                  |                                      |                   |                            |
| 1 meter from Upper Contact                           | Biotite          | 40                                   | 1                 | Anhedral                   |
|  | Augite           | 5                                    | 0.5               | Subhedral                  |
|  | Plagioclase      | 55                                   | 1                 | Subhedral to Euhedral      |
|  | Fe-Ti oxides     | 1                                    | <0.5              | Anhedral to Subhedral      |
|  | Apatite          | <<1                                  | 1                 | Euhedral                   |
| Gabbro from base of granophyre to middle of sill     | Augite           | 55                                   | 3.5               | Poikilitic                 |
|  | Biotite          | ≥2                                   | 1.0               | Poikilitic to Interstitial |
|  | Plagioclase      | 40                                   | 1.0               | Subhedral                  |
|  | Apatite          | ≤1                                   | 1.0               | Euhedral                   |
|  | Fe-Ti oxides     | 2                                    | 1.0               | Euhedral to Subhedral      |
| From middle to base of sill                          | Augite           | 60                                   | <20               | Poikilitic                 |
|  | Biotite          | <1                                   | <0.5              | Anhedral                   |
|  | Plagioclase      | 37                                   | 1.0               | Subhedral to Euhedral      |
|  | Fe-Ti oxides     | 2                                    | 1.0               | Subhedral                  |
|  | Apatite          | <<1                                  | 1.0               | Euhedral                   |
| Layers close to base of Lance Cove sill <sup>4</sup> | Olivine          | 5-80                                 | 2.0               | Cumulus                    |
|  | Augite           | <45                                  | 3.0               | Intercumulus, poikilitic   |
|  | Hornblende       | <12                                  | 2.0               | Intercumulus               |
|  | Biotite          | <5                                   | 1.0               | Intercumulus               |
|  | Plagioclase      | 5-40                                 | 1.0               | Euhedral                   |
|  | Oxides           | 2                                    | <1.0              | Cumulus? + Intercumulus    |
| Base of Gull Cove sill                               | Augite           | 50                                   | 1.5               | Poikilitic                 |
|  | Biotite          | 1                                    | 0.5               | Anhedral                   |
|  | Plagioclase      | 47                                   | 1.0               | Euhedral                   |
|  | Fe-Ti oxides     | 2                                    | 0.5               | Subhedral                  |
| Chilled contact at base of Gull Cove sill            | Olivine?         | ≤5                                   | 1                 | Chloritized phenocrysts    |
|  | Plagioclase      | 15                                   | 1                 | Albitized phenocrysts      |
|  | "Glass"          | 80                                   |                   | Altered                    |

Table 3.4 (Cont'd.)

| Location   | Primary Minerals      | Approximate <sup>1</sup> Percentages | Average Sizes (mm) | Textures   |
|--|-----------------------|--------------------------------------|--------------------|--|
| <u>Granophyres</u>   |                       |                                      |                    |  |
| Top of 3 meter thick granophyre, 5 meters from top of sill | Hornblende            | 15                                   | 0.5x20             | Euhedral needles   |
|  | Augite                | <1                                   | 0.2                | Euhedral needles   |
|  | Fe-Ti oxides          | <1                                   | 0.2                | Euhedral   |
|  | Feldspar <sup>2</sup> | 80                                   | 10                 | Anhedral   |
|  | Apatite               | <1                                   | 5                  | Euhedral   |
|  | Quartz                | <1                                   | 0.2                | Anhedral, Interstitial                                     |
|  | Calcite               | <<1                                  | 0.2                | Anhedral, Interstitial                                     |
| Lower half of thick granophyre                             | Augite                | 35                                   | 7                  | ) Anhedral grains and graphically intergrown with feldspar |
|  | Hornblende            | 3                                    | 1                  |  |
|  | Fe-Ti oxides          | 5                                    | 3.5                |  |
|  | Feldspar              | 55                                   | 10                 | Anhedral   |
|  | Apatite               | 2                                    | 5                  | Euhedral   |
|  | Calcite               | <1                                   | 0.2                | Anhedral, Interstitial                                     |
| Granophyric pods where dikes and thin layers intersect     | Feldspar              | 90                                   | 5                  | Equigranular   |
|  | Quartz                | 5                                    | 2                  | Interstitial   |
|  | Mafics <sup>3</sup>   | 2                                    | <0.5               | Chloritized  |
|  | Calcite               | <<1                                  | 0.2                | Interstitial   |
| Dikes and thin layers within above middle gabbro           | Feldspar              | 70                                   | 5                  | Equigranular, Anhedral                                     |
|  | Quartz                | 5                                    | 2                  | Interstitial   |
|  | Hornblende            | 20                                   | 1                  | Euhedral   |
|  | Augite                | 5                                    | 1                  | Euhedral   |
|  | Biotite               | <1                                   | 0.5                | Anhedral   |
|  | Apatite               | 1                                    | 2                  | Euhedral   |

1 Percentages are estimates of primary composition of samples now altered to varying extents.

2 Entirely altered to albite.

3 Entirely altered to chlorite.

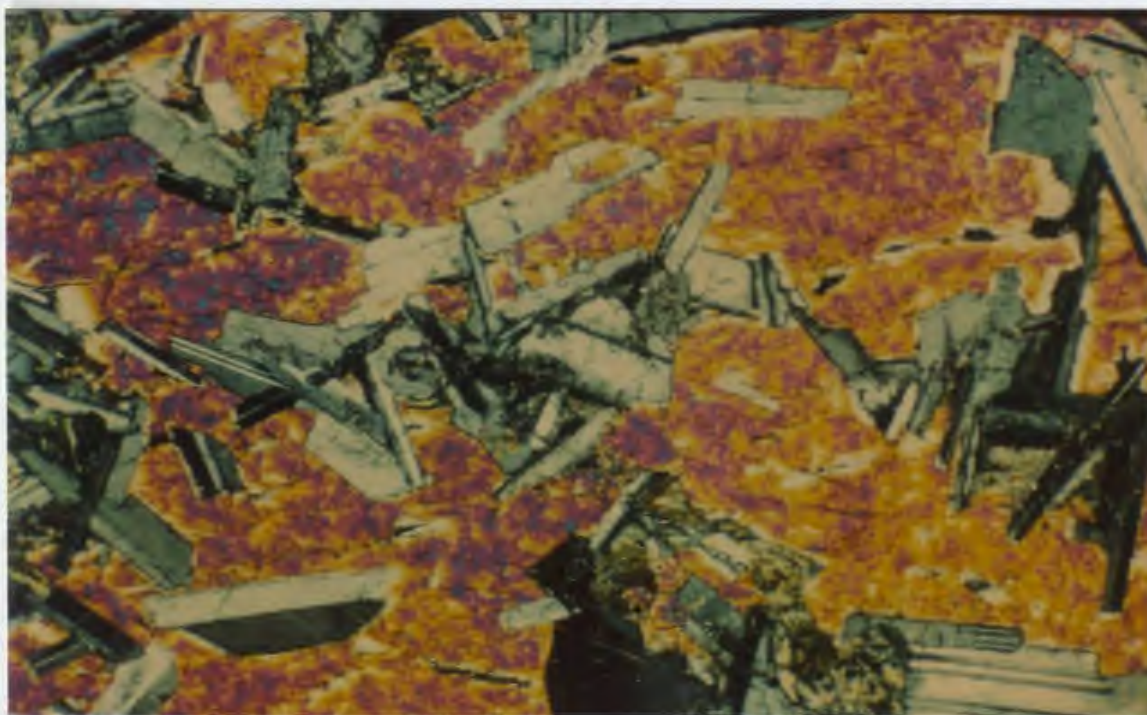
4 Cumulate layers not observed at Gull Cove.

Along with augite, minerals commonly observed in all gabbroic samples include plagioclase, biotite, apatite, and Fe-Ti oxides (Table 3.3). Plagioclase grain sizes remain relatively constant throughout the gabbroic portions of the sill but percentages seem to increase slightly moving up through the lower and middle gabbros. The percentage and grain-size of biotite and apatite rise throughout the lower and middle gabbros, but biotite percentages also appear very high close to the upper shale contact (Table 3.4).

Olivine was not observed in gabbros from the Gull Cove sill but occurs in bands close to the base of a sill near the fish plat at Lance Cove (Plate 3.4, sampling localities SB60 and SB61 Map B). The olivine forms euhedral grains which have a cumulus appearance. Poikilitic grains of augite, hornblende, and biotite, surround the olivine and also enclose euhedral plagioclase grains (Table 3.4, Plate 3.5). Textures in the rocks allow the delineation of a crystallization sequence. Olivine phenocrysts probably existed in the magma at the time of its emplacement, and settled out to form the cumulate layers. Intercumulus augite then started to form, probably with the cessation of olivine precipitation, as the latter does not occur as an intercumulus phase and is not found higher in the sill. The pyroxene is sometimes mantled by hornblende which is mantled by biotite, suggesting that crystallization proceeded in that order. These minerals surround euhedral plagioclase that probably preceded them on the liquidus. Plagioclase

Plate 3.4 A. Olivine Payers in weathered boulders from the base of the sill at Lance Cove (sampling locality SB60 pocket Map B).

B. Photomicrograph of a large poikilitic augite grain in a Gull Cove sill sample (SB7E pocket Map B). Photograph was taken under crossed nicols. Longest dimension of photograph equals 11.6 mm.



does not occur as a cumulus phase, and probably started to crystallize after olivine. In summary, the crystallization sequence would seem to be: olivine, plagioclase, augite, hornblende, biotite.

The absence of olivine in the Gull Cove sill may be explained in several ways. Chlorite pseudomorphs of a mineral with olivine form occur near the base of the Gull Cove sill and suggest that the mineral was present in minor amounts but was entirely altered during metamorphism. Alternatively the Gull Cove sill may have formed from an already fractionated magma, less likely to precipitate olivine. This explanation is perhaps the most reasonable because it also explains why the sill possesses an unusually thick granophyre, (discussed below) though its total thickness appears comparable to others. A third explanation is that there were differences in the mantle derived magmas forming the sills. This explanation is not supported by the geochemistry discussed in the next chapter.

Close to half way up the Gull Cove sill, the lowest "granophyric" dikes and layers appear (sampling locality SB7 Map B). They are usually quite thin (20 to 30 centimeters), define sharp boundaries with the gabbros, and are mineralogically and texturally distinct from the mafic portions of the sill (Table 3.4). Minerals observed in these rocks, in order of abundance, include feldspar (always turbid albite), hornblende, quartz, augite, apatite and

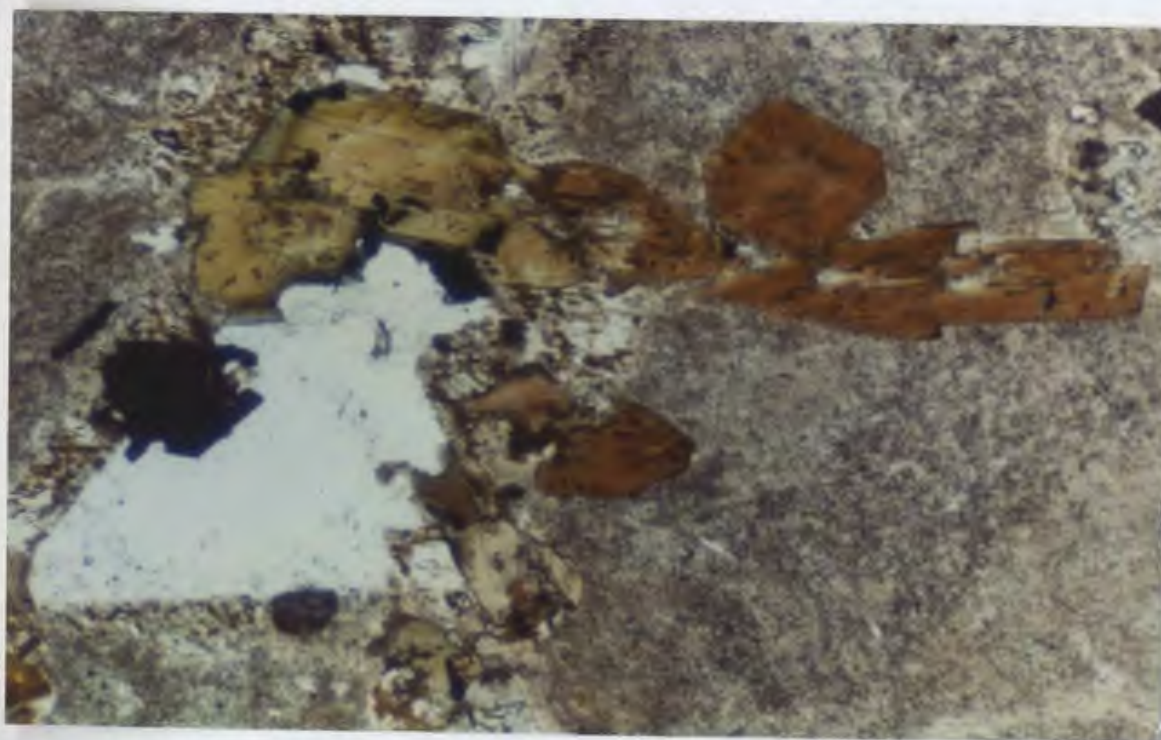
biotite. Baddeleyite ( $ZrO_2$ ) was found in the heavy mineral separate of a similar granophyric layer from Lance Cove (sampling locality SB58 Map B) and a thorough discussion of its composition, appearance, and importance is given in Chapter 4. Granophyric pods, occurring where dikes and layers cross, show the highest percentages of feldspar observed in the Gull Cove sill. Calcite observed in these pods may be a late primary igneous mineral because it texturally resembles the interstitial quartz.

The granophyre near the top of the Gull Cove sill was the thickest (three meters thick) observed in any of the sills. Textural and mineralogical variations between the top and bottom of this layer are summarized in Table 3.4 and details on mineral compositions appear in Chapter 4. The percentage of feldspar is never as high in these rocks as in the "pods", but the grain sizes are the largest observed. Perhaps the most interesting aspects of these rocks are the textural features of the mafic minerals. At the top of the layer pyroxene and amphibole grains form euhedral needles over one centimeter long (Plate 3.5). In samples from its base, these minerals are sometimes graphically intergrown with feldspar, or form euhedral grains, and anhedral interstitial grains. In some cases amphibole occurs as "reaction spots" throughout the large pyroxenes. Similar "albite-diabase pegmatites" have been reported from a differentiated diabase sill in Sierra Ancha (Arizona) by Smith (1970).



Plate 3.5 A. Photomicrograph of olivine bearing sample from the base of the sill at Lance Cove (sample SB60E, pocket Map B). Olivine occurs in the upper right-hand corner of the photo, biotite in the lower right corner, and amphibole mantles an augite grain in the lower left-hand corner. All other minerals are secondary and consist primarily of fine-grained chlorite and albite. Photograph was taken under plane light with the longest dimension equal to 11.6 mm.

B. Photomicrograph showing several amphibole grains in a Gull Cove sill granophyre sample (SB7L pocket Map B). The brown hexagonal form represents a cross-section through a needle-like amphibole grain, at right angles to the c axis. A large interstitial quartz grain is shown below a zoned (yellow-brown to faint green at the edge) amphibole. The remainder of the photograph is mostly albite. The photograph was taken under plane light with the longest dimension equal to 11.6 mm.



With the observation that olivine and quartz occur in the sills, low Ca pyroxene (hypersthene or pigeonite) is also expected, but was never observed. Hornblende and biotite do occur, and it is possible that these minerals took the place of hypersthene in the crystallization sequence.

All of the sill rocks show a certain amount of alteration. The two most common alteration minerals are albite and chlorite which make up over 90 percent of some samples but less than 10 percent of others. The feldspars are commonly altered to albite, and in some cases to prehnite, though primary plagioclase (An 40 to An 80) was observed in many gabbroic samples (Chapter 4). Of the mafic minerals olivine and biotite seem most susceptible to alteration, primarily to chlorite. Some augite remains unaltered in most gabbroic samples but when altered usually forms chlorite and small amounts of actinolite. The mineral assemblage chlorite, actinolite, prehnite, and albite, occurs in all of the sills and indicates very low grade metamorphism (prehnite - pumpellyite facies) at pressures less than 3 kilobars (Winkler, 1976).

### 3.2.5 Dikes

Most of the dikes are highly altered, with no original minerals remaining, and show the mineral assemblage albite, chlorite, calcite, sphene, and Fe-Ti oxides. Dikes of this description are usually found cutting Cambrian shales and

limestones (eg. locality SB26 at St. Brides Map B). Where the dikes intrude sedimentary rocks below the Bonavista Formation (Table 1.3), which are generally more arenaceous, they tend to contain less calcite and sometimes show the low grade metamorphic assemblage epidote, chlorite, albite, actinolite and sphene (eg. locality SB66 Patrick's Cove Map B).

The only primary minerals present in the least altered dikes are high Ca clinopyroxene, and plagioclase. Olivine and low Ca pyroxene were not observed in any of the dikes. The purplish color of the pyroxenes indicates high Ti content, which is confirmed by analyses presented in the next chapter. Primary plagioclase grains show compositions around An60, though the mineral is usually altered to albite. The dikes consist of 40 to 50 percent augite, with most of the rest of the rock plagioclase, and display an aphanitic and sometimes porphyritic texture, with groundmass grain sizes between 0.25 to 0.75 millimeters. Approximately 40 percent of the dikes show feldspar phenocrysts usually 2 to 3 millimeters long, but crystals in a dike at Patricks Cove (sampling locality SB56 Map B) average 2 centimeters and are as much as 30 centimeters in length (Plate 3.6). The phenocrysts are concentrated in the center of the dike, probably as a result of flowage differentiation as described by Bahatbacharji (1967) and Komar (1972). These feldspar phyric dikes, though they appear to have similar orientations to the aphyric dikes, cut the latter at



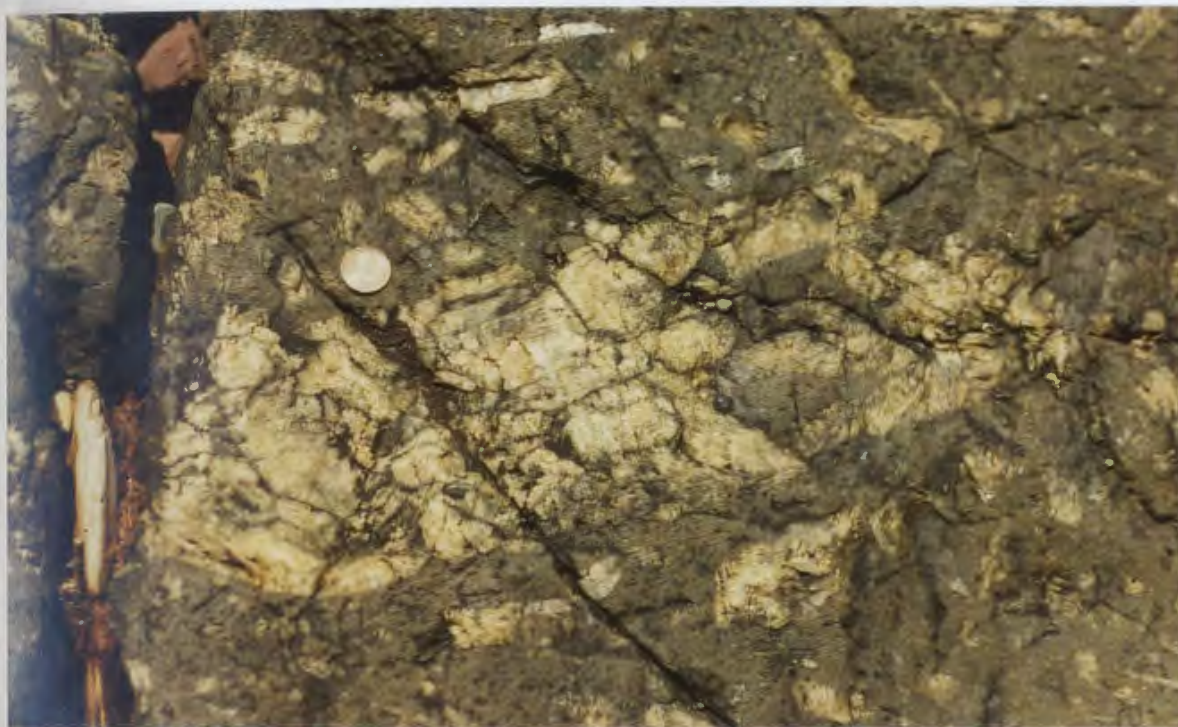


Plate 3.6 Large plagioclase megacryst in a dike at Patricks Cove. The megacryst is zoned and appears to have grown around and trapped some melt within itself. Sampling locality SB56, pocket Map B.

Patricks Cove. Several samples appear to have calcite filled amygdules approximately 0.3 millimeters in diameter, though these could be highly altered feldspar phenocrysts. Petrographically similar rocks have been reported by Wilton (1976) on the Burin Peninsula, and by Jayasinghe (1978) from the shores of Bonavista Bay.

### 3.3 NEW BRUNSWICK

#### 3.3.1 Beaver Harbour Area

As discussed in Chapter 3, the volcanic rocks at Beaver Harbour (Figure 2.2) comprise two units. The pyroclastic unit (C2) shows some textural and mineralogical changes between the bottom and the top. At the base the unit is composed of beds averaging 0.5 m in thickness, with clasts usually less than 4 cm in apparent longest dimension. These vesicular, usually lapilli-sized, clasts constitute 60 percent of most samples, and are suffronded by coarse ash. The vesicles in each clast are less than 0.5 mm across, and tend to be round in the center and stretched out at the edges of the clasts. The vesicle shapes together with the oval appearance of the clasts suggest that the unit formed subaerially.

Minerals present in the samples include hematite (approximately 35%) chlorite (10%) calcite (30%) and sphene (2%). These are probably all secondary but it is possible that the hematite was produced by oxidation at the time of

eruption. Hematite tends to outline the clasts and vesicles, whereas calcite and occasionally albite or chlorite fill the vesicles. The matrix between the clasts is recrystallized, and consists predominantly of albite and hematite together with some chlorite (5%) and calcite (20%). Primary textural features of the rocks appear to be well preserved by the alteration mineralogy.

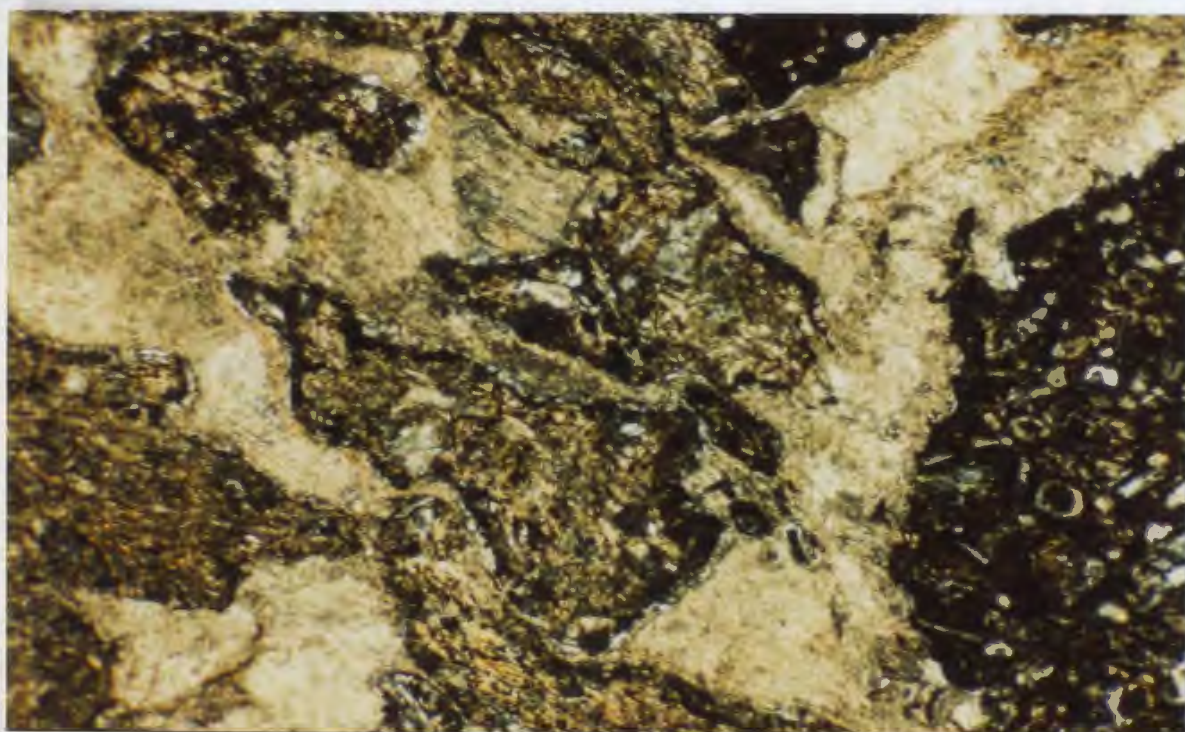
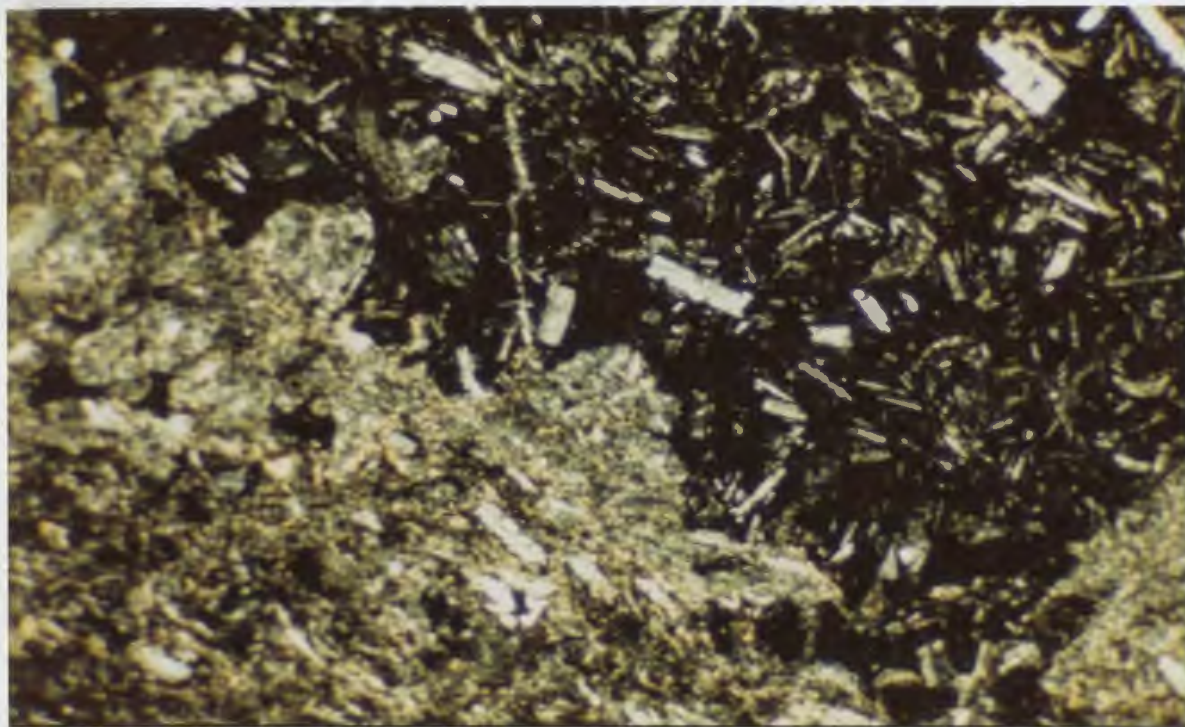
Higher in unit C2 (20 m) the beds tend to decrease in thickness, in some cases to only a few millimeters, and clast sizes decrease to several millimeters or are absent in ash beds. Perhaps the most important change from the basal samples is the appearance of plagioclase phenocrysts (now albite) both in the matrix and within the clasts (Plate 3.7). This mineral also makes up a fine-grained matrix between the phenocrysts within the clasts, and constitutes 40 percent of some samples. In the red colored samples hematite is present (less than 30%) but it is totally replaced by chlorite in the greenish rocks at the top of the section. Calcite comprises between 10 and 30 percent of most samples (Plate 3.7).

The massive flow (C3) is also rich in plagioclase, now altered to albite. Phenocrysts 2 mm across, which sometimes show traces of primary igneous zoning, are surrounded by matrix feldspar (Plate 3.8). All of the primary mafic minerals are altered to chlorite, but the low calcite content of these rocks (<10 %) which is concentrated along

Plate 3.7 A. Photomicrograph of a large hematite-rich clast in a Beaver Harbour volcanoclastic sample (BHR3 Figure 2.2). The black is mostly hematite, and makes up most of the clast which also contains albitized feldspar phenocrysts. The matrix surrounding the clast (upper right-hand portion of the photograph) consists of fine-grained recrystallized plagioclase (albite) with some hematite (black spots). Photograph was taken under crossed nicols with the longest dimension equal to 11.6 mm.

B. Photomicrograph of hematite-rich volcanoclastic sample (BHR5 Figure 2.2) with high carbonate content. Oval to round shapes in the hematitic clast to the left are vesicles filled with carbonate and/or albite. Calcite makes up the large yellow to white patches as well as most of the fine-grained material of the same color within clasts. Photograph was taken under crossed nicols with the longest dimension equal to 11.6 mm.







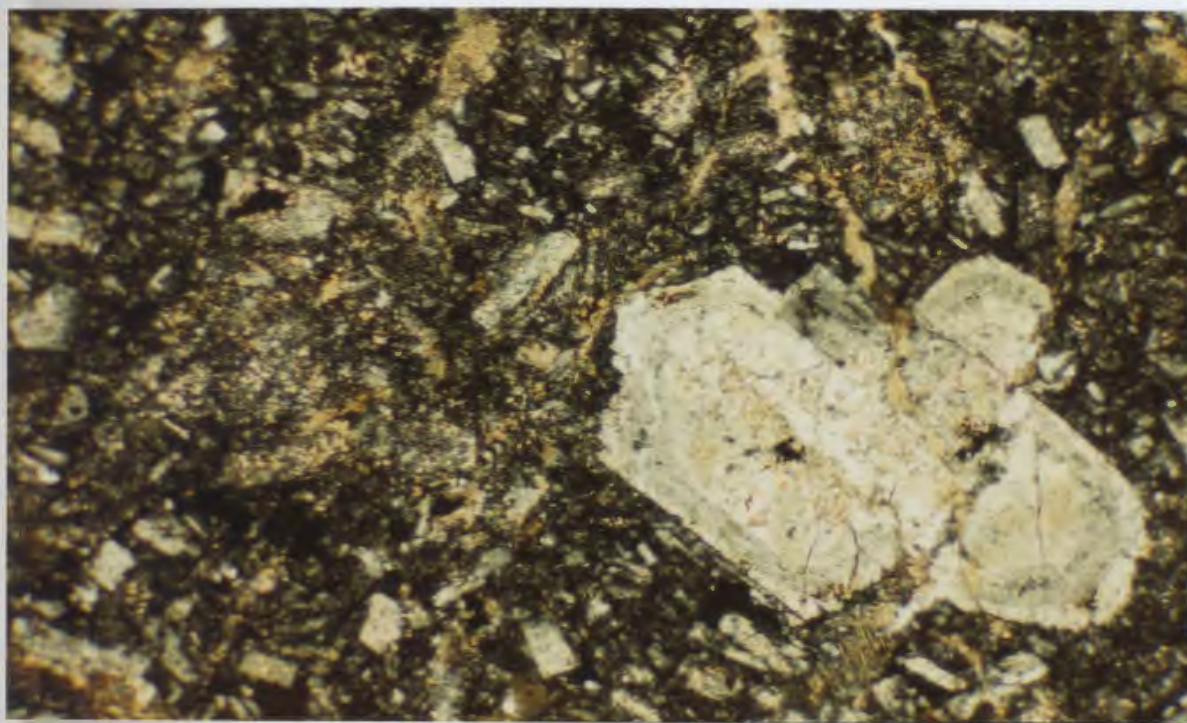


Plate 3.8 Photomicrograph of chlorite rich Beaver Harbour sample (BHR25 Figure 2.2). Dark areas are mostly chlorite. The large phenocryst is entirely altered to albite but the original zoning in the crystal is preserved in the pseudomorph. Fine-grained calcite is disseminated throughout the feldspar rich matrix and fills a crack through the phenocryst. Photograph was taken under crossed nicols with the longest dimension equal to 11.6 mm.

small fractures gives them a relatively unaltered appearance. Some outcrops of this unit, particularly close to the faulted contacts are tectonically brecciated into fist sized clasts with calcite filling voids between the clasts.

### 3.3.2 Long Reach Area

#### Felsic Pyroclastic Rocks

The felsic rocks in the Long Reach area (Figure 2.3) are entirely pyroclastic and display well defined bedding as a result of variations in clast size and color. Individual clasts are typically 10 millimeters by 2 millimeters in size, are usually well sorted, and commonly appear flattened. Feldspar phenocrysts, 2 to 3 millimeters long occur in the clasts and in the ash matrix where shards are difficult to see as a result of recrystallization. The percentage of phenocrysts in the matrix (15%) is equal to or exceeds that in the clasts.

Apart from the feldspar phenocrysts, which are now entirely albite, the samples consist mostly of extremely small (0.01 mm) grains of quartz and albite with hematite forming thin continuous lines or spots through the matrix, and around clasts. The hematite makes up less than 10 percent of each sample but gives the rocks their bright raspberry red color. Chlorite is of minor importance.

There are some textural and mineralogical variations related to height in the section. The percentage of angular clasts that contain clasts themselves may increase up through the section. The mineralogical composition of all parts of these clasts is the same as the surrounding rock, so they probably represent pyroclastic material that solidified close to the vent and was torn apart later in the eruption. The percentage of ash (matrix) appears to increase from 35 percent in the lower portions of the section to 60 percent near the top. The size and percentage of feldspar phenocrysts also tends to increase up through the section. Quartz grains appear near the top of the section and may be detrital in origin. Clasts of foreign (sedimentary) composition were noted in only one of the samples.

#### Mafic Rocks

Basalts from Browns Flat and Beulah Camp (Figure 2.3) show a fine-grained texture with groundmass feldspar (now albite) less than 1 mm in length and augite, the only primary mineral which survived metamorphism, of similar size. A subophitic texture is preserved by chlorite and albite pseudomorphs of pyroxene and feldspar. Vesicles, when present, constitute 1 to 15 percent of the sample, are always less than 5 mm in diameter, and show chlorite or locally quartz fillings.

The mafic extrusive rocks at Browns Flat and Beulah Camp form two mineralogical groups; one with feldspar

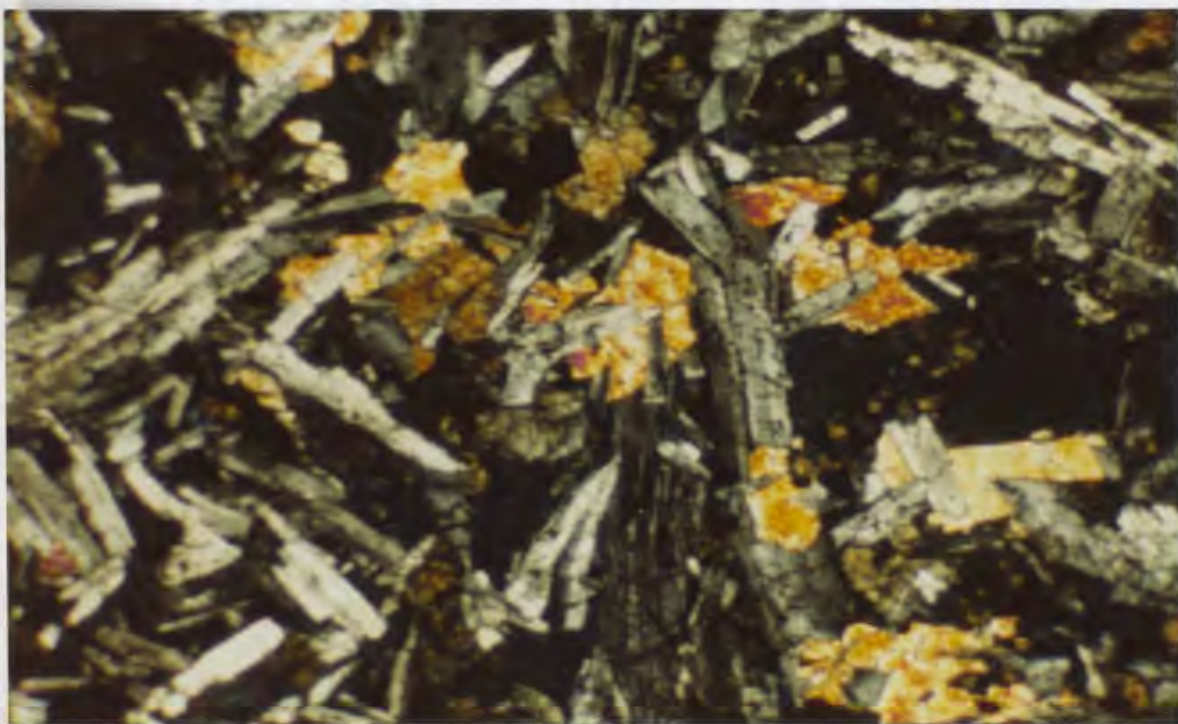
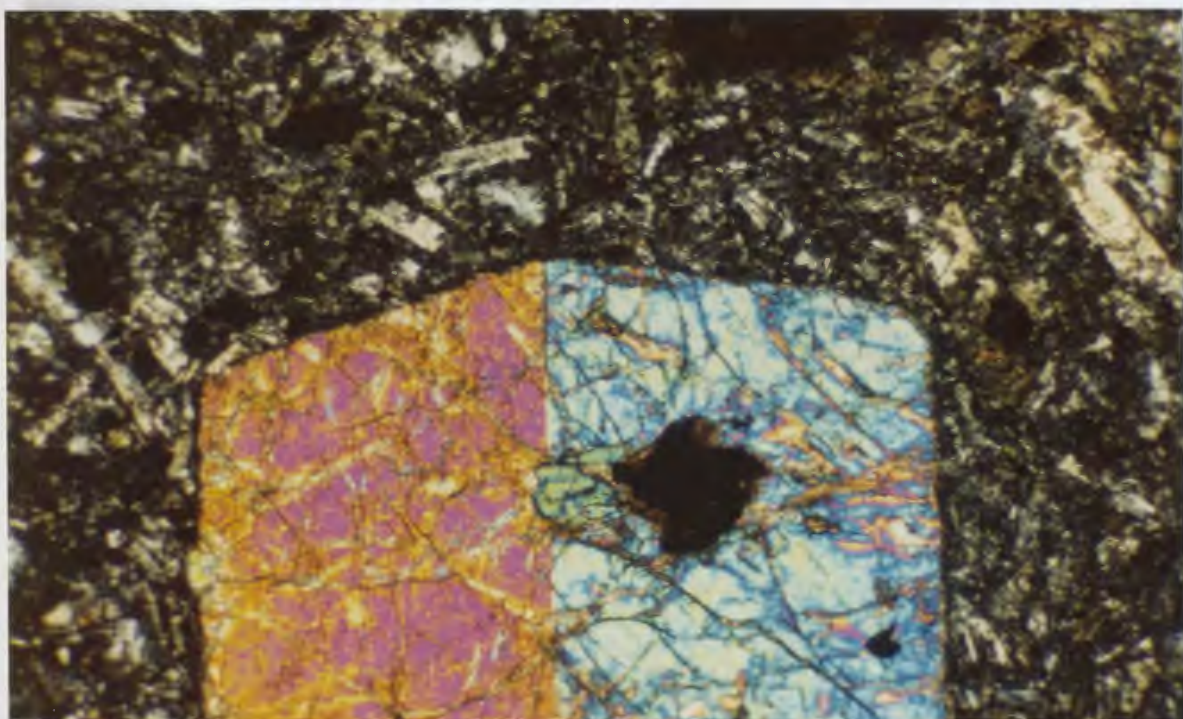
phenocrysts approximately 2 mm in size that make up 10 to 15 percent of the rock (sampling localities GWD4 to GWD7, GWD9 and GWD10 Figure 2.3) and one without feldspar phenocrysts (hereafter termed aphyric, sampling localities GWD8, GWD11, and GWD12 Figure 2.3). Augites in the former group display a purplish pleochroism but in the latter they show only faint coloration (Plate 3.9). Augite phenocrysts, commonly 5.0 mm across, twinned, relatively colorless and sometimes glomeroporphyritic, occasionally occur in the feldspar aphyric samples (Plate 3.9). Another phenocrystic phase, possibly olivine, forms chlorite pseudomorphs rimmed by hematite in some samples.

The mafic volcanic rocks at Greenwich Hill (sampling localities GWD20 to GWD25 Figure 2.3) show colorless augite, and plagioclase (now albite) measuring about 0.05 mm. Augite phenocrysts less than 0.6 mm in size make up less than 1 percent of the rock. McCutcheon (1981) suggested that chlorite spots in the samples may represent altered olivine phenocrysts. Samples from the unit show very little mineralogical or textural variation suggesting it could be a thick flow. A dike cutting red beds below the flow (?) (locality GWD26 Figure 2.3) was probably not a feeder to the latter because it contains 3 to 4 mm feldspar phenocrysts (altered to albite), and augites with a purplish hue. The massive unit shows similar petrographic characteristics to the aphyric basalts at Browns Flat and Beulah Camp, where as the dike resembles the feldspar phyric basalts.

Plate 3.9 A. A large twinned augite phenocryst in one of the feldspar aphyric basalt samples (GWD8 Figure 2.3) from the Long Reach area. The matrix material around the phenocryst consists of very small grains of augite and plagioclase (albite), which form the light colored areas, and chlorite represented by the dark areas. Photograph was taken under crossed nicols with the longest dimension equal to 11.6 mm.

B. Photomicrograph of one of the least altered feldspar aphyric basalt samples (GWD9 Figure 2.3). The high birefringence areas are augite grains, deep blue to black areas are chlorite grains together with extinct plagioclase and clinopyroxene, and the remainder of the photograph is mostly albitized feldspar. Picture was taken under crossed nicols with the longest dimension equal to 11.6 mm.





Alteration minerals commonly observed, though not necessarily present in every sample of the Long Reach volcanic rocks, include chlorite, albite, epidote, actinolite, calcite, quartz, sphene, hematite and possibly prehnite, but in terms of volume, chlorite and albite are the most important. The mineral assemblage chlorite-actinolite-epidote-albite, which indicates low grade (greenschist facies) metamorphic conditions (Winkler, 1976) was observed in one of the samples.

### 3.4 CAPE BRETON, NOVA SCOTIA

The following summary of the Cape Breton rocks is primarily from Cameron (1980) who showed that the Bourinot Group consists of volcanic rocks of basaltic and rhyolitic composition, comprising a bimodal suite. The basalts have a secondary mineralogy consisting predominantly of chlorite, epidote, zoisite, calcite, actinolite, prehnite, and possibly pumpellyite, which are suggestive of very low grade metamorphism. Relict augitic pyroxene, with a purplish-brown color, occurs in some samples and is the only unaltered primary mineral. Analyses of these pyroxenes were made for this study and are discussed in Chapter 5. The basalts are typically aphanitic, and sometimes contain vesicles, commonly filled with calcite. The rhyolites are usually fine-grained as well, and in places show flow banding. They are generally composed of quartz, K-spar, and plagioclase, with the latter now entirely altered to albite.



CHAPTER 4. GEOCHEMISTRY OF LOWER PALEOZOIC  
AVALON ZONE ROCKS

4.1 INTRODUCTION

In this chapter the geochemical characteristics of the Middle Cambrian basaltic flows, and their probable feeders, as well as Silurian sills and Devonian (?) dikes from the Cape St. Mary's study area are examined. Also discussed are Lower to Middle Cambrian basaltic pyroclastic rocks from the Beaver Harbour area and Lower Cambrian, mafic flows and felsic pyroclastic rocks from the Long Reach area in New Brunswick. The geochemical characteristics of Middle Cambrian mafic and felsic rocks from Cape Breton Island in Nova Scotia (Cameron, 1979), Eocambrian basaltic rocks from central Norway (Furnes et al., 1983), and Upper Cambrian basaltic rocks from Poland (Baranowski et al., 1984) are briefly reviewed for comparative purposes. New data on the composition of pyroxenes from the Cape Breton basalts are also presented. The effects of low grade metamorphism on the Avalon Peninsula and southern New Brunswick rocks are discussed prior to the primary geochemistry, but only the Beaver Harbour pyroclastic rocks and Avalon Peninsula flows are discussed in detail.

Representative whole-rock and mineral analyses for each rock group are given in text-tables, but complete listings of all data are given in Appendices B and C. Analytical techniques, precision and accuracy are discussed in Appendix A.

## 4.2 CAMBRIAN FLOWS AND FEEDER PIPES

### 4.2.1 Alteration Of The Flows

Recent studies of element mobility during low grade metamorphism of mafic flows have shown that even elements such as Ti, Zr, Nb, P, Y and the rare earth elements (REE), commonly considered immobile (eg. Pearce and Cann, 1973; Floyd and Winchester, 1975; Winchester and Floyd, 1976, 1977), may in actual fact be very mobile (eg. Vallance, 1974; Floyd, 1977; Hellman et al., 1979; Hynes, 1980). One approach to determining the effects of low grade metamorphism on element concentrations is to identify the primary or parental composition of the rocks involved (cf. Hellman et al., 1979) and then account for volume changes which may have taken place in the altered rocks (Gresens, 1967).

Some studies (eg. Hellman et al., 1979) were based on thick flows with "relict" (relatively unaltered) rocks from the centers of the flows as the parent composition, and these rocks were compared with the more altered external portions of the flows. This may be a poor approach since thick flows of fresh basalts often show large variations in element compositions as a result of differentiation as the flow cooled (eg. Basaltic Volcanism Study Project, 1981, p. 117). In this respect the Cambrian basalts, particularly

from the shores of Chapel Arm are well suited to this type of study because the flows are not very thick, and in most cases consist of quickly cooled pillows, all of which were produced by at most two extrusive events.

Another weakness of these early studies is that the relict rocks nearly always contain a certain percentage (20 percent or more) of alteration minerals. These rocks may not represent the primary rock composition, but they should give the best available estimate of that composition. In this study these samples are referred to as the "least altered" samples.

Most studies of element mobility in mafic rocks fail to take into account volume changes during metamorphism. Apparent losses or gains of particular elements may arise from a volume increase or decrease, respectively, and can result in erroneous conclusions, since the latter must be accounted for (Gresens, 1967). An approach to this problem suggested by Gresens (1967), which involves using changes in the rock density to estimate the volume modification, is used in this study.

#### Presentation Of Data

A total of 45 samples were analyzed for their major and trace element concentrations with the following breakdown according to locality: Chapel Arm, 22; Hopeall Head, 5; Placentia Junction, 4; Cape Dog, 9; and Hay Cove, 5. In

addition some samples from each locality (18, 5, 5, 1, 5, order as above) were analyzed solely for their trace element concentrations. The following discussion concentrates on documenting the alteration effects in the Chapel Arm flows because several samples of these rocks are the least altered of all the Cambrian flows. They contain little carbonate or chlorite, show excellent preservation of primary igneous textures, and contain primary pyroxene, which is largely unaltered (see petrography discussion Chapter 3).

The major element and trace element concentrations in seven meta-basalt samples from Chapel Arm are given in Table 4.1 along with one analysis from Placentia Junction. Sample LC15A represents one of the least altered samples as discussed above whereas CA45 shows alteration of all primary mafic minerals to chlorite. Higher loss on ignition values (LOI) in the remaining samples correspond to higher calcite contents.

The Chapel Arm analyses show apparent decreases in nearly all major and trace elements with increasing LOI, the most important exceptions being CaO, Ni, Cr, Sr, and Zn. These observations do not take into account the volume changes which must have taken place, given the large variations in LOI and specific gravity (Table 4.1). Following Gresens (1967) it may be shown that

$$f_v (g^B/g^A) C_n^B - C_n^A = X_n$$

where  $f_v$  = the volume factor

$g^A$  = specific gravity of the parent rock

$g^B$  = specific gravity of the altered rock

$C_n^A$  = concentration of component n in the parent rock

$C_n^B$  = concentration of component n in the altered rock

$X_n$  = amount of component n lost or gained

The equation was rearranged and solved for  $f_v$  assuming  $X_n = 0$  for each component. Using LC15A as the parent, because it is probably least altered of all the samples,  $f_v$  values were calculated for samples CA45 and CA37 (Figure 4.1) which represent the two ends of the alteration spectrum (ie. chloritized with minor calcite and chloritized with abundant calcite). In the case of CA45 many elements cluster between  $f_v$  values of 0.9 and 1.5, and in the middle of the cluster are  $Al_2O_3$  and Zr with  $f_v$  values of 1.01 and 1.05 respectively. These two elements are often considered immobile and if we assume that the distribution of points in Figure 4.1 is due to the removal of some elements and the addition of others, their position in the middle of the distribution suggests that they were neither added nor subtracted from the rock (Gresens, 1967). Elements with higher  $f_v$  values were removed from the rock whereas those with lower volume factors were added during metasomatism. Assuming a volume factor of 1.01 (a 1 percent increase in

Table 4.1. Major and trace element concentrations in Cambrian meta-basalts.

|                                  | LC15A  | CA45  | PL57B | CA42C | CA58A | CA37  | CA57  | PL150 |
|----------------------------------|--------|-------|-------|-------|-------|-------|-------|-------|
| SiO <sub>2</sub>                 | 51.60  | 49.70 | 45.40 | 47.30 | 41.80 | 42.10 | 27.30 | 52.50 |
| TiO <sub>2</sub>                 | 2.60   | 2.44  | 1.78  | 2.18  | 1.78  | 1.82  | 1.47  | 3.61  |
| Al <sub>2</sub> O <sub>3</sub>   | 13.30  | 13.20 | 12.20 | 12.10 | 10.00 | 9.94  | 9.77  | 12.30 |
| Fe <sub>2</sub> O <sub>3</sub> * | 11.00  | 11.31 | 9.29  | 10.67 | 8.94  | 3.64  | 6.60  | 10.54 |
| MnO                              | 0.21   | 0.52  | 0.22  | 0.42  | 0.21  | 0.11  | 0.51  | 0.07  |
| MgO                              | 6.08   | 6.73  | 7.76  | 3.39  | 5.29  | 1.96  | 1.80  | 7.25  |
| CaO                              | 6.42   | 4.59  | 8.46  | 9.84  | 13.50 | 17.88 | 25.38 | 2.92  |
| Na <sub>2</sub> O                | 4.11   | 3.19  | 2.57  | 3.35  | 2.93  | 5.07  | 3.62  | 3.08  |
| K <sub>2</sub> O                 | 1.96   | 0.02  | 0.05  | 0.02  | 0.06  | 0.20  | 0.07  | 0.12  |
| P <sub>2</sub> O <sub>5</sub>    | 0.52   | 0.44  | 0.95  | 0.37  | 0.47  | 0.48  | 0.42  | 0.60  |
| L.O.I                            | 2.90   | 7.40  | 9.86  | 10.03 | 10.50 | 16.10 | 21.71 | 5.88  |
| Total                            | 100.70 | 99.54 | 98.54 | 99.67 | 98.48 | 99.34 | 98.65 | 98.87 |

|    |      |     |     |     |     |     |     |     |
|----|------|-----|-----|-----|-----|-----|-----|-----|
| Ga | 21   | 20  | 20  | 18  | 20  | 6   | 13  | 23  |
| Sr | 345  | 118 | 334 | 147 | 272 | 326 | 359 | 226 |
| Ba | 1075 | 144 | 260 | 161 | 165 | 242 | 80  | 281 |
| Rb | 21   | 0   | 1   | 1   | 4   | 3   | 0   | 1   |
| Zr | 205  | 196 | 294 | 175 | 163 | 161 | 168 | 473 |
| Nb | 47   | 33  | 52  | 28  | 38  | 36  | 31  | 97  |
| Y  | 29   | 26  | 33  | 24  | 19  | 18  | 22  | 36  |
| V  | 214  | 250 | 220 | 200 | 181 | 120 | 131 | 148 |
| Cr | 75   | 226 | 101 | 154 | 315 | 141 | 140 | 236 |
| Ni | 49   | 128 | 109 | 139 | 260 | 125 | 145 | 187 |
| Cu | 56   | 39  | 43  | 37  | 33  | 30  | 13  | 36  |
| Zn | 109  | 96  | 112 | 210 | 100 | 37  | 106 | 132 |

Density\* 2.79 2.77 2.78 2.75 2.77 2.71 2.77

Major element concentrations in wt. percent. Fe<sub>2</sub>O<sub>3</sub> = total Fe.

Trace element concentrations in ppm.

Density in g/cc.

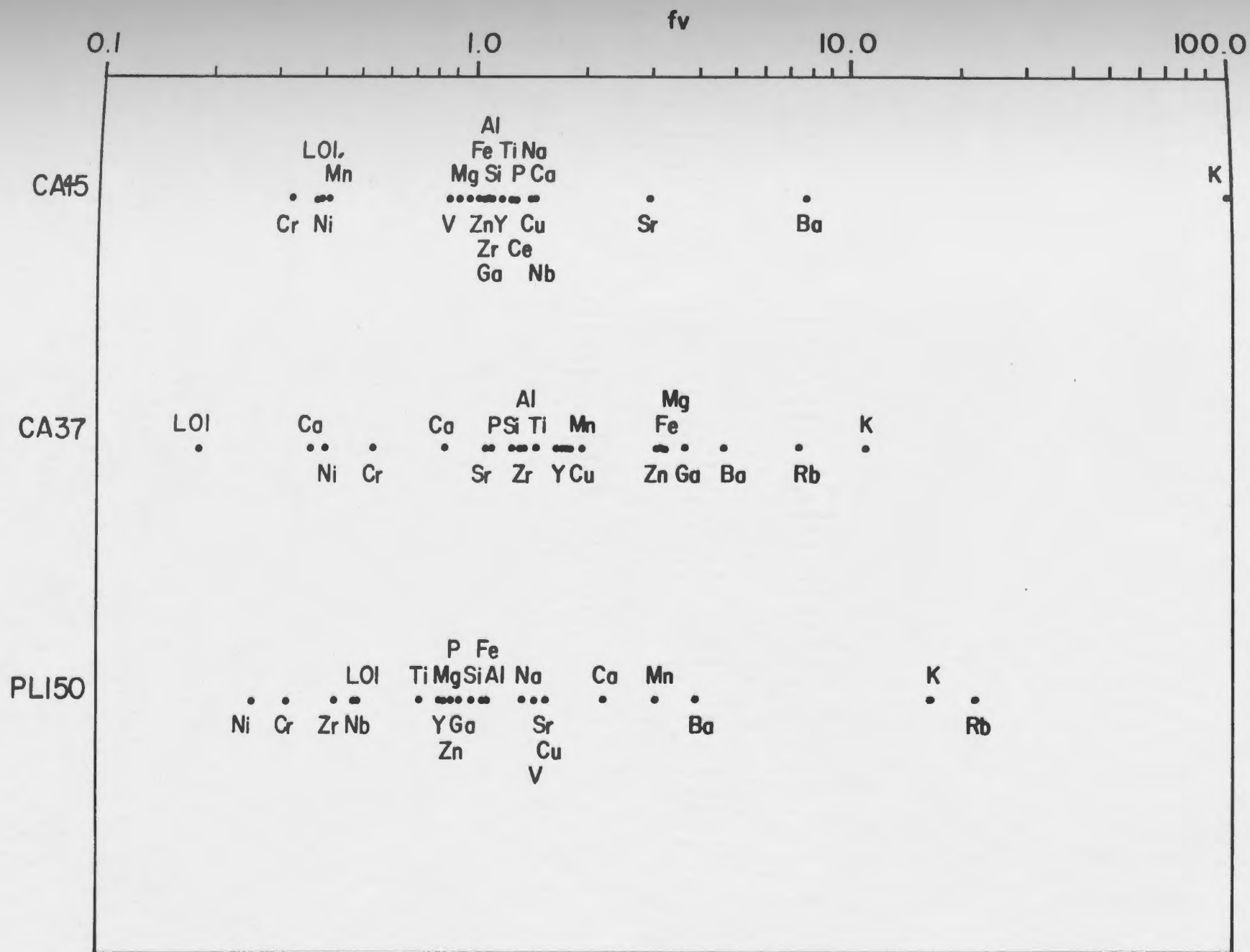
Sample locations: LC15A to CA37 - Chapel Arm

PL150 - Placentia Junction

PL53B - Hopeall Head

See map in pocket for precise locations.

Figure 4.1 Volume factor diagram for three Cambrian basalt samples. The diagram shows the volume change ( $f_v$ ) necessary to account for the concentration of each element in three samples assuming LC15A was the parent rock. Sample CA45 had most of its mafic minerals altered to chlorite but shows very low carbonate content; whereas sample CA37 has a high percentage of calcite. Samples LC15A, CA45 and CA37 are from Chapel Arm whereas sample PL150 is a chloritized volcaniclastic sample from Placentia Junction.





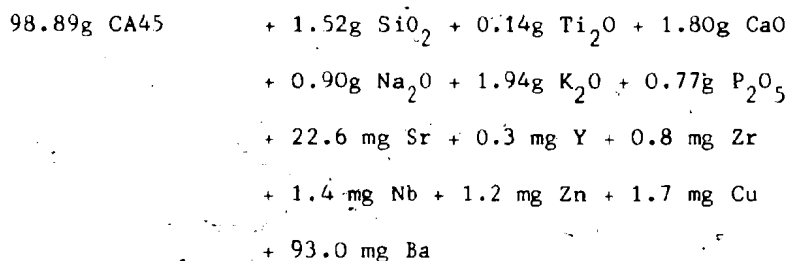
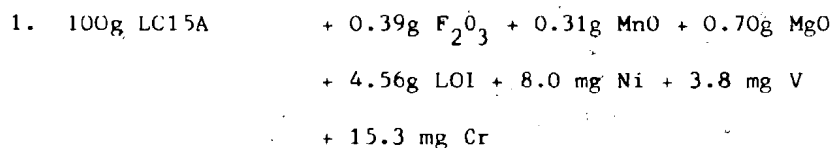
volume) equation 1 in Table 4.2 summarizes the alteration of LC15A to CA45.

Using the same procedure for CA37, a calcite rich sample, the data show a similar distribution but with clustering at higher  $f_v$  values. As with CA45,  $Al_2O_3$  and Zr fall in the center of the graph with factors of 1.38 and 1.31 respectively. Assuming constant Al and  $f_v$  equals 1.38 (38 percent volume increase) equation 2 in Table 4.2 summarizes additions and subtractions from the rock.

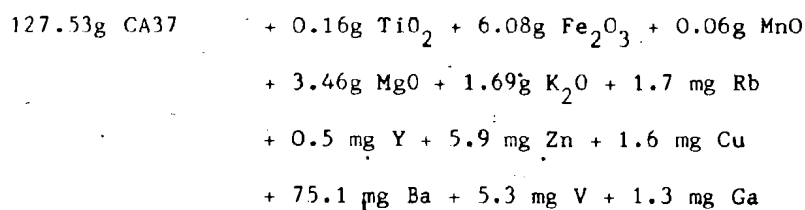
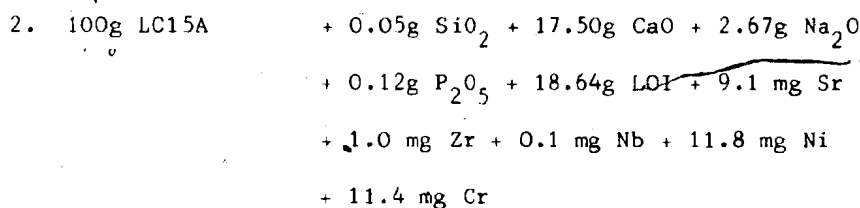
Individual sample pairs for the entire suite of meta-basalts could be compared in this fashion, but a more concise approach, which allows averaging of samples within specific LOI ranges is shown in Figure 4.2. Assuming Al remained constant in each sample, all element concentrations were divided by  $Al_2O_3$ , and the resulting ratios compared with those in the least altered basalt samples (LOI less than 5 wt. %). The samples were placed in groups representing increases in LOI of 2.5 wt. % (ie. 5 to 7.49, 7.5 to 9.99 etc.). Figure 4.2 expresses changes in the ratios between the least altered samples (parent rocks) and the altered rocks as a percentage of those in the least altered samples. Positive values indicate that the ratios increased, and that the element concentrations increased, negative values imply the opposite. Note that the ratios of a few elements (Ca, Mn, etc.) are divided by 10 to allow plotting on the same diagram. The elements are arranged in

Table 4.2 Alteration equations - Cape St. Mary's metabasalts.

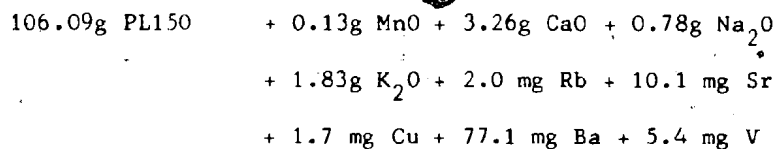
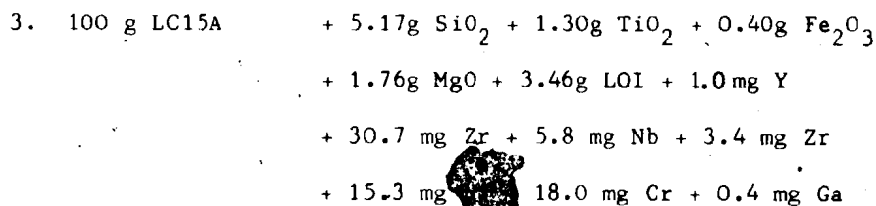
117

Assuming  $\text{Al}_2\text{O}_3$  remained constant.

$$f_v = 1.01$$



$$f_v = 1.38$$



$$f_v = 1.09$$

three groups; the alkaline earth and alkali metals, elements commonly considered immobile, and the transition and chalcophile elements.

With reference to Figure 4.2, those samples with LOI in the range 5 to 7.49 (LLOI samples) are generally depleted in  $\text{CaO}$ ,  $\text{MgO}$ ,  $\text{K}_2\text{O}$ ,  $\text{Sr}$ ,  $\text{Ba}$ , and  $\text{Rb}$  relative to the parent samples, by as much as 100 percent. The immobile elements plot very close to the baseline in the LLOI samples. Elements in the third group tend to be enriched, in some cases more than 100 percent (eg.  $\text{MnO}$ ,  $\text{Cr}$ , and  $\text{Ni}$ ).

The addition of carbonate, as indicated by an increase in LOI, most affected the alkali and alkaline earth metals. Compared to the LLOI samples, those with high LOI (HLOI) are enriched in  $\text{Na}_2\text{O}$ ,  $\text{CaO}$ , and  $\text{Sr}$ , but depleted in  $\text{MgO}$ . Potassium,  $\text{Rb}$ , and  $\text{Ba}$  show little or no relationship to the addition of carbonate, as is the case with all of the immobile elements, and generally true of the transition and chalcophile elements.

Samples from Cape Dog were treated in a similar manner with all element/ $\text{Al}_2\text{O}_3$  ratios related to those in the two least altered Cape Dog samples which show an average LOI value of 4.1. The diagrams (Figure 4.3) are essentially identical to those for Chapel Arm samples with the following exceptions.  $\text{Sr}$  does not increase with the addition of carbonate and  $\text{Cr}$  and  $\text{Ni}$  do not show as much enrichment (relative to the least altered samples) as in the Chapel Arm

Figure 4.2 Diagram showing the effect of metasomatism on the concentration of various elements in Chapel Arm lavas. Samples were grouped according to their LOI values and compared with the average of the two least altered samples LC15A and LC15B. The number of samples in each group is shown in the upper portion of the left rectangle. The diagram assumes that Al<sub>2</sub>O<sub>3</sub> was immobile. See text for discussion.

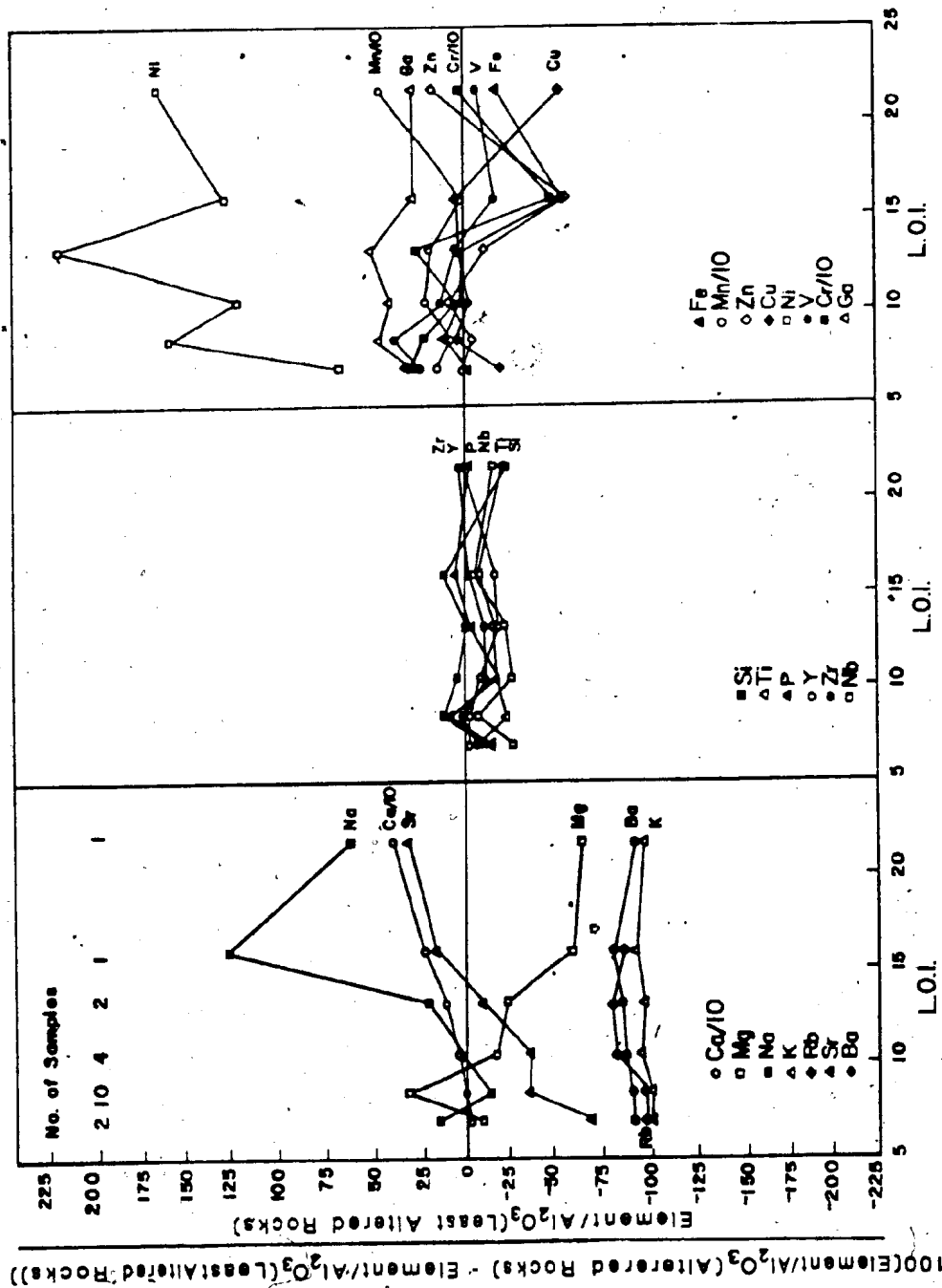
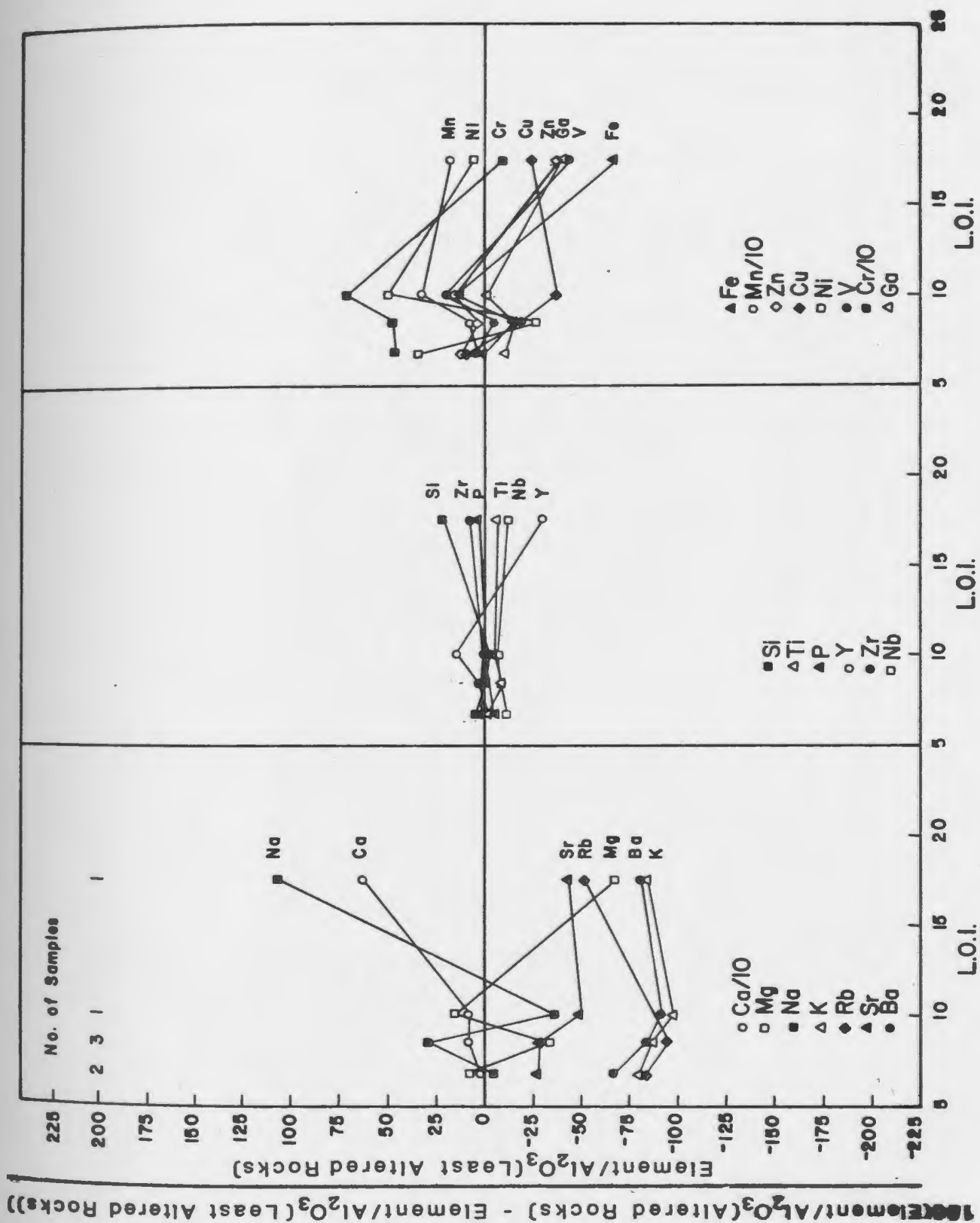


Figure 4.3 Diagram showing the effect of metasomatism on the concentration of various elements in the Cape Dog lavas. The diagram is the same as for the Chapel Arm samples except that the least altered samples are PL38C and PL44 from Cape Dog. See text for discussion.



samples. Lastly, the transition and chalcophile elements show a greater tendency to decrease with the addition of carbonate than they did in the Chapel Arm samples.

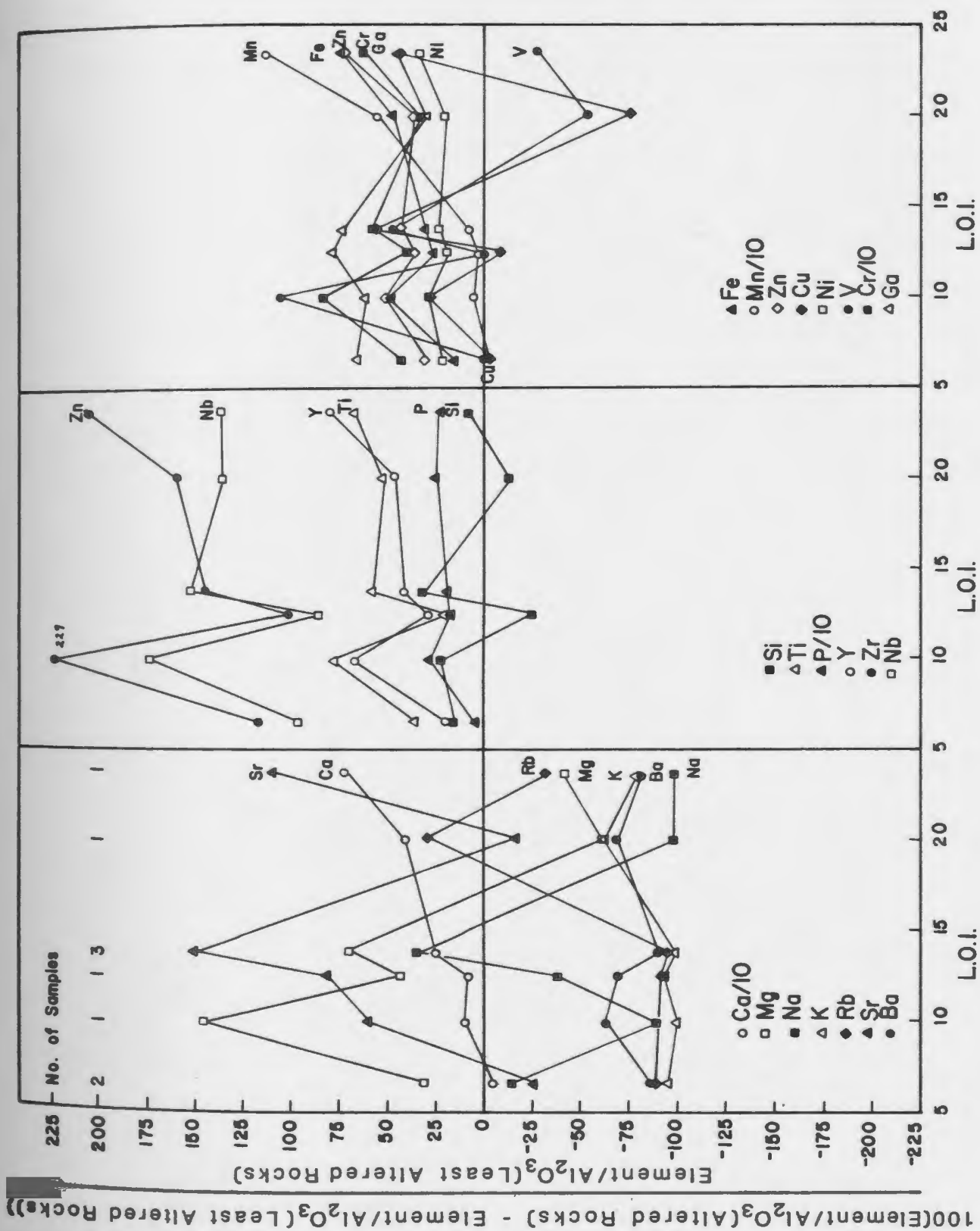
The volcanic rocks at Placentia Junction represent the most southerly extension of the flows and volcanoclastic rocks which start at Chapel Arm, though they are separated from the latter by a series of faults. It is reasonable to assume that these rocks were originally similar to those at Chapel Arm. But a comparison of sample PL150 with LLOI samples from Chapel Arm shows some important differences. In particular the "immobile" elements are all enriched. The volume change necessary to generate the concentrations observed in PL150 from those in LC15A, while constraining gains and losses of each element to 0 are shown in Figure 4.1. As with the Chapel Arm samples Al plots in the middle of the graph suggesting it was immobile, and that there was a 9 percent ( $f_v = 1.09$ ) volume increase.

Assuming that  $Al_2O_3$  was immobile, equation 3 in Table 4.2 relates LC15A to PL150 in terms of additions and subtractions through metasomatism. Note the large additions of  $TiO_2$ , Y, Zr, Nb, and the extremely large removal of CaO necessary to balance the equation.

Samples of the volcanic rocks from Hopeall Head also show high concentrations of the "immobile" elements. This is shown in Figure 4.4 where the concentrations of elements divided by  $Al_2O_3$ , at various LOI values, are compared to



Figure 4.4 Diagram showing the possible effect of metasomatism on the concentration of various elements in the Placentia Junction and Hopeall Head samples. Because relatively unaltered samples were not recovered at either locality the altered rocks were compared to the two least altered samples from Chapel Arm, LC15A and LC15B. The number of samples in each LOI group is given in the left rectangle. See text for discussion.



those in the Chapel Arm basalts. The patterns for the Placentia Junction and Hopeall Head samples are similar to those for Chapel Arm (Figure 4.2) with a few exceptions. Strontium, Rb, and  $\text{Na}_2\text{O}$  show large fluctuations with increasing LOI. Rb tends to increase with increasing LOI but  $\text{Na}_2\text{O}$  shows no overall trend. As in the LLOI Chapel Arm samples, most of the transition and chalcophile elements tend to be slightly (Fe, V, Zn) to strongly enriched (Cr, Ni, Ga). Manganese concentrations increase substantially with increasing LOI but most elements show little or no correlation with LOI.

The most important difference between the Chapel Arm patterns (Figure 4.2) and those for Placentia Junction and Hopeall Head are the unusually high concentrations of Y,  $\text{TiO}_2$ , Nb, Zr, and  $\text{P}_2\text{O}_5$  which show increasing enrichment in that order. The amount of enrichment does not appear related to the LOI values but an increase or decrease of one element between LOI groups tends to parallel similar changes in the other elements.

It is equally probable that the high immobile element concentrations in these samples represent primary differences from the Chapel Arm samples. However, the observation that such ratios as Zr/Y, Nb/Y, and Ti/V (which tend to be relatively unaffected by differentiation) as well as Zr and  $\text{P}_2\text{O}_5$  concentrations are either outside of, or just on the borderline of those observed in igneous (particularly

basaltic) suites suggests that these elements were enriched by secondary processes. Without relatively unaltered samples from either locality it is impossible to conclusively resolve the problem one way or the other.

Chondrite normalized REE patterns from selected Chapel Arm basalts (Figure 4.5, concentrations in Table 4.3) show no relationship with LOI values. Samples LC15A, LC15B, CA45, and PL57H, with LOI values of 2.9, 3.6, 7.4, and 9.5 wt. % respectively show nearly identical REE patterns which would not be appreciably affected if corrected for volume changes. Sample PL44 (LOI = 3.7) from Cape Dog has similar REE concentrations to those in the Chapel Arm lavas but the LREE are slightly enriched and the HREE are depleted in PL38C (LOI = 4.6). Similarly the HREE appear depleted in the Hay Cove sample SB37B2 (LOI = 5.4). Samples from Hopeall Head (PL133B) and Placentia Junction (PL67) are strongly enriched in the LREE and depleted in the HREE relative to the Chapel Arm basalts.

#### Discussion

The alteration of the Cambrian lavas can be separated into two stages, a (early?) phase during which mafic minerals were altered to chlorite, and a (later?) phase when carbonate was added to the rocks. The first phase resulted in the removal of CaO from the rocks and resembles the results of experiments modelling the formation of chlorite in basalts through interaction with seawater (Mottl, 1983).

Table 4.3. Rare earth element concentrations in Cambrian basalt samples.

|    | LC15A <sup>1</sup> | LC15B <sup>1</sup> | CA45 | PL57H | PL133B |
|----|--------------------|--------------------|------|-------|--------|
| La | 16.8               | 13.6               | 12.5 | 17.0  | 59.0   |
| Ce | 48.8               | 39.1               | 34.1 | 43.6  | 142.   |
| Pr | 6.89               | 6.32               | 4.35 | 6.52  | 16.6   |
| Nd | 35.0               | 31.6               | 22.0 | 29.4  | 77.6   |
| Sm | 8.40               | 8.66               | 6.39 | 8.20  | 16.2   |
| Eu | 3.21               | 3.14               | 2.22 | 3.10  | 4.96   |
| Gd | 7.85               | 8.10               | 6.07 | 8.13  | 12.5   |
| Dy | 5.18               | 5.45               | 3.91 | 5.82  | 5.23   |
| Er | 2.20               | 2.23               | 1.31 | 1.75  | 1.42   |
| Yb | 1.16               | 1.09               | 0.86 | 1.34  | 0.00   |

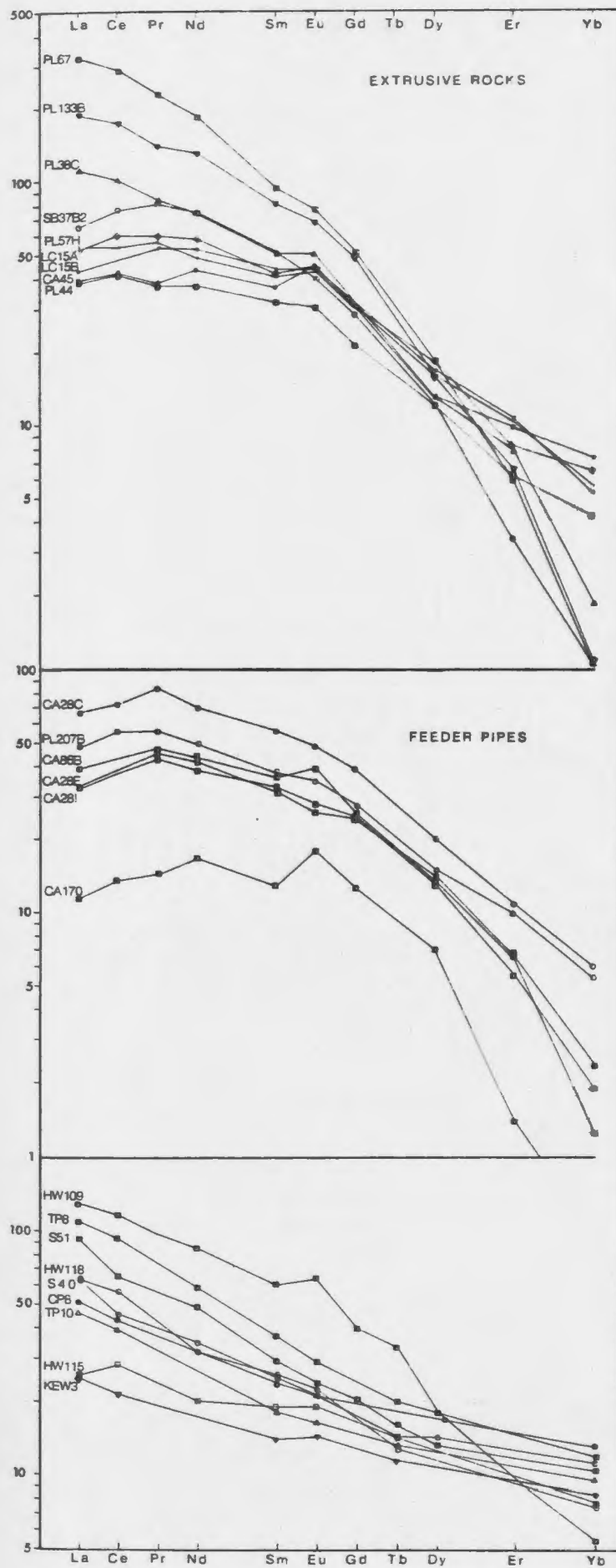
|    | PL38C <sup>1</sup> | PL44 <sup>1</sup> | SB37B2 <sup>1</sup> | PL67 |
|----|--------------------|-------------------|---------------------|------|
| La | 35.2               | 12.4              | 20.7                | 100. |
| Ce | 84.0               | 34.7              | 61.3                | 243. |
| Pr | 9.75               | 4.41              | 9.32                | 26.8 |
| Nd | 44.3               | 25.9              | 44.4                | 112. |
| Sm | 10.0               | 7.29              | 10.1                | 18.4 |
| Eu | 3.66               | 3.28              | 3.02                | 5.50 |
| Gd | 8.03               | 8.02              | 7.47                | 13.2 |
| Dy | 4.32               | 4.26              | 3.92                | 5.93 |
| Er | 1.53               | 2.11              | 0.72                | 1.29 |
| Yb | 0.39               | 1.51              | 0.00                | 0.13 |

Concentrations in ppm.

<sup>1</sup>Least altered basalt samples.

Locations: LC15A, B, CA45, PL57H - Chapel Arm  
 PL133B Hopeall Head  
 PL38C, PL44 - Cape Dog  
 SB37B2 - Hay Cove  
 PL67 - Placentia Junction

Figure 4.5 Chondrite-normalized REE patterns in the Cambrian basalts, feeder pipes, and basalts from various intraplate locations. The intraplate basalts have the following chemical affinities: sample HW109 is a nephelinite; samples TP8, S51, S40, and HW118 are alkali basalts; and samples TP10, KEW3, CP8, and HW115 are tholeiitic basalts. Sources and locations for these basalts are as follows: TP8 and TP10, Rio Grande Rift, Basaltic Volcanism Study Project (1981), p. 116; KEW3, Keweenawan flood basalt, Basaltic Volcanism Study Project (1981), p. 69; CP8, Columbia River flood basalt, Basaltic Volcanism Study Project (1981), p. 85; HW118, HW115, HW109, Hawaiian Islands, Greenough (1979); S40, S51, Afar (Ethiopia), Barberi et al. (1975). The chondrite normalizing values are from Taylor and Gorton, 1977.



These experiments also suggest that the absence of minerals such as epidote and actinolite may be accounted for by large seawater/basalt mass ratios. Whether or not the formation of chlorite was accomplished by interaction with seawater, it was accompanied by leaching of Sr, Ba, Rb, and K from the rocks, presumably because these elements were highly soluble in the passing solutions and do not fit in the chlorite lattice.

Studies of the alteration of basaltic glass through interaction with seawater (eg. Frey et al., 1974) have also noted that CaO decreases but Sr, Ba, Rb, and K tend to be enriched in the altered glass. Possibly these elements are enriched during the formation of albite (the only feldspar observed even in the least altered samples such as LC15A) but removed with the formation of chlorite.

The appearance of chlorite was also accompanied by slight to strong enrichment in Ni, Cr, Ga, V, and Mn in all samples but the effect on the immobile elements differed entirely from one locality to another. LLOI samples from Chapel Arm and Cape Dog show immobile element concentrations which are similar to those in the least altered basalts, but those in the Placentia Junction and Hopeall Head samples show much higher concentrations. If these differences are not due to primary compositional variations, there are several lines of reasoning which may explain the differential response to alteration.



The volcanic rocks from Placentia Junction are made up entirely of chloritized volcanic clasts which were once glassy shards and lapilli. The analyzed samples from Hopeall Head consist of volcanoclastic samples and highly vesicular basalts. Possibly the permeable nature of the volcanoclastic units and highly vesicular basalts allowed larger volumes of fluid to pass through the rocks, and resulted in substantial increases in the immobile element concentrations. Faults adjacent to the volcanic rocks at both Placentia Junction and Hopeall Head may have acted as pathways for metasomatic fluids and led to an increase in the fluid flux at these localities. Studies on the low grade alteration of basalts (eg. Floyd, 1977; Frey et al., 1974) have shown that glasses are much more susceptible to chemical alteration than are crystalline rocks. Furthermore this alteration commonly results in an increase in the LREE, and depletion of the HREE (Frey et al, 1974; Smewing and Potts, 1976; Floyd, 1977; Hellman et al., 1979) as appears to be the case for the Placentia Junction and Hopeall Head samples.

Other possible explanations which might account for the differences between the two groups of samples are: 1) varying metamorphic conditions at some localities that might allow greater stability for minor phases such as sphene and apatite which could selectively remove the "immobile" elements from passing solutions. This suggestion is supported by the observation that the rocks at Hopeall Head are very rich in secondary sphene. 2) differences in the

immobile element concentrations in the alteration fluids. 3) differences in the composition of the fluid phase which resulted in lower fluid/whole-rock partition coefficients for these elements at the Placentia Junction and Hopeall Head localities.

The second phase of alteration involved the addition of carbonate to the samples. This aspect of the alteration most affected the concentrations of  $\text{CaO}$ ,  $\text{Na}_2\text{O}$ , and  $\text{Sr}$ , which tend to be enriched, and  $\text{MgO}$ , which shows depletion with increasing  $\text{LOI}$ . Various studies of alteration where the  $\text{CO}_2$  activity was high show that  $\text{Ca}$ ,  $\text{Sr}$ , and in some cases  $\text{Na}$ , increase during alteration, but in general  $\text{Mg}$  also increases (eg. Kerrich and Fyfe, 1981; Strong, 1982).

Unlike carbonate rich solutions in peralkaline systems (Taylor et al., 1981) those associated with the alteration of the Cambrian lavas did not result in the enrichment of the HREE or in any of the REE. In this respect the alteration resembles that described by Strong (1982). Other immobile elements were similarly unaffected by the carbonate rich fluids. This contrasts sharply with the results of a study by Hynes (1980) where the addition of carbonate to basalts resulted in  $\text{Y}$  and  $\text{Zr}$  depletion and  $\text{Ti}$  enrichment. If the metamorphic phases present in these two groups of rocks are the same, as appears to be the case, the implications are that the fluids passing through the Avalon Peninsula rocks did not contain, or could not carry, these elements.

#### 4.2.2 Alteration Of The Feeder Pipes

The differentiated nature of the feeder pipes complicates the assessment of chemical modification from metamorphism. Both  $MgO$  and  $SiO_2$  show a scattered correlation with loss on ignition (LOI), which might suggest they were affected by metamorphism (Figure 4.6), but there is another, more reasonable, explanation for the correlation. During low grade metamorphism, mafic minerals are usually altered to hydrous minerals such as chlorite and actinolite and the feldspars to (anhydrous) albite. As a result mafic samples (high  $MgO$  and low  $SiO_2$ ) will have high LOI and felsic samples (low  $MgO$  and high  $SiO_2$ ) low LOI, which explains the observed correlation. The feeder pipes are in general much better preserved than the flows, and many samples are texturally and mineralogically as well (or better) preserved as any of the least altered flows. As the following discussion will show, most of the geochemical characteristics of these rocks can best be interpreted in terms of igneous processes.

#### 4.2.3 Primary Whole-Rock Geochemistry

The major element and normative composition of the least altered flow samples and representative feeder pipe samples are given in Tables 4.4 and 4.5, and the trace element concentrations are presented in Table 4.6. Major element and trace element variation diagrams showing all of the samples from the feeder pipes, and the five least

Figure 4.6 Plot of  $\text{SiO}_2$  and  $\text{MgO}$  against LOI for the feeder pipe samples. The metals are shown in oxide wt. %, volatile free, and LOI is in wt. %.

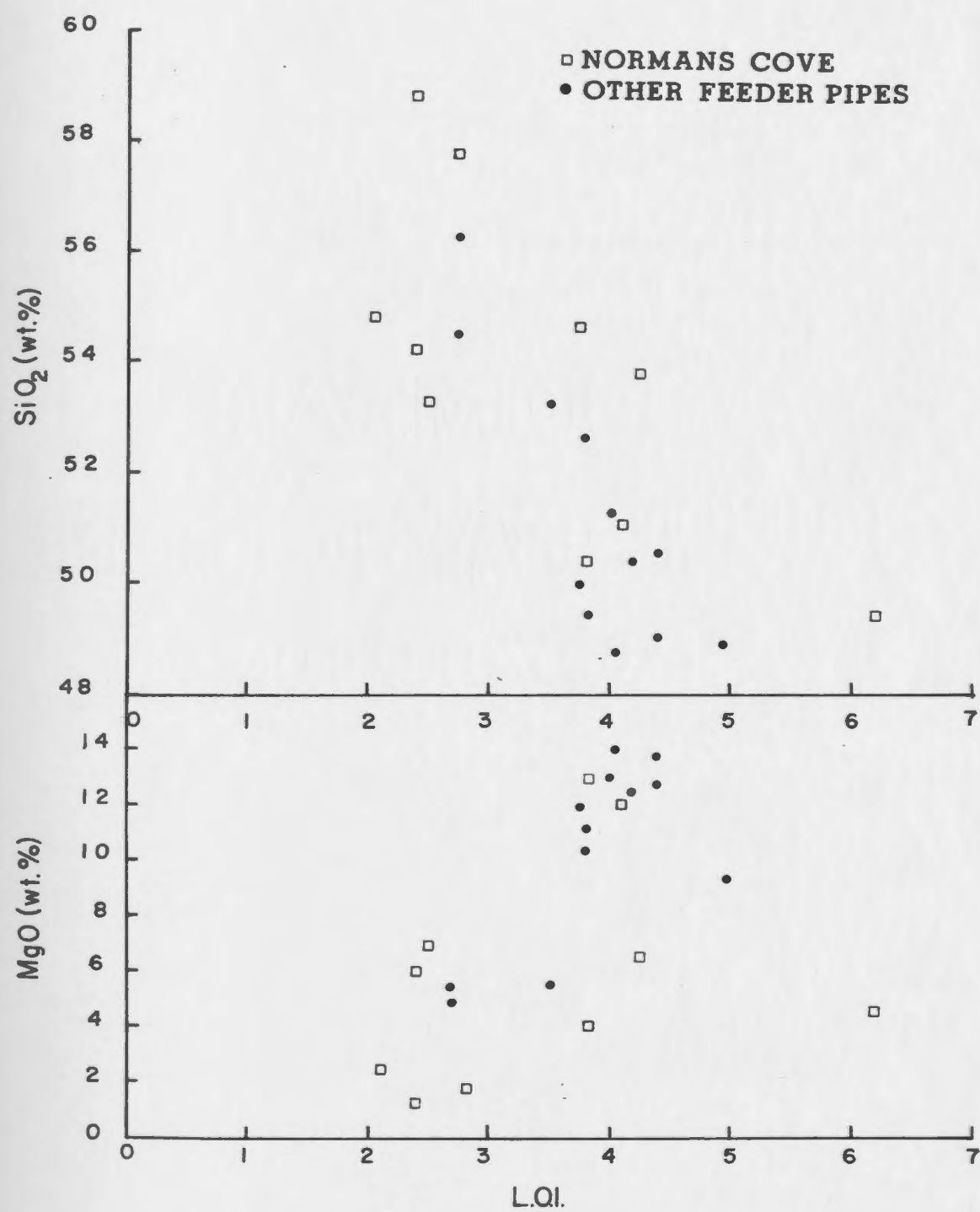


Table 4.4. Major element analyses of least altered extrusive rocks.

|                                | Chapel Arm |       | Cape Dog |       | Hay Cove |
|--------------------------------|------------|-------|----------|-------|----------|
|                                | LC15A      | LC15B | PL44     | PL38C | SB37B2   |
| SiO <sub>2</sub>               | 51.60      | 46.60 | 47.60    | 49.50 | 47.80    |
| TiO <sub>2</sub>               | 2.60       | 2.65  | 2.64     | 2.50  | 2.03     |
| Al <sub>2</sub> O <sub>3</sub> | 13.30      | 12.90 | 13.50    | 12.30 | 12.00    |
| Fe <sub>2</sub> O <sub>3</sub> | 11.00      | 11.12 | 10.57    | 11.90 | 10.54    |
| MnO                            | 0.21       | 0.15  | 0.20     | 0.13  | 0.13     |
| MgO                            | 6.08       | 7.39  | 8.71     | 9.29  | 6.08     |
| CaO                            | 6.42       | 7.06  | 5.85     | 4.74  | 8.03     |
| Na <sub>2</sub> O              | 4.11       | 1.87  | 2.79     | 4.13  | 3.84     |
| K <sub>2</sub> O               | 1.96       | 4.05  | 2.80     | 0.04  | 2.84     |
| P <sub>2</sub> O <sub>5</sub>  | 0.52       | 0.61  | 0.65     | 0.59  | 0.64     |
| L.O.I                          | 2.90       | 3.60  | 3.70     | 4.55  | 5.36     |
| Total                          | 100.70     | 98.00 | 99.01    | 99.67 | 99.29    |
| CIPW Norms                     |            |       |          |       |          |
| OR                             | 10.18      | 21.08 | 14.29    | 0.21  | 14.47    |
| Ab                             | 32.43      | 14.79 | 21.64    | 33.10 | 20.25    |
| An                             | 10.59      | 13.08 | 13.86    | 13.31 | 6.14     |
| Ne                             | 0.00       | 0.00  | 0.00     | 0.00  | 9.49     |
| Q                              | 0.00       | 0.00  | 0.00     | 0.00  | 0.00     |
| Ol                             | 10.23      | 22.71 | 22.81    | 6.20  | 15.30    |
| Hy                             | 10.61      | 1.98  | 8.04     | 31.57 | 0.00     |
| Di                             | 14.73      | 14.81 | 7.96     | 4.33  | 24.82    |
| Il                             | 7.96       | 8.13  | 7.94     | 7.77  | 6.10     |
| Mt                             | 2.30       | 2.30  | 2.26     | 2.33  | 2.25     |
| Ap                             | 0.90       | 1.05  | 1.10     | 1.03  | 1.08     |

Major element oxides in weight percent. Total Fe as Fe<sub>2</sub>O<sub>3</sub>.  
 Norms assume Fe<sub>2</sub>O<sub>3</sub> = 1.5 weight percent and remaining Fe = FeO.

Table 4.5: Major element and normative composition of selected feeder pipe samples.

|                                  | Normans Cove Pipe  |                    |                    | Other Feeder Pipes <sup>4</sup> |                    |                     |
|----------------------------------|--------------------|--------------------|--------------------|---------------------------------|--------------------|---------------------|
|                                  | CA281 <sup>1</sup> | CA28E <sup>2</sup> | CA28C <sup>3</sup> | CA86B <sup>1</sup>              | CA170 <sup>2</sup> | PL207B <sup>3</sup> |
| SiO <sub>2</sub>                 | 51.40              | 48.20              | 53.10              | 50.60                           | 46.0               | 52.60               |
| TiO <sub>2</sub>                 | 1.98               | 1.55               | 1.79               | 1.98                            | 1.12               | 2.80                |
| Al <sub>2</sub> O <sub>3</sub>   | 14.40              | 10.20              | 14.80              | 11.80                           | 11.90              | 13.50               |
| Fe <sub>2</sub> O <sub>3</sub> * | 10.44              | 11.82              | 9.03               | 10.61                           | 10.92              | 12.14               |
| MnO                              | 0.15               | 0.16               | 0.12               | 0.14                            | 0.15               | 0.16                |
| MgO                              | 6.67               | 12.60              | 3.36               | 10.00                           | 13.20              | 5.20                |
| CaO                              | 5.42               | 8.59               | 5.35               | 7.37                            | 9.46               | 4.61                |
| Na <sub>2</sub> O                | 4.54               | 1.77               | 3.64               | 3.30                            | 1.74               | 4.75                |
| K <sub>2</sub> O                 | 2.04               | 1.24               | 5.35               | 0.62                            | 0.62               | 1.28                |
| P <sub>2</sub> O <sub>5</sub>    | 0.37               | 0.33               | 0.80               | 0.38                            | 0.13               | 0.52                |
| L.O.I                            | 2.48               | 3.79               | 2.07               | 3.83                            | 4.05               | 2.67                |
| Total                            | 99.89              | 100.25             | 99.41              | 100.63                          | 99.29              | 100.23              |

## CIPW Norms

|    |       |       |       |       |       |       |
|----|-------|-------|-------|-------|-------|-------|
| OR | 10.39 | 6.20  | 28.64 | 3.20  | 3.06  | 6.86  |
| Ab | 35.13 | 13.44 | 27.60 | 25.86 | 13.05 | 38.71 |
| An | 11.11 | 13.73 | 7.47  | 13.58 | 19.07 | 10.65 |
| Ne | 0.00  | 0.00  | 2.02  | 0.00  | 0.00  | 0.00  |
| Q  | 0.00  | 0.00  | 0.00  | 0.00  | 0.00  | 0.13  |
| Ol | 22.68 | 15.95 | 12.45 | 6.50  | 26.69 | 0.00  |
| Hg | 1.62  | 22.51 | 0.00  | 25.25 | 12.73 | 24.14 |
| Di | 10.20 | 20.72 | 12.31 | 16.57 | 19.65 | 7.29  |
| Il | 5.94  | 4.57  | 5.65  | 6.02  | 3.26  | 8.85  |
| Mt | 2.25  | 2.21  | 2.37  | 2.28  | 2.18  | 2.37  |
| Ap | 0.63  | 0.55  | 1.42  | 0.65  | 0.21  | 0.93  |

1. Gabbro; 2. Cumulate; 3. Felsic differentiate;

4. Locations: CA86B - pipe E of Chapel Arm. CA170 - W of Spread Eagle Peak. PL207B - pipe at Placentia Junction.

See map in pocket for locations.

Total Fe as Fe<sub>2</sub>O<sub>3</sub>.

Table 4.6. Trace element analyses of least altered basalt samples and feeder pipe samples.

|    | LC15A <sup>1</sup> | LC15B <sup>1</sup> | PL44 <sup>1</sup> | PL38C <sup>1</sup> | SB37B <sup>2</sup> |
|----|--------------------|--------------------|-------------------|--------------------|--------------------|
| Rb | 21                 | 39                 | 28                | 1                  | 23                 |
| Sr | 345                | 377                | 429               | 119                | 193                |
| Ba | 1075               | 2213               | 1488              | 88                 | 631                |
| Zr | 205                | 233                | 277               | 267                | 198                |
| Nb | 47                 | 54                 | 57                | 49                 | 48                 |
| Y  | 29                 | 29                 | 31                | 25                 | 22                 |
| Ga | 13                 | 21                 | 25                | 25                 | 17                 |
| V  | 214                | 172                | 229               | 247                | 132                |
| Cr | 75                 | 24                 | 114               | 317                | 138                |
| Ni | 49                 | 97                 | 129               | 230                | 165                |
| Cu | 56                 | 22                 | 62                | 52                 | 27                 |
| Zn | 109                | 129                | 119               | 115                | 165                |

|    | CA28I <sup>3</sup> | CA28E <sup>4</sup> | CA28C <sup>5</sup> | CA86B <sup>3</sup> | CA170 <sup>4</sup> | PL207B <sup>5</sup> |
|----|--------------------|--------------------|--------------------|--------------------|--------------------|---------------------|
| Rb | 21                 | 16                 | 55                 | 8                  | 5                  | 13                  |
| Sr | 331                | 327                | 939                | 662                | 453                | 305                 |
| Ba | 615                | 635                | 777                | 1073               | 578                | 801                 |
| Zr | 121                | 117                | 272                | 158                | 48                 | 218                 |
| Nb | 25                 | 24                 | 52                 | 28 <sup>4</sup>    | 10                 | 41                  |
| Y  | 23                 | 19                 | 36                 | 24                 | 12                 | 34                  |
| Ga | 22                 | 17                 | 23                 | 20                 | 19                 | 29                  |
| V  | 156                | 139                | 122                | 170                | 113                | 279                 |
| Cr | 12                 | 439                | 0                  | 241                | 389                | 0                   |
| Ni | 9                  | 370                | 6                  | 210                | 345                | 23                  |
| Cu | 33                 | 15                 | 21                 | 44                 | 29                 | 39                  |
| Zn | 82                 | 95                 | 77                 | 100                | 124                | 155                 |

Concentrations in ppm.

1. Flow; 2. Bomb; 3. Gabbro; 4. Cumulate; 5. Differentiate.

Locations: See Tables 4.4 and 4.5.



altered basalt samples are presented in Figures 4.7 and 4.8. These diagrams provide fairly conclusive evidence that the pipes were the feeders to the flows. In most cases the flow samples plot along the trend lines defined by the feeder pipes, though they tend to show more scatter (especially on the major element diagrams) than the feeder pipe samples do. Some elements such as  $K_2O$  and Sr show random behaviour in both the flow and feeder pipe samples and reflect altered compositions as is common for these elements (Hughes, 1973).

The Cape St. Mary's Cambrian flows show relatively evolved basalt to basaltic andesite compositions as indicated by their intermediate  $Mg'$  values (0.55 to 0.64 where  $Mg' = Mg / (Mg + 0.9Fe \text{ atomic})$ ) and relatively high  $SiO_2$  contents (50 to 54 wt. %, LOI free). Some of the feeder pipe samples have much higher  $Mg'$  values, but they generally show cumulus pyroxene and olivine textures. The flows and noncumulus feeder pipe samples display a negative correlation between  $Mg'$  values and  $Al_2O_3$  (Figure 4.9). Similarly  $TiO_2$  values tend to increase with decreasing  $Mg'$ , (Figure 4.10) but drop abruptly in those samples with lowest  $Mg'$ . The feeder pipe samples show considerable scatter on a  $Na_2O + K_2O$ ,  $FeO$ ,  $MgO$  (AFM) diagram, but seem to define a trend with little or no Fe enrichment (Figure 4.11). Most of the basalt and feeder pipe samples contain normative Hy and Ol (Tables 4.4 and 4.5).

Figure 4.7 Major element Harker diagrams for Cape St. Mary's feeder pipe rocks. Also shown are the least altered Cambrian flow samples. Concentrations are in wt. % volatile free.

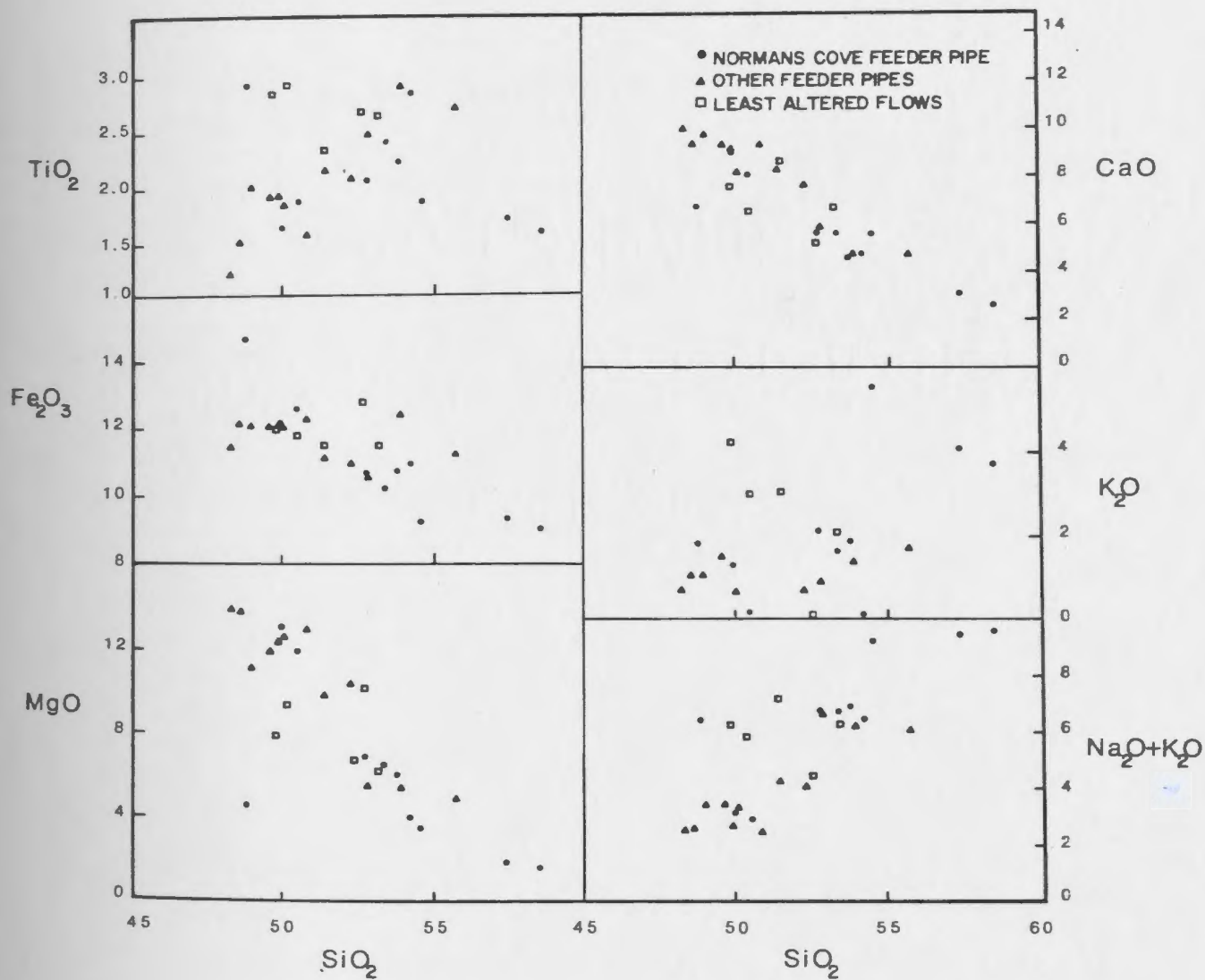


Figure 4.8 Trace element variation diagrams for Cape St. Mary's feeder pipe rocks. Also shown are the least altered Cambrian lava samples.  $TiO_2$  concentrations are in wt. %, volatile free, and all others are in ppm.

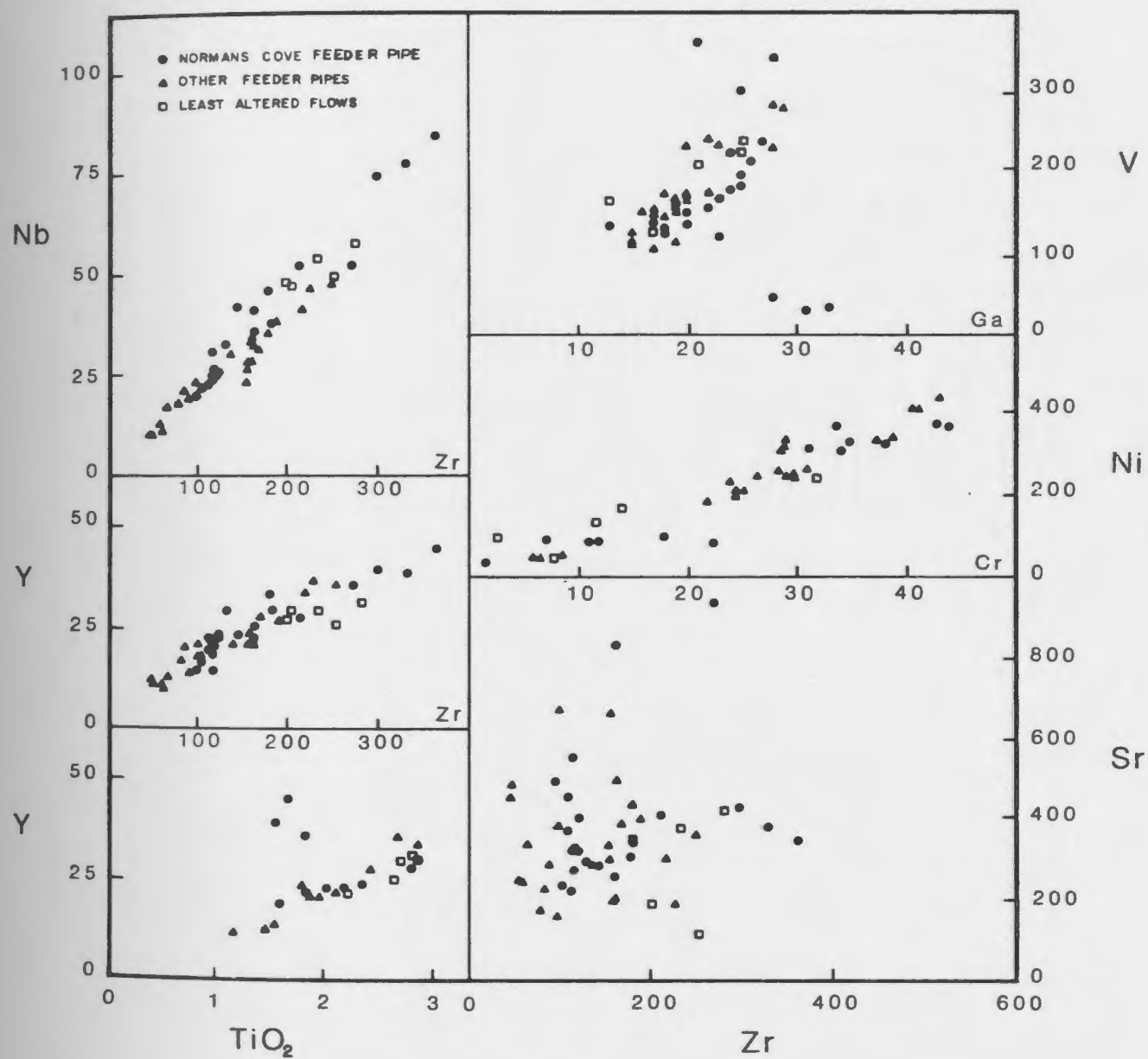


Figure 4.9 Plot of  $Mg'$  versus  $Al_2O_3$  in the feeder pipes, sills, dikes and various basaltic suites. The least altered Cambrian basalts from the Cape St. Mary's area are also shown on the feeder pipe diagram. The Cape St. Mary's samples were plotted volatile free with  $Al_2O_3$  in wt. %. Only non-cumulus samples are plotted on the feeder pipe diagram.  $Mg' = Mg/(Mg+0.9Fe)$  atomic. Sources for the other suites are as follows: Keweenaw, Basaltic Volcanism Study Project (1981), p. 67; Columbia River, Basaltic Volcanism Study Project (1981), p. 82, and Swanson and Wright (1981); Hawaiian Islands, Greenough (1979); Oslo Rift, Weigand (1975); Ethiopian Rift, Barberi et al. (1975) and Di Paola (1972); Rio Grande Rift, Basaltic Volcanism Study Project (1981), p. 115.

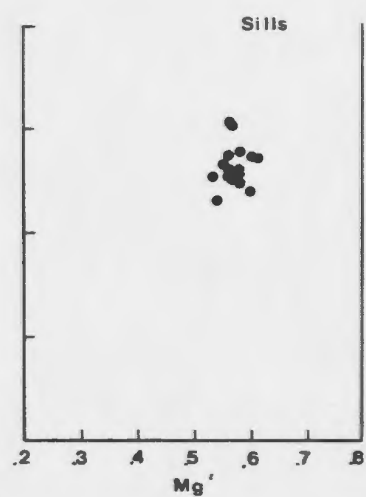
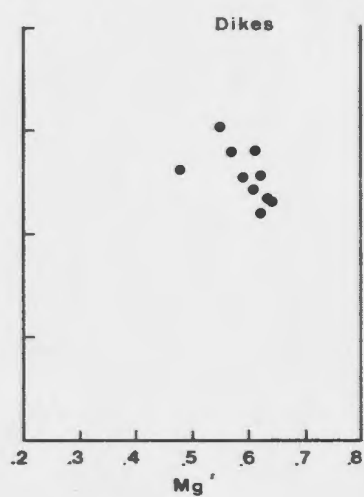
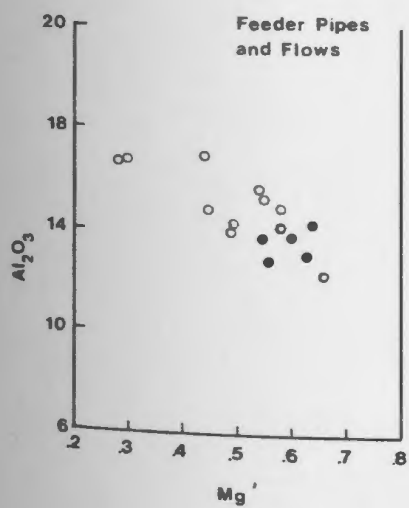
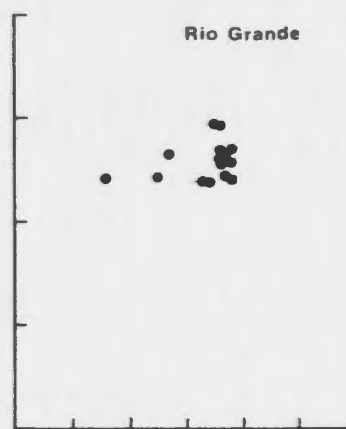
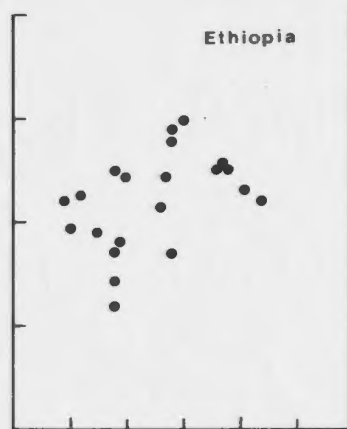
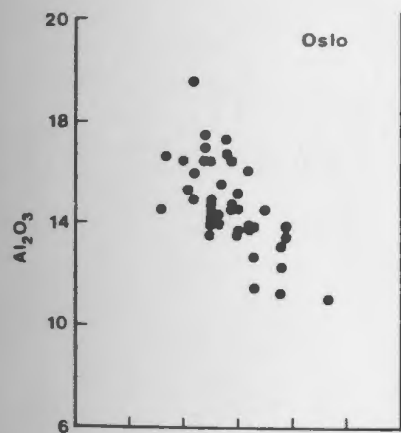
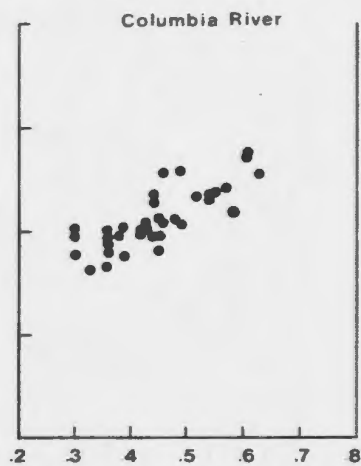
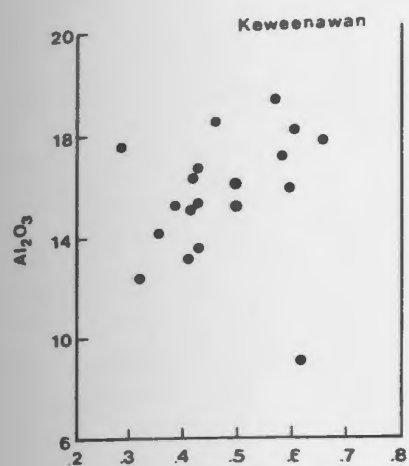


Figure 4.10 Plot of  $Mg'$  versus  $TiO_2$  in the feeder pipes, sills, dikes and various basaltic suites. The least altered Cambrian flow samples are also shown on the feeder pipe diagram. The Cape St. Mary's samples were plotted volatile free with  $TiO_2$  in wt. %.  $Mg' = Mg/(Mg+0.9Fe)$  atomic. Only non-cumulus samples are plotted on the feeder pipe diagram. Sources for the other suites are given in Figure 4.9.



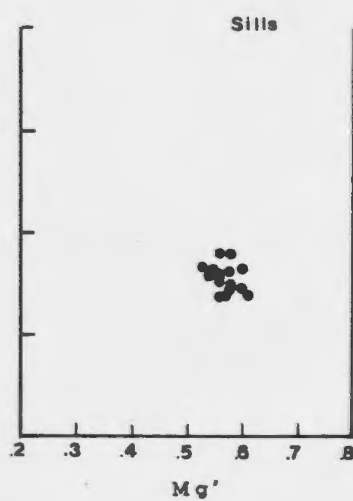
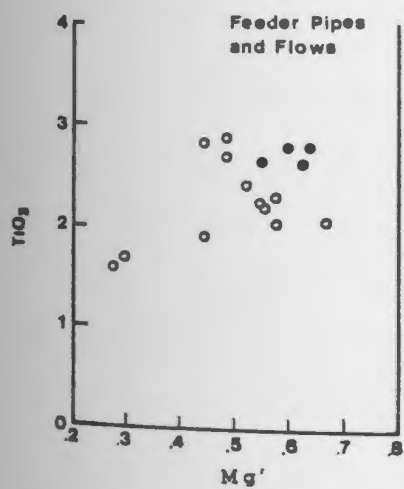
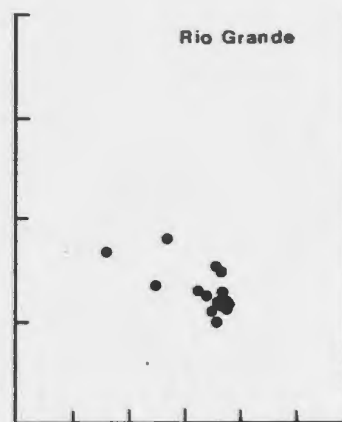
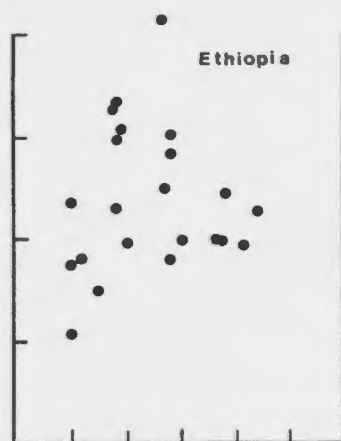
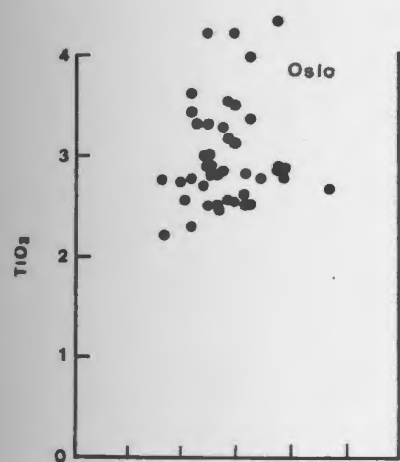
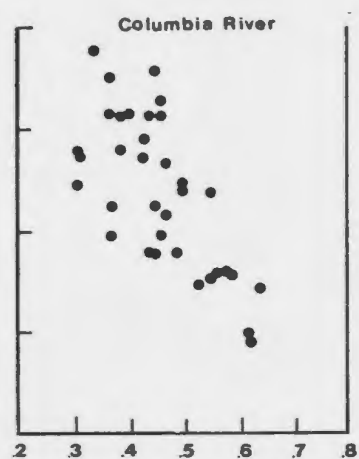
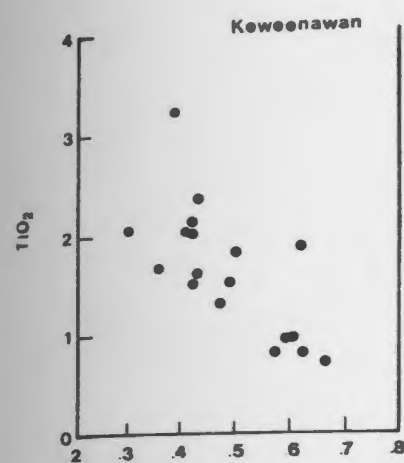
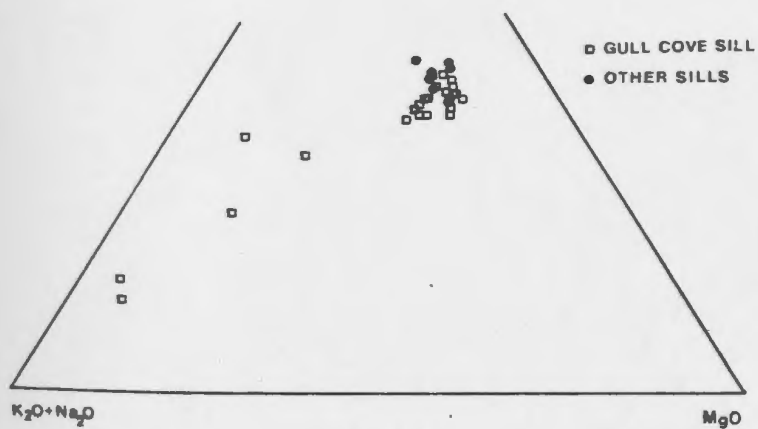
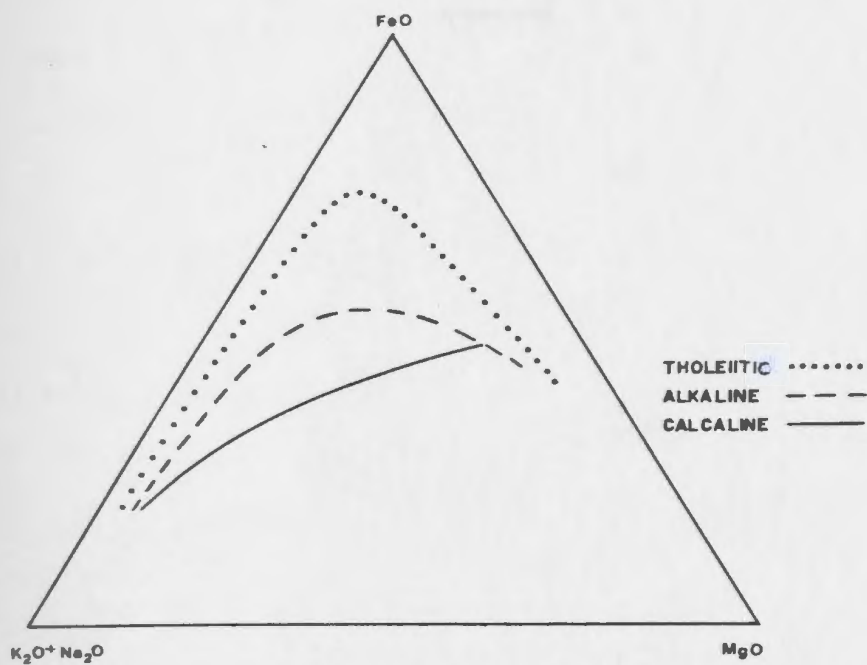


Figure 4.11 AFM diagram for Cape St. Mary's feeder pipe, and sill rocks. The tholeiitic, alkaline and calcalkaline trend lines in the top diagram do not represent particular data sets but are similar to Carmichael et al. (1974) examples.



Incompatible element pairs such as Nb-Zr and Zr-Y show a strong positive correlation on variation diagrams as do Cr and Ni values (Figure 4.8). Niobium, Zr, and Y concentrations (Table 4.6) are highest in the differentiated feeder pipe samples and lowest in the cumulate samples whereas the reverse is true of Cr, and Ni. Zr/Nb ratios (3.9 to 5.5, see Figure 4.12) and Nb/Y ratios (1.6 to 2.2) display very little variation within the suite.

Chondrite-normalized REE patterns (Figure 4.5a concentrations in Table 4.3) for the least altered flow samples (eg. LC15A) tend to be slightly concave upward with low La/Ce ratios (0.34), relatively high La/Yb ratios (13.5) and normalized Yb values less than 10. The feeder pipe gabbros (CA86B and CA28I Figure 4.5b and Table 4.7) along with more evolved samples (PL207B and CA28C) encompass the range of compositions shown by the basalts. All of the REE display elevated concentrations in the evolved samples whereas all are depleted in the cumulate samples (eg. CA170).

#### 4.2.4 Pyroxene Compositions

##### Flows

The only minerals in the extrusive rocks with primary chemistry are pyroxenes. Approximately 100 groundmass pyroxenes in the Chapel Arm, Cape Dog, and Hay Cove basalts were analysed (see Appendix A for experimental methods,

Figure 4.12 Zirconium versus Nb diagrams. Shown are the feeder pipes, sills and dikes as well as other basaltic suites. In the Keweenawan, Hawaii, Rio Grande, and feeder pipe diagrams closed circles represent tholeiites and open circles alkali basalts. The open circle with lowest Zr/Nb on the Rio Grande diagram and the two open circles with lowest Zr/Nb on the Hawaii diagram are nephelinites. On the sill diagram open circles represent fine-grained or contact samples and closed circles gabbro samples. All dike samples were plotted as closed symbols, but samples with low Nb/Y ratios are probably alkaline. Sources for the data are given Figure 4.9.

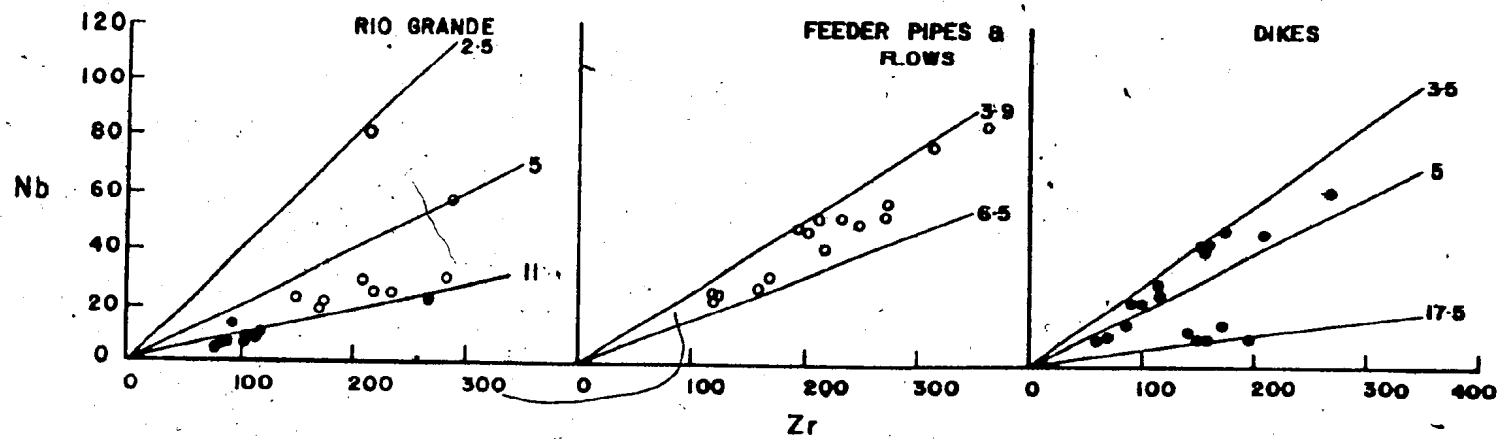
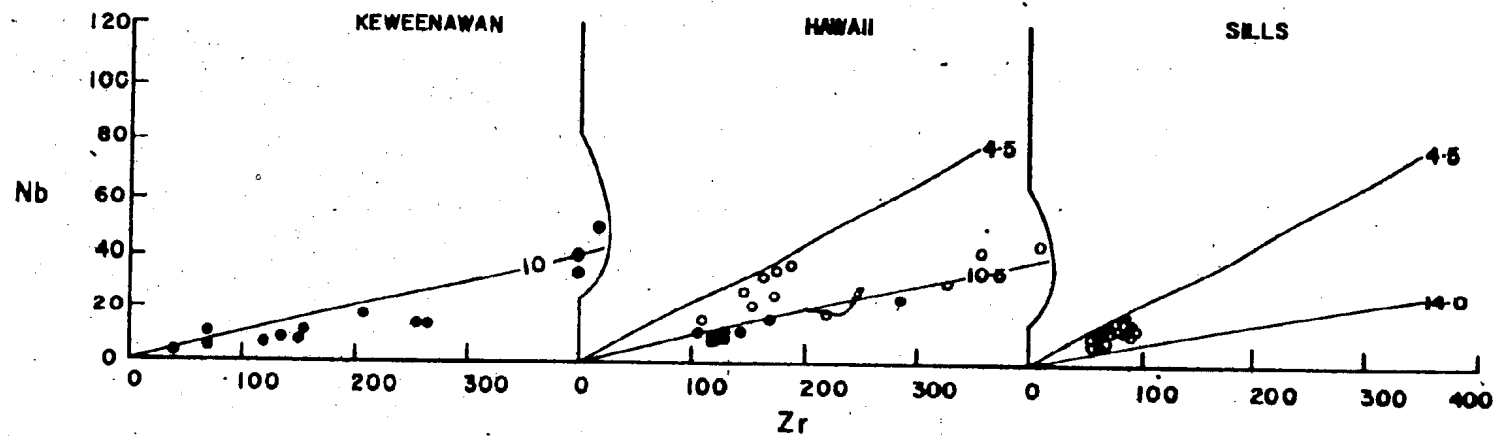


Table 4.7. Rare earth element concentrations in representative feeder pipe samples.

|    | CA28I <sup>1</sup> | CA28E <sup>2</sup> | CA28C <sup>3</sup> | CA86B <sup>1</sup> | CA1702 | PL207B3 |
|----|--------------------|--------------------|--------------------|--------------------|--------|---------|
| La | 10.4               | 11.0               | 19.1               | 12.3               | 3.67   | 15.1    |
| Ce | 31.4               | 31.2               | 58.0               | 35.0               | 11.2   | 44.8    |
| Pr | 5.07               | 5.48               | 9.69               | 5.64               | 1.72   | 6.43    |
| Nd | 23.1               | 25.2               | 41.6               | 26.1               | 10.1   | 29.7    |
| Sm | 6.47               | 6.49               | 11.1               | 7.13               | 2.60   | 7.58    |
| Eu | 2.07               | 1.92               | 3.53               | 2.83               | 1.32   | 2.53    |
| Gd | 6.63               | 6.69               | 10.2               | 6.89               | 3.31   | 7.34    |
| Dy | 4.42               | 4.58               | 6.59               | 4.45               | 2.28   | 4.92    |
| Er | 1.21               | 1.37               | 2.36               | 1.42               | 0.29   | 2.12    |
| Yb | 0.40               | 0.26               | 1.25               | 0.49               | 0.06   | 1.10    |

Concentrations in ppm.

1. Gabbro; 2. Cumulate; 3. Felsic differentiate.

Locations as in Table 4.5.

precision and accuracy) and representative analyses are given in Table 4.8 (see Appendix C for a complete listing of data. In terms of the three main pyroxene components, most analyses fall within the following bounds; Wo 42 to 50 percent, En 34 to 46 percent, and Fs 10 to 20 percent (Figure 4.13). Grains with Wo contents greater than 45 percent are properly termed salites (Deer et al., 1966) but most have augitic compositions.

TiO<sub>2</sub> contents of the pyroxenes show a skewed distribution. Some grains from Chapel Arm have 5 weight percent TiO<sub>2</sub> and are therefore titanaugites (Deer et al., 1966); but TiO<sub>2</sub> is normally between 1 and 2 weight percent. Al<sub>2</sub>O<sub>3</sub> may reach 8 weight percent in the high Ti grains, but concentrations of 3 weight percent, typical of augitic pyroxenes (Nisbet and Pearce, 1977), are the norm. The pyroxenes with high TiO<sub>2</sub> and Al<sub>2</sub>O<sub>3</sub> concentrations (eg. analysis 1 Table 4.8) come from the Chapel Arm sample displaying a variolitic texture as a result of quenching. MnO concentrations are usually less than 0.20 weight percent and Na<sub>2</sub>O values range from 0.20 to 0.70 weight percent; as is characteristic of high Mg pyroxenes (Deer et al., 1966; Nisbet and Pearce, 1977).

#### Feeder Pipes

Representative analyses of the feeder pipe pyroxenes are given in Table 4.9. The Wo, En, and Fs components (Figure 4.13) range from 41 to 44, 33 to 47, and 11 to 25;



Table 4.8. Representative analyses of pyroxenes from the extrusive rocks.

|                                | 1     | 2     | 3      | 4     | 5     | 6      |
|--------------------------------|-------|-------|--------|-------|-------|--------|
| SiO <sub>2</sub>               | 44.18 | 50.72 | 52.56  | 48.97 | 48.93 | 52.05  |
| TiO <sub>2</sub>               | 4.19  | 1.21  | 1.14   | 2.15  | 2.30  | 1.21   |
| Al <sub>2</sub> O <sub>3</sub> | 7.00  | 2.40  | 2.36   | 4.32  | 4.41  | 2.22   |
| Cr <sub>2</sub> O <sub>3</sub> | 0.05  | 0.16  | 0.73   | 0.21  | 0.74  | 0.36   |
| FeO*                           | 10.72 | 7.00  | 7.87   | 7.21  | 6.79  | 7.23   |
| MnO                            | 0.14  | 0.11  | 0.07   | 0.09  | 0.04  | 0.11   |
| MgO                            | 11.23 | 15.22 | 16.62  | 14.13 | 15.00 | 16.84  |
| NiO                            | 0.07  | 0.01  | 0.08   | 0.04  | 0.01  | 0.06   |
| CaO                            | 20.63 | 21.56 | 19.91  | 21.56 | 20.74 | 19.80  |
| Na <sub>2</sub> O              | 0.59  | 0.20  | 0.39   | 0.41  | 0.48  | 0.41   |
| K <sub>2</sub> O               | 0.00  | 0.02  | 0.02   | 0.02  | 0.01  | 0.01   |
| Total                          | 98.79 | 98.62 | 101.75 | 99.11 | 99.44 | 100.31 |
| Si                             | 1.701 | 1.905 | 1.909  | 1.836 | 1.825 | 1.913  |
| Al <sup>iv</sup>               | 0.299 | 0.095 | 0.091  | 0.164 | 0.175 | 0.087  |
| Al <sup>vi</sup>               | 0.018 | 0.010 | 0.009  | 0.026 | 0.018 | 0.009  |
| Ti                             | 0.121 | 0.034 | 0.031  | 0.060 | 0.063 | 0.032  |
| Cr                             | 0.001 | 0.004 | 0.020  | 0.005 | 0.021 | 0.009  |
| Fe                             | 0.344 | 0.219 | 0.239  | 0.226 | 0.211 | 0.222  |
| Mn                             | 0.003 | 0.003 | 0.002  | 0.002 | 0.001 | 0.003  |
| Mg                             | 0.644 | 0.852 | 0.899  | 0.789 | 0.833 | 0.922  |
| Ni                             | 0.001 | 0.000 | 0.002  | 0.001 | 0.000 | 0.001  |
| Ca                             | 0.851 | 0.867 | 0.775  | 0.866 | 0.829 | 0.779  |
| Na                             | 0.042 | 0.014 | 0.026  | 0.029 | 0.034 | 0.029  |
| K                              | 0.000 | 0.000 | 0.000  | 0.000 | 0.000 | 0.000  |
| Total                          | 4.025 | 4.005 | 4.003  | 4.004 | 4.009 | 4.005  |
| Ca                             | 46.2  | 44.7  | 40.5   | 46.0  | 44.2  | 40.4   |
| Mg                             | 35.0  | 43.9  | 46.9   | 41.9  | 44.5  | 47.9   |
| Fe + Mn                        | 18.8  | 11.4  | 12.6   | 12.1  | 11.3  | 11.7   |

1 = Rim Chapel Arm Pyroxene

2 = Core Chapel Arm Pyroxene

3 &amp; 4 = Cape Dog

5 &amp; 6 = Hay Cove

\*FeO = total Fe; Stoichiometry on basis of 6 oxygens.

Major element oxides in weight percent

Figure 4.13 Pyroxene quadrilateral showing pyroxenes from the Cape St. Mary's extrusive rocks and feeder pipes. In the case of the extrusive rocks individual analyses are not shown, but the areas where they plot are outlined, and the number of analyses is given in the table. The fields are labelled after Le Bas (1962).

## Number of Analyses

|                | <u>SUBALKALINE</u> | <u>ALKALINE</u> | <u>PERALKALINE</u> |
|----------------|--------------------|-----------------|--------------------|
| 1 = CHAPEL ARM | 2                  | 39              | 13                 |
| 2 = CAPE DOG   | 7                  | 15              | 0                  |
| 3 = HAY COVE   | 8                  | 13              | 0                  |

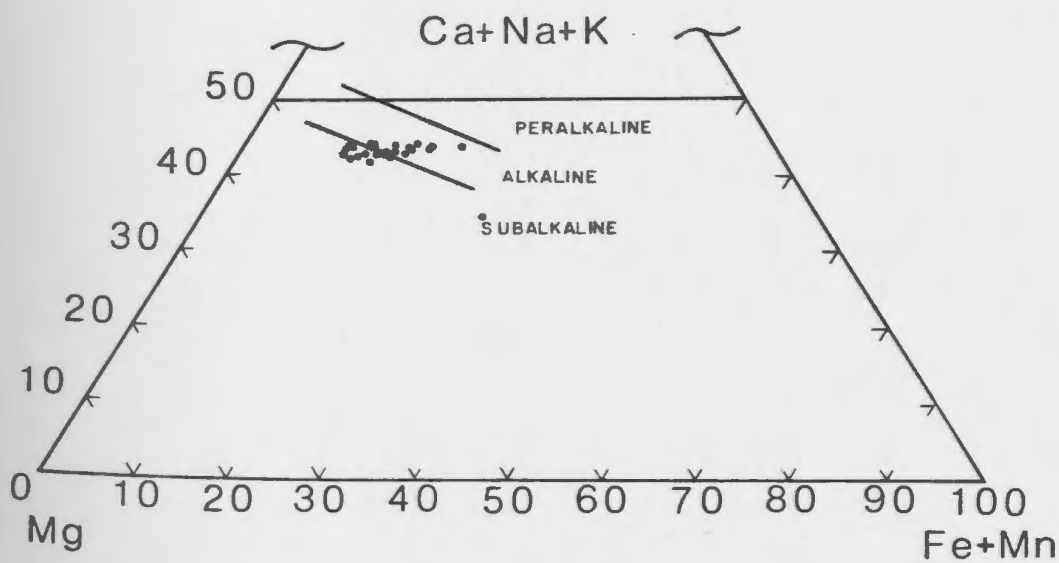
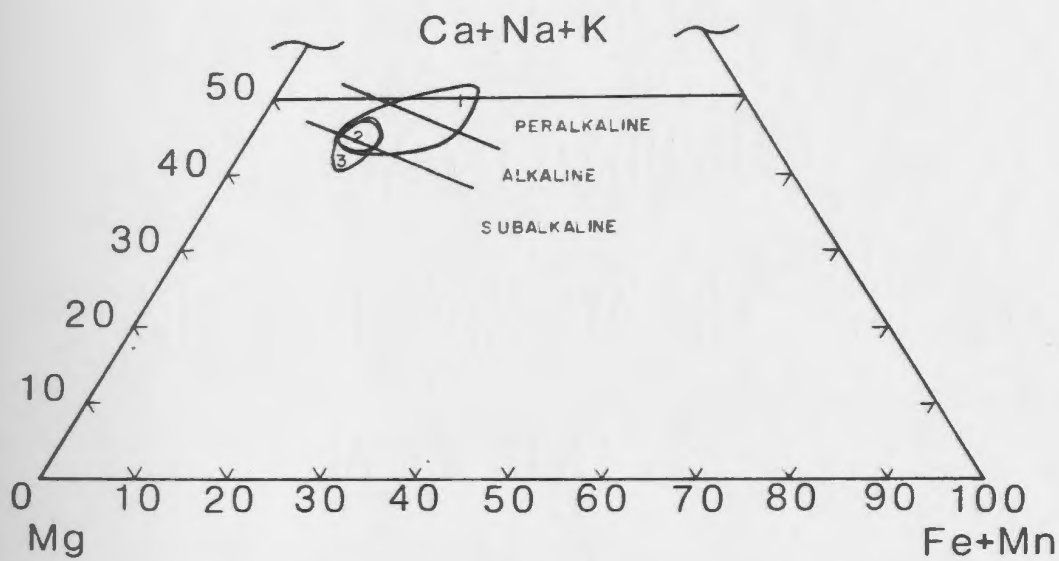


Table 4.9. Representative feeder pipe pyroxene analyses.

|                                | 1      | 2      | 3      | 4     | 5      | 6     |
|--------------------------------|--------|--------|--------|-------|--------|-------|
| SiO <sub>2</sub>               | 52.05  | 50.58  | 51.60  | 52.48 | 49.41  | 50.81 |
| TiO <sub>2</sub>               | 0.70   | 1.54   | 1.17   | 0.63  | 1.87   | 1.33  |
| Al <sub>2</sub> O <sub>3</sub> | 1.05   | 2.73   | 2.71   | 1.11  | 3.48   | 2.49  |
| Cr <sub>2</sub> O <sub>3</sub> | 0.01   | 0.05   | 0.51   | 0.02  | 0.00   | 0.00  |
| FeO*                           | 14.43  | 9.58   | 7.05   | 8.35  | 11.43  | 8.21  |
| MnO                            | 0.26   | 0.20   | 0.17   | 0.16  | 0.14   | 0.11  |
| MgO                            | 11.73  | 14.97  | 15.86  | 15.91 | 12.98  | 14.53 |
| NiO                            | 0.00   | 0.03   | 0.05   | 0.04  | 0.00   | 0.09  |
| CaO                            | 21.16  | 20.60  | 21.40  | 20.22 | 20.45  | 21.50 |
| Na <sub>2</sub> O              | 0.25   | 0.30   | 0.28   | 0.45  | 0.44   | 0.31  |
| K <sub>2</sub> O               | 0.01   | 0.01   | 0.00   | 0.01  | 0.01   | 0.00  |
| Total                          | 101.64 | 100.58 | 100.79 | 99.38 | 100.22 | 99.40 |
| Si                             | 1.923  | 1.881  | 1.896  | 1.958 | 1.862  | 1.903 |
| Al <sup>iv</sup>               | 0.077  | 0.119  | 0.104  | 0.042 | 0.138  | 0.097 |
| Al <sup>vi</sup>               | 0.003  | 0.000  | 0.012  | 0.006 | 0.015  | 0.011 |
| Ti                             | 0.031  | 0.042  | 0.031  | 0.017 | 0.052  | 0.037 |
| Cr                             | 0.000  | 0.001  | 0.014  | 0.000 | 0.000  | 0.000 |
| Fe                             | 0.351  | 0.298  | 0.215  | 0.259 | 0.359  | 0.257 |
| Mn                             | 0.008  | 0.005  | 0.004  | 0.004 | 0.004  | 0.003 |
| Mg                             | 0.741  | 0.829  | 0.868  | 0.885 | 0.729  | 0.812 |
| Ni                             | 0.000  | 0.000  | 0.001  | 0.000 | 0.000  | 0.002 |
| Ca                             | 0.846  | 0.820  | 0.842  | 0.808 | 0.825  | 0.863 |
| Na                             | 0.025  | 0.021  | 0.019  | 0.032 | 0.032  | 0.022 |
| K                              | 0.000  | 0.000  | 0.000  | 0.000 | 0.000  | 0.000 |
| Total                          | 4.005  | 4.018  | 4.007  | 4.011 | 4.016  | 4.007 |
| Ca                             | 43.5   | 42.0   | 43.6   | 41.3  | 43.0   | 44.6  |
| Mg                             | 38.1   | 42.5   | 45.0   | 45.2  | 38.0   | 42.0  |
| Fe+Mn                          | 18.4   | 15.5   | 11.4   | 13.4  | 19.0   | 13.4  |

\*All Fe as FeO, Oxides in weight percent, Stoichiometry calculated on the basis of 6 oxygen.

- 1, 2, & 3 = Normans Cove  
 4 = W. of Spread Eagle Peak  
 5 = SE. of Placentia Junction  
 6 = N. of Spread Eagle Peak

which are augitic compositions (Deer et al., 1966) and the data points define a trend of constant Ca content with decreasing Mg composition. Most  $TiO_2$  concentrations fall between 1 and 2 weight and display a positive correlation with  $Al_2O_3$  values which are generally between 2 and 3 weight percent. The  $Na_2O$  and  $MnO$  concentrations average 0.35 and 0.30 weight percent respectively. The slightly lower  $TiO_2$  concentrations in the feeder pipe pyroxenes as compared with the flows is illustrated in Figure 4.14 but for the most part the feeder pipe pyroxene compositions overlap those of the lava flows.

#### 4.2.5 Discussion - Flows and Feeder Pipes

Mass balance and trace element modelling calculations show that phases present in the melanogabbro samples can be removed from the flows to produce the most differentiated samples. The mass balance calculations were carried out using the petrological mixing model of Le Maitre (1979). Results show that an excellent estimate of the major element composition of the differentiate (Table 4.10) can be produced by removing 45 percent of the melt in the form of augite, plagioclase, Fe-Ti oxide, olivine, and apatite in the proportions 15.1 : 14.3 : 3.8 : 10.9 : 0.9. The residual sum of squares for these calculations is 0.81. The results shown in Table 4.10 are the least squares best fit solution to the problem without weighting any of the oxides. The most serious problem is with  $TiO_2$ , and it could be

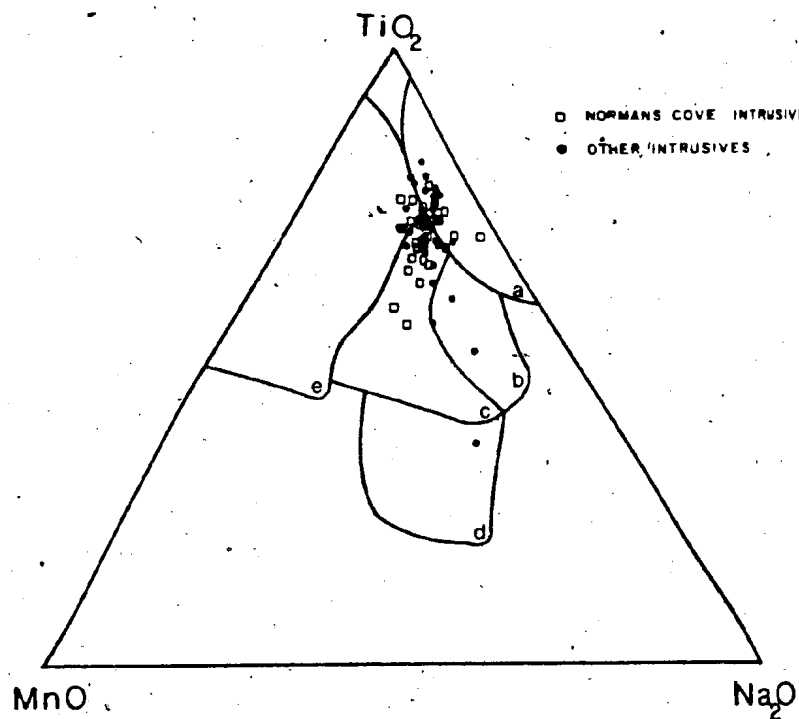
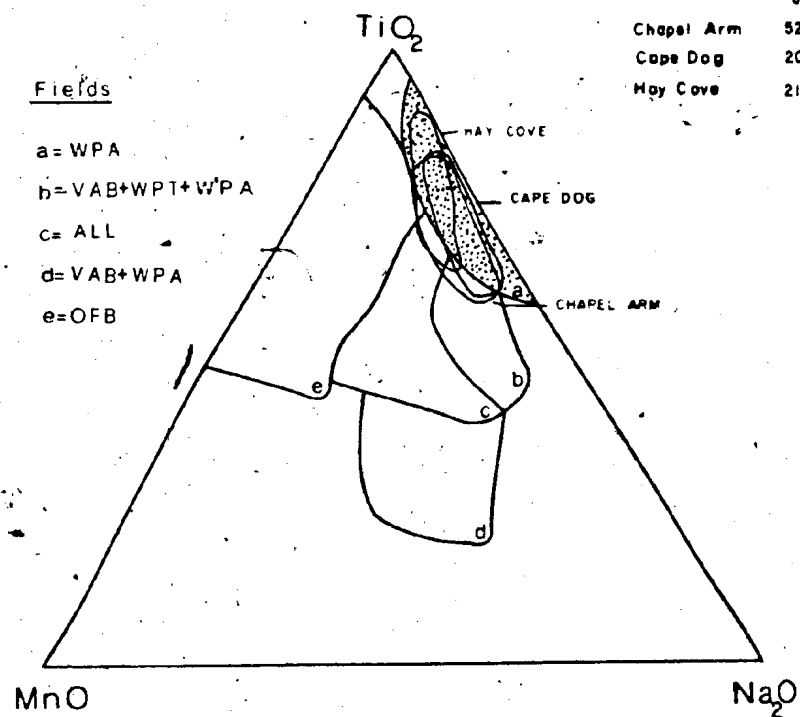
Figure 4.14  $\text{TiO}_2$ - $\text{MnO}$ - $\text{Na}_2\text{O}$  pyroxene discrimination diagram - Cape St. Mary's extrusive rocks and feeder pipe pyroxenes. In the case of the extrusive rocks individual analyses are not shown, but the areas where they plot are outlined, and the number of analyses for each locality is given in the table. For clarity the a field in the upper diagram is stippled. Fields are from Nisbet and Pearce (1977). WPA = within plate alkaline; WPT = within plate tholeiite; VAB = volcanic arc basalt OFB = ocean floor basalt.

## NUMBER OF ANALYSES

|            | Fields |   |   |   |   |
|------------|--------|---|---|---|---|
|            | a      | b | c | d | e |
| Chapel Arm | 52     | 1 | 1 | 0 | 0 |
| Cape Dog   | 20     | 1 | 2 | 0 | 0 |
| May Cove   | 21     | 0 | 0 | 0 | 0 |

## Fields

a = WPA  
 b = VAB+WPT+WPA  
 c = ALL  
 d = VAB+WPA  
 e = OFB



1

163



Table 4.10 (continued)

KD values<sup>8</sup> used in trace element modelling.

|    | Augite | Plagioclase | FeTi Oxide | Olivine | Apatite |
|----|--------|-------------|------------|---------|---------|
| Rb | 0.031  | 0.071       | 0.000      | 0.007   | 0.000   |
| Sr | 0.120  | 1.830       | 0.000      | 0.014   | 1.000   |
| Ba | 0.026  | 0.230       | 0.000      | 0.009   | 0.000   |
| Cr | 10.000 | 0.100       | 96.500     | 2.700   | 0.000   |
| Ni | 4.500  | 0.008       | 23.333     | 23.800  | 0.000   |
| Y  | 0.680  | 0.055       | 0.000      | 0.010   | 50.700  |
| Nb | 0.400  | 0.055       | 0.000      | 0.010   | 50.700  |
| Zr | 0.400  | 0.005       | 0.000      | 0.010   | 0.000   |
| V  | 1.300  | 0.080       | 79.950     | 0.050   | 0.000   |
| Ga | 0.505  | 1.000       | 0.000      | 0.000   | 1.000   |

Major element oxides in weight percent. Trace elements in ppm.

1. Lava = Average of 5 least altered samples, majors recalculated to 100% and Fe<sub>2</sub>O<sub>3</sub> thin recalculated as FeO.
2. Augite = Average of 6 augite analyses from the cumulate sample CA170.
3. Plagioclase = Analysis 3 from Hawaiian basalt, Basaltic Volcanism Study Project, 1981, p. 182, with similar An content to normative feldspar for flows.
4. FeTi Oxide = Analysis 2 from Hawaiian basalt, Basaltic Volcanism Study Project, 1981, p. 186.
5. Olivine = Analysis 14 from Hawaiian basalt, *ibid.*, p. 180.
6. Apatite = Analysis 1 from quartz diorite as presented in Deer *et al.*, 1966, p. 506.
7. Differentiate = Average of two most extreme differentiates, LC8F and LC8G, majors recalculated to 100% and Fe<sub>2</sub>O<sub>3</sub> then recalculated as FeO.
8. KD values from Arth (1976), Jensen (1973), Ewart and Taylor (1969), Henderson and Dale (1969), Delong (1974), Duke (1976), Dudas *et al.* (1971), Arth (1976). See Evans (1981) for details.

significantly improved, without appreciably affecting the other oxides, by increasing the percentage of Fe-Ti oxide removed.

The trace elements were modelled for both surface and total equilibrium fractionation conditions assuming 45 percent fractionation of the melt, with minerals in the same proportions as indicated from the mass balance calculations. Sources for the partition coefficients used are given in Table 4.10. Calculations were carried out using a computer program written by Evans (1978) and the results, which are in reasonable agreement with the observed concentrations in the differentiate, are given in Table 4.10. The most serious problem is with Nb, an element very sensitive to the proportion of apatite removed. A small decrease in the amount of apatite subtracted would bring the Nb values more in line with those observed as well as raising the Y concentrations.

#### 4.3 CAPE ST. MARY'S SILLS

##### 4.3.1 Whole-Rock Geochemistry

Although most sill samples show a certain amount of mineralogical alteration, the whole-rock chemistry does not appear seriously affected by the metamorphism. All samples show less than 4.0 wt. % LOI and a few less than 2.0 wt. %. The coherent behaviour of most elements on variation diagrams (Figures 4.15 and 4.16) is best interpreted in

Figure 4.15 Major element Harker diagrams for the Gull Cove sill. The lines on the diagrams represent a least squares fit through the feeder pipe data and the diamonds mark the mean feeder pipe compositions. Correlation coefficients for the lines are as follows: Ti, 0.53; Fe, 0.76; Mn, 0.04; Mg, 0.84; Al, 0.76; P, 0.50; Ca, 0.92; K, 0.60; Na, 0.78. All concentrations are in wt. % volatile free.

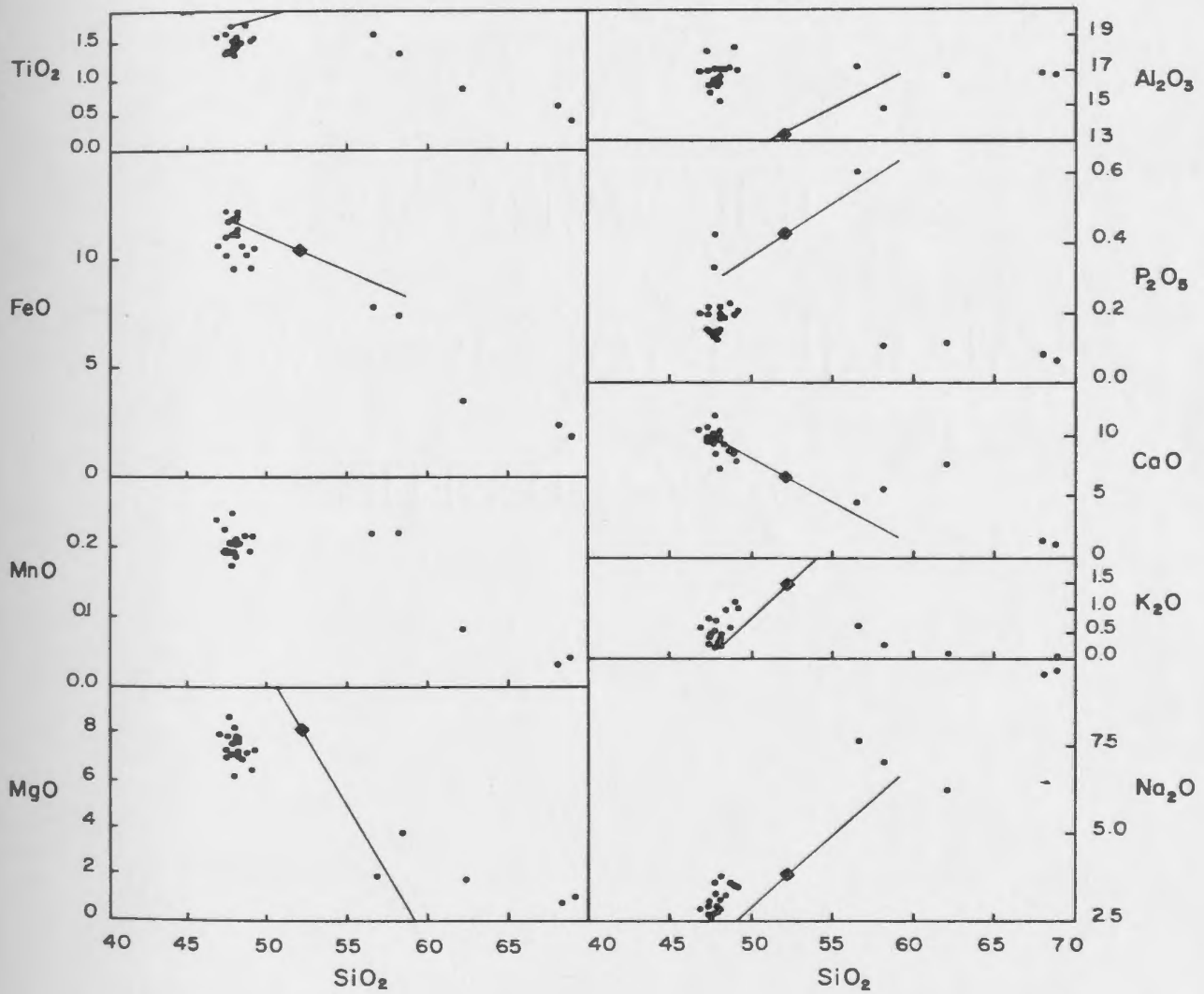
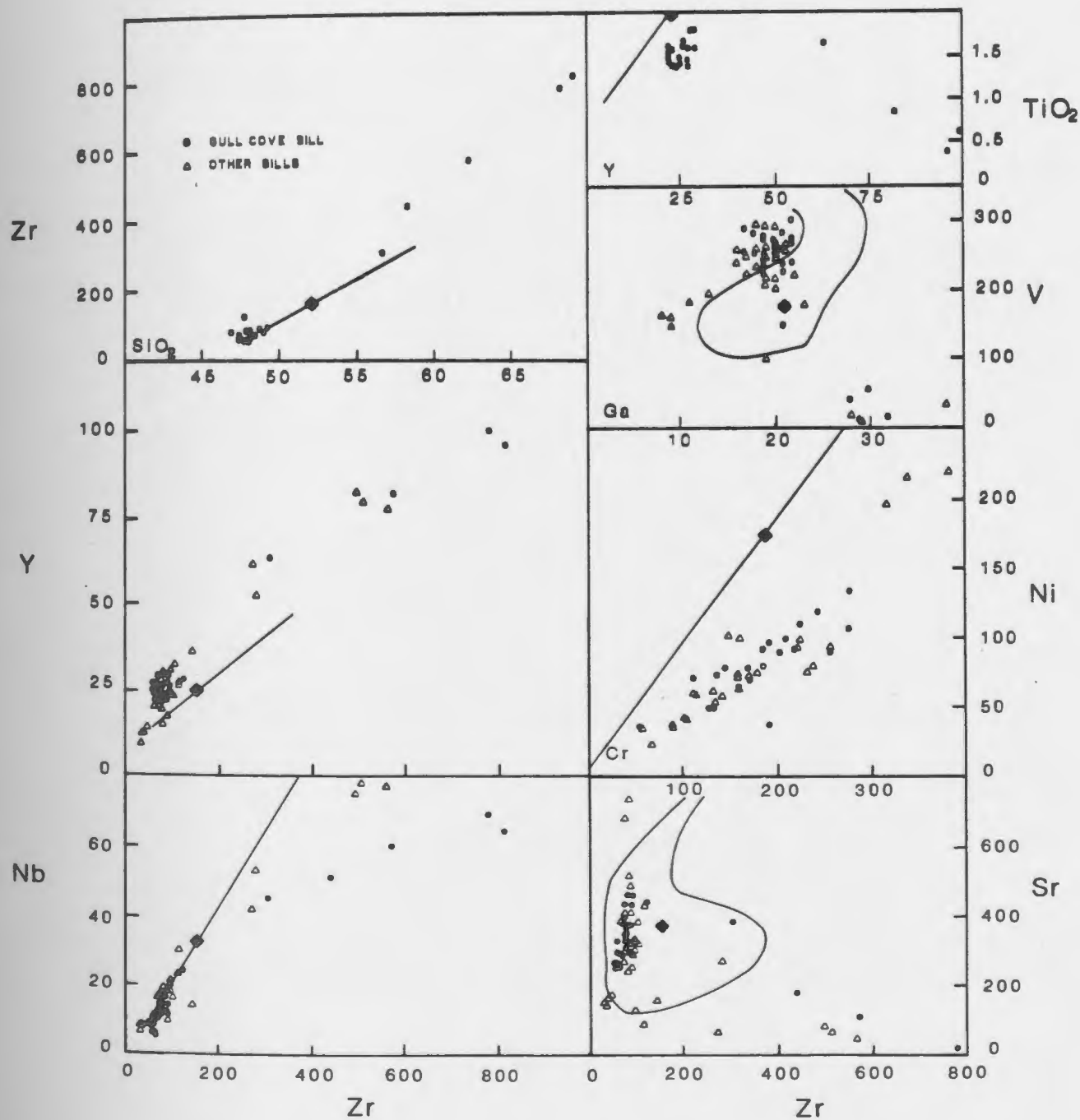


Figure 4.16 Trace element variation diagrams showing sill data. The lines on the diagram represent a least squares fit through the feeder pipe data with the diamonds marking the mean composition. Correlation coefficients for the lines are as follows:  $\text{SiO}_2$ -Zr, 0.85; Zr-Y, 0.93; Zr-Nb, 0.96; Y- $\text{TiO}_2$ , 0.76; Cr-Ni, 0.97. Data for the two element pairs showing poor correlation were marked off as fields and the mean composition shown with a diamond. The  $\text{TiO}_2$  and  $\text{SiO}_2$  concentrations are in wt. %, volatile free, and all others are in ppm.



terms of primary igneous processes.

170

Representative major and trace element analyses of sill samples are presented in Tables 4.11 and 4.12 and along with the variation diagrams shown in Figures 4.15 and 4.16 illustrate a number of the more important characteristics of these rocks. Granophyric samples plot at higher  $\text{SiO}_2$  values than the mafic samples in Figure 4.15. The figure illustrates that there is little variation in the major element composition of the mafic samples despite the fact that some samples represent contact rocks, or are from the base of the sill, and still others were taken from the middle to upper portions of the sill next to the granophyres. However, there are small variations in the major element composition of the mafic rocks, and the significance of these is discussed below. Mafic sill samples show relatively low  $\text{SiO}_2$  concentrations and their  $\text{Mg}'$  values ( $\text{Mg}' = \text{Mg}/(\text{Mg} + 0.9\text{Fe})$  atomic) are also quite low (0.5 to 0.6).

On an AFM diagram the sills define an Fe depletion trend (Figure 4.11) However, the trend line is based on granophyric samples which may not represent residual melts in terms of classical fractionation models. The granophyre samples display high  $\text{Na}_2\text{O}$  and low  $\text{K}_2\text{O}$  concentrations that tend to correlate with  $\text{SiO}_2$  values (Figure 4.15).

Zr and Nb concentrations (Table 4.12) in the sills are relatively low in comparison with the Cape St. Mary's flows

Table 4.11. Major element and normative composition of representative sill samples.

|                                | SB6E   | SB7I  | SB7L  | SB7G  |
|--------------------------------|--------|-------|-------|-------|
| SiO <sub>2</sub>               | 47.60  | 45.90 | 55.30 | 67.00 |
| TiO <sub>2</sub>               | 1.57   | 1.34  | 1.30  | 0.37  |
| Al <sub>2</sub> O <sub>3</sub> | 14.90  | 16.30 | 13.90 | 16.00 |
| Fe <sub>2</sub> O <sub>3</sub> | 13.36  | 10.93 | 7.86  | 2.06  |
| MnO                            | 0.21   | 0.19  | 0.21  | 0.04  |
| MgO                            | 7.19   | 7.67  | 3.62  | 1.02  |
| CaO                            | 10.72  | 10.76 | 5.62  | 1.14  |
| Na <sub>2</sub> O              | 2.78   | 2.58  | 6.68  | 9.40  |
| K <sub>2</sub> O               | 0.25   | 0.79  | 0.27  | 0.04  |
| P <sub>2</sub> O <sub>3</sub>  | 0.15   | 0.19  | 0.10  | 0.06  |
| L.O.I.                         | 1.84   | 2.97  | 3.20  | 1.77  |
| Total                          | 100.57 | 99.56 | 98.06 | 98.92 |
| CIPW Norms                     |        |       |       |       |
| Or                             | 1.27   | 4.00  | 1.49  | 0.17  |
| Ab                             | 21.41  | 17.99 | 56.21 | 60.89 |
| An                             | 23.54  | 26.21 | 6.70  | 0.97  |
| Ne                             | 0.00   | 1.87  | 0.00  | 0.00  |
| A                              | 0.00   | 0.00  | 0.00  | 30.61 |
| Ol                             | 19.15  | 24.63 | 3.82  | 0.00  |
| Hy                             | 6.04   | 0.00  | 5.85  | 1.55  |
| Di                             | 21.35  | 18.67 | 18.91 | 1.97  |
| Il                             | 4.69   | 4.00  | 4.24  | 0.11  |
| Mt                             | 2.24   | 2.24  | 2.45  | 0.00  |
| Ap                             | 0.25   | 0.32  | 0.18  | 0.08  |
| Sp                             | -      | -     | -     | 0.87  |
| Hm                             | -      | -     | -     | 2.59  |

Oxides in weight percent. All Fe as Fe<sub>2</sub>O<sub>3</sub>.

Norms calculated assuming Fe<sub>2</sub>O<sub>3</sub> = 1.5 weight percent, remaining

Fe = FeO

SB6E - Gabbro near base

SB7I - Gabbro immediately below granophyre

SB7L - Thick granophyre

SB7G - Granophyric dike



Table 4.12. Representative trace element analyses of sill rocks.

|    | SB60F | SB6E | SB7I | SB7L | SB7G |
|----|-------|------|------|------|------|
| Sr | 164   | 249  | 393  | 176  | 19   |
| Ba | 95    | 162  | 252  | 184  | 46   |
| Rb | 6     | 6    | 13   | 6    | 0    |
| Zr | 37    | 68   | 77   | 444  | 816  |
| Nb | 8     | 5    | 14   | 51   | 64   |
| Y  | 12    | 29   | 23   | 119  | 96   |
| Ga | 9     | 19   | 19   | 21   | 29   |
| V  | 146   | 275  | 231  | 148  | 12   |
| Cr | 1514  | 186  | 219  | 53   | 0    |
| Ni | 730   | 79   | 91   | 36   | 1    |
| Cu | 45    | 64   | 58   | 12   | 78   |
| Zn | 86    | 95   | 81   | 90   | 35   |

- SB60F - Olivine cumulate from sill at Lance Cove.  
 SB6E - Gabbro near base of Gull Cove sill.  
 SB7I - Gabbro just below thick granophyre in Gull Cove sill.  
 SB7L - Granophyre in Gull Cove sill.  
 SB7G - Granophyric dike in Gull Cove sill.

All concentrations in ppm.

and feeder pipes. The Nb/Y ratios vary from 0.1 to 1.0 and Zr/Nb ratios range from 4.5 to 14 (Figure 4.12); values much lower and higher (respectively) than Cape St. Mary's flows and feeder pipes. The chondrite-normalized REE patterns (Figure 4.17, concentrations in Table 4.13) for samples from (or close to) the contact of the Gull Cove sill (representing the least evolved samples) show relatively flat REE patterns with or without a small Eu anomaly (eg. SB6D and SB6E). Gabbros from the middle of the sill tend to show slight LREE enrichment (SB7I). The granophyres display patterns with similar slopes to the basal samples, but all of the REE, with the exception of Eu, are significantly enriched (SB7G and SB7I).

#### 4.3.2 Mineral Chemistry

##### Plagioclase

Representative analyses of plagioclase cores from various levels in the Gull Cove sill are given in Table 4.14. The An contents of plagioclase cores are shown in Figure 4.18 arranged according to their relative positions in the sills at Lance Cove and Gull Cove.

There appears to be a relationship between the average An content of the plagioclase cores and their height in the sills. Lines connecting the maximum and minimum An content of the samples tend to be parallel (Figure 4.18) and suggest that the observed compositional differences between the

Figure 4.17 Chondrite-normalized REE patterns in the sill and dike rocks. The normalizing values are from Taylor and Gorton, 1977.

U

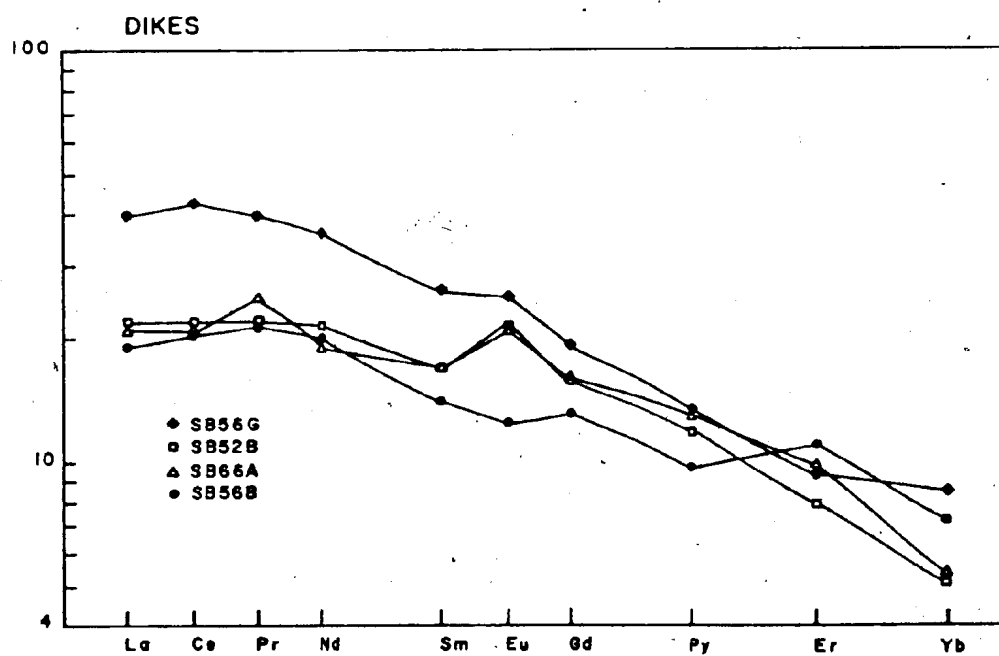
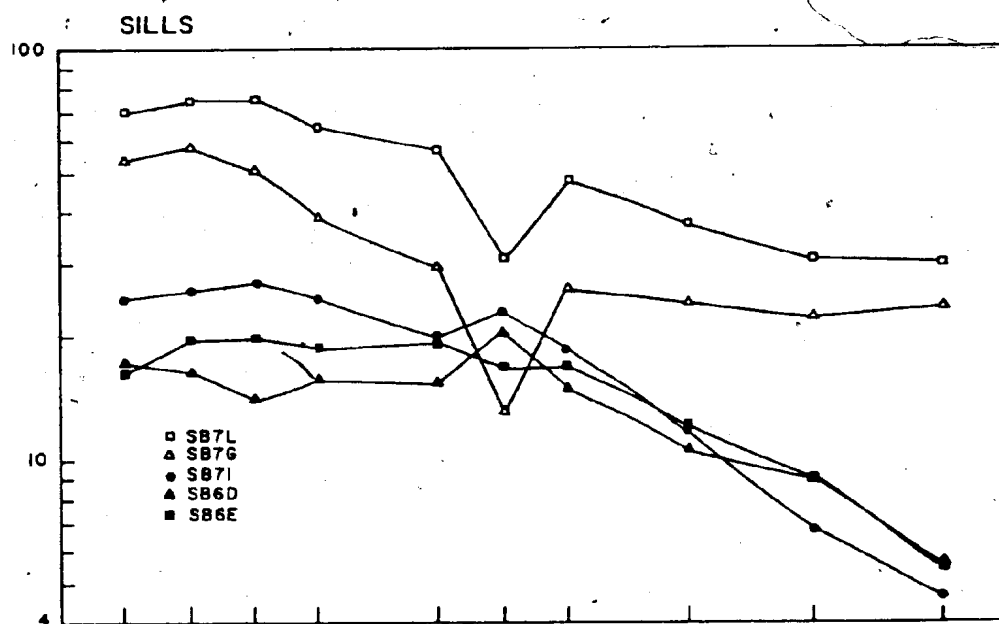


Table 4.13. Rare earth element concentrations in representative sill samples.

|    | Sb6D | SB6E | SB7I | SB7G | SB7L |
|----|------|------|------|------|------|
| La | 5.54 | 5.17 | 7.77 | 17.2 | 22.2 |
| Ce | 13.5 | 16.3 | 21.4 | 47.1 | 62.1 |
| Pr | 1.64 | 2.36 | 3.22 | 5.90 | 8.83 |
| Nd | 0.51 | 11.6 | 14.8 | 23.5 | 39.1 |
| Sm | 3.04 | 3.87 | 3.96 | 5.81 | 11.3 |
| Eu | 1.59 | 1.22 | 1.69 | 0.95 | 2.27 |
| Gd | 3.88 | 4.56 | 4.91 | 6.77 | 12.6 |
| Dy | 3.46 | 4.01 | 3.96 | 7.81 | 12.2 |
| Er | 1.95 | 1.93 | 1.45 | 4.72 | 6.81 |
| Yb | 1.14 | 1.21 | 0.99 | 4.97 | 6.15 |

Concentrations in ppm.

All samples from Gull cove (pocket Map B).

Table 4.14. Representative analyses of sill plagioclases.

|                                | SB7K          | SB7I          | SB6K          | SB6E          | SB6D          | SB60F         |
|--------------------------------|---------------|---------------|---------------|---------------|---------------|---------------|
| SiO <sub>2</sub>               | 68.50         | 50.21         | 58.05         | 52.98         | 52.92         | 52.45         |
| CaO                            | 0.73          | 15.38         | 8.43          | 13.67         | 11.06         | 12.49         |
| K <sub>2</sub> O               | 0.07          | 0.09          | 0.46          | 0.08          | 0.15          | 0.07          |
| Al <sub>2</sub> O <sub>3</sub> | 20.80         | 31.51         | 27.64         | 29.48         | 28.45         | 29.91         |
| FeO                            | 0.13          | 0.44          | 0.31          | 0.41          | 0.65          | 0.34          |
| Na <sub>2</sub> O              | 10.69         | 3.09          | 6.44          | 4.21          | 4.86          | 4.27          |
| Total                          | <u>100.91</u> | <u>100.79</u> | <u>101.32</u> | <u>100.84</u> | <u>98.09</u>  | <u>99.53</u>  |
| Si                             | 11.844        | 9.119         | 10.275        | 9.566         | 9.769         | 9.541         |
| Ca                             | 0.132         | 2.990         | 1.595         | 2.643         | 2.183         | 2.437         |
| K                              | 0.010         | 0.016         | 0.099         | 0.016         | 0.032         | 0.016         |
| Al                             | 4.237         | 6.758         | 7.009         | 6.271         | 6.188         | 6.418         |
| Fe                             | 0.015         | 0.063         | 0.042         | 0.058         | 0.097         | 0.048         |
| Na                             | 3.583         | 1.087         | 2.208         | 1.472         | 1.733         | 1.501         |
| Total                          | <u>19.820</u> | <u>20.033</u> | <u>19.983</u> | <u>20.027</u> | <u>20.002</u> | <u>19.969</u> |
| Or                             | 0.003         | 0.004         | 0.025         | 0.004         | 0.008         | 0.004         |
| An                             | 0.035         | 0.730         | 0.409         | 0.640         | 0.553         | 0.616         |
| Ab                             | 0.962         | 0.266         | 0.566         | 0.356         | 0.439         | 0.380         |

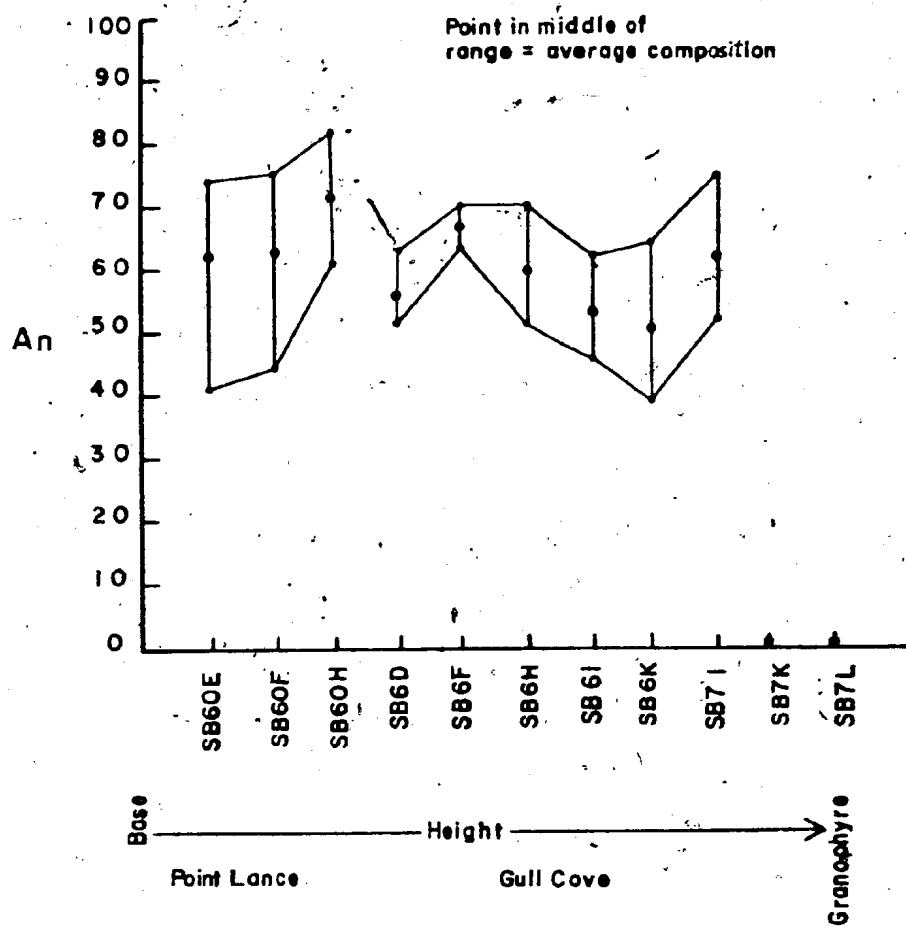
Stoichiometry based on 32 oxygen.

SB7K = Plagioclase in granophyre.

SB7I to SB6D = Samples from just below granophyre to the base of the sill at Gull Cove.

SB60F = Feldspar in Olivine cumulate at the base of Lance Cove sill.

Figure 4.18 An content of sill plagioclases. SB60 samples are from the base of the sill at Lance Cove and all others are from the Gull Cove sill. SB7K and SB7L are samples of the granophyre near the top of the Gull Cove sill. The upper and lower dots for each sample represent the range of compositions observed, and the dot between is the average composition for that sample. All compositions were determined by electron microprobe.





samples are probably significant. Relative to samples from slightly higher in the Lance Cove sill those closest to the contact (SB60E and SB60F) show lower An content than those from several meters inside the sill (SB60H). Although the average, An content for corresponding rocks from the base of the Gull Cove sill show lower average An contents than those from the Lance Cove sill, samples from the contact (SB6D) still show lower average An content than those slightly higher in the sill (SB6F). At increasingly higher locations in the Gull Cove sill the average An content of the plagioclase cores systematically decreases, though this trend is reversed in SB7I.

The extent of plagioclase composition variation in layered mafic sills appears very closely related to their thickness. The cores of plagioclases from thicker sills (greater than 300 meters), such as the Palisades sill (Walker, 1969a,b), or the Endion sill (Ernest, 1960), have compositions of An70 to An85 at the base, and then decrease in An content up through the sill. Thinner sills (less than 100 meters) such as the Logan sills (Blackadar, 1956) or the sill from site 169 of DSDP Leg 17 (Myers et al., 1975) show rather constant An content of plagioclase cores from the bottom to the top of the sill. For such relatively thin sills the Cape St. Mary's sills show a large variation in their plagioclase core compositions.

## Olivine

Representative analyses of the olivines from the base of the sill at Lance Cove are given in Table 4.15. All olivines in the samples show similar forsterite compositions between Fo71 and Fo80 (Figure 4.19) and zoning is negligible, as shown by the SB60H analyses in Table 4.15. The Mn content in the olivines ranges from 0.002 to 0.011 atoms per formula unit (based on 4 O) and Ca varies from 0.002 to 0.007 atoms per formula unit. The CaO concentrations (0.25 weight percent) are typical of olivines from hypabyssal intrusions which generally contain over 0.1 weight percent CaO (Simkin and Smith 1970).

Olivines with similar Fo compositions occur near the base of many layered tholeiitic sills, such as the Palisades sill (Walker, 1969) and alkali - olivine basalt sills (Myers et al., 1975). In cases where olivine only occurs near the base of layered mafic intrusions (eg. Palisades and Endion sills) it is generally believed the mineral was present as phenocrysts at the time of intrusion and settled out early in the crystallization history. Olivine occurs throughout the tholeiitic Logan sills (Blackadar, 1956), but examples of sills where it only occurs sporadically, or not at all, include the Tasmanian dolerites (McDougall, 1962 and Gunn, 1962) and the Tumatumari - Kopinang sill (Hawkes, 1966). In some thick layered intrusions, olivine (Fo80) occurs at the base, disappears in the middle, and then reappears much more

Table 4.15. Representative analyses of sill olivine.

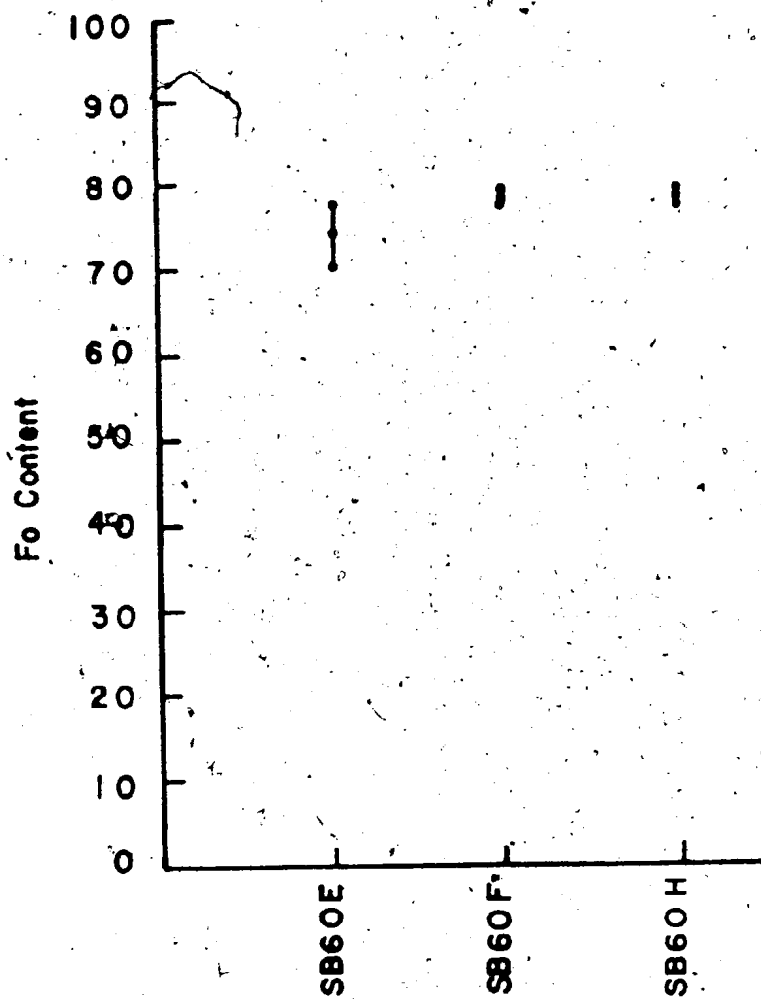
|                                | SB60E  | SB60F  | Core<br>SB60H | Rim<br>SB60H |
|--------------------------------|--------|--------|---------------|--------------|
| SiO <sub>2</sub>               | 38.30  | 38.21  | 38.88         | 38.77        |
| TiO <sub>2</sub>               | 0.00   | 0.04   | 0.04          | 0.04         |
| Al <sub>2</sub> O <sub>3</sub> | 0.02   | 0.02   | 0.00          | 0.04         |
| Cr <sub>2</sub> O <sub>3</sub> | 0.02   | 0.00   | 0.05          | 0.00         |
| FeO                            | 23.08  | 20.41  | 19.03         | 20.65        |
| MnO                            | 0.21   | 0.23   | 0.11          | 0.30         |
| MgO                            | 38.54  | 38.21  | 41.97         | 41.75        |
| CaO                            | 0.23   | 0.25   | 0.30          | 0.18         |
| Na <sub>2</sub> O              | 0.00   | 0.00   | 0.00          | 0.06         |
| K <sub>2</sub> O               | 0.00   | 0.02   | 0.00          | 0.00         |
| NiO                            | 0.16   | 0.14   | 0.15          | 0.20         |
| Total                          | 100.57 | 101.17 | 100.53        | 102.00       |
| Si                             | 0.995  | 0.976  | 0.990         | 0.987        |
| Ti                             | 0.000  | 0.000  | 0.000         | 0.000        |
| Al                             | 0.000  | 0.000  | 0.000         | 0.000        |
| Cr                             | 0.000  | 0.002  | 0.000         | 0.000        |
| Fe                             | 0.500  | 0.435  | 0.405         | 0.435        |
| Mn                             | 0.004  | 0.004  | 0.002         | 0.006        |
| Mg                             | 1.492  | 1.593  | 1.593         | 1.569        |
| Ca                             | 0.006  | 0.006  | 0.007         | 0.004        |
| Na                             | 0.000  | 0.000  | 0.000         | 0.002        |
| K                              | 0.000  | 0.000  | 0.000         | 0.000        |
| Ni                             | 0.003  | 0.002  | 0.003         | 0.003        |
| Total                          | 3.000  | 3.017  | 3.001         | 3.007        |
| Fo                             | 75     | 79     | 80            | 78           |

Oxides = weight percent. All Fe as FeO.

Formula based on 4 oxygen.

SB60E = Lowest in sill, SB60F and SB60H slightly higher.

Figure 4.19 Fo content of olivines from a sill at Lance Cove. For each sample the range of compositions is shown as well as the mean. The analyses were done by electron microprobe.



iron rich (Fo40), in the upper portions of the intrusions (Wager and Brown, 1967). Differentiated alkaline sills, such as the sill at Site 169, DSDP Leg 17 (Myers et al., 1975) and the Shiant sill (Walker, 1930) contain olivine throughout. The Cape St. Mary's sills most closely resemble the tholeiitic Palisades or Tasmanian sills which either lack olivine, or contain cumulus olivine only at their bases.

#### Pyroxene

Representative analyses of the high Ca pyroxenes from the Cape St. Mary's sills are given in Table 4.16. The Ca contents of the pyroxenes often exceed 45 percent Wo making them salites (Deer et al., 1966) and typical of pyroxenes from alkaline rocks (Figure 4.20). The Wo, En and atomic Ti contents of the pyroxenes, are plotted against height in the sills in Figure 4.21 with samples (containing olivine) from near the base of the Lance Cove sill (SB60E and SB60H) shown below the lowest Gull Cove samples (SB6D and SB6E). Basal pyroxenes contain Wo contents between 43 and 50 percent, but at higher levels in the sill Wo drops to about 41 percent and then rises slightly in the upper mafic and felsic samples to between 40 and 43 percent. Although Wo contents typically decrease, and then rise again in tholeiitic intrusions such as Skaergaard (Brown and Vincent, 1963) and Bushveld (Atkins, 1969), the Fs content also rises to 30 or 40 percent. Pyroxenes with this high a Fs content do not

Table 4.16. Representative analyses of sill pyroxenes.

|                                | SB6D  | SB6F   | SB6H  | SB7I  | SB7L   |
|--------------------------------|-------|--------|-------|-------|--------|
| SiO <sub>2</sub>               | 49.43 | 49.92  | 50.29 | 49.31 | 51.34  |
| TiO <sub>2</sub>               | 1.45  | 1.22   | 1.13  | 1.17  | 0.22   |
| Al <sub>2</sub> O <sub>3</sub> | 3.62  | 2.81   | 2.21  | 3.45  | 0.36   |
| Cr <sub>2</sub> O <sub>3</sub> | 0.05  | 0.07   | 0.00  | 0.04  | 0.01   |
| FeO                            | 9.73  | 10.47  | 11.34 | 8.29  | 11.99  |
| MnO                            | 0.26  | 0.25   | 0.28  | 0.17  | 0.20   |
| MgO                            | 12.55 | 13.68  | 13.89 | 14.07 | 12.34  |
| CaO                            | 21.97 | 21.20  | 19.60 | 22.12 | 23.60  |
| Na <sub>2</sub> O              | 0.41  | 0.40   | 0.48  | 0.39  | 0.58   |
| K <sub>2</sub> O               | 0.04  | 0.00   | 0.03  | 0.02  | 0.00   |
| NiO                            | 0.11  | 0.00   | 0.00  | 0.00  | 0.00   |
| Total                          | 99.62 | 100.01 | 99.25 | 99.03 | 100.64 |
| Si                             | 1.868 | 1.881  | 1.909 | 1.864 | 1.947  |
| Aliv                           | 0.132 | 0.119  | 0.091 | 0.136 | 0.015  |
| Alvi                           | 0.029 | 0.005  | 0.007 | 0.017 | 0.000  |
| Ti                             | 0.041 | 0.034  | 0.031 | 0.032 | 0.005  |
| Cr                             | 0.001 | 0.001  | 0.000 | 0.001 | 0.000  |
| Fe                             | 0.307 | 0.329  | 0.359 | 0.262 | 0.379  |
| Mn                             | 0.007 | 0.007  | 0.009 | 0.004 | 0.005  |
| Mg                             | 0.707 | 0.767  | 0.785 | 0.793 | 0.698  |
| Ca                             | 0.889 | 0.855  | 0.796 | 0.895 | 0.958  |
| Na                             | 0.030 | 0.028  | 0.034 | 0.029 | 0.042  |
| K                              | 0.001 | 0.000  | 0.001 | 0.000 | 0.000  |
| Ni                             | 0.002 | 0.000  | 0.000 | 0.000 | 0.000  |
| Total                          | 4.013 | 4.027  | 4.021 | 4.032 | 4.050  |
| Wo                             | 47    | 44     | 42    | 46    | 47     |
| En                             | 37    | 39     | 40    | 41    | 34     |
| Fs                             | 16    | 17     | 18    | 13    | 19     |

Oxides = Weight percent; All Fe as FeO; Recalculated on basis 6 oxygen.

SB6D = base of LGB  
 SB6F = middle of LGB  
 SB6H = top of LGB  
 SB7I = top of MGB  
 SB7L = top of granophyre

Figure 4.20 Pyroxene quadrilateral showing pyroxenes from the Cape St. Mary's sill rocks. The fields are labelled after Le Bas (1962).



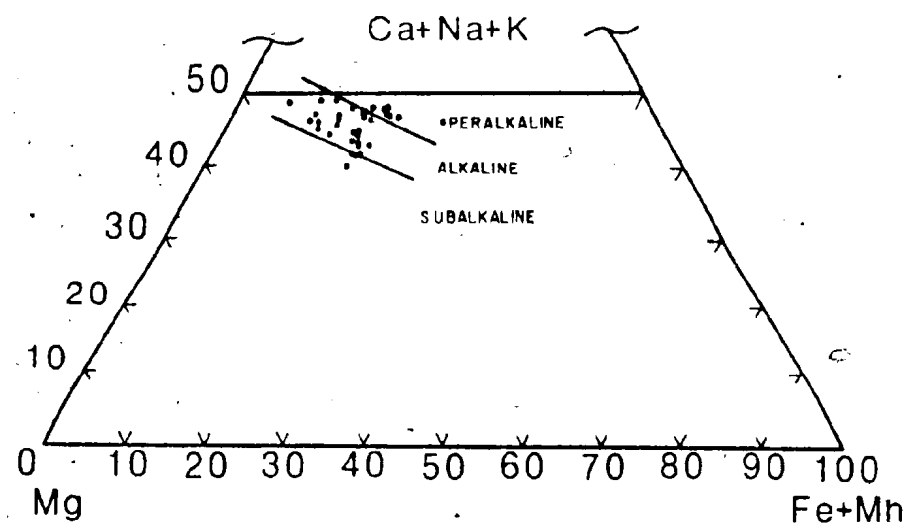
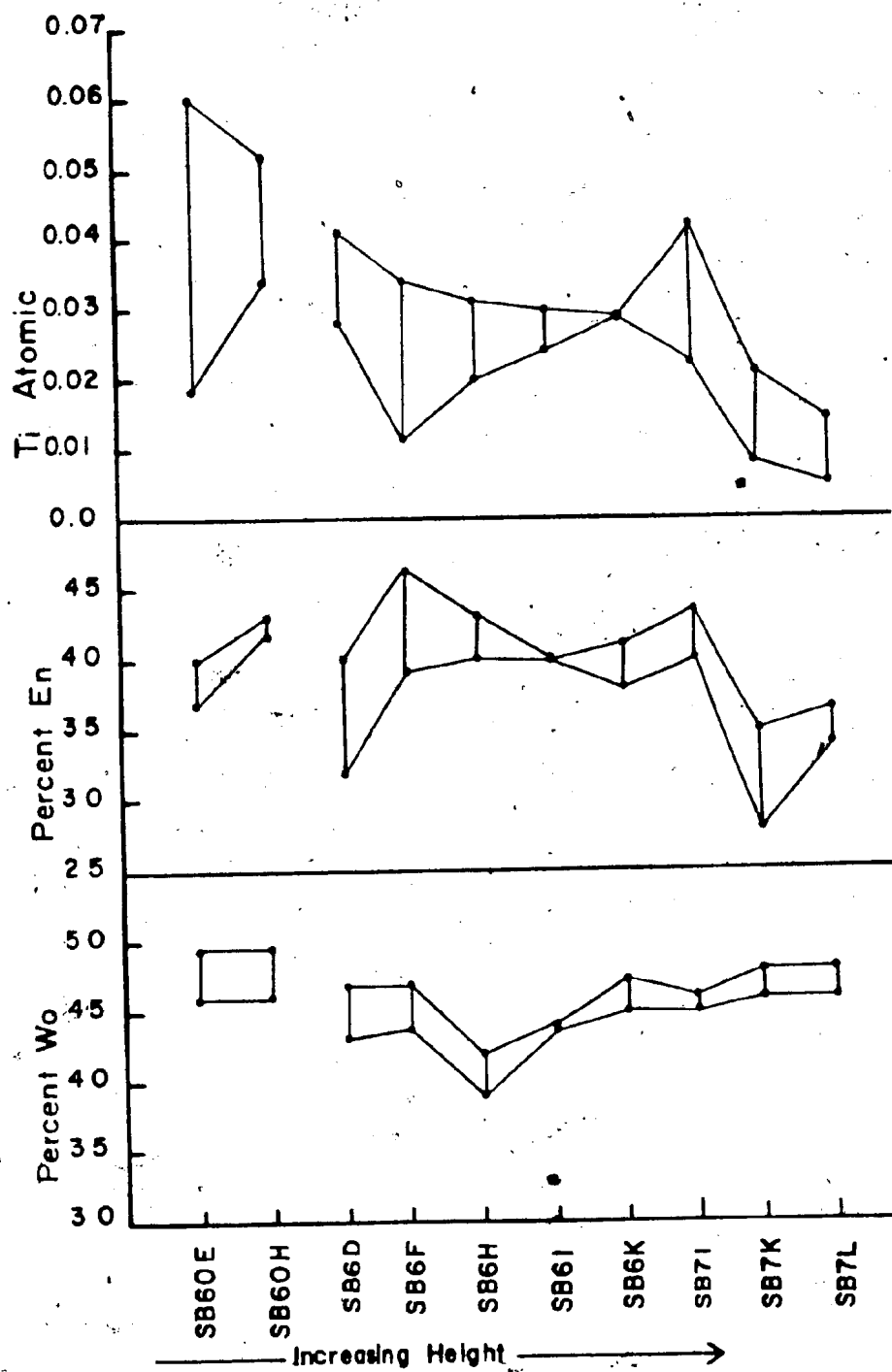


Figure 4.21 Wo, En, and Ti (atomic) content of Cape St. Mary's sill pyroxenes. The range of compositions in each sample is shown. SB60 samples are from the base of the sill at Lance Cove and all others are from the sill at Gull Cove.

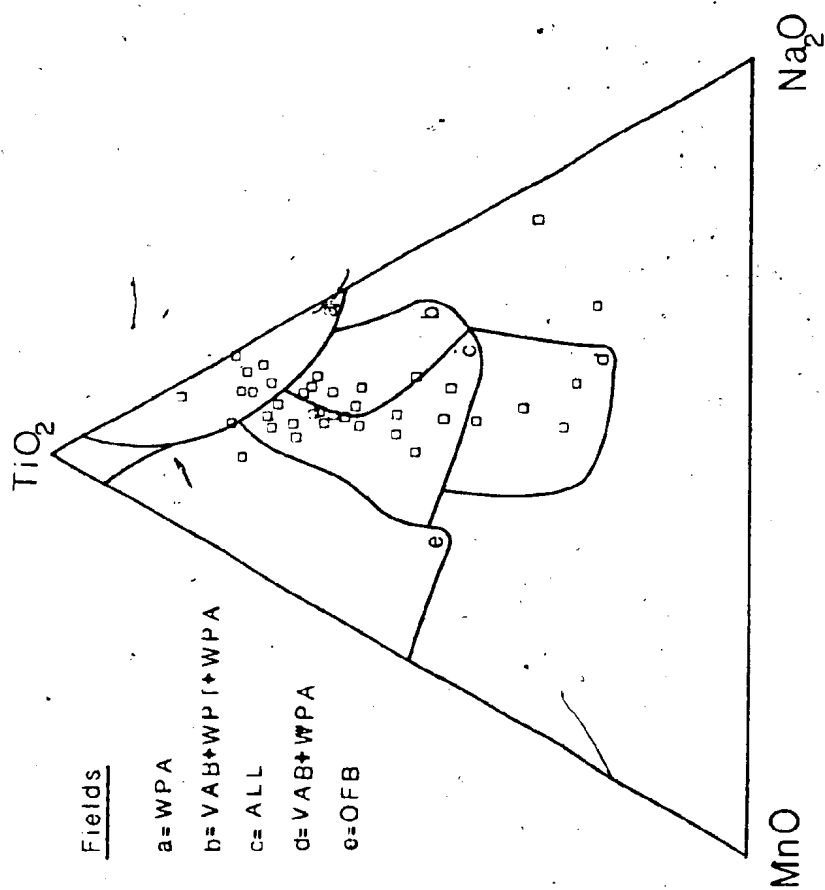


occur in the Cape St. Mary's sills. Despite the slight decrease in Wo content in the middle of the Gull Cove sill, it remains relatively high and constant even in the late felsic samples (SB7K and SB7L).

En contents tend to decline with increasing height in the sill, but fluctuations occur that are similar to those observed for plagioclase compositions (compare Figures 4.18 and 4.21). Pyroxenes from low in the Lance Cove sill (SB60E) show lower En contents than those slightly higher in the intrusion (SB60H). The same relationship exists in the Gull Cove sill as shown by the contact sample SB6D and sample SB6F, which comes from a few meters above the base. Samples from a few meters inside the sills show the highest average En contents observed. Similarly the An content of plagioclase in these samples exceeded that in other samples. The average En content of pyroxenes in the middle portions of the Gull Cove sill declines from about 43 to 39 percent (SB6F to SB6K), increases close to the granophyre (SB7I), and is lowest in the granophyre. The An content of plagioclases behaves similarly (Figure 4.18).

The average (as well as highest) Ti content (atomic) of sill pyroxenes decreases with height in the intrusions (Figure 4.21). The only exception, a single analysis from SB7I, shows unusually high Ti. Some indication of the variation in sill pyroxene compositions may be garnered from their Ti-Mn-Na proportions shown in Figure 4.22.

Figure 4.22  $\text{TiO}_2$ - $\text{MnO}$ - $\text{Na}_2\text{O}$  pyroxene discrimination diagram - Cape St. Mary's sill pyroxenes. Diagram after Nisbet and Pearce (1977). WPA = within plate alkaline; WPT = within plate tholeiite; VAB = volcanic arc basalt; OFB = ocean floor basalt.



## Amphiboles

Magmatic amphiboles occur in the olivine cumulate layers at Lance Cove and in the felsic granophyres of the Gull Cove sill. Amphiboles in the cumulus rocks are mainly intercumulus and/or poikilitic, as much as 5 millimeters across, show only slight undulatory extinction, and the following pleochroic scheme: alpha = faint tan; beta = faint tan; gamma = dark orange brown. Amphiboles in the granophyres display a much wider range of textural features. In sample SB7L they form euhedral needles as much as 3 centimeters long and 1 millimeter wide which show limited undulatory extinction and the following pleochroic scheme: alpha = faint tan; beta = faint tan; gamma = orange brown. These amphiboles (SB7L2, Table 4.17) are similar in composition to those from the cumulates (SB60F2) except their FeO/MgO ratios are higher, and Cr<sub>2</sub>O<sub>3</sub> concentrations lower. Names were derived for the amphiboles (Table 4.17) following Leake (1978) and assuming Fe<sup>3+</sup> is between 0 and 1/2 of the total Fe (atomic).

Along with the needles of amphibole in SB7L, there are anhedral interstitial masses of the mineral, showing strong undulatory extinction, and a wide range of pleochroic schemes. The centers display similar pleochroism and composition to the needles described above, but toward the rim they change as shown by data in Table 4.17 (SB7L2, SB7L1, and SB7L4). Between the center and the rim Al<sub>2</sub>O<sub>3</sub>,

Table 4.17. Amphibole pleochroism and composition.

|                                | SB60F2<br>Poikilitic<br>in Olivine<br>Cumulate | SB7L2<br>Cores and<br>Euhedral<br>Needles | SB7L1<br>Between rim<br>and core of<br>Anhedral Grain | SB7L4<br>Rim of<br>Anhedral<br>Grain | SB7K8<br>Rim of<br>Zoned<br>Grain |
|--------------------------------|--|---|---|--------------------------------------|-----------------------------------|
| $\alpha$                       | faint tan                                      | faint tan                                 | faint tan   | faint green                          | faint green                       |
| $\beta$                        | faint tan                                      | faint tan                                 | pinkish<br>brown                                      | faint green                          | lt. olive<br>green                |
| $\gamma$                       | dark or-<br>ange brown                         | orange<br>brown                           | yellow<br>olive<br>green                              | deep blue<br>green                   | forest<br>green                   |
| SiO <sub>2</sub>               | 43.90  | 40.82                                     | 48.66   | 47.13                                | 36.84                             |
| TiO <sub>2</sub>               | 3.62   | 4.77                                      | 1.90  | 2.06                                 | 1.26                              |
| Al <sub>2</sub> O <sub>3</sub> | 9.66   | 10.77                                     | 3.16  | 1.10                                 | 11.99                             |
| Cr <sub>2</sub> O <sub>3</sub> | 0.39   | 0.02                                      | 0.00  | 0.03                                 | 0.00                              |
| FeO                            | 9.07   | 15.18                                     | 17.70   | 27.79                                | 30.05                             |
| MnO                            | 0.05   | 0.14                                      | 0.37  | 0.34                                 | 0.27                              |
| MgO                            | 15.70  | 11.75                                     | 12.17   | 5.13                                 | 0.99                              |
| CaO                            | 10.64  | 11.49                                     | 8.95  | 4.61                                 | 16.33                             |
| Na <sub>2</sub> O              | 3.31   | 3.32                                      | 5.01  | 5.04                                 | 2.87                              |
| K <sub>2</sub> O               | 0.63   | 0.68                                      | 0.86  | 0.80                                 | 1.16                              |
| NiO                            | 0.10   | 0.05                                      | 0.01  | 0.03                                 | 0.03                              |
| Total                          | 97.06  | 98.93                                     | 98.79   | 94.07                                | 96.81                             |

(Cont'd.)

Oxides in weight percent. All Fe as FeO.

Formula calculated on the basis of 23 oxygen.

Names determined by assuming Fe<sub>2</sub>O<sub>3</sub> is between 0 and 1/2 total Fe.

See text.

SB60F = Base of sill at Lance Cove.

SB7L = Top of thick granophyre at Gull Cove.

SB7K = Bottom of thick granophyre at Gull Cove.



Table 4.17 (Cont'd.)

|                     | SB60F2                                 | SB7L2      | SB7L1        | SB7L4                        | SB7K8                      |
|---------------------|--|------------|--------------|------------------------------|----------------------------|
| Si                  | 6.438                                  | 6.091      | 7.269        | 7.702                        | 6.081                      |
| Aliv                | 1.562                                  | 1.878      | 0.557        | 0.211                        | 1.919                      |
| Fe <sup>3+</sup>    | 0.000                                  | 0.031      | 0.171        | 0.087                        | 0.000                      |
| $\Sigma$ Tet.       | 8.000                                  | 8.000      | 8.000        | 8.000                        | 8.000                      |
| Alvi                | 0.104                                  | 0.000      | 0.000        | 0.000                        | 0.411                      |
| Cr                  | 0.043                                  | 0.000      | 0.000        | 0.000                        | 0.000                      |
| Ti                  | 0.396                                  | 0.534      | 0.207        | 0.249                        | 0.135                      |
| Mg                  | 3.430                                  | 2.656      | 2.709        | 1.247                        | 0.242                      |
| Fe <sup>2+</sup>    | 1.027                                  | 0.861      | 2.038        | 3.504                        | 3.952                      |
| Mn                  | 0.000                                  | 0.000      | 0.043        | 0.000                        | 0.034                      |
| $\Sigma$ Oct        | 5.000                                  | 5.000      | 4.997        | 5.000                        | 4.794                      |
| Fe <sup>2+</sup>    | 0.083                                  | 0.051      | 0.000        | 0.207                        | 0.000                      |
| Mn                  | 0.004                                  | 0.017      | 0.000        | 0.043                        | 0.000                      |
| Ca                  | 1.669                                  | 1.834      | 1.429        | 0.806                        | 2.001                      |
| Na                  | 0.244                                  | 0.098      | 0.571        | 0.944                        | 0.000                      |
| $\Sigma$ M4         | 2.000                                  | 2.000      | 2.000        | 2.000                        | 2.001                      |
| Na                  | 0.694                                  | 0.861      | 0.876        | 0.653                        | 0.916                      |
| K                   | 0.116                                  | 0.127      | 0.162        | 0.163                        | 0.242                      |
| $\Sigma$ A          | 0.810                                  | 0.988      | 1.038        | 0.816                        | 1.158                      |
| Mg                  | 0.77                                   | .58-.24    | .55          | 25.40                        | .05-.10                    |
| Mg+Fe <sup>2+</sup> |  |            |              |                              |                            |
| Name                | Magnesio<br>Hastingsitic<br>Hornblende | Kaersutite | Eden-<br>ite | Silicic<br>Ferro-<br>edenite | Hastingsitic<br>Hornblende |

MgO, and CaO decrease, while FeO, MnO, Na<sub>2</sub>O, and K<sub>2</sub>O tend to increase. The high Ti content of the cores gives them kaersutitic compositions (SB7L2) whereas the outer portions of the anhedral grains (SB7L1 and SB7L4) have edenitic, and silicic ferro - edenitic compositions.

Large zoned amphiboles in SB7K (same granophyre) display similar pleochroism to the amphiboles in SB7L. The centers of these amphiboles have similar compositions to SB7L cores, but their rims are markedly different (compare SB7L4 and SB7K8 in Table 4.17). Aluminum, and the FeO/MgO ratio are much higher, and Na<sub>2</sub>O much lower in SB7K8.

Amphiboles commonly occur in the felsic differentiates of sills, or occasionally as small interstitial grains throughout a sill (Myers et al., 1975). In most cases their occurrence is attributed to high PH<sub>2</sub>O. Their occurrence in the olivine cumulates of the Cape St. Mary's sills is extremely unusual.

#### Biotite

Biotite occurs as a minor (less than 1 percent) primary phase throughout the sills, though its percentage increases near the sill - sediment contacts (especially upper contact) as well as close to the granophyres. It usually forms small, anhedral, interstitial grains, but close to the granophyres, and in the olivine cumulate samples from Lance Cove the grains may be poikilitic and 4 millimeters in diameter.

All biotites show the same pleochroism (alpha = faint tan, beta = orange brown, gamma = deep red brown) but there are large variations in their composition between rock types (Table 4.18). The ranges of FeO/MgO ratios in biotites from various sill samples are shown in Figure 4.23, arranged according to height in the sills. Biotites from the olivine cumulate layers (SB60E,F,H) show FeO/MgO ratios less than 1. Those from the mafic portion of the Gull Cove sill (SB6D to SB7I) have FeO/MgO ratios between 1 and 3. The rise in FeO/MgO ratios may reflect an increase in melt FeO/MgO ratios, as well as a decrease in temperature.

The abundance of biotite suggests the sills had relatively high water contents. Examples of other sills showing similar biotite abundances and textures were not found.

#### Baddeleyite ( $\text{ZrO}_2$ )

In an attempt to obtain zircons for radiometric dating purposes, a clear, reddish brown to yellow brown mineral was found in the nonmagnetic heavy mineral fraction of a felsic granophyre from Lance Cove. Electron microprobe analysis of several grains revealed a mineral composed primarily of  $\text{ZrO}_2$ , and it was positively identified as baddeleyite using X-ray diffraction techniques.

The baddeleyite forms equant grains, typically only 0.1 to 0.2 millimeters across; though 1 millimeter grains do.

Table 4.18. Representative analyses of sill biotites.

|                                | SB60H | SB6D1 | SB6D2 | SB7I2 |
|--------------------------------|-------|-------|-------|-------|
| SiO <sub>2</sub>               | 36.45 | 33.18 | 35.89 | 36.89 |
| TiO <sub>2</sub>               | 6.80  | 5.42  | 5.13  | 5.32  |
| Al <sub>2</sub> O <sub>3</sub> | 14.16 | 11.98 | 12.94 | 13.77 |
| Cr <sub>2</sub> O <sub>3</sub> | 0.06  | 0.10  | 0.00  | 0.01  |
| FeO                            | 10.20 | 25.27 | 18.33 | 17.53 |
| MnO                            | 0.04  | 0.08  | 0.08  | 0.13  |
| MgO                            | 17.70 | 8.14  | 12.06 | 13.91 |
| CaO                            | 0.02  | 0.20  | 0.06  | 0.04  |
| Na <sub>2</sub> O              | 1.61  | 0.41  | 0.42  | 0.78  |
| K <sub>2</sub> O               | 9.13  | 8.82  | 9.73  | 8.32  |
| NiO                            | 0.00  | 0.04  | 0.00  | 0.00  |
| Total                          | 96.15 | 93.64 | 94.64 | 96.70 |
| FeO/MgO                        | 0.58  | 3.10  | 1.52  | 1.26  |

Water content of biotites = 3.5 to 4.5 weight percent  
(Deer et al., 1966).

All elements in oxide weight percent.

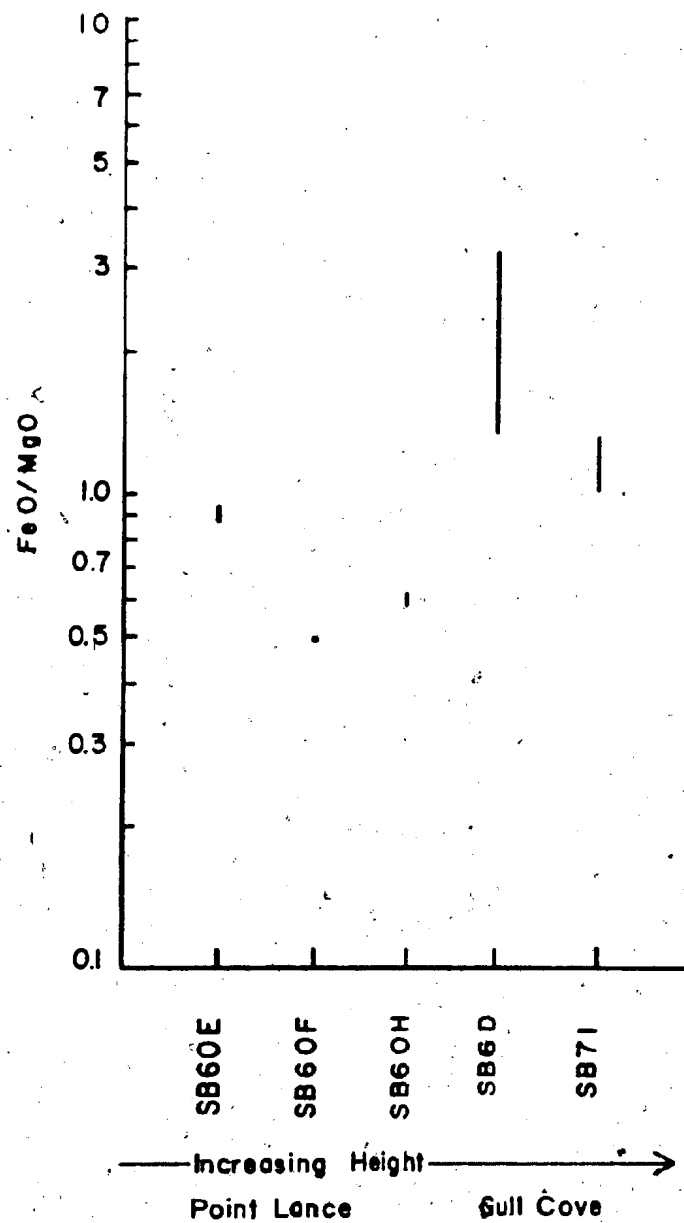
FeO = total Fe.

SB60H = Olivine cumulate Lance Cove.

SB6D = Base of Gull Cove.

SB7I = Top of MGB, Gull Cove.

Figure 4.23 FeO/MgO ratios in biotites from the Cape St.  
Mary's sills.



occur. They show striations caused by twinning, and occasionally have some zircon attached on one side which probably formed by baddeleyite reacting with the melt. Under the electron microprobe beam, the baddeleyite shows a characteristic blue - green luminescence.

Several analyses of the baddeleyite (Table 4.19) show that  $ZrO_2$  usually constitutes over 95 weight percent of the mineral. The most important element to substitute for Zr is Hf, which as an oxide makes up 1 to 4 weight percent of the mineral. The next most abundant oxide is  $TiO_2$  followed by FeO, both of which make up less than 1 percent of the mineral. Silicon was detected in only a few grains.

Most terrestrial occurrences of baddeleyite are in highly undersaturated rocks such as kimberlites (eg. Nixon et al., 1963; Kreston, 1973; Fiermans and Ottenburgs, 1979) carbonatites (Hiemstra, 1955; Paarma, 1970), and alkali syenites (Widenfalk and Gorbátshev, 1971). Although baddeleyite has commonly been observed in the mesostasis of lunar basalts (eg. Ramdohr and El Goresy, 1970; Lovering et al., 1972; Hinthorne et al., 1979), only recently has it been reported from, or in association with, terrestrial rocks of basaltic composition (eg. Keil and Fricker, 1974; Suvola, 1977; Williams, 1978). The occurrence of this rare mineral in the Cape St. Mary's sills further emphasizes their unusual chemical characteristics.

Table 4.19. Baddeleyite analyses.

|                  | 1             | 2            | 3            |
|------------------|---------------|--------------|--------------|
| SiO <sub>2</sub> | 0.01          | 0.00         | 0.00         |
| TiO <sub>2</sub> | 0.23          | 0.14         | 0.64         |
| HfO <sub>2</sub> | 1.34          | 3.82         | 0.90         |
| FeO              | 0.11          | 0.04         | 0.22         |
| ZrO <sub>2</sub> | 98.54         | 95.01        | 97.39        |
| Total            | <u>100.24</u> | <u>99.01</u> | <u>99.15</u> |
| Si               | 0.000         | 0.000        | 0.000        |
| Ti               | 0.004         | 0.004        | 0.012        |
| Hf               | 0.008         | 0.023        | 0.004        |
| Fe               | 0.000         | 0.000        | 0.004        |
| Zr               | 0.988         | 0.973        | 0.984        |
| Total            | <u>1.000</u>  | <u>1.000</u> | <u>1.004</u> |

Stoichiometry on basis of 2 oxygen.



The presence of Baddeleyite indicates low silica activity (Nicholls et al., 1971), but it does not mean the rocks are critically undersaturated (ie. alkaline). Occurrences reported by Keil and Fricker (1974), and Suvola (1977), unequivocally show that quartz can occur in the same rock as baddeleyite. The crystallization sequence reported by these authors is baddeleyite, zircon, quartz, indicating increasingly higher silica activity.

#### 4.3.3 Differentiation of the Sills

##### Endmember Rock Types

The sill at Gull Cove was extensively sampled from bottom to top, and an analysis of textural, mineralogical, and geochemical data shows that the sill can be divided into 5 endmember rock types. Averages of samples representing the endmember types are given in Table 4.20.

1. The contact rocks are fine-grained samples from (or close to) the lower chilled margin of the sill and should closely represent the parent magma composition.
2. Samples taken 2 to 3 meters inside the sill, at the base of the lower gabbro (BLGB), show plagioclase and augite cores with the highest An and En contents observed in the sill. They could represent cumulus samples, but do not show

Table 4.20. Endmember rock types in Gull Cove Sill.

|                                | CR <sup>1</sup> | BLGB <sup>2</sup> | EMGB <sup>3</sup> | DMGB <sup>4</sup> | GR <sup>5</sup> | Sediment |
|--------------------------------|-----------------|-------------------|-------------------|-------------------|-----------------|----------|
| SiO <sub>2</sub>               | 48.46           | 48.69             | 49.59             | 47.77             | 68.73           |          |
| TiO <sub>2</sub>               | 1.50            | 1.46              | 1.68              | 1.52              | 0.50            |          |
| Al <sub>2</sub> O <sub>3</sub> | 16.77           | 16.41             | 17.59             | 17.05             | 16.58           |          |
| FeO                            | 11.75           | 11.36             | 10.22             | 10.51             | 2.15            |          |
| MnO                            | 0.21            | 0.20              | 0.21              | 0.22              | 0.04            |          |
| MgO                            | 7.42            | 7.97              | 7.08              | 8.06              | 0.91            |          |
| CaO                            | 10.57           | 10.65             | 8.93              | 11.17             | 1.35            |          |
| Na <sub>2</sub> O              | 2.89            | 2.78              | 3.56              | 2.77              | 9.64            |          |
| K <sub>2</sub> O               | 0.27            | 0.34              | 0.93              | 0.72              | 0.03            |          |
| P <sub>2</sub> O <sub>5</sub>  | 0.16            | 0.14              | 0.21              | 0.20              | 0.07            |          |
| Rb                             | 5               | 5                 | 19                | 13                | 0               | 82       |
| Sr                             | 270             | 263               | 448               | 379               | 18              | 113      |
| Ba                             | 194             | 129               | 284               | 245               | 39              | 625      |
| Cr                             | 215             | 225               | 145               | 48                | 0               | 88       |
| Ni                             | 98              | 109               | 56                | 82                | 0               | 28       |
| Y                              | 28              | 27                | 26                | 22                | 98              | 43       |
| Nb                             | 6               | 8                 | 12                | 14                | 66              | 16       |
| Zr                             | 66              | 58                | 91                | 78                | 798             | 151      |
| V                              | 257             | 233               | 256               | 241               | 14              | 102      |
| Ga                             | 20              | 19                | 21                | 18                | 30              | 22       |
| Cu                             | 58              | 64                | 51                | 59                | 45              | -        |
| Zn                             | 102             | 86                | 99                | 85                | 46              | -        |
| Mg <sup>1</sup>                | 0.56            | 0.58              | 0.58              | 0.60              | 0.46            |          |
| Norm. Hy                       | 5.0             | 6.0               | 0.0               | 0.0               |                 |          |
| Ne                             | 0.0             | 0.0               | 0.7               | 1.4               |                 |          |

1. CR = Contact Rocks = average of SB6C and SB6D.
2. BLGB = Base of Lower Gabbro = SB6F.
3. EMGB = Enriched Middle Gabbro = average of SB6I, SB6J and SB7E.
4. DMGB = Depleted Middle Gabbro = average of SB6K and SB7I.
5. GR = Granophyre = average of SB7G and SB7J.

Major element oxides in weight percent, recalculated to 100%, volatile free. Total Fe as FeO. Trace elements in ppm.

classical cumulus textures.

3. Near the top of the lower gabbro and at the base of the middle gabbro are rocks enriched in (EMGB)  $\text{SiO}_2$ ,  $\text{TiO}_2$ ,  $\text{Al}_2\text{O}_3$ ,  $\text{Na}_2\text{O}$ ,  $\text{K}_2\text{O}$ ,  $\text{P}_2\text{O}_5$ , Rb, Sr, Ba, Nb, Zr, V, and Ca, and depleted in FeO, MgO, CaO, Cr, Ni, and Y, relative to the basal gabbro. There is a continuum of compositions between the BLGB and the EMGB.
4. Above the EMGB and close to the granophyres are gabbros depleted (DMGB) in many of the elements the EMGB is enriched in, but significantly enriched in MgO and CaO.
5. The granophyres are (generally) greatly enriched in many of the elements showing depletion in the DMGB and enrichment in the EMGB. The most important exceptions to this rule are  $\text{K}_2\text{O}$ , Rb, and Sr. Elements with high concentrations in the DMGB (eg. MgO and CaO) tend to show very low concentrations in the granophyres.

#### Models for Differentiation

There are various possible processes which can be called on to produce the rock types in the Gull Cove sill:

Assimilation of Sediment The sills intrude Upper

Cambrian siltstones and shales and, because the granophyres and EMGB tend to show high Si and Al, one might hypothesize that the sedimentary rocks had an important effect on the chemical evolution of the sill. This idea would seem unlikely, however, in view of the fact that xenoliths were never observed either in the field or in thin sections. Secondly the hypothesis does little to explain the gradual change in compositions up through the lower gabbro or the presence of the DMGB in the middle of the sill where it is surrounded by granophyres. Thirdly it is impossible to mix trace element concentrations in the sediments (Table 4.20) with those from the contact to help produce the granophyres or EMGB.

Multiple Magma Injection. This hypothesis is at first glance appealing because it would help explain the presence of rocks enriched in MgO and CaO (DMGB) and somewhat depleted in elements such as Na<sub>2</sub>O and K<sub>2</sub>O, in the middle of the sill. However, there are a number of problems with the hypothesis. Chilled margins indicative of the late intrusion of another liquid, or even gradual textural changes which one could use to support the hypothesis are absent. Indeed, the occurrence of the granophyres primarily in association with, and cutting these rocks is difficult to reconcile in terms of simple magma injection. Perhaps more difficult to understand is why plagioclase and augite cores from one DMGB sample (SB6K) with high MgO and CaO, display the lowest An and En contents (respectively) in the mafic

portions of the sill. If this portion of the sill represents a second intrusion of hot primitive magma one might expect mineral compositions to closely resemble SB6F. It is also difficult to explain the regular increase in grain-sizes and gradual changes in composition throughout the lower gabbro in terms of a multiple injection model.

Crystal Settling and Fractionation In these models it is assumed that minerals forming either in the melt or on the floor of the magma chamber were in equilibrium with the melt from which they formed. Components not used in forming these minerals were enriched in the residual melt. Evidence in the form of cumulus olivine textures at the base of the Lance Cove sill suggests that crystal settling processes played an important role in the early formation of the sills. However, cumulus textures are absent in the Cull Cove sill; the implications being that a model representing crystallization from the sill floor, roofward, may be more applicable.

The following paragraphs outline evidence suggesting that the model for simple crystallization from the floor upward is not totally applicable. A trace element modelling program written by Evans (1978) was used to model trace element concentrations in the granophyres, which in any simple crystallization model must represent the last residual melt, from those in the contact rocks. Modelling parameters are presented in Table 4.21 along with the

Table 4.21. Modelling of sill trace element concentrations.

## Granophyre

|    | Surface Equilibrium |  | Total Equilibrium   |  | observed concentration |
|----|---------------------|--|---------------------|--|------------------------|
|    | 94% Crystallization | Crystallization observed concentration found | 94% Crystallization | % Crystallization observed concentration found |                        |
| Rb | 95                  | A  | 27                  | A  | 0                      |
| Sr | 351                 | A  | 297                 | A  | 18                     |
| Ba | 1354                | A  | 575                 | A  | 39                     |
| Cr | 0                   | 58%  | 28                  | B  | 0                      |
| Ni | 0                   | 90%  | 29                  | B  | 0                      |
| Y  | 173                 | 86%  | 74                  | C  | 98                     |
| Nb | 54                  | 96%  | 24                  | C  | 66                     |
| Zr | 587                 | 96%  | 260                 | C  | 798                    |
| V  | 0                   | 70%  | 77                  | B  | 14                     |
| Ga | 33                  | 98%  | 24                  | C  | 30                     |

## Enriched Middle Gabbro

| Melt Composition (Surface Equilibrium) |  |     | Solid Composition                        |  |                        |
|--|--|-----|--|--|------------------------|
| 50 Percent Crystallization             | % Crystallization observed concentration found |     | Solid Composition at 50% crystallization | % Crystallization observed concentration found | observed concentration |
| Rb                                     | 10   | 76% | 1  | 96%  | 19                     |
| Sr                                     | 283  | C   | 256                                      | C  | 448                    |
| Ba                                     | 356  | 36% | 410                                      | 83%  | 284                    |
| Cr                                     | 2  | 6%  | 15                                       | 30%  | 145                    |
| Ni                                     | 26   | 26% | 89                                       | 72%  | 56                     |
| Y                                      | 44   | A   | 15                                       | 78%  | 26                     |
| Nb                                     | 10   | 59% | 2  | 77%  | 12                     |
| Zr                                     | 115  | 83% | 26                                       | 90%  | 91                     |
| V                                      | 61   | 3%  | 208                                      | 46%  | 256                    |
| Ga                                     | 24   | 16% | 20                                       | 56%  | 21                     |

Table 4.21 (continued)  
Phases Removed and Proportions

|                                    | Augite | Plagioclase | Fe-Ti oxides | Biotite |
|------------------------------------|--------|-------------|--------------|---------|
| Granophyre Model                   | 47.8   | 46.2        | 3.0          | 3.0     |
| Melt Composition<br>Middle Gabbro  | 49.3   | 47.7        | 3.0          |         |
| Proportions of<br>Phases in Solid* | 47.8   | 46.2        | 3.0          | 3.0     |

Partitioning Coefficients

|    |        |       |        |        |
|----|--------|-------|--------|--------|
| Pb | 0.031  | 0.071 | 0.000  | 3.260  |
| Sr | 0.120  | 1.830 | 0.000  | 0.120  |
| Ba | 0.026  | 0.230 | 0.000  | 6.360  |
| Cr | 10.000 | 0.100 | 96.500 | 12.600 |
| Ni | 4.500  | 0.008 | 23.333 | 20.000 |
| V  | 0.680  | 0.055 | 0.000  | 0.097  |
| Ch | 0.400  | 0.055 | 0.000  | 0.097  |
| Zr | 0.400  | 0.005 | 0.000  | 1.000  |
| V  | 1.300  | 0.080 | 79.950 | 12.000 |
| Ca | 0.505  | 1.000 | 0.000  | 4.000  |

Concentrations in ppm

\*Rock composition was calculated from the estimated melt composition using the bulk  $k_d$  value assuming biotite was a precipitating phase. The melt composition was calculated assuming no biotite was removed (see Melt Composition Middle Gabbro, above).

A Model predicts concentration should increase.

B Model predicts concentrations will not decrease to observed concentration.

C Model predicts concentrations will not increase to observed concentration.

Sources for partitioning coefficients: Arth (1976) Ewart and Taylor (1969) Henderson and Pale (1969) Delong (1974) Duke (1976) Jensen (1973). Values used are for average basalt as reviewed by Evaps (1978).

numerical results. Estimates of the phases and their relative percentages were made with reference to the petrography. Partition coefficients are those compiled by Evans (1978) for average basalt. The granophyres represent a small portion of the sill so the modelled concentrations in a residual liquid after 94% crystallization are presented in the table. Also shown are the percentages of fractionation at which the observed and modelled concentrations match.

Inspection of Table 4.21 shows that a total equilibrium crystallization model cannot explain trace element concentrations in the granophyres. The concentrations of some elements can be modelled assuming surface equilibrium but Rb, Sr, and Ba, behave antithetically to the model. It is impossible to change the partition coefficients or the percentages of minerals crystallizing (within reason) to significantly improve the model. Similarly the decrease in P in the sill is difficult to explain in view of the fact that Y concentrations increase.

Also difficult to explain in terms of crystal fractionation processes are the observations that the granophyres form sharp contacts with the gabbros and intermediate or transitional rocks are rare. The process provides no insight into the formation of the depleted gabbros adjacent to the granophyres which are not transitional to the latter but among the most mafic (ie high MgO and CaO) in the sill.



Elements such as Rb, Sr, Ba, P, Nb and Zr show substantial enrichment over the contact rocks in some middle gabbros. It is unknown whether these rocks represent a pure melt, pure cumulates or cumulates with intercumulus phases representing some trapped melt. The two limiting conditions were modelled and show that it is unlikely crystal fractionation processes can explain the EMGB trace element concentrations. The EMGB occurs approximately half way up the sill, and if crystallization proceeded from the floor upwards (as suggested by presence of the thickest granophyre 5 meters from the top of the sill) these rocks must have formed after approximately 50 percent crystallization of the sill. Table 4.21 shows an estimate of the melts composition after crystallizing 50% of the starting magma (contact rocks) in the form of augite, plagioclase and Fe-Ti oxides. The modelled concentrations bear little resemblance to those observed. The percentages of fractionation where the modelled melt concentrations match the observed concentrations in the EMGB range from 3% to 100% and in some cases can not be reproduced.

Table 4.21 shows the trace element composition of a modelled EMGB rock containing augite, plagioclase, biotite and Fe-Ti oxides which precipitated from a residual melt produced by crystallizing 50% of the starting magma in the form of augite, plagioclase, and Fe-Ti oxides. In general, correspondence between the observed and estimated concentrations at 50% crystallization is poor. Better

correspondence for many elements may be found at higher percentages of crystallization. In some cases (eg. Rb, Sr, Ba, and Zr) the percentages of crystallization where the model and observed concentrations match are unrealistic. Mixing the estimated melt and liquid compositions does nothing to improve the modelling of some elements (Cr, Sr, V, Zr). The models for both the residual melt and the solid attempt to bring modelled Rb and Ba concentrations in line with those observed. If in the modelling some biotite is removed, as the petrography suggests it should be, estimates of the Rb and Ba concentrations in the pure melt and pure cumulate would be even further (lower) from those observed. Sr concentrations cannot be modelled, they are simply too high. Lastly the concentration of Y actually dropped, a situation difficult to reconcile with P increasing. Collectively the above evidence appears to eliminate simple crystallization from the floor roofward as the primary process controlling element variation in the sills.

Thermogravitational Fractionation and Volatile Complexing The inability of the processes discussed above to explain the zonation and distribution of rock types in the Cape St. Mary's sills suggests that mechanisms similar to those invoked by Hildreth (1979, 1981) to explain the chemical variation in silicic magma chambers may also be applicable to mafic systems. Possible processes include Soret diffusion, diffusion across convecting thermal and chemical boundary layers, volatile complexing and transport

of elements by the diffusive mechanisms or by a free volatile phase, and preference of some elements for particular melt structural sites, the availability of which will be dependent on zonation in the magma.

It is presently difficult to test for the relative importance of the above mechanisms because their effects are at best poorly understood. Unless there was a free volatile phase present in the sills, convection probably played an important role in early differentiation processes because simple diffusion rates in a stagnant magma are too low to effect differentiation (Hofmann, 1980). There is textural evidence that convection is common in large mafic magma chambers (Irvine, 1983,a,b; Wager and Brown, 1968). It is unlikely that layering in the Cape St. Mary's sills, which primarily reflects small variations in pyroxene grain-sizes, is due to sorting of crystals on the floor of the magma chamber because the textures observed are ophitic. McBirney and Noyes (1979) have proposed that the layering in mafic magma chambers may be due to in situ gravitational stratification of the magma through diffusion, convection, nucleation, and growth of crystals within discrete boundary layers.

Thermogravitative processes similar to those proposed by McBirney and Noyes (1979) or Irvine (1983,a,b) may have established compositional gradients within the sill magma chamber in the early stages of cooling, but the

morphological characteristics of the granophyric dikes and layers place constraints on how long these processes remained operative. The dikes occur in various orientations, in some cases normal to the roof of the sill at Gull Cove. Obviously convection had ceased by the time they formed and so other processes are necessary to explain their formation.

The following paragraphs present evidence suggesting that the sill at Gull Cove developed gradients in volatile components. The concentration of hydrous minerals (primarily biotite) tends to increase up through the lower gabbro and into the middle gabbro. Above the EMGB, in the granophyres, amphiboles form the most important mafic minerals. These observations attest to an increase in  $H_2O$  upward in the sill.

Pyroxene grain sizes show an overall tendency to increase up through the lower gabbro and into the middle gabbro. The grain size of any igneous rock is a function of cooling rates, composition, viscosity, and volatile content of the magma, number of crystal nuclei, and movement of the magma (Hyndman, 1972, page 46). Thick sills (which cool slowly) such as the Tasmanian dolerite show pyroxene grains as much as 5 mm in length (McDougall, 1962). The relatively thin Cape St. Mary's sills show pyroxene grain sizes (in the middle) exceeding 10 mm! Though the other variables mentioned above cannot be eliminated, the best explanation for the coarseness of the middle gabbros would seem to be a

high volatile content. According to Hyndman (1972, page 47), volatiles tend to limit crystal nucleation by weakening the bonds between silica tetrahedra. Secondly, they increase the rate of crystal growth by lowering magma viscosity, and increasing ion diffusion rates. The net result is rapid growth of a few crystals to produce a coarse-grained texture.

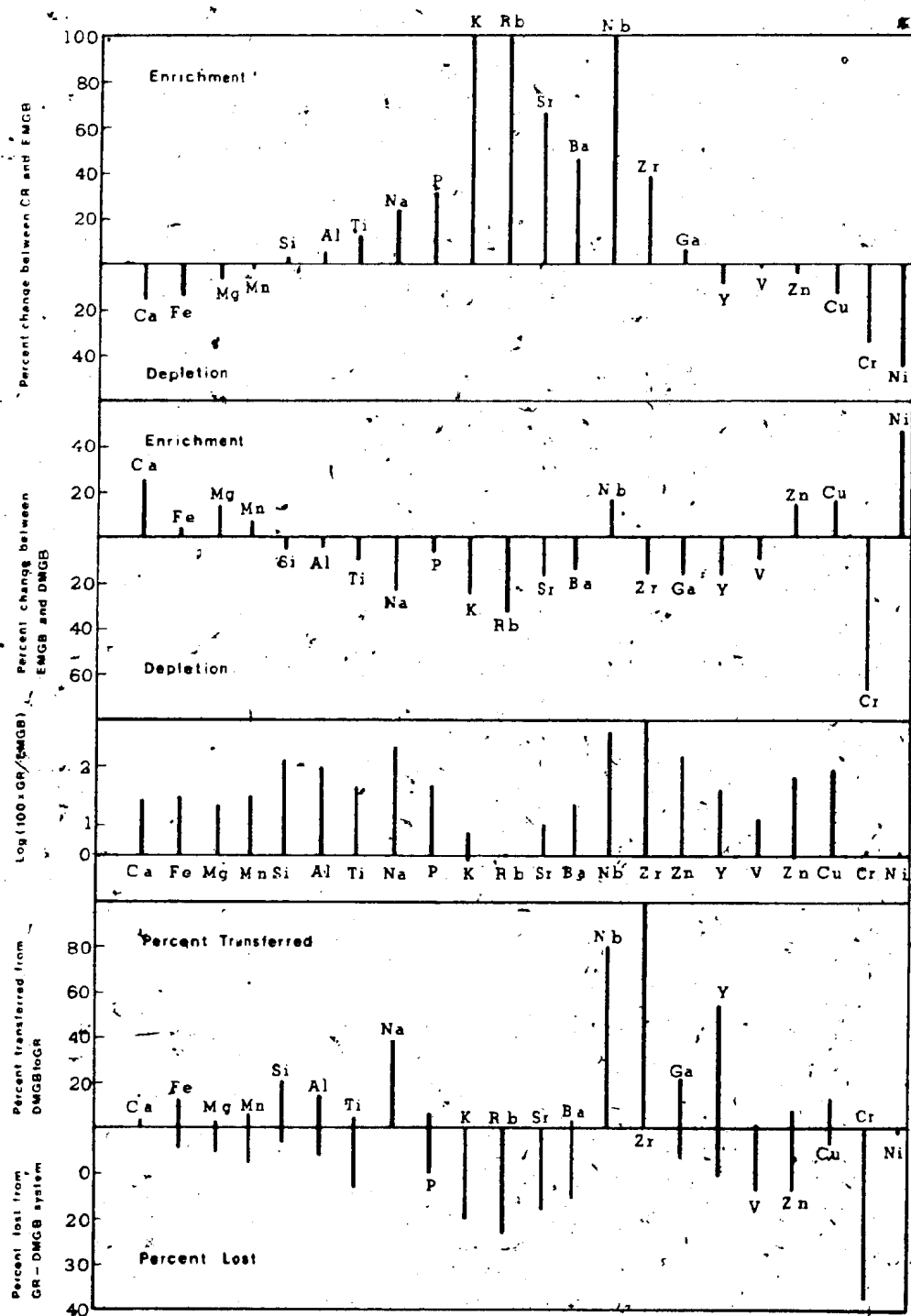
The fluctuations in both plagioclase and augite compositions may be related to gradients in the volatile content of the sill magma. The composition of plagioclase precipitating from a silicate melt is controlled by the composition and temperature of the melt (Bowen, 1913; Kudo and Weill, 1970; Wood and Banno, 1973), and the temperature at which precipitation begins is dependent on the volatile content of the system. The extent of reequilibration between mineral cores and the cooling magma, and the rate of crystallization, are increased with high volatile percentages. If the felsic dikes and layers high in the sills acted as "drainage routes" for volatiles, then the relatively high average An and En contents of plagioclase and pyroxene cores in SB71 (which is closest to the granophyres) may be explained in terms of volatile loss in this portion of the sill. A loss of volatiles might have prevented reequilibration of mineral cores with the melt.

The occurrence of baddeleyite, zircon, and quartz in the granophyres records a wide range of silica activities

which may be related to increasing water pressures as the sills crystallized. Nicholls et al. (1977) suggest that an increase in the water content of a felsic liquid, increases the activity of silica. It seems likely that the occurrence of baddeleyite in the Cape St. Mary's sills records fairly low silica activity, and that zircon formed on the baddeleyite as silica activity rose, possibly in response to increasing water pressure. Although quartz was not observed in the granophyre containing the baddeleyite, it commonly occurs in some of the granophyres at Gull Cove, possibly because  $\text{PH}_2\text{O}$  was even higher in these rocks.

The importance of volatile complexing of elements to differentiation of the Gull Cove sill may be reflected in the relative enrichment/depletion of elements in the endmember rock types (Figure 4.24). Nearly every element which shows enrichment in the EMGB (Figure 4.24a) is proportionally depleted in the DMGB (Figure 4.24b) and those depleted in the EMGB are enriched in the DMGB. Inspection of Table 4.20 shows that elements enriched in the DMGB generally occur at low concentrations in the granophyres. Similarly elements such as Si, Al, Ti, Na, Zr, and Ga make up large proportions of (or show high concentrations in) the granophyres but are depleted in the DMGB. However, the alkali and alkaline earth metals, which display remarkable enrichment in the EMGB, are proportionally depleted in the granophyres (Figure 4.24c). These observations suggest:

Figure 4.24 Bar-graphs showing the movement of elements within the Gull Cove sill. Abbreviations used are as follows: contact rocks, CR; granophyres, GR; depleted middle gabbro, DMGB; enriched middle gabbro, EMGB. See text for discussion.





1. After emplacement of the magma, thermogravitative processes moved such elements as Si, Al, Ti, Na, P, K, Rb, Sr, Ba, Nb, Zr, Ga, and Y upward and concentrated them in the upper levels of the sill. Elements such as Ca, Fe, and Mg, which were not appreciably carried were diluted in the resulting rock.

2. Above the EMGB volatiles were apparently concentrated along certain pathways which now make up the granophyres. As a result the gabbros closest to the granophyres (the DMGB) were depleted in most of the elements found enriched in the EMGB.

3. Some of the elements carried by the volatiles were largely deposited in the granophyres (eg. Si, Al, Na, Nb, Zr), where as others (eg. K, Rb, Sr, Ba) were apparently carried out of the sill system entirely.

4. Implicit in the above statements is the conclusion that volatile complexing was important in determining which elements were enriched/depleted during the early stages of differentiation when thermogravitative processes may have been operative. The elements showing

enrichment in the early formed EMGB are similarly enriched in the granophyres or apparently removed from the sills system.

In order to show which elements were concentrated in the granophyre, and which elements were removed from the system entirely, the following calculations were made and plotted in Figure 4.24d. Mass balance calculations show that a mix of approximately 80 percent of the DMGB plus 20 percent of the granophyres will yield a rock similar to the EMGB. The two elements which fit the worst in these calculations (based solely on the major elements) are Ca, which shows the greatest enrichment in the DMGB, and Na which shows the greatest propensity for concentration in the granophyres. These two elements were most conserved by the system as a whole. Solving for Na and Ca:

|    |           |   |            |   |      |
|----|-----------|---|------------|---|------|
|    | DMGB      | + | Granophyre | = | EMGB |
| Ca | 11.17X    | + | 1.35Y      | = | 8.93 |
| Na | 2.77X     | + | 9.64Y      | = | 3.56 |
|    | X = 0.782 |   | Y = 0.145  |   |      |

It is possible to rationalize the fact that X and Y do not total 1.0 by assuming that all elements were removed to some extent from the system as a whole, and because the chemical analyses for each rock must sum to 100 the CaO and Na<sub>2</sub>O are overestimated. The relative percentage loss of each oxide, and the percentage transferred from the gabbro to the

granophyre were calculated as follows:

$$(0.782(A)DMGB + 0.145(A)GR - (A)EMGB)/(A)EMGB =$$

Percentage of A lost from system.

$$0.145(A)GR/(A)EMGB =$$

Percentage of A transferred from the gabbros to the GR

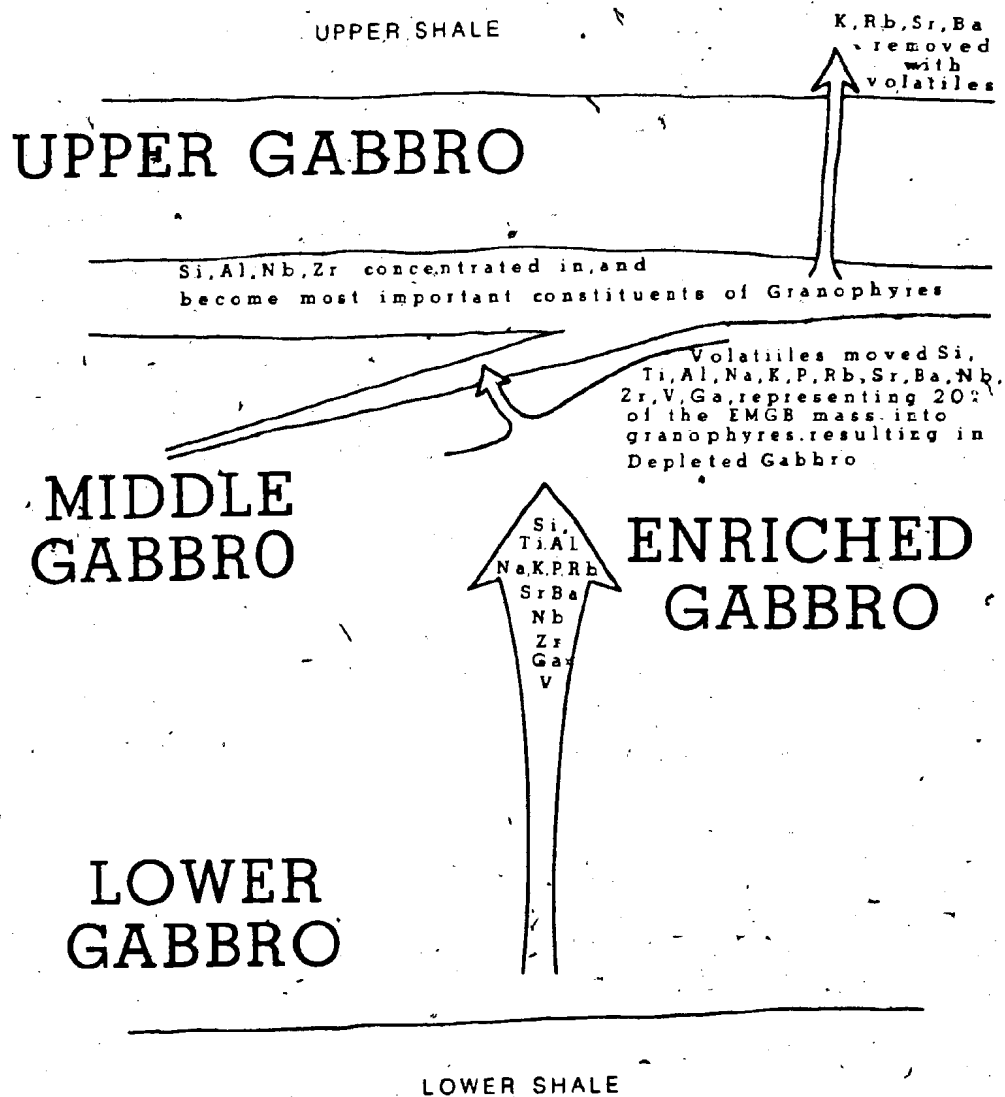
where GR = granophyre

A = each major element oxide.

The same calculations were also made for the trace elements. The results show that large percentages of Ti, P, K, Rb, Sr, Ba, Y, V, and Zn were lost from the system. Sodium, Nb, Zr, and Y show the greatest propensity for concentration in the granophyre. The above observations are summarized in pictorial form in Figure 4.25.

The extent to which any particular mobile element was lost as opposed to concentrated in the granophyre appears related to the stability of phases in the granophyre. Albite is volumetrically the most important mineral in the granophyres, and its formation effectively removed a large portion of the Na in passing solutions. Phases such as zircon, baddeleyite, and sphene, found in heavy mineral separates of a granophyre from Lance Cove, were responsible for removing Zr, Nb, and Y, as well as the REE (see Figure 4.17). Phases such as biotite, or K-feldspar, which could have removed K, Rb, and Sr, were apparently not stable in the granophyre system.

Figure 4.25 Schematic diagram illustrating the movement of elements within the Gull Cove sill.



#### 4.3.4 Discussion of Sills

During the 1940's, 1950's, and 1960's numerous studies documented the variations in texture, sequence of mineral formation, and differentiation trends in layered intrusions. The Cape St. Mary's sills show various characteristics in common with sills in general. For example, Wager and Brown (1968) pointed out that crystal settling is probably not an important process in the differentiation of most sills and is restricted to the early removal of phenocrysts present at the time of magma emplacement. This appears applicable to the Cape St. Mary's sills as does the observation that the last felsic (pegmatitic) differentiates, nearly always occur 2/3 to 3/4 of the way up most sills (Wager and Brown 1968). However, the Cape St. Mary's Sills show many textural, mineralogical, and chemical features which set them apart from the norm and these are summarized below.

1. The Cape St. Mary's sills are much coarser-grained than is normally the case for most sills regardless of their thickness.
2. Hydrous minerals, especially biotite, occur in relatively large quantities throughout the mafic portions of the sills. Magmatic amphiboles occur in the olivine cumulates at the base of the sill at point Lance.

3. Plagioclase cores show a relatively large range of compositions given that the sills are relatively thin. The compositions are related to height in the sill and the proportions of volatile minerals such as biotite.
4. Only high Ca pyroxene occurs in the sills despite the fact that the whole-rock chemistry of contact rocks resembles that of subalkaline rocks and is Hy normative. Furthermore, quartz occurs in some of the late differentiates.
5. The high Ca pyroxenes commonly show salitic compositions indicative of low silica activities and representative of alkaline rocks.
6. The presence of baddeleyite, olivine, zircon, and quartz attests to a wide range of silica activities during the course of crystallization.
7. The Fe depletion trend shown by samples on an AFM diagram (if representative of liquids) may indicate  $fO_2$  was very high. The trend is clearly unlike that normally seen in either tholeiitic or alkaline sills.
8. Trace element concentrations and ratios in the

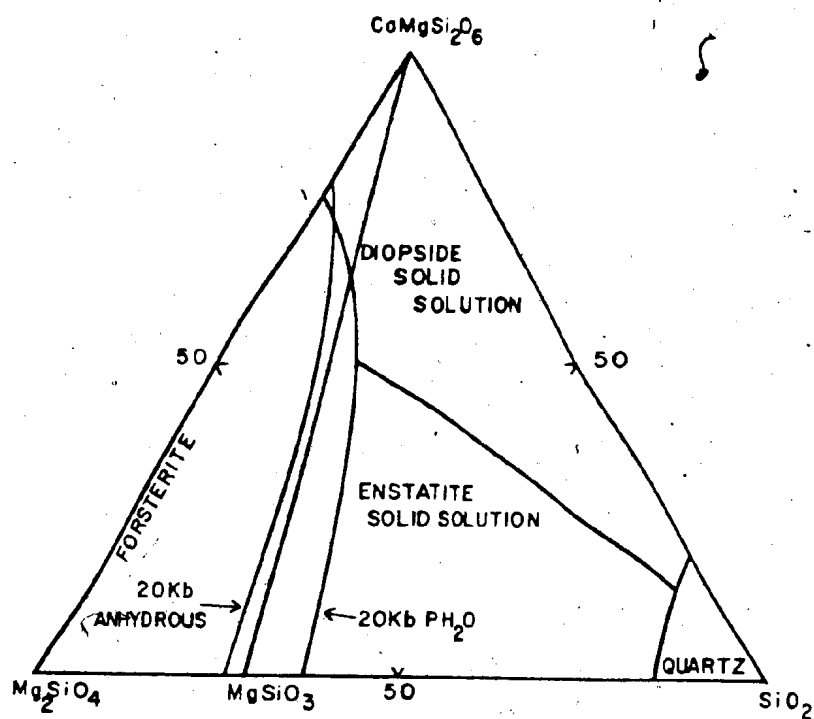
contact rocks are representative of those associated with tholeiitic or mildly alkaline rocks.

9. Evidence presented above suggests that volatile complexing of elements was an important process in differentiation of the sills.

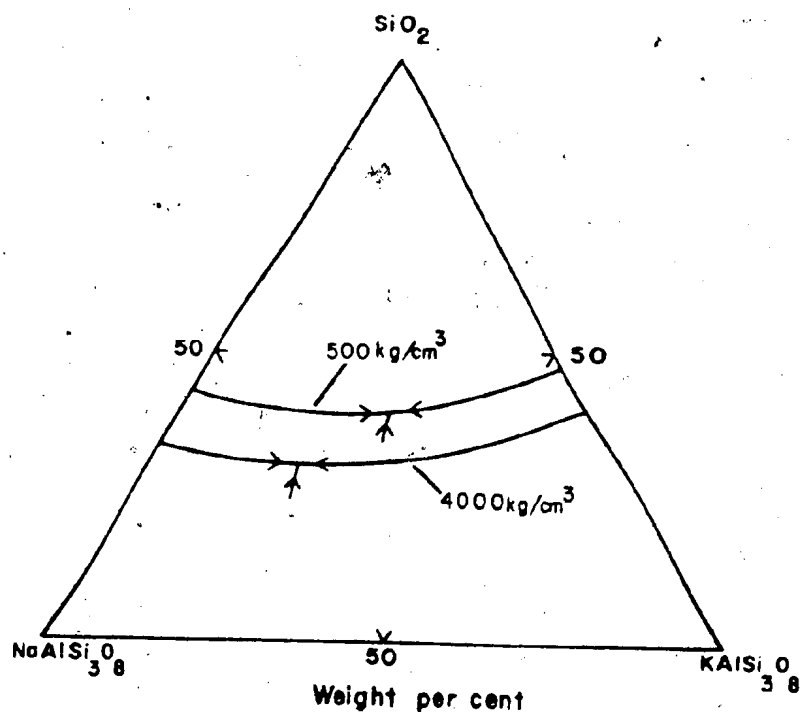
Several of the above items (1, 2, 7, and 9) support the idea that the Cape St. Mary's sills had unusually high water contents. The following discussion examines the possibility that high volatile concentrations might also account for some of the unusual mineralogical attributes of the sills (3, 4, 5, and 6 above). The work of Kushiro (1969) shows that high water pressure causes the forsterite - enstatite boundary curve to move to higher silica contents (Figure 4.26a). In other words, in basaltic systems, high water pressure tends to lower the activity of silica. But in felsic systems, high water pressure tends to increase the activity of silica as shown by movement of the "granite" minimum away from  $\text{SiO}_2$  (Figure 4.26b after Tuttle and Bowen, 1958). Analogies with the sills must be made carefully because water pressure cannot exceed lithostatic pressure, and in the case of the sills, the 3000 meters of overlying Lower Ordovician strata suggest pressures may have been about 1000 bars. However even at these low pressures the amount of water that will dissolve in a basaltic melt is substantially higher than at atmospheric pressure (see



Figure 4.26 Ternary diagrams showing the effect of water pressure on silica activity. The top diagram, after Kushiro (1969) illustrates the effect of water in a mafic system and the lower diagram, after Tuttle and Bowen (1958), shows its effect in a felsic system.



Weight per cent



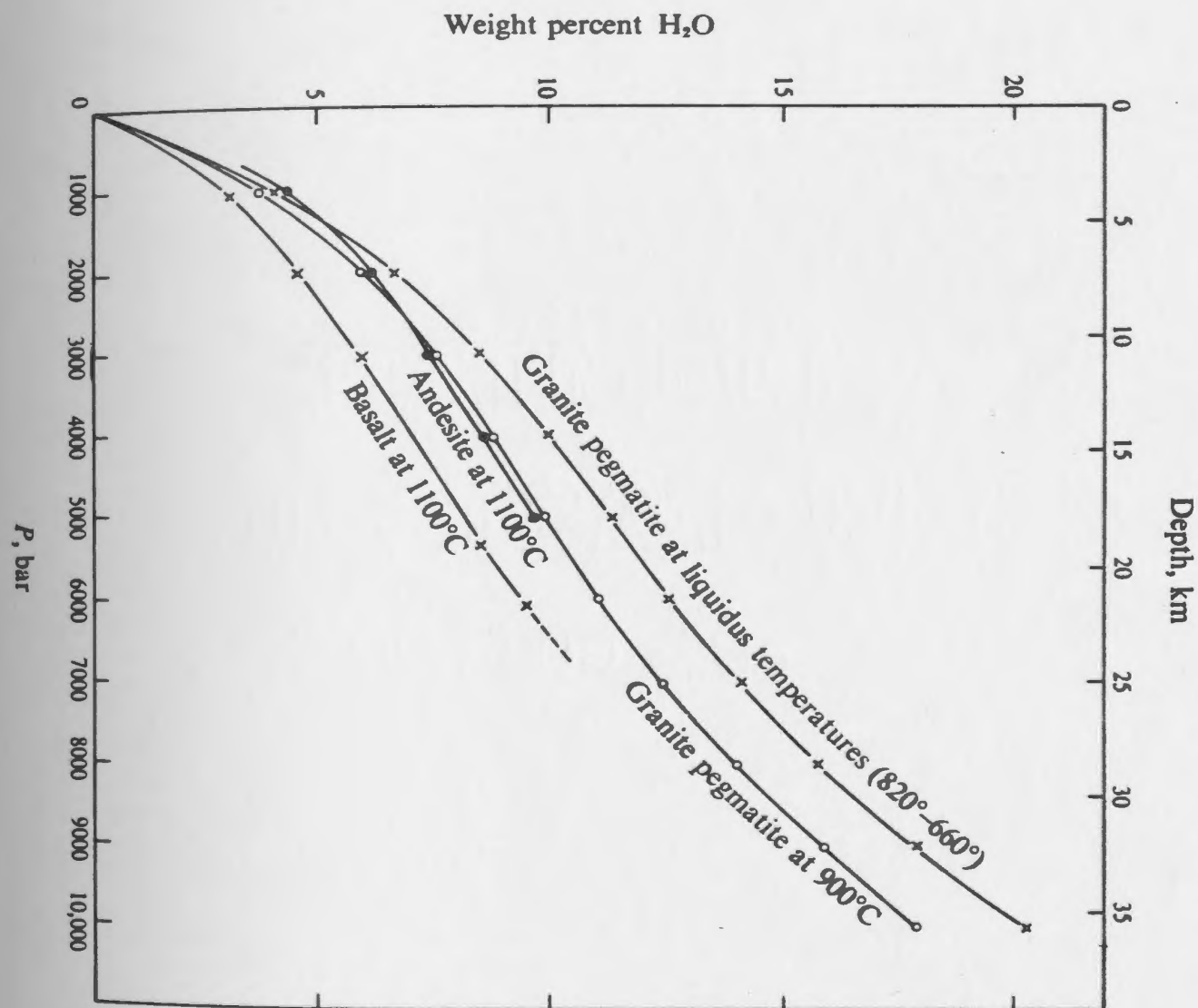
Weight per cent

Figure 4.27).

It appears that the starting sill magma was subalkaline, but had low enough silica activity to precipitate olivine during the early stages of crystallization. It also had high water content, possibly as a result of intrusion into wet unconsolidated sediments. In a "normal" subalkaline magma, low Ca pyroxene would have been precipitated, but the high water content of the sill magma depressed the activity of silica preventing its formation, and enhancing the formation of hydrous minerals, particularly biotite. The low silica activity also led to the formation of some clinopyroxenes with salitic compositions.

Constituents not used in the formation of minerals in the mafic portions of the sills were possibly moved through thermogravitational transport of volatile complexes in a manner similar to that described by Hildreth (1981) for silicic systems. In the upper regions of the sills the volatiles followed specific paths and formed the granophyric dikes and layers. Mafic minerals forming in this felsic system were mostly hydrous (amphibole) as a result of the high water content. The water content of the system probably increased as crystallization proceeded, and led to an increasing silica activity in the felsic rocks, and ended with the precipitation of quartz.

Figure 4.27 Solubility of water in various magma types at constant temperature and varying pressure. From Carmichael et al., 1974, page 323.



#### 4.4 CAPE ST. MARY'S DIKES

##### 4.4.1 Whole-Rock Geochemistry

Over 100 samples of the dikes were collected and petrographically examined but only four were found with primary pyroxenes. Most samples show alteration resembling that observed in the Cambrian flows; that is, large amounts of carbonate have been added to the rocks. The freshest samples are emphasized in the following discussion but another problem which complicates interpretation of the dike chemistry is the accumulation of feldspar. These problems leave a number of questions regarding the geochemistry and origin of these rocks unanswered, however some generalizations are possible.

The major element and normative compositions of the three least altered dike samples are given in Table 4.22, and trace element concentrations are presented in Table 4.23. A complete listing of all data is given in Appendix B. Few of the major elements show any correlation with  $\text{SiO}_2$  on variation diagrams (Figure 4.28). In general, samples without plagioclase accumulations (hereafter referred to as noncumulus) show 14 to 16 wt %  $\text{Fe}_2\text{O}_3$  (total Fe, LOI free) and between 14 and 16 wt %  $\text{Al}_2\text{O}_3$  (LOI free). Samples with plagioclase phenocrysts (cumulus samples) display higher  $\text{Al}_2\text{O}_3$  and lower  $\text{Fe}_2\text{O}_3$ . Noncumulus samples seem to show a negative correlation between  $\text{SiO}_2$  and CaO (Figure 4.28) whereas cumulus samples plot above these.

Table 4.22. Major element and normative composition of least altered dike samples.

|                                | SB66A | SB56B | SB56G |
|--------------------------------|-------|-------|-------|
| SiO <sub>2</sub>               | 43.40 | 45.20 | 46.50 |
| TiO <sub>2</sub>               | 1.26  | 1.20  | 1.75  |
| Al <sub>2</sub> O <sub>3</sub> | 14.50 | 16.10 | 17.10 |
| Fe <sub>2</sub> O <sub>3</sub> | 14.30 | 12.92 | 10.97 |
| MnO                            | 0.21  | 0.20  | 0.17  |
| MgO                            | 11.67 | 9.25  | 6.17  |
| CaO                            | 8.96  | 6.27  | 7.37  |
| Na <sub>2</sub> O              | 1.34  | 2.18  | 3.64  |
| K <sub>2</sub> O               | 0.06  | 0.60  | 0.46  |
| P <sub>2</sub> O <sub>5</sub>  | 0.20  | 0.30  | 0.53  |
| 1.0.I.                         | 4.08  | 4.34  | 3.92  |
| Total                          | 99.98 | 98.56 | 98.58 |
| CIPW Norms                     |       |       |       |
| OR                             | 0.30  | 3.17  | 2.47  |
| Ab                             | 10.23 | 17.51 | 29.67 |
| An                             | 28.37 | 26.51 | 26.30 |
| Ne                             | 0.00  | 0.00  | 0.00  |
| Q                              | 0.00  | 0.00  | 0.00  |
| Ol                             | 26.95 | 15.10 | 18.89 |
| Hy                             | 19.36 | 28.55 | 9.76  |
| Di                             | 8.40  | 0.00  | 4.01  |
| Il                             | 3.73  | 3.74  | 5.53  |
| Mt                             | 2.22  | 2.34  | 2.37  |
| Ap                             | 0.33  | 0.53  | 0.94  |

Oxides in weight percent, Fe<sub>2</sub>O<sub>3</sub> = Total Fe.  
 Norms calculated assuming Fe<sub>2</sub>O<sub>3</sub> = 1.5 weight percent and remaining Fe was FeO. All samples from Patricks Cove (pocket Map B).

Table 4.23. Trace element composition of least altered dike samples.

|    | SB66A | SB56B | SB56G |
|----|-------|-------|-------|
| Sr | 245   | 395   | 650   |
| Ba | 83    | 1610  | 195   |
| Rb | 1     | 7     | 4     |
| Zr | 60    | 93    | 157   |
| Nb | 9     | 23    | 10    |
| Y  | 23    | 30    | 36    |
| Ga | 18    | 19    | 20    |
| V  | 222   | 276   | 218   |
| Cr | 352   | 248   | 186   |
| Ni | 287   | 185   | 149   |
| Cu | 72    | 69    | 47    |
| Zn | 101   | 88    | 82    |

All concentrations in ppm.

All samples from Patricks Cove. Note SB56G cuts SB56B.

Table 4.24. REE concentrations in four dike samples.

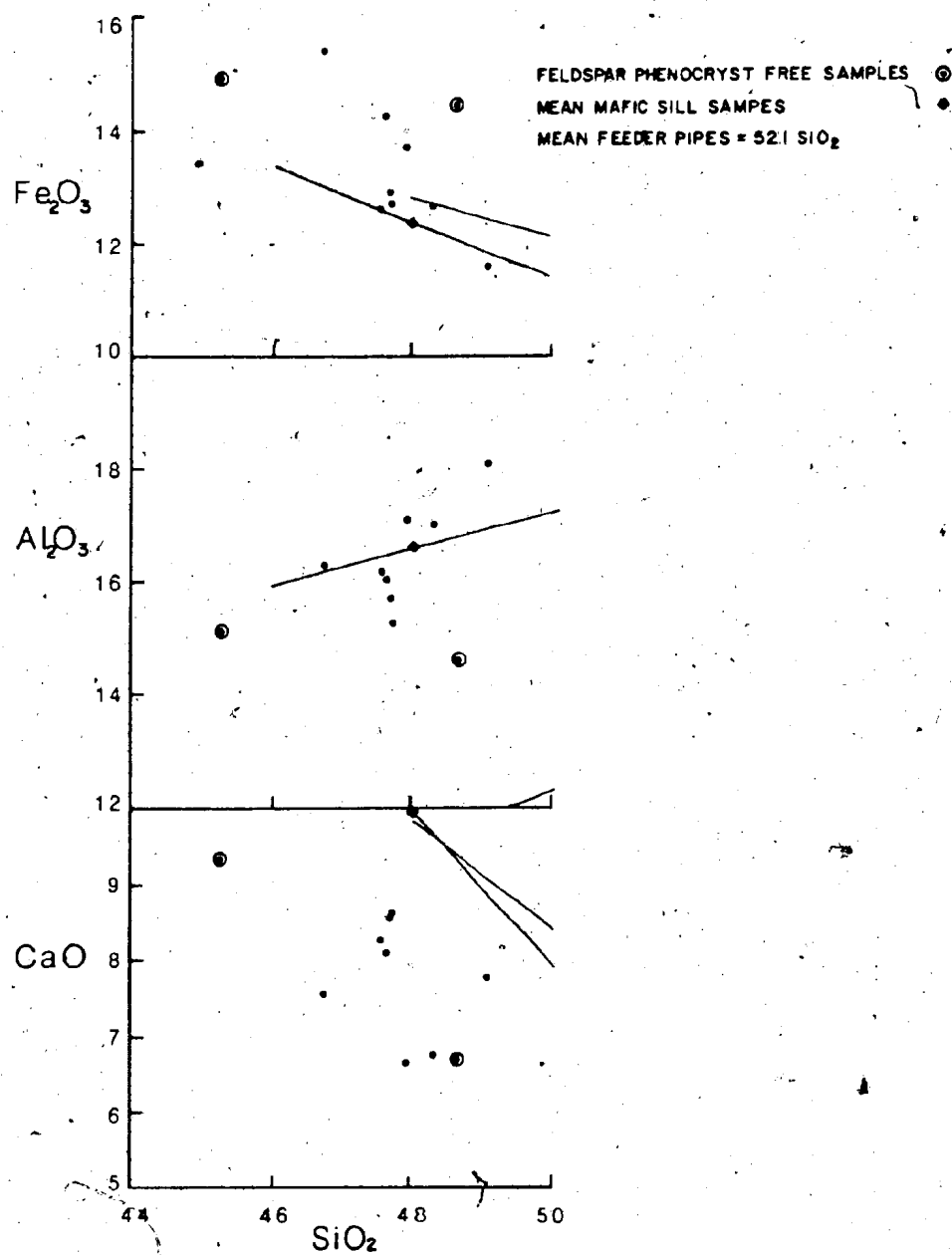
|    | SB66A | SB56B | SB56G | SB52B |
|----|-------|-------|-------|-------|
| La | 6.59  | 6.27  | 12.6  | 6.81  |
| Ce | 17.0  | 17.0  | 34.3  | 17.6  |
| Pr | 2.97  | 2.49  | 4.56  | 2.56  |
| Nd | 11.4  | 12.0  | 21.8  | 12.9  |
| Sm | 3.39  | 2.78  | 5.12  | 3.50  |
| Eu | 1.52  | 0.92  | 1.80  | 1.68  |
| Gd | 4.14  | 3.42  | 5.13  | 4.20  |
| Dy | 4.28  | 3.15  | 4.36  | 3.98  |
| Er | 2.10  | 2.33  | 2.00  | 1.69  |
| Yb | 1.12  | 1.49  | 1.82  | 0.99  |

Concentrations in ppm.

All samples from Patricks Cove (pocket Map B).



Figure 4.28 Variation diagrams for selected major elements - Cape St. Mary's dike samples. Also shown are least squares lines through the feeder pipe and non-granophyric sill data with the mean compositions plotted on the sill lines. Correlation coefficients of the lines are for the feeder pipes and sills respectively:  $\text{Fe}_2\text{O}_3$ , 0.76, 0.30;  $\text{Al}_2\text{O}_3$ , 0.76, 0.24;  $\text{CaO}$ , 0.93, 0.58. All concentrations are in wt. %, volatile free.



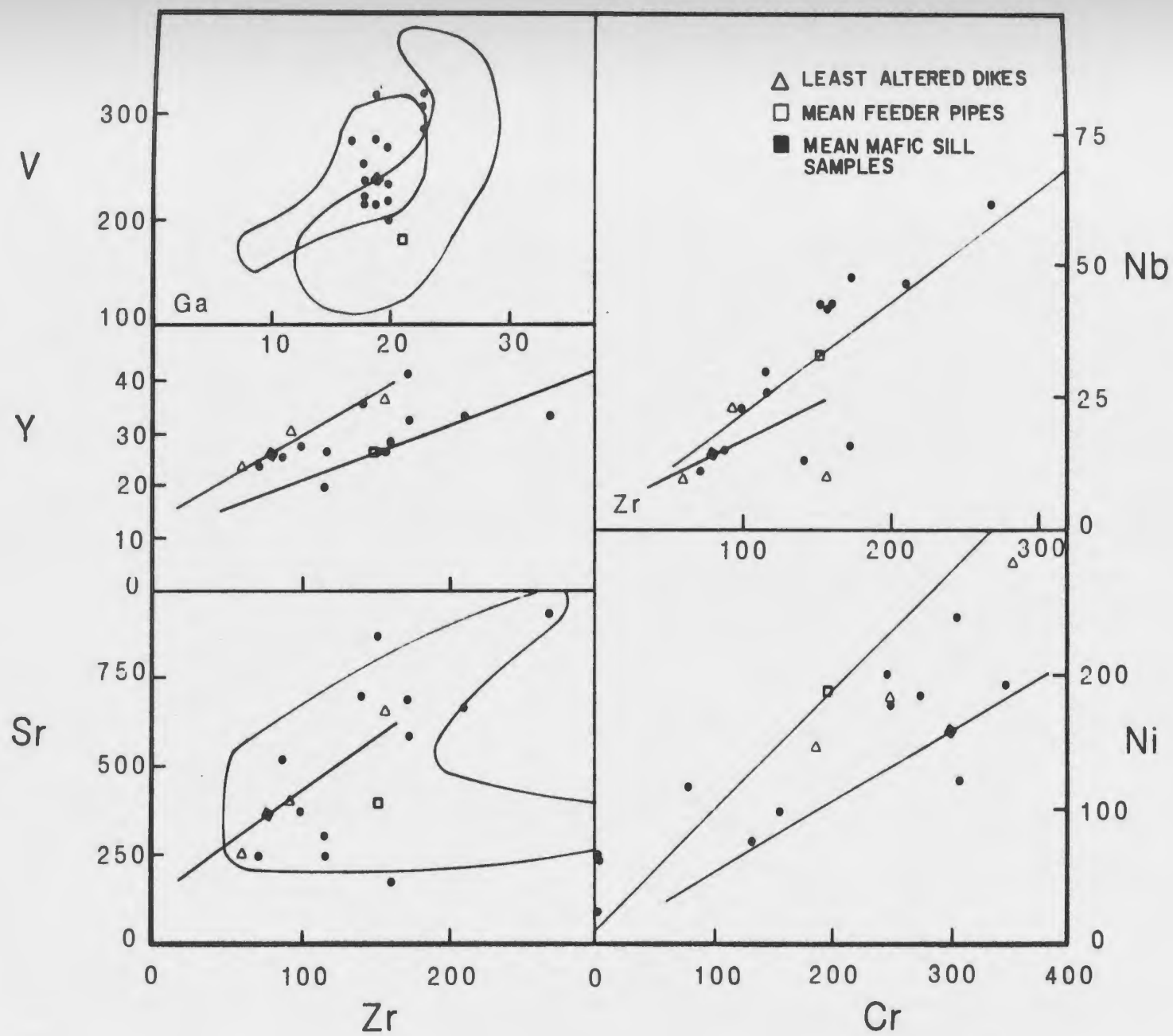
In comparison with the sills these rocks show lower  $\text{CaO}$  and higher  $\text{Fe}_2\text{O}_3$ . The Cambrian lavas and feeder pipes exhibit much higher  $\text{SiO}_2$ , and lower  $\text{Fe}_2\text{O}_3$  and  $\text{Al}_2\text{O}_3$  than the dikes. The  $\text{TiO}_2$  concentrations are generally between those observed in the Cambrian flows and those of the sills. The rocks show a range of  $\text{Mg}'$  values (0.48 to 0.64) which should not be substantially affected by feldspar accumulation in the samples. Figures 4.9 and 4.10 illustrate that both  $\text{Al}_2\text{O}_3$  and  $\text{TiO}_2$  display a negative correlation with  $\text{Mg}'$ . The correlation with  $\text{Al}_2\text{O}_3$  cannot (entirely) be due to feldspar accumulation because noncumulus samples occur at both ends of the trend line.

Trace element concentrations in the dikes (Table 4.23) show some interesting, and in particular cases enigmatic, characteristics. Most elements show concentrations which are similar to, or between, those of the sills and the Cambrian flows and feeder pipes (Figure 4.29). The  $\text{Zr/Nb}$  ratios mostly lie between 3.5 and 5.0, but three samples with low  $\text{Zr}$  show higher ratios. The chondrite-normalized REE patterns for the dikes show a range of slopes (Figure 4.23 and Table 4.24) and normalized heavy REE concentrations less than 10.

#### 4.4.2 Mineral Chemistry

Representative analyses of groundmass pyroxenes from two dike samples, SB66A and SB56A, with different bulk rock chemistry (SB56A similar to SB56G, Tables 4.22 and 4.23) are

Figure 4.29 Variation diagrams for selected trace elements - Cape St. Mary's dike samples. Also shown are least squares lines through the feeder pipe and non-granophyric sill data with the mean compositions plotted on the lines. Fields surrounding the feeder pipe or sill data are shown where the correlation coefficients are low. Correlation coefficients of the lines for the feeder pipes and sills (respectively) are as follows: Ga-V, 0.26, 0.15; Zr-Y, 0.93, 0.67; Zr-Sr, 0.20, 0.58; Zr-Nb, 0.96, 0.50; Cr-Ni, 0.97, 0.96. All concentrations are in ppm.



given in Table 4.25. Pyroxenes from sample SB66A have Wo, En, and Fs proportions of about 42, 41, and 17, where as in SB56A they average 49, 33, and 18 (Figure 4.30). Pyroxenes in SB66A are nearly all augites, but in SB56A the Wo component is usually over 45 percent giving most grains salitic compositions. Some SB56A grains have more than 50 percent Wo, and Al<sup>IV</sup> over 0.25 (atomic); they appear to be fassaites (Deer et al., 1978). The concentrations of TiO<sub>2</sub>, Na<sub>2</sub>O, and MnO (Figure 4.31) also serve to distinguish SB66A augites (1.00, 0.40, and 0.20 weight percent) from the salitic grains in SB56A (3.00, 0.65, 0.15 weight percent).

#### 4.4.3 Discussion of Dikes

The small number of relatively unaltered samples makes it difficult to establish the genetic relationships between the dikes. The following points appear valid. The range of Mg values show that the rocks are variably evolved as a result of the precipitation of ferromagnesian. Variations in Ni concentrations illustrate that olivine was probably removed and corresponding changes in Cr values suggest that clinopyroxene and/or Cr-spinel were precipitated. Many samples contain plagioclase phenocrysts which show that the mineral was on the liquidus at the time of emplacement, but the lack of a significant negative Eu anomaly in any of chondrite-normalized REE patterns (Figure 4.23) suggests that substantial amounts of the mineral could not have been removed prior to emplacement.

Table 4.25. Representative analyses of dike pyroxenes.

|                                | SB66A5 | SB66A6 | SB66A8 | SB56A16 | SB56A15 | SB56A18 |
|--------------------------------|--------|--------|--------|---------|---------|---------|
| SiO <sub>2</sub>               | 51.91  | 49.86  | 48.21  | 45.95   | 45.61   | 44.79   |
| TiO <sub>2</sub>               | 0.63   | 1.08   | 1.46   | 2.64    | 3.06    | 3.66    |
| N <sub>2</sub> O <sub>3</sub>  | 2.09   | 3.76   | 4.81   | 6.91    | 7.14    | 7.71    |
| Cr <sub>2</sub> O <sub>3</sub> | 0.20   | 0.18   | 0.39   | 0.02    | 0.02    | 0.02    |
| FeO                            | 8.93   | 9.40   | 9.79   | 9.83    | 9.95    | 10.00   |
| MnO                            | 0.19   | 0.16   | 0.18   | 0.16    | 0.11    | 0.14    |
| MgO                            | 15.65  | 14.06  | 13.46  | 11.28   | 10.57   | 10.11   |
| NiO                            | 0.05   | 0.08   | 0.07   | 0.03    | 0.04    | 0.00    |
| CaO                            | 19.27  | 20.47  | 20.23  | 21.95   | 22.40   | 21.22   |
| Na <sub>2</sub> O              | 0.35   | 0.37   | 0.37   | 0.64    | 0.57    | 0.69    |
| K <sub>2</sub> O               | 0.00   | 0.00   | 0.02   | 0.00    | 0.00    | 0.02    |
| Total                          | 99.26  | 99.41  | 98.99  | 99.40   | 99.47   | 98.34   |
| Si                             | 1.936  | 1.875  | 1.829  | 1.751   | 1.740   | 1.126   |
| Al <sup>iv</sup>               | 0.064  | 0.125  | 0.171  | 0.249   | 0.260   | 0.274   |
| Al <sup>vi</sup>               | 0.028  | 0.041  | 0.043  | 0.061   | 0.061   | 0.075   |
| Ti                             | 0.017  | 0.030  | 0.041  | 0.075   | 0.087   | 0.105   |
| Cr                             | 0.005  | 0.004  | 0.011  | 0.000   | 0.000   | 0.000   |
| Fe                             | 0.278  | 0.295  | 0.309  | 0.313   | 0.317   | 0.321   |
| Mn                             | 0.005  | 0.004  | 0.005  | 0.004   | 0.003   | 0.000   |
| Mg                             | 0.870  | 0.788  | 0.761  | 0.640   | 0.600   | 0.580   |
| Ni                             | 0.001  | 0.002  | 0.001  | 0.000   | 0.000   | 0.000   |
| Ca                             | 0.770  | 0.824  | 0.821  | 0.896   | 0.916   | 0.875   |
| Na                             | 0.025  | 0.370  | 0.026  | 0.047   | 0.041   | 0.051   |
| K                              | 0.000  | 0.000  | 0.000  | 0.000   | 0.000   | 0.000   |
| Total                          | 3.999  | 4.016  | 4.019  | 4.035   | 4.025   | 4.012   |
| Ca                             | 40.0   | 43.2   | 43.3   | 48.4    | 49.9    | 49.3    |
| Mg                             | 45.3   | 41.2   | 40.1   | 34.5    | 32.6    | 32.7    |
| Fe+Mn                          | 14.7   | 15.6   | 16.6   | 17.1    | 17.4    | 18.1    |

All samples from Patricks Cove (pocket Map B).  
 Oxides in weight percent, all Fe as FeO.  
 Recalculated on the basis of 6 oxygen.

Figure 4.30 Pyroxene quadrilateral showing pyroxenes from the Cape St. Mary's dike rocks. The fields are labelled after Le Bas (1962).



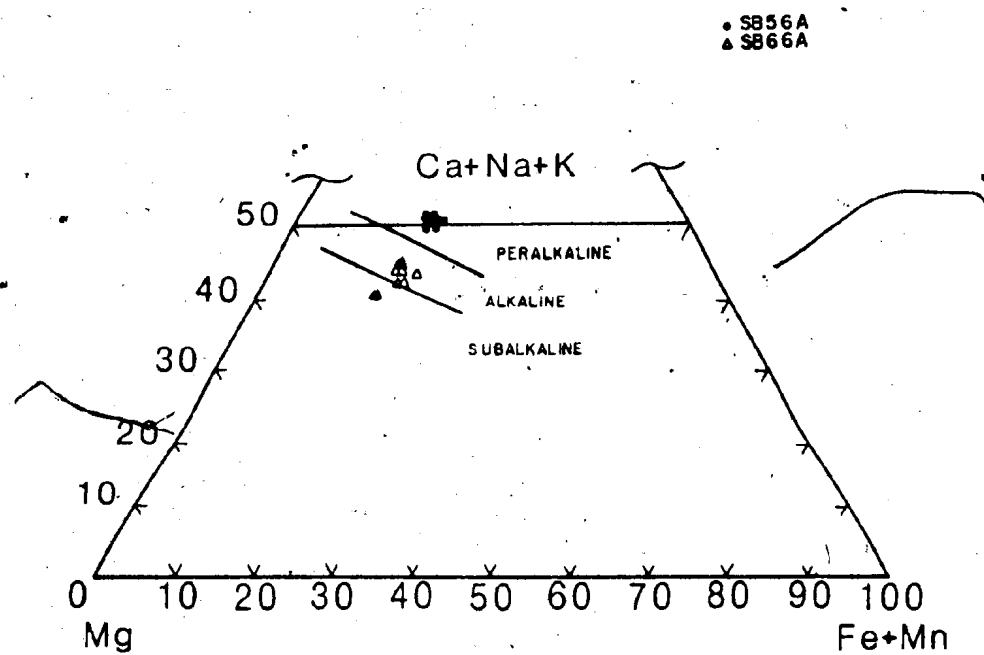
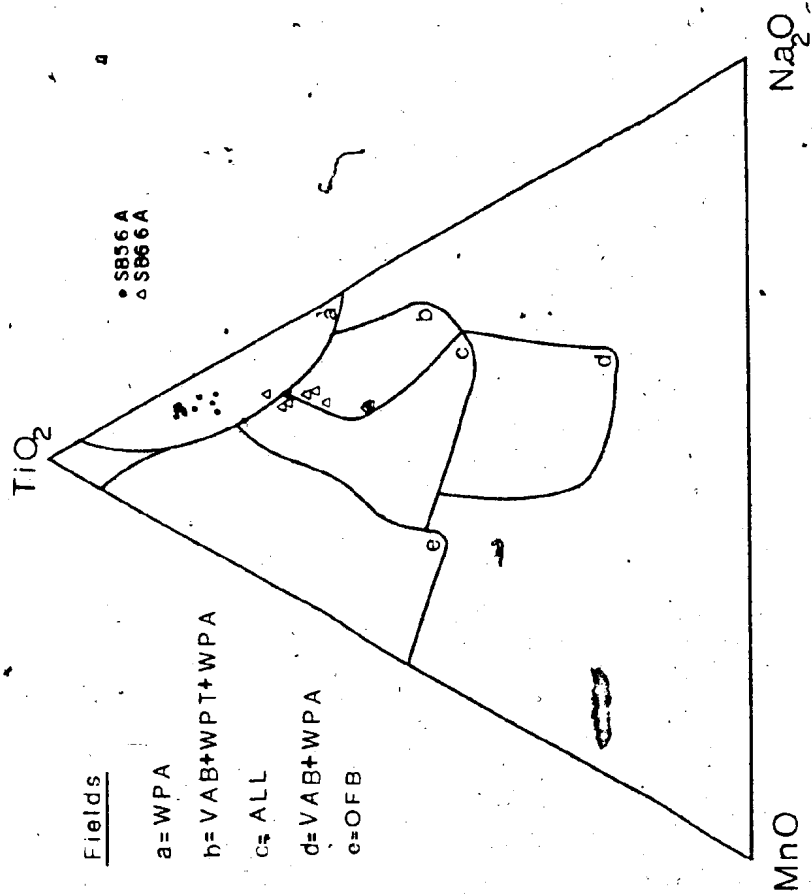


Figure 4.31  $\text{TiO}_2$ - $\text{MnO}$ - $\text{Na}_2\text{O}$  pyroxene discrimination diagram - Cape St. Mary's dike, pyroxenes. Diagram after Nisbet and Pearce (1977). WPA = within plate alkaline; WPT = within plate tholeiite; VAB = volcanic arc basalt OFB = ocean floor basalt.



Elements such as Nb, Zr, and Y generally behave as incompatible elements, during low pressure differentiation, as most minerals commonly found precipitating from mafic magmas (ie. olivine, pyroxene, plagioclase) display low mineral/melt  $kD$  values (cf. Table 4.10). Ratios between the elements remain relatively unaffected, as do the slopes on the REE patterns (Figure 4.23), by the precipitation of these minerals (cf. Figure 4.8). However the ratios in the dike samples show a relatively large range of values (eg. Zr/Nb Figure 4.12), as do the slopes on the REE patterns (Figure 4.23), which are probably related to mantle melting processes (eg. Kay and Gast, 1973; Langmuir et al., 1977; and Pearce and Norry, 1979). These variations suggest that the dikes represent 2 or more magma batches from the mantle. The differences in SB56A and SB66A pyroxene compositions (Figures 4.30 and 4.31) could be related to the low pressure fractionation processes and/or high pressure (mantle melting) processes.

#### 4.5 NEW BRUNSWICK VOLCANIC ROCKS

##### 4.5.1 Alteration Geochemistry - Beaver Harbour Area

A great deal of the compositional variation observed in the Beaver Harbour volcanic rocks (Table 4.26) can be related to the alteration mineralogy observed. In general, samples with high hematite content show high  $TiO_2$  and  $Fe_2O_3$  compared to chlorite rich samples with similar loss on ignition (LOI) values and from the same stratigraphic unit

Table 4:26 Representative analyses of Beaver Harbour meta-volcanic rocks.

|                                  | BHR3  | BHR1  | BHR5  | BHR8  | BHR12B | BHR24 |
|----------------------------------|-------|-------|-------|-------|--------|-------|
| SiO <sub>2</sub>                 | 51.70 | 47.40 | 43.00 | 55.10 | 54.50  | 52.60 |
| TiO <sub>2</sub>                 | 2.08  | 2.38  | 1.40  | 0.68  | 0.58   | 0.55  |
| Al <sub>2</sub> O <sub>3</sub>   | 19.80 | 17.40 | 13.60 | 20.00 | 20.80  | 18.20 |
| Fe <sub>2</sub> O <sub>3</sub> * | 12.36 | 12.50 | 10.86 | 6.11  | 7.53   | 6.08  |
| MnO                              | 0.03  | 0.14  | 0.11  | 0.04  | 0.16   | 0.07  |
| MgO                              | 1.31  | 2.77  | 1.51  | 4.04  | 2.85   | 3.96  |
| CaO                              | 1.14  | 4.72  | 12.06 | 1.30  | 1.75   | 3.97  |
| Na <sub>2</sub> O                | 5.35  | 1.96  | 4.29  | 6.17  | 6.62   | 7.22  |
| K <sub>2</sub> O                 | 2.54  | 2.99  | 1.47  | 1.49  | 1.29   | 0.13  |
| P <sub>2</sub> O <sub>5</sub>    | 0.12  | 0.42  | 0.57  | 0.23  | 0.08   | 0.27  |
| L.O.I                            | 3.12  | 7.23  | 10.92 | 3.43  | 4.19   | 5.04  |
| Total                            | 99.55 | 99.91 | 99.79 | 98.59 | 100.35 | 98.09 |
| Density <sup>†</sup>             | 2.840 |       | 2.825 | 2.622 |        | 2.585 |
| Rb                               | 73    | 89    | 41    | 59    | 37     | 0     |
| Sr                               | 274   | 109   | 230   | 434   | 465    | 631   |
| Ba                               | 327   | 489   | 148   | 363   | 336    | 125   |
| Zr                               | 296   | 223   | 209   | 129   | 81     | 121   |
| Nb                               | 16    | 12    | 10    | 18    | 7      | 14    |
| Y                                | 28    | 46    | 51    | 15    | 6      | 13    |
| Ga                               | 29    | 23    | 22    | 28    | 24     | 20    |
| V                                | 159   | 84    | 89    | 138   | 131    | 120   |
| Cr                               | 0     | 57    | 0     | 27    | 20     | 25    |
| Ni                               | 0     | 56    | 0     | 58    | 48     | 44    |
| Cu                               | 0     | 0     | 0     | 8     | 35     | 10    |
| Zn                               | 87    | 104   | 76    | 94    | 74     | 75    |

\*Major elements in oxide wt. %. Total Fe as Fe<sub>2</sub>O<sub>3</sub>.Trace elements in ppm. <sup>†</sup>Density in g/cc.

Samples BHR3, BHR1 and BHR5 are hematite bearing.

Samples BHR8, BHR12B and BHR24 are chlorite bearing.

(compare BHR3 and BHR8, Table 4.26). Some of the compositional variation can be related to the addition of carbonate (as shown by increasing LOI values) to the rocks with the most important effect being an increase in CaO with LOI (compare BHR3 to BHR5 and BHR8 to BHR24). Chlorite rich samples from unit C3 (eg. BHR24) cannot be distinguished from chlorite rich samples from unit C2 (eg. BHR8 and BHR12B), possibly because metasomatism has homogenized the compositions, or alternatively because they were originally similar in composition. The observation that both rocks contain abundant albitized phenocrysts supports the latter hypothesis.

In discussing the effects of metasomatism an approach similar to that discussed for the Cape St. Mary's extrusive rocks is employed. The least altered samples are identified and compared, while accounting for volume changes, with samples showing greater alteration. In the case of the Beaver Harbour volcanic rocks this is difficult because samples containing primary minerals were not observed. All of the chlorite rich samples probably have highly altered compositions because their  $Mg'$  values ( $Mg' = Mg/Mg + 0.9Fe$  atomic), which are about 0.65, are unreasonable given their relatively high  $SiO_2$  contents (55 to 60 wt. % volatile free). Similarly their  $TiO_2$  concentrations are unreasonably low given that Nb/Y (1.2) ratios are representative of alkaline rocks.

Samples of the hematite rich rocks with low LOI (eg. BHR3) show unusual compositions, but they are not unreasonable. They are comparable to some of the highly evolved feeder pipe samples from Cape St. Mary's as well as some Cambrian flows from Norway (see section 4.7). Internal consistency between the major and trace element indications of petrogenetic character as well as the degree of evolution (section 4.5.3) suggests that the rocks may represent (relatively) primary compositions. Although it is impossible to prove this, these rocks are clearly better candidates than the chlorite rich samples.

#### Presentation of Data

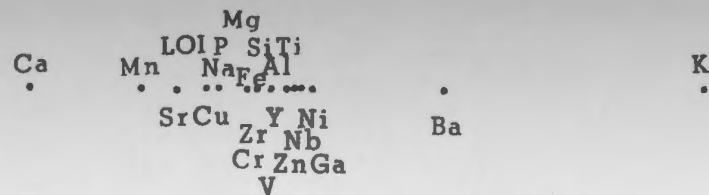
The following discussion documents 1) the relationship between the hematite rich samples and chlorite rich samples, 2) the effect of carbonate addition on the chlorite rich samples, and 3) the effect of carbonate addition on the hematite rich samples. In order to account for volume changes, methods described by Gresens (1967) are used (see section 4.2.1 for details of approach).

A plot of volume changes ( $f_v$  values) necessary to account for the concentrations of various elements in the chlorite sample BHR8, assuming it was derived from a rock with a composition represented by the hematite rich sample BHR3, are shown in Figure 4.32. Elements with low  $f_v$  values have probably been added to BHR8, and those with high values metasomatically removed. In the middle of the distribution

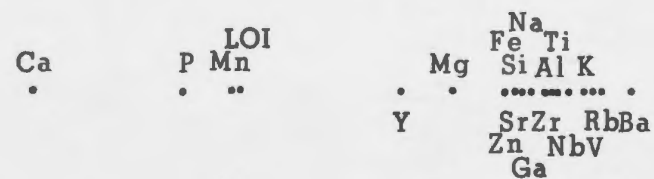
Figure 4.32 Volume factor diagram for three Cambrian basalt samples from Beaver Harbour. The diagram shows the volume change ( $f_v$ ) necessary to account for the concentration of each element in three samples assuming BHR3 was the parent rock for "a" and "b" and BHR8 was the parent in case "c". See text for discussion.



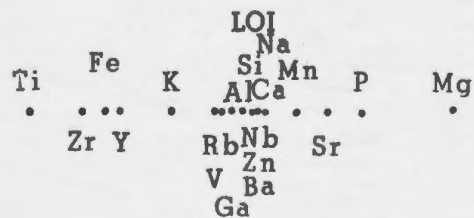
BHR 8 → BHR 24



BHR 3 → BHR 5



BHR 3 → BHR 8



fv

.1

1

10

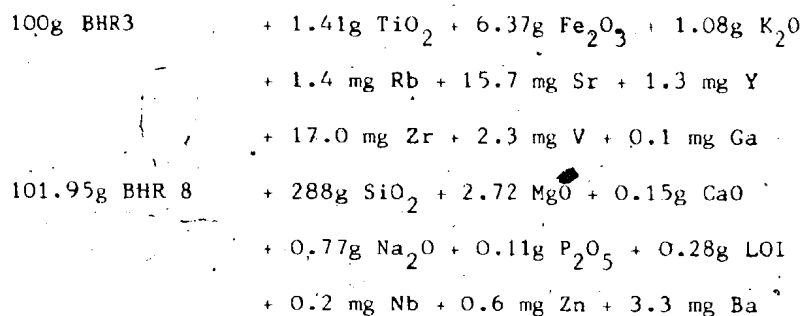
of points, and in the center of where elements tend to cluster is Al with an  $f_v$  value of 0.933. Apparently this element was relatively unaffected by the metasomatic reactions which produced BHR8. Assuming constant Al and a 7 percent volume decrease, an equation may be written which relates additions and subtractions of each element (Equation 1 Table 4.27). These results are graphically displayed in Figure 4.33a where the values of each element divided by  $Al_2O_3$  in BHR8, are compared by division to the element/ $Al_2O_3$  ratio in BHR3. Elements plotting above the line, in particular Mg, Sr, P, and Mn were added to BHR8. Those elements which show depleted concentrations in BHR8 plot below the line and include K, Rb, Ti, Zr, V, and Fe.

The effects of metasomatic reactions which added carbonate to both the chlorite rich and hematite rich samples are remarkably different from those associated with the formation of the chlorite rich samples discussed above. Plots of  $f_v$  assuming constant volume for each element (Figure 4.32b and 4.32c) show similar patterns for both the hematite rich rocks (BHR3 yields BHR5) and the chlorite rich samples (BHR8 yields BHR24). Note, however, that much less carbonate was added to BHR24 than to BHR5 (compare LOI in Table 4.26).

The  $f_v$  diagrams show that Ca was almost certainly added to the rocks during metasomatism. The diagrams also show that if Al remained constant certain amounts of all of the

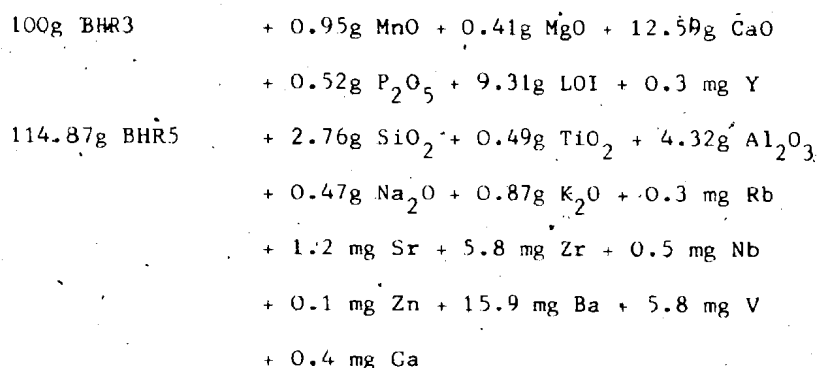
Table 4.2 7' Alteration equations - Beaver Harbour metavolcanic rocks.

## Equation 1



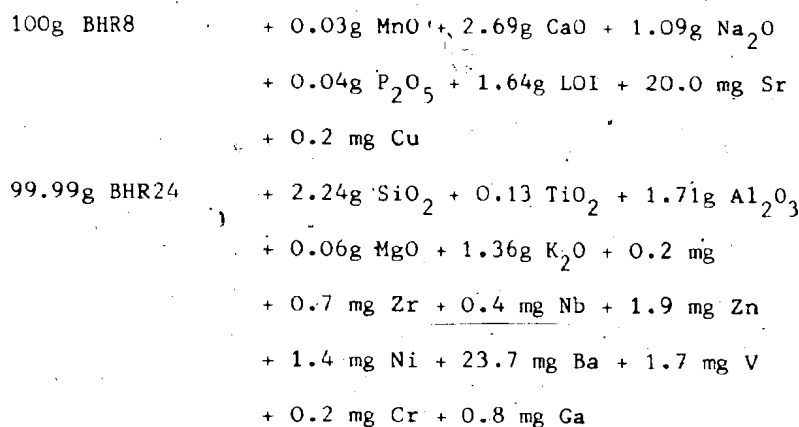
$f_v = 0.933$  assuming  $\text{Al}_2\text{O}_3$  assuming  $\text{Al}_2\text{O}_3$  was constant.

## Equation 2



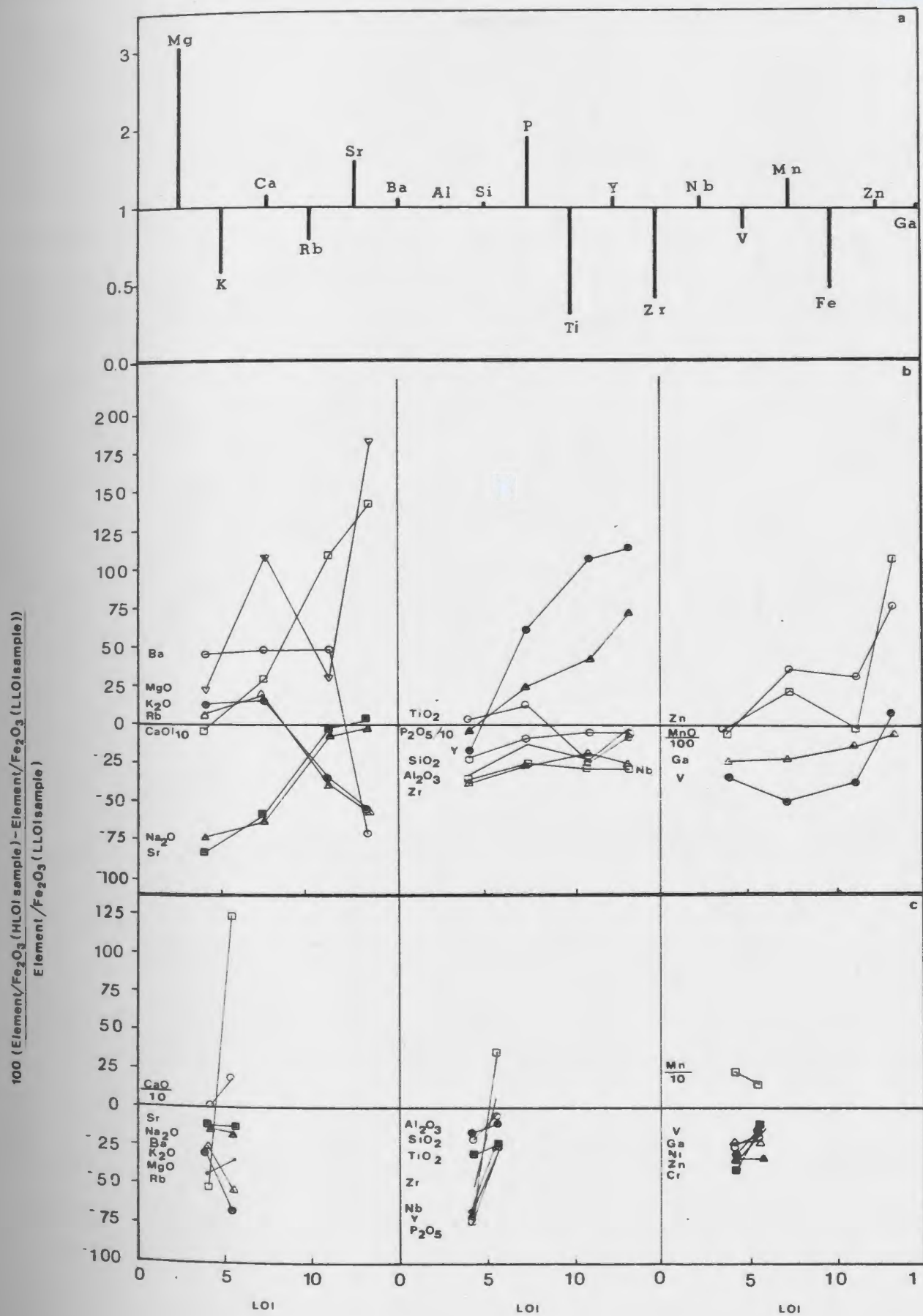
$f_v = 1.14$  assuming  $\text{Fe}_2\text{O}_3$  was constant.

## Equation 3



$f_v = 1.01$  assuming  $\text{Fe}_2\text{O}_3$  was constant.

Figure 4.33 Diagram showing the effect of metasomatism on Beaver Harbour samples. A. Enrichment/depletion diagram showing the effect of chlorite formation. Elements plotting above the base line were enriched and those below depleted in the chlorite rich sample BHR8 assuming that  $\text{Al}_2\text{O}_3$  remained constant and BHR3 represents the parent rock. The B. and C. portions of the diagram show the effect of adding carbonate to the hematite rich and the chlorite rich samples (respectively) assuming  $\text{Fe}_2\text{O}_3$  remained constant. See text for discussion.



major elements, with the exceptions of Ti and K, would have to be added as a result of carbonation. Although this is possible, a better assumption may be that an element with a slightly lower  $f_v$  value remained constant. Iron is an important constituent of both chlorite and hematite, and although it was probably mobile during the reactions which led to the formation of chlorite from hematite, the presence of one of the two minerals during carbonation reactions may have resulted in its relative immobility. Supporting this argument is the observation that Fe plots in the middle of the point distribution shown in Figures 4.32b and 4.32c.

Assuming that Fe remained constant during the carbonate metasomatism of both the chlorite bearing and hematite bearing samples, equations 2 and 3 (Table 4.27) relate the additions and subtractions involved in the reactions. The percentage changes in element/ $\text{Fe}_2\text{O}_3$  ratios between sample BHR3 and other hematite bearing samples with various LOI contents are shown in Figure 4.33b. Elements plotting above the baseline were enriched in the more altered samples, assuming  $\text{Fe}_2\text{O}_3$  was immobile.

Elements commonly considered immobile are shown in the middle of Figure 4.33b. Some such as Al, Si, Zr, and Nb plot relatively close to the baseline and do not change appreciably with LOI. This suggests that the carbonate metasomatism had very little effect on their concentrations, or on the Fe concentrations, since they are divided by the

latter. Elements such as P, and Y, as well as Zn, and Mn have apparently been increasingly added with the carbonate. It is important to note that the effect of using any of the above elements as the immobile element would result in only slight shifts in where all other elements plot relative to the baseline. Even more importantly, the direction of change with increasing LOI, of elements such as P, would not be affected.

The alkaline and alkaline earth elements were most affected by the addition of carbonate as shown in the first section of Figure 4.33b. Although Na and Sr were initially strongly depleted, their concentrations show a regular increase with LOI. Both Ca and Mg show an overall tendency to increase with LOI but Ba, Rb, and K tend to decrease.

A similar diagram was constructed for the chlorite rich samples but the range of LOI values in the analyzed samples is much smaller than in the hematite rich samples, and two samples had nearly identical LOI values. As a result only two sets of data representing a limited range of LOI values are shown in Figure 4.33c. This makes it difficult to draw conclusions as to whether elements show any correlation with LOI. However the direction of movement of most elements appears to be the same as in Figure 4.33b, the most notable exceptions being Rb, Nb, Zr, and Mn.

The chondrite normalized REE patterns for two chlorite rich samples (BHR8 and BHR25) and two hematite rich samples

(BHR3 and BHR23) are shown in Figure 4.34 (concentrations given in Table 4.28). The patterns for BHR8 and BHR23 differ from those normally seen in unaltered basalts and andesites in that they are not smooth curves. Hematite rich samples show patterns which are convex upward with the highest normalized concentrations between Sm and Gd. The chlorite rich samples tend to show straighter patterns and one (BHR25) shows LREE enrichment.

#### Discussion

The alteration of the Beaver Harbour volcanic rocks resembles that of the Cambrian lavas in Newfoundland (Chapter 4) in that the reactions can be separated into two parts. The first and probably early phase resulted in the formation of chlorite especially in samples from the upper portions of unit C2 and all of unit C3. The second phase, carbonate metasomatism, resulted in the addition of carbonate to the rocks, and variably affected all portions of units C2 and C3.

Metasomatic reactions which led to the formation of chlorite resulted in major additions of Mg, Sr, P, and Mn, and removal of K, Rb, Ti, Zr, V, and Fe (Figure 4.33a). These observations resemble the results of experimental studies on basaltic rocks which modelled the formation of chlorite through interaction with seawater (Mottl, 1983). The experiments indicate that Mg is greatly enriched in the altered rocks and that Ca, K, Mn, Fe, and Si are leached.



Figure 4.34 Chondrite-normalized REE patterns of Beaver Harbour metabasalts. The normalizing values are from Taylor and Gorton (1977).

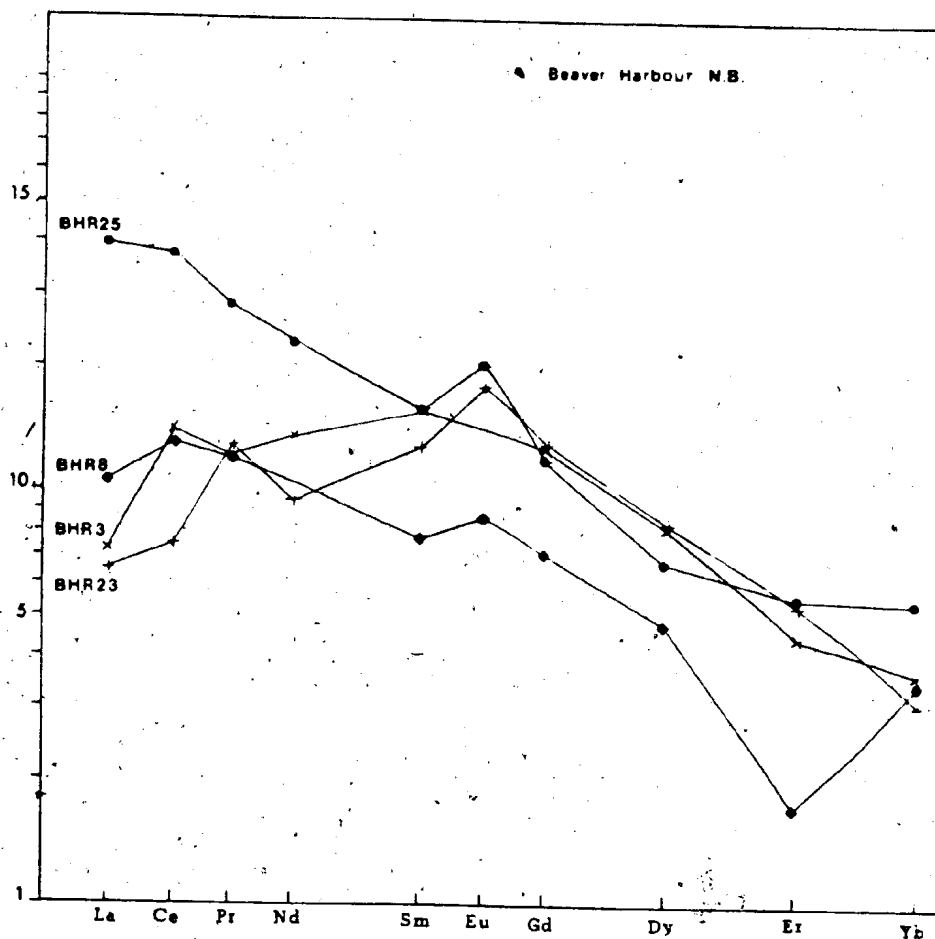


Table 4.28. Rare earth element concentrations in four Beaver Harbour meta-basalt samples.

|                        | BHR3     | BHR23    | BHR8     | BHR25    |
|------------------------|----------|----------|----------|----------|
| Rock Type <sup>1</sup> | Hematite | Hematite | Chlorite | Chlorite |
| L.O.I. <sup>2</sup>    | 3.12     | 3.99     | 3.43     | 5.45     |
| La                     | 2.24     | 2.04     | 3.37     | 12.6     |
| Ce                     | 11.2     | 6.01     | 10.7     | 30.1     |
| Pr                     | 1.43     | 1.19     | 1.50     | 3.26     |
| Nd                     | 8.20     | 5.65     | 6.35     | 14.0     |
| Sm                     | 3.04     | 2.53     | 1.55     | 3.10     |
| Eu                     | 1.01     | 1.26     | 0.62     | 1.46     |
| Gd                     | 3.32     | 3.39     | 1.83     | 3.11     |
| Dy                     | 2.69     | 2.70     | 1.56     | 2.20     |
| Er                     | 1.15     | 6.97     | 0.37     | 1.17     |
| Yb                     | 0.67     | 0.77     | 0.73     | 1.13     |

1. Rock type refers to whether the samples are hematite rich or chlorite rich.
2. L.O.I. values in wt. %.
3. REE concentrations in ppm.

Important differences between the experiments and the Beaver Harbour rocks are that Ca, Si and Mn are enriched in the latter. The differences (particularly in the case of Ca and Mn) may be ascribed to minor overprinting by the carbonate metasomatism.

In natural systems Fe commonly increases in response to the formation of chlorite. According to Mottl (1983) this results from the fixation of Fe through pyrite precipitation. Pyrite did not form in appreciable quantities during the metasomatism of the Beaver Harbour rocks, possibly because the passing solutions were  $H_2S$  poor. Another explanation might be that the highly oxidized nature of the primary Beaver Harbour rocks (as indicated by the abundance of hematite) prevented reducing conditions necessary for the precipitation of pyrite.

The elements Sr, Ba, Rb, and K are commonly enriched during the alteration of basaltic glass by seawater (eg. Frey et al., 1974). In the case of the Beaver Harbour rocks only the first two were enriched and in the Newfoundland lavas all four elements were leached during the chloritization reactions. These observations are probably related to the fact that primary feldspar (which might be expected to hold the elements) no longer exists even in the least altered samples from the two areas. Chromium, Ni, and Cu concentrations tend to be very low in the hematite rich samples but show higher concentrations in the chloritized

rocks. These elements were also added during the formation of chlorite in the Chapel Arm basalts (Chapter 4).

It is apparent that the "immobile" elements did not behave as such during the formation of chlorite (Figure 4.33a). Titanium and Zr were substantially depleted and P enriched. Hellman et al. (1979) report that Ti, Zr, and P are depleted in the Maddina metabasalts (Australia) as a result of metasomatism. The behaviour of these elements apparently varies considerably from one locality to another. These variations could be related to differences in the composition of the volatile phase (ie.  $H_2O$ ,  $CO_2$ , F, and Cl content), the concentration of each element in the volatile phase when it enters the volcanic rocks, the phases present in the rocks, and pressure and temperature differences affecting partitioning between the mineral and fluid phases. Until the effects of each of these variables are better understood, the implications of differences in element behaviour will remain unknown.

The behaviour of the LREE in BHR3 (originally a vitric lapilli tuff) is identical to that observed in altered ocean floor basaltic glass (cf. Frey et al., 1974). Lanthanum is depleted and Ce enriched to produce a Ce anomaly (Figure 4.34). Depletion of the HREE commonly accompanies the La removal and Ce enrichment but it is impossible to prove that this has happened in BHR3. Frey et al. (1974) and Floyd (1977) report that the alteration of crystalline rocks

results in LREE enrichment, which may explain the REE pattern shown by BHR25.

In summary a comparison of the low carbonate hematite rich rocks with low carbonate chlorite rich rocks shows that the latter were probably derived from the former through metasomatism. The most important evidence in favour of this is that Mg was substantially enriched and Fe depleted. A cursory review of the literature shows that the behaviour of most other elements varies considerably from one locality to another and that there is nothing particularly unusual about the Beaver Harbour samples.

The effects of the carbonate metasomatism overprint those of chlorite formation and can be seen in both the chlorite and hematite rich rocks. This phase of metasomatism can be viewed as a cumulative and progressive process which led to a suite of rocks with variable carbonate contents. The following discussion relates primarily to the hematite rich samples and their characteristics as displayed in Figure 4.33b.

Although most of the important changes in element concentrations shown in Figure 4.33b can be related to the addition of carbonate, there are a few, which will be dealt with first, that may be related to other processes. All samples shown are compared to BHR3 which has the lowest LOI (3.12 wt. %) observed. Sodium and Sr are substantially depleted in the sample with lowest LOI shown in Figure 4.33b

(4 wt. %). As LOI increases both Sr and Na increase such that it is difficult to explain their initial large depletion in terms of carbonate addition. Processes such as the breakdown of feldspars to form albite, as well as the formation of some chlorite may account for the initial large depletion of Na and Sr. However, the strong correlation between LOI and the elements Rb, Sr, Na, and K suggests that all carbonated samples were initially affected by these processes.

The addition of carbonate had its most important effects on the alkali and alkaline earth metals as was observed for the Chapel Arm and Cape Dog lavas discussed in Chapter 4. As in the Newfoundland metabasalts Ca, Sr and Na show a positive correlation with LOI. One of the most important differences between the two localities is that MgO increases in the Beaver Harbour samples. Similarly Ba, K, and Rb decrease with LOI in the Beaver Harbour rocks but remain relatively constant in the Chapel Arm and Cape Dog samples.

The differences in behaviour are probably related to dolomite stability during the metasomatism. In the Newfoundland samples only calcite was observed. Metasomatic reactions involving high  $\text{CO}_2$  activity commonly produce increases in Ca, Sr, Na, and Mg and a loss of K and Rb (eg. Kerrich and Fyfe, 1981; Strong, 1982).

It appears that Ti, Si, Al, Zr, and Fe remained relatively immobile during the carbonate metasomatism of the Beaver Harbour rocks. Hynes (1980) found that Ti, was enriched and Zr, and Y depleted during carbonatization of some metabasalts from Quebec. Yttrium however is strongly enriched with increasing LOI in the Beaver Harbour samples, as is P. The precipitation of apatite can account for both of these observations and may also indicate that F concentrations were high because this element commonly shows high concentrations in apatite (cf. Deer et al., 1966). The enrichment of Na, Y, P, Zn, Sr, Mg, and Ca, as well as removal of Ba, Rb, and K, closely resembles that observed in peralkaline systems where  $\text{CO}_2$  and F are important constituents of the volatile fluids (eg. Taylor et al., 1981; Strong, 1982). It is unlikely that the metasomatic solutions had a magmatic source which implies that high  $\text{CO}_2$  and F rich solutions need not occur solely in igneous settings.

#### 4.5.2 Alteration Geochemistry - Long Reach Area

As a group the volcanic rocks from the Long Reach area in New Brunswick are much better preserved than those from Beaver Harbour (see petrography Chapter 3). Most samples show less than 5 wt. % LOI and many of the basaltic samples contain primary pyroxenes. As the following discussion will show, most of the geochemical characteristics of the Long Reach rocks can best be interpreted in terms of primary



igneous processes.

#### 4.5.3 Primary Whole-Rock Geochemistry

The major element and normative compositions of representative samples of the New Brunswick volcanic rocks, which have relatively low LOI values and in most cases some relict pyroxene grains, are given in Table 4.29. Trace element analyses are presented in Table 4.30, and REE data for the Long Reach samples may be found in Table 4.31. Appendix A contains a description of the analytical methods used, and a complete listing of all bulk-rock data is given in Appendix B. In confirmation of indications from the petrography, major element and trace element variation diagrams (Figures 4.35 and 4.36) show that the New Brunswick rocks can be separated into four groups; the feldspar phyric basalts, the aphyric basalts and the felsic rocks from the Long Reach area, and the Beaver Harbour basalts.

#### Beaver Harbour Samples

Only two of the non-chloritized Beaver Harbour basalts showed LOI values less than 5 wt. % LOI. The norms for these rocks show large amounts of Hy. Their low CaO and MgO, high  $Al_2O_3$ , FeO, and  $TiO_2$ , and low Mg' values (0.22 to 0.18) show that they are highly evolved basalts or basaltic andesites (Table 4.29 and Figures 4.35, 4.37, and 4.38). The  $Al_2O_3$  values of some of the differentiated Cambrian volcanic rocks from Newfoundland approach those of the Beaver Harbour rocks

Table 4.29. Major element composition of least altered New Brunswick volcanic rocks.

|                                | BHR3  | BHR23 | GWD4  | GWD9  | GWD8   | GWD12 | GWD23 | GWD14 | GWD17 |
|--------------------------------|-------|-------|-------|-------|--------|-------|-------|-------|-------|
| SiO <sub>2</sub>               | 51.70 | 51.70 | 52.00 | 47.20 | 50.70  | 47.90 | 48.20 | 64.20 | 73.10 |
| TiO <sub>2</sub>               | 2.08  | 2.73  | 2.10  | 2.36  | 0.75   | 0.66  | 1.05  | 0.59  | 0.32  |
| Al <sub>2</sub> O <sub>3</sub> | 19.80 | 17.00 | 12.70 | 12.80 | 16.20  | 17.00 | 16.00 | 13.60 | 13.80 |
| Fe <sub>2</sub> O <sub>3</sub> | 12.36 | 15.60 | 15.72 | 17.24 | 8.35   | 9.57  | 9.43  | 8.96  | 2.04  |
| MnO                            | 0.03  | 0.02  | 0.11  | 0.28  | 0.28   | 0.21  | 0.17  | 0.06  | 0.06  |
| MgO                            | 1.31  | 2.05  | 1.55  | 6.33  | 8.50   | 7.83  | 9.58  | 2.51  | 1.19  |
| CaO                            | 1.14  | 1.04  | 4.65  | 5.89  | 7.60   | 9.20  | 10.29 | 0.60  | 0.97  |
| Na <sub>2</sub> O              | 5.35  | 1.89  | 6.27  | 4.07  | 3.17   | 3.44  | 1.93  | 0.68  | 2.93  |
| K <sub>2</sub> O               | 2.54  | 3.67  | 0.11  | 0.42  | 0.16   | 0.01  | 0.28  | 3.65  | 1.74  |
| P <sub>2</sub> O <sub>5</sub>  | 0.12  | 0.15  | 0.34  | 0.33  | 0.11   | 0.14  | 0.10  | 0.25  | 0.05  |
| L.O.I.                         | 3.12  | 3.99  | 2.61  | 2.59  | 4.50   | 3.76  | 2.58  | 3.19  | 2.00  |
| Total                          | 99.55 | 99.84 | 98.16 | 99.51 | 100.32 | 99.72 | 99.53 | 98.29 | 98.20 |
| Mg <sup>1</sup>                | 0.18  | 0.22  | .18   | .45   | .69    | .64   | .69   | -     | -     |
| CIPW Norms                     |       |       |       |       |        |       |       |       |       |
| Or                             | 12.79 | 12.96 | 0.61  | 2.13  | 0.87   | 0.05  | 1.48  | 8.69  | 3.73  |
| Ab                             | 40.96 | 10.14 | 52.85 | 31.42 | 26.11  | 27.31 | 15.48 | 2.46  | 9.53  |
| An                             | 4.29  | 2.59  | 5.81  | 13.26 | 27.07  | 27.34 | 30.53 | 0.59  | 1.71  |
| Ne                             | 0.00  | 0.00  | 0.00  | 0.00  | 0.00   | 0.00  | 0.00  | 0.00  | 0.00  |
| Q <sup>1</sup>                 | 2.54  | 37.94 | 0.00  | 0.00  | 1.45   | 0.00  | 0.00  | 69.52 | 76.49 |
| Ol                             | 0.00  | 0.00  | 7.47  | 25.82 | 0.00   | 21.98 | 5.82  | 0.00  | 0.00  |
| Hy                             | 15.84 | 15.31 | 9.43  | 7.26  | 32.43  | 6.36  | 26.23 | 7.84  | 1.49  |
| Di                             | 0.00  | 0.00  | 13.85 | 10.18 | 6.99   | 12.33 | 14.59 | 0.00  | 0.00  |
| Il                             | 6.18  | 5.68  | 6.87  | 7.07  | 2.40   | 2.03  | 3.27  | 0.83  | 0.09  |
| Mt                             | 2.23  | 1.56  | 2.45  | 2.25  | 2.40   | 2.31  | 2.34  | 1.05  | 0.00  |
| Ap                             | 0.20  | 0.18  | 0.63  | 0.56  | 0.20   | 0.24  | 0.18  | 0.20  | 0.04  |

Table 4.29(continued)

\*Total Fe as  $\text{Fe}_2\text{O}_3$ . Oxides in weight percent.

Norm calculated assuming  $\text{Fe}_2\text{O}_3 = 1.5$  weight percent and remaining Fe = FeO.

BHR3 + BHR23 = Beaver Harbour basalts.

GWD4 + GWD9 = FeldsparPhyric basalts at Browns Flat.

GWD8 + GWD12 = Aphyric basalts at Browns Flat.

GWD23 = Aphyric flow (?) at Greenwich Hills.

GWD14 + GWD17 = Felsic volcaniclastics at Browns Flat.

Table 4.30. Trace element concentrations in least altered New Brunswick volcanic rocks.

|    | BHR3 | BHR23 | GWD7 | GWD9 | GWD8 | GWD12 | GWD23 | GWD14 | GWD17 |
|----|------|-------|------|------|------|-------|-------|-------|-------|
| Rb | 73   | 99    | 18   | 14   | 3    | 1     | 6     | 144   | 67    |
| Sr | 274  | 58    | 344  | 323  | 344  | 327   | 213   | 19    | 228   |
| Ba | 327  | 601   | 454  | 346  | 111  | 82    | 149   | 82    | 748   |
| Zr | 296  | 245   | 185  | 149  | 54   | 49    | 47    | 166   | 143   |
| Nb | 16   | 13    | 8    | 8    | 3    | 3     | 4     | 31    | 10    |
| Y  | 28   | 29    | 73   | 66   | 22   | 17    | 12    | 60    | 50    |
| Ga | 29   | 28    | 24   | 21   | 17   | 16    | 13    | 17    | 19    |
| V  | 159  | 135   | 539  | 509  | 222  | 253   | 204   | 65    | 13    |
| Cr | 0    | 2     | 61   | 38   | 308  | 173   | 311   | 0     | 0     |
| Ni | 0    | 22    | 83   | 50   | 69   | 63    | 125   | 18    | 2     |
| Cu | 0    | 0     | 34   | 17   | 46   | 10    | 43    | 32    | 13    |
| Zn | 87   | 107   | 230  | 199  | 81   | 76    | 70    | 86    | 51    |

Locations as in Table 4.29.  
Element concentrations in ppm.

Table 4.31. REE concentrations in Long Reach basalt samples.

|    | GWD4 | GWD9 | GWD8 | GWD12 | GWD23 |
|----|------|------|------|-------|-------|
| La | 9.78 | 11.3 | 4.84 | 7.60  | 5.61  |
| Ce | 28.3 | 31.2 | 13.7 | 21.6  | 15.5  |
| Pr | 4.09 | 4.32 | 1.63 | 3.17  | 2.31  |
| Nd | 18.3 | 21.2 | 9.71 | 12.7  | 10.6  |
| Sm | 5.28 | 6.49 | 2.68 | 3.19  | 3.04  |
| Eu | 1.63 | 2.59 | 1.15 | 1.08  | 1.61  |
| Gd | 6.42 | 7.71 | 3.05 | 3.03  | 3.34  |
| Dy | 6.65 | 7.95 | 2.83 | 2.64  | 2.73  |
| Er | 3.89 | 4.41 | 1.63 | 1.26  | 0.95  |
| Yb | 3.02 | 4.18 | 1.00 | 0.68  | 0.85  |

Figure 4.35 Major element variation diagram - New Brunswick volcanic rocks. All concentrations are in wt. %, volatile free.

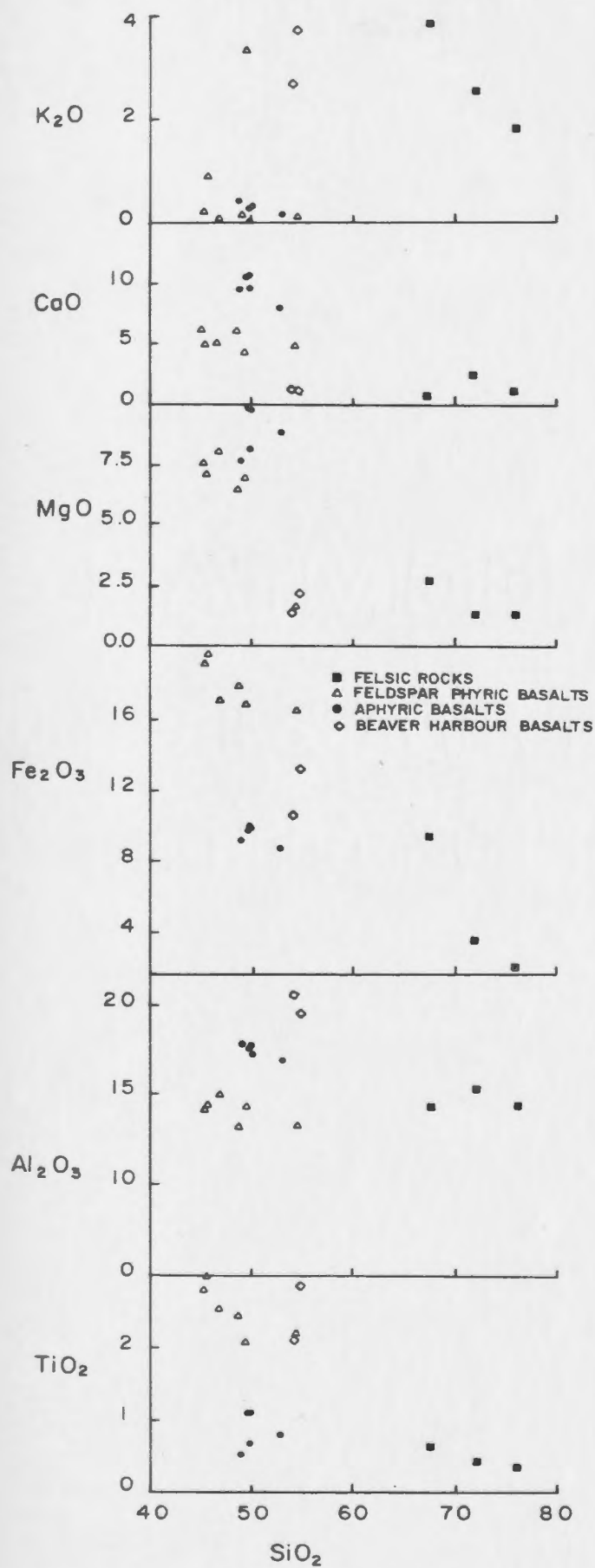


Figure 4.36 Trace element variation diagram - New Brunswick volcanic rocks. The  $\text{TiO}_2$  concentrations are in wt. %, volatile free and all others are in ppm.

X Beaver Harbour    Δ Feldspar Phyric Basalt  
 • Aphyrlic Basalt    ■ Felsic Rocks

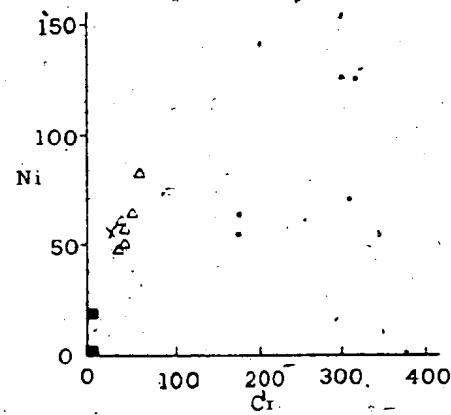
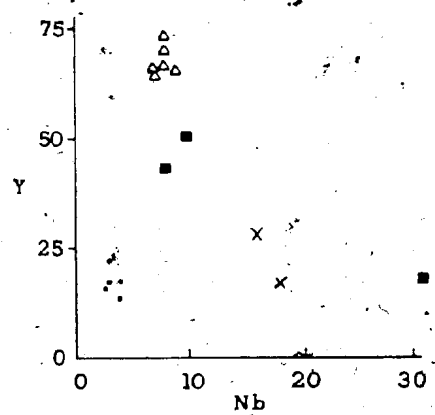
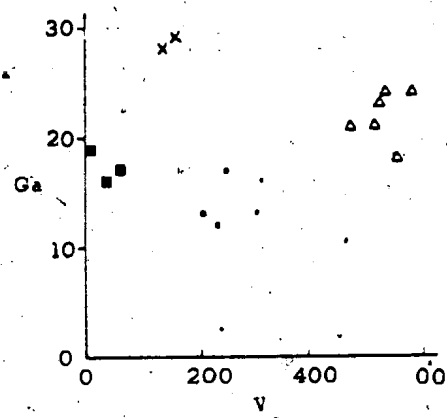
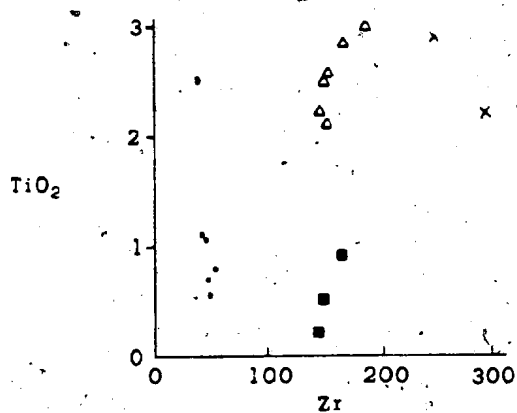




Figure 4.37 Mg' versus  $Al_2O_3$  diagrams. The  $Al_2O_3$  concentrations are in wt. %, volatile free. The information for the Cape Breton rocks is from Cameron (1980), for the Norwegian basalts from Furnes et al. (1983) and for the Avalon Cambrian rocks from this study.

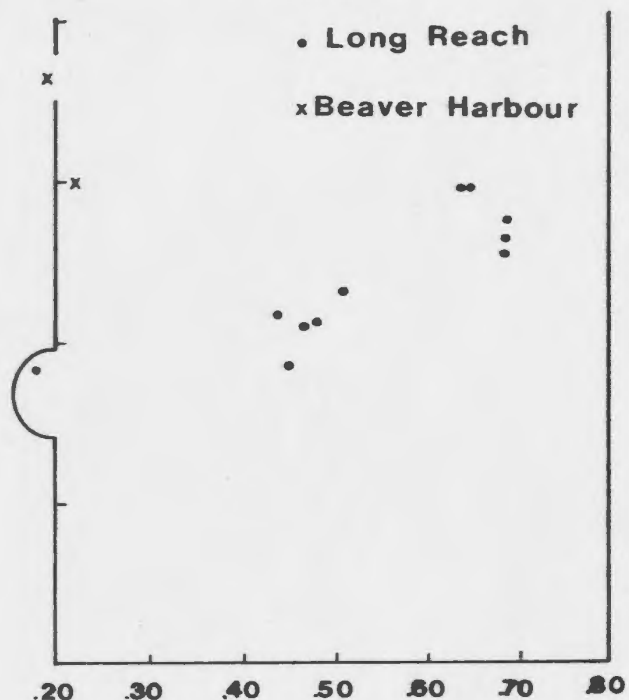
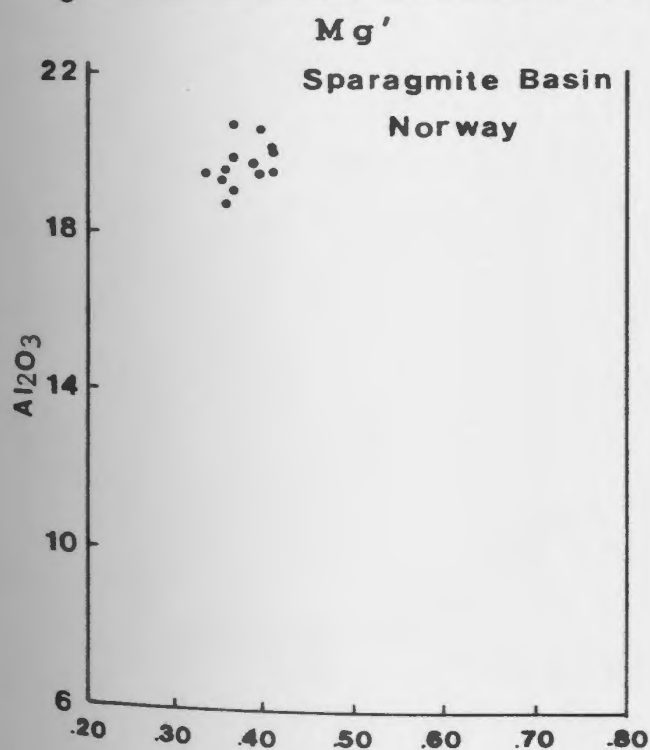
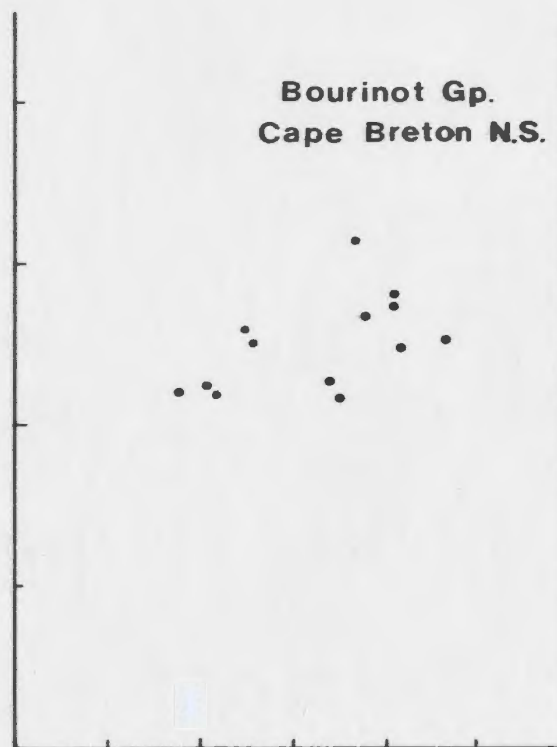
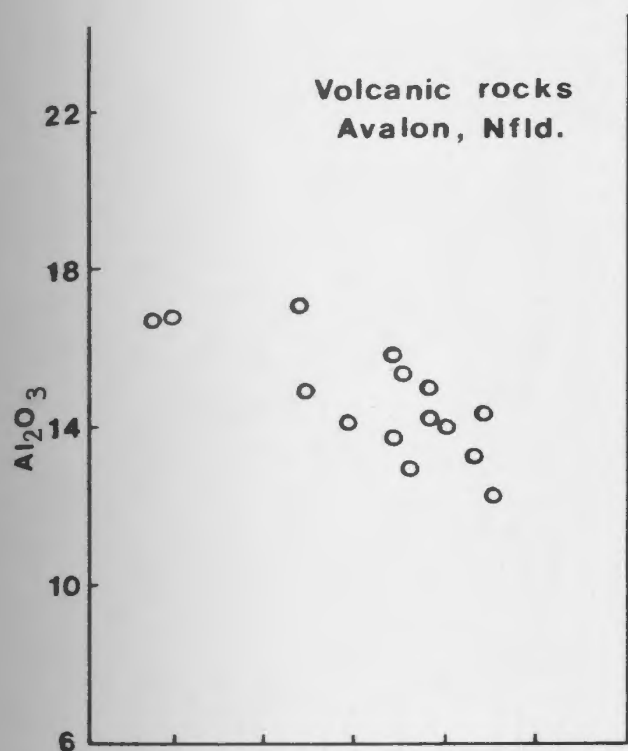
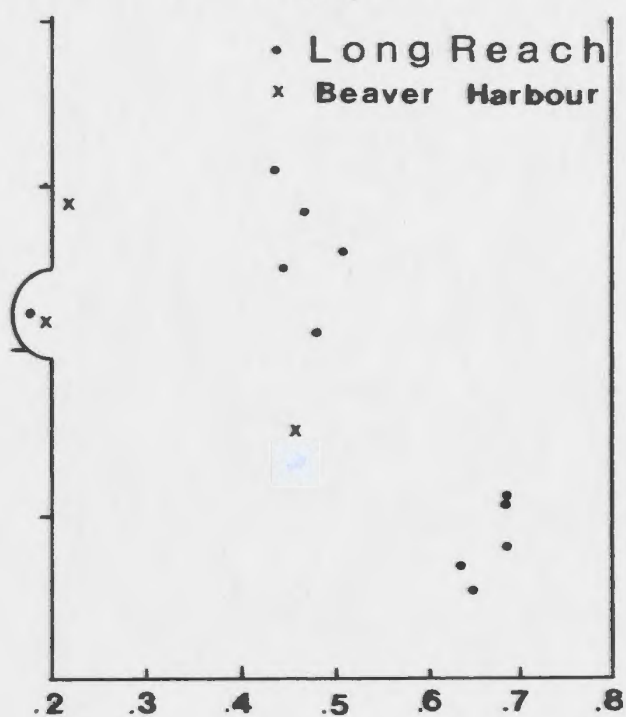
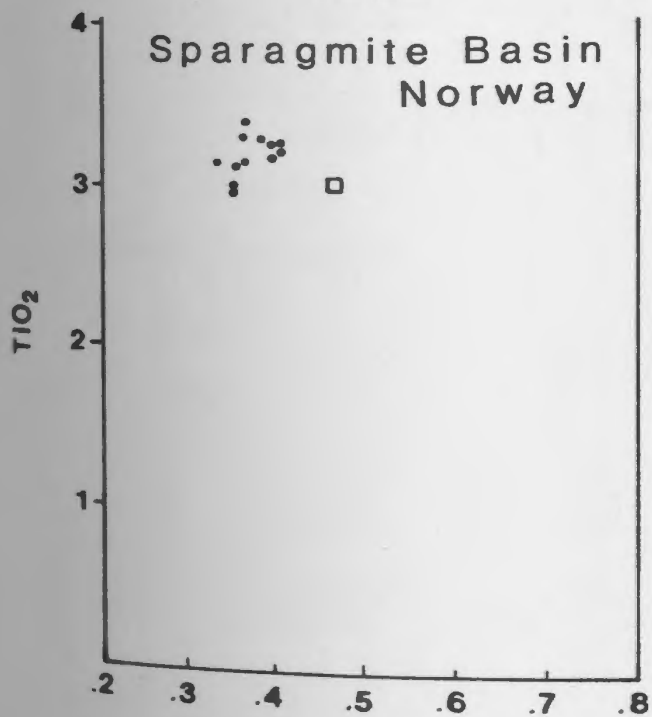
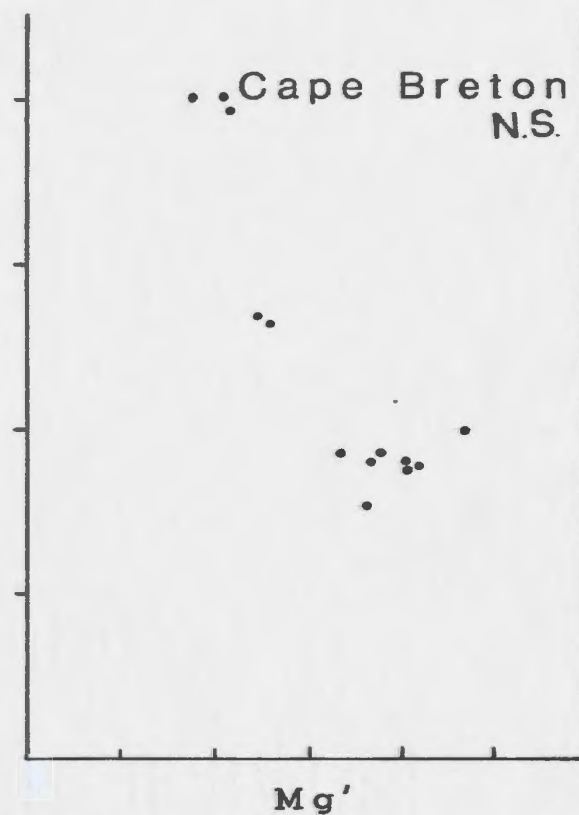
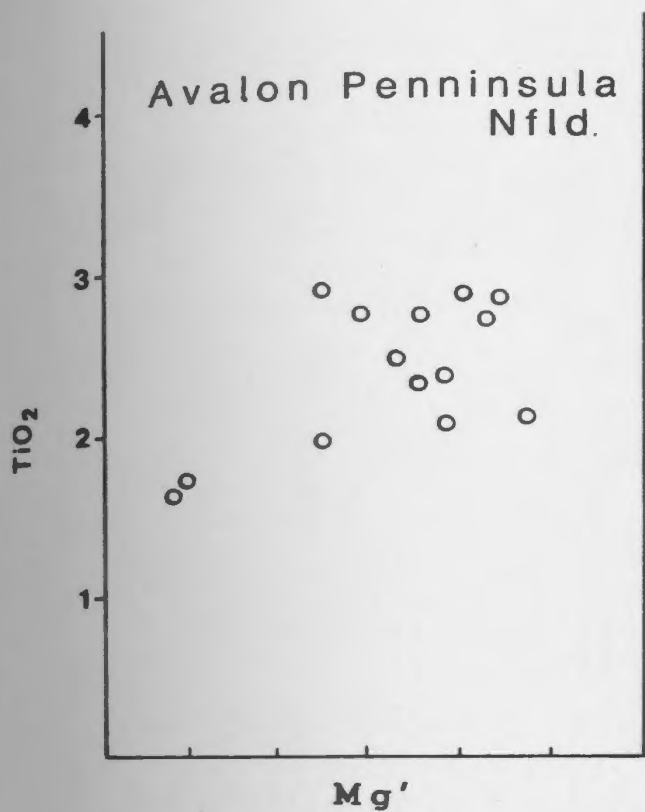


Figure 4.38 Mg' versus  $\text{TiO}_2$  diagrams. The  $\text{TiO}_2$  concentrations are in wt. %, volatile free. Data sources as in Figure 4.37.



and would probably equal the latter at lower  $Mg'$  values (Figure 4.37). Evolved basalts from the Sparagmite basin in Norway also show similar  $Al_2O_3$  values to those in the Beaver Harbour rocks.

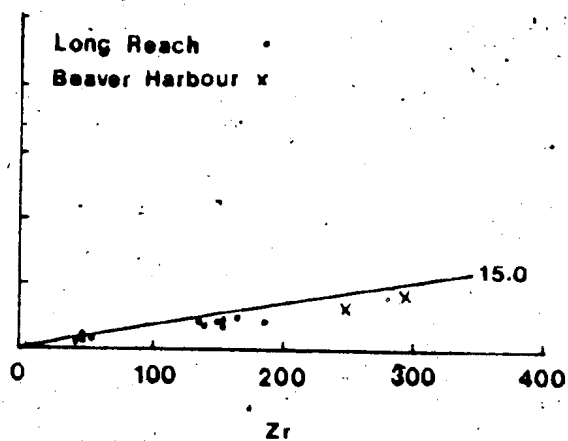
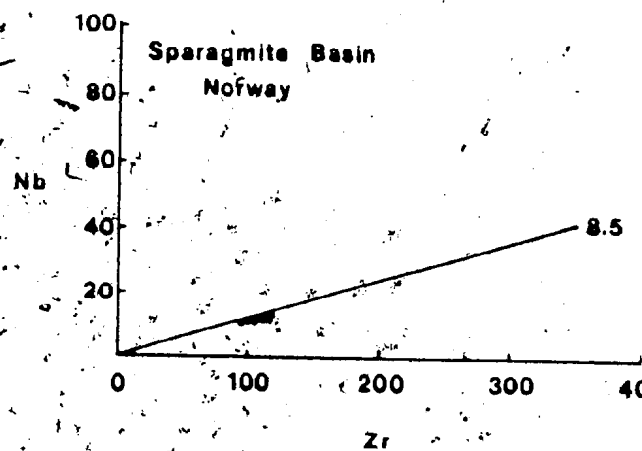
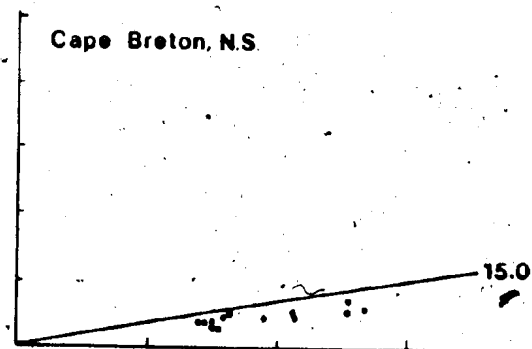
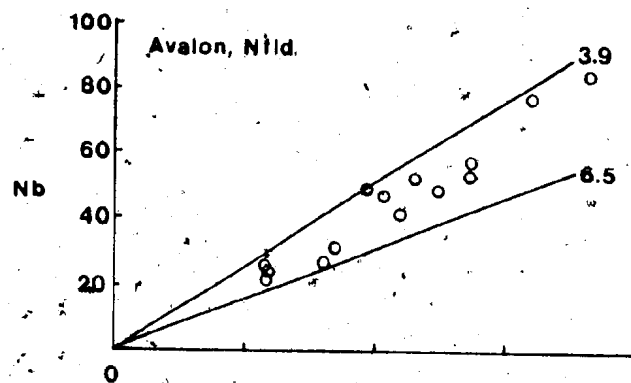
Low concentrations of  $Cr$  and  $Ni$ , and relatively high  $Ga$  and  $Zr$  also suggest that the rocks are highly evolved (Table 4.30 and Figure 4.36). The  $Zr/Nb$  ratios are approximately 18 (Figure 4.39) and  $Nb/Y$  ratios appear close to 0.5.

#### Long Reach Phyric Basalts

Although they are not nearly so evolved as the Beaver Harbour samples, the feldspar phyric basalts from the Long Reach area show low  $CaO$  and  $MgO$  as well as relatively low  $Mg'$  values (0.18 to 0.51) representative of differentiated basalts (Table 4.29 and Figures 4.35, 4.37, and 4.38). It is possible  $Mg$  was leached from sample GWD4 because the other geochemical characteristics of this rock are comparable to the other feldspar phyric basalts. The single most important difference between these evolved rocks and the Beaver Harbour samples is their lower  $Al_2O_3$  concentrations. Note that the rocks are  $H_y$  normative.

Trace element ratios such as  $Nb/Y$  (0.1 to 0.2) and  $Zr/Nb$  (15 to 18 see Figure 4.39) are similar to those in the Beaver Harbour rocks but concentrations of  $Zr$  and  $Nb$  are much lower (Table 4.30). Both  $Cr$  and  $Y$  show higher values in the Long Reach phyric basalts than the Beaver Harbour

Figure 4.39 Zr versus Nb diagrams. The Avalon volcanic rocks are distinguished from the other samples to emphasize their alkaline characteristics. All concentrations are in ppm, and data sources are the same as for Figure 4.37.



basalts. The Cr, V and Ti concentrations are in keeping with an evolved origin for the basalts. The chondrite normalized REE patterns for these basalts are flat (Figure 4.40, concentrations in Table 4.31). As is typical of evolved basalts the normalized heavy REE concentrations are above 10. The samples show only small Eu anomalies (both positive and negative).

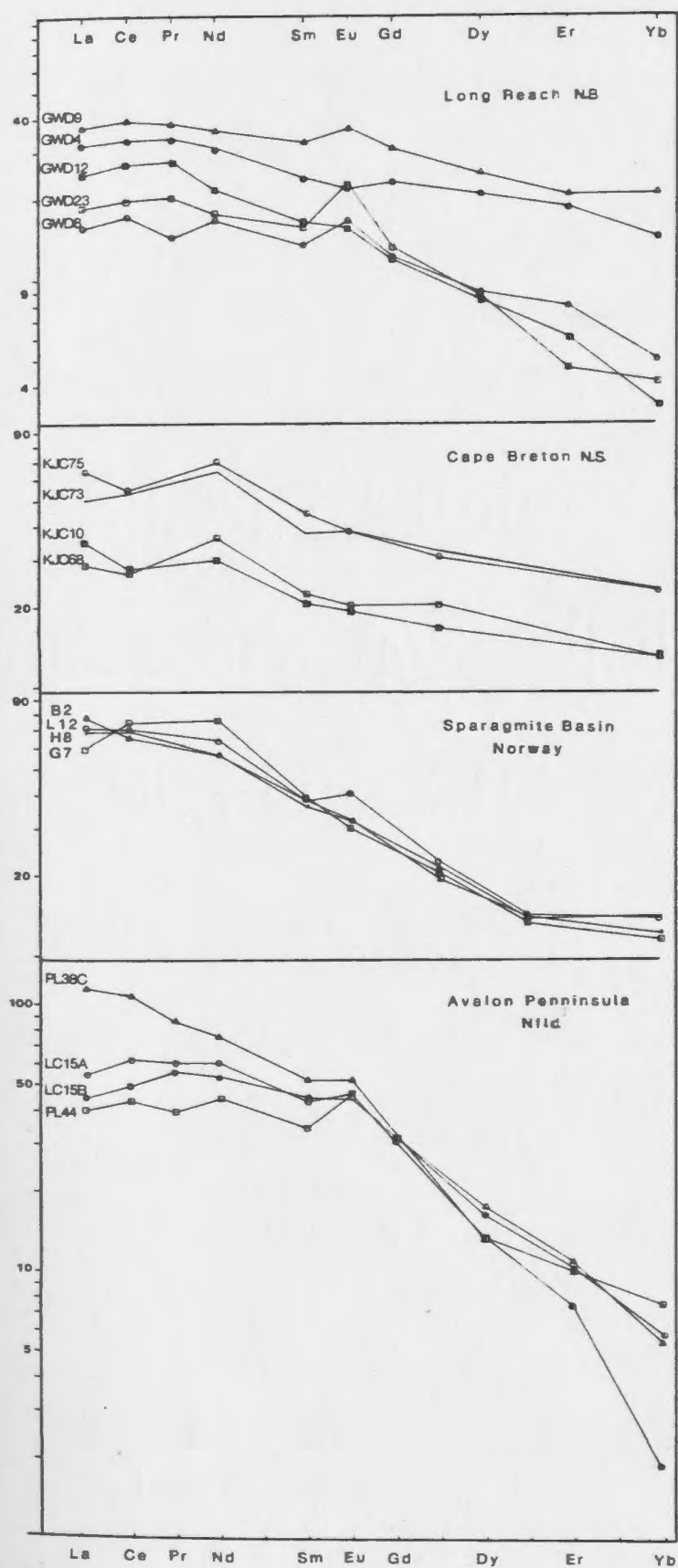
#### Long Reach Aphyric Basalts

In comparison with the other New Brunswick basalts the aphyric basalts display primitive compositions. Their Mg values are high (0.64 to 0.69), and  $TiO_2$  and  $P_2O_5$  concentrations low (Table 4.29 and Figures 4.35, 4.37, 4.38). All of the samples are hypersthene normative.

Concentrations of incompatible elements such as Nb, Zr, and Y are lower than in the other New Brunswick basalts (Table 4.30 and Figure 4.36). The Nb/Y ratios (0.14 to 0.33) tend to be slightly higher than in the feldspar phyric basalts but Zr/Nb ratios are similar in the two (Figure 4.39). Nickel and Cr show a range of concentrations in the aphyric basalts all of which are higher than in the other New Brunswick basalts. The chondrite normalized REE patterns for these rocks (Figure 4.40) show slightly steeper slopes than the feldspar phyric basalts, and the low heavy REE concentrations reflect the unevolved nature of the rocks. All of the samples show a small positive Eu anomaly.



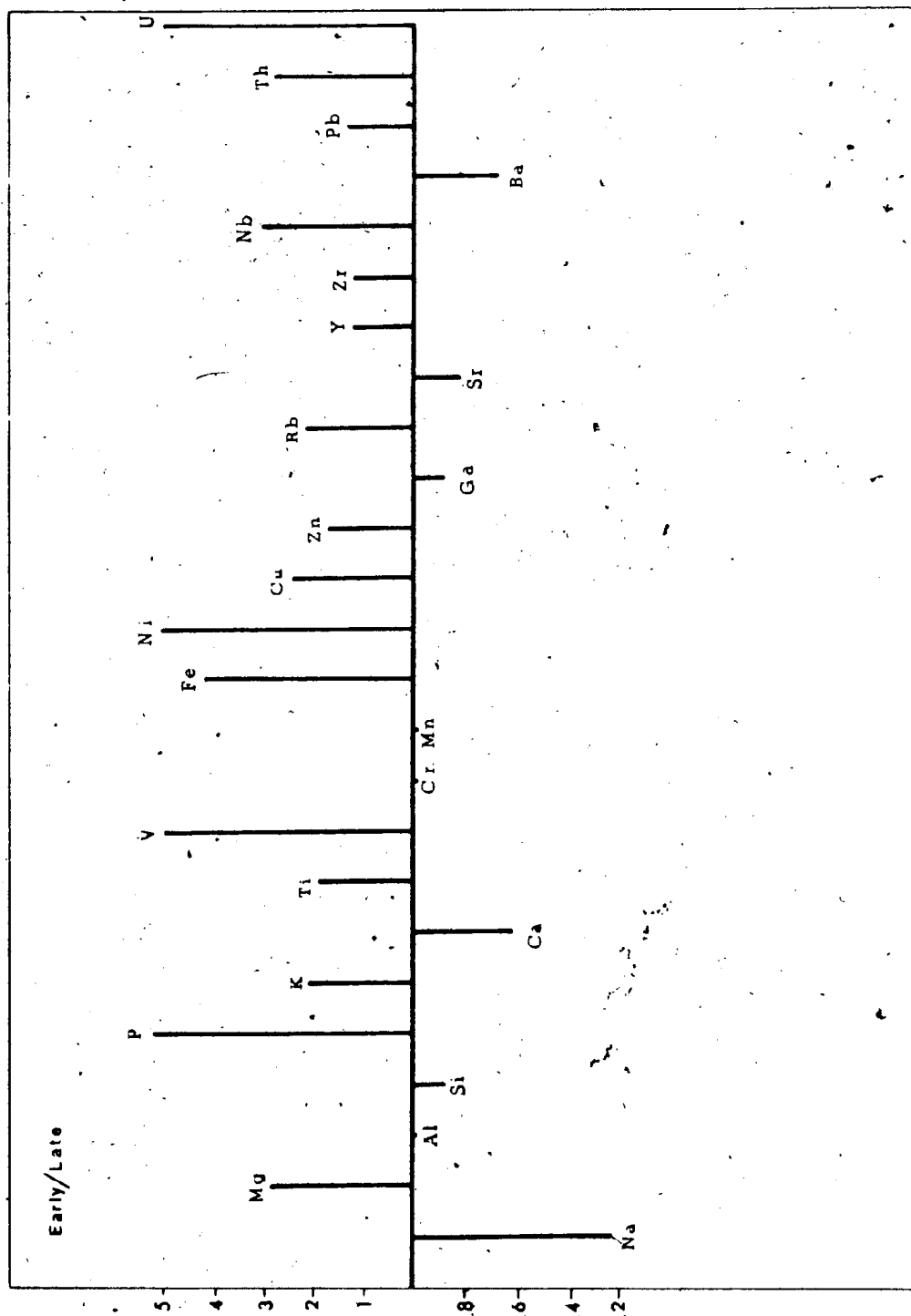
Figure 4.40 Chondrite-normalized REE patterns of Cambrian basalts from various localities. The normalizing values are from Taylor and Gorton, 1977. Data sources as in Figure 4.37.



Intermediate rocks are missing in the Long Reach area, but the presence of felsic rocks makes the suite bimodal. These pyroclastic rocks are peraluminous and show Nb/Y ratios less than 1. The  $\text{SiO}_2$  values range from 64 to 73 wt. % and increase from the bottom to the top of the section. With the exception of  $\text{SiO}_2$  and  $\text{Na}_2\text{O}$  Ba and Sr, most elements tend to decrease up through the section (Tables 4.29 and 4.30).

Compositional variation is common within felsic tuff piles, and frequently related to differentiation and volatile complexing within a pre-eruptive magma chamber (Hildreth, 1979, 1981). In this case the changes are probably not due to this process for two reasons; 1) the silica values increase rather than decrease up through the section, 2) the distribution of early/late factors (Figure 4.41) does not in any way resemble that normally seen in felsic sections, which tend to be quite similar (Hildreth, 1981). Nearly all elements are enriched in the early rocks which is the type of pattern one might expect if detrital quartz and possibly some feldspar were mixed in with the volcanic rocks at the top of the section. This would result in a net dilution of most elements. Another explanation might be that metasomatic solutions added quartz and albite to rocks near the top of the section.

Figure 4.41 Enrichment/depletion diagram for the Long Reach felsic rocks. The concentration of each element at the base of the felsic section is divided by its concentration at the top of the section and the resulting enrichment/depletion factors are shown by the bars.



#### 4.5.4 Pyroxene Compositions in Long Reach Basalts

Pyroxenes were never observed in the Beaver Harbour volcanic rocks but the feldspar phyric and aphyric lavas in the Long Reach area contain relict grains of the mineral. Representative major element electron microprobe analyses of these pyroxenes are presented in Table 4.32, and all analyses are listed in Appendix C. Refer to Appendix A for experimental methods, precision and accuracy.

Pyroxenes from the dike at Greenwich Hill were found to closely resemble the feldspar phyric basalt pyroxenes and so the two are grouped together in the following discussion. For the same reason pyroxenes from the flow (?) at Greenwich Hill are discussed with those from the aphyric basalts. Figure 4.42 shows that Wo, En, and Fs range from 35 to 45, 35 to 45, and 16 to 29 percent in the phyric basalt pyroxenes (PBP). Wo is similar in the aphyric basalt pyroxenes (ABP) but En tends to be higher (45 to 51) and Fs lower (7 to 20). These characteristics reflect the more evolved nature of the phyric basalts. Two analyses (approximately 2 percent of the total), one from each rock type, show low Ca (pigeonite) compositions.

The  $\text{TiO}_2$  contents of the pyroxenes reflect concentrations in the lavas. They average 1.87 wt. % in PBP (standard deviation, SD. = 0.51), which is much higher than the mean for ABP (0.41 wt. %, SD. = 0.12). The proportion of MnO and  $\text{Na}_2\text{O}$  to  $\text{TiO}_2$  in the PBP tends to be much lower

Table 4.32 Representative analyses of Long Reach pyroxenes.

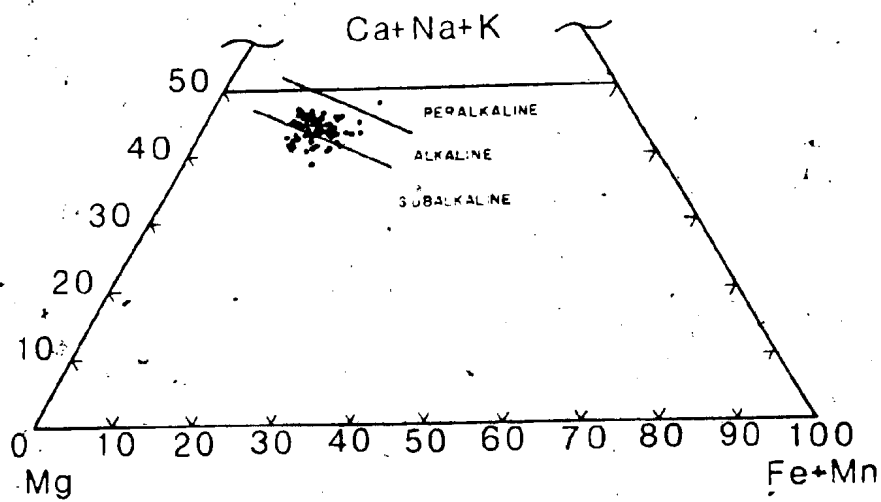
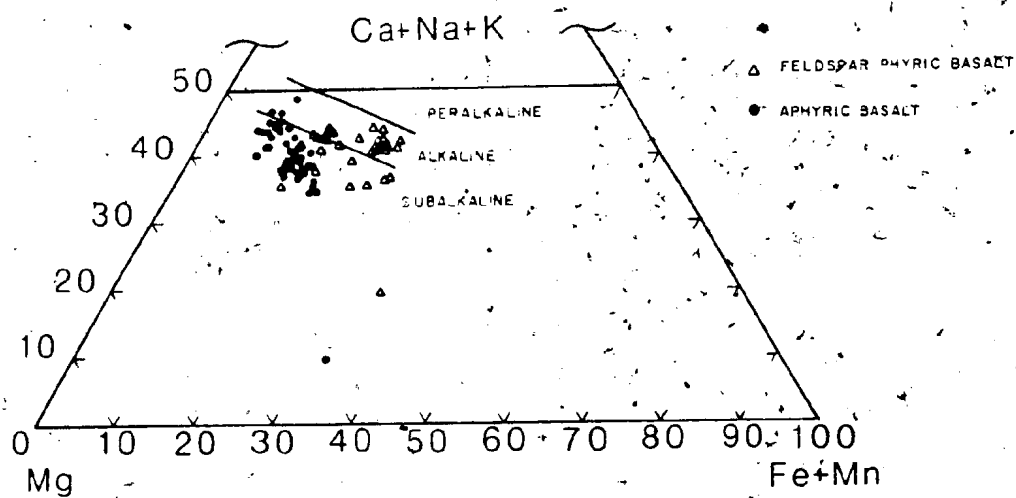
|                                | GWD20 | GWD25  | GWD12  | GWD8   | GWD26 | GWD9  |
|--------------------------------|-------|--------|--------|--------|-------|-------|
| SiO <sub>2</sub>               | 53.21 | 52.23  | 53.53  | 51.28  | 48.60 | 47.77 |
| TiO <sub>2</sub>               | 0.52  | 0.38   | 0.36   | 0.60   | 2.00  | 2.66  |
| Al <sub>2</sub> O <sub>3</sub> | 0.91  | 1.75   | 1.82   | 4.11   | 4.28  | 4.38  |
| Cr <sub>2</sub> O <sub>3</sub> | 0.02  | 0.29   | 0.26   | 0.27   | 0.38  | 0.11  |
| FeO*                           | 19.75 | 9.14   | 7.96   | 6.42   | 8.47  | 12.35 |
| MnO                            | 0.39  | 0.17   | 0.14   | 0.10   | 0.20  | 0.20  |
| MgO                            | 20.24 | 16.66  | 16.56  | 16.02  | 14.58 | 11.42 |
| NiO                            | 0.00  | 0.03   | 0.03   | 0.01   | 0.02  | 0.01  |
| CaO                            | 4.34  | 19.30  | 19.54  | 21.31  | 20.20 | 19.40 |
| Na <sub>2</sub> O              | 0.05  | 0.12   | 0.19   | 0.18   | 0.28  | 0.45  |
| K <sub>2</sub> O               | 0.08  | 0.02   | 0.00   | 0.00   | 0.00  | 0.00  |
| Total                          | 99.50 | 100.08 | 100.38 | 100.30 | 99.00 | 98.68 |
| Si                             | 1.987 | 1.936  | 1.961  | 1.880  | 1.832 | 1.837 |
| Al <sup>iv</sup>               | 0.013 | 0.064  | 0.039  | 0.120  | 0.168 | 0.163 |
| Al <sup>vi</sup>               | 0.026 | 0.012  | 0.039  | 0.057  | 0.021 | 0.034 |
| Ti                             | 0.014 | 0.010  | 0.009  | 0.016  | 0.056 | 0.074 |
| Cr                             | 0.000 | 0.007  | 0.006  | 0.007  | 0.011 | 0.002 |
| Fe                             | 0.616 | 0.283  | 0.243  | 0.197  | 0.266 | 0.396 |
| Mn                             | 0.012 | 0.004  | 0.004  | 0.002  | 0.005 | 0.005 |
| Mg                             | 1.126 | 0.920  | 0.904  | 0.876  | 0.818 | 0.654 |
| Ni                             | 0.000 | 0.000  | 0.000  | 0.000  | 0.000 | 0.000 |
| Ca                             | 0.173 | 0.766  | 0.767  | 0.837  | 0.815 | 0.799 |
| Na                             | 0.003 | 0.008  | 0.013  | 0.012  | 0.020 | 0.033 |
| K                              | 0.003 | 0.001  | 0.000  | 0.000  | 0.000 | 0.000 |
| Total                          | 3.973 | 4.010  | 3.985  | 4.005  | 4.012 | 3.998 |
| Ca                             | 9.0   | 38.8   | 40.0   | 43.8   | 42.8  | 43.1  |
| Mg                             | 58.4  | 46.6   | 47.1   | 45.8   | 43.0  | 35.3  |
| Fe+Mn                          | 32.6  | 14.6   | 12.9   | 10.4   | 14.2  | 21.6  |

All oxides in weight percent, FeO = total Fe; stoichiometry on basis of 6 oxygen.

GWD20 and 25 from flow at Greenwich Hills; GWD26 from dike below flow at Greenwich Hills; GWD8, 9, and 12 from flows at Browns Flat.

Figure 4.42 Pyroxene quadrilateral showing pyroxenes from the Long Reach area and from the Bourinot basalts in Cape Breton. The fields are labelled after Le Bas (1962).





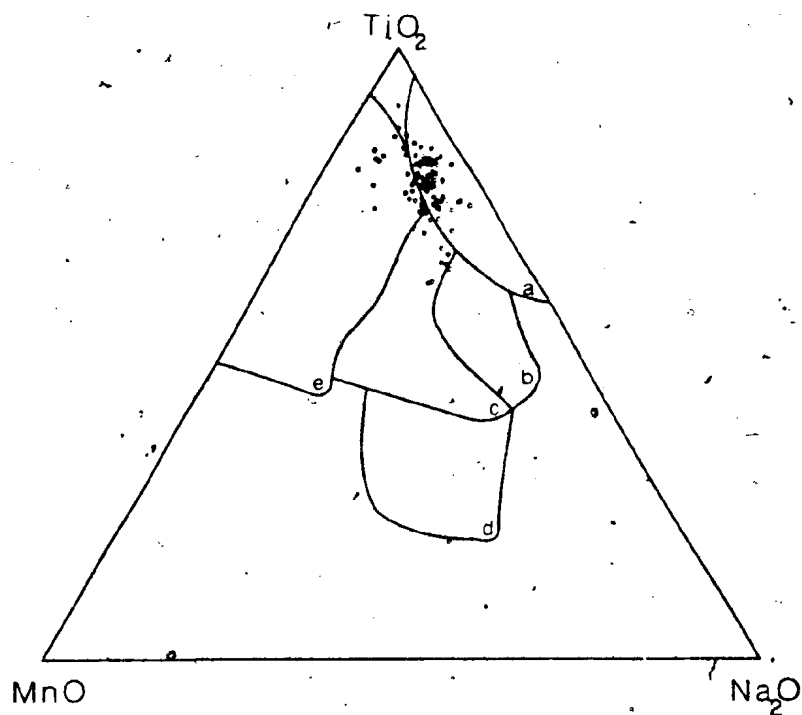
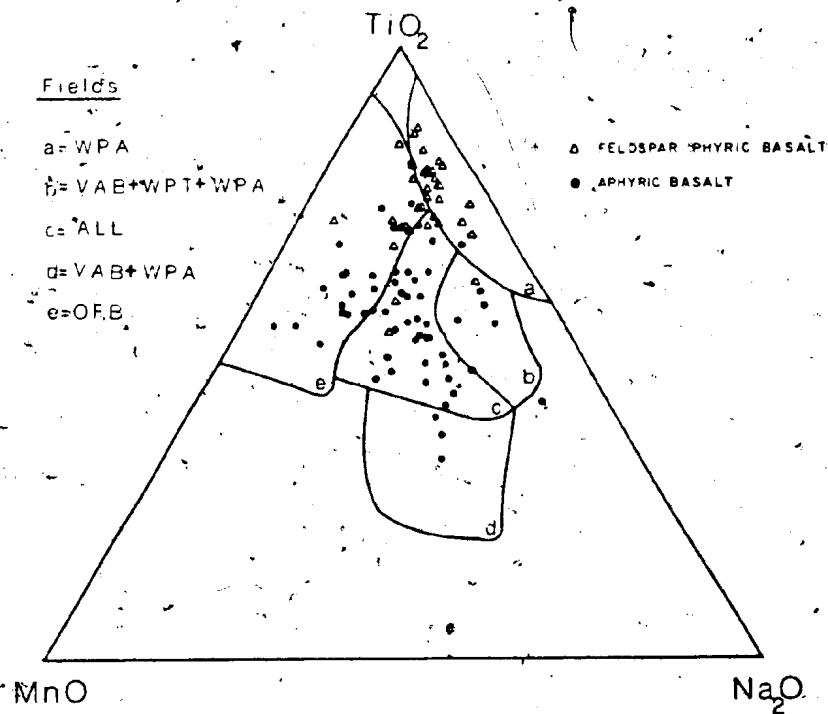
and more regular than the proportion in the ABP (Figure 4.43).

#### 4.5.5 Discussion

The aphyric basalts show the highest Mg values, highest Cr and Ni concentrations, and lowest Nb and Zr concentrations of the New Brunswick basalts indicating that they are the least evolved (Figures 4.37, 4.36, and 4.39). The basalts from Beaver Harbour show the opposite characteristics suggesting that they are the most evolved. Olivine removal can explain the low Ni concentrations in the Long Reach phyrific and Beaver Harbour basalts and clinopyroxene and/or Cr-spinel precipitation may explain their low Cr concentrations. Plagioclase removal could not have been an important process in the evolution of the phyrific basalts because the chondrite normalized REE patterns do not show a large negative Eu anomaly (Figure 4.40). It is difficult to evaluate the importance of plagioclase fractionation in the case of the Beaver Harbour basalts because the REE concentrations have probably been altered (see section 4.5.1).

The observation that the ratios of  $TiO_2/Zr$ , Nb/Y, and Zr/Nb are similar in both the aphyric and phyrific basalts (Figure 4.36 and 4.39) suggests that the basalts may be comagmatic as these ratios commonly remain constant in differentiated basalt suites (Pearce and Cann, 1973;

Figure 4.43  $\text{TiO}_2$ - $\text{MnO}$ - $\text{Na}_2\text{O}$  pyroxene discrimination diagram - Long Reach and Bourinot pyroxenes. Diagram after Nisbet and Pearce (1977). WPA = within plate alkaline; WPT = within plate tholeiite; VAB = volcanic arc basalt OFB = ocean floor basalt.



Winchester and Floyd, 1977). Closer inspection of the ratios shows that the averages for the aphyric basalts ( $\text{TiO}_2/\text{Zr} = 0.019$ ,  $\text{Nb/Y} = 0.19$ , and  $\text{Zr/Nb} = 15$ ) indicate greater alkalinity (Ibid.) than those for the phyric basalts (0.016, 0.12, 20). Although these differences are only small, they support the more significant observation that the chondrite normalized REE patterns of the aphyric basalts show steeper slopes (indicative of greater alkalinity) than those of the phyric basalts suggesting that they are not comagmatic (Kay and Gast, 1973; Langmuir et al., 1977).

Ratios of elements indicative of alkalinity (eg.  $\text{Nb/Y}$ ) commonly show similar values in both the basalts and rhyolites of bimodal suites (Winchester and Floyd, 1977) and this appears to be the case with the Long Reach rocks. Some authors have suggested that a fractional crystallization model can explain these observations (eg. Barberi et al., 1975). Hildreth (1981) proposed that the composition of the volatile flux from basalts, which in his model heat and melt the crust to produce the rhyolites, controls the composition and subalkaline/peralkaline character of the rhyolites. It is impossible to distinguish between these two models on the basis of the data presented here, but similarities between the basalts and rhyolites in such element ratios as  $\text{Nb/Y}$  imply a cause and effect relationship between the two rock types.

#### 4.6 CAPE BRETON VOLCANIC ROCKS

##### 4.6.1 Whole-Rock Geochemistry

Cameron (1980) found that Cambrian volcanic rocks from Cape Breton Island in Nova Scotia comprise a basalt-rhyolite bimodal suite. He showed that the basalts may be separated into two distinct groups (Table 4.33) both of which are representative of continental tholeiites. The rhyolites, he concluded, were probably the result of melting of the lower crust as a result of basalt intrusion. Because these rocks are of similar age to those from Cape St. Mary's and southern New Brunswick and because they also occur in the Avalon Zone, they are discussed here for comparison with the former two localities. The more important characteristics of the basalts include:

1. Intermediate to low concentrations of CaO, MgO, Cr, and Ni, (Table 4.33) high to very high  $TiO_2$ , and intermediate to low Mg' values show that the basalts possess evolved to highly evolved compositions (Figures 4.37 and 4.38).
2. Trace element ratios such as Nb/Y and Zr/Nb (Figure 4.39) as well as the relatively low slopes of chondrite normalized REE patterns (Figure 4.40) are very similar to those of the Long Reach basalts.

Table 4.33. Composition of representative Cambrian basalts from Poland, Norway and Nova Scotia.

|   | Poland <sup>4</sup> | / | Norway | /      | Cape Breton |       |        |       |
|---|---------------------|---|--------|--------|-------------|-------|--------|-------|
|   |                     |   | G7     | H8     | KJC68       | KJC66 | KJC75  | KJC73 |
| SiO <sub>2</sub>                            | 49.4                |   | 48.06  | 47.29  | 48.00       | 51.90 | 48.00  | 50.30 |
| TiO <sub>2</sub>                            | 2.6                 |   | 3.21   | 2.96   | 1.69        | 1.79  | 3.77   | 3.88  |
| Al <sub>2</sub> O <sub>3</sub> <sup>1</sup> | 16.1                |   | 20.36  | 19.30  | 16.20       | 14.50 | 14.10  | 14.30 |
| Fe <sub>2</sub> O <sub>3</sub>              | 11.7                |   | 2.88   | 3.76   | 5.39        | 7.67  | 6.72   | 6.67  |
| FeO   | 0.0                 |   | 11.56  | 13.11  | 4.70        | 2.70  | 6.85   | 5.80  |
| MnO   | 0.2                 |   | 0.20   | 0.31   | 0.21        | 0.15  | 0.23   | 0.20  |
| MgO   | 6.7                 |   | 4.90   | 4.75   | 8.01        | 5.69  | 4.75   | 3.60  |
| CaO   | 8.3                 |   | 1.35   | 0.87   | 4.71        | 5.12  | 5.82   | 5.66  |
| Na <sub>2</sub> O                           | 4.1                 |   | 1.42   | 3.29   | 3.86        | 6.49  | 4.37   | 4.77  |
| K <sub>2</sub> O                            | 0.4                 |   | 5.50   | 3.80   | 1.82        | 0.18  | 0.30   | 0.27  |
| P <sub>2</sub> O <sub>5</sub>               | 0.5                 |   | 0.54   | 0.55   | 0.28        | 0.28  | 0.58   | 0.59  |
| L.O.I. <sup>2</sup>                         | -                   |   | 2.68   | 5.50   | 4.55        | 3.02  | 4.56   | 3.42  |
| Total <sup>3</sup>                          | 100.0               |   | 100.00 | 100.00 | 99.42       | 99.49 | 100.05 | 99.46 |
| Hg <sup>1</sup>                             | 0.56                |   | 0.41   | 0.36   | 0.62        | 0.55  | 0.42   | 0.38  |
| Pb  | 5                   |   | 267    | 173    | 81          | 5     | 4      | 11    |
| Sr  | 274                 |   | 136    | 144    | 334         | 241   | 248    | 324   |
| Ba  | 65                  |   | 616    | 839    | 499         | 127   | 146    | 127   |
| Zr  | 187                 |   | 116    | 97     | 131         | 138   | 246    | 257   |
| Hf  | -                   |   | 13     | 11     | 5           | 3     | 9      | 9     |
| Y   | 30                  |   | 26     | 22     | 38          | 37    | 64     | 66    |
| Ga  | 20                  |   | -      | -      | 17          | 13    | 23     | 21    |
| V   | 292                 |   | 295    | 279    | 234         | 213   | 455    | 444   |
| Cr  | 164                 |   | 59     | 56     | 130         | 129   | 4      | 9     |
| Ni  | 149                 |   | -      | -      | 65          | 70    | 16     | 18    |
| Cu  | 38                  |   | -      | -      | 0           | 11    | 14     | 8     |
| Zn  | 66                  |   | -      | -      | 123         | 95    | 118    | 108   |

Major element oxides in weight percent, trace elements in ppm.

1. Total Fe as Fe<sub>2</sub>O<sub>3</sub> unless shown otherwise.
2. L.O.I. = Loss on ignition. Poland, not given. Sum of H<sub>2</sub>O + CO<sub>2</sub> for Norway + Cape Breton.
3. Analyses for Norwegian basalts were recalculated CO<sub>2</sub> and H<sub>2</sub>O free, to 100% in source paper.
4. Average of 17 analyses recalculated volatile free.

Sources: Poland - Baranowski et al. (1984)

Norway - Farnes et al. (1983).

Cape Breton - Major elements from Cameron (1980); trace elements determined for this study from powders provided courtesy of K.J. Cameron.

3. The range of basalt compositions can be related to olivine and clinopyroxene precipitation. Titanium and V behaved as incompatible elements and exclude Fe-Ti oxide precipitation as an important process. On the basis of the REE patterns Cameron (1980) concluded that appreciable amounts of plagioclase could not have been precipitated. The behaviour of Ga as an incompatible element (Table 4.33) supports these conclusions.

#### 4.6.2 Pyroxene Compositions

Cameron (1980) reported relict pyroxenes in the Cape Breton basalts and provided samples for analysis here. Representative analyses of the Cape Breton pyroxenes are presented in Table 4.34 and approximately 100 additional analyses from six samples are given in Appendix C. The pyroxenes have Wo, En, and Fs compositions of 40 to 47, 38 to 45, and 11 to 19 percent respectively (Figure 4.42). Most are augites, but approximately 10 percent show salitic (Wo exceeds 45 percent) compositions. These pyroxenes show higher Wo contents than those from the aphyric basalts from New Brunswick, and higher Wo and En contents than the phyric basalt pyroxenes. They are, however, very similar to pyroxenes from lavas at Cape Dog in the Cape St. Mary's study area (Figure 4.13).



Table 5.8: Representative analyses of Cape Breton pyroxenes.

|                                | 1     | 2     | 3     | 4      | 5     | 6     |
|--------------------------------|-------|-------|-------|--------|-------|-------|
| SiO <sub>2</sub>               | 49.96 | 50.84 | 51.85 | 50.65  | 48.71 | 49.33 |
| TiO <sub>2</sub>               | 1.76  | 1.27  | 0.88  | 1.63   | 2.56  | 2.26  |
| Al <sub>2</sub> O <sub>3</sub> | 3.09  | 3.39  | 1.94  | 3.50   | 3.82  | 2.87  |
| Cr <sub>2</sub> O <sub>3</sub> | 0.41  | 0.87  | 0.41  | 0.36   | 0.27  | 0.03  |
| FeO                            | 7.20  | 6.54  | 7.71  | 7.65   | 8.02  | 10.02 |
| MnO                            | 0.13  | 0.19  | 0.14  | 0.09   | 0.14  | 0.23  |
| MgO                            | 14.80 | 15.30 | 16.34 | 14.70  | 13.98 | 13.62 |
| NiO                            | 0.05  | 0.02  | 0.00  | 0.00   | 0.05  | 0.01  |
| CaO                            | 21.51 | 20.97 | 19.64 | 21.24  | 21.51 | 20.70 |
| Na <sub>2</sub> O              | 0.36  | 0.36  | 0.20  | 0.46   | 0.40  | 0.42  |
| K <sub>2</sub> O               | 0.03  | 0.03  | 0.05  | 0.01   | 0.03  | 0.01  |
| Total                          | 99.30 | 99.79 | 99.16 | 100.29 | 99.50 | 99.48 |
| Si                             | 1.870 | 1.883 | 1.929 | 1.876  | 1.831 | 1.865 |
| Al <sup>iv</sup>               | 0.130 | 0.117 | 0.071 | 0.124  | 0.168 | 0.127 |
| Al <sup>vi</sup>               | 0.006 | 0.030 | 0.013 | 0.028  | 0.000 | 0.000 |
| Ti                             | 0.049 | 0.035 | 0.024 | 0.044  | 0.071 | 0.063 |
| Cr                             | 0.011 | 0.025 | 0.012 | 0.010  | 0.007 | 0.000 |
| Fe                             | 0.225 | 0.202 | 0.239 | 0.237  | 0.251 | 0.316 |
| Mn                             | 0.003 | 0.005 | 0.004 | 0.002  | 0.003 | 0.006 |
| Mg                             | 0.825 | 0.845 | 0.906 | 0.811  | 0.783 | 0.767 |
| Ni                             | 0.001 | 0.001 | 0.000 | 0.000  | 0.001 | 0.000 |
| Ca                             | 0.862 | 0.832 | 0.783 | 0.842  | 0.866 | 0.837 |
| Na                             | 0.025 | 0.026 | 0.014 | 0.032  | 0.028 | 0.030 |
| K                              | 0.001 | 0.001 | 0.002 | 0.000  | 0.001 | 0.000 |
| Total                          | 4.009 | 4.001 | 3.997 | 4.007  | 4.012 | 4.011 |
| Ca                             | 45.0  | 44.1  | 40.5  | 44.5   | 45.5  | 43.5  |
| Mg                             | 43.1  | 44.9  | 46.9  | 42.9   | 41.2  | 39.8  |
| Fe+Mn                          | 11.9  | 11.0  | 12.6  | 12.6   | 13.3  | 16.7  |

Major element oxides in weight percent; FeO = total Fe.  
Stoichiometry on basis of 6 oxygen.

Most grains show a purplish brown pleochroism as a result of relatively high  $TiO_2$  concentrations that average 1.8 weight percent but range from 0.80 to 2.60. These  $TiO_2$  concentrations reflect the relatively high  $TiO_2$  concentrations observed in the lavas (Figure 4.38). As with the phyric basalt pyroxenes from New Brunswick, the high  $TiO_2$  concentrations of the pyroxenes tend to control where they plot on some discrimination diagrams (Figure 4.43).

#### 4.7 NORWEGIAN BASALTS

The Norwegian basalts studied by Furnes et al. (1983) are probably not Cambrian, but they are intimately associated with faulting and graben forming events that started just prior to the Cambrian and continued into the Cambrian (Bjorlykke, 1978; Ramberg and Larsen, 1978; Nystuen, 1982). Representative analyses of these rocks are presented in Table 4.33 for comparison with the Cambrian basalts from eastern North America discussed above. Some of their more important characteristics include:

1. They show very high concentrations of  $TiO_2$  and  $Al_2O_3$  (Figures 4.37, and 4.38) as well as low CaO and MgO indicating they are highly evolved (Furnes et al., 1983).
2. Trace element ratios such as Nb/Y (0.5) are comparable to those in the Cape Breton and New Brunswick basalts but Zr/Nb ratios (9) may be

slightly lower (Figure 4.39).

3. The basalts owe their evolved compositions primarily to olivine and clinopyroxene precipitation. High Ti and V preclude substantial Fe-Ti oxide removal. A few samples show positive Eu anomalies, but there is little evidence (ie. negative anomalies) that large quantities of plagioclase were removed prior to extrusion (Figure 4.40).

#### 4.8 POLISH VOLCANIC ROCKS

Cambrian rocks in Poland belong to the Acado-Baltic province as do all of the rocks studied in this chapter (see paleogeography Chapter 1). Polish volcanic rocks recently discussed by Baranowski et al. (1984) are therefore of interest for comparison with the other volcanic rocks. Baranowski et al. (1984) established that the volcanic rocks display a bimodal basalt-rhyolite distribution with the basaltic rocks volumetrically most important. Unfortunately, only an average composition for the 17 basalt samples analyzed is presented in the Baranowski et al. paper making it difficult to determine how altered the rocks are on the range of compositions. The average analysis is presented in Table 4.33 and the following points seem valid:

1. The average major element composition of the Polish basalts is very similar to compositions

shown by the Cape St. Mary's flows and feeder pipes (compare Tables 4.33 and 4.4). Perhaps the most important difference is that Al concentrations are slightly higher in the Polish rocks.

2. Trace element concentrations also appear quite similar in the two groups of rocks (compare Tables 4.33 and 4.6) as do element ratios indicative of petrogenetic character (ie.  $Zr/Y$ ,  $Zr/P_2O_5$ ,  $Zr/TiO_2$  and  $V/TiO_2$ ).

## CHAPTER 5 TECTONICS AND PETROGENETIC CONSIDERATIONS

### 5.1 INTRODUCTION

In Chapter 1, the distribution and characteristics of Acado-Baltic Cambrian rocks from around the North Atlantic were reviewed. The review pointed out that these rocks display many lithologic, stratigraphic, paleontologic, and volcanologic similarities implying that they formed under similar environmental conditions which were in part tectonically controlled. In this chapter the characteristics of the volcanic rocks and their association with the stratigraphy are examined in detail with the intention of developing tectonic and volcanologic models for the Acado-Baltic province during the Cambrian. The Cape St. Mary's sills (Silurian) and dikes (Devonian?) provide information of a local nature on tectonism during the Lower Paleozoic.

### 5.2 SIMILARITIES TO PLATFORMS

The sedimentary rocks of the Acado-Baltic province have been termed platformal because of their relatively thin stratigraphy and the areal extensiveness of individual lithotypes (Kay and Colbert, 1965; Dore 1977). Platforms are areas where essentially flat lying, areally extensive, and slowly accumulated sedimentary rocks, often thousands of meters thick, lie relatively undisturbed atop polydeformed rocks for periods of time, sometimes, in excess of a billion

years. Many platformal Precambrian rocks consist largely of quartzites and other arenaceous rocks with some conglomerates, limestones and dolomites. Paleozoic successions tend to have a much higher proportion of limestones and dolomites with siliciclastics of lesser importance (Clark and Stearn, 1968). The absence of volcanic rocks from platformal successions of all ages is in keeping with a stable tectonic environment.

The Cambrian sedimentary rocks show many characteristics in common with platformal rocks in general. Sedimentation rates must have been relatively low (15 - 20 micrometers per year) given that sections are typically about 1000 meters thick and the Cambrian lasted on the order of 70 million years (Van Eysinga, 1975). In contrast, rifts such as the East African rift show sedimentation rates ranging from 70 to over 1000 micrometers per year (Tiercelin and Faure, 1977). The Cambrian rocks show individual units, such as the manganese beds, which are traceable for thousands of kilometers. Sedimentary rocks from the northern portion of the Acado Baltic province may resemble Precambrian platformal deposits because, for the most part, they show few carbonates. Those from the southern portion of the province more closely resemble Paleozoic platforms because of their higher percentages of carbonate rocks. The single most important aspect of the Cambrian successions, which sets them apart from platformal rocks, is their associated volcanic rocks.

### 5.3 EVIDENCE FOR TENSION

#### 5.3.1 Style Of Volcanism

Volcanic rocks occur within the Cambrian stratigraphy at just about every broad locality examined in this report and they tend to display a bimodal distribution, or consist solely of basaltic rocks, (Table 1.1). In the northern portion of the province basalts tend to predominate over the felsic rocks, at localities where both are present, but in the southern portion the felsic rocks tend to dominate. Czechoslovakia is unique in that the rocks show a unimodal distribution with the felsic rocks dominant.

The Cambrian volcanic rocks at many localities consist of only a few flows or tuffaceous beds which represent single eruptive episodes with limited areal extent (Table 1.1). Volcanic rocks related to extensional tectonism may be voluminous and products of numerous eruptions, such as the Deccan Traps and the Columbia River flood basalts (Basaltic Volcanism Study Project, 1981). Alternatively the volcanic rocks may be small in volume and quite localized, such as in the Oslo rift (Segalstad, 1977), parts of the Rio Grande rift (Baldrige, 1979; Basaltic Volcanism Study Project, 1981, p. 108), and the Kenyan rift (Bailey, 1974). Back-arc basins are characterized by copious volumes of basaltic magma (Tarney et al., 1977) which sets the Cambrian rocks apart from this environment. In most cases the Cambrian rocks are clearly unlike volcanic arcs which tend to form

sequences that are several kilometers thick, of wide aerial extent and are the result of numerous eruptions from the same volcanic center (eg. Carmichael et al., 1974, pages 528 to 557). The thickest sequences are developed in Poland and Czechoslovakia possibly indicating a different tectonic setting for these rocks.

The textural characteristics of volcanic rocks can act as guides to their tectonic setting (eg. Ricketts et al., 1982; Ayres, 1982). As a generalized statement the Cambrian rocks show an intermediate proportion of flows to volcanoclastic rocks (Table 1.1). This argues against an ocean floor or marginal basin environment because high water pressures in these settings prevent the formation of pyroclastic rocks (Moore and Fiske, 1969; Ayres, 1982; Ricketts et al., 1982). Continental and island arc settings show high proportions of fragmental rocks (Ricketts et al., 1982). Only in some mid-plate settings are intermediate proportions of flows to volcanoclastic rocks common (Ibid.).

All of the preserved Cambrian volcanic rocks on the Avalon Peninsula occur in a narrow belt in Cape St. Mary's study area. It is conceivable that volcanic rocks once occurred outside of the narrow belt and have since been eroded away, but the preserved distribution resembles the linear chain of volcanic centers commonly seen along rift axes (eg. Afar, Mohr, 1978; Benue Trough, Fitton, 1980; Rio Grande rift, Baldrige, 1979; Monteregian Hills, Philpotts,



1974). In rifts the volcanic centers are usually parallel to normal faults which define the rift valley and probably control magma emplacement. Evidence for Cambrian faulting is absent in the Cape St. Mary's study area, nevertheless the volcanism suggests that there was a linear zone of weakness which controlled emplacement of the magmas. Such linear control of magma emplacement has also been noted for the Cambrian volcanic rocks, in Czechoslovakia (Palicova and Stovickova, 1968; Waldhausrova, 1971; Fiala, 1978a).

#### 5.3.2 Chemical Characteristics Of Volcanic Rocks

Perhaps the most important characteristics of the volcanic rocks relating them to their environment of formation are their geochemical characteristics. In the following discussion, differentiation processes affecting the volcanic rocks discussed in Chapter 4 are used to derive their petrogenetic and tectonic affinities. In a similar manner attributes related to mantle melting processes provide further information on their probable tectonic setting.

All of the Cambrian basaltic rocks from New Brunswick, Nova Scotia, Cape St. Mary's (Newfoundland), and Norway as well as the Cape St. Mary's sills and dikes show similar minerals controlling their pre-extrusion/emplacement evolution. Chromium and Ni concentrations tend to be low to very low in all of the rocks and provide evidence for olivine and clinopyroxene precipitation. The observation

that  $\text{TiO}_2$  and V behave as incompatible elements in each group of rocks (Figures 4.10 and 4.38) suggests that Fe-Ti oxides were not important in the evolution of most of the basalts. Only in some of the more evolved Newfoundland samples do  $\text{TiO}_2$  concentrations drop, giving evidence for magnetite and/or ilmenite removal. It is also possible that a certain percentage of these minerals were precipitated prior to extrusion of the highly evolved Beaver Harbour rocks as Ti is relatively low given the Mg' values observed. The chondrite normalized REE patterns indicate that plagioclase fractionation was not an important process in the formation of most of the lavas, even those which are relatively evolved such as the Norwegian basalts (Figure 4.40).

The unimportance of plagioclase and Fe-Ti oxide precipitation, except in highly evolved basalts, is a characteristic common to most basaltic rocks from mid-plate or tensional tectonic environments (cf., Basaltic Volcanism Study Project, 1981, p. 78, 161; Barberi et al., 1975). In contrast, the consistently low concentrations (< 1 wt. %) of Ti in volcanic arc basalts indicate the significance of Fe-Ti oxide precipitation in the generation of these rocks. Plagioclase phenocrysts usually occur in both ocean floor and volcanic arc basalts, even in relatively unevolved lavas, pointing to the importance of the mineral in their formation.

Some indication of the degree of evolution undergone by any basalt may be garnered from its  $Mg'$  value ( $Mg' = Mg/(Mg+0.9Fe)$  atomic). The  $Mg'$  values commonly associated with primitive (ie. unfractionated) basaltic magmas are about 0.70 to 0.72 as these are expected of melts in equilibrium with lherzolite containing olivine with Fo90 composition (eg. Green, 1971; Hanson and Langmuir, 1978). This ratio will be very sensitive to fractionation of olivine and/or other ferro-magnesian minerals such as augite and hypersthene. The observations that  $Mg'$  values rarely exceed 0.60 in flood basalt provinces (Basaltic Volcanism Study Project 1981 p. 103) but may be higher in rift and oceanic island basalts, have led some authors (eg. Wilkinson and Binns, 1977; Swanson and Wright, 1980; Basaltic Volcanism Study Project, 1981, pages 101 to 105) to suggest that continental flood basalts have Fe rich sources. However, the mantle xenoliths from various kinds of alkaline rocks rarely show Fe rich compositions and thus do not support this hypothesis. Apparently the distances involved in passing through thickened continental lithosphere make it unlikely that primitive flood basalts will arrive at the surface. Because rifts tend to show some basalts with ratios above 0.60, the implications are that the continental crust is thinner in rift zones, or that faults allow magmas to reach the surface faster, than in continental flood basalt provinces.

The most primitive basalts studied in this report are the aphyric basalts from the Long Reach area which show  $Mg'$  values between 0.65 and 0.70. Some samples of the Cape St. Mary's dikes, the Cambrian Cape St. Mary's flows and feeder pipes, and Cambrian flows from Cape Breton display  $Mg'$  values between 0.60 and 0.65 (Figures 4.10 and 4.38). It follows that none of these rocks resemble flood basalts (in this respect) and that they are more likely associated with continental rifting and rupture. The low  $Mg'$  values ( $< 0.40$ ) shown by some of the feeder pipes, the Norwegian basalts, and the Beaver Harbour basalts demonstrate that they are highly evolved.

The Cape St. Mary's flows and feeder pipes and dikes display a negative correlation between  $Mg'$  values and  $Al_2O_3$  (Figure 4.9). It is possible to infer that  $Al_2O_3$  values probably increased during differentiation to produce the Norwegian and Beaver Harbour basalts (Figure 4.37) because evolved basalts produced from primitive basalts with such high  $Al_2O_3$  values generally show lower  $Al_2O_3$  concentrations. For example, flood basalts (eg. Keweenaw and Columbia River, Figure 4.9, see Basaltic Volcanism Study Project, 1981, p. 48, 100) usually show a positive correlation between  $Mg'$  and  $Al_2O_3$ , and some rift basalts (Ethiopia, Figure 4.9) may display a similar correlation. Primarily oceanic island and rift basalts (Hail and Oslo, Figure 4.9) show a negative correlation between  $Al_2O_3$  concentrations and  $Mg'$  values. These observations support a

rift origin for the Cambrian basalts from Beaver Harbour, Norway and Newfoundland, and leave open such a possibility for the Long Reach and Cape Breton basalts. The reason for these correlations is somewhat enigmatic. The most logical explanation is that the positive correlations reflect plagioclase precipitation, but the lack of a negative Eu anomaly in most flood basalts places limits on the amount of plagioclase removal that is possible.

Suites of rocks thought to be comagmatic produce trends on  $\text{Na}_2\text{O} + \text{K}_2\text{O}$ ,  $\text{FeO}$ ,  $\text{MgO}$  (AFM) diagrams that can be used to indicate the petrogenetic character of the suite. The Cape St. Mary's feeder pipe samples show considerable scatter on an AFM diagram but seem to define a trend representative of alkaline rocks, with little or no Fe enrichment (Figure 4.11). The sill rocks exhibit an Fe depletion trend - (Figure 4.11) similar to that shown by calcalkaline suites, but the unusual geochemical characteristics and fractionation processes shown by the sills complicate interpretation of the diagram.

Nearly all of the Cambrian basalts examined in this report (ie. Cape St. Mary's, New Brunswick, Cape Breton, and Norway) as well as the sills and dikes contain normative Hy making them tholeiites according to the Yoder and Tilley (1962) classification. However, the proportion of Hy is very sensitive to the  $\text{Fe}^{2+}/\text{Fe}^{3+}$  ratio (Coombs, 1963) and for this reason it is difficult to use norms to petrogenetically

classify the rocks.

Low pressure fractionation cannot account for many of the differences in composition shown by the basalts under study here, and in some cases these differences can probably be related to mantle melting processes. Various trace element ratios commonly used as alkalinity indicators such as Nb/Y, Zr/Nb, Zr/Y, V/Ti, Zr/P<sub>2</sub>O<sub>5</sub>, and Zr/TiO<sub>2</sub> reflect the controls of mantle processes on basalt magma geochemistry and help petrogenetically and tectonically classify basalts (Pearce and Cann, 1973; Floyd and Winchester, 1976; Winchester and Floyd, 1977, 1976; Pearce and Norry, 1979).

Of all the basalts studied in this report the Cape St. Mary's flows show the most alkaline compositions and all of the above alkalinity indicators show that the rocks are alkali basalts. The extreme compositions are indicated by the Zr/Nb ratios which tend to be within the range of nephelinites observed in the Hawaiian Islands (Figure 4.12). Based on ratios such as V/Ti, Zr/P<sub>2</sub>O<sub>5</sub>, and Zr/TiO<sub>2</sub> the Polish basalts would appear to show similarly alkaline compositions (Baranowski et al., 1984). The association of continental alkali basalts with rifting environments is well established.

The Cape St. Mary's dikes display a wide range of Nb/Y (0.1 to 2.0) and Zr/Nb ratios (3.5 to 17.5) indicating both alkali basalt and tholeiitic basalt compositions (Figure 4.12). In contrast non-differentiated sill samples show

Zr/Nb and Nb/Y ratios transitional between alkalic and tholeiitic within-plate basalts. The basalts from Cape Breton (Cameron, 1980), Norway (Furnes et al., 1983), and New Brunswick have tholeiitic compositions (Figure 4.39). but in many cases tend to plot in the ocean floor basalt fields on many "discrimination" diagrams (eg. Pearce and Cann, 1973; Pearce and Norry, 1979). Various authors have shown that continental tholeiites associated with rupture and rifting commonly have incompatible element concentrations and ratios similar to ocean floor basalts (eg. Papezik and Hodych, 1980; Wark and Clark, 1980; Holm, 1982).

Variations in the slope on chondrite normalized REE patterns probably reflect differences in the percentage of mantle melting (Kay and Gast, 1973; Langmuir et al., 1977), the proportion of garnet to clinopyroxene in the mantle (Kay and Gast, 1973), the concentration of each element in the source as a result of previous melt extraction (Pearce and Norry, 1979), the mode of melt removal (Gast, 1968), and metasomatic and volatile effects both pre- and syn-magma genesis (Chauvel and Jahn, 1984). Numerical experiments modelling the slope of REE patterns (eg. Kay and Gast, 1973; Langmuir et al., 1977) show that of these the percentage of melting is probably the most important process. If the REE patterns (Figures 4.5, 4.17, and 4.40) indicate an increase in the percentage of melting (and decrease in alkalinity) approximately as follows: Cape St. Mary's flows

(lowest), Norway = dikes = sills = Long Reach aphyric basalts, Cape Breton, Long Reach phyrlic basalts (highest). The slopes on the Cape St. Mary's flows are similar to those for some alkali basalts (Figure 4.5) whereas the remainder of the patterns appear transitional between alkali and tholeiitic basalts, or similar to continental tholeiites.

Two interesting characteristics of the chondrite normalized REE patterns of most of the above rock groups are that the patterns are convex upward and they show normalized Yb concentrations less than 10. These characteristics are atypical of ocean floor basalts, volcanic arc basalts, and basalts from flood basalt provinces (Basaltic Volcanism Study Project, 1981 p. 145, 202, 86). Both characteristics are common in Hawaiian Islands alkaline and tholeiitic basalts as well as some rift rocks (cf. Kay and Gast, 1973; Basaltic Volcanism Study Project, 1981, p. 172). Trace element modelling experiments suggest that both of these characteristics can be related to high proportions of garnet to clinopyroxene in the mantle (Kay and Gast, 1973; Greenough, 1979).

The compositions of clinopyroxenes in the basaltic rocks reflect both the whole rock geochemistry of their host magmas and cooling rates. Le Bas (1962) observed that the Wo component of pyroxenes increases with lava alkalinity, and allows the definition of magma type fields on the pyroxene quadrilateral (Figure 4.13). In the case of the



Cape St Mary's flows, the Le Bas diagram indicates that the lavas are alkaline, but Cape Dog and Hay Cove analyses straddle the subalkaline - alkaline boundary and some from Chapel Arm plot in the peralkaline field. The feeder pipe pyroxenes fall in both the alkaline and subalkaline fields (Figure 4.13), but perhaps more importantly they define a trend of constant Ca content (as opposed to declining Ca) with decreasing Mg composition; a characteristic which is commonly associated with alkaline rocks. The  $\text{TiO}_2$  -  $\text{MnO}$  -  $\text{Na}_2\text{O}$  pyroxene discrimination diagram of Nisbet and Pearce (1977) illustrates the high Ti nature of the lava pyroxenes as is characteristic of alkali basalts (Figure 4.14). The feeder pipe pyroxenes tend to have lower Ti contents but over 80 percent of them fall in either the alkaline or the "neutral" field of the Nisbet and Pearce (1977) diagram. In keeping with their alkaline characteristics, low Ca pyroxenes were never identified any of these rocks.

Chapel Arm pyroxenes plotting in the peralkaline field of the Le Bas (1962) diagram also show unusually high  $\text{TiO}_2$  and  $\text{Al}_2\text{O}_3$  and come from a sample displaying a variolitic texture indicative of quenching. Although quenched clinopyroxenes from tholeiitic flows commonly show lowered Ca, Al, and Ti contents (Robinson, 1980) the opposite effect in alkaline lavas has to the author's knowledge never been documented. The slowly cooled feeder pipe pyroxenes tend to show lower Ca, Al, Na and Ti as well as higher Si and Mn than the flow pyroxenes. Similar observations were made by

317

Foder et al. (1975) in a study of phenocryst and matrix clinopyroxenes in lavas.

Clinopyroxenes from the aphyric Long Reach basalts mostly plot in the subalkaline field of the Le Bas (1962) diagram where as those from both the phyrlic Long Reach basalts and Cape Breton basalts straddle the subalkaline - alkaline boundary, presumably reflecting the mildly alkaline characteristics of these continental tholeiitic basalts (Figure 4.42). Similarly the phyrlic basalts and Cape Breton basalts mostly plot in the alkaline field of the Nisbet and Pearce (1977) discrimination diagram (Figure 4.43) but those from the aphyric basalts fall in nearly all fields of the diagram. Analyses of pigeonite from both the phyrlic and aphyric basalts confirm that the rocks are tholeiitic.

Clinopyroxenes from two Cape St. Mary's dikes reflect the diverse range of compositions shown by these rocks. As a result of their high Ca contents, pyroxenes from one dike (SB56A) plot in the peralkaline field of the pyroxene quadrilateral and in the alkaline field of the Nisbett and Pearce (1977) diagram (Figures 4.30 and 4.31). Some of these pyroxenes have fassaitic compositions. Fassaites are most commonly found within eclogite or clinopyroxenite nodules in nephelinitic rocks, and the only occurrence similar to the Cape St Mary's dikes is in a dolerite at Vilyuy, Yakutia (as reviewed in Deer et al., 1978). These extreme compositions

confirm that some of the dikes have alkaline characteristics. In contrast, the diagrams indicate that pyroxenes from the other dike (SB66A) show mildly alkaline to subalkaline compositions (Figures 4.30 and 4.31).

Pyroxenes from the Cape St. Mary's sills show a wide range of compositions (Figures 4.20, 4.21, 4.22) probably related to variations in the water content and silica activity within individual sills (see section 4.3.3).

The Cambrian volcanic rocks over most of the Acado-Baltic province show a basalt-rhyolite bimodal distribution as is common in continental tensional environments (Martin and Piwinski, 1972). Rhyolites in present day rift systems, such as the East African rift, are usually peralkaline, but the rhyolites can be subalkaline (or peraluminous) in which case they are usually associated with tholeiitic basalts (Eichleberger, 1978; Hanson and Al-Shaieb, 1980; Cameron, 1980; Easton, 1981, 1982; Hildreth, 1981; Tankard et al., 1982). Although some researchers have argued that the rhyolites are derived from the basalts by fractional crystallization (eg. Barberi et al. 1975), most researchers suggest that they are produced by melting of the lower crust in response to injection of high temperature basaltic magmas (eg. Eichleberger, 1978; Cameron, 1980; Easton, 1981, 1982; Hildreth, 1981). The extensional environment allows both magma types to rise quickly to the surface, with little or no mixing, and

results in a bimodal distribution of rock types. In the subduction zone environment melts get to the surface with greater difficulty, which results in mixing between the basaltic and rhyolitic magma types and intermediate andesitic volcanism (eg. Eichelberger, 1978; Hildreth, 1981).

Models for volcanism in tensional zones suggest that the volume and composition of the Cambrian volcanic rocks should act as indicators of the amount of extension that took place (Jarvis and McKenzie, 1980; Le Pichon and Sibuet, 1981; Wendlandt and Podpora, 1982). In any rift, as the lithosphere is stretched by a factor of about 2, hot asthenosphere moves in to replace it, and begins to melt in response to decreased lithospheric pressure. Early magmas should be highly alkaline as they are produced at relatively high pressures by small amounts of melting (Green and Ringwood, 1967). Because the volume of melting is small, and the distance to the surface is still large, the probability of a melt getting to the surface is low. As the amount of lithospheric stretching increases, the distance from the asthenosphere to the surface decreases, pressure decreases, the percentage of melting increases, and eventually tholeiitic magmas are produced. The probability of eruption increases because the volume of magma generated is greater, and the distance to the surface is lower.

The small stretching factor indicated by the relatively thin stratigraphic sections over most of the Acado-Baltic province (see section 5.3.4) predicts that both the volume of lava, and the frequency of eruption should be low, as seems to be the case. In the Cape St. Mary's study area and Poland the Cambrian basaltic rocks are alkaline and in keeping with a low stretching factor (Le Pichon and Sibuet, 1981). At all other localities the volcanic rocks are subalkaline, thus refuting the model. If the arrival of basaltic magmas on the surface is related to fracturing which extends in the upper mantle, the composition of the volcanic rocks may reflect how far down into the mantle the faults extend. Possibly the depth of faulting is not only related to the amount of extension but the rate of extension.

The composition of volcanism commonly varies across rift zones with the most alkaline rocks generally occurring on the flanks of the rift and less alkaline rocks (in some cases tholeiites) appearing in the rift axis (Lippard and Truckle, 1978; Neumann and Ramberg, 1978; Basaltic Volcanism Study Project, 1981, p. 109, 111). This generalization does not appear applicable to the Early Mesozoic graben system of eastern North America as the volcanic rocks are generally more alkaline on the continental shelves than they are on land (L. Jansa, personal communication, 1984). Because it is impossible to reconstruct the paleogeography of the Acado-Baltic province in detail, and because an actual rift

or rifted continental margin has not been identified within the province, it is impossible to determine if there was any spatial relationship between the composition of volcanism and possible focal points of tension.

### 5.3.3 Relationship To Underlying Stratigraphy

Many rifts, such as the East African rift (Bailey, 1974; King, 1978) and the St. Lawrence graben (Doig, 1970; Kumarapeli, 1977), are characterized by very long histories of development with reactivation occurring repeatedly. Possibly the NNW trending, bimodal (basalt-rhyolite) volcanic rocks of the Bull Arm Formation (McCartney, 1967; Hughes and Malpas, 1971), provide evidence for an earlier tensional event within the Cape St. Mary's study area. Studies of volcanic rocks and stratigraphy at other localities in the Avalon Zone of Newfoundland indicate the area experienced tensional tectonism throughout most of the Late Precambrian (Eg. Papezik, 1970, 1972; O'Driscoll and Strong, 1979; Strong et al., 1978; King, 1980). In southern New Brunswick, Cambrian volcanic rocks may also represent small-scale reactivation of an older rift system as they overlie the Coldbrook volcanic rocks which Giles and Ruitenberg (1977) related to intracratonic rifting. In a review of Proterozoic stratigraphy and volcanism on Avalonian terrane in general, Strong (1979) suggested that most of the area underwent a prolonged period of extensional tectonism with local rupturing. The Cambrian volcanic rocks

support continuation of a tensional tectonic regime into the Early Paleozoic.

#### 5.3.4 Taphrogenic Features

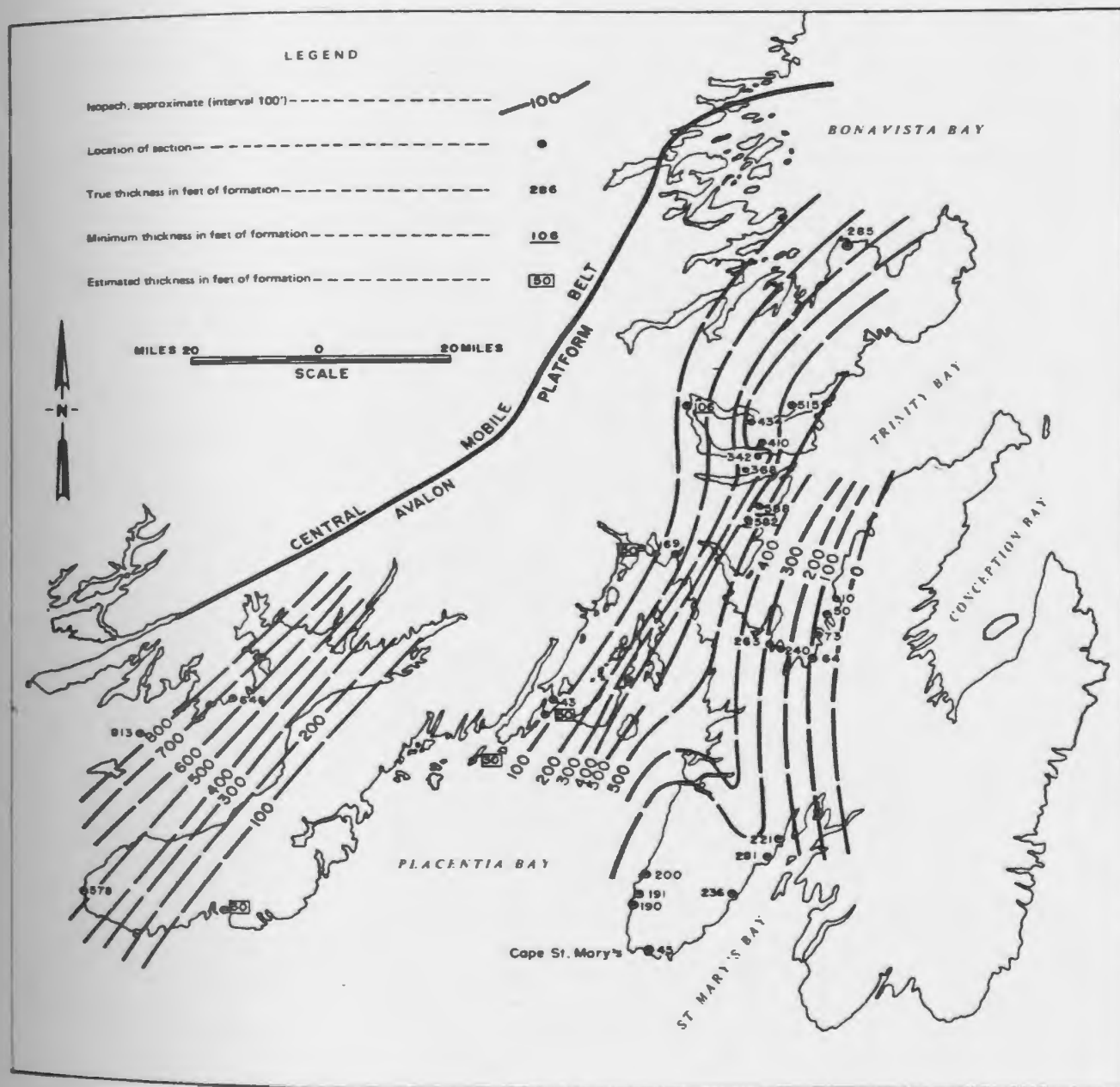
Taphrogenic features common to many active rifts include doming, basin subsidence, faulting, volcanism, positive Bouguer gravity anomalies, magnetic anomalies, low electrical conductivity, and high heat flow. In ancient, or dormant rifts, the latter two features have usually long since disappeared, but many others sometimes remain. They provide a means of identifying and ascertaining the importance of the Cambrian tensional event.

Doming may be very difficult or impossible to identify in most of the Cambrian sections for two reasons: it does not always take place during a tensional event (Easton, personal communication, 1982), and identifying unconformities related to uplift is complicated by the presence of unconformities produced by global changes in sea level during the Cambrian (Vail et al., 1977).

Isopach maps of the Cambrian sedimentation in the Cape St. Mary's study area may provide evidence for tension and small-scale basin subsidence. An isopach map of the Random Formation (Figure 5.1 after Butler and Greene, 1976) shows that the preserved Random is thickest in a narrow trough slightly west of the belt of Middle Cambrian volcanic rocks and in a second trough west of Placentia Bay. The

Figure 5.1<sup>a</sup> Isopach map of the Random Formation. After Butler and Greene (1976).



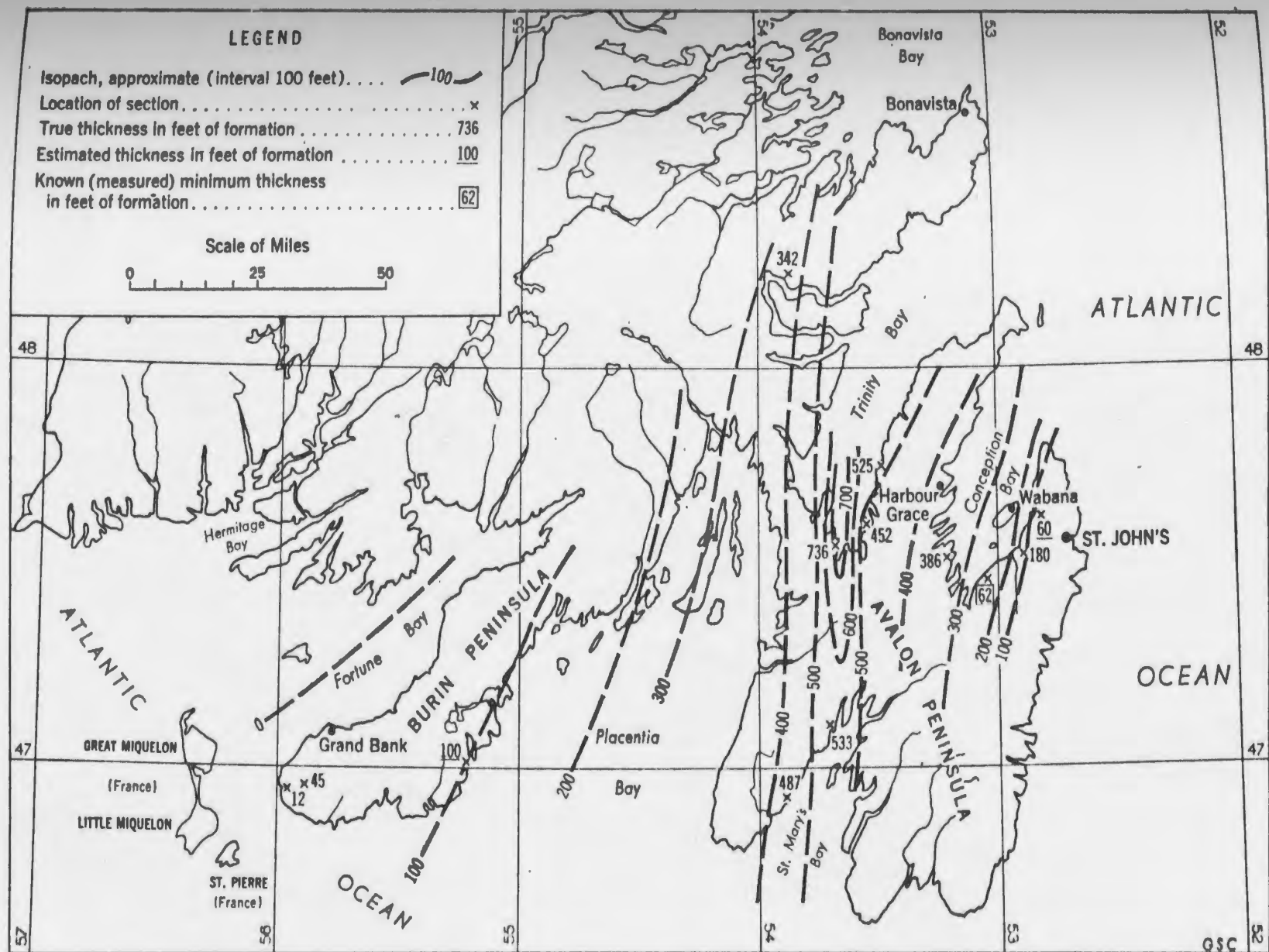


differential thickness of the Random Formation resulted from two separate processes: sedimentation was greatest in areas where the preserved Random is thickest, and pre-Bonavista erosion was most extensive east and west of the trough axis (Hiscott, 1982; Anderson, 1981; Butler and Greene, 1976; Greene and Williams, 1974). These observations suggest that there was a trough shaped basin and that areas east and west of the trough axis defined topographic (bathymetric) highs (the edges of the basin) which were later affected by greatest erosion.

Isopach maps for other Lower and Middle Cambrian sedimentary rocks in the Cape St. Mary's study area (Hutchinson, 1962) show that the basins may have persisted until Upper Cambrian time (eg. Figure 5.2). It could be argued such a small percentage of the original Cambrian cover is preserved that the isopach maps may not accurately represent the paleobathymetry. More detailed but local studies by Fletcher (1972) demonstrated that there are problems with the maps. Nevertheless, all four of Hutchinson's maps for different Cambrian formations indicate the presence of a N to NNW trending trough. The evidence that they collectively provide for a slowly subsiding basin in the study area cannot be ignored.

Cambrian sedimentary rocks, found in Cape Breton were deposited in two basins which may have resembled those in the Cape St. Mary's study area (Hutchinson, 1952). Hayes and

Figure 5.2 Isopach map of the Brigus Formation. After Hutchinson (1962).



Howell (1937) proposed that the Cambrian rocks in southern New Brunswick formed in eight or more basins having an average northeast trend and a total width in excess of 100 km.

In Norway a rifting event that started during the Late Precambrian, resulted in N to NNW trending, fault-bounded, grabens approximately 30 to 60 kilometers wide (Henningsmoen, 1956; Bjorlykke, 1978). As these grabens formed, they filled with the "sparagmite" sediments, and they continued to develop throughout Cambrian time experiencing the minor tholeiitic volcanism (discussed above) as well as alkaline plutonism (Ramberg and Larsen, 1978).

Cambrian sedimentation in Spain was preceded by extensive rift-related block-faulting, subsidence, and clastic sedimentation (Vegas, 1978, 1980). This tectonic regime probably persisted up until the Early Cambrian by which time faulting, and the development of a deep subsiding basin in northern Spain (Zamarreno, 1972; Baldwin, 1975; Julivert, 1979) suggests the existence of a rift valley (Van Calsteren and Den Tex, 1978; Den Tex, 1979). During Cambrian time, subsidence continued, but probably slowed as two basins developed, one in the north, and one in southern Spain.

McKenzie (1978) proposed a model for basin formation which relates crustal thickness, high heat flow and

subsidence to lithospheric stretching and replacement by hot asthenosphere. As the asthenosphere slowly cools it contracts causing the subsidence. The model has been favorably tested in the North Sea by Christie and Sclater (1980), on the Nova Scotia and Labrador shelves by Royden and Keen (1980) and on the Armorican and Galicia continental margins by Le Pichon and Sibuet (1981). According to the model low Cambrian sedimentation rates suggest that the lithosphere was stretched only a small amount resulting in very little subsidence. Curves given by McKenzie (1978), which relate the thermal subsidence in a sediment-loaded basin, to the amount of stretching, show that a stretching factor of only 1.25 can account for the observed thickness (1000 - 1500 m) of Cambrian sedimentary rocks.

According to Jarvis and McKenzie (1980), subsidence is also reduced if extension takes place over time periods on the order of 100 million years. It is unlikely that the low subsidence can be related to higher heat flow and reduced lithospheric thickness during the Cambrian, because McKenzie et al. (1980) were unable to demonstrate that the thicknesses of successions in Archean and Proterozoic basins are any different from those of today.

Very little subsidence will take place if the sediment input is low (McKenzie, 1978) and this is controlled by factors such as petrology of the source area, climate, topography and relief (Tiercelin and Faure, 1977). The red

color of the Lower Cambrian, and some Middle Cambrian rocks on the Avalon Peninsula suggests that they were deposited under arid conditions (Walker, 1967) where low rainfall may have hampered the transportation of clastic material to the basin. Secondly, with the exception of the mature Random Formation clastics, most of the Cambrian sedimentary rocks are shales. The paucity of coarse grained clastic rocks implies there was a sediment supply problem between the Cambrian basin and the source area, possibly as a result of a distal relationship between the two. These explanations for the low subsidence might be useful on a local basis but most of the Acado-Baltic province shows relatively thin stratigraphic sections indicative of relatively low sedimentation (subsidence) rates. The implications are that only a small amount of stretching took place. As discussed above in the geochemistry section, the small volume of the Cambrian volcanic rocks at most localities in the Acado-Baltic province is consistent with a small amount of stretching.

Several of the Cambrian localities discussed above (Avalon Peninsula, Cape Breton, New Brunswick, Spain) show evidence for more than one basin. Estimates of the basin widths are difficult to make but in the case of the Avalon Peninsula they appear to be about 50 to 60 km wide (uncorrected for Devonian deformation). Most rifts consist of one graben a few tens of kilometers wide (Kumarapeli, 1978) but some, such as the Baikal rift, may be up to 200 km

in width (Logatchev et al., 1978) with volcanism across the entire valley. The early Mesozoic graben system on the east coast of North America, which appears related to opening of the Atlantic Ocean, consists of numerous parallel grabens, as much as 500 kilometers inside the continent (Burke, 1976; Robbins, 1982). The Cambrian basins may have formed a system similar to that of the eastern North American graben system except that in the latter subsidence was much greater as a result of large amounts of lithospheric stretching which culminated in rifting. Similarities in the volcanism associated with these two tensional events were discussed above.

Rifts such as the Oslo rift, the East African rift, and the Central North American rift are characterized by a large positive Bouguer gravity anomaly over the rift axis, which is flanked by gravity minima (Girdler, 1978). The gravity high is attributed to thinning of the crust and intrusion of mafic rocks into the lower crust. The Bouguer gravity anomaly map of the Appalachian Orogen, compiled by Haworth et al. (1980), shows that there is no clear gravity evidence for Cambrian tensional basins in New Brunswick, Cape Breton, or the Avalon Peninsula. However, gravity highs at Bonavista Bay and Cape St. Mary's (Avalon Peninsula) tend to define a trend parallel to the basin axis, which could be interpreted as consistent with the tensional hypothesis.



Rifts commonly show a magnetic anomaly produced by igneous rocks with a remnant magnetism (Halls, 1978; Girdler, 1978). Magnetic highs on Cape Bonavista and on the west side of Cape St Mary's (Zietz et al., 1980), define a trend which closely corresponds with the Cambrian basin axis, and could be interpreted as consistent with the tensional hypothesis. No such trends exist in either New Brunswick or Cape Breton. Neither the gravity nor magnetic anomalies define strong unbroken trends at any of the localities (including the Avalon Peninsula) but all of these areas have been affected by Devonian deformation, metamorphism, and plutonism which could have disrupted any such trends.

#### 5.4 SUMMARY AND DISCUSSION

From a review of Acado-Baltic stratigraphy, lithologies, faunas, and paleomagnetism it was concluded in Chapter 1 that lithological and faunal differences between the northern and southern portions of the Acado-Baltic province are more likely due to paleoenvironmental differences rather than the result of formation on separate continental blocks. The sedimentary rocks covering most of the Acado-Baltic landmass can best be described as platformal and record relatively stable tectonic conditions. However, Lower and Middle Cambrian volcanic rocks, showing compositions (where known) and style consistent with derivation in a tensional environment are common, though not

abundant, and they occur in most areas of the Acado-Baltic province (Table 1.1).

The volcanic rocks are usually bimodal, volumetrically small, of limited areal extent, and show an intermediate proportion of volcanoclastic rocks to flows, all of which is consistent with a tensional environment. Where determined, the geochemistry of the mafic rocks most closely resembles that of volcanic rocks associated with rift zones.

The extension did not produce a classical rift valley, such as the East African rift, but appears to have been spread out over a broad continental area. Locally, narrow basins developed, which in a few cases, such as in Norway, are partially fault-controlled. The Cambrian sequences are generally quite thin, contain few arenaceous rocks, and formed under low sedimentation rates. There are local exceptions to this rule, such as in northern Spain, where a relatively deep trough developed and filled with coarse clastic sediments (Vegas, 1978, 1980). Rift valleys and rifted continental margins usually have high subsidence rates which produce thick (several kilometers in an equivalent time span) clastic sequences. Models for the Cambrian basins show that the thin sequences, low sedimentation rates, and low volumes of volcanic rocks can be related to small amounts of lithospheric stretching.

Volcanism was apparently most common in the Middle Cambrian (most number of localities), and least common in

the Late Cambrian (Table 1.1). If volcanism can be used as an indicator (cf. Sengor and Burke, 1978; Baker and Morgan, 1982), it appears that tension persisted throughout the Early and Middle Cambrian, but may have waned in the Late Cambrian. This possibly occurred in direct or indirect response to closing of the Iapetus Ocean which primarily took place during the Ordovician (Stevens, 1970). The thickest volcanic sections occur in Czechoslovakia and Poland where the volcanism is Middle to Late Cambrian and may have been accompanied, in the later stages, by compressive tectonic movements. Although this change in the style of volcanism implies that these rocks formed under a different tectonic regime, the geochemical composition of the rocks from Poland suggests a continuation of tensional tectonism. The Lower and Middle Cambrian volcanic rocks studied here represent a small-scale continuation of the extensional tectonic regime prevalent on Pan African terrane during the Late Precambrian. Sills and dikes in the Cape St. Mary's study area provide local evidence for occasional reactivation of the tensional regime during the Lower Paleozoic.

It is unlikely that the Cambrian tensional event can be related to rifting between the St. Lawrence Platform and Pan African terrane because their Late Precambrian sequences are quite different and preclude their juxtaposition (Rast et al., 1976; Strong, 1977). Although the formation of slowly subsiding basins and the occurrence of small-scale volcanism

supports a tensional tectonic regime over most of the Acado-Baltic province during the Lower and Middle Cambrian, the absence of thick rift sequences indicates lithospheric rupturing may have never taken place. The situation may have been analagous to that for Africa today where the continent is predominantly surrounded by oceanic crust forming part of the same lithospheric plate (Le Pichon, 1968). The plate is in a state of quasi-tension despite being largely surrounded by ocean ridge rift zones.

The Cambrian may have been a time of world wide tensional tectonism as volcanic rocks of this derivation occur at various localities around the globe. Examples include the flood basalts in Australia and Pakistan (Veevers, 1976) and the basalts in Mongolia (Dergunov, 1980). Most paleomagnetic reconstructions indicate that the continents were lined up around the equator during the Cambrian (cf. Smith et al., 1980; Ziegler, 1981). This situation would leave very little room for any major ocean basins (longitudinally) between the continents. If the present day north-south orientation of subduction zones is a product of long-lived convection patterns in the mantle, then the equatorial positioning of the continents during the Cambrian may help explain the importance of (Cambrian) tensional tectonism.

## CHAPTER 6 CONCLUSIONS

1. Cambrian basaltic flows and volcanoclastic rocks on the Avalon Peninsula of Newfoundland show two phases of alteration which resulted in the formation of chlorite and carbonate in most of the rocks. Calculations which account for volume changes in the rocks show that during the phase resulting in the formation of chlorite, Ca, Sr, Ba, Rb, and K were removed from the rocks and Ni, Cr, ~~Co~~, V, and Mn were added. The effects of metasomatism resemble those produced by the interaction of seawater with basalts. The chlorite metasomatism may have also resulted in enrichment of Y, Ti, Nb, Zr, and P at some localities, such as Placentia Junction and Hopeall Head, but it is impossible to show this conclusively because relatively unaltered samples were not found at these localities. The carbonate metasomatism resulted in the addition of Ca, Na, Sr, and  $\text{CO}_2$  and removal of Mg. With the exception of the Mg removal, the behaviour of these elements resembles that observed in systems with high  $\text{CO}_2$  activity.

2. Variation diagrams show that subvolcanic pipes in the area of the flows were probably their feeders. The volcanic rocks display high Nb/Y and low Zr/Nb ratios, steep REE patterns, and high concentrations of incompatible elements such as Nb and Zr which are typical of alkaline rocks. The compositions of relict clinopyroxenes in some of the samples are consistent with these conclusions. Relatively low Mg

values, low CaO and high  $TiO_2$  concentrations show that the flows represent evolved compositions. Petrographic evidence along with mass balance and trace element modelling calculations demonstrate that the range of bulk rock compositions in the feeder pipes can be related to precipitation of augite, plagioclase, and olivine as well as late removal of Fe-Ti oxides and apatite.

3. Silurian sills on Cape St. Mary's show relatively unaltered compositions with primary plagioclase, olivine, clinopyroxene, amphibole, and biotite present in some samples. The very coarse-grained nature of the thicker sills, abundance of hydrous minerals, variation in mineral compositions with height in the sills, lack of low Ca pyroxene, presence of minerals indicative of a wide range of  $SiO_2$  activities (baddeleyite and quartz) and a Fe depletion AFM trend, give direct and indirect evidence for high volatile content in the sills. Mass balance and trace element modelling calculations show that assimilation of sediment, multiple magma injection and crystal fractionation processes cannot account for the range of bulk rock compositions observed in the sills. The transport of Si, Al, Ti, Na, P, K, Rb, Sr, Ba, Nb, Zr, Ga and Y roofward, through thermogravitative processes probably involving volatile complexing, resulted in these elements being concentrated in the middle portions of the sills. Above these rocks the volatiles moved along specific paths in the sills and produced granophyres. Elements such as Si, Al, Na, Nb and Zr

remained in the granophyres whereas some such as K, Rb, Sr and Ba were mostly removed from the sill system. Gabbros immediately adjacent to the granophyres were depleted in all of the elements complexed by the volatiles. The parental sill magma was tholeiitic, as shown by low Nb/Y and high Zr/Nb ratios as well as flat REE patterns. The magma was somewhat evolved at the time of emplacement as evidenced by the Mg' values. The high water content of the magma may have been an intrinsic mantle-derived property or it could have been derived from injection into wet unconsolidated sediments.

4. Dikes on Cape St. Mary's show a range of bulk rock compositions which reflect varying degrees of plagioclase accumulation and ferromagnesian mineral removal in rocks representing two or more magma batches. These rocks resemble Devonian dikes along the shores of Bonavista Bay and can be distinguished from the sills by their lower CaO, and higher  $\text{Fe}_2\text{O}_3$  and  $\text{TiO}_2$  concentrations. The range of Mg' values shown by the dikes are indicative of slightly evolved to highly evolved compositions. Variations in the Nb/Y and Zr/Nb ratios, as well as in the slopes of the REE patterns suggest that the dikes represent various magma batches with compositions ranging from tholeiitic basalts to alkali basalts.

5. Samples of late Lower to Middle Cambrian volcanic rocks at Beaver Harbour (New Brunswick) show a range of compositions which can be related to alteration reactions that led to the formation of chlorite and carbonate in the rocks. Chlorite forming reactions resulted in the addition of Mg, Sr, P, and Mn and the removal of K, Rb, Ti, Zr, V, and Fe from the rocks, as is sometimes observed during the alteration of basalts by seawater. Carbonate metasomatic reactions affected most of the rocks and led to the addition of Ca, Sr, Na, Mg, P, Y, and Zn as well as the removal of Ba, Rb, and K in proportion to the amount of carbonate added to the rocks. The behaviour of these elements closely resembles that observed in peralkaline systems where  $\text{CO}_2$  and F are important constituents of the metasomatic fluids.

6. The least altered Beaver Harbour basalt samples show very low CaO, MgO, Cr, and Ni and high  $\text{Al}_2\text{O}_3$ , FeO,  $\text{TiO}_2$ , Ga, and Zr concentrations as well as low Mg values indicating that they are highly evolved. The high Zr/Nb and low Nb/Y ratios of these rocks are representative of tholeiitic basalts.

7. Volcanic rocks from the Long Reach area (New Brunswick) comprise a bimodal suite, the basaltic portion of which can be petrographically and geochemically separated into two groups. The feldspar phyric basalts show higher  $\text{TiO}_2$ ,  $\text{Fe}_2\text{O}_3$ ,  $\text{P}_2\text{O}_5$ , Y, Nb, and Zr, lower MgO, CaO, Ni, and REE concentrations and lower Mg values than the aphyric



basalts. The former represent relatively evolved rocks where as the latter show unevolved compositions for continental basalts. The slightly lower Nb/Y and higher Zr/Nb ratios of the phyric basalts as well as their flatter REE patterns illustrate that the two groups of basalts are probably not comagmatic, although both are tholeiitic.

8. A review of information on the Precambrian stratigraphy, Cambrian lithologies, fauna, and stratigraphy, as well as paleomagnetic information shows that areas belonging to the Acado-Baltic province in western Europe and eastern North America probably formed one large continental block which remained at lower latitudes throughout the Cambrian. Some lithologic, fauna, and stratigraphic differences between areas to the north (eg. Britain) and the south (eg. France) imply that there were climatic or environmental differences between the two. However, both areas show platformal type sedimentation; stratigraphic units are traceable over great distances and sedimentation rates were low.

9. The platformal sedimentation is consistent with stable tectonic conditions but the presence of volcanic rocks at just about every broad locality examined in this report gives evidence for some tectonism. The volcanic rocks are usually small in volume, in some areas consisting of only one or two flows, and they frequently show a basalt-rhyolite bimodal distribution. These attributes are

commonly found in rifting environments.

10. The petrography and geochemistry of Cambrian basaltic rocks from southern New Brunswick, Cape Breton, Cape St. Mary's, Poland and Norway as well as the Cape St. Mary's dikes and sills show that olivine and clinopyroxene controlled low pressure fractionation of the magmas. The Mg values of some of the basalts and dikes from Cape St. Mary's, as well as flows from Cape Breton, and the Long Reach area exceed 0.60 suggesting that these rocks should not be correlated with flood basalts but with rift basalts. Another similarity with rift-type basalts is the negative correlation between Mg values and  $Al_2O_3$  concentrations shown by the Cape St. Mary's basalts and dikes and inferred for the Beaver Harbour and Norwegian basalts. The alkaline nature of some of the dikes from Cape St. Mary's as well as the flows from Cape St. Mary's and Poland serves to relate them to rift basalts. The Cape St. Mary's sills and some of the dikes display tholeiitic trace element characteristics resembling basalts from continental tensional environments in general. Similar conclusions apply to the Cambrian basalts from Cape Breton, southern New Brunswick and Norway. The compositions of pyroxenes from these rocks tend to confirm indications from the whole rock geochemistry on the alkaline versus tholeiitic nature of each rock group. However, the pyroxenes also reflect the cooling rates of the rocks and this complicates their use as indicators of petrogenetic character. Chondrite normalized REE patterns

for many of these Avalonian rocks are convex upward and normalized Yb values for the Cape St. Mary's dikes, sills and flows and Long Reach aphyric basalts are less than 10. These characteristics may be related to a high proportion of garnet to clinopyroxene in the mantle source region for the rocks. More importantly, from the point of view of correlation, continental basalts showing such patterns are most commonly found in rifting environments.

11. The small volume of the Acado-Baltic Cambrian volcanic rocks at most localities in western Europe and eastern North America is consistent with the relatively thin Acado-Baltic stratigraphy in indicating that the tension produced only small amounts of lithospheric stretching. Alkali basalts in Newfoundland and Poland support this model for tension induced volcanism but the tholeiitic nature of the basalts in southern New Brunswick, Cape Breton and Norway suggests that other factors, such as the depth of extension-related fracturing, may control the composition of the volcanism.

12. Very few of the localities examined here show Upper Cambrian volcanic rocks but Lower and/or Middle Cambrian extrusive rocks occur at most of them. If volcanism can be used as an indicator, it appears that tension persisted throughout the Lower and Middle Cambrian, but may have waned in the Upper Cambrian possibly in direct or indirect response to closing of the Iapetus Ocean. The tension did

not produce a classical rift valley, such as the East African rift, but affected a broad continental area and produced numerous narrow basins or graben (eg. Cape St. Mary's basin, or the Sparagmite basins) where the volcanic rocks appear to be concentrated. In summary the tectonic environment would appear to be very similar to that associated with platforms except that small amounts of tension affecting most portions of the Acado-Baltic province resulted in the formation of shallow basins and small volumes of volcanic rocks geochemically resembling rift basalts.

REFERENCES CITED

Allen, P.M., and Jackson, A.A., 1978. Bryn-teg borehole, North Wales. Bulletin of the Geological Survey of Great Britain, Bulletin 61, London, 51 p.

Anderson, M.M. 1981. The Random Formation of southeastern Newfoundland: A discussion aimed at establishing its age and relationship to bounding formations. American Journal of Science, Volume 281, pp. 807 to 830.

Anderton, R. 1980. Did Iapetus start to open during the Cambrian? Nature, Volume 286, pp. 706 to 708.

Arth, J.G. 1976. Behaviour of trace elements during magmatic processes - a summary of the theoretical models and their applications. Journal of Research United States Geological Survey, Volume 4, Number 1, pp. 41 to 47.

Atkins, F.B. 1969. Pyroxenes of the Bushveld intrusion, South Africa. Journal of Petrology, Volume 10, pp. 222 to 249.

Ayres, L.D. 1982. Pyroclastic rocks in the geologic record. In Pyroclastic Volcanism and Deposits Of Cenozoic Intermediate to Felsic Volcanic Islands With Implications For Greenstone-Belt Volcanoes. Edited by L.D. Ayres. Geological Association of Canada Short Course Notes, Volume 2, pp. 1 to 17.

Bahatbacharji, S. 1967. Mechanics of flow differentiation in ultramafic and mafic sills. Journal of Geology, Volume 75, pp. 101 to 112.

Bailey, D.K., 1974. Continental rifting and alkaline magmatism. In The Alkaline Rocks. Edited by H. Sorensen. John Wiley and Sons, London, pp. 148 to 159.

Baker, B.H., and Morgan, P. 1982. Continental rifting: Progress and outlook. EOS, Volume 62, pp. 585.

Baldrige, W.S. 1979. Petrology and petrogenesis of Plio-Pleistocene basaltic rocks from the central Rio Grande rift, New Mexico, and their relation to rift structure. In Rio Grande Rift: Tectonics and Magmatism. Edited by Robert E. Riecker. American Geophysical Union, Washington, D.C., pp. 323 to 353.

Baldwin, C.T. 1975. The stratigraphy of the Cabos series in the section between Cadavedo and Luarca, province of Oviedo, N.W. Spain. Breviora Geologica Asturica, Volume 19, pp. 4 to 9.

Banks, N.L., Edwards, M.B., Geddes, W.P., Hobday, D.K., and Reading, H.G. 1971. Late Precambrian and Cambro-Ordovician sedimentation in East Finnmark. In *The Caledonian Geology of Northern Norway*. Edited by David Roberts and Magne Gustavson. Norges Geologiske Undersøkelse, Nr. 269, pp. 197 to 236.

Baranowski, Z., Lorenc, S., Heinisch, H., and Schmidt, K. 1984. The Cambrian volcanism of the Kaczawa Mountains (Kaczawskie Gory, West Sudetes, Poland). *Neues Jahrbuch für Geologie und Paläontologie Monatshefte*, Volume 1, pp. 1 to 26.

Barberi, F., Ferrara, G., Santacroce, R., Treuil, M., Varet, J. 1975. A transitional basalt-pantellerite sequence of fractional crystallization, the Boina Centre (Afar Rift Ethiopia). *Journal of Petrology*, Volume 16, pp. 22 to 56.

Basaltic Volcanism Study Project, (1981) *Basaltic Volcanism on the Terrestrial Planets*. Pergamon Press, Inc., New York, 1286 p.

Bengston, S., and Fletcher, T.P. 1981. The succession of skeletal fossils in the basal Lower Cambrian of the Southeastern Newfoundland. In *Short Papers For the Second International Symposium on the Cambrian System*. Edited by M.E. Taylor. United States Geological Survey Open File Report 81-743, p 18.

Benziane, F., Prost, A.E., Yazidi, A. 1983. Le passage du Précambrien au Cambrien précoce volcanique et sédimentaire de l'Anti-Atlas oriental; comparaisons avec l'Anti-Atlas occidental. *Société Géologique de France, Bulletin, Series 7*, Volume 25, pp. 549 to 556.

Berthelsen, A. 1980. Towards a palinspastic analysis of the Baltic Shield. In *Colloque C6: Géologie de l'Europe du Précambrien aux bassins sédimentaires post-hercyniens*. Edited by Jean Cogné, and Maurice Slansky. 26<sup>th</sup>. *Congrès Géologique International*, pp. 5 to 21.

Bird, J.M. and Dewey, J.F. 1970. Lithosphere plate - continental margin tectonics and the evolution of the Appalachian orogen. *Geological Society of America Bulletin*, Volume 81, pp. 1031 to 1060.

Bjørlykke, K. 1978. The eastern marginal zone of the Caledonide orogen in Norway. In *Caledonian - Appalachian Orogen of the North Atlantic Region*. IGCP Project 27, Geological Survey of Canada, Paper 78-13, pp. 49 to 55.

Black, W.W. 1980. Chemical characteristics of metavolcanics in the Carolina Slate Belt. In Proceedings "The Caledonides In the U.S.A." Edited by David R. Wones. IGCP Project 27: Caledonide Orogen. Department of Geological Sciences, Virginia Polytechnic Institute and State University, Memoir Number 2, pp. 271 to 278.

Blackadar, R.G. 1956. Differentiation and assimilation in the Logan Sills, Lake Superior District, Ontario. American Journal of Science, Volume 254, pp. 623 to 645.

Bland, A.E., and Blackburn, W.H. 1980. Geochemical studies on the greenstones of the Atlantic seaboard volcanic province, south-central Appalachians. In Proceedings "The Caledonides In the U.S.A." Edited by David R. Wones. IGCP Project 27: Caledonide Orogen. Department of Geological Sciences, Virginia Polytechnic Institute and State University, Memoir Number 2, pp. 263 to 270.

Bowen, N.L. 1913. The melting phenomena of the plagioclase feldspars. American Journal of Science, Series 4, Volume 40, pp. 161 to 185.

Boyer, C. 1966. Etude des keratophyres de la region de Radon (Paleozoique Inferieur du Massif Armoricaire). Societe Geologique de France, Bulletin, Series 7, Volume 8, pp. 288 to 297.

Boyer, C. 1974. Vulcanismes Acides Paleozoiques Dans Le Massif Amoricain. Ph.D. Thesis, L'Universite De Paris-Sud Centre D'Orsay. 384 p.

Boyer, C., Autran, A., Auvray, B., Guillot, P.-L., et Le Gall, J. 1979. Bilan et synthese des paleovulcanismes Ante Devonian en France. Societe Geologique de France, Bulletin, Number 6, pp. 695 to 708.

Brasier, M.D. 1980. The Lower Cambrian transgression and glauconite - phosphate facies in western Europe. Journal of the Geological Society of London, Volume 137, pp. 695 to 703.

Brown, G.M., and Vincent, E.A. 1963. Pyroxenes from the late stages of fractionation of the Skaergaard intrusion, east Greenland. Journal of Petrology, volume 4, pp. 175 to 197.

Bullard, E., Everett, J.E., and Smith, A.G. 1965. The fit of the continents around the Atlantic. In A Symposium On Continental Drift. Edited by P.M.S. Blackett, E. Bullard, and S.K. Runcorn. The Royal Society, London, pp. 41 to 51.

Burke, K. 1976. Development of graben associated with the initial ruptures of the Atlantic Ocean. *Tectonophysics*, Volume 36, pp. 93 to 112.

Burke, K., and Dewey, J.F. 1973. Plume generated triple junctions: key indicators in applying plate tectonics to old rocks. *Journal of Geology*, Volume 81, pp. 406 to 433.

Burrett, C., and Richardson, R. 1980. Trilobite biogeography and Cambrian tectonic models. *Tectonophysics*, Volume 63, pp. 155 to 192.

Butler, A.J., and Greene, B.A. 1976. Silica Resources of Newfoundland. Report 76-2, Mineral Development Division, Department of Mines and Energy, Government of Newfoundland and Labrador, 68 p.

Butler, J.R., and Ragland, P.C. 1969. Petrology and chemistry of meta-igneous rocks in the Albemarle area, North Carolina Slate Belt. *American Journal of Science*, Volume 267, pp. 700 to 726.

Cameron, Kevin J. 1980. Geochemistry and Petrogenesis of Volcanic Rocks From the Bourinot Group, Cape Breton, Nova Scotia. B.Sc. Thesis (Honours), Saint Mary's University, Halifax, Nova Scotia, 114 p.

Carmichael, Ian S.E., Turner, Francis J., and Verhoogen, John. 1974. *Igneous Petrology*. McGraw - Hill, New York, 739 p.

Chauvel, J.J. 1979. A cross section through the Armorican Massif. *Krystalinikum*, Volume 14, pp. 8 to 17.

Chauvel, C. and Jahn, Bor-Ming. 1984. Nd-Sr isotope and REE geochemistry of alkali basalts from the Massif Central, France. *Geochimica et Cosmochimica Acta*, Volume 48, pp. 93 to 110.

Chlebowski, Roman. 1978. Petrographic study of Early Paleozoic tuffogenic rocks from the Holy Cross Mts. *Archivum Mineralogiczne*, Volume 34, pp. 70 to 131.

Christie, P.A.F. and Sclater, J.G. 1980. An extensional origin for the Buchan and Witchgroud Graben in the North Sea. *Nature*, Volume 283, pp. 729 to 732.

Claesson, K.C., and Turner, P., 1980, Diagenetic magnetization of the Caerfai Bay shales (Cambrian), South Wales. *Geophysical Journal*; Volume 60, pp. 95 to 106.



Clark, Thomas H., and Stearn, Colin W., 1968. Geological Evolution of North America. 2nd edition, New York, Ronald Press Company, 570 p.

Coombs, D.S. 1963. Trends and affinities of basaltic magmas and pyroxenes as illustrated on the diopside - olivine - silica diagram. Mineralogical Society of America Special Paper 1, pp. 227 to 250.

Costello, O.P., Secor, D.T., Snoke, A.W. 1981. Structural relationships as a key to stratigraphic sequences in the Carolina Slate Belt Lake Murray, South Carolina. Southeastern Geology, Volume 22, pp. 139 to 146.

Crandell, D.R. 1971. Postglacial Lahars From Mount Rainier Volcano, Washington. United States Geological Survey Professional Paper 667, 75 p.

Currie, K.L., Nance, R.D., Pajari, G.E. Jr., Pickerill, R.K. 1981. Some aspects of the pre-Carboniferous geology of Saint John, New Brunswick. In Current Research, Part A., Geological Survey of Canada, Paper 81-1a, pp. 23 to 30.

Daly, L., and Pozzi, J.P. 1977. Determination d'un nouveau pôle paleomagnetique Africain sur des formations Cambriennes du Maroc. Earth and Planetary Science Letters, Volume 34, pp. 264 to 272.

Deer, W.A., Howie, R.A., and Zussman, J. 1966. An Introduction to the Rock Forming Minerals. Longman Limited, London, 528 p.

Deer, W.A., Howie, R.A., and Zussman, J. 1978. Rock Forming Minerals, Volume 2A, Single - Chain Silicates, 2nd. edition, Longman Limited, London, 668 p.

Delong, S.E., 1974. Distribution of Rb, Sr, and Nd in igneous rocks, central and western islands, Alaska. Geochimica et Cosmochimica Acta, Volume 38, pp. 245 to 266.

Den Tex, E. 1979. A pre-Variscan continental rift system in N.W. Spain. Krystalinikum, Volume 14, pp. 19 to 31.

Dergunov, A.B. 1980. Structure, of the Caledonides and the development of the earth's crust in West Mongolia and the Altai-Sayan area, USSR. In Proceedings "The Caledonides In the U.S.A." Edited by David R. Wones. IGCP Project 27: Caledonide Orogen. Department of Geological Sciences, Virginia Polytechnic Institute and State University, Memoir Number 2, pp. 197 to 203.

Dimroth, E., Cousineau, P., Leduc, M., and Sanschagrin, Y. 1978. Structure and organization of Archean subaqueous basalt flows, R  gion - Noranda area, Quebec, Canada. Canadian Journal of Earth Sciences, Volume 15, Pages 902 to 918.

Di Paola, G.M. 1972. The Ethiopian Rift Valley (between 7 degrees 00 minutes and 8 degrees 41 minutes lat. north). Bulletin Volcanologique, Volume 36, pp. 517 to 560.

Doig, R. 1970. An alkaline rock province linking Europe and North America. Canadian Journal of Earth Sciences, Volume 7, Pages 22 to 28.

Dore, F. 1977. L'Europe Moyenne Cambrian, les modeles sedimentaires leur zonalite, leur controle. In La Cha  ne Varisque d'Europe Moyenne Et Occidentale, Colloque International Du Centre National De La Recherche Scientifique, No 243, pp. 143 to 155.

Dore F., Giordano, R., et Le Gall, J. 1972. Mise au point sur la position stratigraphique des volcanites Cambriennes de l'est de Massif Armorica  n. Bulletin Soci  te Linneenne De Normandie, Caen, Volume 103, pp. 29 to 45.

Douglas, John Leslie. 1981. Geochemistry of the Cambrian Manganese Deposits of Eastern Newfoundland. Ph.D. Thesis, Memorial University of Newfoundland, St. John's Newfoundland, 271 p.

Dudas, M.J., Schmitt, R.A., Harward, M.E. 1971. Trace element partitioning between volcanic plagioclase and dacitic plagioclase matrix. Earth and Planetary Science Letters, Volume 11, pp. 440 to 446.

Duke, J.M. 1976. Experimental determination of partition coefficients of period 4 transition elements in olivine and clinopyroxene. Journal of Petrology, Volume 17, pp. 499 to 521.

Dupont, R., and Vegas, R. 1978. Le Cambrien Inferior du sud de la Province de Badajoz (sud-ouest d'Espagne), distribution des series sedimentaires et volcaniques associees. Academie des Sciences, Comptes Rendus, Series. D, Volume 286, pp. 447 to 450.

Dypvik, H. 1977. Mineralogical and geochemical studies of Lower Paleozoic rocks from the Trondheim and Oslo Regions, Norway. Norsk Geologisk Tidsskrift, Volume 57, pp. 205 to 241.

Easton, R.M. 1981. Stratigraphy of the Akaitcho Group and the development of an Early Proterozoic continental margin, Wopmay Orogen, Northwest Territories. In Proterozoic Basins of Canada. Edited by F.H.A. Campbell. Geological Survey of Canada Paper 81-10, pp. 79 to 95.

Easton, R.M. 1982. Tectonic Significance of the Akaitcho Group, Wopmay Orogen, Northwest Territories, Canada. Ph.D. Thesis, Memorial University of Newfoundland, St. John's, Newfoundland, 432 p.

Eichelberger, J.C., 1978. Andesitic volcanism and crustal evolution. *Nature*, Volume 275, pp. 21 to 27.

Elias, P.N., and Strong, D.F. 1982. Timing of arrival of the Avalon Zone in the northern Appalachians: a new look at the Straddling Granite. *Canadian Journal of Earth Sciences*, Volume 19, pp. 1088 to 1094.

Ernst, W.G. 1960. Diabase - granophyre relations in the Endion Sill, Duluth, Minnesota. *Journal of Petrology*, Volume 1, pp. 286 to 303.

Evans, J.L. 1978. An alkalic volcanic suite of the Labrador Trough, Labrador. M.Sc. Thesis, Memorial University of Newfoundland, St. John's, Newfoundland, Canada. 382 p.

Ewart, A., and Taylor, S.R., 1969. Trace element geochemistry of the rhyolitic volcanic rocks, central North Island, New Zealand: phenocryst data. *Contributions to Mineralogy and Petrology*, Volume 22, pp. 127 to 146.

Fiala, Frantisek. 1978a. Proterozoic and Early Paleozoic Volcanism of the Barrandian - Zelezne hory zone. *Sbornik Geologických Ved: Geologie*, Volume 31, pp. 71 to 90.

Fiala, Frantisek. 1978b. The TiO<sub>2</sub>-K<sub>2</sub>O-P<sub>2</sub>O<sub>5</sub> Diagram and tectonomagmatic relations of the volcanics of the Barrandian area. *Vestník Ustředního Ústavu Geologického*, Volume 53, pp. 333 to 346.

Fieremans, M., and Ottenburgs, R. 1979. The occurrence of zircon and baddeleyite in the kimberlite formations at Mbuji - Mayi (Bakwanga, Zaire). *Bulletin de la Société belge de Géologie*, Volume 8, pp. 25 to 31.

Fisher, R.V. 1961. Proposed classification of volcanoclastic sediments and rocks. *Geological Society of America Bulletin*, Volume 72, pp. 1409 to 1414.

Fitton, J.G. 1980. The Benue Trough and Cameroon line - A migrating rift system in West Africa. *Earth and Planetary Science Letters*, Volume 51, pp. 132 to 138.

Fletcher, Terence Patrick. 1972. *Geology and Lower to Middle Cambrian Trilobite Faunas of the Southwest Avalon, Newfoundland*. Ph.D. Thesis, University of Cambridge, part one 236 p.

Floyd, P.A. 1977 Rare earth element mobility and geochemical characterization of spilitic rocks. *Nature*, Volume 269, pp. 134 to 137.

Floyd, P.A. and Winchester, J.A. 1975. Magma type and tectonic setting discrimination using immobile elements. *Earth and Planetary Science Letters*, Volume 27, pp. 211 to 218.

Fodor, R.V., Keil, Klaus, and Bunch, T.E. 1975. Contributions to the mineral chemistry of Hawaiian rocks. *Contributions to Mineralogy and Petrology*, Volume 50, pp. 173 to 195.

Frey, F.A., Bryan, W.B., and Thompson, G. 1974. Atlantic Ocean floor: Geochemistry and petrology of basalts from Legs 2 and 3 of the Deep Sea Drilling Project. *Journal of Geophysical Research*, Volume 79, pp. 5507 to 5528.

Fryer, B.J. 1977. Rare earth evidence in iron formations for changing oxidation states. *Geochimica et Cosmochimica Acta*, Volume 41, pp. 361 to 367.

Furnes, H., Nystuen, J.P., Brunfelt, A.O., and Solheim, S. 1983. Geochemistry of an Upper Riphean-Vendian basalt associated with the "sparagmites" of southern Norway. *Geological Magazine*, Volume 120, pp. 349 to 361.

Furon, Raymond. 1956. Le Cambrien du Sahara et de l'Ouest Africa. In *XX Congress Geologico Internacional, Mexico. El Sistema Cambrico, Su Paleogeografia y el Problema de Su Base*, Volume 1, pp. 243 to 260.

Furon, Raymond. 1963. *Geology of Africa*. Hofner Publishing Company, New York, 377p.

Gale, G.H., and Roberts, D. 1974. Trace element geochemistry of Norwegian Lower Palaeozoic basic volcanics and its tectonic implications. *Earth and Planetary Science Letters*, Volume 22, pp. 380 to 390.

Gale, G.H., and Pearce, J.A. 1982. Geochemical patterns in Norwegian greenstones. Canadian Journal of Earth Sciences. Volume 19, pp. 385 to 397.

Gast, P.W. 1968. Trace element fractionation and the origin of tholeiitic and alkaline magma types. Geochimica et Cosmochimica Acta, Volume 32, pp. 1057 to 1086.

Geze, Bernard. 1956. Les Terrains Cambriens et Antecambrian dans le sud du Massif Central Français (montagne Noire et Cévennes Méridionales). In XX Congress Geologico Internacional, Mexico. El Sistema Cambrico, Su Paleogeografía y el Problema de Su Base, Volume 1, pp. 185 to 234.

Giles, P.S. and Ruitenberg, A.A. 1977. Stratigraphy, paleogeography, and tectonic setting of the Coldbrook Group in the Caledonia Highlands of southern New Brunswick. Canadian Journal of Earth Sciences, Volume 14, pp. 1263 to 1275.

Girdler, R.W. 1978. Comparison of the East African rift system and the Permian Oslo rift. In Tectonics and Geophysics of Continental Rifts. Edited by I.B. Ramberg and E.R. Neumann. D. Reidel Publishing Company, Dordrecht, Holland, pp. 329 to 346.

Green, D.H. 1971. Composition of basaltic magmas as indicators of conditions of origin: Application to oceanic volcanism. Philosophical Transactions of the Royal Society of London, Volume A268, pp. 70 to 725.

Green, D.H. 1973. Experimental melting studies on a model upper mantle composition at high pressure under water-saturated and water-undersaturated conditions. Earth and Planetary Science Letters, Volume 19, pp. 37 to 53.

Green, D.H., and Ringwood, A.E., 1967. The genesis of basaltic magmas. Contributions to Mineralogy and Petrology, Volume 15, pp. 103 to 190.

Greene, B., and Williams, H. 1974. New fossil localities and the base of the Cambrian in southeastern Newfoundland. Canadian Journal of Earth Sciences, Volume 11, pp. 319 to 323.

Greenly, E. 1944. The Cambrian rocks of Arvon. Geological Magazine, Volume 81, pp. 170 to 174.

Greenly, E. 1945. The Arvonian rocks of Arvon. Quarterly Journal of the Royal Society of London, 1945, pp. 269 to 287.

Greenough, John D. 1979. The Geochemistry of Hawaiian Lavas. M.Sc. Thesis, Department of Geology, Carleton University, 104 p.

Grenne, T., and Roberts, D. 1980. Geochemistry and volcanic setting of the Ordovician Forbordfjell and Jonsvaen greenstones, Trondheim region, central Norwegian Caledonides. Contributions to Mineralogy and Petrology, Volume 74, pp. 375 to 386.

Gresens, R.L., 1967. Composition-volume relationships of metasomatism. Chemical Geology, Volume 2, pp. 47 to 65.

Guilhou, Jean-Jacques. 1971. Variations chimiques portant sur Zn, Cu, Sb, Hg, d'un type morphologique de gite syngenétique selon son contexte sédimentaire ou volcanique - sédimentaire (Cambrien inférieur du sud de la Péninsule Iberique). Académie des Sciences Comptes Rendus, Série D, Volume 272, pp. 1829 to 1832.

Gunn, B.G. 1962. Differentiation in Farrar dolerites Antarctica. New Zealand Journal of Geology and Geophysics, Volume 5, pp. 820 to 863.

Hallam, A., 1972. Continental drift and the fossil record. In Continents Adrift and Continents Aground. W.H. Freeman and Company, New York, pp. 186 to 195.

Halls, H.C. 1978. The Late Precambrian central North American rift system - A survey of recent geological and geophysical investigations. In Tectonics and Geophysics of Continental Rifts. Edited by I.B. Ramberg and E.R. Neumann. D. Reidel Publishing Company, Dordrecht, Holland, pp. 111 to 124.

Hanson, G.N., and Langmuir, C.H., 1978. Modelling of major elements in mantle-melt systems using trace element approaches. Geochimica et Cosmochimica Acta, Volume 42, pp. 725 to 742.

Hanson, R.E., and Al-Shaieb, Z. 1980. Voluminous subalkaline silicic magmas related to intracontinental rifting in the southern Oklahoma aulacogen. Geology, Volume 8, pp. 480 to 484.

Hawkes, D.D. 1966. Differentiation of the Tumatumari - Kopinang dolerite intrusion, British Guiana. Geological Society of America, Volume 77, pp. 1131 to 1158.

Hawkins, James W. Jr. 1977. Petrologic and geochemical characteristics of marginal basin basalts. In Island Arcs, Deep Sea Trenches, and Back - Arc Basins. Edited by Manik Talwani, and Walter C. Pitman. American Geophysical Union, Washington D.C., pp. 355 to 365.

Haworth, R.T., Daniels, D.L., Williams, H., Zietz, I., 1980. Bouger Gravity Anomaly Map of the Appalachian Orogen. Memorial University of Newfoundland, St. John's, Newfoundland.

Hayes, A.O., and Howell, B.F. 1937. Geology Of Saint John New Brunswick. Geological Society of America Special Paper Number 5, 146 p. plus map.

Heiken, G. 1972. Morphology and petrography of volcanic ashes. Geological Society of America Bulletin, Volume 83, pp. 1961 to 1988.

Hellman, P.L., Smith, R.E., Henderson, P. 1979. The mobility of the rare earth elements: Evidence and implications from selected terrains affected by burial metamorphism. Contributions to Mineralogy and Petrology, Volume 71, pp. 23 to 44.

Helmstaedt, H. 1968. Structural Analysis Of the Beaver Harbour Area, Charlotte County, New Brunswick. Ph.D. Thesis, University of New Brunswick, Fredericton, New Brunswick, 196 p. plus map.

Helmstaedt, H., and Tella, S. 1973. Pre-Carboniferous structural history of S.E. Cape Breton Island, Nova Scotia. Maritime Sediments, Volume 9, pp. 88 to 99.

Henderson, P., and Dale, I.M. 1969. The partitioning of selected transition element ions between olivine and the groundmass of oceanic basalts. Chemical Geology, Volume 5, pp. 267 to 274.

Henningsmoen, Gunnar. 1956. The Cambrian of Norway. In XX Congress Geológico Internacional, Mexico. El Sistema Cambrico, Su Paleogeografía y el Problema de Su Base, Volume 1, pp. 45 to 57.

Henningsmoen, Gunnar. 1969. Short account of Cambrian and Tremadocian of Acado - Baltic province. In North Atlantic - Geology and Continental Drift; A Symposium. American Association of Petroleum Geologists, Memoir 12, pp. 110 to 114.

Hiemstra, S.A., 1955. Baddeleyite from Phalaborwa, Eastern Transvaal. American Mineralogist, Volume 40, pp. 275 to 282.

Hildreth, W. 1979. The Bishop Tuff: Evidence for the origin of compositional zonation in silicic magma chambers. Geological Society of America Special Paper 180, pp. 43 to 75.

Hildreth, W. 1981. Gradients in silicic magma chambers: Implications for lithospheric magmatism. *Journal of Geophysical Research*, Volume 86, pp. 10153 to 10192.

Hinthorne, J.R., Andersen, C.A., Conrad, R.L., and Lovering, J.F. 1979. Single-grain  $^{207}\text{Pb}/^{206}\text{Pb}$  and  $\text{U}/\text{Pb}$  age determinations with a 10- $\mu\text{m}$  spatial resolution using the ion microprobe mass analyzer (IMMA). *Chemical Geology*, Volume 25, pp. 271 to 303.

Hiscott, Richard N. 1982 Tidal deposits of the Lower Cambrian Random Formation, eastern Newfoundland: Facies and paleoenvironments. *Canadian Journal of Earth Sciences*, Volume 19 pp. 2028 to 2042.

Hodych, J.P., and Patzold, R. 1980. Paleomagnetism of folded Lower Palaeozoic sills of the Avalon Peninsula. (Abstract) *EOS*, Volume 61 p. 220.

Hoffman, H.J. 1974. Stromatolites from the Proterozoic Greenhead Group, New Brunswick. Geological Association of Canada - Mineralogical Association of Canada, 1974 Annual Meeting, Program Abstracts, p. 43.

Hofmann, A. W. 1980. Diffusion in natural silicate melts: A critical review. In *Physics of Magmatic Processes*. Edited by Hargraves, R.B. Princeton University Press, Princeton, N.J., pp. 385 to 417.

Holm, P.E., 1982. Non-recognition of continental tholeiites using the Ti-Y-Zr diagram. *Contributions to Mineralogy and Petrology*, Volume 79, pp. 308 to 310.

Hubert, C., Lajoie, J., and Leonard, M.A. 1970. Deep sea sediments in the Lower Paleozoic Quebec Supergroup. In *Flysch Sedimentology in North America*. Edited by J. Lajoie. Geological Association of Canada, Special Paper 7, pp. 103 to 125.

Hughes, C.J. 1973. Spilites, keratophyres, and the igneous spectrum. *Geological Magazine*, Volume 109, pp. 513 to 527.

Hughes, C.J., and Malpas, J.G. 1971. Metasomatism in the Late Precambrian Bull Arm Formation in southeastern Newfoundland: Recognition and implications. *Geological Association of Canada Proceedings*, Volume 24, Number 1, pp. 85 to 93.

Hughes, C.P. 1981. Paleozoic faunas. In *Paleoreconstruction of the Continents*. Geodynamic Series, Volume 2, American Geophysical Union, Washington D.C., pp. 27 to 30.



Hutchinson, R.D. 1952. The Stratigraphy and Trilobite Faunas of the Cambrian Sedimentary Rocks of Cape Breton Island, Nova Scotia. Geological Survey of Canada Memoir 263, 124 p. plus maps.

Hutchinson, R.D. 1962. Cambrian Stratigraphy and Trilobite Faunas of Southeastern Newfoundland. Geological Survey of Canada Bulletin 88, 156 p. plus plates.

Hyndman, Donald W. 1972. Petrology of Igneous and Metamorphic Rocks. McGraw-Hill, New York, 533 p.

Hynes, Andrew. 1980. Carbonatization and mobility of Ti, Y, and Zr, in Ascot Formation metabasalts, S.E. Quebec. Contributions to Mineralogy and Petrology, Volume 75, pp. 79 to 87.

Irvine, T.N. 1983a. Observations on the origins of Skaergaard layering. In Annual Report of the Director - Geophysical Laboratory 1982 - 1983. Geophysical Laboratory, Carnegie Institution, Washington, D.C., pp. 284 to 289.

Irvine, T.N. 1983b. Skaergaard trough-layering structures. In Annual Report of the Director - Geophysical Laboratory 1982 - 1983. Geophysical Laboratory, Carnegie Institution, Washington, D.C., pp. 289 to 295.

Jarvis, G.T., and McKenzie, D.P. 1980. Sedimentary basin formation with finite extension rates. Earth and Planetary Science Letters, Volume 48, pp. 42 to 52.

Jayasinghe, N.R. 1978. Devonian alkali basalt dikes of northeastern Newfoundland: Evidence of a tensional environment. Canadian Journal of Earth Sciences, Volume 15, pp. 848 to 853.

Jenness, Stuart E. 1963. Terra Nova and Bonavista Map Areas, Newfoundland. Geological Survey of Canada Memoir 327, 184 p.

Jensen, B.B. 1973. Patterns of trace element partitioning. Geochimica et Cosmochimica Acta, Volume 37, pp. 2227 to 2242.

Johnson, Rex, and Van Der Voo, R. 1983. A paleomagnetically determined position for the Avalon terrane in the early paleozoic. (Abstract) Geological Society of America Abstracts with Programs, Volume 15, p. 605.

Jones, J.C. 1969. Pillow lavas as depth indicators. American Journal of Science, Volume 267, pp. 181 to 195.

Julivert, M. 1979. A cross-section through the northern part of the Iberian Massif: Its position within the Hercynian fold belt. *Krystalinikum*, Volume 14, pp. 51 to 67.

Juskowiak, O., and Ryka, W. 1967. Volcanogenic rocks and adjacent sedimentary rock-complex in bore-holes, Kruszyneany and Mielnik (northeastern Poland). *Instytut Geologiczny Biuletyn*, Volume 1, pp. 69 to 114.

Kay, M., and Colbert, E.H. 1965. *Stratigraphy and Life*. John Wiley and Sons, New York, 736 p.

Kay, R.W., and Gast, P.W., 1973. The rare earth content and origin of alkali - rich basalts. *Journal of Geology*, Volume 81, pp. 653 to 682.

Kaye, C.A., and Zartman, R.E. 1980. A Late Proterozoic to Cambrian age for the stratified rocks of the Boston Basin, Massachusetts, U.S.A. In *Proceedings "The Caledonides In the U.S.A."* Edited by David R. Wones. IGCP Project 27: Caledonide Orogen. Department of Geological Sciences, Virginia Polytechnic Institute and State University, Memoir Number 2, pp. 257 to 261.

Kanasewich, E.R., Havskow, J., and Evans, M.E. 1978. Plate Tectonics in the Phanerozoic. *Canadian Journal of Earth Sciences*, Volume 15, pp. 919 to 955.

Keil, K., and Fricker, P.E. 1974. Baddeleyite (ZrO<sub>2</sub>) in gabbroic rocks from Axel Heiberg Island, Canadian Arctic Archipelago. *American Mineralogist*, Volume 59, pp. 249 to 253.

Keppie, J.D. 1982. Cape Breton Island. In *Field Guide For Avalon and Meguma Zones*. Edited by A.F. King. The Caledonide Orogen, IGCP Project 27, Earth Sciences Department, Memorial University of Newfoundland, St. John's, Newfoundland, pp. 141 to 152.

Keppie, J., and Dostal, J. 1980. Paleozoic volcanic rocks of Nova Scotia. In *Proceedings "The Caledonides In the U.S.A."* Edited by David R. Wones. IGCP Project 27: Caledonide Orogen. Department of Geological Sciences, Virginia Polytechnic Institute and State University, Memoir Number 2, pp. 249 to 256.

Keppie, J.D., Dostal, J., and Murphy, J.B., 1979. Petrology of the Late Precambrian Forchu Group in the Louisbourg area, Cape Breton Island. Nova Scotia Department of Mines, Paper 79-1.

Kerrick, R. and Fyfe, W.S. 1981. The gold - carbonate association: Source of CO<sub>2</sub> and CO<sub>2</sub> fixation reactions in Archean lode deposits. *Chemical Geology*, Volume 33, pp. 265 to 294.

King, Arthur F., 1980. The birth of the Caledonides: Late Precambrian rocks of the Avalon Peninsula, Newfoundland, and their correlatives in the Appalachian Orogen. In *Proceedings "The Caledonides In the U.S.A."* Edited by David R. Wones. IGCP Project 27: Caledonide Orogen. Department of Geological Sciences, Virginia Polytechnic Institute and State University, Memoir Number 2, pp. 3 to 8.

King, A.F., Brueckner, W.D., Anderson, M.M., and Fletcher, T. 1974. Late Precambrian and Cambrian sedimentary sequences of eastern Newfoundland: Guidebook for field trip B-6. Geological and Mineralogical Associations of Canada Joint Meeting, St. John's, Newfoundland, 59 p.

King, B.C. 1978. A comparison between the older (Karoo) rifts and the younger (Cenozoic) rifts of eastern Africa. In *Tectonics and Geophysics of Continental Rifts*. Edited by I.B. Ramberg and E.R. Neumann. D. Reidel Publishing Company, Dordrecht, Holland, pp. 347 to 350.

Komar, P.D. 1972. Mechanical interactions and flow differentiation of igneous dikes and sills. *Geological Society of America Bulletin*, Volume 83, pp. 973 to 988.

Kresten, P. 1973. The coating of kimberlitic zircons: A preliminary study. In *Lesotho Kimberlites*. Edited by P.H. Nixon. pp. 220 to 223.

Kudo, A.M., and Weill, D.F. 1970. An igneous plagioclase thermometer. *Contributions to Mineralogy and Petrology*, Volume 25, pp. 52 to 65.

Kumarapeli, P.S. 1978. The St. Lawrence paleo-rift system: A comparative study. In *Tectonics and Geophysics of Continental Rifts*. Edited by I.B. Ramberg and E.R. Neumann. D. Reidel Publishing Company, Dordrecht, Holland, pp. 367 to 384.

Kushiro, I. 1969. The system forsterite - diopside - silica with and without water at high pressures. *American Journal of Science*, Volume 267A, pp. 269 to 294.

Langmuir C.H., Bender, J.F., Bence, A.E., Hanson, G.N., and Taylor, S.R. 1977. Petrogenesis of basalts from the FAMOUS area: Mid-Atlantic Ridge. *Earth and Planetary Science Letters*, Volume 36, pp. 133 to 156.

Lajoie, Jean. 1979. Volcaniclastic rocks. In Facies Models. Edited by Roger G. Walker. Geoscience Canada Reprint Series 1, Geological Association of Canada, Toronto, pp. 191 to 200.

Leake, Bernard E. 1978. Nomenclature of amphiboles. Canadian Mineralogist, Volume 16, pp. 501 to 520.

Le Bas, M.J. 1962. The role of aluminum in igneous clinopyroxenes with relation to their parentage. American Journal of Science, Volume 260, pp. 267 to 288.

Le Gall, Jean. 1978. Les pyroclastites acides de Cambrien de la Charnie (E du massif Armoricaïn): petrographie; encadrement lithostratigraphique. Societe Linneenne de Normandie, Caen - Bulletin, Volume 106, pp. 27 to 34.

Le Gall, J., Dore, F., Giordano, R., and Pottier, Y. 1975. Position stratigraphique et cadre tectono - sedimentaire des manifestations volcaniques Cambriennes dan le nord-est du Massif Armoricaïn. Societe Geologique de France Bulletin, Volume 7, pp. 1101 to 1109.

Le Maitre, R.W. 1979. A new generalized petrological mixing model. Contributions to Mineralogy and Petrology, Volume 71, pp. 133 to 137.

Lenk, C., Strother, P.K., Kaye, C.A., and Barghoorn, E.S. 1982. Precambrian age of the Boston Basin: New Evidence from microfossils. Science, Volume 216, pp. 619 to 620.

Le Pichon, X. and Sibuet, J-C. 1981. Passive margins: A model of formation. Journal of Geophysical Research, Volume 86, pp. 3708 to 3720.

Le Pichon, X. 1968. Sea-floor spreading and continental drift. Journal of Geophysical Research, Volume 73, pp. 3661 to 3697.

Lippard, S.J. 1977. Spatial and temporal variations in basalt geochemistry in the N. Kenya rift. In Petrology and Geochemistry of Continental Rifts. Edited by E.-R. Neumann and I.B. Ramberg. D. Reidel Publishing Company, Dordrecht, Holland, pp. 209 to 216.

Lofgren, Gary. 1971. Spherulitic textures in glassy and crystalline rocks. Journal of Geophysical Research, Volume 76, pp. 5635 to 5648.

Logatchev, N.A., Rogozhina, V.A., Solonenko, V.P., and Zorin, Yu.A. 1978. Deep structure and evolution of the Baikal rift zone. In *Tectonics and Geophysics of Continental Rifts*. Edited by I.B. Ramberg and E.R. Neumann. D. Reidel Publishing Company, Dordrecht, Holland, pp. 49 to 61.

Lovering, J.F., Wark, D.A., Gleadow, A.J.W. and Sewell, D.K.B. 1972. Uranium and potassium fractionation in pre-Imrian lunar crustal rocks. *Proceedings of the Third Lunar Science Conference, Geochimica et Cosmochimica Acta Supplement 3, Volume 1*, pp. 281 to 294.

McBirney, A.R. and Noyes, R.M. 1979. Crystallization and layering of the Skaergaard intrusion. *Journal of Petrology*, Volume 20, pp. 487 to 554.

McCartney, W.D. 1967. Whitbourne Map-Area, Newfoundland. *Geological Survey of Canada Memoir 341*, 135 p. plus map.

McCutcheon, S.R. 1981. Revised stratigraphy of the Long Reach area, southern New Brunswick: Evidence for major northwestward - directed Acadian thrusting. *Canadian Journal of earth Sciences*, Volume 18, pp. 646 to 656.

McDougall, Ian. 1962. Differentiation of the Tasmanian dolerites: Red Hill dolerite - granophyre association. *Geological Society of America Bulletin*, Volume 73, pp. 279 to 316.

McKenzie, D. 1978. Some remarks on the development of sedimentary basins. *Earth and Planetary Science Letters*, Volume 40, pp. 25 to 32.

McKenzie, D., Nisbet, E., and Sclater, J.G. 1980. Sedimentary basin development in the Archean. *Earth and Planetary Science Letters*, Volume 48, pp. 35 to 41.

Maher, H.D., Palmer, A.R., Secor, D.T., and Snoke, A.W., 1981. New trilobite locality in the Piedmont of south Carolina, and its regional implications. *Geology*, Volume 9, pp. 34 to 36.

Martin, R.F., and Piwinski, A.J. 1972. Magmatism and tectonic settings. *Journal of Geophysical Research*, Volume 77, pp. 4966 to 4975.

Maxwell, John A. 1968. *Rock and Mineral Analysis*. John Wiley and Sons, New York, 584 p.

Michard, A. 1976. *Elements de Geologie Marocaine. Notes et Memoires du Service Geologique du Maroc*, No 252, 408 p.

- Mohr, Paul. 1978. Afar. Annual Review of Earth and Planetary Sciences, Volume 6, pp. 145 to 172.
- Moore, James G. 1965. Petrology of deep-sea basalt near Hawaii. American Journal of Science, Volume 263, pp. 40 to 52.
- Moore, James G. 1979. Vesicularity and CO<sub>2</sub> in mid-ocean ridge basalt. Nature, Volume 282, pp. 250 to 253.
- Moore, J.G., Clague, D.A., and Normark, W.R. 1982. Diverse basalt types from Loihi Seamount, Hawaii. Geology, Volume 10, pp. 88 to 92.
- Moore, J.G., and Fiske, R.S. 1969. Volcanic substructure inferred from dredge samples and ocean - bottom photographs, Hawaii. Geological Society of America Bulletin, Volume 80, pp. 1191 to 1202.
- Morel, P., and Irving, E. 1978. Tentative paleocontinental maps for the Early Phanerozoic and Proterozoic, Journal of Geology, Volume 86, pp. 535 to 561.
- Mottl, M.J. 1983. Metabasalts, axial hot springs, and structure of hydrothermal systems at mid-ocean ridges. Geological Society of America Bulletin, Volume 94, pp. 161 to 180.
- Myers, C.W., Bence, A.E., Papike, J.J., Ayuso, R.A. 1975. Petrology of an alkali - olivine basalt sill from Site 169 of DSDP Leg 17: The central Pacific Basin. Journal of Geophysical Research, Volume 80, pp. 807 to 822.
- Nairn, I.A., and Self, S. 1978. Explosive eruptions and pyroclastic avalanches from Ngauruhoe in February, 1975. Journal of Volcanology and Geothermal Research, Volume 3, pp. 39 to 60.
- Neumann, E.R., and Ramberg, I.B. 1978. Paleorifts - Concluding remarks. In Tectonics and Geophysics of Continental Rifts. Edited by I.B. Ramberg and E.R. Neumann. D. Reidel Publishing Company, Dordrecht, Holland, pp. 409 to 424.
- Nicholls, J., Carmichael, I.S.E., and Stormer, J.C. 1971. Silica activity and P<sub>total</sub> in igneous rocks. Contributions to Mineralogy and Petrology, Volume 33, pp. 1 to 20.
- Nisbet, E.G., and Pearce, J.A. 1977. Clinopyroxene composition in mafic lavas from different tectonic settings. Contributions to Mineralogy and Petrology, Volume 63, pp. 149 to 160.

Nixon, P.H., Knorring, O. Von, and Rooke, J.M. 1963. Kimberlites and associated inclusions of Basutoland: A mineralogical and geochemical study. *American Mineralogist*, Volume 48, pp. 1090 to 1132.

Nystuen, J.P. 1981. The Late Precambrian "sparagmite" of southern Norway: A major Caledonian allochthon - The Osen-Roa Nappe Complex. *American Journal of Science*, Volume 281, pp. 69 to 94.

Nystuen, J.P. 1982. Late Proterozoic basin evolution on the Baltoscandian craton: The Hedmark Group, southern Norway. *Norges Geologiske Undersokelse*, Volume 375, pp. 1 to 75.

O'Brien, S., and King, A.F. 1982. The Avalon zone in Newfoundland. In *Field Guide For Avalon and Meguma Zones*. Edited by A.F. King. The Caledonide Orogen, IGCP Project 27, Earth Sciences Department, Memorial University of Newfoundland, St. John's, Newfoundland, pp. 1 to 28.

O'Driscoll, C.F., and Strong, D.F. 1979. Geology and geochemistry of Late Precambrian volcanic and intrusive rocks of southwestern Avalon zone in Newfoundland. *Precambrian Research*, Volume 8, pp. 19 to 48.

Olszewski, W.J. Jr., and Gaudette, H.E. 1982. Age of the Brookville Gneiss and associated rocks, southeastern New Brunswick. *Canadian Journal of Earth Science*, Volume 19, pp. 2158 to 2166.

Olszewski, W.J., Gaudette, H.E., Keppie, J.D. and Donahoe, H.V. 1981. Rb-Sr whole rock age of the Kelly's Mountain basement complex, Cape Breton Island. *Geological Society of America Abstracts*, Volume 13, p. 13.

Paarma, H. 1970. A new find of carbonatite in North Finland; the Sokli plug in Savukoski. *Lithos*, Volume 3, pp. 129 to 133.

Palicova, M., and Stovickova, N. 1968. Volcanism and plutonism of the Bohemian Massif from the aspect of its segmented structure. *Krystalinikum*, Volume 6, pp. 169 to 199.

Palmer, A.R. 1971. Cambrian of the Appalachian and eastern New England regions, eastern United States. In *Cambrian of the New World*. Edited by C.H. Holland. John Wiley and Sons, New York, pp. 169 to 218.

Palmer, A.R. 1972. Problems of Cambrian biogeography. In *International Geological Congress 24th session, Montreal, Section 7*, pp. 310 to 315.

Palmer, A.R. 1977 Biostratigraphy of the Cambrian system - A progress report. Annual Reviews of Earth and Planetary Sciences, Volume 5, pp. 13 to 33.

Papezik, V.S. 1970. Petrochemistry of volcanic rocks of the Harbour Main Group, Avalon Peninsula, Newfoundland. Canadian Journal of Earth Sciences, Volume 7, pp. 1485 to 1498.

Papezik, V.S. 1972. Late Precambrian ignimbrites in eastern Newfoundland, and their tectonic significance. Proceedings of the International Geological Congress, 24th session, Section 1, pp. 147 to 152.

Papezik, V.S., and Hodych, J.P. 1980. Early Mesozoic diabase dikes of the Avalon Peninsula, Newfoundland: Petrochemistry, mineralogy, and origin. Canadian Journal of Earth Sciences, Volume 17, pp. 1417 to 1430.

Parga, J.B. 1969. Sobre la distribution de las manifestaciones efusivas en el Combrico do Portugal. Servicos geologicos Comunicacoes, Volume 53, pp. 43 to 56.

Pearce, J.A., and Cann, J.R. 1973. Tectonic setting of basic volcanic rocks determined using trace element analyses. Earth and Planetary Science Letters, Volume 19, pp. 290 to 300.

Pearce, J.A., and Norry, M.J. 1979. Petrogenic implications of Ti, Zr, Y, and Nb variations in volcanic rocks. Contributions to Mineralogy and Petrology, Volume 69, pp. 33 to 47.

Philpotts, A.R. 1974. The Montereian Province. In The Alkaline Rocks. Edited by H. Sorensen. John Wiley and Sons, London, pp. 293 to 310.

Pringle, I.R., Miller, J.A., Warrell, D.M. 1971. Radiometric age determinations from the Long Range Mountains, Newfoundland. Canadian Journal of Earth Sciences, Volume 8, pp. 1325 to 1330.

Ramberg, I.B., and Barth, T.F.W. 1966. Eocambrian volcanism in southern Norway. Norsk Geologisk Tidsskrift, Volume 46, pp. 219 to 236.

Ramberg, I.B., and Larsen, B.T. 1978. Tectonomagmatic evolution In The Oslo Paleorift - A Review and Guide to Excursions. Edited by Johannes A. Dons and Bjorn T. Larsen. Inter - Union Commission on Geodynamics, Scientific Report No. 46, Universitetsforlaget. pp. 55 to 73.



Ramdohr, P., and ElGorsey, A. 1970. Opaque minerals of the Lunar rocks and dust from the Mare Tranquillitatis. *Science (AAAS)*, Volume 167, pp. 615 to 618.

Rankin, D.W., 1976. Appalachian salients and recesses: Late Precambrian continental breakup and the opening of the Iapetus Ocean. *Journal of Geophysical Research*, Volume 81, pp. 5605 to 5619.

Rast, Nicholas, Dickson, W.L., and Grant, R.H. 1978. Precambrian basement in southwestern New Brunswick. In *Geological Bulletin No. 6, Guidebook For Field Trips In Southeastern Maine and Southwestern New Brunswick*. Edited by Allan Ludman. New England Intercollegiate Geological Conference, 70th Annual Meeting, pp. 108 to 119.

Rast, N., O'Brien, B.H., and Wardle, R.J. 1976. Relationships between Precambrian and Lower Palaeozoic rocks of the "Avalon Platform" in New Brunswick, the northeast Appalachians, and the British Isles. *Tectonophysics*, Volume 30, pp. 315 to 338.

Ricketts, B.D., Ware, M.J., and Donaldson, J.A. 1982. Volcaniclastic rocks and volcaniclastic facies in the Middle Precambrian (Aphebian) Belcher Group, Northwest Territories, Canada. *Canadian Journal of Earth Sciences*, Volume 19, pp. 1275 to 1294.

Robbins, E.I., 1982. A preliminary account of the Newark rift system. In *Papers Presented to the Conference on the Processes of Planetary Rifting*. Edited by K. Hrametz. Lunar and Planetary Institute, Houston, pp. 107 to 109.

Roberts, D., and Gale, G.H. 1977. The Caledonian - Appalachian Iapetus Ocean. In *The Evolution of the Earth's Crust*. Edited by D.H. Tarling. Academic Press, New York, 255 to 341.

Robinson, Peter. 1980. The composition of terrestrial pyroxenes - internal and external limits. In *Reviews in Mineralogy*, Volume 7, Pyroxenes. Mineralogical Society of America, Washington, pp. 419 to 490.

Royden, L., and Keen, C.E. 1980. Rifting process and thermal evolution of the continental margin of eastern Canada determined from subsidence curves. *Earth and Planetary Science Letters*, Volume 51, pp. 343 to 361.

Ruitenberg, A.A., Fyffe, L.R., McCutcheon, S.R., St. Peter, C.J., Irrinki, R.R., and Venugopal, D.V. 1977. Evolution of the Pre-Carboniferous tectonostratigraphic zones in the New Brunswick Appalachians. *Geoscience Canada*, Volume 4, pp. 171 to 181.

Ruitenberg, A.A., and Ludman, A. 1978. Stratigraphy and tectonic setting of early Paleozoic sedimentary rocks of the Wirral - Big Lake area southwestern New Brunswick and southeastern Maine. *Canadian Journal of Earth Sciences*, Volume 15, pp. 22 to 32.

Rushton, A.W.A. 1974. The Cambrian of Wales and England. In *Cambrian of the British Isles, Norden, and Spitsbergen*. John Wiley and Sons, Toronto, pp. 43 to 121.

Samson S.L., Secor, D.T., and Snoke, A.W. 1982. Geological Implications of recently discovered Middle Cambrian trilobites in the Carolina Slate Belt (Abstract). *Geological Society of America Abstracts With Programs*, Volume 14, p. 607.

Samsonowicz, Jan. 1956. Cambrian paleogeography and the Cambrian System in Poland. In *XX Congress Geologico Internacional, Mexico. El Sistema Cambrico, Su Paleogeografia y el Problema de Su Base*, Volume 1, pp. 127 to 160.

Schenk, P.E. 1971. Southeastern Atlantic Canada, northwestern Africa, and continental drift. *Canadian Journal of Earth Sciences*, Volume 8, pp. 1218 to 1251.

Scotese, C.R., Bambach, R.K., Barton, C., Van der Voo, R. and Ziegler, A.M. 1979. Paleozoic base maps. *Journal of Geology*, Volume 87, pp. 217 to 277.

Segalstad, T.V. 1977. Petrology of the Skien basaltic rocks and the early basaltic (B1) volcanism of the Permian Oslo rift. In *Petrology and Geochemistry of Continental Rifts*. Edited by E.-R. Neumann and I.B. Ramberg. D. Reidel Publishing Company, Dordrecht, Holland, pp. 209 to 216.

Self, S. 1982. Terminology and classification for pyroclastic deposits. In *Pyroclastic Volcanism and Deposits Of Cenozoic Intermediate to Felsic Volcanic Islands With Implications For Greenstone-Belt Volcanoes*. Edited by L.D. Ayres. Geological Association of Canada Short Course Notes, Volume 2, pp. 1 to 17.

Sengor, A.M.C., and Burke, K. 1978. Relative timing of rifting and volcanism on earth and its tectonic implications. *Geophysical Research Letters*, Volume 5, pp. 419 to 421.

Sheridan, M.F. 1971. Particle-size characteristics of pyroclastic tuffs. *Journal of Geophysical Research*, Volume 76, pp. 5627 to 5634.

Simkin, T., and Smith, J.V. 1970. Minor element distribution in olivine. *Journal of Geology*, Volume 78, pp. 304 to 325.

- Skehan, S.J., J.W., Murray, D.P., Palmer, A.R., and Smith, A.T. 1977. The geological significance of Middle Cambrian trilobite - bearing phylites from southern Narragansett Basin, Rhode Island. Geological Society of America Abstracts with Programs, Volume 9, 319.
- Skehan, S.J., J.W., Murray, D.P., Palmer, A.R., Smith, A.T. and Belt, E.S. 1978. Significance of fossiliferous Middle Cambrian rocks of Rhode Island to the history of the Avalonian microcontinent. *Geology*, Volume 6, pp. 694 to 698.
- Skehan, S.J., J.W., Rast, N. and Logue, D.F. 1981. The geology of the Cambrian rocks of Conanicut Island, Jamestown, Rhode Island. In Hermes, O.D., and Boothroyd, J.C. (Editors) *Guidebook to Geologic Field Studies in Rhode Island and Adjacent Areas*, New England Intercollegiate Geological Conference, 73rd Annual Meeting, University of Rhode Island, Kingston, Rhode Island, pp. 237 to 264.
- Smewing J.D., and Potts, P.J., 1976. Rare-earth abundances in basalts and metabasalts from the Troodos Massif, Cyprus. *Contributions to Mineralogy and Petrology*, Volume 57, pp. 245 to 258.
- Smith, A.G., Hurley, A.M., and Briden, J.C. 1980. *Phanerozoic Paleogeographic World Maps*. Cambridge University Press, Cambridge, 98 p.
- Smith, D. 1970. Petrology of the diabasic rocks in a differentiated olivine diabase sill complex, Sierra Ancha, Arizona. *Contributions to Mineralogy and Petrology*, Volume 27, pp. 95 to 113.
- Sparks, R.S.J. 1976. Grain size variations in ignimbrites and implications for the transport of pyroclastic flows. *Sedimentology*, Volume 23, 147 to 188.
- Sparks, R.S.J., Self, S., and Walker, G.P.L. 1973. Products of ignimbrite eruptions. *Geology*, Volume 1, pp. 115 to 122.
- Stevens, R.K. 1970. Cambro-Ordovician flysch sedimentation and tectonics in west Newfoundland and their possible bearing on a Proto - Atlantic Ocean. In *Flysch Sedimentology in North America*. Edited by J. Lajoie. Geological Association of Canada Special Paper 7, pp. 165 to 177.
- St. Jean, J. 1973. A new Cambrian trilobite from the Piedmont of North Carolina. *American Journal of Science*, Volume 273-A, pp. 196 to 216.
- Stringer, P., and Pajari, G.E. 1981. Age of pre-Triassic rocks and polyphase deformation, Grand Manan, New Brunswick. In *Current Research. Geological Survey of Canada Paper 81-1C*, pp. 9 to 15.

Stromquist, A.A., and Sundelius, H.W. 1969. Stratigraphy of the Albemarle Group of the Carolina Slate Belt in Central North Carolina. United States Geological Survey Bulletin; 1274-B, 22 p.

Strong, D.F. 1977. Volcanic regimes of the Newfoundland Appalachians. In Volcanic Regimes in Canada. Edited by W.R.A. Baragar, L.C. Coleman, and J.M. Hall. Geological Association of Canada Special Paper Number 16, pp. 61 to 90.

Strong, D.F. 1979. Proterozoic tectonics of northwestern Gondwanaland: New evidence from eastern Newfoundland. Tectonophysics, Volume 54, pp. 81 to 101.

Strong, D.F. 1982. Carbothermal metasomatism of alaskitic granite, St. Lawrence, Newfoundland, Canada. Chemical Geology, Volume 35, pp. 97 to 114.

Strong, D.F., O'Brien, S.J., Taylor, S.W., Strong, P.G., and Wilton, D.H. 1978. Aborted Proterozoic rifting in eastern Newfoundland. Canadian Journal of Earth Sciences, Volume 15, pp. 117 to 131.

Strong, D.F., O'Brien, S.J., Taylor, S.W., Strong, P.G., and Wilton, D.H. 1978. Geology of the Marystown (1M/3) and St. Lawrence (1L/14) Map Areas, Newfoundland. Department of Mines and Energy, Government of Newfoundland and Labrador, Report 77-8, St. John's, Newfoundland, 81p.

Strong, D.F., and Williams, H. 1971. Early Paleozoic flood basalts of northwestern Newfoundland: Their petrology and significance. Geological Association of Canada Special Paper 25, pp. 43 to 54.

Stubblefield, C.J. 1956 Cambrian paleogeography in Britain. In XX Congress Geologico Internacional, Mexico. El Sistema Cambrico, Su Paleogeografia y el Problema de Su Base, Volume 1, pp. 1 to 43.

Sundelius, H.W. 1970. The Carolina Slate Belt. In Studies of Appalachian Geology: Central and Southern. Edited by G.W. Fisher, F.J. Pettijohn, J.C. Reed, and K.N. Weaver. John Wiley and Sons, New York, pp. 351 to 367.

Suvola, Jaakko 1977. Baddeleyite -  $ZrO_2$  - from Lovasjarvi diabase, southeastern Finland. Bulletin, Geological Society of Finland, Volume 49. pp. 59 to 64.

Svoboda, J. 1966. Regional Geology of Czechoslovakia, Part 1, The Bohemian Massif. Geological Survey of Czechoslovakia Publishing House, Prague,

Swanson, D.A., and Wright, T.L., 1981. Guide to geologic field trip between Lewiston, Idaho, and Kimberly, Oregon emphasizing the Columbia River Basalt Group. United States Geological Survey Circular 838, pp. 1 to 14.

Tankard, A.J., Jackson, M.P.A., Eriksson, K.A., Hobday, D.K., Hunter, D.R., and Minter, W.E.L., 1982. Crustal Evolution of South Africa. Springer - Verlag, New York, 523 p.

Tarney, J., Saunders, A.D., and Weaver, S.D. 1977. Geochemistry of volcanic rocks from the island arcs and marginal basins of the Scotia Arc region. In Island Arcs, Deep Sea Trenches, and Back - Arc Basins. Edited by Manik Talwani, and Walter C. Pitman. American Geophysical Union, Washington D.C., pp. 367 to 377.

Taylor, R.P., Strong, D.F., and Fryer, B.J. 1981. Volatile control of contrasting rare element distributions in peralkaline granitic and volcanic rocks. Contributions to Mineralogy and Petrology, Volume 77, pp. 267 to 271.

Taylor, S.R., and Gorton, M.P. 1977. Geochemical application of spark source mass spectrography - III Element sensitivity, precision, and accuracy. *Geochimica et Cosmochimica Acta*, Volume 41, pp. 1375 to 1380.

Teisseyre, J. 1968. On the old Paleozoic initial volcanism in the West Sudetes. *Acta Geologica Polonica*, Volume 18, pp. 239 to 256.

Teixeira, C. 1956. Le Cambrien Portugais et ses problemes. In XX Congress Geologico Internacional, Mexico. El Sistema Cambrico, Su Paleogeografia y el Problema de Su Base, Volume 1, pp. 235 to 242.

Teixeira, C. 1968. Quelques problemes de la geologie du Portugal. International Geological Congress, 23rd, Czechoslovakia, Section 13 of Proceedings, pp. 233 to 242.

Termier, H., and Termier, G. 1966. Le Cambrien Inferieur au Voisinage du Massif Granitodioritique du Tichka (Haut Atlas Marocain). *Academie des Sciences, Comptes Rendus, Series D*, Volume 262, pp. 843 to 845.

Theokritoff, G. 1968. Cambrian biogeography and biostratigraphy in New England. In Studies of Appalachian Geology: Northern and Maritime. Edited by E-an Zen, W.S. White, J.B. Hadley, and J.B. Thompson Jr. Interscience Publishers, New York, p. 9 to 22.

Teircelin, J.J., and Faure, H., 1977. Rates of sedimentation in neorifts and paleorifts. In Tectonics and Geophysics of Continental Rifts. Edited by I.B. Ramberg and E.R. Neumann. D. Reidel Publishing Company, Dordrecht, Holland, pp. 41 to 48.

Tuttle, O.F., and Bowen, N.L. 1958. Origin Of Granite in the Light of Experimental Studies in the System  $\text{NaAlSi}_3\text{O}_8$  -  $\text{KAlSi}_3\text{O}_8$  -  $\text{SiO}_2$  -  $\text{H}_2\text{O}$ . Geological Society of America Memoir 74, 153 p.

Vail, P.R., Mitchum, R.M., and Thompson, S. 1977. Seismic stratigraphy and global changes of sea level, part 3: Relative changes of sea level from coastal onlap and part 4: Global cycles of relative changes of sea level. In Seismic Stratigraphy - Applications to Hydrocarbon Exploration. Edited by C.E. Payton. American Association of Petroleum Geologists, Memoir 26, pp. 63 to 98.

Vallance, T.G. 1974. Spilitic degradation of a tholeiitic basalt. Journal of Petrology, Volume 15, pp. 79 to 96.

Van Calstern, P.W.C., and Den Tex, E. 1978. An Early Paleozoic continental rift system in Galicia (NW Spain). In Tectonics and Geophysics of Continental Rifts. Edited by I.B. Ramberg and E.R. Neumann. D. Reidel Publishing Company, Dordrecht, Holland, pp. 125 to 132.

Van Der Voo, Rob, Briden, J.C., and Duff, B.A. 1980. Late Precambrian and Paleozoic paleomagnetism of the Atlantic - bordering continents. In Colloque C6: Geologie de l'Europe du Precambrien aux bassins sedimentaires post-hercyniens. Edited by Jean Cogne, and Maurice Slansky. 26th Congres Geologique International, pp. 203 to 212.

Van Eysinga, F.W.B. (Compiler) 1975. Geological Time Table, 3rd edition, Elsevier, Amsterdam.

Veevers, J.J. 1976. Early Phanerozoic events along the Australasian - Antarctic Platform. Geological Society of Australia Journal, Volume 23, pp. 183 to 206.

Vegas, Ramon. 1978. Sedimentation and tectonism in the Iberian Massif prior to the Hercynian deformation (Late Precambrian to Silurian Times) In Geologia de la Parte Norte del Mocizo Iberico. Cuadernos del Seminario de Estudios Ceramicos de Sargadelos, Number 27, Sada (La Coruna), Ediciones del Castro, pp. 271 to 286.

Vegas, Ramon. 1980. Carboniferous subduction complex in the South Portuguese zone coeval with basement reactivation and uplift in the Iberian Massif. In Publicacions do Seminario de Estudos Galegos, Castro/Moret, Sada - La Coruna, pp. 187 to 202.

Vidal, Ph., Auvray, B., Charlot, R., Fediuk, F., Hameurt, J., and Waldhausrova, J. 1975. Radiometric age of volcanics of the Cambrian "Krivoklat - Rokycany" complex (Bohemian Massif). *Geologische Rundschau*, Volume 64, pp. 565 to 570.

Vokes, F.M., and Gale, G.H. 1976. Metallogeny related to global tectonics in southern Scandinavia. In *Metallogeny and Plate Tectonics*. Edited by D.F. Strong. Geological Association of Canada Special Paper Number 14, pp. 413 to 441.

Wager, L.R. and Brown, G.M., 1967. *Layered Igneous Rocks*. Oliver and Boyd Limited, London, 588 p.

Waldhausrova, J. 1966. The volcanites of the Krivoklat - Rokycany zone. Paleovolcanites of the Bohemian Massif. Edited by F. Fediuk, M. Fiserá, and J. Kasakova. Praha, p. 145 to 151.

Waldhausrova, J. 1971. The chemistry of the Cambrian volcanics in the Barrandian area. *Krystalinikum*, Volume 8, pp. 45 to 75.

Walker, F. 1930. The geology of the Shiant Isles (Hebrides). *Quarterly Journal of the Geological Society of London*, Volume 86, pp. 355 to 398.

Walker, G.P.L. 1971. Grain-size characteristics of pyroclastic deposits. *Journal of Geology*, Volume 79, pp. 696 to 714.

Walker, G.P.L. and Croasdale, R. 1971. Characteristics of some basaltic pyroclastics. *Bulletin Volcanologique*, Volume 35, pp. 303 to 317.

Walker, K.R. 1969. A mineralogical, petrological, and geochemical investigation of the Palisades Sill, New Jersey. *Geological Society of America Memoir*, Number 115, pp. 175 to 187.

Walker, K.R. 1969. The Palisades Sill, New Jersey: A reinvestigation. *Geological Society of America Special Paper* Number 111, 178 p.

Walker, T.R. 1967. Formation of red beds in modern and ancient deserts. *Geological Society of America Bulletin*, Volume 78, pp. 353 to 368.

Wark, J.M., and Clark, D.B. 1980. Geochemical discriminators and the palaeotectonic environment of the North Mountain Basalts, Nova Scotia. *Canadian Journal of Earth Sciences*, Volume 17, pp. 1740 to 1745.

Weigand, P.W. 1975. Geochemistry of the Oslo Basaltic Rocks. Norske Videnskaps - Akademi / Oslo Matematisk Naturvidenskabelig Klass, Skrifter, Number 35, 38 p.

Wendlandt, R.F. and Podpora, C. 1982. Magma composition variations along hotspot traces: Paleolithospheric thickness and compositions of the LVZ. In Papers Presented to the Conference on the Processes of Planetary Rifting. Lunar and Planetary Institute, Houston, pp. 192 to 198.

Widenfalk, L. and Gorbatshev, R. 1971. A note on a new occurrence of baddeleyite in larvikite from Larvik. Norway. Norsk Geologisk Tidsskrift, Volume 51, pp. 193 to 194.

Wilkinson, J.F.K., and Binns, R.A. 1977. Relatively iron-rich lherzolite xenoliths of the Cr-diopside suite: A guide to the primary nature of anorogenic tholeiitic magmas. Contributions to Mineralogy and Petrology, Volume 65, pp. 199 to 212.

Williams, C.T. 1978. Uranium - enriched minerals in mesostasis areas of the Rhum layered pluton. Contributions to Mineralogy and Petrology, Volume 66, pp. 29 to 39.

Williams, Harold. 1978a. Tectonic - Lithofacies Map of the Appalachian Orogen. Memorial University of Newfoundland, Map No. 1.

Williams, Harold. 1978b. Geological development of the northern Appalachians: its bearing on the evolution of the British Isles. In Crustal Evolution in Northwestern Britain and Adjacent Regions. Edited by D.R. Bowes and B.E. Leake. Geological Journal Special Issue Number 10, pp. 1 to 22 plus maps.

Williams, Harold. 1979. Appalachian orogen in Canada. Canadian Journal of Earth Sciences, Volume 16, pp. 792 to 807.

Williams, Harold, and Hatcher, R.D. 1982. Suspect terranes and accretionary history of the Appalachian orogen. Geology, Volume 10, pp. 530 to 536.

Wilson, J.T. 1966. Did the Atlantic close and then re-open? Nature, Volume 211, pp. 676 to 681.

Wilton, D.H. 1976. Petrological Studies of the Southeast Part of the Burin Group, Burin Peninsula, Newfoundland. B.Sc. Thesis (Honours), Memorial University of Newfoundland, St. John's, Newfoundland, 115 p.



Winchester, J.A. and Floyd, P.A. 1976. Geochemical magma type discrimination: Application to altered and metamorphosed basic igneous rocks. *Earth and Planetary Science Letters*, Volume 28, pp. 459 to 469.

Winchester, J.A. and Floyd, P.A. 1977. Geochemical discrimination of different magma series and their differentiation products using immobile elements. *Chemical Geology*, Volume 20, pp. 325 to 343.

Winkler, H.G.F. 1976. *Petrogenesis of Metamorphic Rocks*. Fourth edition. Springer - Verlag, New York, 334 p.

Wood, B.J. and Banno, S. 1973. Garnet - orthopyroxene relationships and orthopyroxene - clinopyroxene relationships in simple and complex systems. *Contributions to Mineralogy and Petrology*, Volume 42, pp. 109 to 124.

Yoder, H.S. and Tilley, C.E. 1962. Origin of basaltic magmas: An experimental study of natural and synthetic rock systems. *Journal of Petrology*, Volume 3, pp. 342 to 532.

Zamarreno, I. 1972. Las lithofacies carbonatadas del Cámbrico de la zona Cantábrica (NW España) y su distribución paleogeográfica. *Trabajos de Geología*, No. 5., 118 p.

Ziegler, A.M. 1981. Paleozoic paleogeography. In *Paleoreconstruction of the Continents*. Geodynamics Series, Volume 2. American Geophysical Union, Washington D.C., pp. 31 to 37.

Ziegler, A.M., Scotese, C.R., McKerrow, W.S., Johnson, M.E., Bamback, R.K. 1977. Paleozoic biogeography of continents bordering the Iapetus (pre-Caledonian) and Rheic (pre-Hercynian) Oceans. In *Paleontology and Plate Tectonics*. Edited by R.M. West. Milwaukee Public Museum Special Publications in Biology and Geology, Number 2, pp. 1 to 22.

Ziegler, A.M., Scotese, C.R., McKerrow, W.S., Johnson, M.E., Bamback, R.K. 1979. Paleozoic paleogeography. *Annual Review of Earth and Planetary Sciences*, Volume 7, pp. 473 to 502.

Zietz, I., Haworth, R.T., Williams, H. and Daniels, D.L. 1980. Magnetic Anomaly Map of the Appalachians. Memorial University of Newfoundland, St. John's, Newfoundland.

Znoska, Jery. 1965. Sinian and Cambrian in the north-eastern area of Poland. *Kwartalnik Geologiczny*, Volume 9, pp. 465 to 488.

Zoubek, V. 1977. Remarks to the problem of subdivision of the Precambrian. In Correlation of the Precambrian. Edited by A.V. Sidorenko. Nauka, Moscow, pp. 62 to 93.

APPENDIX A - EXPERIMENTAL METHODSWHOLE ROCK ANALYSES

Rocks analyzed for their major and/or trace element and REE contents were first prepared by carefully removing all weathered surfaces, and any veins of secondary nature along jointing planes. The samples were then crushed in a jaw crusher to coarse gravel size chips and then powdered to 200 mesh in a tungsten carbide Bleuler mill. All equipment was meticulously washed with distilled water and dilute hydrochloric acid after each sample in order to minimize contamination.

Major Elements

The major elements were determined by atomic absorption on a Perkin Elmer 360 at The Memorial University of Newfoundland. 0.1 grams of each sample were accurately weighed out and dissolved in 5.0 ml. of hydrofluoric acid and 50 ml. of saturated boric acid solution and made up to 200 ml. with distilled water. Samples were compared with a suite of standards with approximately the same concentrations as the samples. FeO was determined by titration using the method described by Maxwell (1968, p.419). Analysis for P2O5 was carried out colorimetrically following the method outlined by Maxwell (1968, p.394). Loss on ignition was determined by weighing a portion of powder in a porcelain crucible, heating to 1050 degrees C.

for two hours, cooling in a dessicator, and weighing again to determine the percentage of volatiles lost. Precision and accuracy for each the major elements are better than or equal to 2 percent.

#### Trace Elements

Pressed powder pellets were made by mechanically mixing approximately 1 gram of phenyl formaldehyde thermal binding agent with 10 grams of rock powder, compacting the mixture to form a disc, and baking for 10 minutes at 200 C. These pellets were analyzed for their trace element contents at The Memorial University of Newfoundland on a Phillips 1450 automatic X-ray fluorescence spectrometer. The peak intensities were compared with those of U.S.G.S. rock standards. The correction for mass absorption was based on measurements of the Compton scatter peak of the rhodium tube. Precision and accuracy as determined from standards run with the samples are as follows:  $\pm 50$  to 100 percent for Pb, Th, and U,  $\pm 2$  ppm for Rb and Nb,  $\pm 2$  percent for Sr and Zr,  $\pm 2$  to 6 ppm for V, Cr, Zn, Cu, Ga, Y, and Ni,  $\pm 10$  percent for Ba, and  $\pm 20$  percent for La and Ce.

#### Rare Earth Element Analyses

Samples were analyzed for their rare earth element contents using a method similar to that described by Fryer (1977). In summary, approximately 1 gram of rock powder was accurately weighed out into a teflon beaker and 50  $\mu\text{g}$  of Tm

in solution accurately added to the powder. The sample was taken into solution using HF and HClO<sub>4</sub> acid, evaporated to dryness, and then fluorides were converted to chlorides using HCl and evaporating to dryness. The resulting powder was put into solution using HCL, centrifuged, and then loaded onto cation exchange columns. The collected solution was evaporated to dryness. Distilled water and H<sub>2</sub>SO<sub>4</sub> were added, and the solution filtered to remove Ba. To ensure that the samples were clean they were loaded onto the columns a second time, evaporated to dryness, and then pipetted onto cation exchange papers using weak HCL. Analysis was carried out on a Philips 1450 X-ray fluorescence spectrometer using thin-film methods.

As a check on precision, and to compare the method with instrumental neutron activation analyses a sample analyzed by Greenough (1979) using the latter method, was analyzed three times (disolution through X-ray analysis) using the method of Fryer (1977). The following table summarizes the results.

|    | Sample by<br>INAA. | Average of<br>3 Analyses | Standard<br>Deviation | Percent<br>S.d. |
|----|--------------------|--------------------------|-----------------------|-----------------|
| La | 21                 | 25.4                     | 5.2                   | 21              |
| Ce | 81                 | 68.8                     | 13.3                  | 19              |
| Pr |                    | 9.15                     | 2.15                  | 22              |
| Nd | 32                 | 44.6                     | 7.7                   | 17              |
| Sm | 11                 | 10.8                     | 1.5                   | 14              |
| Eu | 3.1                | 3.58                     | 0.53                  | 15              |
| Gd |                    | 10.4                     | 1.72                  | 12              |
| Dy |                    | 7.35                     | 0.90                  | 12              |
| Er |                    | 2.96                     | 0.34                  | 12              |
| Yb | 3.0                | 1.85                     | 0.33                  | 18              |

#### ELECTRON MICROPROBE MINERAL ANALYSES

Mineral compositions were determined using a fully automated JEOL JXA-50A electron probe microanalyser with Kriesel software run on a PDP-11 computer. In most cases beam width was approximately 1 micron, the beam current 0.20 to 0.22 microamps, and the accelerating voltage 15 KV. Counting time was 30 seconds, or until 60,000 counts were obtained. The values were corrected using the ALPHA correction procedure, or in the case of baddeleyite the MAGIC program. Precision and accuracy on the oxides is better than, or equal to, 2 percent. The instrument was calibrated using known standards as follows:

Clinopyroxene, olivine, amphibole, and biotite: Si, Al, Mg, Ca = pyroxene; Fe, Mn = hedenbergite; Na = jadeitic pyroxene; K = orthoclase; Ti = titanpyroxene; Cr = chromian spinel; Ni = nickel olivine.

Feldspar: Si, Al, Na = anorthoclase; K = orthoclase; Ca

- plagioclase; Fe = hedenbergite.

Baddeleyite: Zr = zirconium metal; Hf = hafnium metal;

Si, Ti, Fe = coesite.

APPENDIX B WHOLE ROCK ANALYSES

This appendix contains major element and trace element analyses of all rocks analyzed for the thesis. Brief sample descriptions precede the analyses which are arranged according to rock type and location in the following order: Cambrian extrusive rocks on Cape St. Mary's in Newfoundland, feeder pipe analyses, Cape St. Mary's sills, Cape St. Mary's dikes, Cambrian extrusive rocks at Beaver Harbour, New Brunswick, and Cambrian volcanic rocks from the Long Reach area in New Brunswick. Samples analyzed for both the major and trace elements are presented first, and those examined for their trace element concentrations alone are presented at the end.



CAPE ST. MARY'S CAMBRIAN EXTRUSIVE ROCKS

| Samples Analyzed For<br>Major and Trace Elements | Trace Elements  | Locations      |
|--|-----------------|----------------|
| CHA2, CHA3, ETC. to PL57I                        | CHA5A to PL57J  | Chapel Arm     |
| PL153B to PL133B                                 | PL53P to PL132J | Hopeall Head   |
| PL67 to PL167                                    | PL64 to PL163   | Placentia Jct. |
| PL31C1 to PL44                                   | PL37B           | Cape Dog       |
| SB37B1 to SB40D                                  | SB38C to SB43B  | Hay Cove       |

CHA2 to CHA7. Vesicular metabasalt. Minerals: chlorite, albite, calcite, Fe-Ti oxides, sphene + quartz. Calcite chlorite and sometimes albite and quartz fill vesicles. Total % calcite = 20 to 30%. Texture: Aphanitic, vesicular.

LC15A, B. Metabasalt. Primary minerals: Clinopyroxene, Fe-Ti oxides. Secondary minerals: albite, chlorite, epidote, actinolite, Fe-Ti oxides, calcite. Albite pseudomorphs primary plagioclase. Chlorite = 5 - 10%, each of remaining phases < 1%. Texture: Clinopyroxene and Fe-Ti oxides form variolitic texture. Vesicles = 5%, and are filled with albite.

CA15. Vesicular metabasalt. Primary minerals: Clinopyroxene = 5%. Secondary minerals: albite, chlorite, calcite (5%), sphene. Texture: Aphanitic, vesicular. Comments: Vesicles filled with calcite and chlorite, = 5%.

CA18 to PL57J. Vesicular metabasalt. Secondary minerals: Albite, chlorite, calcite, sphene. Texture: Aphanitic, vesicular, preserved by secondary minerals.

Comments: Vesicles filled with calcite, chlorite and sometimes albite. Calcite = 10 to 40% of rock.

PL54B, C, PL128C, F. Vesicular metabasalt. Secondary minerals: Albite, chlorite, calcite, quartz, sphene. Texture: Aphanitic, vesicular, preserved by secondary minerals. Comments: Vesicles filled with calcite, chlorite and sometimes quartz. Calcite forms from 10 to 30% of rock.

PL53B, P, I, PL132D, J, PL133B. Metalapilli tuff. Secondary minerals: Chlorite, calcite, albite, quartz, sphene + quartz, + hematite. Texture: Highly vesicular lapilli clasts are surrounded by tuffaceous matrix largely replaced by calcite. Clasts replaced by chlorite, vesicles filled with chlorite, albite, calcite. Calcite approaches 50% of some samples, forms equigranular texture, sometimes replaces clasts.

PL64, 67, 77, 83, 150, 144M, 157, 163, 167. Metalapilli tuff. Secondary minerals: Chlorite, calcite, albite, sphene. Texture: Similar to samples PL53B, P, etc.

PL31H0, 34B, 39A. Metalapilli tuff. Primary minerals: Clinopyroxene (< 1%, PL31H0 only). Secondary minerals: Chlorite, albite, calcite, sphene Fe-Ti oxides. Texture: Highly vesicular lapilli clasts are surrounded by mud - tuff matrix which is sometimes replaced by calcite. Clasts replaced by chlorite. Vesicles filled with calcite, chlorite.

PL37A, 37C, 38A. Vesicular metabasalt. Secondary minerals: Chlorite, albite, calcite, sphene. Texture: Aphanitic, vesicular, preserved by secondary minerals. Comments: Vesicles filled with calcite. Calcite forms from 15 to 25% of rock.

PL31CL, 34C, 38C, 44. Metabasalt. Primary Minerals: Clinopyroxene (< 1 %, < 5%, 30%, 40% respectively). Secondary minerals: Albite, chlorite, actinolite (< 1%, PL44 only), sphene, Fe-Ti oxides, calcite. Texture: Aphanitic, PL31CL highly vesicular bomb with calcite and chlorite filled vesicles. Calcite comprises 20%, 10%, 5%, <5% (respectively) of each sample.

SB37B1, B2. Metabasalt. Primary Minerals: Clinopyroxene < 1%. Secondary minerals: Chlorite, albite, calcite, sphene. Texture: Secondary minerals very fine grained. Large vesicles filled with calcite, small ones with chlorite.

SB38C, D. Sills. Primary Minerals: Augite, plagioclase, Fe-Ti oxides. Secondary Minerals: chlorite, albite, actinolite. Texture: ophitic.

SB39C Metatuff. Minerals: Chlorite, albite, calcite. Texture: fine grained shards recrystallized with primary texture obscured.

SB39D to 43B. Metalapilli tuff. Secondary minerals: Chlorite, calcite, albite, Fe-Ti oxides,  $\pm$  sphene,  $\pm$  hematite. Texture: Highly vesicular lapilli clasts are

surrounded by tuffaceous matrix commonly replaced by calcite. Clasts replaced by chlorite, vesicles filled with chlorite, albite, quartz. Calcite content varies 10 to 40%.

|       | CHA2  | CHA3  | CHA4  | CHA7  | LC15A  | LC15B | CA15  | CA18  | CA37  | CA40  |
|-------|-------|-------|-------|-------|--------|-------|-------|-------|-------|-------|
| SiO2  | 49.30 | 50.70 | 47.20 | 48.40 | 51.60  | 46.60 | 43.10 | 40.20 | 42.10 | 51.30 |
| TiO2  | 1.60  | 1.34  | 1.44  | 2.22  | 2.60   | 2.65  | 2.77  | 2.54  | 1.82  | 1.20  |
| Al2O3 | 12.60 | 11.10 | 11.60 | 11.80 | 13.30  | 12.90 | 15.70 | 14.70 | 9.94  | 10.10 |
| Fe2O3 | 10.92 | 11.09 | 11.09 | 11.34 | 11.00  | 11.12 | 12.17 | 14.90 | 3.68  | 12.66 |
| FeO   | 0.00  | 0.00  | 0.00  | 0.00  | 0.00   | 0.00  | 0.00  | 0.00  | 0.00  | 0.00  |
| MnO   | .19   | .17   | .28   | .21   | .21    | .04   | .16   | .12   | .11   | .16   |
| MgO   | 7.47  | 8.46  | 9.21  | 9.77  | 6.08   | 7.39  | 6.44  | 5.81  | 1.96  | 9.74  |
| CaO   | 5.91  | 5.37  | 6.23  | 5.16  | 6.42   | 7.06  | 5.93  | 8.43  | 17.88 | 3.85  |
| Na2O  | 2.66  | 1.90  | 2.00  | 1.20  | 4.11   | 1.87  | 4.48  | 4.34  | 5.07  | 1.16  |
| K2O   | .04   | .04   | .08   | .06   | 1.96   | 4.05  | .07   | .03   | .20   | .02   |
| P2O5  | .49   | .44   | .43   | .61   | .52    | .61   | .63   | .65   | .48   | .33   |
| LOI   | 8.70  | 8.74  | 10.27 | 8.96  | 2.90   | 3.60  | 6.65  | 8.27  | 16.10 | 7.74  |
| Total | 99.88 | 99.35 | 99.83 | 99.75 | 100.70 | 97.89 | 98.10 | 99.99 | 99.34 | 98.26 |
| Pb    | 5     | 2     | 2     | 5     | 10     | 3     | 11    | .4    | 2     | 0     |
| Th    | 5     | 3     | 6     | 6     | 7      | 0     | 3     | 2     | 0     | 0     |
| U     | 2     | 1     | 0     | 2     | 3      | 0     | 3     | 0     | 0     | 0     |
| Rb    | 0     | 0     | 1     | 1     | 21     | 39    | 1     | 1     | 3     | 1     |
| Sr    | 218   | 235   | 252   | 182   | 345    | 377   | 125   | 175   | 326   | 145   |
| Y     | 27    | 26    | 27    | 28    | 29     | 29    | 36    | 25    | 18    | 26    |
| Zr    | 200   | 200   | 184   | 211   | 205    | 233   | 241   | 211   | 181   | 149   |
| Nb    | 51    | 51    | 48    | 60    | 47     | 54    | 47    | 48    | 36    | 24    |
| Zn    | 100   | 101   | 104   | 87    | 109    | 129   | 169   | 104   | 37    | 100   |
| Cu    | 28    | 28    | 27    | 37    | 56     | 22    | 27    | 41    | 30    | 32    |
| Ni    | 147   | 134   | 148   | 80    | 49     | 97    | 137   | 259   | 125   | 274   |
| La    | 40    | 34    | 44    | 37    | 55     | 42    | 56    | 57    | 32    | 49    |
| Ba    | 112   | 121   | 106   | 122   | 1075   | 2213  | 133   | 82    | 242   | 90    |
| V     | 248   | 235   | 230   | 256   | 214    | 172   | 284   | 309   | 120   | 233   |
| Ce    | 26    | 23    | 27    | 19    | 121    | 62    | 121   | 96    | 72    | 82    |
| Cr    | 262   | 212   | 272   | 165   | 75     | 24    | 207   | 332   | 141   | 410   |
| Ga    | 17    | 11    | 14    | 15    | 21     | 13    | 29    | 29    | 6     | 20    |

|       | CA42C | CA45  | CA57  | CA58A | CA65  | CA67B | CA80  | PL55A | PL55E | PL56A |
|-------|-------|-------|-------|-------|-------|-------|-------|-------|-------|-------|
| SiO2  | 47.30 | 49.70 | 27.30 | 41.80 | 52.40 | 53.40 | 53.00 | 41.20 | 45.90 | 47.90 |
| TiO2  | 2.18  | 2.44  | 1.47  | 1.78  | 1.56  | 1.64  | 2.13  | 1.91  | 2.04  | 2.04  |
| Al2O3 | 12.10 | 13.20 | 9.77  | 10.00 | 10.00 | 12.40 | 10.40 | 12.50 | 12.00 | 12.00 |
| Fe2O3 | 10.67 | 11.31 | 6.60  | 8.94  | 11.68 | 9.07  | 7.78  | 10.06 | 9.70  | 9.91  |
| FeO   | 0.00  | 0.00  | 0.00  | 0.00  | 0.00  | 0.00  | 0.00  | 0.00  | 0.00  | 0.00  |
| MnO   | .42   | .52   | .51   | .21   | .25   | .18   | .18   | .44   | .48   | .37   |
| MgO   | 3.39  | 6.73  | 1.80  | 5.29  | 8.87  | 7.01  | 5.33  | 3.08  | 2.64  | 4.28  |
| CaO   | 9.84  | 4.59  | 25.38 | 13.50 | 4.74  | 4.67  | 7.43  | 13.13 | 11.23 | 9.23  |
| Na2O  | 3.35  | 3.19  | 3.62  | 2.93  | .50   | 3.40  | 2.97  | 3.33  | 3.04  | 2.68  |
| K2O   | .02   | .02   | .07   | .06   | .03   | .02   | .03   | .13   | .29   | .15   |
| P2O5  | .37   | .44   | .42   | .47   | .36   | .42   | .57   | .47   | .43   | .43   |
| LOI   | 10.03 | 7.40  | 21.71 | 13.50 | 8.34  | 7.72  | 8.34  | 12.99 | 11.27 | 10.36 |
| Total | 99.67 | 99.54 | 98.65 | 98.48 | 98.73 | 99.93 | 98.16 | 99.24 | 99.02 | 99.35 |
| Pb    | 0     | 5     | 0     | 0     | 0     | 3     | 1     | 4     | 3     | 2     |
| Th    | 0     | 0     | 0     | 0     | 0     | 0     | 0     | 6     | 0     | 0     |
| U     | 0     | 1     | 0     | 0     | 0     | 0     | 0     | 0     | 0     | 4     |
| Rb    | 1     | 0     | 0     | 4     | 0     | 2     | 0     | 7     | 13    | 6     |
| Sr    | 147   | 118   | 359   | 272   | 128   | 195   | 153   | 275   | 189   | 222   |
| Y     | 24    | 26    | 22    | 19    | 17    | 22    | 18    | 21    | 22    | 21    |
| Zr    | 175   | 196   | 168   | 163   | 151   | 177   | 186   | 164   | 171   | 177   |
| Nb    | 28    | 33    | 31    | 38    | 29    | 30    | 41    | 26    | 26    | 30    |
| Zn    | 210   | 96    | 106   | 100   | 105   | 98    | 82    | 72    | 72    | 95    |
| Cu    | 37    | 39    | 13    | 33    | 26    | 46    | 36    | 35    | 36    | 38    |
| Ni    | 139   | 128   | 145   | 260   | 251   | 122   | 129   | 123   | 164   | 132   |
| La    | 45    | 44    | 38    | 40    | 44    | 48    | 32    | 46    | 62    | 45    |
| Ba    | 161   | 144   | 80    | 165   | 104   | 154   | 223   | 247   | 275   | 295   |
| V     | 200   | 250   | 131   | 181   | 201   | 217   | 220   | 159   | 175   | 192   |
| Ce    | 82    | 93    | 59    | 69    | 73    | 86    | 90    | 67    | 117   | 86    |
| Cr    | 154   | 226   | 140   | 315   | 298   | 215   | 189   | 176   | 243   | 233   |
| Ga    | 18    | 20    | 13    | 20    | 16    | 19    | 18    | 16    | 16    | 17    |

|       | PL57B | PL57I | PL53B | PL53I | PL54B | PL128F | PL133B | PL67  | PL83  | PL150 |
|-------|-------|-------|-------|-------|-------|--------|--------|-------|-------|-------|
| SiO2  | 45.40 | 47.50 | 26.00 | 28.90 | 42.60 | 41.70  | 39.00  | 50.00 | 34.40 | 52.50 |
| TiO2  | 1.78  | 1.56  | 2.16  | 2.71  | 2.13  | 3.26   | 3.00   | 2.92  | 2.95  | 3.61  |
| Al2O3 | 12.20 | 12.00 | 6.47  | 8.93  | 6.64  | 9.11   | 8.68   | 11.60 | 12.30 | 12.30 |
| Fe2O3 | 9.29  | 10.98 | 9.40  | 11.00 | 8.45  | 11.41  | 8.90   | 12.83 | 12.97 | 10.54 |
| FeO   | 0.00  | 0.00  | 0.00  | 0.00  | 0.00  | 0.00   | 0.00   | 0.00  | 0.00  | 0.00  |
| MnO   | .22   | .20   | .76   | .56   | .13   | .13    | .12    | .11   | .14   | .07   |
| MgO   | 7.76  | 8.08  | 1.94  | 1.73  | 7.71  | 11.55  | 6.67   | 8.86  | 9.10  | 7.25  |
| CaO   | 8.46  | 6.15  | 27.25 | 22.55 | 15.40 | 9.89   | 15.68  | 3.59  | 10.86 | 2.92  |
| Na2O  | 2.57  | 2.53  | .02   | .04   | .34   | .22    | 1.86   | 1.54  | 1.70  | 3.08  |
| K2O   | .05   | .02   | .29   | .77   | .01   | .02    | .01    | .15   | .20   | .12   |
| P2O5  | .95   | .69   | .95   | 1.36  | 1.06  | 1.45   | 1.09   | .76   | 1.30  | .60   |
| LOI   | 9.86  | 8.64  | 23.28 | 19.71 | 14.47 | 9.78   | 13.14  | 6.97  | 12.34 | 5.88  |
| Total | 98.54 | 98.35 | 98.52 | 98.26 | 98.94 | 98.52  | 98.15  | 99.33 | 98.26 | 98.87 |
| Pb    | 5     | 1     | 10    | 27    | 14    | 1      | 4      | 13    | 4     | 11    |
| Th    | 3     | 0     | 1     | 1     | 3     | 1      | 1      | 6     | 0     | 4     |
| U     | 0     | 2     | 0     | 5     | 0     | 0      | 0      | 0     | 0     | 0     |
| Rb    | 1     | 1     | 10    | 27    | 1     | 0      | 0      | 5     | 2     | 1     |
| Sr    | 334   | 267   | 373   | 204   | 502   | 406    | 682    | 257   | 632   | 226   |
| Y     | 33    | 28    | 26    | 29    | 27    | 34     | 24     | 28    | 35    | 36    |
| Zr    | 294   | 191   | 332   | 386   | 326   | 502    | 372    | 397   | 415   | 473   |
| Nb    | 52    | 28    | 65    | 81    | 79    | 96     | 90     | 83    | 88    | 97    |
| In    | 112   | 118   | 100   | 110   | 97    | 124    | 104    | 151   | 151   | 132   |
| Cu    | 43    | 49    | 31    | 6     | 42    | 35     | 43     | 32    | 33    | 36    |
| Ni    | 109   | 150   | 158   | 155   | 138   | 199    | 182    | 203   | 192   | 187   |
| La    | 82    | 34    | 62    | 61    | 72    | 82     | 70     | 119   | 95    | 115   |
| Ba    | 260   | 76    | 148   | 346   | 35    | 419    | 84     | 98    | 464   | 281   |
| V     | 220   | 245   | 68    | 59    | 206   | 277    | 193    | 199   | 180   | 148   |
| Ce    | 133   | 93    | 116   | 121   | 151   | 171    | 135    | 231   | 184   | 255   |
| Cr    | 101   | 253   | 129   | 143   | 234   | 315    | 226    | 223   | 220   | 236   |
| Ga    | 20    | 23    | 12    | 15    | 17    | 19     | 18     | 28    | 28    | 23    |

|       | PL167 | PL31CL | PL31HO | PL34C | PL37A | PL37C | PL38A | PL38C | PL39A | PL44  |
|-------|-------|--------|--------|-------|-------|-------|-------|-------|-------|-------|
| SiO2  | 39.50 | 36.00  | 49.50  | 47.10 | 42.90 | 42.90 | 47.40 | 49.50 | 50.30 | 47.60 |
| TiO2  | 2.87  | 1.47   | 2.10   | 2.40  | 2.15  | 2.20  | 2.50  | 2.50  | 2.45  | 2.64  |
| Al2O3 | 10.20 | 7.83   | 11.90  | 12.00 | 13.90 | 11.70 | 11.80 | 12.30 | 12.40 | 13.50 |
| Fe2O3 | 10.15 | 2.18   | 5.01   | 11.05 | 12.00 | 11.75 | 10.85 | 11.90 | 10.31 | 10.57 |
| FeO   | 0.00  | 0.00   | 0.00   | 0.00  | 0.00  | 0.00  | 0.00  | 0.00  | 0.00  | 0.00  |
| MnO   | .13   | .28    | .19    | .20   | .63   | .64   | .10   | .13   | .26   | .20   |
| MgO   | 7.17  | 1.72   | 3.78   | 9.68  | 6.55  | 9.45  | 6.59  | 9.29  | 8.63  | 8.71  |
| CaO   | 13.00 | 23.50  | 11.28  | 6.00  | 6.83  | 7.89  | 8.26  | 4.74  | 5.26  | 5.85  |
| Na2O  | 1.81  | 4.38   | 5.65   | 3.41  | 3.93  | 2.00  | 4.08  | 4.13  | 2.42  | 2.79  |
| K2O   | .07   | .13    | .38    | .40   | .03   | .02   | .03   | .04   | .06   | 2.80  |
| P2O5  | .84   | .39    | .55    | .54   | .63   | .56   | .60   | .59   | .52   | .65   |
| LOI   | 13.50 | 17.61  | 8.85   | 6.77  | 8.68  | 10.10 | 7.77  | 4.55  | 6.61  | 3.70  |
| Total | 99.24 | 95.49  | 99.19  | 99.55 | 98.23 | 99.21 | 99.98 | 99.67 | 99.22 | 99.01 |
| Pb    | 1     | 17     | 0      | 5     | 2     | 14    | 0     | 0     | 12    | 4     |
| Th    | 5     | 2      | 0      | 0     | 2     | 1     | 0     | 0     | 3     | 0     |
| U     | 0     | 5      | 0      | 0     | 0     | 3     | 0     | 0     | 0     | 0     |
| Rb    | 2     | 4      | 0      | 3     | 2     | 0     | 0     | 1     | 1     | 28    |
| Sr    | 514   | 237    | 274    | 175   | 121   | 120   | 129   | 119   | 178   | 429   |
| Y     | 26    | 12     | 26     | 24    | 33    | 29    | 25    | 25    | 28    | 31    |
| Zr    | 320   | 173    | 241    | 241   | 267   | 239   | 253   | 250   | 267   | 277   |
| Nb    | 71    | 28     | 40     | 43    | 50    | 45    | 49    | 49    | 45    | 57    |
| Zn    | 124   | 43     | 116    | 119   | 135   | 123   | 104   | 115   | 131   | 119   |
| Cu    | 28    | 26     | 48     | 49    | 34    | 32    | 51    | 52    | 47    | 62    |
| Ni    | 153   | 117    | 183    | 227   | 261   | 249   | 238   | 230   | 239   | 129   |
| La    | 66    | 49     | 60     | 59    | 61    | 70    | 74    | 78    | 67    | 75    |
| Ba    | 145   | 75     | 164    | 170   | 54    | 55    | 91    | 88    | 280   | 1488  |
| V     | 118   | 82     | 157    | 231   | 279   | 256   | 231   | 247   | 238   | 229   |
| Ce    | 127   | 56     | 111    | 115   | 131   | 133   | 107   | 127   | 124   | 120   |
| Cr    | 131   | 120    | 244    | 278   | 362   | 344   | 349   | 317   | 333   | 114   |
| Ga    | 21    | 9      | 20     | 21    | 23    | 22    | 18    | 25    | 21    | 25    |



|       | SB37B1 | SB37B2 | SB39C | SB40A | SB40D |
|-------|--------|--------|-------|-------|-------|
| SiO2  | 46.00  | 47.80  | 69.40 | 28.40 | 26.70 |
| TiO2  | 1.93   | 2.03   | 1.55  | 1.02  | .76   |
| Al2O3 | 11.60  | 12.00  | 9.78  | 6.63  | 8.59  |
| Fe2O3 | 9.79   | 10.54  | 5.97  | 6.88  | 12.28 |
| FeO   | 0.00   | 0.00   | 0.00  | 0.00  | 0.00  |
| MnO   | .13    | .13    | .04   | .13   | .12   |
| MgO   | 6.00   | 6.08   | 5.25  | 3.92  | 4.75  |
| CaO   | 9.45   | 8.03   | 1.08  | 27.10 | 23.15 |
| Na2O  | 3.56   | 3.84   | .19   | .79   | .48   |
| K2O   | 3.25   | 2.84   | .47   | .10   | .10   |
| P2O5  | .67    | .64    | .23   | .29   | .22   |
| LOI   | 7.31   | 5.36   | 5.10  | 24.42 | 22.25 |
| Total | 99.69  | 99.29  | 99.06 | 99.68 | 99.40 |
| Pb    | 4      | 0      | 4     | 4     | 4     |
| Th    | 4      | 2      | 0     | 0     | 0     |
| U     | 1      | 1      | 0     | 0     | 7     |
| Rb    | 27     | 23     | 14    | 6     | 6     |
| Sr    | 179    | 193    | 12    | 318   | 169   |
| Y     | 21     | 22     | 15    | 13    | 11    |
| Zr    | 184    | 198    | 128   | 90    | 64    |
| Nb    | 41     | 48     | 24    | 16    | 14    |
| Zn    | 119    | 165    | 108   | 91    | 93    |
| Cu    | 29     | 27     | 50    | 29    | 17    |
| Ni    | 151    | 165    | 74    | 104   | 287   |
| La    | 41     | 36     | 23    | 25    | 26    |
| Ba    | 638    | 631    | 258   | 225   | 69    |
| V     | 125    | 132    | 157   | 85    | 84    |
| Ce    | 78     | 88     | 55    | 32    | 29    |
| Cr    | 147    | 138    | 214   | 125   | 96    |
| Ga    | 15     | 17     | 17    | 15    | 16    |

|    | CHA5A | CHA5C | CHA6B | CA36 | CA42D | CA67C | PL55B | PL55F | PL55G |
|----|-------|-------|-------|------|-------|-------|-------|-------|-------|
| Pb | 3     | 4     | 4     | 100  | 3     | 7     | 1     | 0     | 3     |
| Th | 3     | 6     | 8     | 3    | 1     | 1     | 0     | 3     | 1     |
| U  | 2     | 1     | 2     | 0    | 0     | 4     | 0     | 3     | 0     |
| Rb | 1     | 1     | 1     | 0    | 0     | 1     | 15    | 8     | 16    |
| Sr | 360   | 257   | 212   | 127  | 211   | 129   | 169   | 172   | 174   |
| Y  | 26    | 24    | 36    | 40   | 27    | 27    | 22    | 20    | 21    |
| Zr | 178   | 169   | 259   | 274  | 202   | 263   | 151   | 153   | 165   |
| Nb | 45    | 45    | 68    | 48   | 32    | 41    | 27    | 24    | 28    |
| Zn | 97    | 94    | 68    | 109  | 138   | 99    | 68    | 66    | 52    |
| Cu | 25    | 36    | 23    | 68   | 43    | 38    | 29    | 13    | 25    |
| Ni | 152   | 165   | 110   | 252  | 202   | 179   | 105   | 114   | 116   |
| La | 42    | 35    | 52    | 57   | 52    | 66    | 28    | 39    | 41    |
| Ba | 124   | 112   | 128   | 51   | 129   | 114   | 389   | 263   | 415   |
| V  | 221   | 245   | 210   | 215  | 259   | 259   | 156   | 153   | 162   |
| Ce | 26    | 30    | 31    | 112  | 97    | 125   | 60    | 66    | 73    |
| Cr | 317   | 313   | 120   | 301  | 324   | 295   | 200   | 189   | 218   |
| Ga | 12    | 19    | 17    | 25   | 21    | 24    | 13    | 15    | 16    |

|    | PL56B | PL56C | PL57A | PL57C | PL57E | PL57F | PL57G | PL57H | PL57J |
|----|-------|-------|-------|-------|-------|-------|-------|-------|-------|
| Pb | 0     | 6     | 1     | 7     | 1     | 8     | 5     | 6     | 6     |
| Th | 0     | 0     | 1     | 5     | 3     | 0     | 2     | 4     | 5     |
| U  | 3     | 5     | 3     | 2     | 9     | 0     | 1     | 6     | 1     |
| Rb | 0     | 0     | 1     | 3     | 4     | 0     | 0     | 3     | 0     |
| Sr | 159   | 233   | 272   | 158   | 271   | 148   | 212   | 370   | 68    |
| Y  | 22    | 26    | 28    | 27    | 27    | 25    | 26    | 31    | 25    |
| Zr | 163   | 178   | 267   | 248   | 179   | 185   | 176   | 187   | 177   |
| Nb | 28    | 29    | 45    | 41    | 28    | 25    | 29    | 28    | 28    |
| Zn | 104   | 111   | 106   | 102   | 111   | 120   | 104   | 118   | 99    |
| Cu | 33    | 34    | 43    | 38    | 37    | 40    | 45    | 46    | 41    |
| Ni | 133   | 152   | 164   | 223   | 196   | 166   | 143   | 143   | 146   |
| La | 40    | 51    | 66    | 44    | 56    | 48    | 43    | 44    | 37    |
| Ba | 190   | 249   | 162   | 126   | 155   | 98    | 104   | 108   | 75    |
| V  | 199   | 201   | 250   | 255   | 231   | 253   | 220   | 242   | 249   |
| Ce | 77    | 89    | 117   | 98    | 85    | 87    | 82    | 86    | 88    |
| Cr | 236   | 251   | 236   | 373   | 298   | 215   | 236   | 248   | 260   |
| Ga | 20    | 19    | 22    | 19    | 19    | 19    | 20    | 23    | 23    |

|    | PL53P | PL54C | PL128C | PL132D | PL132J | PL64 | PL77 | PL144M | PL157 |
|----|-------|-------|--------|--------|--------|------|------|--------|-------|
| Pb | 7     | 11    | 9      | 8      | 8      | 7    | 10   | 0      | 5     |
| Th | 4     | 1     | 9      | 0      | 0      | 2    | 3    | 4      | 2     |
| U  | 2     | 0     | 7      | 0      | 4      | 2    | 9    | 1      | 0     |
| Rb | 34    | 0     | 0      | 32     | 4      | 3    | 14   | 0      | 0     |
| Sr | 200   | 478   | 590    | 352    | 287    | 176  | 447  | 416    | 354   |
| Y  | 35    | 33    | 35     | 19     | 19     | 28   | 32   | 25     | 25    |
| Zr | 429   | 445   | 495    | 282    | 264    | 380  | 379  | 285    | 372   |
| Nb | 99    | 105   | 95     | 57     | 60     | 82   | 80   | 60     | 79    |
| Zn | 92    | 129   | 109    | 54     | 103    | 149  | 130  | 107    | 133   |
| Cu | 8     | 41    | 41     | 7      | 5      | 30   | 35   | 31     | 26    |
| Ni | 99    | 209   | 190    | 76     | 145    | 185  | 170  | 121    | 230   |
| La | 75    | 84    | 97     | 62     | 56     | 108  | 77   | 66     | 78    |
| Ba | 450   | 47    | 110    | 329    | 103    | 285  | 121  | 92     | 160   |
| V  | 52    | 261   | 191    | 98     | 165    | 196  | 161  | 98     | 137   |
| Ce | 148   | 169   | 173    | 89     | 79     | 197  | 160  | 119    | 181   |
| Cr | 165   | 288   | 275    | 57     | 96     | 243  | 202  | 135    | 255   |
| Ga | 14    | 23    | 16     | 11     | 13     | 25   | 27   | 21     | 26    |

|    | PL163 | PL37B | SB38C | SB38D | SB39D | SB40C | SB43B |
|----|-------|-------|-------|-------|-------|-------|-------|
| Pb | 7     | 14    | 8     | 0     | 8     | 4     | 45    |
| Th | 3     | 14    | 4     | 0     | 0     | 0     | 4     |
| U  | 1     | 1     | 1     | 1     | 4     | 4     | 1     |
| Rb | 1     | 97    | 8     | 6     | 5     | 36    | 3     |
| Sr | 474   | 66    | 440   | 467   | 300   | 169   | 56    |
| Y  | 29    | 24    | 25    | 26    | 12    | 19    | 17    |
| Zr | 356   | 91    | 112   | 115   | 74    | 120   | 119   |
| Nb | 78    | 11    | 21    | 20    | 13    | 25    | 24    |
| Zn | 121   | 87    | 86    | 89    | 93    | 103   | 105   |
| Cu | 28    | 7     | 64    | 62    | 32    | 46    | 30    |
| Ni | 174   | 39    | 151   | 60    | 113   | 219   | 183   |
| La | 77    | 50    | 27    | 31    | 27    | 33    | 21    |
| Ba | 157   | 475   | 376   | 489   | 95    | 433   | 181   |
| V  | 99    | 114   | 251   | 180   | 72    | 122   | 143   |
| Ce | 149   | 94    | 63    | 60    | 35    | 45    | 53    |
| Cr | 221   | 72    | 220   | 115   | 115   | 200   | 171   |
| Ga | 20    | 21    | 18    | 23    | 12    | 19    | 16    |

CAPE ST. MARY'S FEEDER PIPE ANALYSES

| Samples Analyzed For<br>Major and Trace Elements               | Trace Elements                                 | Locations  |
|--|--|--|
| LC8C, LC8F, etc. to CA28I<br>CA86B and CA89<br>CA162 and CA164 | CA25 to PL7<br>CA86A to CA88<br>CA163 to CA165 | Normans Cove<br>McLeod Point<br>Spread Eagle<br>Peak |
| CA170 and CA173  | CA169 to CA174                                 | W. of Spread<br>Eagle Peak                           |
| CA178 and CA180  | CA179  | N. of Spread<br>Eagle Peak                           |
| PL106 and PL108  | PL105 to PL107                                 | S.E. of<br>Placentia<br>Junction                     |
| PL207B and PL210   | PL207A to PL211                                | Placentia<br>Junction                                |

LC8C, F, G, CA25, 28C, 33, PL6, 7. Leucogabbro. Primary minerals: Clinopyroxene, Fe-Ti oxides, apatite. Secondary minerals: Chlorite, albite,  $\pm$  epidote  $\pm$  actinolite  $\pm$  quartz,  $\pm$  sphene,  $\pm$  calcite. Texture: Phaneritic, equigranular. Comments: Ferromagnesian minerals < than 30%.

CA26, 27, 28A, 28E, 29, 34, 36. Melanogabbro. Primary minerals: Clinopyroxene, Fe-Ti oxides. Secondary minerals: Chlorite, albite, actinolite, serpentine. Texture: Phaneritic, altered, olivine phenocrysts, clinopyroxene porphyritic and sometimes glomeroporphyritic. Comments: Mafic minerals up to 80%.

CA28D, F, G, H, I, 32G, 143. Gabbro. Primary minerals: Clinopyroxene, Fe-Ti oxides, apatite. Secondary minerals: Chlorite, albite,  $\pm$  epidote  $\pm$  sphene,  $\pm$  calcite. Texture: Phaneritic, sometimes clinopyroxene porphyritic and, less

commonly serpentized olivine phenocrysts. Comments: Mafic minerals > 30% and < 60%.

CA86B, 87, 89, 165. Gabbro. Primary minerals: Clinopyroxene, Fe-Ti oxides, apatite. Secondary minerals: Chlorite, albite, actinolite  $\pm$  prehnite,  $\pm$  sphene,  $\pm$  calcite. Texture: Phaneritic, sometimes clinopyroxene porphyritic and less commonly serpentized olivine phenocrysts. Comments: Mafic minerals > 30% and < 60%.

CA86A, 162, 163, 164, 169, 170, 172, 173, 174, 178, 179, 180, PL105, 106, 107. Melanogabbro. Primary minerals: Clinopyroxene, Fe-Ti oxides. Secondary minerals: Chlorite, albite, actinolite, serpentine, sphene,  $\pm$  prehnite,  $\pm$  biotite,  $\pm$  calcite,  $\pm$  quartz. Texture: Phaneritic, altered olivine phenocrysts, clinopyroxene porphyritic and sometimes glomeroporphyritic. Comments: Mafic minerals up to 80%.

PL108, 207A, 207B, 209, 210, 211. Leucogabbro. Primary minerals: Clinopyroxene, Fe-Ti oxides, apatite. Secondary Minerals: Chlorite, albite,  $\pm$  actinolite  $\pm$  sphene,  $\pm$  calcite. Texture: Phaneritic, equigranular. Comments: Ferromagnesian minerals < than 30%.

|       | LC8C   | LC8F  | LC8G  | CA26  | CA28C | CA28E  | CA28F | CA28G  | CA28H | CA28I |
|-------|--------|-------|-------|-------|-------|--------|-------|--------|-------|-------|
| SiO2  | 52.30  | 55.20 | 56.30 | 47.70 | 53.10 | 48.20  | 45.70 | 51.50  | 52.30 | 51.40 |
| TiO2  | 2.71   | 1.62  | 1.51  | 1.74  | 1.79  | 1.55   | 2.70  | 2.28   | 2.13  | 1.98  |
| Al2O3 | 15.20  | 15.90 | 15.90 | 11.00 | 14.80 | 10.20  | 14.00 | 14.20  | 14.80 | 14.40 |
| Fe2O3 | 10.62  | 8.99  | 8.71  | 11.96 | 9.03  | 11.82  | 13.80 | 9.91   | 10.50 | 10.44 |
| FeO   | 0.00   | 0.00  | 0.00  | 0.00  | 0.00  | 0.00   | 0.00  | 0.00   | 0.00  | 0.00  |
| MnO   | .44    | .19   | .17   | .15   | .12   | .16    | .17   | .16    | .17   | .15   |
| MgO   | 3.83   | 1.76  | 1.51  | 11.19 | 3.36  | 12.60  | 4.25  | 6.25   | 5.83  | 6.67  |
| CaO   | 4.49   | 2.93  | 2.46  | 7.59  | 5.35  | 8.59   | 6.29  | 5.35   | 4.43  | 5.42  |
| Na2O  | 6.14   | 5.22  | 5.71  | 2.57  | 3.64  | 1.77   | 4.35  | 4.94   | 4.93  | 4.54  |
| K2O   | .10    | 3.87  | 3.51  | .16   | 5.35  | 1.24   | 1.68  | 1.56   | 1.80  | 2.04  |
| P2O5  | .63    | .51   | .49   | .36   | .80   | .33    | .67   | .32    | .35   | .37   |
| LOI   | 3.76   | 2.77  | 2.40  | 4.13  | 2.07  | 3.79   | 6.18  | 4.25   | 2.42  | 2.48  |
| Total | 100.22 | 98.96 | 98.67 | 98.55 | 99.41 | 100.25 | 99.79 | 100.72 | 99.66 | 99.89 |
| Pb    | 0      | 4     | 2     | 7     | 0     | 1      | 4     | 0      | 1     | 5     |
| Th    | .0     | 4     | 0     | 4     | 0     | 0      | 2     | 1      | 0     | 1     |
| U     | 0      | 1     | 0     | 4     | 1     | 1      | 0     | 7      | 0     | 1     |
| Rb    | 1      | 54    | 48    | 4     | 55    | 16     | 20    | 18     | 20    | 21    |
| Sr    | 414    | 351   | 385   | 226   | 939   | 327    | 297   | 327    | 407   | 331   |
| Y     | 28     | 45    | 39    | 22    | 36    | 19     | 30    | 24     | 23    | 23    |
| Zr    | 213    | 364   | 332   | 115   | 272   | 117    | 132   | 123    | 124   | 121   |
| Nb    | 52     | 84    | 77    | 25    | 52    | 24     | 33    | 25     | 26    | 25    |
| Zn    | 105    | 140   | 111   | 74    | 77    | 95     | 112   | 80     | 96    | 82    |
| Cu    | 44     | 16    | 17    | 16    | 21    | 15     | 39    | 33     | 51    | 33    |
| Ni    | 26     | 0     | 0     | 327   | 6     | 370    | 86    | 88     | 93    | 89    |
| La    | 63     | 58    | 56    | 31    | 120   | 29     | 43    | 26     | 30    | 38    |
| Ba    | 108    | 1157  | 1385  | 98    | 777   | 635    | 509   | 444    | 726   | 615   |
| V     | 215    | 35    | 31    | 162   | 122   | 139    | 225   | 169    | 180   | 156   |
| Ce    | 103    | 110   | 112   | 68    | 100   | 64     | 86    | 61     | 69    | 68    |
| Cr    | 0      | 0     | 0     | 382   | 0     | 439    | 224   | 111    | 73    | 120   |
| Ga    | 26     | 33    | 31    | 19    | 23    | 17     | 24    | 23     | 24    | 22    |



|       | CA86B  | CA89   | CA162  | CA164 | CA170 | CA173  | CA178  | CA180  | PL106 | PL108 |
|-------|--------|--------|--------|-------|-------|--------|--------|--------|-------|-------|
| SiO2  | 50.60  | 48.90  | 48.00  | 48.60 | 46.00 | 46.80  | 47.20  | 48.00  | 47.60 | 53.50 |
| TiO2  | 1.98   | 2.01   | 1.81   | 1.47  | 1.12  | 1.41   | 1.89   | 1.81   | 1.71  | 2.57  |
| Al2O3 | 11.80  | 11.80  | 11.20  | 9.95  | 11.90 | 11.30  | 11.80  | 11.00  | 11.00 | 13.50 |
| Fe2O3 | 10.61  | 10.58  | 11.65  | 11.72 | 10.92 | 11.71  | 11.64  | 11.68  | 11.46 | 10.82 |
| FeO   | 0.00   | 0.00   | 0.00   | 0.00  | 0.00  | 0.00   | 0.00   | 0.00   | 0.00  | 0.00  |
| MnO   | .14    | .27    | .19    | .19   | .15   | .23    | .14    | .15    | .22   | .14   |
| MgO   | 10.00  | 9.28   | 11.84  | 12.32 | 13.20 | 13.20  | 10.64  | 11.44  | 11.92 | 4.64  |
| CaO   | 7.37   | 7.85   | 8.75   | 8.87  | 9.46  | 8.93   | 9.40   | 8.99   | 7.73  | 4.49  |
| Na2O  | 3.30   | 4.00   | 2.53   | 2.28  | 1.74  | 1.46   | 2.28   | 1.87   | 2.55  | 4.22  |
| K2O   | .62    | .02    | .02    | .03   | .62   | .98    | .98    | 1.42   | .59   | 1.58  |
| P2O5  | .38    | .38    | .22    | .16   | .13   | .25    | .38    | .40    | .29   | .54   |
| LOI   | 3.83   | 4.96   | 4.17   | 4.02  | 4.05  | 4.38   | 3.83   | 3.75   | 4.41  | 2.69  |
| Total | 100.63 | 100.05 | 100.38 | 99.61 | 99.29 | 100.65 | 100.18 | 100.51 | 99.48 | 98.69 |
| Pb    | 8      | 5      | 0      | 6     | 3     | 0      | 0      | 3      | 9     | 3     |
| Th    | 1      | 1      | 0      | 2     | 0     | 0      | 0      | 1      | 0     | 0     |
| U     | 1      | 1      | 0      | 1     | 0     | 4      | 0      | 0      | 0     | 0     |
| Rb    | 8      | 0      | 0      | 3     | 5     | 23     | 13     | 15     | 4     | 15    |
| Sr    | 662    | 259    | 162    | 289   | 453   | 338    | 200    | 205    | 218   | 361   |
| Y     | 24     | 22     | 21     | 14    | 12    | 13     | 21     | 21     | 24    | 36    |
| Zr    | 158    | 162    | 100    | 90    | 48    | 67     | 162    | 163    | 118   | 252   |
| Nb    | 28     | 28     | 23     | 19    | 10    | 17     | 33     | 34     | 31    | 47    |
| Zn    | 100    | 106    | 128    | 108   | 124   | 107    | 113    | 107    | 129   | 128   |
| Cu    | 44     | 40     | 62     | 42    | 29    | 19     | 41     | 58     | 28    | 29    |
| Ni    | 210    | 196    | 339    | 310   | 345   | 336    | 233    | 244    | 248   | 13    |
| La    | 45     | 36     | 25     | 21    | 14    | 23     | 45     | 45     | 42    | 54    |
| Ba    | 1073   | 64     | 42     | 63    | 578   | 342    | 305    | 624    | 451   | 866   |
| V     | 170    | 166    | 145    | 126   | 113   | 134    | 158    | 167    | 174   | 233   |
| Ge    | 73     | 76     | 54     | 41    | 39    | 53     | 77     | 78     | 72    | 116   |
| Cr    | 246    | 246    | 292    | 288   | 389   | 375    | 241    | 300    | 266   | 0     |
| Ga    | 20     | 20     | 18     | 15    | 19    | 17     | 19     | 19     | 18    | 20    |

|       | PL207B | PL210 |
|-------|--------|-------|
| SiO2  | 52.60  | 50.60 |
| TiO2  | 2.80   | 2.33  |
| Al2O3 | 13.50  | 14.90 |
| Fe2O3 | 12.14  | 10.14 |
| FeO   | 0.00   | 0.00  |
| MnO   | .16    | .16   |
| MgO   | 5.20   | 5.20  |
| CaO   | 4.61   | 5.59  |
| Na2O  | 4.75   | 5.56  |
| K2O   | 1.28   | .80   |
| P2O5  | .52    | .50   |
| LOI   | 2.67   | 3.52  |
| Total | 100.23 | 99.30 |

|    |     |     |
|----|-----|-----|
| Pb | 1   | 4   |
| Th | 0   | 1   |
| U  | 1   | 0   |
| Rb | 13  | 8   |
| Sr | 305 | 391 |
| Y  | 34  | 28  |
| Zr | 218 | 170 |
| Nb | 41  | 31  |
| Zn | 155 | 106 |
| Cu | 39  | 43  |
| Ni | 23  | 51  |
| La | 62  | 53  |
| Ba | 801 | 448 |
| V  | 279 | 234 |
| Ce | 113 | 97  |
| Cr | 0   | 88  |
| Ga | 29  | 23  |

|    | CA25 | CA27 | CA28A | CA28D | CA29A | CA32 | CA33 | CA34 | CA36 |
|----|------|------|-------|-------|-------|------|------|------|------|
| Pb | 2    | 17   | 0     | 0     | 0     | 0    | 1    | 0    | 6    |
| Th | 0    | 0    | 0     | 0     | 0     | 0    | 0    | 5    | 0    |
| U  | 5    | 0    | 0     | 0     | 0     | 0    | 6    | 0    | 0    |
| Rb | 42   | 10   | 27    | 21    | 14    | 23   | 15   | 5    | 6    |
| Sr | 433  | 279  | 458   | 834   | 376   | 556  | 288  | 497  | 242  |
| Y  | 40   | 21   | 20    | 26    | 23    | 15   | 24   | 15   | 17   |
| Zr | 300  | 119  | 112   | 164   | 112   | 117  | 145  | 98   | 105  |
| Nb | 74   | 27   | 23    | 36    | 23    | 31   | 42   | 20   | 22   |
| Zn | 113  | 164  | 109   | 91    | 102   | 122  | 131  | 100  | 108  |
| Cu | 23   | 55   | 49    | 58    | 53    | 103  | 24   | 32   | 51   |
| Ni | 0    | 316  | 310   | 101   | 333   | 68   | 3    | 377  | 372  |
| La | 60   | 25   | 33    | 35    | 32    | 46   | 50   | 31   | 31   |
| Ba | 1000 | 617  | 1026  | 776   | 838   | 908  | 371  | 365  | 386  |
| V  | 47   | 151  | 137   | 184   | 132   | 362  | 343  | 135  | 125  |
| Ce | 117  | 61   | 55    | 87    | 67    | 110  | 112  | 56   | 57   |
| Cr | 0    | 313  | 342   | 179   | 350   | 0    | 0    | 428  | 338  |
| Ga | 28   | 20   | 20    | 25    | 18    | 21   | 28   | 13   | 18   |

|    | CA143 | PL6 | PL7 | CA86A | CA87 | CA88 | CA163 | CA165 | CA169 |
|----|-------|-----|-----|-------|------|------|-------|-------|-------|
| Pb | 14    | 8   | 1   | 2     | 6    | 0    | 0     | 5     | 0     |
| Th | 11    | 7   | 7   | 5     | 3    | 0    | 0     | 2     | 0     |
| U  | 5     | 5   | 0   | 0     | 2    | 0    | 0     | 0     | 0     |
| Rb | 18    | 29  | 21  | 2     | 3    | 0    | 8     | 0     | 7     |
| Sr | 346   | 262 | 309 | 336   | 496  | 303  | 670   | 384   | 488   |
| Y  | 30    | 23  | 34  | 21    | 23   | 21   | 18    | 18    | 11    |
| Zr | 183   | 163 | 180 | 156   | 165  | 157  | 103   | 101   | 50    |
| Nb | 38    | 41  | 46  | 23    | 32   | 26   | 21    | 20    | 10    |
| Zn | 115   | 135 | 130 | 96    | 120  | 113  | 116   | 103   | 112   |
| Cu | 36    | 20  | 28  | 18    | 37   | 42   | 57    | 48    | 27    |
| Ni | 40    | 11  | 0   | 264   | 183  | 209  | 318   | 247   | 444   |
| La | 46    | 49  | 55  | 43    | 35   | 35   | 33    | 37    | 28    |
| Ba | 406   | 663 | 461 | 98    | 245  | 89   | 600   | 85    | 291   |
| V  | 199   | 302 | 239 | 151   | 176  | 174  | 145   | 149   | 105   |
| Ce | 95    | 109 | 109 | 77    | 84   | 79   | 63    | 59    | 40    |
| Cr | 16    | 0   | 0   | 285   | 219  | 253  | 290   | 292   | 431   |
| Ga | 25    | 25  | 27  | 19    | 22   | 20   | 18    | 17    | 17    |

|    | CA172 | CA174 | CA169 | PL105 | PL107 | PL207A | PL209 | PL211 |
|----|-------|-------|-------|-------|-------|--------|-------|-------|
| Pb | 0     | 0     | 2     | 2     | 2     | 2      | 4     | 5     |
| Th | 1     | 4     | 0     | 0     | 0     | 0      | 0     | 3     |
| U  | 0     | 0     | 0     | 0     | 2     | 1      | 0     | 0     |
| Rb | 5     | 3     | 9     | 0     | 1     | 11     | 10    | 12    |
| Sr | 249   | 245   | 288   | 178   | 228   | 438    | 194   | 400   |
| Y  | 11    | 10    | 21    | 17    | 20    | 30     | 37    | 27    |
| Zr | 59    | 62    | 139   | 81    | 86    | 181    | 228   | 190   |
| Nb | 13    | 11    | 30    | 18    | 21    | 35     | 46    | 38    |
| Zn | 107   | 111   | 127   | 119   | 108   | 110    | 133   | 120   |
| Cu | 21    | 22    | 57    | 49    | 37    | 42     | 35    | 44    |
| Ni | 413   | 416   | 266   | 339   | 252   | 46     | 23    | 46    |
| La | 18    | 17    | 42    | 31    | 36    | 52     | 63    | 50    |
| Ba | 431   | 415   | 500   | 216   | 136   | 559    | 555   | 951   |
| V  | 110   | 111   | 153   | 114   | 151   | 230    | 284   | 241   |
| Ce | 37    | 39    | 65    | 48    | 51    | 92     | 117   | 93    |
| Cr | 413   | 407   | 311   | 380   | 299   | 61     | 0     | 69    |
| Ga | 15    | 15    | 17    | 15    | 16    | 28     | 28    | 22    |

CAPE ST. MARY'S SILL ANALYSES

The sill at Gull Cove was systematically sampled at two locations. Analyses numbered SB6C, SB6D, etc. are from progressively higher levels in the lower two-thirds of the sill, and the SB7 series samples are from the upper three-quarters of the sill. The remaining samples are from various sills around Lance Cove.

| Samples Analyzed For<br>Major and Trace Elements | Trace Elements | Locations  |
|--|----------------|------------|
| SB6C to SB70                                     | SB7R           | Gull Cove  |
| SB15A to 26.7.7                                  | SB12 to SB60H  | Lance Cove |

SB6C. Sill margin. Secondary minerals: Chlorite, albite, Fe-Ti oxides. Texture: Very fine grained chlorite - albite after glass, altered olivine? phenocrysts, and small minor plagioclase (now albite) phenocrysts.

SB6D. Gabbro. Primary minerals: Plagioclase, clinopyroxene, biotite, Fe-Ti oxides, apatite. Secondary minerals: Chlorite, albite. Texture: phaneritic, ophitic, minor plagioclase phenocrysts.

SB6E, F, G, H, I, J, K, SB7A, B, C, D, E, F, I, O, 26.7.7, 5.9.79, 26.7.7B. Gabbro. Primary minerals: Plagioclase, clinopyroxene, biotite, Fe-Ti oxides, apatite. Secondary minerals: Chlorite, albite, prehnite, actinolite, minor sphene. Texture: phaneritic, poikilitic augite, and in upper samples poikilitic biotite. Grain sizes shown in

Figure 3.2.

SB7M. Diabase. Primary minerals: Plagioclase, clinopyroxene, biotite, Fe-Ti oxides. Secondary minerals: Chlorite, albite, minor calcite. Fine grained, subophitic.

SB7N. Diabase. Primary minerals: Plagioclase, biotite, clinopyroxene, Fe-Ti oxides. Secondary minerals: Chlorite, albite. Fine grained, subophitic. Comments: Biotite 40%.

SB7G, J. Granophyre. Primary minerals: Albite, quartz, Fe-Ti oxides, apatite, calcite. Secondary minerals: Chlorite, actinolite. Texture: Phaneritic, equigranular.

SB7H, K, L. Granophyre. Primary minerals: Albite, amphibole, clinopyroxene, Fe-Ti oxides, biotite, apatite, + quartz, calcite. Secondary minerals: Chlorite, actinolite, + prehnite. Texture: Phaneritic, equigranular. Mafic minerals form thin needles in SB7L, large anhedral grains in SB7H, and 7K.

SB7R, 12, 13, 14. Diabase. Clinopyroxene, plagioclase, Fe-Ti oxides + amphibole, + biotite. Secondary minerals: Albite, chlorite, calcite. Texture: Fine-grained, subophitic. Comments: Calcite = 5 to 15%.

SB15A, C, E, F, H, J, K, 16A, B, 18, 19, 20, 22, 24A, 48A, 48B, 48C, 48D, 48E, 48F, 48G, 48I, J, L, 50A, B1, B2, C, D, 58Q, 60C. Gabbro. Primary minerals: Plagioclase, clinopyroxene, biotite, Fe-Ti oxides, apatite. Secondary minerals:

Chlorite, albite,  $\pm$  calcite,  $\pm$  prehnite,  $\pm$  actinolite.  
Texture: phaneritic, poikilitic augite, sometimes biotite.  
Augite grain sizes vary from 1 to 20 mm.

SB17, 21. Granophyre. Primary minerals: Albite, quartz, biotite, Fe-Ti oxides, apatite, calcite?. Secondary minerals: Chlorite, prehnite. Texture: Phaneritic, equigranular. Comments: Calcite forms interstitial grains and may be primary.

SB58F, J, 60E, F, G, H. Gabbro. Primary minerals: Olivine, clinopyroxene, amphibole, biotite, Fe-Ti oxides, plagioclase. Secondary minerals: Chlorite, albite, prehnite, actinolite, serpentine. Texture: Olivine is cumulus; augite, amphibole, biotite intercumulus and poikilitic. Percentage olivine varies from 5 to 80%.



|       | SB6C  | SB6D   | SB6E   | SB6F  | SB6G  | SB6H  | SB6I   | SB6J   | SB6K  | SB7A  |
|-------|-------|--------|--------|-------|-------|-------|--------|--------|-------|-------|
| SiO2  | 46.40 | 46.10  | 47.80  | 46.90 | 46.60 | 45.90 | 47.70  | 47.70  | 44.90 | 46.50 |
| TiO2  | 1.53  | 1.34   | 1.57   | 1.41  | 1.37  | 1.41  | 1.56   | 1.52   | 1.55  | 1.32  |
| Al2O3 | 16.30 | 17.50  | 14.90  | 15.80 | 15.70 | 15.70 | 16.40  | 17.70  | 16.10 | 15.50 |
| Fe2O3 | 12.76 | 11.89  | 13.36  | 12.16 | 12.82 | 12.63 | 11.29  | 10.40  | 11.29 | 12.66 |
| FeO   | 0.00  | 0.00   | 0.00   | 0.00  | 0.00  | 0.00  | 0.00   | 0.00   | 0.00  | 0.00  |
| MnO   | .20   | .19    | .21    | .19   | .19   | .24   | .21    | .19    | .23   | .20   |
| MgO   | 7.41  | 7.16   | 7.19   | 7.68  | 7.42  | 7.92  | 7.08   | 6.30   | 7.65  | 7.58  |
| CaO   | 7.38  | 9.74   | 10.72  | 10.26 | 10.35 | 8.56  | 8.06   | 8.71   | 10.47 | 9.94  |
| Na2O  | 3.63  | 2.81   | 2.78   | 2.68  | 2.62  | 2.78  | 3.35   | 3.41   | 2.69  | 2.65  |
| K2O   | .45   | .28    | .25    | .33   | .21   | .41   | .97    | 1.11   | .59   | .29   |
| P2O5  | .19   | .15    | .15    | .14   | .13   | .14   | .20    | .19    | .19   | .12   |
| LOI   | 3.41  | 2.84   | 1.84   | 1.99  | 2.43  | 3.58  | 3.43   | 3.48   | 3.17  | 2.61  |
| Total | 99.66 | 100.00 | 100.57 | 99.54 | 99.84 | 99.27 | 100.25 | 100.71 | 98.83 | 99.37 |
| Pb    | 3     | 0      | 0      | 4     | 5     | 4     | 4      | 3      | 3     | 0     |
| Th    | 0     | 0      | 0      | 0     | 2     | 5     | 0      | 1      | 0     | 0     |
| U     | 0     | 0      | 0      | 0     | 7     | 10    | 0      | 1      | 1     | 0     |
| Rb    | 13    | 4      | 6      | 5     | 9     | 9     | 22     | 23     | 13    | 9     |
| Sr    | 370   | 291    | 249    | 263   | 249   | 324   | 456    | 459    | 365   | 261   |
| Y     | 27    | 27     | 29     | 27    | 25    | 25    | 26     | 23     | 22    | 24    |
| Zr    | 90    | 63     | 68     | 58    | 59    | 62    | 96     | 84     | 82    | 61    |
| Nb    | 12    | 6      | 5      | 8     | 6     | 8     | 11     | 12     | 14    | 6     |
| Zn    | 110   | 95     | 95     | 86    | 100   | 103   | 117    | 87     | 89    | 107   |
| Cu    | 61    | 54     | 64     | 64    | 53    | 61    | 34     | 60     | 59    | 46    |
| Ni    | 106   | 118    | 79     | 109   | 91    | 96    | 69     | 49     | 73    | 99    |
| La    | 38    | 24     | 20     | 20    | 11    | 37    | 34     | 29     | 24    | 27    |
| Ba    | 353   | 226    | 162    | 129   | 146   | 175   | 332    | 302    | 238   | 180   |
| V     | 299   | 239    | 275    | 233   | 257   | 266   | 271    | 224    | 251   | 280   |
| Ce    | 48    | 33     | 44     | 38    | 36    | 49    | 51     | 45     | 49    | 35    |
| Cr    | 277   | 244    | 186    | 225   | 186   | 193   | 172    | 129    | 137   | 210   |
| Ga    | 22    | 22     | 19     | 19    | 21    | 22    | 20     | 21     | 18    | 18    |

|       | SB7B  | SB7C  | SB7D  | SB7E  | SB7F  | SB7G  | SB7H  | SB7I  | SB7J  | SB7K  |
|-------|-------|-------|-------|-------|-------|-------|-------|-------|-------|-------|
| SiO2  | 46.30 | 46.70 | 46.90 | 47.00 | 46.30 | 67.00 | 60.00 | 45.90 | 66.50 | 54.20 |
| TiO2  | 1.39  | 1.43  | 1.49  | 1.73  | 1.52  | .39   | .84   | 1.34  | .59   | 1.57  |
| Al2O3 | 15.20 | 15.70 | 16.40 | 16.40 | 16.40 | 16.00 | 15.90 | 16.30 | 16.20 | 16.30 |
| Fe2O3 | 12.70 | 11.96 | 11.42 | 10.93 | 10.27 | 2.06  | 3.80  | 10.93 | 2.58  | 8.33  |
| FeO   | 0.00  | 0.00  | 0.00  | 0.00  | 0.00  | 0.00  | 0.00  | 0.00  | 0.00  | 0.00  |
| MnO   | .19   | .20   | .20   | .21   | .17   | .04   | .08   | .19   | .03   | .21   |
| MgO   | 8.54  | 7.59  | 6.70  | 6.97  | 6.00  | 1.02  | 1.75  | 7.67  | .75   | 1.86  |
| CaO   | 9.86  | 9.91  | 9.39  | 8.87  | 11.71 | 1.14  | 7.77  | 10.76 | 1.49  | 4.60  |
| Na2O  | 2.49  | 2.72  | 3.11  | 3.46  | 3.13  | 9.40  | 6.01  | 2.58  | 9.32  | 7.30  |
| K2O   | .48   | .46   | .94   | .59   | .73   | .04   | .11   | .79   | .01   | .64   |
| P2O5  | .14   | .18   | .18   | .22   | .41   | .06   | .11   | .19   | .08   | .58   |
| LOI   | 2.63  | 2.95  | 3.01  | 3.24  | 3.30  | 1.77  | 3.32  | 2.97  | 1.90  | 2.87  |
| Total | 99.92 | 99.80 | 99.74 | 99.62 | 99.94 | 98.92 | 99.69 | 99.62 | 99.45 | 98.46 |
| Pb    | 10    | 2     | 5     | 4     | 3     | 12    | 10    | 0     | 3     | 4     |
| Th    | 1     | 0     | 1     | 1     | 0     | 11    | 8     | 0     | 9     | 2     |
| U     | 1     | 0     | 3     | 0     | 3     | 1     | 4     | 1     | 5     | 5     |
| Rb    | 10    | 8     | 22    | 11    | 13    | 0     | 1     | 13    | 0     | 13    |
| Sr    | 289   | 350   | 432   | 430   | 373   | 19    | 109   | 393   | 18    | 380   |
| Y     | 22    | 22    | 22    | 29    | 22    | 96    | 82    | 23    | 100   | 63    |
| Zr    | 65    | 81    | 76    | 93    | 88    | 816   | 575   | 77    | 781   | 310   |
| Nb    | 9     | 12    | 12    | 14    | 16    | 64    | 60    | 14    | 69    | 45    |
| Zn    | 98    | 96    | 108   | 92    | 82    | 35    | 47    | 81    | 58    | 107   |
| Cu    | 53    | 57    | 46    | 58    | 54    | 78    | 12    | 58    | 11    | 12    |
| Ni    | 133   | 89    | 64    | 49    | 37    | 1     | 7     | 91    | 0     | 1     |
| La    | 18    | 23    | 29    | 37    | 29    | 46    | 47    | 20    | 60    | 55    |
| Ba    | 140   | 172   | 345   | 220   | 195   | 46    | 66    | 252   | 32    | 496   |
| V     | 221   | 241   | 251   | 273   | 236   | 12    | 55    | 231   | 15    | 41    |
| Ce    | 40    | 39    | 42    | 59    | 48    | 104   | 94    | 46    | 112   | 84    |
| Cr    | 278   | 204   | 160   | 134   | 192   | 0     | 0     | 249   | 0     | 0     |
| Ga    | 19    | 19    | 19    | 22    | 21    | 29    | 30    | 19    | 32    | 28    |

|       | SB7L  | SB7M  | SB7N  | SB7D  | SB15A | SB15H | SB15J | SB15K | 26.7.7 | 5.9.79 |
|-------|-------|-------|-------|-------|-------|-------|-------|-------|--------|--------|
| SiO2  | 55.30 | 45.90 | 46.00 | 46.30 | 45.40 | 45.90 | 45.20 | 45.80 | 46.90  | 47.20  |
| TiO2  | 1.30  | 1.61  | 1.72  | 1.55  | 1.43  | 1.38  | 1.38  | 1.47  | 1.98   | 1.52   |
| Al2O3 | 13.90 | 15.50 | 15.70 | 15.90 | 16.30 | 16.00 | 15.20 | 15.20 | 14.30  | 15.70  |
| Fe2O3 | 7.86  | 13.12 | 11.90 | 12.10 | 11.38 | 11.96 | 13.02 | 12.56 | 13.84  | 13.23  |
| FeO   | 0.00  | 0.00  | 0.00  | 0.00  | 0.00  | 0.00  | 0.00  | 0.00  | 0.00   | 0.00   |
| MnO   | .21   | .22   | .20   | .18   | .19   | .18   | .20   | .21   | .17    | .24    |
| MgO   | 3.62  | 6.80  | 6.88  | 6.80  | 7.33  | 6.67  | 6.75  | 6.50  | 6.00   | 6.85   |
| CaO   | 5.62  | 9.94  | 9.47  | 9.71  | 10.47 | 10.47 | 9.88  | 10.84 | 9.00   | 9.65   |
| Na2O  | 6.68  | 2.95  | 3.44  | 2.94  | 2.60  | 2.88  | 2.98  | 2.77  | 3.16   | 2.36   |
| K2O   | .27   | .41   | .54   | .38   | .54   | .52   | .54   | .42   | .37    | .16    |
| P2O5  | .10   | .21   | .32   | .21   | .20   | .21   | .23   | .23   | .27    | .18    |
| LOI   | 3.20  | 2.96  | 2.64  | 2.76  | 3.72  | 3.63  | 3.31  | 3.77  | 3.35   | 3.02   |
| Total | 98.06 | 99.62 | 98.81 | 98.83 | 99.56 | 99.80 | 98.69 | 99.77 | 99.34  | 100.11 |
| Pb    | 11    | 5     | 0     | 6     | 3     | 2     | 7     | 0     | 5      | 3      |
| Th    | 3     | 2     | 4     | 0     | 2     | 0     | 0     | 0     | 3      | 2      |
| U     | 1     | 7     | 0     | 0     | 0     | 3     | 3     | 0     | 1      | 0      |
| Rb    | 6     | 13    | 10    | 7     | 11    | 11    | 13    | 4     | 7      | 1      |
| Sr    | 176   | 285   | 437   | 335   | 353   | 336   | 327   | 319   | 322    | 241    |
| Y     | 119   | 26    | 28    | 22    | 21    | 22    | 24    | 27    | 32     | 30     |
| Zr    | 444   | 73    | 126   | 79    | 76    | 78    | 78    | 75    | 104    | 80     |
| Nb    | 51    | 10    | 24    | 11    | 16    | 14    | 15    | 16    | 0      | 0      |
| Zn    | 90    | 105   | 95    | 98    | 88    | 95    | 95    | 97    | 99     | 103    |
| Cu    | 12    | 53    | 53    | 56    | 80    | 59    | 57    | 70    | 0      | 0      |
| Ni    | 36    | 78    | 78    | 71    | 100   | 58    | 42    | 40    | 14     | 73     |
| La    | 50    | 37    | 38    | 28    | 27    | 32    | 34    | 24    | 0      | 0      |
| Ba    | 184   | 201   | 229   | 162   | 204   | 236   | 270   | 176   | 0      | 0      |
| V     | 148   | 270   | 281   | 253   | 214   | 245   | 256   | 292   | 0      | 0      |
| Ce    | 88    | 38    | 68    | 55    | 44    | 47    | 54    | 49    | 0      | 0      |
| Cr    | 53    | 147   | 170   | 112   | 149   | 116   | 103   | 106   | 0      | 0      |
| Ga    | 21    | 19    | 21    | 17    | 20    | 19    | 16    | 18    | 21     | 21     |

26.7.7

|       |       |
|-------|-------|
| SiO2  | 47.30 |
| TiO2  | 1.43  |
| Al2O3 | 15.70 |
| Fe2O3 | 12.97 |
| FeO   | 0.00  |
| MnO   | .20   |
| MgO   | 6.85  |
| CaO   | 9.88  |
| Na2O  | 2.39  |
| K2O   | .16   |
| P2O5  | .16   |
| LOI   | 2.93  |
| Total | 99.97 |

|    |     |
|----|-----|
| Pb | 2   |
| Th | 1   |
| U  | 0   |
| Rb | 0   |
| Sr | 255 |
| Y  | 28  |
| Zr | 88  |
| Nb | 0   |
| Zn | 100 |
| Cu | 0   |
| Ni | 79  |
| La | 0   |
| Ba | 0   |
| V  | 0   |
| Ce | 0   |
| Cr | 0   |
| Ga | 22  |

|    | SB7R | SB12 | SB13 | SB14 | SB15C | SB15E | SB15F | SB16A | SB16B |
|----|------|------|------|------|-------|-------|-------|-------|-------|
| Pb | 0    | 0    | 11   | 0    | 7     | 4     | 1     | 9     | 9     |
| Th | 0    | 0    | 0    | 0    | 0     | 9     | 0     | 1     | 0     |
| U  | 1    | 4    | 5    | 0    | 0     | 0     | 1     | 0     | 0     |
| Rb | 0    | 9    | 16   | 8    | 17    | 0     | 13    | 11    | 9     |
| Sr | 306  | 269  | 411  | 293  | 408   | 64    | 340   | 320   | 304   |
| Y  | 26   | 26   | 22   | 24   | 23    | 79    | 20    | 29    | 30    |
| Zr | 30   | 72   | 87   | 73   | 74    | 512   | 71    | 83    | 95    |
| Nb | 14   | 13   | 17   | 14   | 15    | 78    | 16    | 19    | 20    |
| Zn | 76   | 94   | 101  | 90   | 86    | 37    | 91    | 98    | 100   |
| Cu | 57   | 57   | 50   | 56   | 54    | 6     | 52    | 55    | 55    |
| Ni | 89   | 76   | 92   | 70   | 73    | 3     | 74    | 34    | 36    |
| La | 38   | 28   | 33   | 25   | 41    | 43    | 29    | 38    | 32    |
| Ba | 138  | 167  | 362  | 224  | 290   | 38    | 244   | 220   | 245   |
| V  | 287  | 231  | 254  | 255  | 245   | 19    | 257   | 290   | 289   |
| Ce | 56   | 35   | 48   | 48   | 56    | 88    | 43    | 58    | 44    |
| Cr | 257  | 170  | 221  | 159  | 139   | 0     | 231   | 91    | 90    |
| Ga | 17   | 18   | 21   | 18   | 20    | 28    | 18    | 19    | 20    |

|    | SB17 | SB18 | SB19 | SB20 | SB21 | SB22 | SB24A | SB48A | SB48C |
|----|------|------|------|------|------|------|-------|-------|-------|
| Pb | 0    | 4    | 6    | 1    | 2    | 3    | 14    | 9     | 10    |
| Th | 0    | 0    | 2    | 0    | 6    | 0    | 10    | 0     | 0     |
| U  | 5    | 0    | 5    | 0    | 3    | 0    | 2     | 4     | 0     |
| Rb | 7    | 19   | 10   | 10   | 0    | 8    | 39    | 9     | 12    |
| Sr | 66   | 384  | 318  | 328  | 46   | 335  | 158   | 684   | 380   |
| Y  | 61   | 20   | 26   | 25   | 77   | 24   | 36    | 19    | 21    |
| Zr | 273  | 69   | 81   | 75   | 564  | 95   | 143   | 76    | 75    |
| Nb | 42   | 15   | 16   | 16   | 77   | 14   | 14    | 17    | 17    |
| Zn | 31   | 77   | 89   | 82   | 31   | 96   | 87    | 106   | 79    |
| Cu | 0    | 32   | 53   | 53   | 17   | 46   | 15    | 59    | 47    |
| Ni | 0    | 72   | 59   | 57   | 0    | 73   | 34    | 212   | 61    |
| La | 53   | 33   | 33   | 32   | 44   | 38   | 43    | 41    | 35    |
| Ba | 40   | 411  | 268  | 326  | 52   | 240  | 571   | 366   | 366   |
| V  | 33   | 237  | 249  | 221  | 10   | 249  | 98    | 220   | 216   |
| Ce | 66   | 51   | 45   | 53   | 91   | 51   | 85    | 54    | 52    |
| Cr | 0    | 140  | 113  | 143  | 0    | 159  | 57    | 433   | 133   |
| Ga | 38   | 16   | 19   | 17   | 29   | 20   | 19    | 22    | 19    |

|    | SB48D | SB48F | SB48G | SB48I | SB48J | SB48L | SB50A | SB50B1 | SB50B2 |
|----|-------|-------|-------|-------|-------|-------|-------|--------|--------|
| Pb | 0     | 1     | 0     | 0     | 1     | 0     | 0     | 0      | 3      |
| Th | 1     | 0     | 0     | 0     | 0     | 4     | 0     | 0      | 0      |
| U  | 0     | 2     | 0     | 0     | 2     | 1     | 8     | 5      | 0      |
| Rb | 8     | 1     | 4     | 12    | 17    | 2     | 6     | 7      | 0      |
| Sr | 516   | 130   | 269   | 489   | 739   | 90    | 327   | 288    | 295    |
| Y  | 23    | 29    | 52    | 17    | 23    | 27    | 23    | 24     | 26     |
| Zr | 83    | 97    | 282   | 88    | 85    | 114   | 98    | 92     | 86     |
| Nb | 17    | 21    | 53    | 18    | 17    | 23    | 18    | 10     | 15     |
| Zn | 91    | 58    | 112   | 83    | 86    | 98    | 90    | 89     | 91     |
| Cu | 49    | 46    | 17    | 54    | 53    | 39    | 53    | 66     | 68     |
| Ni | 71    | 40    | 3     | 53    | 78    | 22    | 74    | 99     | 93     |
| La | 44    | 38    | 51    | 31    | 29    | 37    | 41    | 27     | 33     |
| Ba | 241   | 70    | 196   | 208   | 2866  | 66    | 178   | 212    | 156    |
| V  | 245   | 254   | 176   | 206   | 246   | 290   | 264   | 260    | 263    |
| Ce | 48    | 59    | 86    | 51    | 60    | 61    | 59    | 51     | 50     |
| Cr | 171   | 105   | 0     | 135   | 238   | 67    | 179   | 161    | 256    |
| Ga | 20    | 21    | 23    | 19    | 17    | 19    | 20    | 19     | 21     |

|    | SB50C | SB50D | SB58F | SB58J | SB58Q | SB60C | SB60E | SB60F | SB60G | SB60H |
|----|-------|-------|-------|-------|-------|-------|-------|-------|-------|-------|
| Pb | 1     | 7     | 0     | 5     | 1     | 9     | 5     | 7     | 0     | 2     |
| Th | 0     | 3     | 0     | 8     | 0     | 4     | 0     | 8     | 0     | 0     |
| U  | 0     | 3     | 0     | 0     | 1     | 3     | 0     | 2     | 0     | 0     |
| Rb | 13    | 8     | 7     | 0     | 15    | 14    | 15    | 6     | 4     | 7     |
| Sr | 336   | 384   | 174   | 83    | 289   | 431   | 331   | 164   | 153   | 141   |
| Y  | 26    | 23    | 14    | 82    | 20    | 26    | 15    | 12    | 9     | 12    |
| Zr | 79    | 101   | 45    | 497   | 61    | 115   | 78    | 37    | 30    | 34    |
| Nb | 11    | 16    | 8     | 75    | 11    | 30    | 14    | 8     | 6     | 8     |
| Zn | 81    | 89    | 86    | 60    | 55    | 99    | 84    | 86    | 84    | 88    |
| Cu | 58    | 62    | 62    | 21    | 47    | 47    | 83    | 45    | 31    | 39    |
| Ni | 98    | 63    | 538   | 0     | 219   | 195   | 386   | 730   | 746   | 823   |
| La | 23    | 24    | 20    | 0     | 23    | 40    | 37    | 17    | 29    | 25    |
| Ba | 392   | 319   | 126   | 0     | 237   | 553   | 265   | 95    | 103   | 91    |
| V  | 253   | 272   | 180   | 0     | 200   | 260   | 192   | 146   | 162   | 158   |
| Ce | 40    | 42    | 39    | 0     | 43    | 71    | 41    | 27    | 28    | 28    |
| Cr | 224   | 160   | 744   | 0     | 382   | 317   | 504   | 1514  | 1580  | 1103  |
| Ga | 20    | 19    | 11    | 0     | 20    | 20    | 13    | 9     | 8     | 9     |



CAPE ST. MARY'S DIKE ANALYSES

412

| Samples Analyzed For<br>Major and Trace Elements | Trace Elements  | Locations      |
|--|-----------------|----------------|
| SB35A and SB52B                                  | SB52A           | Cuslette Cove  |
| SB56A and SB56G                                  | SB56C and SB56D | Patrick's Cove |
| SB63A and SB64C                                  | SB63B           | Branch Cove    |
| SB65A to SB66A                                   | SB65B and SB65C | Patrick's Cove |

SB35A, 52A, B, 56A, C, D, 63A, B, 64C, 65B, C. Mafic dikes. Secondary minerals: Albite, chlorite, sphene, Fe-Ti oxides. Texture: Fine-grained, varying percentages of plagioclase phenocrysts often altered to albite and sometimes calcite. Original textures often obscured as a result of recrystallization.

SB56B, G, 65A, D, 66A. Mafic dikes. Primary minerals: augite, sometimes plagioclase (SB56G, 66A). Secondary minerals: albite chlorite, actinolite, sphene, Fe-Ti oxides, calcite. Texture: Fine-grained, subophitic, feldspar porphyric (SB56B, 56G, 65D).

|       | SB35A | SB52B | SB56A | SB56B | SB56G | SB63A | SB64C | SB65A | SB65D | SB66A |
|-------|-------|-------|-------|-------|-------|-------|-------|-------|-------|-------|
| SiO2  | 44.90 | 44.60 | 44.10 | 45.20 | 46.50 | 42.40 | 43.30 | 43.80 | 44.20 | 43.40 |
| TiO2  | 2.06  | 1.37  | 1.64  | 1.20  | 1.75  | 1.40  | 2.16  | 1.65  | 2.61  | 1.26  |
| Al2O3 | 15.80 | 15.00 | 14.10 | 16.10 | 17.10 | 14.40 | 13.00 | 14.40 | 15.40 | 14.50 |
| Fe2O3 | 11.76 | 13.34 | 11.73 | 12.92 | 10.97 | 11.24 | 12.86 | 11.85 | 14.57 | 14.30 |
| FeO   | 0.00  | 0.00  | 0.00  | 0.00  | 0.00  | 0.00  | 0.00  | 0.00  | 0.00  | 0.00  |
| MnO   | .21   | .28   | .24   | .20   | .17   | .38   | .27   | .32   | .24   | .21   |
| MgO   | 7.00  | 8.58  | 9.08  | 9.25  | 6.17  | 8.33  | 9.50  | 8.42  | 6.00  | 11.67 |
| CaO   | 6.27  | 7.59  | 7.97  | 6.27  | 7.37  | 7.37  | 5.95  | 7.86  | 7.14  | 8.96  |
| Na2O  | 3.87  | 1.88  | 2.26  | 2.18  | 3.64  | 2.35  | 1.31  | 2.71  | 3.41  | 1.34  |
| K2O   | .31   | .70   | .73   | .60   | .46   | .86   | .17   | .21   | .27   | .06   |
| P2O5  | .70   | .21   | .48   | .30   | .53   | .33   | .45   | .53   | .67   | .20   |
| LOI   | 6.19  | 6.17  | 7.49  | 4.34  | 3.92  | 10.70 | 9.98  | 7.37  | 4.79  | 4.08  |
| Total | 99.07 | 99.72 | 99.82 | 98.56 | 98.58 | 99.76 | 98.95 | 99.12 | 99.30 | 99.98 |
| Pb    | 6     | 5     | 6     | 6     | 4     | 3     | 7     | 13    | 1     | 2     |
| Th    | 0     | 0     | 0     | 0     | 0     | 0     | 0     | 0     | 0     | 0     |
| U     | 3     | 0     | 0     | 3     | 1     | 5     | 2     | 0     | 1     | 0     |
| Rb    | 3     | 19    | 9     | 7     | 4     | 22    | 9     | 3     | 2     | 0     |
| Sr    | 923   | 244   | 862   | 395   | 650   | 294   | 169   | 1087  | 682   | 245   |
| Y     | 33    | 23    | 26    | 30    | 36    | 19    | 28    | 26    | 41    | 23    |
| Zr    | 269   | 72    | 153   | 93    | 157   | 116   | 161   | 158   | 173   | 60    |
| Nb    | 62    | 11    | 43    | 23    | 10    | 30    | 43    | 42    | 16    | 9     |
| Zn    | 91    | 114   | 80    | 88    | 99    | 82    | 105   | 86    | 115   | 101   |
| Cu    | 32    | 62    | 58    | 69    | 51    | 47    | 45    | 56    | 52    | 72    |
| Ni    | 99    | 124   | 182   | 185   | 66    | 149   | 248   | 185   | 62    | 287   |
| La    | 58    | 18    | 44    | 23    | 33    | 27    | 52    | 39    | 40    | 17    |
| Ba    | 532   | 281   | 2037  | 1610  | 195   | 384   | 161   | 1223  | 191   | 83    |
| V     | 200   | 286   | 215   | 276   | 218   | 238   | 307   | 222   | 319   | 222   |
| Ce    | 106   | 46    | 73    | 60    | 68    | 69    | 96    | 69    | 94    | 29    |
| Cr    | 156   | 307   | 249   | 248   | 2     | 186   | 305   | 248   | 4     | 352   |
| Ga    | 20    | 23    | 18    | 19    | 20    | 18    | 23    | 18    | 23    | 18    |

|    | SB52A | SB56C | SB56D | SB63B | SB65B | SB65C |
|----|-------|-------|-------|-------|-------|-------|
| Pb | 5     | 8     | 11    | 7     | 12    | 1     |
| Th | 0     | 0     | 0     | 3     | 4     | 4     |
| U  | 0     | 0     | 3     | 5     | 4     | 3     |
| Rb | 10    | 4     | 6     | 10    | 7     | 1     |
| Sr | 514   | 692   | 368   | 237   | 658   | 581   |
| Y  | 25    | 35    | 27    | 26    | 33    | 32    |
| Zr | 88    | 142   | 100   | 117   | 211   | 174   |
| Nb | 15    | 13    | 23    | 26    | 47    | 48    |
| Zn | 91    | 202   | 111   | 86    | 93    | 108   |
| Cu | 53    | 55    | 72    | 136   | 35    | 59    |
| Ni | 77    | 118   | 188   | 204   | 25    | 196   |
| La | 15    | 30    | 19    | 40    | 58    | 42    |
| Ba | 3003  | 170   | 185   | 152   | 257   | 223   |
| V  | 269   | 234   | 318   | 275   | 214   | 254   |
| Ce | 61    | 66    | 57    | 68    | 119   | 75    |
| Cr | 132   | 78    | 274   | 246   | 1     | 346   |
| Ga | 20    | 20    | 19    | 17    | 19    | 18    |

Samples labelled BHR are from the Beaver Harbour area whereas those labelled GWD are from the Long Reach area.

| Samples Analyzed For<br>Major and Trace Elements  | Trace Elements                            | Locations                                       |
|---|---|---|
| GWD4, GWD5 etc. to GWD10<br>GWD11 and GWD12       | -<br>-                                    | Browns Flat<br>Road to Beulah<br>Camp           |
| GWD20 to GWD23<br>GWD14 to GWD17<br>BHR1 to BHR25 | GWD21 to GWD26<br>GWD15<br>BHR2 to BHR21A | Greenwich Hill<br>Beulah Camp<br>Beaver Harbour |

GWD4, 5, 6, 7, 9, 10. Metabasalt. Primary minerals: Clinopyroxene (sample GWD9). Secondary minerals: Albite, chlorite, epidote, actinolite, Fe-Ti oxides, hematite. Texture: Aphanitic, slightly feldspar porphyritic. GWD7 slightly vesicular. Comments: Feldspar = 60% in most samples.

GWD8, 11, 12. Metabasalt. Primary minerals: Clinopyroxene (samples GWD8, 12). Secondary minerals: Albite, chlorite, epidote, actinolite, Fe-Ti oxides, hematite. Texture: Aphanitic, large augite phenocrysts and glomeroporphyritic texture in GWD8. Comments: Calcite = 10% of GWD11.

GWD20, 21, 22, 23, 24, 25. Metabasalt. Primary minerals: Clinopyroxene. Secondary minerals: Albite, chlorite, epidote, actinolite, prehnite, Fe-Ti oxides. Texture: Aphanitic, small augite phenocrysts (< 1%).

416

GWD26. Metadiabase dike. Primary minerals: Clinopyroxene. Secondary minerals: Albite, chlorite, epidote, actinolite, prehnite, Fe-Ti oxides. Texture: Aphanitic, feldspar (now albite) porphyric.

GWD14, 15, 16. Felsic pyroclastic rock. Minerals: Albite, quartz, hematite, prehnite. Texture: Lapilli tuff, vesicular clasts flattened, clasts feldspar porphyric, matrix shards (recrystallized) = 35%. Hematite outlines clasts.

GWD17. Felsic pyroclastic rock. Comments: Same as GWD14, 15 etc. above except quartz grains more apparent, and fine grained matrix = 65%.

BHR1, 2, 3, 4, 5, 20, 21A, 21B, 22 23. Metalapilli tuff. Minerals: Albite, hematite, calcite, chlorite, actinolite, sphene. Texture: Lapilli clasts surrounded by hematite-rich ash. Comments: Clasts consist largely of hematite with microphenocrysts of feldspar (albite). Clasts are vesicular in BHR1 and 2 but non-vesicular in remaining samples. Samples BHR21A and 21B finer grained, tending to tuffs. Sample BHR20 shows extremely high calcite and higher chlorite content than other samples.

BHR8, 9, 10, 11, 12A, 12B, 14. Metalapilli tuff. Minerals: Albite, chlorite, actinolite, calcite. Texture: Lapilli clasts surrounded by chlorite-rich ash. Clasts consist largely of chlorite and phenocrysts of feldspar

(albite). Large phenocrysts may show zoning.

BHR15. Metalapilli tuff. Minerals: Albite, chlorite, calcite. Texture: Feldspar rich, fine-grained tuff with broken feldspar phenocrysts.

BHR24, 25. Metabasalt. Minerals: Albite, chlorite, clacite. Texture: Aphanitic, feldspar porphyric. Comments: Only samples of the flow unit.

|       | GWD4  | GWD5   | GWD6  | GWD7  | GWD8   | GWD9  | GWD10 | GWD11 | GWD12 | GWD20 |
|-------|-------|--------|-------|-------|--------|-------|-------|-------|-------|-------|
| SiO2  | 52.00 | 44.20  | 41.90 | 43.30 | 50.70  | 47.20 | 47.10 | 43.70 | 47.90 | 48.20 |
| TiO2  | 2.10  | 2.40   | 2.59  | 2.86  | .75    | 2.36  | 1.98  | .47   | .66   | 1.05  |
| Al2O3 | 12.70 | 14.20  | 13.10 | 13.70 | 16.20  | 12.80 | 13.70 | 15.90 | 17.00 | 15.50 |
| Fe2O3 | 15.72 | 16.04  | 17.56 | 18.54 | 8.35   | 17.24 | 15.96 | 8.21  | 9.57  | 9.50  |
| FeO   | 0.00  | 0.00   | 0.00  | 0.00  | 0.00   | 0.00  | 0.00  | 0.00  | 0.00  | 0.00  |
| MnO   | .11   | .30    | .34   | .27   | .28    | .28   | .24   | .42   | .21   | .16   |
| MgO   | 1.55  | 7.67   | 7.00  | 6.75  | 8.50   | 6.33  | 6.67  | 6.83  | 7.83  | 9.42  |
| CaO   | 4.65  | 4.82   | 5.71  | 4.69  | 7.60   | 5.89  | 4.06  | 8.51  | 9.20  | 10.29 |
| Na2O  | 6.27  | 4.31   | 3.71  | 3.45  | 3.17   | 4.07  | 2.07  | 4.93  | 3.44  | 1.87  |
| K2O   | .11   | .08    | .20   | .86   | .16    | .42   | 3.19  | .14   | .01   | .32   |
| P2O5  | .34   | .41    | .41   | .46   | .11    | .33   | .32   | .15   | .14   | .09   |
| LOI   | 2.61  | 5.77   | 6.97  | 3.72  | 4.50   | 2.59  | 3.70  | 9.85  | 3.76  | 2.90  |
| Total | 98.16 | 100.20 | 99.49 | 98.60 | 100.32 | 99.51 | 98.99 | 99.11 | 99.72 | 99.30 |
| Pb    | 10    | 13     | 17    | 10    | 0      | 9     | 15    | 5     | 1     | 5     |
| Th    | 1     | 0      | 0     | 0     | 0      | 2     | 1     | 0     | 2     | 0     |
| U     | 0     | 5      | 1     | 4     | 0      | 9     | 7     | 0     | 0     | 2     |
| Rb    | 4     | 7      | 11    | 18    | 3      | 14    | 70    | 2     | 1     | 6     |
| Sr    | 135   | 92     | 129   | 184   | 344    | 323   | 171   | 217   | 327   | 278   |
| Y     | 64    | 66     | 65    | 73    | 22     | 66    | 70    | 17    | 17    | 16    |
| Zr    | 141   | 154    | 166   | 185   | 54     | 149   | 153   | 48    | 49    | 43    |
| Nb    | 7     | 7      | 9     | 8     | 3      | 8     | 8     | 4     | 3     | 3     |
| Zn    | 72    | 179    | 163   | 230   | 81     | 199   | 155   | 82    | 76    | 72    |
| Cu    | 0     | 66     | 9     | 34    | 17     | 46    | 66    | 47    | 10    | 42    |
| Ni    | 58    | 63     | 57    | 83    | 69     | 50    | 46    | 54    | 63    | 124   |
| La    | 45    | 44     | 54    | 49    | 18     | 45    | 54    | 13    | 31    | 31    |
| Ba    | 99    | 121    | 138   | 454   | 111    | 346   | 1719  | 149   | 82    | 142   |
| V     | 554   | 530    | 585   | 539   | 222    | 509   | 474   | 250   | 253   | 229   |
| Ce    | 76    | 73     | 85    | 95    | 25     | 88    | 74    | 27    | 35    | 28    |
| Cr    | 38    | 50     | 40    | 61    | 308    | 38    | 33    | 175   | 173   | 323   |
| Ga    | 18    | 23     | 24    | 24    | 17     | 21    | 21    | 13    | 16    | 12    |

|       | GWD23 | GWD14 | GWD16 | GWD17 | BHR1  | BHR3  | BHR5BH | BHR8  | BHR12B | BHR15 |
|-------|-------|-------|-------|-------|-------|-------|--------|-------|--------|-------|
| SiO2  | 48.20 | 64.20 | 69.10 | 73.10 | 47.40 | 51.70 | 43.00  | 55.10 | 54.50  | 38.00 |
| TiO2  | 1.05  | .59   | .40   | .32   | 2.38  | 2.08  | 1.40   | .68   | .58    | 1.52  |
| Al2O3 | 16.00 | 13.60 | 14.70 | 13.80 | 17.40 | 19.80 | 13.60  | 20.00 | 20.80  | 14.70 |
| Fe2O3 | 9.43  | 8.96  | 3.49  | 2.04  | 12.50 | 12.36 | 10.86  | 6.11  | 7.53   | 9.53  |
| FeO   | 0.00  | 0.00  | 0.00  | 0.00  | 0.00  | 0.00  | 0.00   | 0.00  | 0.00   | 0.00  |
| MnO   | .17   | .06   | .06   | .06   | .14   | .03   | .11    | .04   | .16    | .20   |
| MgO   | 9.58  | 2.51  | 1.19  | 1.19  | 2.77  | 1.31  | 1.51   | 4.04  | 2.85   | 2.85  |
| CaO   | 10.29 | .60   | 2.23  | .97   | 4.72  | 1.14  | 12.06  | 1.30  | 1.75   | 13.45 |
| Na2O  | 1.93  | .68   | 2.25  | 2.93  | 1.96  | 5.35  | 4.29   | 6.17  | 6.62   | 4.02  |
| K2O   | .28   | 3.65  | 2.42  | 1.74  | 2.99  | 2.54  | 1.47   | 1.49  | 1.29   | .91   |
| P2O5  | .10   | .25   | .12   | .05   | .42   | .12   | .57    | .23   | .08    | .76   |
| LOI   | 2.58  | 3.19  | 3.26  | 2.00  | 7.23  | 3.12  | 10.92  | 3.43  | 4.19   | 13.79 |
| Total | 99.61 | 98.29 | 99.22 | 98.20 | 99.91 | 99.55 | 99.79  | 98.59 | 100.35 | 99.73 |
| Pb    | 3     | 17    | 6     | 13    | 0     | 14    | 11     | 3     | 0      | 0     |
| Th    | 0     | 20    | 1     | 7     | 1     | 4     | 3      | 1     | 0      | 0     |
| U     | 0     | 5     | 0     | 0     | 2     | 4     | 3      | 0     | 0      | 0     |
| Rb    | 6     | 144   | 111   | 67    | 89    | 73    | 41     | 59    | 37     | 25    |
| Sr    | 213   | 19    | 120   | 228   | 109   | 274   | 230    | 434   | 465    | 213   |
| Y     | 12    | 60    | 43    | 50    | 46    | 28    | 51     | 15    | 6      | 46    |
| Zr    | 47    | 166   | 150   | 143   | 223   | 296   | 209    | 129   | 81     | 170   |
| Nb    | 4     | 31    | 8     | 10    | 12    | 16    | 10     | 18    | 7      | 9     |
| Zn    | 70    | 86    | 76    | 51    | 104   | 87    | 76     | 94    | 74     | 143   |
| Cu    | 43    | 32    | 17    | 13    | 0     | 0     | 0      | 8     | 35     | 0     |
| Ni    | 125   | 18    | 1     | 2     | 56    | 0     | 0      | 58    | 48     | 4     |
| La    | 32    | 51    | 35    | 35    | 50    | 48    | 40     | 36    | 20     | 39    |
| Ba    | 149   | 516   | 551   | 748   | 489   | 327   | 148    | 363   | 336    | 78    |
| V     | 204   | 65    | 37    | 13    | 84    | 159   | 89     | 138   | 131    | 132   |
| Ce    | 26    | 64    | 54    | 63    | 77    | 92    | 58     | 46    | 25     | 62    |
| Cr    | 311   | 0     | 0     | 0     | 57    | 0     | 0      | 27    | 20     | 0     |
| Ga    | 13    | 17    | 16    | 19    | 23    | 29    | 22     | 28    | 24     | 21    |



|       | BHR20 | BHR23 | BHR24 | BHR25 |
|-------|-------|-------|-------|-------|
| SiO2  | 44.40 | 51.70 | 52.60 | 54.20 |
| TiO2  | .76   | 2.73  | .55   | .55   |
| Al2O3 | 8.22  | 17.00 | 18.20 | 18.50 |
| Fe2O3 | 4.75  | 15.60 | 6.08  | 6.20  |
| FeO   | 0.00  | 0.00  | 0.00  | 0.00  |
| MnO   | .09   | .02   | .07   | .11   |
| MgO   | 1.82  | 2.05  | 3.96  | 5.51  |
| CaO   | 19.25 | 1.04  | 3.97  | 3.75  |
| Na2O  | .76   | 1.89  | 7.22  | 5.27  |
| K2O   | 1.92  | 3.67  | .13   | .49   |
| P2O5  | .10   | .15   | .27   | .18   |
| LOI   | 17.91 | 3.99  | 5.04  | 5.20  |
| Total | 99.98 | 99.84 | 98.09 | 99.96 |
| Pb    | 1     | 2     | 6     | 2     |
| Th    | 0     | 1     | 4     | 2     |
| U     | 0     | 0     | 0     | 0     |
| Rb    | 55    | 99    | 0     | 11    |
| Sr    | 116   | 58    | 631   | 995   |
| Y     | 15    | 29    | 13    | 21    |
| Zr    | 70    | 245   | 121   | 134   |
| Nb    | 2     | 13    | 14    | 14    |
| Zn    | 49    | 107   | 75    | 81    |
| Cu    | 1     | 0     | 10    | 16    |
| Ni    | 34    | 22    | 44    | 40    |
| La    | 25    | 43    | 30    | 34    |
| Ba    | 175   | 601   | 125   | 175   |
| V     | 41    | 135   | 120   | 116   |
| Ce    | 22    | 91    | 47    | 49    |
| Cr    | 20    | 2     | 25    | 22    |
| Ga    | 9     | 28    | 20    | 24    |

|    | GWD21 | GWD22 | GWD24 | GWD25 | GWD26 | GWD15 | BHR2 | BHR4 | BHR9 |
|----|-------|-------|-------|-------|-------|-------|------|------|------|
| Pb | 1     | 0     | 6     | 0     | 14    | 23    | 0    | 0    | 0    |
| Th | 5     | 0     | 5     | 0     | 1     | 10    | 0    | 0    | 2    |
| U  | 3     | 0     | 0     | 0     | 2     | 9     | 0    | 1    | 0    |
| Rb | 6     | 8     | 2     | 3     | 4     | 91    | 43   | 17   | 21   |
| Sr | 231   | 368   | 188   | 192   | 247   | 101   | 176  | 223  | 401  |
| Y  | 17    | 14    | 18    | 14    | 37    | 45    | 12   | 64   | 18   |
| Zr | 43    | 43    | 46    | 41    | 138   | 159   | 83   | 153  | 123  |
| Nb | 3     | 2     | 3     | 3     | 8     | 10    | 2    | 9    | 15   |
| Zn | 69    | 71    | 73    | 73    | 92    | 78    | 53   | 88   | 75   |
| Cu | 32    | 61    | 22    | 148   | 51    | 41    | 0    | 0    | 17   |
| Ni | 117   | 125   | 125   | 134   | 33    | 37    | 32   | 0    | 42   |
| La | 15    | 25    | 13    | 16    | 44    | 36    | 27   | 30   | 38   |
| Ba | 129   | 146   | 120   | 111   | 123   | 277   | 138  | 74   | 144  |
| V  | 221   | 227   | 233   | 236   | 332   | 175   | 55   | 64   | 127  |
| Ce | 22    | 26    | 30    | 22    | 58    | 57    | 26   | 52   | 47   |
| Cr | 322   | 310   | 341   | 381   | 125   | 67    | 17   | 0    | 27   |
| Ga | 13    | 15    | 13    | 16    | 20    | 16    | 11   | 16   | 22   |

|    | BHR10 | BHR11 | BHR12A | BHR14 | BHR21A        | BHR21B | BHR22 |
|----|-------|-------|--------|-------|---------------|--------|-------|
| Pb | 0     | 0     | 6      | 0     | 3             | 0      | 0     |
| Th | 0     | 0     | 0      | 6     | 0             | 0      | 0     |
| U  | 0     | 0     | 0      | 0     | 0             | 0      | 0     |
| Rb | 27    | 13    | 15     | 20    | <del>77</del> | 24     | 51    |
| Sr | 412   | 319   | 421    | 198   | 101           | 101    | 131   |
| Y  | 11    | 12    | 12     | 24    | 51            | 53     | 20    |
| Zr | 130   | 108   | 49     | 118   | 248           | 178    | 90    |
| Nb | 17    | 15    | 5      | 7     | 11            | 8      | 4     |
| Zn | 63    | 79    | 53     | 89    | 116           | 192    | 48    |
| Cu | 52    | 3     | 13     | 71    | 0             | 2      | 0     |
| Ni | 24    | 36    | 22     | 62    | 18            | 10     | 31    |
| La | 34    | 31    | 25     | 33    | 44            | 38     | 28    |
| Ba | 369   | 184   | 134    | 92    | 251           | 102    | 150   |
| V  | 117   | 70    | 64     | 169   | 330           | 295    | 56    |
| Ce | 57    | 43    | 21     | 37    | 93            | 59     | 26    |
| Cr | 26    | 13    | 11     | 52    | 0             | 0      | 26    |
| Ga | 23    | 19    | 8      | 11    | 29            | 14     | 11    |

APPENDIX C MINERAL ANALYSES

Mineral analyses collected for the study are given in this appendix. Most of the data are pyroxene analyses but biotite, olivine, amphibole, and feldspar data are presented for the Cape St. Mary's sills. Analytical procedures are discussed in Appendix A.

CAMBRIAN EXTRUSIVE ROCKS, CAPE ST. MARY'S

| Location   | Sample Number | Analysis Numbers |
|------------|---------------|------------------|
| Chapel Arm | LC15A         | 1 to 18          |
|            | LC15B         | 19 to 27         |
|            | LC15C         | 28 to 37         |
|            | LC15D         | 38 to 48         |
| Cape Dog   | PL38C         | 49 to 57         |
|            | PL34C         | 58 to 64         |
|            | PL31          | 65 to 73         |
| Hay Cove   | SB37B2        | 74 to 94         |

|       | 1     | 2     | 3     | 4     | 5     | 6     | 7     | 8     | 9     | 10    |
|-------|-------|-------|-------|-------|-------|-------|-------|-------|-------|-------|
| SiO2  | 44.18 | 47.36 | 44.63 | 46.45 | 50.18 | 50.72 | 48.77 | 48.37 | 50.14 | 50.02 |
| TiO2  | 4.19  | 2.80  | 4.05  | 2.63  | 1.55  | 1.41  | 2.07  | 2.45  | 1.71  | 1.70  |
| Al2O3 | 7.00  | 4.27  | 7.46  | 4.26  | 2.63  | 2.40  | 4.44  | 4.94  | 3.88  | 3.95  |
| Cr2O3 | 0.00  | 0.00  | 0.00  | 0.00  | 0.00  | .10   | .20   | 0.00  | .50   | .60   |
| FeO   | 10.72 | 11.71 | 10.67 | 11.02 | 8.10  | 7.00  | 7.56  | 7.67  | 6.68  | 6.96  |
| MnO   | .14   | .21   | .11   | .21   | .14   | .11   | .11   | .14   | .13   | .08   |
| MgO   | 11.23 | 11.34 | 11.54 | 12.43 | 15.02 | 15.22 | 14.09 | 13.45 | 14.68 | 14.36 |
| NiO   | 0.00  | 0.00  | 0.00  | 0.00  | 0.00  | 0.00  | 0.00  | 0.00  | 0.00  | 0.00  |
| CaO   | 20.63 | 21.00 | 20.55 | 20.67 | 20.68 | 21.56 | 21.33 | 21.66 | 21.69 | 21.68 |
| Na2O  | .59   | .48   | .57   | .53   | .26   | .20   | .40   | .36   | .30   | .35   |
| K2O   | 0.00  | .02   | 0.00  | 0.00  | .01   | .02   | .01   | 0.00  | 0.00  | 0.00  |
| Total | 98.75 | 99.23 | 99.63 | 98.20 | 98.61 | 98.55 | 98.98 | 99.07 | 99.71 | 99.72 |

|       |       |       |       |       |       |       |       |       |       |       |
|-------|-------|-------|-------|-------|-------|-------|-------|-------|-------|-------|
| Si    | 1.704 | 1.818 | 1.702 | 1.798 | 1.893 | 1.907 | 1.836 | 1.822 | 1.864 | 1.862 |
| AlIV  | .296  | .182  | .298  | .194  | .107  | .093  | .164  | .178  | .136  | .138  |
| AlVI  | .023  | .011  | .037  | 0.000 | .010  | .014  | .033  | .041  | .034  | .036  |
| Ti    | .122  | .081  | .116  | .077  | .044  | .034  | .059  | .069  | .048  | .048  |
| Cr    | 0.000 | 0.000 | 0.000 | 0.000 | 0.000 | .003  | .006  | 0.000 | .015  | .018  |
| Fe    | .346  | .376  | .340  | .357  | .256  | .220  | .238  | .242  | .208  | .217  |
| Mn    | .005  | .007  | .004  | .007  | .004  | .004  | .004  | .004  | .004  | .003  |
| Mg    | .646  | .649  | .656  | .717  | .845  | .853  | .790  | .755  | .813  | .797  |
| Ni    | 0.000 | 0.000 | 0.000 | 0.000 | 0.000 | 0.000 | 0.000 | 0.000 | 0.000 | 0.000 |
| Ca    | .853  | .864  | .840  | .857  | .836  | .869  | .860  | .874  | .864  | .865  |
| Na    | .044  | .036  | .042  | .040  | .019  | .015  | .029  | .026  | .022  | .025  |
| K     | 0.000 | .001  | 0.000 | 0.000 | .000  | .001  | .000  | 0.000 | 0.000 | 0.000 |
| Total | 4.037 | 4.023 | 4.035 | 4.048 | 4.014 | 4.012 | 4.019 | 4.012 | 4.007 | 4.007 |

|       |      |      |      |      |      |      |      |      |      |      |
|-------|------|------|------|------|------|------|------|------|------|------|
| Ca    | 46.1 | 45.6 | 45.6 | 44.2 | 43.1 | 44.7 | 45.5 | 46.6 | 45.7 | 46.0 |
| Mg    | 34.9 | 34.2 | 35.7 | 37.0 | 43.5 | 43.9 | 41.8 | 40.3 | 43.1 | 42.4 |
| Fe+Mn | 19.0 | 20.2 | 18.7 | 18.8 | 13.4 | 11.5 | 12.8 | 13.1 | 11.2 | 11.7 |

|                                | 11    | 12    | 13    | 14    | 15    | 16    | 17    | 18    | 19     | 20     |
|--------------------------------|-------|-------|-------|-------|-------|-------|-------|-------|--------|--------|
| SiO <sub>2</sub>               | 50.16 | 45.23 | 46.31 | 48.11 | 51.25 | 51.55 | 46.61 | 51.53 | 45.84  | 43.62  |
| TiO <sub>2</sub>               | 1.21  | 3.47  | 3.15  | 2.41  | 1.10  | 1.07  | 2.82  | 1.18  | 3.18   | 4.54   |
| Al <sub>2</sub> O <sub>3</sub> | 2.09  | 6.20  | 5.76  | 3.85  | 2.09  | 2.48  | 4.27  | 2.12  | 7.20   | 8.11   |
| Cr <sub>2</sub> O <sub>3</sub> | 0.00  | 0.00  | 0.00  | 0.00  | .40   | .20   | 0.00  | .20   | 0.00   | .02    |
| FeO                            | 10.49 | 11.34 | 11.10 | 12.84 | 6.45  | 6.82  | 10.77 | 7.11  | 11.12  | 10.79  |
| MnO                            | .21   | .15   | .13   | .22   | .10   | .12   | .14   | .07   | .13    | .23    |
| MgO                            | 12.54 | 11.74 | 11.79 | 10.86 | 15.65 | 15.34 | 12.62 | 15.15 | 12.18  | 11.04  |
| NiO                            | 0.00  | 0.00  | 0.00  | 0.00  | 0.00  | 0.00  | 0.00  | 0.00  | .07    | 0.00   |
| CaO                            | 20.93 | 20.79 | 20.57 | 20.63 | 20.84 | 21.81 | 20.70 | 21.30 | 20.01  | 21.18  |
| Na <sub>2</sub> O              | .35   | .54   | .50   | .46   | .31   | .33   | .51   | .30   | .53    | .64    |
| K <sub>2</sub> O               | 0.00  | .01   | .01   | .02   | 0.00  | .02   | .01   | 0.00  | .02    | 0.00   |
| Total                          | 98.05 | 99.52 | 99.32 | 99.47 | 98.19 | 99.74 | 98.45 | 98.96 | 100.28 | 100.17 |

|       |       |       |       |       |       |       |       |       |       |       |
|-------|-------|-------|-------|-------|-------|-------|-------|-------|-------|-------|
| Si    | 1.926 | 1.733 | 1.769 | 1.847 | 1.925 | 1.913 | 1.797 | 1.926 | 1.732 | 1.663 |
| Al IV | .074  | .267  | .231  | .153  | .075  | .087  | .194  | .074  | .268  | .337  |
| Al VI | .021  | .014  | .029  | .021  | .017  | .021  | 0.000 | .020  | .053  | .027  |
| Ti    | .035  | .100  | .091  | .070  | .031  | .030  | .082  | .033  | .090  | .130  |
| Cr    | 0.000 | 0.000 | 0.000 | 0.000 | .012  | .006  | 0.000 | .006  | 0.000 | .001  |
| Fe    | .337  | .363  | .355  | .412  | .203  | .212  | .347  | .222  | .351  | .344  |
| Mn    | .007  | .005  | .004  | .007  | .003  | .004  | .005  | .002  | .004  | .007  |
| Mg    | .718  | .671  | .671  | .621  | .876  | .848  | .725  | .844  | .686  | .627  |
| Ni    | 0.000 | 0.000 | 0.000 | 0.000 | 0.000 | 0.000 | 0.000 | 0.000 | .002  | 0.000 |
| Ca    | .861  | .854  | .842  | .848  | .839  | .867  | .855  | .853  | .810  | .865  |
| Na    | .026  | .040  | .037  | .034  | .023  | .024  | .038  | .022  | .039  | .047  |
| K     | 0.000 | .000  | .000  | .001  | 0.000 | .001  | .000  | 0.000 | .001  | 0.000 |
| Total | 4.005 | 4.047 | 4.029 | 4.014 | 4.003 | 4.013 | 4.044 | 4.002 | 4.037 | 4.048 |

|       |      |      |      |      |      |      |      |      |      |      |
|-------|------|------|------|------|------|------|------|------|------|------|
| Ca    | 44.8 | 45.1 | 45.0 | 44.9 | 43.7 | 44.9 | 44.3 | 44.4 | 43.8 | 46.9 |
| Mg    | 37.3 | 35.4 | 35.9 | 32.9 | 45.6 | 43.9 | 37.5 | 43.9 | 37.0 | 34.0 |
| Fe+Mn | 17.9 | 19.5 | 19.2 | 22.2 | 10.7 | 11.2 | 18.2 | 11.7 | 19.2 | 19.1 |

|       | 21    | 22     | 23    | 24    | 25    | 26    | 27     | 28     | 29    | 30    |
|-------|-------|--------|-------|-------|-------|-------|--------|--------|-------|-------|
| SiO2  | 42.00 | 44.41  | 43.68 | 44.24 | 43.17 | 45.14 | 45.40  | 48.30  | 47.87 | 45.96 |
| TiO2  | 5.52  | 4.76   | 5.09  | 4.06  | 4.41  | 4.23  | 3.89   | 2.33   | 2.18  | 3.35  |
| Al2O3 | 8.56  | 7.09   | 7.52  | 7.09  | 7.98  | 6.27  | 6.73   | 4.86   | 4.68  | 6.04  |
| Cr2O3 | .01   | 0.00   | 0.00  | 0.00  | 0.00  | .04   | 0.00   | .66    | .37   | .02   |
| FeO   | 11.13 | 11.15  | 10.37 | 10.32 | 10.34 | 9.18  | 11.50  | 6.95   | 7.90  | 8.35  |
| MnO   | .18   | .14    | .17   | .14   | .17   | .14   | .13    | .03    | .13   | .14   |
| MgO   | 10.63 | 11.72  | 11.20 | 11.33 | 10.80 | 12.44 | 10.28  | 14.30  | 14.09 | 12.44 |
| NiO   | 0.00  | .10    | .03   | .02   | .03   | 0.00  | .03    | .03    | .03   | .04   |
| CaO   | 20.59 | 20.73  | 20.95 | 21.21 | 21.09 | 21.39 | 21.75  | 22.20  | 21.87 | 22.06 |
| Na2O  | .71   | .59    | .29   | .57   | .68   | .41   | .58    | .37    | .31   | .47   |
| K2O   | .01   | .01    | .02   | .03   | .05   | 0.00  | .04    | .02    | .02   | .01   |
| Total | 99.34 | 100.70 | 99.32 | 99.01 | 98.72 | 99.24 | 100.33 | 100.05 | 99.45 | 98.88 |

|       |       |       |       |       |       |       |       |       |       |       |
|-------|-------|-------|-------|-------|-------|-------|-------|-------|-------|-------|
| Si    | 1.621 | 1.683 | 1.674 | 1.701 | 1.668 | 1.720 | 1.729 | 1.802 | 1.804 | 1.752 |
| Al IV | .380  | .317  | .326  | .299  | .332  | .280  | .271  | .198  | .196  | .248  |
| Al VI | .010  | .000  | .013  | .022  | .031  | .002  | .032  | .016  | .012  | .023  |
| Ti    | .160  | .136  | .147  | .117  | .128  | .121  | .111  | .065  | .062  | .096  |
| Cr    | .000  | 0.000 | 0.000 | 0.000 | 0.000 | .001  | 0.000 | .019  | .011  | .001  |
| Fe    | .359  | .353  | .332  | .332  | .334  | .293  | .366  | .217  | .249  | .266  |
| Mn    | .006  | .004  | .006  | .005  | .006  | .005  | .004  | .001  | .004  | .005  |
| Mg    | .611  | .662  | .640  | .649  | .622  | .707  | .584  | .795  | .791  | .707  |
| Ni    | 0.000 | .003  | .001  | .001  | .001  | 0.000 | .001  | .001  | .001  | .001  |
| Ca    | .851  | .842  | .860  | .874  | .873  | .873  | .888  | .887  | .883  | .901  |
| Na    | .053  | .043  | .022  | .042  | .051  | .030  | .043  | .027  | .023  | .035  |
| K     | .000  | .000  | .001  | .001  | .002  | 0.000 | .002  | .001  | .001  | .000  |
| Total | 4.051 | 4.045 | 4.021 | 4.043 | 4.049 | 4.032 | 4.030 | 4.030 | 4.037 | 4.034 |

|       |      |      |      |      |      |      |      |      |      |      |
|-------|------|------|------|------|------|------|------|------|------|------|
| Ca    | 46.6 | 45.2 | 46.8 | 47.0 | 47.6 | 46.5 | 48.2 | 46.7 | 45.8 | 48.0 |
| Mg    | 33.5 | 35.6 | 34.8 | 34.9 | 33.9 | 37.6 | 31.7 | 41.8 | 41.1 | 37.6 |
| Fe+Mn | 20.0 | 19.2 | 18.4 | 18.1 | 18.5 | 15.8 | 20.1 | 11.5 | 13.1 | 14.4 |

|       | 31     | 32    | 33     | 34    | 35    | 36    | 37    | 38    | 39     | 40    |
|-------|--------|-------|--------|-------|-------|-------|-------|-------|--------|-------|
| SiO2  | 51.04  | 49.33 | 47.82  | 48.25 | 45.15 | 45.40 | 46.29 | 50.80 | 49.79  | 46.36 |
| TiO2  | 1.22   | 1.66  | 2.88   | 1.95  | 3.24  | 3.36  | 3.23  | 1.21  | 1.73   | 3.42  |
| Al2O3 | 2.27   | 2.71  | 5.55   | 4.16  | 5.74  | 6.00  | 5.89  | 2.16  | 3.08   | 5.73  |
| Cr2O3 | .44    | .19   | .39    | .76   | .32   | .23   | .07   | .45   | .05    | .14   |
| FeO   | 6.60   | 7.71  | 7.75   | 6.56  | 8.27  | 8.33  | 8.52  | 6.59  | 8.02   | 8.88  |
| MnO   | .13    | .11   | .09    | .10   | .11   | .11   | .11   | .13   | .16    | .17   |
| MgO   | 15.83  | 15.42 | 13.88  | 14.71 | 12.91 | 13.20 | 13.02 | 15.86 | 15.26  | 12.44 |
| NiO   | 0.00   | .01   | 0.00   | .12   | 0.00  | .05   | .03   | .01   | .01    | .04   |
| CaO   | 22.47  | 21.32 | 21.71  | 22.45 | 21.89 | 21.82 | 22.34 | 22.30 | 21.81  | 22.25 |
| Na2O  | .25    | .29   | .50    | .39   | .50   | .41   | .36   | .36   | .29    | .45   |
| K2O   | .01    | .01   | .01    | .02   | 0.00  | .01   | .01   | 0.00  | .01    | 0.00  |
| Total | 100.26 | 98.76 | 100.58 | 99.47 | 98.13 | 98.92 | 99.87 | 99.87 | 100.21 | 99.88 |

|       |       |       |       |       |       |       |       |       |       |       |
|-------|-------|-------|-------|-------|-------|-------|-------|-------|-------|-------|
| Si    | 1.890 | 1.863 | 1.779 | 1.812 | 1.738 | 1.732 | 1.748 | 1.890 | 1.856 | 1.754 |
| Al IV | .099  | .121  | .221  | .184  | .260  | .268  | .252  | .095  | .135  | .246  |
| Al VI | 0.000 | 0.000 | .023  | 0.000 | 0.000 | .002  | .010  | 0.000 | 0.000 | .010  |
| Ti    | .034  | .047  | .081  | .055  | .094  | .096  | .092  | .034  | .049  | .097  |
| Cr    | .013  | .006  | .011  | .023  | .010  | .007  | .002  | .013  | .001  | .004  |
| Fe    | .204  | .244  | .241  | .206  | .266  | .266  | .269  | .205  | .250  | .281  |
| Mn    | .004  | .004  | .003  | .003  | .004  | .004  | .004  | .004  | .005  | .005  |
| Mg    | .874  | .868  | .770  | .824  | .741  | .751  | .733  | .879  | .848  | .702  |
| Ni    | 0.000 | .000  | 0.000 | .004  | 0.000 | .002  | .001  | .000  | .000  | .001  |
| Ca    | .892  | .863  | .866  | .904  | .903  | .892  | .904  | .889  | .871  | .902  |
| Na    | .018  | .021  | .036  | .028  | .037  | .030  | .026  | .026  | .021  | .033  |
| K     | .000  | .000  | .000  | .001  | 0.000 | .000  | .000  | 0.000 | .000  | 0.000 |
| Total | 4.029 | 4.037 | 4.031 | 4.044 | 4.052 | 4.049 | 4.041 | 4.035 | 4.038 | 4.035 |

|       |      |      |      |      |      |      |      |      |      |      |
|-------|------|------|------|------|------|------|------|------|------|------|
| Ca    | 45.2 | 43.6 | 46.1 | 46.7 | 47.2 | 46.7 | 47.3 | 45.0 | 44.1 | 47.7 |
| Mg    | 44.3 | 43.9 | 41.0 | 42.5 | 38.7 | 39.3 | 38.4 | 44.5 | 43.0 | 37.1 |
| Fe+Mn | 10.6 | 12.5 | 13.0 | 10.8 | 14.1 | 14.1 | 14.3 | 10.6 | 12.9 | 15.2 |



|       | 41    | 42    | 43    | 44    | 45     | 46     | 47    | 48    | 49    | 50    |
|-------|-------|-------|-------|-------|--------|--------|-------|-------|-------|-------|
| SiO2  | 47.02 | 49.05 | 47.85 | 45.11 | 49.10  | 50.39  | 45.69 | 47.68 | 50.75 | 51.19 |
| TiO2  | 2.75  | 1.64  | 2.16  | 3.52  | 1.89   | 1.49   | 3.66  | 1.93  | 1.31  | 1.17  |
| Al2O3 | 4.84  | 2.36  | 4.64  | 6.26  | 2.29   | 2.46   | 6.16  | 4.27  | 2.00  | 1.88  |
| Cr2O3 | .05   | 0.00  | .23   | .05   | .02    | .02    | .07   | .39   | .10   | .20   |
| FeO   | 8.18  | 9.25  | 7.80  | 8.48  | 11.63  | 9.66   | 8.78  | 7.02  | 7.60  | 6.77  |
| MnO   | .05   | .11   | .10   | .11   | .24    | .10    | .10   | .13   | .13   | .05   |
| MgO   | 13.71 | 14.88 | 14.09 | 12.87 | 13.42  | 14.70  | 12.87 | 14.40 | 15.32 | 15.80 |
| NiO   | 0.00  | .09   | .05   | 0.00  | 0.00   | .05    | .05   | 0.00  | 0.00  | 0.00  |
| CaO   | 22.37 | 21.29 | 22.47 | 22.14 | 21.35  | 21.11  | 22.14 | 22.50 | 20.75 | 21.60 |
| Na2O  | .42   | .33   | .25   | .41   | .45    | .36    | .43   | .45   | .36   | .29   |
| K2O   | .01   | 0.00  | 0.00  | .01   | .02    | .02    | .01   | .01   | 0.00  | 0.00  |
| Total | 99.40 | 99.00 | 99.64 | 98.96 | 100.41 | 100.36 | 99.96 | 98.78 | 98.38 | 99.07 |
| Si    | 1.780 | 1.863 | 1.801 | 1.722 | 1.860  | 1.884  | 1.728 | 1.808 | 1.915 | 1.915 |
| AlIV  | .216  | .106  | .199  | .278  | .102   | .108   | .272  | .191  | .085  | .083  |
| AlVI  | 0.000 | 0.000 | .007  | .004  | 0.000  | 0.000  | .002  | 0.000 | .004  | 0.000 |
| Ti    | .078  | .047  | .061  | .101  | .054   | .042   | .104  | .055  | .037  | .033  |
| Cr    | .001  | 0.000 | .007  | .002  | .001   | .001   | .002  | .012  | .003  | .006  |
| Fe    | .259  | .294  | .246  | .271  | .368   | .302   | .278  | .223  | .240  | .212  |
| Mn    | .002  | .004  | .003  | .004  | .008   | .003   | .003  | .004  | .004  | .002  |
| Mg    | .774  | .843  | .791  | .732  | .758   | .819   | .725  | .814  | .862  | .881  |
| Ni    | 0.000 | .003  | .002  | 0.000 | 0.000  | .002   | .002  | 0.000 | 0.000 | 0.000 |
| Ca    | .907  | .867  | .906  | .906  | .867   | .846   | .897  | .914  | .839  | .866  |
| Na    | .031  | .024  | .018  | .030  | .033   | .026   | .032  | .033  | .026  | .021  |
| K     | .000  | 0.000 | 0.000 | .000  | .001   | .001   | .000  | .000  | 0.000 | 0.000 |
| Total | 4.049 | 4.049 | 4.040 | 4.050 | 4.052  | 4.033  | 4.046 | 4.053 | 4.015 | 4.018 |
| Ca    | 46.7  | 43.2  | 46.6  | 47.4  | 43.3   | 42.9   | 47.1  | 46.8  | 43.1  | 44.2  |
| Mg    | 39.8  | 42.0  | 40.6  | 38.3  | 37.9   | 41.6   | 38.1  | 41.6  | 44.3  | 44.9  |
| Fe+Mn | 13.4  | 14.8  | 12.8  | 14.3  | 18.8   | 15.5   | 14.8  | 11.6  | 12.5  | 10.9  |

|       | 51    | 52    | 53    | 54     | 55    | 56    | 57    | 58    | 59    | 60    |
|-------|-------|-------|-------|--------|-------|-------|-------|-------|-------|-------|
| SiO2  | 48.97 | 51.86 | 50.83 | 51.27  | 51.82 | 50.58 | 51.71 | 50.99 | 50.52 | 49.87 |
| TiO2  | 2.15  | 1.16  | 1.14  | 1.37   | 1.18  | 1.14  | 1.21  | 1.23  | 1.25  | 1.38  |
| Al2O3 | 4.32  | 1.70  | 2.07  | 2.60   | 1.73  | 2.01  | 1.90  | 1.92  | 1.95  | 2.49  |
| Cr2O3 | .20   | .40   | .40   | .50    | .20   | .30   | .30   | 0.00  | .20   | .40   |
| FeO   | 7.21  | 6.54  | 6.45  | 6.84   | 6.99  | 6.91  | 7.22  | 7.98  | 6.99  | 6.86  |
| MnO   | .09   | .10   | .09   | .11    | .11   | .05   | .08   | .11   | .13   | .17   |
| MgO   | 14.13 | 15.77 | 15.66 | 15.46  | 15.65 | 16.19 | 15.82 | 15.50 | 15.83 | 15.51 |
| NiO   | 0.00  | 0.00  | 0.00  | 0.00   | 0.00  | 0.00  | 0.00  | 0.00  | 0.00  | 0.00  |
| CaO   | 21.56 | 20.97 | 21.70 | 21.95  | 21.22 | 21.55 | 21.25 | 21.10 | 21.21 | 21.80 |
| Na2O  | .41   | .34   | .34   | .36    | .36   | .36   | .27   | .38   | .37   | .31   |
| K2O   | .02   | 0.00  | 0.00  | 0.00   | 0.00  | 0.00  | 0.00  | .01   | .02   | 0.00  |
| Total | 99.10 | 98.84 | 98.68 | 100.56 | 99.31 | 99.18 | 99.85 | 99.26 | 98.50 | 98.79 |

|       |       |       |       |       |       |       |       |       |       |       |
|-------|-------|-------|-------|-------|-------|-------|-------|-------|-------|-------|
| Si    | 1.840 | 1.935 | 1.907 | 1.893 | 1.930 | 1.895 | 1.919 | 1.911 | 1.903 | 1.878 |
| Al IV | .160  | .065  | .092  | .107  | .070  | .089  | .081  | .085  | .087  | .111  |
| Al VI | .031  | .010  | 0.000 | .006  | .006  | 0.000 | .002  | 0.000 | 0.000 | 0.000 |
| Ti    | .061  | .033  | .032  | .038  | .033  | .032  | .034  | .035  | .035  | .039  |
| Cr    | .006  | .012  | .012  | .015  | .006  | .009  | .009  | 0.000 | .006  | .012  |
| Fe    | .227  | .204  | .202  | .211  | .218  | .216  | .224  | .250  | .220  | .216  |
| Mn    | .003  | .003  | .003  | .003  | .003  | .002  | .003  | .003  | .004  | .005  |
| Mg    | .791  | .877  | .876  | .851  | .869  | .904  | .875  | .866  | .889  | .870  |
| Ni    | 0.000 | 0.000 | 0.000 | 0.000 | 0.000 | 0.000 | 0.000 | 0.000 | 0.000 | 0.000 |
| Ca    | .868  | .838  | .872  | .868  | .847  | .865  | .845  | .847  | .856  | .879  |
| Na    | .030  | .025  | .025  | .026  | .026  | .026  | .019  | .028  | .027  | .023  |
| K     | .001  | 0.000 | 0.000 | 0.000 | 0.000 | 0.000 | 0.000 | .000  | .001  | 0.000 |
| Total | 4.017 | 4.001 | 4.021 | 4.018 | 4.009 | 4.037 | 4.011 | 4.026 | 4.029 | 4.033 |

|       |      |      |      |      |      |      |      |      |      |      |
|-------|------|------|------|------|------|------|------|------|------|------|
| Ca    | 46.0 | 43.6 | 44.7 | 44.9 | 43.7 | 43.5 | 43.4 | 43.1 | 43.5 | 44.6 |
| Mg    | 41.9 | 45.6 | 44.8 | 44.0 | 44.9 | 45.5 | 45.0 | 44.0 | 45.1 | 44.2 |
| Fe+Mn | 12.1 | 10.8 | 10.5 | 11.1 | 11.4 | 11.0 | 11.6 | 12.9 | 11.4 | 11.2 |

|       | 61    | 62    | 63    | 64    | 65     | 66     | 67     | 68     | 69     | 70     |
|-------|-------|-------|-------|-------|--------|--------|--------|--------|--------|--------|
| SiO2  | 49.30 | 51.53 | 51.68 | 51.44 | 52.11  | 50.81  | 51.89  | 51.57  | 51.52  | 51.62  |
| TiO2  | 1.86  | 1.11  | 1.15  | 1.09  | 1.19   | 1.61   | 1.45   | 1.36   | 1.33   | 1.45   |
| Al2O3 | 3.31  | 1.95  | 1.68  | 1.60  | 1.64   | 2.50   | 2.19   | 2.29   | 2.01   | 2.35   |
| Cr2O3 | 0.00  | .40   | .20   | .30   | .40    | .40    | .50    | .40    | .50    | .50    |
| FeO   | 8.54  | 6.70  | 6.79  | 6.99  | 7.66   | 8.09   | 7.84   | 7.79   | 7.41   | 7.34   |
| MnO   | .11   | .07   | .04   | .14   | .09    | .11    | .10    | .13    | .19    | .13    |
| MgO   | 14.48 | 15.70 | 15.37 | 15.75 | 16.07  | 15.54  | 15.57  | 15.99  | 15.43  | 15.71  |
| NiO   | 0.00  | 0.00  | 0.00  | 0.00  | 0.00   | 0.00   | 0.00   | 0.00   | 0.00   | 0.00   |
| CaO   | 20.96 | 21.62 | 21.27 | 21.08 | 20.79  | 21.41  | 21.39  | 21.28  | 21.15  | 21.70  |
| Na2O  | .41   | .36   | .30   | .36   | .62    | .28    | .43    | .32    | .70    | .34    |
| K2O   | .01   | 0.00  | 0.00  | .01   | .05    | .02    | .02    | .04    | .10    | .04    |
| Total | 98.98 | 99.47 | 98.49 | 98.76 | 100.67 | 100.82 | 101.46 | 101.27 | 100.34 | 101.22 |

|       |       |       |       |       |       |       |       |       |       |       |
|-------|-------|-------|-------|-------|-------|-------|-------|-------|-------|-------|
| Si    | 1.861 | 1.918 | 1.938 | 1.928 | 1.921 | 1.880 | 1.903 | 1.895 | 1.909 | 1.895 |
| Al IV | .139  | .082  | .062  | .071  | .071  | .109  | .095  | .099  | .088  | .102  |
| Al VI | .008  | .003  | .012  | 0.000 | 0.000 | 0.000 | 0.000 | 0.000 | 0.000 | 0.000 |
| Ti    | .053  | .031  | .032  | .031  | .033  | .045  | .040  | .038  | .037  | .040  |
| Cr    | 0.000 | .012  | .006  | .009  | .012  | .012  | .014  | .012  | .015  | .015  |
| Fe    | .270  | .209  | .213  | .219  | .236  | .250  | .240  | .239  | .230  | .225  |
| Mn    | .004  | .002  | .001  | .004  | .003  | .003  | .003  | .004  | .006  | .004  |
| Mg    | .815  | .871  | .859  | .880  | .883  | .857  | .851  | .876  | .852  | .860  |
| Ni    | 0.000 | 0.000 | 0.000 | 0.000 | 0.000 | 0.000 | 0.000 | 0.000 | 0.000 | 0.000 |
| Ca    | .848  | .862  | .855  | .847  | .821  | .849  | .840  | .838  | .840  | .854  |
| Na    | .030  | .026  | .022  | .026  | .044  | .020  | .031  | .023  | .050  | .024  |
| K     | .000  | 0.000 | 0.000 | .000  | .002  | .001  | .001  | .002  | .005  | .002  |
| Total | 4.028 | 4.016 | 4.000 | 4.015 | 4.027 | 4.026 | 4.018 | 4.025 | 4.030 | 4.020 |

|       |      |      |      |      |      |      |      |      |      |      |
|-------|------|------|------|------|------|------|------|------|------|------|
| Ca    | 43.8 | 44.4 | 44.3 | 43.4 | 42.3 | 43.3 | 43.4 | 42.8 | 43.6 | 43.9 |
| Mg    | 42.1 | 44.8 | 44.6 | 45.1 | 45.4 | 43.7 | 44.0 | 44.8 | 44.2 | 44.3 |
| Fe+Mn | 14.1 | 10.8 | 11.1 | 11.5 | 12.3 | 13.0 | 12.6 | 12.4 | 12.2 | 11.8 |

|       | 71     | 72     | 73     | 74     | 75    | 76     | 77     | 78     | 79     | 80    |
|-------|--------|--------|--------|--------|-------|--------|--------|--------|--------|-------|
| SiO2  | 52.56  | 52.38  | 52.39  | 52.33  | 51.18 | 52.22  | 50.26  | 52.39  | 51.67  | 49.16 |
| TiO2  | 1.14   | 1.16   | 1.02   | 1.27   | 1.18  | 1.69   | 1.67   | 1.31   | 1.42   | 2.18  |
| Al2O3 | 2.36   | 1.92   | 1.89   | 1.82   | 2.34  | 2.92   | 3.51   | 2.06   | 2.54   | 4.11  |
| Cr2O3 | .70    | .40    | .40    | .09    | .74   | .29    | .83    | .09    | .41    | .33   |
| FeO   | 7.87   | 6.24   | 6.81   | 7.68   | 6.05  | 6.87   | 6.27   | 7.79   | 6.93   | 6.79  |
| MnO   | .07    | .16    | .41    | .09    | .14   | .07    | .11    | .07    | .10    | .04   |
| MgO   | 16.62  | 16.40  | 15.80  | 16.03  | 15.89 | 15.18  | 15.39  | 15.74  | 15.64  | 14.96 |
| NiO   | 0.00   | 0.00   | 0.00   | 0.00   | .03   | 0.00   | 0.00   | .11    | .02    | .04   |
| CaO   | 19.91  | 21.68  | 21.79  | 20.86  | 21.07 | 21.44  | 21.66  | 20.48  | 21.10  | 21.23 |
| Na2O  | .39    | .44    | .39    | .68    | .63   | .61    | .43    | .59    | .58    | .41   |
| K2O   | .02    | .06    | .01    | .02    | 0.00  | .01    | .01    | .03    | .01    | .03   |
| Total | 101.72 | 100.89 | 100.96 | 100.87 | 99.25 | 101.30 | 100.14 | 100.66 | 100.42 | 99.28 |

|       |       |       |       |       |       |       |       |       |       |       |
|-------|-------|-------|-------|-------|-------|-------|-------|-------|-------|-------|
| Si    | 1.912 | 1.918 | 1.923 | 1.923 | 1.905 | 1.905 | 1.860 | 1.927 | 1.904 | 1.838 |
| Al IV | .088  | .082  | .077  | .077  | .095  | .095  | .140  | .073  | .096  | .162  |
| Al VI | .013  | .001  | .005  | .001  | .007  | .030  | .013  | .016  | .014  | .019  |
| Ti    | .031  | .032  | .028  | .035  | .033  | .046  | .046  | .036  | .039  | .061  |
| Cr    | .020  | .012  | .012  | .003  | .022  | .008  | .024  | .003  | .012  | .010  |
| Fe    | .239  | .191  | .209  | .236  | .188  | .210  | .194  | .240  | .214  | .212  |
| Mn    | .002  | .005  | .013  | .003  | .004  | .002  | .003  | .002  | .003  | .001  |
| Mg    | .901  | .895  | .864  | .878  | .881  | .825  | .849  | .863  | .859  | .834  |
| Ni    | 0.000 | 0.000 | 0.000 | 0.000 | .001  | 0.000 | 0.000 | .003  | .001  | .001  |
| Ca    | .776  | .851  | .857  | .821  | .840  | .838  | .859  | .807  | .833  | .851  |
| Na    | .027  | .031  | .028  | .048  | .045  | .043  | .031  | .042  | .041  | .030  |
| K     | .001  | .003  | .000  | .001  | 0.000 | .000  | .000  | .001  | .000  | .001  |
| Total | 4.011 | 4.020 | 4.016 | 4.026 | 4.023 | 4.004 | 4.020 | 4.013 | 4.017 | 4.021 |

|       |      |      |      |      |      |      |      |      |      |      |
|-------|------|------|------|------|------|------|------|------|------|------|
| Ca    | 40.4 | 43.8 | 44.1 | 42.4 | 43.9 | 44.7 | 45.1 | 42.2 | 43.6 | 44.8 |
| Mg    | 47.0 | 46.1 | 44.5 | 45.3 | 46.0 | 44.0 | 44.6 | 45.1 | 45.0 | 43.9 |
| Fe+Mn | 12.6 | 10.1 | 11.4 | 12.3 | 10.1 | 11.3 | 10.4 | 12.6 | 11.4 | 11.3 |

|       | 81    | 82    | 83     | 84    | 85     | 86     | 87     | 88     | 89     | 90    |
|-------|-------|-------|--------|-------|--------|--------|--------|--------|--------|-------|
| SiO2  | 49.89 | 50.33 | 48.20  | 49.52 | 51.35  | 51.72  | 50.76  | 50.27  | 49.29  | 47.71 |
| TiO2  | 1.95  | 1.68  | 2.98   | 1.74  | 1.63   | 1.48   | 1.84   | 2.66   | 2.41   | 2.43  |
| Al2O3 | 4.09  | 3.20  | 4.81   | 3.13  | 2.56   | 2.30   | 3.40   | 4.77   | 5.30   | 4.93  |
| Cr2O3 | .59   | .77   | .51    | .78   | .23    | .36    | .78    | .36    | .89    | .84   |
| FeO   | 6.52  | 6.31  | 8.23   | 5.91  | 6.96   | 6.90   | 6.01   | 7.15   | 6.38   | 6.49  |
| MnO   | .09   | .04   | .10    | .07   | .13    | .11    | .11    | .09    | .11    | .07   |
| MgO   | 14.70 | 15.65 | 14.13  | 15.73 | 16.22  | 16.24  | 15.85  | 14.37  | 15.87  | 14.64 |
| NiO   | .07   | .06   | .05    | 0.00  | .04    | 0.00   | 0.00   | .07    | .03    | .07   |
| CaO   | 20.83 | 21.23 | 20.58  | 21.47 | 20.52  | 20.56  | 21.41  | 21.13  | 20.32  | 20.86 |
| Na2O  | .79   | .41   | .64    | .58   | .46    | .39    | .55    | .66    | .54    | .57   |
| K2O   | .02   | .02   | .02    | .02   | 0.00   | .01    | .01    | .02    | .02    | .01   |
| Total | 99.54 | 99.70 | 100.25 | 98.95 | 100.10 | 100.07 | 100.72 | 101.55 | 101.16 | 98.62 |

|       |       |       |       |       |       |       |       |       |       |       |
|-------|-------|-------|-------|-------|-------|-------|-------|-------|-------|-------|
| Si    | 1.857 | 1.869 | 1.799 | 1.855 | 1.896 | 1.908 | 1.863 | 1.837 | 1.803 | 1.800 |
| AlIV  | .143  | .131  | .201  | .138  | .104  | .092  | .137  | .163  | .197  | .200  |
| AlVI  | .036  | .009  | .011  | 0.000 | .007  | .008  | .010  | .042  | .031  | .019  |
| Ti    | .055  | .047  | .084  | .049  | .045  | .041  | .051  | .073  | .066  | .069  |
| Cr    | .017  | .023  | .015  | .023  | .007  | .011  | .023  | .010  | .026  | .025  |
| Fe    | .203  | .196  | .257  | .185  | .215  | .213  | .185  | .218  | .195  | .205  |
| Mn    | .003  | .001  | .003  | .002  | .004  | .003  | .003  | .003  | .003  | .002  |
| Mg    | .815  | .866  | .786  | .878  | .893  | .893  | .867  | .783  | .865  | .823  |
| Ni    | .002  | .002  | .002  | 0.000 | .001  | 0.000 | 0.000 | .002  | .001  | .002  |
| Ca    | .830  | .845  | .823  | .862  | .812  | .813  | .842  | .827  | .796  | .843  |
| Na    | .057  | .030  | .046  | .042  | .033  | .028  | .039  | .047  | .038  | .042  |
| K     | .001  | .001  | .001  | .001  | 0.000 | .000  | .000  | .001  | .001  | .000  |
| Total | 4.019 | 4.018 | 4.027 | 4.037 | 4.016 | 4.010 | 4.021 | 4.006 | 4.023 | 4.030 |

|       |      |      |      |      |      |      |      |      |      |      |
|-------|------|------|------|------|------|------|------|------|------|------|
| Ca    | 44.9 | 44.3 | 44.0 | 44.7 | 42.2 | 42.3 | 44.4 | 45.2 | 42.8 | 45.0 |
| Mg    | 44.0 | 45.4 | 42.1 | 45.6 | 46.4 | 46.5 | 45.7 | 42.7 | 46.5 | 43.9 |
| Fe+Mn | 11.1 | 10.3 | 13.9 | 9.7  | 11.4 | 11.3 | 9.9  | 12.1 | 10.7 | 11.0 |

|       | 91    | 92     | 93    | 94     |
|-------|-------|--------|-------|--------|
| SiO2  | 48.37 | 49.73  | 48.93 | 52.05  |
| TiO2  | 2.23  | 2.36   | 2.30  | 1.21   |
| Al2O3 | 4.38  | 4.74   | 4.41  | 2.22   |
| Cr2O3 | .59   | .38    | .74   | .36    |
| FeO   | 6.38  | 6.81   | 6.79  | 7.23   |
| MnO   | .08   | .11    | .04   | .11    |
| MgO   | 14.45 | 14.66  | 15.00 | 16.84  |
| NiO   | .06   | .01    | .01   | .06    |
| CaO   | 21.06 | 21.20  | 20.74 | 19.80  |
| Na2O  | .61   | .39    | .48   | .41    |
| K2O   | .02   | .01    | .01   | .01    |
| Total | 98.23 | 100.40 | 99.45 | 100.30 |

|       |       |       |       |       |
|-------|-------|-------|-------|-------|
| Si    | 1.829 | 1.835 | 1.826 | 1.914 |
| AlIV  | .171  | .165  | .174  | .086  |
| AlVI  | .024  | .041  | .020  | .010  |
| Ti    | .063  | .065  | .065  | .033  |
| Cr    | .018  | .011  | .022  | .010  |
| Fe    | .202  | .210  | .212  | .222  |
| Mn    | .003  | .003  | .001  | .003  |
| Mg    | .814  | .806  | .834  | .923  |
| Ni    | .002  | .000  | .000  | .002  |
| Ca    | .853  | .838  | .829  | .780  |
| Na    | .045  | .028  | .035  | .029  |
| K     | .001  | .000  | .000  | .000  |
| Total | 4.024 | 4.005 | 4.019 | 4.014 |

|       |      |      |      |      |
|-------|------|------|------|------|
| Ca    | 45.6 | 45.1 | 44.2 | 40.4 |
| Mg    | 43.5 | 43.4 | 44.5 | 47.9 |
| Fe+Mn | 10.9 | 11.5 | 11.4 | 11.7 |

CAPE ST. MARY'S FEEDER PIPE PYROXENES

| Location                   | Sample Number | Analysis Numbers |
|----------------------------|---------------|------------------|
| Normans Cove               | CA28I         | 1 to 11          |
|                            | CA28E         | 12 to 21         |
|                            | CA28          | 22 to 24         |
|                            | LC8D          | 25 to 32         |
| Placentia Jct.             | PL210         | 33 to 42         |
| S.E. of Placentia Junction | PL108         | 43 to 47         |
| N. of Spread               |               |                  |
| Eagle Peak                 | CA178         | 48 to 52         |
| W. of Spread               |               |                  |
| Eagle Peak                 | CA170         | 53 to 58         |
| Spread Eagle Peak          | CA164         | 59 to 64         |
| McLeod Point               | CA87          | 65 to 69         |

|       | 1     | 2     | 3     | 4     | 5     | 6      | 7     | 8     | 9     | 10    |
|-------|-------|-------|-------|-------|-------|--------|-------|-------|-------|-------|
| SiO2  | 50.95 | 51.47 | 50.31 | 50.52 | 49.34 | 51.69  | 49.64 | 51.05 | 50.59 | 50.29 |
| TiO2  | 1.13  | 1.14  | 1.46  | 1.09  | 1.18  | 1.16   | 1.30  | 1.04  | 1.43  | 1.63  |
| Al2O3 | 2.23  | 1.95  | 2.69  | 1.96  | 2.17  | 2.04   | 2.59  | 1.91  | 2.50  | 3.26  |
| Cr2O3 | 0.00  | 0.00  | 0.00  | 0.00  | 0.00  | 0.00   | 0.00  | 0.00  | .10   | .10   |
| FeO   | 9.16  | 8.32  | 8.30  | 9.68  | 10.81 | 9.57   | 8.70  | 10.08 | 8.53  | 8.91  |
| MnO   | .14   | .16   | .17   | .14   | .18   | .14    | .10   | .20   | .13   | .14   |
| MgO   | 15.17 | 15.44 | 14.92 | 14.66 | 13.88 | 14.78  | 14.84 | 14.21 | 14.85 | 14.77 |
| NiO   | 0.00  | 0.00  | 0.00  | 0.00  | 0.00  | 0.00   | 0.00  | 0.00  | 0.00  | 0.00  |
| CaO   | 20.40 | 20.50 | 20.88 | 20.66 | 20.30 | 20.41  | 20.64 | 20.41 | 20.54 | 20.13 |
| Na2O  | .40   | .28   | .37   | .26   | .34   | .31    | .37   | .36   | .50   | .40   |
| K2O   | 0.00  | 0.00  | .01   | .01   | .01   | .02    | .02   | .01   | .01   | .01   |
| Total | 99.58 | 99.31 | 99.11 | 99.00 | 98.21 | 100.12 | 98.20 | 99.36 | 99.18 | 99.64 |

|       |       |       |       |       |       |       |       |       |       |       |
|-------|-------|-------|-------|-------|-------|-------|-------|-------|-------|-------|
| Si    | 1.909 | 1.925 | 1.891 | 1.911 | 1.895 | 1.926 | 1.888 | 1.926 | 1.900 | 1.880 |
| AlIV  | .091  | .075  | .109  | .087  | .098  | .074  | .112  | .074  | .100  | .120  |
| AlVI  | .007  | .011  | .010  | 0.000 | 0.000 | .015  | .004  | .011  | .011  | .024  |
| Ti    | .032  | .032  | .041  | .031  | .034  | .032  | .037  | .030  | .040  | .046  |
| Cr    | 0.000 | 0.000 | 0.000 | 0.000 | 0.000 | 0.000 | 0.000 | 0.000 | .003  | .003  |
| Fe    | .287  | .260  | .261  | .306  | .347  | .298  | .277  | .318  | .268  | .279  |
| Mn    | .004  | .005  | .005  | .004  | .006  | .004  | .003  | .006  | .004  | .004  |
| Mg    | .847  | .861  | .836  | .827  | .794  | .821  | .841  | .799  | .831  | .823  |
| Ni    | 0.000 | 0.000 | 0.000 | 0.000 | 0.000 | 0.000 | 0.000 | 0.000 | 0.000 | 0.000 |
| Ca    | .819  | .821  | .841  | .837  | .835  | .815  | .841  | .825  | .827  | .806  |
| Na    | .029  | .020  | .027  | .019  | .025  | .022  | .027  | .026  | .036  | .029  |
| K     | 0.000 | 0.000 | .000  | .000  | .000  | .001  | .001  | .000  | .000  | .000  |
| Total | 4.025 | 4.010 | 4.022 | 4.024 | 4.035 | 4.009 | 4.031 | 4.016 | 4.021 | 4.015 |

|       |      |      |      |      |      |      |      |      |      |      |
|-------|------|------|------|------|------|------|------|------|------|------|
| Ca    | 41.8 | 42.2 | 43.3 | 42.4 | 42.1 | 42.0 | 42.9 | 42.3 | 42.8 | 42.2 |
| Mg    | 43.3 | 44.2 | 43.0 | 41.9 | 40.1 | 42.3 | 42.9 | 41.0 | 43.1 | 43.0 |
| Fe+Mn | 14.9 | 13.6 | 13.7 | 15.7 | 17.8 | 15.6 | 14.3 | 16.6 | 14.1 | 14.8 |



|       | 11    | 12     | 13     | 14    | 15     | 16     | 17     | 18     | 19     | 20     |
|-------|-------|--------|--------|-------|--------|--------|--------|--------|--------|--------|
| SiO2  | 49.67 | 51.86  | 51.57  | 51.85 | 51.31  | 51.88  | 51.60  | 51.28  | 44.26  | 52.19  |
| TiO2  | 1.73  | 1.19   | 1.14   | 1.25  | 1.68   | 1.06   | 1.17   | 1.00   | 4.19   | 1.11   |
| Al2O3 | 3.02  | 1.89   | 2.71   | 1.64  | 2.51   | 2.29   | 2.71   | 2.24   | 10.43  | 2.64   |
| Cr2O3 | .10   | 0.00   | .40    | 0.00  | 0.00   | .20    | .50    | .30    | .10    | .30    |
| FeO   | 8.94  | 9.17   | 7.01   | 7.75  | 8.53   | 6.89   | 7.05   | 7.66   | 16.72  | 7.35   |
| MnO   | .18   | .20    | .19    | .19   | .13    | .11    | .17    | .20    | .15    | .13    |
| MgO   | 14.60 | 16.14  | 16.06  | 15.66 | 15.32  | 16.27  | 15.86  | 16.60  | 11.24  | 16.14  |
| NiO   | 0.00  | 0.00   | 0.00   | 0.00  | 0.00   | 0.00   | 0.00   | 0.00   | 0.00   | 0.00   |
| CaO   | 20.02 | 20.66  | 21.41  | 20.23 | 21.20  | 21.02  | 21.40  | 20.64  | 11.64  | 21.51  |
| Na2O  | .43   | .35    | .25    | .21   | .35    | .30    | .28    | .32    | 1.71   | .25    |
| K2O   | .02   | .01    | .01    | .01   | 0.00   | .01    | 0.00   | .01    | .40    | .02    |
| Total | 98.80 | 101.51 | 100.75 | 98.83 | 101.03 | 100.07 | 100.79 | 100.25 | 100.89 | 101.69 |

|       |       |       |       |       |       |       |       |       |       |       |
|-------|-------|-------|-------|-------|-------|-------|-------|-------|-------|-------|
| Si    | 1.878 | 1.906 | 1.895 | 1.940 | 1.892 | 1.915 | 1.897 | 1.898 | 1.674 | 1.901 |
| Al IV | .122  | .082  | .105  | .060  | .108  | .085  | .103  | .098  | .326  | .099  |
| Al VI | .013  | 0.000 | .013  | .012  | .001  | .014  | .014  | 0.000 | .139  | .015  |
| Ti    | .049  | .033  | .032  | .035  | .047  | .029  | .032  | .028  | .119  | .030  |
| Cr    | .003  | 0.000 | .012  | 0.000 | 0.000 | .006  | .015  | .009  | .003  | .009  |
| Fe    | .283  | .282  | .215  | .243  | .263  | .213  | .217  | .237  | .529  | .224  |
| Mn    | .006  | .006  | .006  | .006  | .004  | .003  | .005  | .006  | .005  | .004  |
| Mg    | .823  | .884  | .880  | .873  | .842  | .895  | .869  | .916  | .634  | .876  |
| Ni    | 0.000 | 0.000 | 0.000 | 0.000 | 0.000 | 0.000 | 0.000 | 0.000 | 0.000 | 0.000 |
| Ca    | .811  | .814  | .843  | .811  | .838  | .831  | .843  | .818  | .472  | .840  |
| Na    | .032  | .025  | .018  | .015  | .025  | .021  | .020  | .023  | .125  | .018  |
| K     | .001  | .000  | .000  | .000  | 0.000 | .000  | 0.000 | .000  | .019  | .001  |
| Total | 4.020 | 4.033 | 4.018 | 3.996 | 4.019 | 4.014 | 4.015 | 4.033 | 4.045 | 4.016 |

|       |      |      |      |      |      |      |      |      |      |      |
|-------|------|------|------|------|------|------|------|------|------|------|
| Ca    | 42.2 | 41.0 | 43.4 | 42.0 | 43.0 | 42.8 | 43.6 | 41.4 | 28.8 | 43.2 |
| Mg    | 42.8 | 44.5 | 45.3 | 45.2 | 43.3 | 46.1 | 44.9 | 46.3 | 38.7 | 45.1 |
| Fe+Mn | 15.0 | 14.5 | 11.4 | 12.9 | 13.7 | 11.1 | 11.5 | 12.3 | 32.6 | 11.7 |

|       | 21     | 22     | 23     | 24    | 25     | 26     | 27     | 28     | 29     | 30     |
|-------|--------|--------|--------|-------|--------|--------|--------|--------|--------|--------|
| SiO2  | 52.15  | 51.62  | 50.58  | 50.36 | 49.88  | 51.69  | 52.05  | 52.24  | 50.93  | 51.99  |
| TiO2  | .96    | 1.37   | 1.54   | 1.30  | 1.32   | 1.14   | .70    | 1.00   | 1.04   | .84    |
| Al2O3 | 2.14   | 2.29   | 2.73   | 2.20  | 2.06   | 1.82   | 1.05   | 1.57   | 1.73   | 1.16   |
| Cr2O3 | .20    | 0.00   | 0.00   | 0.00  | 0.00   | 0.00   | 0.00   | 0.00   | 0.00   | 0.00   |
| FeO   | 7.08   | 9.91   | 9.58   | 10.13 | 12.61  | 11.28  | 14.43  | 10.98  | 11.54  | 12.56  |
| MnO   | .14    | .13    | .20    | .25   | .25    | .29    | .26    | .25    | .23    | .32    |
| MgO   | 16.72  | 15.03  | 14.97  | 14.85 | 13.31  | 13.38  | 11.73  | 13.81  | 14.02  | 13.07  |
| NaO   | 0.00   | 0.00   | 0.00   | 0.00  | 0.00   | 0.00   | 0.00   | 0.00   | 0.00   | 0.00   |
| CaO   | 21.11  | 21.01  | 20.60  | 20.59 | 21.20  | 21.23  | 21.16  | 21.09  | 21.28  | 21.31  |
| Na2O  | .25    | .37    | .30    | .28   | .36    | .35    | .25    | .36    | .30    | .36    |
| K2O   | 0.00   | .01    | .01    | .02   | .02    | 0.00   | .01    | .01    | .01    | 0.00   |
| Total | 100.78 | 101.82 | 100.54 | 99.99 | 101.01 | 101.18 | 101.64 | 101.31 | 101.12 | 101.63 |

|       |       |       |       |       |       |       |       |       |       |       |
|-------|-------|-------|-------|-------|-------|-------|-------|-------|-------|-------|
| Si    | 1.913 | 1.900 | 1.883 | 1.892 | 1.882 | 1.926 | 1.956 | 1.939 | 1.906 | 1.941 |
| AlIV  | .087  | .099  | .117  | .097  | .092  | .074  | .044  | .061  | .076  | .051  |
| AlVI  | .005  | 0.000 | .003  | 0.000 | 0.000 | .006  | .002  | .007  | 0.000 | 0.000 |
| Ti    | .026  | .038  | .043  | .037  | .037  | .032  | .020  | .028  | .029  | .024  |
| Cr    | .006  | 0.000 | 0.000 | 0.000 | 0.000 | 0.000 | 0.000 | 0.000 | 0.000 | 0.000 |
| Fe    | .217  | .305  | .298  | .318  | .398  | .352  | .453  | .341  | .361  | .392  |
| Mn    | .004  | .004  | .006  | .008  | .008  | .009  | .008  | .008  | .007  | .010  |
| Mg    | .914  | .825  | .831  | .831  | .748  | .743  | .657  | .764  | .782  | .727  |
| Ni    | 0.000 | 0.000 | 0.000 | 0.000 | 0.000 | 0.000 | 0.000 | 0.000 | 0.000 | 0.000 |
| Ca    | .830  | .828  | .822  | .829  | .857  | .848  | .852  | .839  | .853  | .852  |
| Na    | .018  | .026  | .022  | .020  | .026  | .025  | .018  | .026  | .022  | .026  |
| K     | 0.000 | .000  | .000  | .001  | .001  | 0.000 | .000  | .000  | .000  | 0.000 |
| Total | 4.021 | 4.026 | 4.025 | 4.034 | 4.049 | 4.015 | 4.011 | 4.012 | 4.038 | 4.023 |

|       |      |      |      |      |      |      |      |      |      |      |
|-------|------|------|------|------|------|------|------|------|------|------|
| Ca    | 42.2 | 42.2 | 42.0 | 41.7 | 42.6 | 43.4 | 43.2 | 43.0 | 42.6 | 43.0 |
| Mg    | 46.5 | 42.0 | 42.4 | 41.9 | 37.2 | 38.1 | 33.3 | 39.2 | 39.0 | 36.7 |
| Fe+Mn | 11.3 | 15.8 | 15.6 | 16.4 | 20.2 | 18.5 | 23.4 | 17.9 | 18.4 | 20.3 |

|       | 31    | 32     | 33     | 34     | 35     | 36     | 37     | 38     | 39    | 40    |
|-------|-------|--------|--------|--------|--------|--------|--------|--------|-------|-------|
| SiO2  | 51.11 | 50.73  | 50.71  | 51.80  | 50.74  | 51.92  | 51.03  | 50.83  | 50.52 | 48.69 |
| TiO2  | 1.02  | 1.03   | 1.68   | 1.25   | 1.74   | 1.35   | 1.33   | 1.28   | .93   | 2.09  |
| Al2O3 | 1.57  | 1.70   | 3.35   | 1.74   | 3.24   | 1.79   | 2.71   | 2.82   | 1.84  | 3.13  |
| Cr2O3 | 0.00  | 0.00   | .09    | 0.00   | 0.00   | 0.00   | .19    | .36    | .17   | .02   |
| FeO   | 9.97  | 11.25  | 7.80   | 11.18  | 10.55  | 10.25  | 7.46   | 7.55   | 7.71  | 10.60 |
| MnO   | .26   | .20    | .11    | .23    | .23    | .21    | .09    | .09    | .20   | .22   |
| MgO   | 14.28 | 14.11  | 14.95  | 14.75  | 13.91  | 14.73  | 16.00  | 15.57  | 16.29 | 13.98 |
| NiO   | 0.00  | 0.00   | .02    | 0.00   | 0.00   | 0.00   | .08    | 0.00   | .07   | .04   |
| CaO   | 21.21 | 21.61  | 21.37  | 19.99  | 21.07  | 20.21  | 21.79  | 21.89  | 20.63 | 20.73 |
| Na2O  | .31   | .29    | .27    | .39    | .46    | .26    | .30    | .30    | .24   | .36   |
| K2O   | 0.00  | .01    | 0.00   | .02    | .01    | .01    | 0.00   | 0.00   | .01   | .01   |
| Total | 99.77 | 100.93 | 100.35 | 101.35 | 101.95 | 100.73 | 100.98 | 100.69 | 98.61 | 99.87 |

|       |       |       |       |       |       |       |       |       |       |       |
|-------|-------|-------|-------|-------|-------|-------|-------|-------|-------|-------|
| Si    | 1.924 | 1.902 | 1.878 | 1.920 | 1.872 | 1.927 | 1.879 | 1.879 | 1.904 | 1.842 |
| AlIV  | .070  | .075  | .122  | .076  | .128  | .073  | .118  | .121  | .082  | .140  |
| AlVI  | 0.000 | 0.000 | .024  | 0.000 | .013  | .005  | 0.000 | .001  | 0.000 | 0.000 |
| Ti    | .029  | .029  | .047  | .035  | .048  | .038  | .037  | .036  | .026  | .059  |
| Cr    | 0.000 | 0.000 | .003  | 0.000 | 0.000 | 0.000 | .006  | .011  | .005  | .001  |
| Fe    | .314  | .353  | .242  | .347  | .326  | .318  | .230  | .233  | .243  | .335  |
| Mn    | .008  | .006  | .003  | .007  | .007  | .007  | .003  | .003  | .006  | .007  |
| Mg    | .801  | .788  | .825  | .815  | .765  | .815  | .878  | .858  | .915  | .788  |
| Ni    | 0.000 | 0.000 | .001  | 0.000 | 0.000 | 0.000 | .002  | 0.000 | .002  | .001  |
| Ca    | .855  | .868  | .848  | .794  | .833  | .804  | .860  | .867  | .833  | .840  |
| Na    | .023  | .021  | .019  | .028  | .033  | .019  | .021  | .021  | .018  | .026  |
| K     | 0.000 | .000  | 0.000 | .001  | .000  | .000  | 0.000 | 0.000 | .000  | .000  |
| Total | 4.024 | 4.043 | 4.011 | 4.022 | 4.026 | 4.006 | 4.033 | 4.030 | 4.035 | 4.042 |

|       |      |      |      |      |      |      |      |      |      |      |
|-------|------|------|------|------|------|------|------|------|------|------|
| Ca    | 43.2 | 43.1 | 44.2 | 40.5 | 43.1 | 41.4 | 43.6 | 44.2 | 41.7 | 42.6 |
| Mg    | 40.5 | 39.1 | 43.0 | 41.5 | 39.6 | 41.9 | 44.6 | 43.7 | 45.8 | 40.0 |
| Fe+Mn | 16.3 | 17.8 | 12.8 | 18.0 | 17.2 | 16.7 | 11.8 | 12.0 | 12.5 | 17.4 |

|       | 41    | 42    | 43    | 44    | 45     | 46    | 47    | 48    | 49    | 50    |
|-------|-------|-------|-------|-------|--------|-------|-------|-------|-------|-------|
| SiO2  | 49.49 | 49.91 | 47.68 | 48.00 | 49.41  | 49.26 | 49.34 | 51.62 | 49.47 | 49.12 |
| TiO2  | 1.25  | 1.32  | 2.18  | 2.14  | 1.87   | 1.47  | 1.40  | .67   | 1.02  | 1.49  |
| Al2O3 | 1.84  | 1.89  | 3.78  | 3.79  | 3.48   | 2.69  | 2.52  | .95   | 2.29  | 3.01  |
| Cr2O3 | .02   | 0.00  | 0.00  | .04   | 0.00   | 0.00  | .02   | 0.00  | 0.00  | .04   |
| FeO   | 10.08 | 10.44 | 11.72 | 9.99  | 11.43  | 11.60 | 12.36 | 10.58 | 10.09 | 8.36  |
| MnO   | .17   | .21   | .22   | .14   | .14    | .27   | .20   | .38   | .31   | .19   |
| MgO   | 15.20 | 15.08 | 13.00 | 13.93 | 12.98  | 12.84 | 13.14 | 14.00 | 13.68 | 14.48 |
| NiO   | 0.00  | 0.00  | .02   | 0.00  | 0.00   | .02   | 0.00  | 0.00  | 0.00  | .07   |
| CaO   | 20.30 | 19.35 | 20.33 | 20.54 | 20.45  | 20.71 | 19.98 | 20.63 | 20.72 | 21.46 |
| Na2O  | .32   | .37   | .55   | .53   | .44    | .35   | .46   | .82   | .51   | .37   |
| K2O   | .01   | .01   | .02   | 0.00  | .01    | 0.00  | .01   | 0.00  | 0.00  | 0.00  |
| Total | 98.68 | 98.58 | 99.50 | 99.10 | 100.21 | 99.21 | 99.43 | 99.65 | 98.09 | 98.59 |

|       |       |       |       |       |       |       |       |       |       |       |
|-------|-------|-------|-------|-------|-------|-------|-------|-------|-------|-------|
| Si    | 1.886 | 1.900 | 1.822 | 1.826 | 1.863 | 1.881 | 1.883 | 1.950 | 1.899 | 1.865 |
| AlIV  | .083  | .085  | .170  | .170  | .137  | .119  | .113  | .042  | .101  | .135  |
| AlVI  | 0.000 | 0.000 | 0.000 | 0.000 | .017  | .002  | 0.000 | 0.000 | .003  | .000  |
| Ti    | .036  | .038  | .063  | .061  | .053  | .042  | .040  | .019  | .029  | .043  |
| Cr    | .001  | 0.000 | 0.000 | .001  | 0.000 | 0.000 | .001  | 0.000 | 0.000 | .001  |
| Fe    | .321  | .332  | .375  | .318  | .360  | .371  | .394  | .334  | .324  | .266  |
| Mn    | .005  | .007  | .007  | .005  | .004  | .009  | .006  | .012  | .010  | .006  |
| Mg    | .863  | .856  | .740  | .790  | .729  | .731  | .747  | .788  | .783  | .820  |
| Ni    | 0.000 | 0.000 | .001  | 0.000 | 0.000 | .001  | 0.000 | 0.000 | 0.000 | .002  |
| Ca    | .829  | .789  | .832  | .837  | .826  | .847  | .817  | .835  | .852  | .873  |
| Na    | .024  | .027  | .041  | .039  | .032  | .026  | .034  | .060  | .038  | .027  |
| K     | .000  | .000  | .001  | 0.000 | .000  | 0.000 | .000  | 0.000 | 0.000 | 0.000 |
| Total | 4.048 | 4.034 | 4.051 | 4.047 | 4.023 | 4.029 | 4.037 | 4.040 | 4.039 | 4.038 |

|       |      |      |      |      |      |      |      |      |      |      |
|-------|------|------|------|------|------|------|------|------|------|------|
| Ca    | 41.1 | 39.8 | 42.6 | 42.9 | 43.0 | 43.3 | 41.6 | 42.4 | 43.3 | 44.4 |
| Mg    | 42.8 | 43.1 | 37.9 | 40.5 | 38.0 | 37.3 | 38.0 | 40.0 | 39.8 | 41.7 |
| Fe+Mn | 16.2 | 17.1 | 19.5 | 16.5 | 19.0 | 19.4 | 20.4 | 17.6 | 17.0 | 13.8 |

|       | 51    | 52    | 53    | 54    | 55    | 56     | 57    | 58    | 59    | 60    |
|-------|-------|-------|-------|-------|-------|--------|-------|-------|-------|-------|
| SiO2  | 50.81 | 49.78 | 50.28 | 50.92 | 52.48 | 51.95  | 50.35 | 51.16 | 51.02 | 52.09 |
| TiO2  | 1.33  | 1.31  | 1.09  | .70   | .63   | 1.25   | 1.23  | .96   | 1.16  | 1.05  |
| Al2O3 | 2.49  | 2.51  | 1.93  | 2.23  | 1.11  | 2.07   | 2.02  | 1.57  | 2.02  | 1.98  |
| Cr2O3 | 0.00  | 0.00  | .08   | .49   | .02   | .08    | .05   | .04   | .10   | .19   |
| FeO   | 8.21  | 7.98  | 8.22  | 6.79  | 8.35  | 8.43   | 8.18  | 8.68  | 8.14  | 7.10  |
| MnO   | .11   | .13   | .18   | .14   | .16   | .13    | .16   | .21   | .13   | .16   |
| MgO   | 14.53 | 15.27 | 15.89 | 16.20 | 15.91 | 16.34  | 16.15 | 16.03 | 16.23 | 16.55 |
| NiO   | .09   | 0.00  | .11   | .04   | .04   | .09    | .03   | 0.00  | .02   | .07   |
| CaO   | 21.50 | 21.58 | 20.00 | 20.25 | 20.22 | 19.98  | 19.68 | 19.53 | 19.81 | 20.30 |
| Na2O  | .31   | .38   | .32   | .34   | .45   | .20    | .35   | .38   | .32   | .27   |
| K2O   | 0.00  | 0.00  | 0.00  | .01   | .01   | .01    | 0.00  | 0.00  | .01   | .02   |
| Total | 99.38 | 98.94 | 98.10 | 98.11 | 99.38 | 100.53 | 98.20 | 98.56 | 98.96 | 99.78 |

|       |       |       |       |       |       |       |       |       |       |       |
|-------|-------|-------|-------|-------|-------|-------|-------|-------|-------|-------|
| Si    | 1.905 | 1.878 | 1.906 | 1.916 | 1.957 | 1.915 | 1.904 | 1.928 | 1.912 | 1.926 |
| AlIV  | .095  | .112  | .086  | .084  | .043  | .085  | .090  | .070  | .088  | .074  |
| AlVI  | .015  | 0.000 | 0.000 | .015  | .006  | .005  | 0.000 | 0.000 | .001  | .012  |
| Ti    | .037  | .037  | .031  | .020  | .018  | .035  | .035  | .027  | .033  | .029  |
| Cr    | 0.000 | 0.000 | .002  | .015  | .001  | .002  | .001  | .001  | .003  | .006  |
| Fe    | .257  | .252  | .261  | .214  | .260  | .260  | .259  | .274  | .255  | .219  |
| Mn    | .003  | .004  | .006  | .004  | .005  | .004  | .005  | .007  | .004  | .005  |
| Mg    | .812  | .859  | .898  | .909  | .884  | .898  | .910  | .900  | .906  | .912  |
| Ni    | .003  | 0.000 | .003  | .001  | .001  | .003  | .001  | 0.000 | .001  | .002  |
| Ca    | .864  | .872  | .812  | .817  | .808  | .789  | .797  | .789  | .795  | .804  |
| Na    | .023  | .028  | .024  | .025  | .033  | .014  | .026  | .028  | .023  | .019  |
| K     | 0.000 | 0.000 | 0.000 | .000  | .000  | .000  | 0.000 | 0.000 | .000  | .001  |
| Total | 4.014 | 4.042 | 4.030 | 4.020 | 4.017 | 4.011 | 4.028 | 4.023 | 4.022 | 4.009 |

|       |      |      |      |      |      |      |      |      |      |      |
|-------|------|------|------|------|------|------|------|------|------|------|
| Ca    | 44.6 | 43.9 | 41.1 | 42.0 | 41.3 | 40.5 | 40.4 | 40.0 | 40.6 | 41.4 |
| Mg    | 41.9 | 43.2 | 45.4 | 46.8 | 45.2 | 46.0 | 46.2 | 45.7 | 46.2 | 47.0 |
| Fe+Mn | 13.5 | 12.9 | 13.5 | 11.2 | 13.6 | 13.5 | 13.4 | 14.2 | 13.2 | 11.6 |

|       | 61     | 62    | 63    | 64    | 65    | 66    | 67    | 68    | 69    |
|-------|--------|-------|-------|-------|-------|-------|-------|-------|-------|
| SiO2  | 51.85  | 51.73 | 51.07 | 52.41 | 48.84 | 49.59 | 51.87 | 50.48 | 50.61 |
| TiO2  | 1.11   | .86   | .96   | .76   | 2.19  | 1.70  | .87   | 1.58  | .99   |
| Al2O3 | 1.84   | 1.90  | 2.11  | 2.00  | 3.83  | 3.18  | 2.29  | 3.16  | 2.55  |
| Cr2O3 | 0.00   | .27   | .31   | .49   | 0.00  | .05   | .38   | .05   | .51   |
| FeO   | 8.96   | 6.65  | 6.82  | 6.62  | 9.27  | 8.04  | 6.70  | 8.00  | 6.25  |
| MnO   | .24    | .16   | .19   | .13   | .16   | .16   | .09   | .14   | .14   |
| MgO   | 15.87  | 16.55 | 16.32 | 16.73 | 14.22 | 15.00 | 16.18 | 14.92 | 15.79 |
| NiO   | 0.00   | 0.00  | 0.00  | .04   | .04   | .06   | 0.00  | 0.00  | 0.00  |
| CaO   | 19.98  | 20.23 | 20.40 | 20.38 | 20.16 | 20.97 | 20.68 | 20.84 | 21.01 |
| Na2O  | .28    | .31   | .20   | .21   | .41   | .35   | .31   | .38   | .31   |
| K2O   | .02    | .01   | 0.00  | .02   | .01   | .01   | 0.00  | 0.00  | .02   |
| Total | 100.15 | 98.67 | 98.38 | 99.79 | 99.13 | 99.11 | 99.37 | 99.55 | 98.18 |

|       |       |       |       |       |       |       |       |       |       |
|-------|-------|-------|-------|-------|-------|-------|-------|-------|-------|
| Si    | 1.924 | 1.930 | 1.916 | 1.932 | 1.845 | 1.865 | 1.923 | 1.884 | 1.904 |
| Al IV | .076  | .070  | .084  | .068  | .155  | .135  | .077  | .116  | .096  |
| Al VI | .005  | .014  | .009  | .019  | .015  | .006  | .024  | .023  | .017  |
| Ti    | .031  | .024  | .027  | .021  | .062  | .048  | .024  | .044  | .028  |
| Cr    | 0.000 | .008  | .009  | .014  | 0.000 | .001  | .011  | .001  | .015  |
| Fe    | .278  | .208  | .214  | .204  | .293  | .253  | .208  | .250  | .197  |
| Mn    | .008  | .005  | .006  | .004  | .005  | .005  | .003  | .004  | .004  |
| Mg    | .878  | .921  | .913  | .919  | .800  | .841  | .894  | .830  | .885  |
| Ni    | 0.000 | 0.000 | 0.000 | .001  | .001  | .002  | 0.000 | 0.000 | 0.000 |
| Ca    | .794  | .809  | .820  | .805  | .816  | .845  | .822  | .834  | .847  |
| Na    | .020  | .022  | .015  | .015  | .030  | .026  | .022  | .028  | .023  |
| K     | .001  | .000  | 0.000 | .001  | .000  | .000  | 0.000 | 0.000 | .001  |
| Total | 4.015 | 4.011 | 4.013 | 4.004 | 4.023 | 4.028 | 4.008 | 4.015 | 4.016 |

|       |      |      |      |      |      |      |      |      |      |
|-------|------|------|------|------|------|------|------|------|------|
| Ca    | 40.6 | 41.7 | 42.0 | 41.7 | 42.6 | 43.5 | 42.6 | 43.5 | 43.8 |
| Mg    | 44.8 | 47.4 | 46.7 | 47.6 | 41.8 | 43.3 | 46.4 | 43.3 | 45.8 |
| Fe+Mn | 14.6 | 10.9 | 11.3 | 10.8 | 15.6 | 13.3 | 10.9 | 13.3 | 10.4 |

CAPE ST. MARY'S SILL MINERALS

442

Pyroxenes, olivines, amphiboles, biotites and plagioclases were analyzed from the sills on Cape St. Mary's. The following table gives locations and rock types for each of the samples examined. In the case of the Gull Cove sill, the samples are listed from near the top (granophyre) to the base of the sill. The analysis numbers are applicable to the pyroxene data only, but the rock type and sample location information is the same for all of the mineral analyses which follow the pyroxenes.

| Location   | Sample Number | Rock Type  | Pyroxene Analysis Nos. |
|------------|---------------|------------|------------------------|
| Gull Cove  | SB7L          | Granophyre | 1                      |
|            | SB7K          | Granophyre | 2 to 4                 |
|            | SB7I          | Gabbro     | 5 and 6                |
|            | SB6K          | Gabbro     | 7 and 8                |
|            | SB6I          | Gabbro     | 9 and 10               |
|            | SB6H          | Gabbro     | 11 to 15               |
|            | SB6F          | Gabbro     | 16 to 18               |
|            | SB6D          | Gabbro     | 19 to 21               |
|            | SB6OE         | Cumulate   | 22                     |
|            | SB6OF         | Cumulate   | -                      |
| Lance Cove | SB6OH         | Cumulate   | 23 to 25               |
|            | 5.9.79.6      | Gabbro     | 26 to 29               |
|            | 23.5.79.2     | Gabbro     | 30 to 35               |
|            | 5.9.79.2      | Gabbro     | 36 to 43               |
|            | 5.9.79.8      | Gabbro     | 44 to 49               |
|            | 5.9.79.10     | Gabbro     | 50 to 56               |

|       | 1      | 2      | 3      | 4      | 5      | 6     | 7      | 8     | 9     | 10     |
|-------|--------|--------|--------|--------|--------|-------|--------|-------|-------|--------|
| SiO2  | 51.34  | 50.34  | 51.67  | 51.04  | 49.88  | 49.31 | 50.90  | 48.98 | 51.29 | 51.05  |
| TiO2  | .22    | .65    | .85    | .43    | 1.48   | 1.17  | 1.06   | 1.04  | .87   | 1.11   |
| Al2O3 | .36    | 1.39   | 1.80   | .95    | 3.63   | 3.45  | 2.95   | 2.18  | 1.81  | 2.45   |
| Cr2O3 | .01    | 0.00   | 0.00   | 0.00   | .02    | .04   | 0.00   | .02   | .04   | 0.00   |
| FeO   | 11.99  | 13.00  | 10.54  | 16.02  | 8.19   | 8.29  | 8.48   | 9.04  | 10.01 | 10.13  |
| MnO   | .20    | .34    | .23    | .51    | .14    | .17   | .17    | .21   | .28   | .16    |
| MgO   | 12.34  | 11.51  | 13.60  | 9.40   | 13.95  | 14.07 | 14.34  | 13.32 | 13.71 | 13.84  |
| NiO   | 0.00   | 0.00   | .08    | .07    | .01    | 0.00  | .05    | 0.00  | 0.00  | .01    |
| CaO   | 23.60  | 22.51  | 21.69  | 21.38  | 22.18  | 22.12 | 21.75  | 22.95 | 20.21 | 21.22  |
| Na2O  | .58    | .48    | .42    | .63    | .54    | .39   | .43    | .49   | .40   | .52    |
| K2O   | 0.00   | 0.00   | 0.00   | 0.00   | .01    | .02   | 0.00   | 0.00  | .01   | .05    |
| Total | 100.64 | 100.22 | 100.88 | 100.43 | 100.03 | 99.03 | 100.13 | 98.23 | 98.63 | 100.54 |

|       |       |       |       |       |       |       |       |       |       |       |
|-------|-------|-------|-------|-------|-------|-------|-------|-------|-------|-------|
| Si    | 1.948 | 1.924 | 1.928 | 1.965 | 1.865 | 1.865 | 1.897 | 1.883 | 1.945 | 1.907 |
| Al IV | .016  | .063  | .072  | .035  | .135  | .135  | .103  | .099  | .055  | .093  |
| Al VI | 0.000 | 0.000 | .007  | .008  | .025  | .018  | .027  | 0.000 | .026  | .015  |
| Ti    | .006  | .019  | .024  | .012  | .042  | .033  | .030  | .030  | .025  | .031  |
| Cr    | .000  | 0.000 | 0.000 | 0.000 | .001  | .001  | 0.000 | .001  | .001  | 0.000 |
| Fe    | .381  | .415  | .329  | .516  | .256  | .262  | .264  | .291  | .317  | .316  |
| Mn    | .006  | .011  | .007  | .017  | .004  | .005  | .005  | .007  | .009  | .005  |
| Mg    | .698  | .656  | .756  | .540  | .777  | .793  | .797  | .763  | .775  | .771  |
| Ni    | 0.000 | 0.000 | .002  | .002  | .000  | 0.000 | .001  | 0.000 | 0.000 | .000  |
| Ca    | .960  | .922  | .867  | .882  | .888  | .896  | .869  | .945  | .821  | .849  |
| Na    | .043  | .036  | .030  | .047  | .039  | .029  | .031  | .037  | .029  | .038  |
| K     | 0.000 | 0.000 | 0.000 | 0.000 | .000  | .001  | 0.000 | 0.000 | .000  | .002  |
| Total | 4.058 | 4.044 | 4.024 | 4.024 | 4.033 | 4.039 | 4.024 | 4.055 | 4.004 | 4.028 |

|       |      |      |      |      |      |      |      |      |      |      |
|-------|------|------|------|------|------|------|------|------|------|------|
| Ca    | 46.9 | 46.0 | 44.2 | 45.1 | 46.1 | 45.8 | 44.9 | 47.1 | 42.7 | 43.7 |
| Mg    | 34.1 | 32.7 | 38.6 | 27.6 | 40.4 | 40.5 | 41.2 | 38.0 | 40.3 | 39.7 |
| Fe+Mn | 18.9 | 21.3 | 17.2 | 27.3 | 13.5 | 13.7 | 13.9 | 14.8 | 17.0 | 16.6 |



|       | 11    | 12    | 13    | 14    | 15    | 16    | 17     | 18    | 19    | 20    |
|-------|-------|-------|-------|-------|-------|-------|--------|-------|-------|-------|
| SiO2  | 50.41 | 51.77 | 48.93 | 50.29 | 50.07 | 51.18 | 49.92  | 51.01 | 49.13 | 48.34 |
| TiO2  | 1.08  | .72   | 1.13  | 1.13  | 1.11  | .46   | 1.22   | .41   | .98   | 1.25  |
| Al2O3 | 2.23  | 1.73  | 2.63  | 2.21  | 2.79  | 5.12  | 2.81   | 2.23  | 2.30  | 3.59  |
| Cr2O3 | 0.00  | 0.00  | 0.00  | 0.00  | .03   | .65   | .07    | .23   | .05   | 0.00  |
| FeO   | 11.08 | 10.81 | 11.08 | 11.34 | 10.75 | 3.81  | 10.47  | 8.30  | 14.76 | 10.76 |
| MnO   | .27   | .28   | .31   | .28   | .26   | .07   | .25    | .14   | .42   | .19   |
| MgO   | 13.95 | 14.71 | 14.13 | 13.89 | 14.34 | 15.45 | 13.68  | 14.91 | 10.94 | 13.69 |
| NiO   | .01   | .01   | 0.00  | 0.00  | 0.00  | .05   | 0.00   | .05   | 0.00  | 0.00  |
| CaO   | 20.43 | 18.67 | 19.38 | 19.60 | 19.91 | 21.64 | 21.20  | 21.43 | 20.68 | 20.43 |
| Na2O  | .42   | .43   | .50   | .48   | .34   | .95   | .40    | .31   | .53   | .37   |
| K2O   | 0.00  | 0.00  | .03   | .03   | .01   | 0.00  | 0.00   | 0.00  | 0.00  | 0.00  |
| Total | 99.88 | 99.13 | 98.12 | 99.25 | 99.61 | 99.38 | 100.02 | 99.02 | 99.79 | 98.62 |

|       |       |       |       |       |       |       |       |       |       |       |
|-------|-------|-------|-------|-------|-------|-------|-------|-------|-------|-------|
| Si    | 1.903 | 1.950 | 1.881 | 1.909 | 1.889 | 1.881 | 1.882 | 1.920 | 1.895 | 1.851 |
| AlIV  | .097  | .050  | .119  | .091  | .111  | .119  | .118  | .080  | .105  | .149  |
| AlVI  | .002  | .027  | .000  | .007  | .013  | .102  | .006  | .019  | 0.000 | .013  |
| Ti    | .031  | .020  | .033  | .032  | .031  | .013  | .035  | .012  | .028  | .036  |
| Cr    | 0.000 | 0.000 | 0.000 | 0.000 | .001  | .019  | .002  | .007  | .002  | 0.000 |
| Fe    | .350  | .340  | .356  | .360  | .339  | .117  | .330  | .261  | .476  | .345  |
| Mn    | .009  | .009  | .010  | .009  | .008  | .002  | .008  | .004  | .014  | .006  |
| Mg    | .785  | .826  | .810  | .786  | .806  | .846  | .769  | .836  | .629  | .781  |
| Ni    | .000  | .000  | 0.000 | 0.000 | 0.000 | .001  | 0.000 | .002  | 0.000 | 0.000 |
| Ca    | .826  | .753  | .798  | .797  | .805  | .852  | .856  | .864  | .855  | .838  |
| Na    | .031  | .031  | .037  | .035  | .025  | .068  | .029  | .023  | .040  | .027  |
| K     | 0.000 | 0.000 | .001  | .001  | .000  | 0.000 | 0.000 | 0.000 | 0.000 | 0.000 |
| Total | 4.033 | 4.007 | 4.046 | 4.028 | 4.030 | 4.020 | 4.035 | 4.027 | 4.043 | 4.046 |

|       |      |      |      |      |      |      |      |      |      |      |
|-------|------|------|------|------|------|------|------|------|------|------|
| Ca    | 42.0 | 39.1 | 40.4 | 40.8 | 41.1 | 46.9 | 43.6 | 43.9 | 43.3 | 42.5 |
| Mg    | 39.9 | 42.8 | 41.6 | 40.3 | 41.2 | 46.6 | 39.2 | 42.5 | 31.9 | 39.7 |
| Fe+Mn | 18.2 | 18.1 | 18.6 | 18.9 | 17.7 | 6.6  | 17.2 | 13.5 | 24.8 | 17.8 |

|       | 21    | 22     | 23    | 24     | 25    | 26    | 27    | 28    | 29    | 30    |
|-------|-------|--------|-------|--------|-------|-------|-------|-------|-------|-------|
| SiO2  | 49.43 | 51.95  | 49.85 | 50.48  | 49.86 | 51.02 | 50.34 | 50.96 | 45.81 | 51.16 |
| TiO2  | 1.45  | .69    | 1.37  | 1.95   | 1.22  | .91   | 1.04  | .76   | 2.64  | .87   |
| Al2O3 | 3.62  | 2.89   | 4.23  | 3.30   | 3.86  | 1.67  | 2.71  | 1.36  | 6.84  | 2.19  |
| Cr2O3 | .05   | .37    | .52   | .10    | .45   | 0.00  | 0.00  | 0.00  | .20   | 0.00  |
| FeO   | 9.73  | 6.36   | 6.34  | 5.93   | 6.07  | 10.69 | 8.94  | 11.20 | 11.50 | 10.88 |
| MnO   | .26   | .11    | .01   | .09    | .09   | .18   | .14   | .25   | .19   | .21   |
| MgO   | 12.55 | 15.81  | 14.70 | 14.92  | 14.23 | 13.47 | 13.81 | 12.72 | 11.50 | 13.45 |
| NiO   | .11   | 0.00   | 0.00  | .05    | 0.00  | 0.00  | 0.00  | 0.00  | 0.00  | 0.00  |
| CaO   | 21.97 | 22.74  | 21.96 | 24.16  | 23.02 | 21.17 | 21.32 | 21.07 | 19.44 | 20.71 |
| Na2O  | .41   | .30    | .47   | .66    | .36   | .39   | .37   | .50   | .91   | .37   |
| K2O   | .04   | .04    | 0.00  | 0.00   | 0.00  | 0.00  | .01   | 0.00  | .08   | .01   |
| Total | 99.62 | 101.26 | 99.45 | 101.64 | 99.16 | 99.50 | 98.71 | 98.82 | 99.15 | 99.85 |

|       |       |       |       |       |       |       |       |       |       |       |
|-------|-------|-------|-------|-------|-------|-------|-------|-------|-------|-------|
| Si    | 1.870 | 1.899 | 1.857 | 1.850 | 1.866 | 1.930 | 1.907 | 1.947 | 1.755 | 1.926 |
| AlIV  | .130  | .101  | .143  | .143  | .134  | .070  | .093  | .053  | .245  | .074  |
| AlVI  | .031  | .023  | .043  | 0.000 | .037  | .005  | .028  | .008  | .064  | .023  |
| Ti    | .041  | .019  | .038  | .054  | .034  | .026  | .030  | .022  | .076  | .025  |
| Cr    | .001  | .011  | .015  | .003  | .013  | 0.000 | 0.000 | 0.000 | .006  | 0.000 |
| Fe    | .308  | .194  | .198  | .182  | .190  | .338  | .283  | .358  | .368  | .343  |
| Mn    | .008  | .003  | .000  | .003  | .003  | .006  | .004  | .008  | .006  | .007  |
| Mg    | .708  | .861  | .816  | .815  | .794  | .760  | .780  | .724  | .657  | .755  |
| Ni    | .003  | 0.000 | 0.000 | .001  | 0.000 | 0.000 | 0.000 | 0.000 | 0.000 | 0.000 |
| Ca    | .890  | .891  | .877  | .949  | .923  | .858  | .865  | .862  | .798  | .835  |
| Na    | .030  | .021  | .034  | .047  | .026  | .029  | .027  | .037  | .068  | .027  |
| K     | .002  | .002  | 0.000 | 0.000 | 0.000 | 0.000 | .000  | 0.000 | .004  | .000  |
| Total | 4.023 | 4.026 | 4.021 | 4.047 | 4.021 | 4.021 | 4.017 | 4.019 | 4.047 | 4.015 |

|       |      |      |      |      |      |      |      |      |      |      |
|-------|------|------|------|------|------|------|------|------|------|------|
| Ca    | 46.5 | 45.7 | 46.4 | 48.7 | 48.3 | 43.7 | 44.8 | 44.2 | 43.6 | 43.1 |
| Mg    | 37.0 | 44.2 | 43.2 | 41.8 | 41.6 | 38.7 | 40.3 | 37.1 | 35.9 | 38.9 |
| Fe+Mn | 16.5 | 10.1 | 10.5 | 9.5  | 10.1 | 17.5 | 14.9 | 18.7 | 20.5 | 18.0 |

|       | 31     | 32    | 33    | 34    | 35    | 36     | 37    | 38    | 39    | 40     |
|-------|--------|-------|-------|-------|-------|--------|-------|-------|-------|--------|
| SiO2  | 50.81  | 49.86 | 51.22 | 52.06 | 50.54 | 47.82  | 46.44 | 47.06 | 49.04 | 49.27  |
| TiO2  | 1.02   | 1.02  | .88   | .46   | .75   | 1.81   | 2.47  | 2.09  | 1.28  | 1.55   |
| Al2O3 | 2.84   | 2.40  | 2.14  | .97   | 2.04  | 5.24   | 5.44  | 4.87  | 3.26  | 3.78   |
| Cr2O3 | 0.00   | 0.00  | 0.00  | 0.00  | 0.00  | 0.00   | 0.00  | 0.00  | 0.00  | 0.00   |
| FeO   | 9.94   | 9.85  | 10.49 | 12.35 | 11.14 | 10.92  | 11.07 | 11.17 | 11.77 | 11.69  |
| MnO   | .20    | .19   | .20   | .28   | .28   | .14    | .11   | .16   | .24   | .20    |
| MgO   | 13.75  | 13.50 | 13.56 | 12.34 | 12.86 | 12.59  | 11.35 | 11.48 | 12.47 | 12.61  |
| NiO   | 0.00   | 0.00  | 0.00  | 0.00  | 0.00  | 0.00   | 0.00  | 0.00  | 0.00  | 0.00   |
| CaO   | 21.05  | 20.88 | 20.03 | 20.57 | 21.07 | 21.26  | 21.14 | 21.04 | 20.93 | 20.58  |
| Na2O  | .38    | .46   | .47   | .58   | .39   | .48    | .48   | .53   | .60   | .48    |
| K2O   | .02    | 0.00  | .01   | .02   | 0.00  | .01    | 0.00  | 0.00  | 0.00  | .01    |
| Total | 100.01 | 98.16 | 99.00 | 99.63 | 99.07 | 100.27 | 98.58 | 98.40 | 99.63 | 100.21 |

|       |       |       |       |       |       |       |       |       |       |       |
|-------|-------|-------|-------|-------|-------|-------|-------|-------|-------|-------|
| Si    | 1.904 | 1.907 | 1.937 | 1.976 | 1.925 | 1.806 | 1.791 | 1.816 | 1.869 | 1.861 |
| AlIV  | .096  | .093  | .063  | .024  | .075  | .194  | .209  | .184  | .131  | .139  |
| AlVI  | .030  | .016  | .033  | .019  | .017  | .039  | .038  | .037  | .016  | .030  |
| Ti    | .029  | .029  | .025  | .013  | .021  | .051  | .072  | .061  | .037  | .044  |
| Cr    | 0.000 | 0.000 | 0.000 | 0.000 | 0.000 | 0.000 | 0.000 | 0.000 | 0.000 | 0.000 |
| Fe    | .312  | .315  | .332  | .392  | .355  | .345  | .357  | .360  | .375  | .369  |
| Mn    | .006  | .006  | .006  | .009  | .009  | .004  | .004  | .005  | .008  | .006  |
| Mg    | .768  | .770  | .765  | .698  | .730  | .709  | .652  | .660  | .708  | .710  |
| Ni    | 0.000 | 0.000 | 0.000 | 0.000 | 0.000 | 0.000 | 0.000 | 0.000 | 0.000 | 0.000 |
| Ca    | .845  | .856  | .812  | .836  | .860  | .860  | .873  | .870  | .855  | .833  |
| Na    | .028  | .034  | .034  | .043  | .029  | .035  | .036  | .040  | .044  | .035  |
| K     | .001  | 0.000 | .000  | .001  | 0.000 | .000  | 0.000 | 0.000 | 0.000 | .000  |
| Total | 4.018 | 4.026 | 4.007 | 4.011 | 4.022 | 4.044 | 4.032 | 4.033 | 4.043 | 4.028 |

|       |      |      |      |      |      |      |      |      |      |      |
|-------|------|------|------|------|------|------|------|------|------|------|
| Ca    | 43.8 | 44.0 | 42.4 | 43.2 | 44.0 | 44.8 | 46.3 | 45.9 | 43.9 | 43.4 |
| Mg    | 39.8 | 39.5 | 39.9 | 36.1 | 37.4 | 36.9 | 34.6 | 34.8 | 36.4 | 37.0 |
| Fe+Mn | 16.5 | 16.5 | 17.7 | 20.7 | 18.6 | 18.2 | 19.1 | 19.3 | 19.7 | 19.6 |

|                                | 41    | 42    | 43    | 44    | 45    | 46    | 47     | 48    | 49    | 50    |
|--------------------------------|-------|-------|-------|-------|-------|-------|--------|-------|-------|-------|
| SiO <sub>2</sub>               | 50.89 | 46.95 | 48.52 | 48.25 | 47.63 | 47.53 | 49.93  | 49.49 | 47.98 | 50.13 |
| TiO <sub>2</sub>               | .82   | 2.01  | 1.60  | 1.52  | 1.45  | 1.70  | 1.25   | 1.04  | 1.45  | .75   |
| Al <sub>2</sub> O <sub>3</sub> | 2.72  | 6.12  | 4.69  | 4.34  | 3.81  | 4.33  | 2.68   | 2.38  | 3.67  | 1.64  |
| Cr <sub>2</sub> O <sub>3</sub> | .30   | .10   | .10   | 0.00  | 0.00  | 0.00  | 0.00   | 0.00  | 0.00  | 0.00  |
| FeO                            | 9.30  | 10.55 | 10.52 | 12.59 | 12.59 | 12.11 | 14.06  | 14.14 | 12.32 | 12.22 |
| MnO                            | .16   | .19   | .18   | .20   | .19   | .16   | .27    | .29   | .21   | .26   |
| MgO                            | 15.60 | 12.26 | 13.19 | 11.73 | 11.68 | 11.81 | 11.95  | 11.46 | 12.18 | 12.30 |
| NiO                            | 0.00  | 0.00  | 0.00  | 0.00  | 0.00  | 0.00  | 0.00   | 0.00  | 0.00  | 0.00  |
| CaO                            | 19.53 | 20.69 | 20.38 | 20.45 | 20.11 | 20.55 | 19.92  | 20.07 | 20.43 | 20.69 |
| Na <sub>2</sub> O              | .30   | .38   | .38   | .47   | .54   | .71   | .46    | .39   | .46   | .33   |
| K <sub>2</sub> O               | 0.00  | .01   | .01   | .01   | .03   | .11   | .01    | .02   | .02   | 0.00  |
| Total                          | 99.67 | 99.26 | 99.58 | 99.56 | 98.05 | 99.01 | 100.55 | 99.32 | 98.72 | 98.36 |

|       |       |       |       |       |       |       |       |       |       |       |
|-------|-------|-------|-------|-------|-------|-------|-------|-------|-------|-------|
| Si    | 1.902 | 1.787 | 1.835 | 1.844 | 1.851 | 1.829 | 1.895 | 1.906 | 1.850 | 1.934 |
| Al IV | .098  | .213  | .165  | .156  | .149  | .171  | .105  | .094  | .150  | .066  |
| Al VI | .022  | .061  | .044  | .039  | .026  | .025  | .015  | .014  | .017  | .008  |
| Ti    | .023  | .058  | .045  | .044  | .042  | .049  | .036  | .030  | .042  | .022  |
| Cr    | .009  | .003  | .003  | 0.000 | 0.000 | 0.000 | 0.000 | 0.000 | 0.000 | 0.000 |
| Fe    | .291  | .336  | .333  | .402  | .409  | .390  | .446  | .455  | .397  | .394  |
| Mn    | .005  | .006  | .006  | .006  | .006  | .005  | .009  | .009  | .007  | .008  |
| Mg    | .869  | .695  | .743  | .668  | .677  | .677  | .676  | .658  | .700  | .707  |
| Ni    | 0.000 | 0.000 | 0.000 | 0.000 | 0.000 | 0.000 | 0.000 | 0.000 | 0.000 | 0.000 |
| Ca    | .782  | .844  | .826  | .837  | .837  | .847  | .810  | .828  | .844  | .855  |
| Na    | .022  | .028  | .028  | .035  | .041  | .053  | .034  | .029  | .034  | .025  |
| K     | 0.000 | .000  | .000  | .000  | .001  | .005  | .000  | .001  | .001  | 0.000 |
| Total | 4.022 | 4.031 | 4.028 | 4.032 | 4.040 | 4.053 | 4.026 | 4.025 | 4.042 | 4.020 |

|       |      |      |      |      |      |      |      |      |      |      |
|-------|------|------|------|------|------|------|------|------|------|------|
| Ca    | 40.2 | 44.9 | 43.3 | 43.7 | 43.4 | 44.1 | 41.7 | 42.5 | 43.3 | 43.5 |
| Mg    | 44.6 | 37.0 | 39.0 | 34.9 | 35.1 | 35.3 | 34.8 | 33.7 | 35.9 | 36.0 |
| Fe+Mn | 15.2 | 18.2 | 17.7 | 21.4 | 21.5 | 20.6 | 23.4 | 23.8 | 20.7 | 20.5 |

|       | 51    | 52    | 53    | 54    | 55    | 56    |
|-------|-------|-------|-------|-------|-------|-------|
| SiO2  | 50.33 | 50.14 | 50.26 | 49.85 | 48.17 | 50.25 |
| TiO2  | 1.03  | 1.19  | .81   | 1.09  | 1.29  | 1.00  |
| Al2O3 | 2.95  | 2.93  | 1.92  | 2.87  | 4.00  | 2.88  |
| Cr2O3 | 0.00  | 0.00  | 0.00  | 0.00  | .10   | 0.00  |
| FeO   | 8.87  | 10.11 | 11.49 | 9.45  | 10.36 | 9.64  |
| MnO   | .20   | .21   | .23   | .19   | .13   | .19   |
| MgO   | 14.23 | 12.82 | 12.63 | 13.53 | 14.32 | 13.76 |
| NiO   | 0.00  | 0.00  | 0.00  | 0.00  | 0.00  | 0.00  |
| CaO   | 20.81 | 20.78 | 20.59 | 21.14 | 19.86 | 21.05 |
| Na2O  | .39   | .46   | .31   | .45   | .45   | .46   |
| K2O   | 0.00  | .01   | .01   | .01   | 0.00  | .03   |
| Total | 98.85 | 98.67 | 98.34 | 98.58 | 98.70 | 99.32 |

|       |       |       |       |       |       |       |
|-------|-------|-------|-------|-------|-------|-------|
| Si    | 1.900 | 1.908 | 1.931 | 1.896 | 1.837 | 1.898 |
| Al IV | .100  | .092  | .069  | .104  | .163  | .102  |
| Al VI | .032  | .039  | .018  | .025  | .017  | .026  |
| Ti    | .029  | .034  | .023  | .031  | .037  | .028  |
| Cr    | 0.000 | 0.000 | 0.000 | 0.000 | .003  | 0.000 |
| Fe    | .280  | .322  | .369  | .301  | .330  | .305  |
| Mn    | .006  | .007  | .007  | .006  | .004  | .006  |
| Mg    | .801  | .727  | .723  | .767  | .814  | .775  |
| Ni    | 0.000 | 0.000 | 0.000 | 0.000 | 0.000 | 0.000 |
| Ca    | .842  | .847  | .848  | .862  | .812  | .852  |
| Na    | .029  | .034  | .023  | .033  | .033  | .034  |
| K     | 0.000 | .000  | .000  | .000  | 0.000 | .001  |
| Total | 4.019 | 4.010 | 4.013 | 4.025 | 4.051 | 4.027 |

|       |      |      |      |      |      |      |
|-------|------|------|------|------|------|------|
| Ca    | 43.6 | 44.5 | 43.5 | 44.5 | 41.4 | 44.0 |
| Mg    | 41.5 | 38.2 | 37.1 | 39.6 | 41.5 | 40.0 |
| Fe+Mn | 14.8 | 17.3 | 19.3 | 15.8 | 17.1 | 16.0 |

Sill Olivines\*

|                                | SB60E2       | SB60E3       | SB60E4        | SB60F1        | SB60F2        | SB60F3        | SB60F4        |
|--------------------------------|--------------|--------------|---------------|---------------|---------------|---------------|---------------|
| SiO <sub>2</sub>               | 38.03        | 36.59        | 38.30         | 39.28         | 39.20         | 38.24         | 38.21         |
| TiO <sub>2</sub>               | 0.08         | 0.00         | 0.00          | 0.05          | 0.01          | 0.04          | 0.04          |
| Al <sub>2</sub> O <sub>3</sub> | 0.05         | 0.02         | 0.02          | 0.04          | 0.00          | 0.02          | 0.02          |
| Cr <sub>2</sub> O <sub>3</sub> | 0.09         | 0.00         | 0.02          | 0.00          | 0.00          | 0.00          | 0.00          |
| FeO                            | 20.36        | 25.95        | 23.08         | 20.41         | 20.67         | 19.57         | 20.41         |
| MnO                            | 0.28         | 0.50         | 0.21          | 0.16          | 0.22          | 0.23          | 0.23          |
| MgO                            | 39.92        | 35.43        | 38.54         | 41.89         | 41.20         | 42.71         | 38.21         |
| CaO                            | 0.21         | 0.09         | 0.23          | 0.29          | 0.20          | 0.24          | 0.25          |
| Na <sub>2</sub> O              | 0.02         | 0.04         | 0.00          | 0.01          | 0.00          | 0.01          | 0.00          |
| K <sub>2</sub> O               | 0.00         | 0.03         | 0.00          | 0.00          | 0.00          | 0.08          | 0.02          |
| NiO                            | 0.00         | 0.03         | 0.00          | 0.08          | 0.00          | 0.08          | 0.03          |
| Total                          | <u>99.25</u> | <u>98.73</u> | <u>100.57</u> | <u>102.22</u> | <u>101.64</u> | <u>101.27</u> | <u>101.17</u> |
| Si                             | .990         | .986         | .995          | .989          | .994          | .972          | .976          |
| Ti                             | .001         | -            | -             | -             | -             | -             | -             |
| Al                             | .001         | -            | -             | -             | -             | -             | .002          |
| Cr                             | .001         | -            | -             | .007          | -             | -             | .002          |
| Fe                             | .443         | .584         | .500          | .429          | .438          | .416          | .435          |
| Mn                             | .006         | .011         | .004          | .003          | .004          | .004          | .004          |
| Mg                             | 1.550        | 1.422        | 1.492         | 1.573         | 1.558         | 1.618         | 1.593         |
| Ca                             | .005         | .002         | .006          | .007          | .005          | .006          | .006          |
| Na                             | -            | .001         | -             | -             | -             | -             | -             |
| K                              | -            | -            | -             | -             | -             | .002          | -             |
| Ni                             | .003         | .001         | .003          | .001          | .002          | .002          | .002          |
|                                | <u>3.002</u> | <u>3.008</u> | <u>3.000</u>  | <u>3.004</u>  | <u>3.001</u>  | <u>3.021</u>  | <u>3.017</u>  |
| Fo                             | .778         | .708         | .749          | .786          | .751          | .795          | .786          |

\*formula based on 4 oxygen.

Sill Olivines

|                                | SB60H1 | SB60H2 | SB60H3 | SB60H4 |
|--------------------------------|--------|--------|--------|--------|
| SiO <sub>2</sub>               | 38.88  | 38.45  | 38.60  | 39.14  |
| TiO <sub>2</sub>               | 0.04   | 0.05   | 0.00   | 0.04   |
| Al <sub>2</sub> O <sub>3</sub> | 0.00   | 0.02   | 0.04   | 0.04   |
| Cr <sub>2</sub> O <sub>3</sub> | 0.05   | 0.02   | 0.03   | 0.00   |
| FeO                            | 19.03  | 20.54  | 20.30  | 20.65  |
| MnO                            | 0.11   | 0.18   | 0.27   | 0.30   |
| MgO                            | 41.17  | 42.30  | 41.95  | 41.75  |
| CaO                            | 0.30   | 0.23   | 0.21   | 0.18   |
| Na <sub>2</sub> O              | 0.00   | 0.02   | 0.07   | 0.06   |
| K <sub>2</sub> O               | 0.00   | 0.06   | 0.00   | 0.00   |
| NiO                            | 0.15   | 0.21   | 0.16   | 0.20   |
| Total                          | 100.53 | 102.09 | 101.62 | 102.37 |
| Si                             | .990   | .974   | .980   | .987   |
| Ti                             | -      | -      | -      | -      |
| Al                             | -      | -      | -      | -      |
| Cr                             | -      | -      | -      | -      |
| Fe                             | .405   | .435   | .431   | .435   |
| Mn                             | .002   | .003   | .005   | .006   |
| Mg                             | 1.593  | 1.597  | 1.588  | 1.569  |
| Ca                             | .007   | .006   | .005   | .004   |
| Na                             | -      | -      | .003   | .002   |
| K                              | -      | -      | -      | -      |
| Ni                             | .003   | .003   | .003   | .003   |
|                                | 3.001  | 3.020  | 3.015  | 3.007  |
| Fe                             | .797   | .786   | .786   | .783   |

Sill Amphiboles (Magmatic)\*

|                                | SB7L1        | SB7L2        | SB7L3        | SB7L4        | SB7L5        | SB7K1         | SB7K2        |
|--------------------------------|--------------|--------------|--------------|--------------|--------------|---------------|--------------|
| SiO <sub>2</sub>               | 48.66        | 40.82        | 49.28        | 47.13        | 48.14        | 41.57         | 39.31        |
| TiO <sub>2</sub>               | 1.90         | 4.77         | 1.41         | 2.06         | 2.11         | 4.36          | 3.68         |
| Al <sub>2</sub> O <sub>3</sub> | 3.16         | 10.77        | 2.95         | 1.10         | 1.16         | 9.47          | 9.43         |
| Cr <sub>2</sub> O <sub>3</sub> | 0.00         | 0.02         | 0.03         | 0.03         | 0.07         | 0.01          | 0.03         |
| FeO                            | 17.70        | 15.18        | 17.70        | 27.79        | 26.88        | 21.92         | 21.49        |
| MnO                            | 0.37         | 0.14         | 0.34         | 0.34         | 0.43         | 0.24          | 0.29         |
| MgO                            | 12.17        | 11.75        | 12.63        | 5.13         | 4.69         | 6.63          | 7.13         |
| CaO                            | 8.95         | 11.49        | 7.77         | 4.61         | 5.61         | 11.54         | 10.86        |
| Na <sub>2</sub> O              | 5.01         | 3.32         | 4.65         | 5.04         | 5.57         | 3.66          | 3.58         |
| K <sub>2</sub> O               | 0.86         | 0.68         | 0.84         | 0.80         | 1.05         | 1.16          | 1.21         |
| NiO                            | 0.01         | 0.05         | 0.00         | 0.03         | 0.02         | 0.00          | 0.00         |
| Total                          | <u>98.79</u> | <u>98.93</u> | <u>97.58</u> | <u>94.07</u> | <u>95.73</u> | <u>100.57</u> | <u>96.99</u> |

1 = in Qtz; 2 = in feldspar; 3 = center + 4+5 rim of zoned grain.

|       |               |               |               |               |               |               |               |
|-------|---------------|---------------|---------------|---------------|---------------|---------------|---------------|
| Si    | 7.269         | 6.091         | 7.396         | 7.702         | 7.717         | 6.311         | 6.212         |
| Ti    | 0.210         | 0.534         | 0.158         | 0.249         | 0.254         | 0.494         | 0.436         |
| Al    | 0.557         | 1.874         | 0.520         | 0.211         | 0.216         | 1.692         | 1.753         |
| Cr    | 0.000         | 0.000         | 0.000         | 0.000         | 0.004         | 0.000         | 0.000         |
| Fe    | 2.209         | 1.892         | 2.220         | 3.798         | 3.602         | 2.779         | 2.839         |
| Mn    | 0.043         | 0.017         | 0.040         | 0.043         | 0.056         | 0.026         | 0.037         |
| Mg    | 2.709         | 2.610         | 2.824         | 1.247         | 1.119         | 1.496         | 1.675         |
| Ni    | 0.000         | 0.004         | 0.000         | 0.000         | 0.000         | 0.000         | 0.000         |
| Ca    | 1.429         | 1.834         | 1.247         | 0.806         | 0.959         | 1.875         | 1.837         |
| Na    | 1.447         | 0.959         | 1.352         | 1.597         | 1.730         | 1.078         | 0.095         |
| K     | 0.162         | 0.127         | 0.158         | 0.163         | 0.211         | 0.223         | 0.241         |
| Total | <u>16.036</u> | <u>15.947</u> | <u>15.914</u> | <u>15.814</u> | <u>15.870</u> | <u>15.974</u> | <u>16.126</u> |

\*Formula based on 23 oxygen.



Sill Amphiboles (Magmatic)

|                                | SB7K3         | SB7K4         | SB7K5         | SB7K6         | SB7K7         | SB60E1        | SB60E2        |
|--------------------------------|---------------|---------------|---------------|---------------|---------------|---------------|---------------|
| SiO <sub>2</sub>               | 39.88         | 37.72         | 37.19         | 42.65         | 36.84         | 39.87         | 42.90         |
| TiO <sub>2</sub>               | 4.59          | 1.80          | 2.48          | 4.31          | 1.26          | 4.89          | 5.02          |
| Al <sub>2</sub> O <sub>3</sub> | 9.91          | 11.08         | 10.79         | 9.13          | 11.99         | 10.25         | 11.30         |
| Cr <sub>2</sub> O <sub>3</sub> | 0.00          | 0.00          | 0.00          | 0.00          | 0.00          | 0.05          | 0.00          |
| FeO                            | 20.98         | 29.51         | 29.46         | 15.82         | 30.05         | 12.32         | 11.64         |
| MnO                            | 0.25          | 0.20          | 0.27          | 0.31          | 0.27          | 0.11          | 0.04          |
| MgO                            | 7.21          | 2.00          | 1.79          | 10.81         | 0.99          | 12.95         | 13.80         |
| CaO                            | 11.42         | 11.34         | 11.62         | 11.71         | 11.33         | 12.25         | 12.39         |
| Na <sub>2</sub> O              | 3.54          | 3.21          | 3.08          | 3.38          | 2.87          | 3.65          | 3.73          |
| K <sub>2</sub> O               | 0.71          | 1.14          | 1.18          | 0.84          | 1.16          | 0.66          | 0.84          |
| NiO                            | 0.04          | 0.04          | 0.01          | 0.07          | 0.03          | 0.01          | 0.05          |
| Total                          | <u>98.53</u>  | <u>98.04</u>  | <u>97.86</u>  | <u>98.50</u>  | <u>96.81</u>  | <u>97.00</u>  | <u>101.71</u> |
| Si                             | 6.159         | 6.119         | 6.064         | 6.393         | 6.081         | 6.022         | 6.123         |
| Ti                             | 0.530         | 0.219         | 0.301         | 0.484         | 0.155         | 0.554         | 0.536         |
| Al                             | 1.804         | 2.119         | 2.072         | 1.610         | 2.330         | 1.823         | 1.897         |
| Cr                             | 0.000         | 0.000         | 0.000         | 0.000         | 0.000         | 0.004         | 0.000         |
| Fe                             | 2.710         | 4.004         | 4.016         | 1.980         | 4.147         | 1.557         | 1.386         |
| Mn                             | 0.031         | 0.023         | 0.033         | 0.040         | 0.034         | 0.013         | 0.004         |
| Mg                             | 1.659         | 0.480         | 0.431         | 2.416         | 0.242         | 2.918         | 2.936         |
| Ni                             | 0.004         | 0.004         | 0.000         | 0.004         | 0.000         | 0.000         | 0.004         |
| Ca                             | 1.885         | 1.971         | 2.029         | 1.791         | 2.001         | 1.982         | 1.893         |
| Na                             | 1.060         | 1.009         | 0.972         | 0.981         | 0.916         | 1.068         | 1.030         |
| K                              | 0.136         | 0.233         | 0.244         | 0.158         | 0.242         | 0.124         | 0.150         |
| Total                          | <u>15.978</u> | <u>16.182</u> | <u>16.162</u> | <u>15.856</u> | <u>16.147</u> | <u>16.066</u> | <u>15.957</u> |

Sill Amphiboles (Magmatic)

|                                | SB60E3        | SB60F1        | SB60F2        | SB60H1        |
|--------------------------------|---------------|---------------|---------------|---------------|
| SiO <sub>2</sub>               | 40.27         | 40.44         | 43.90         | 42.26         |
| TiO <sub>2</sub>               | 4.79          | 5.04          | 3.62          | 4.38          |
| Al <sub>2</sub> O <sub>3</sub> | 11.11         | 10.81         | 9.66          | 10.65         |
| Cr <sub>2</sub> O <sub>3</sub> | 0.00          | 0.18          | 0.39          | 0.04          |
| FeO                            | 11.16         | 9.26          | 9.07          | 8.87          |
| MnO                            | 0.05          | 0.05          | 0.05          | 0.02          |
| MgO                            | 13.18         | 14.97         | 15.70         | 14.55         |
| CaO                            | 11.40         | 12.24         | 10.64         | 11.05         |
| Na <sub>2</sub> O              | 3.43          | 3.10          | 3.31          | 3.55          |
| K <sub>2</sub> O               | 0.93          | 0.73          | 0.63          | 0.64          |
| NiO                            | 0.09          | 0.05          | 0.10          | 0.09          |
| Total                          | <u>96.40</u>  | <u>96.88</u>  | <u>97.06</u>  | <u>96.11</u>  |
| Si                             | 6.070         | 6.020         | 6.438         | 6.278         |
| Ti                             | 0.540         | 0.563         | 0.396         | 0.488         |
| Al                             | 1.973         | 1.896         | 1.666         | 1.861         |
| Cr                             | 0.000         | 0.017         | 0.043         | 0.000         |
| Fe                             | 1.407         | 1.148         | 1.110         | 1.099         |
| Mn                             | 0.004         | 0.004         | 0.004         | 0.000         |
| Mg                             | 2.960         | 3.320         | 3.430         | 3.222         |
| Ni                             | 0.009         | 0.004         | 0.008         | 0.008         |
| Ca                             | 1.840         | 1.948         | 1.669         | 1.757         |
| Na                             | 1.000         | 0.891         | 0.938         | 1.020         |
| K                              | 0.177         | 0.135         | 0.116         | 0.118         |
| Total                          | <u>15.979</u> | <u>15.946</u> | <u>15.818</u> | <u>15.852</u> |

Sill Biotites

|                                | SB7K1 | SB7I2 | SB6D1 | SB6D2 | SB6D3 | SB6OE1 | SB6OE2 | SB6OF1 | SB6OH1 | SB6OH2 |
|--------------------------------|-------|-------|-------|-------|-------|--------|--------|--------|--------|--------|
| SiO <sub>2</sub>               | 36.89 | 36.89 | 33.18 | 35.89 | 38.41 | 36.16  | 35.54  | 38.75  | 36.45  | 39.38  |
| TiO <sub>2</sub>               | 5.32  | 5.32  | 5.42  | 5.13  | 5.20  | 6.96   | 6.24   | 3.91   | 6.80   | 4.65   |
| Al <sub>2</sub> O <sub>3</sub> | 13.77 | 13.77 | 11.98 | 12.94 | 12.87 | 14.18  | 13.58  | 15.81  | 14.16  | 12.14  |
| Cr <sub>2</sub> O <sub>3</sub> | 0.01  | 0.01  | 0.10  | 0.00  | 0.02  | 0.00   | 0.00   | 0.10   | 0.06   | 0.00   |
| FeO                            | 17.53 | 17.53 | 25.27 | 18.33 | 18.53 | 13.69  | 13.90  | 9.18   | 10.20  | 11.28  |
| MnO                            | 0.13  | 0.13  | 0.08  | 0.08  | 0.17  | 0.08   | 0.07   | 0.02   | 0.04   | 0.01   |
| MgO                            | 13.91 | 13.91 | 8.14  | 12.06 | 13.51 | 14.89  | 15.72  | 20.98  | 17.70  | 19.20  |
| CaO                            | 0.04  | 0.04  | 0.20  | 0.06  | 0.02  | 0.00   | 0.00   | 0.11   | 0.02   | 0.00   |
| Na <sub>2</sub> O              | 0.78  | 0.78  | 0.41  | 0.42  | 0.58  | 1.48   | 1.38   | 1.96   | 1.61   | 1.48   |
| K <sub>2</sub> O               | 8.32  | 8.32  | 8.82  | 9.73  | 8.53  | 7.40   | 9.04   | 7.43   | 9.13   | 6.59   |
| NiO                            | 0.00  | 0.00  | 0.04  | 0.00  | 0.12  | 0.16   | 0.06   | 0.11   | 0.00   | 0.06   |
| Total                          | 96.70 | 96.70 | 93.64 | 94.64 | 97.96 | 95.01  | 95.53  | 98.35  | 96.15  | 93.80  |

Water content of Biotites  $\approx$  3.5 to 4.5, percent (Deer et al., 1966).

Sill Feldspars\*

|                                | SB7L1  | SB7L2  | SB7K1  | SB7K2  | SB7K3  | SB7I1  | SB7I2  | SB7I3  | SB7I4  |
|--------------------------------|--------|--------|--------|--------|--------|--------|--------|--------|--------|
| SiO <sub>2</sub>               | 70.50  | 69.39  | 68.50  | 68.12  | 67.82  | 48.93  | 52.81  | 55.16  | 50.21  |
| CaO                            | 0.05   | 0.03   | 0.73   | 0.50   | 0.29   | 16.44  | 12.39  | 12.52  | 15.38  |
| K <sub>2</sub> O               | 0.05   | 0.10   | 0.07   | 0.02   | 0.05   | 0.15   | 0.29   | 0.11   | 0.09   |
| Al <sub>2</sub> O <sub>3</sub> | 20.14  | 20.18  | 20.80  | 20.12  | 20.53  | 31.75  | 28.27  | 29.24  | 31.57  |
| FeO                            | 0.07   | 0.06   | 0.13   | 1.17   | 0.07   | 0.45   | 0.26   | 0.38   | 0.44   |
| Na <sub>2</sub> O              | 11.27  | 11.03  | 10.69  | 10.51  | 10.64  | 2.82   | 4.91   | 4.99   | 3.09   |
| Total                          | 102.09 | 100.79 | 100.91 | 100.45 | 99.40  | 100.54 | 98.93  | 102.39 | 100.79 |
| Stoi-<br>chiometry             | 19.806 | 19.802 | 19.820 | 19.817 | 19.795 | 20.117 | 20.120 | 20.033 | 20.033 |
| Si                             | 12.017 | 11.978 | 11.844 | 11.874 | 11.879 | 8.953  | 9.710  | 9.772  | 9.119  |
| Ca                             | .005   | .005   | .132   | .092   | .051   | 3.222  | 2.438  | 2.375  | 2.990  |
| K                              | .010   | .020   | .010   | .000   | .010   | .032   | .064   | .021   | .016   |
| Al                             | 4.047  | 4.103  | 4.237  | 4.133  | 4.235  | 6.848  | 6.123  | 6.103  | 6.758  |
| Fe                             | .005   | .005   | .015   | .168   | .005   | 0.064  | .038   | .052   | .063   |
| Na                             | 3.722  | 3.692  | 3.583  | 3.550  | 3.614  | .999   | 1.748  | 1.710  | 1.087  |
| OR                             | .003   | .005   | .003   | .000   | .003   | .008   | .015   | .005   | .004   |
| An                             | .001   | .001   | .035   | .025   | .014   | .757   | .574   | .578   | .730   |
| Ab                             | .995   | .993   | .962   | .975   | .983   | .235   | .411   | .417   | .266   |

\*Formula based on 32 oxygen.

Sill-Feldspars

|                                | SB7I5  | SB7I6  | SB7I7  | SB7I8  | SB7I9  | SB7I10 | SB6I1  | SB6I2  | SB6I3  | SB6I4  |
|--------------------------------|--------|--------|--------|--------|--------|--------|--------|--------|--------|--------|
| SiO <sub>2</sub>               | 54.25  | 53.68  | 50.57  | 52.04  | 53.69  | 53.32  | 52.39  | 53.56  | 52.63  | 57.35  |
| CaO                            | 12.27  | 11.18  | 15.89  | 15.37  | 12.62  | 13.32  | 9.85   | 9.00   | 12.94  | 9.67   |
| K <sub>2</sub> O               | 0.16   | 0.21   | 0.04   | 0.08   | 0.26   | 0.28   | 1.80   | 1.64   | 0.17   | 0.30   |
| Al <sub>2</sub> O <sub>3</sub> | 29.55  | 27.96  | 30.41  | 30.71  | 28.54  | 29.91  | 29.99  | 30.11  | 30.36  | 27.83  |
| FeO                            | 0.55   | 0.45   | 0.20   | 0.32   | 0.50   | 0.36   | 0.57   | 0.71   | 0.43   | 0.34   |
| Na <sub>2</sub> O              | 5.04   | 5.30   | 3.15   | 3.47   | 4.95   | 4.60   | 4.02   | 4.27   | 4.00   | 5.84   |
| Total                          | 101.84 | 98.79  | 100.26 | 102.00 | 100.55 | 101.76 | 98.62  | 99.29  | 100.53 | 101.32 |
| Stoi-<br>chiometry             | 20.081 | 20.078 | 20.027 | 20.014 | 20.117 | 20.103 | 20.016 | 19.945 | 19.968 | 19.935 |
| Si                             | 9.672  | 9.843  | 9.232  | 9.319  | 9.719  | 9.542  | 9.639  | 9.746  | 9.507  | 10.168 |
| Ca                             | 2.343  | 2.195  | 3.107  | 2.949  | 2.444  | 2.547  | 1.938  | 1.751  | 2.501  | 1.837  |
| K                              | .036   | .048   | .005   | .016   | .058   | .063   | .421   | .379   | .037   | .067   |
| Al                             | 6.209  | 6.043  | 6.542  | 6.480  | 6.089  | 6.307  | 6.501  | 6.457  | 6.460  | 5.813  |
| Fe                             | .078   | .064   | .026   | .047   | .074   | .052   | .086   | .106   | .063   | .046   |
| Na                             | 1.742  | 1.883  | 1.114  | 1.204  | 1.732  | 1.591  | 1.431  | 1.506  | 1.399  | 2.003  |
| OR                             | .009   | .012   | .001   | .004   | .015   | .015   | .111   | .104   | .009   | .017   |
| An                             | .569   | .532   | .735   | .707   | .545   | .606   | .511   | .481   | .635   | .470   |
| Ab                             | .423   | .456   | .263   | .289   | .440   | .379   | .378   | .414   | .355   | .513   |

Sill Feldspars

|                                | SB6I5  | SB6I6  | SB6I7  | SB6K1  | SB6K2  | SB6K3  | SB6K4  | SB6K5  | SB6H1  |
|--------------------------------|--------|--------|--------|--------|--------|--------|--------|--------|--------|
| SiO <sub>2</sub>               | 53.73  | 51.28  | 54.47  | 50.58  | 52.90  | 54.76  | 58.05  | 61.50  | 54.86  |
| CaO                            | 11.37  | 13.16  | 11.45  | 12.77  | 12.58  | 12.18  | 8.43   | 6.20   | 12.33  |
| K <sub>2</sub> O               | 0.16   | 0.17   | 0.15   | 0.10   | 0.16   | 0.20   | 0.46   | 0.47   | 0.07   |
| Al <sub>2</sub> O <sub>3</sub> | 29.14  | 30.98  | 28.52  | 30.25  | 30.15  | 29.55  | 27.64  | 25.21  | 28.77  |
| FeO                            | 0.50   | 0.51   | 0.51   | 0.39   | 0.47   | 0.45   | 0.31   | 0.38   | 0.58   |
| Na <sub>2</sub> O              | 5.19   | 4.24   | 5.20   | 3.98   | 4.66   | 4.59   | 6.44   | 7.52   | 5.25   |
| Total                          | 100.07 | 100.34 | 100.29 | 99.46  | 100.91 | 101.73 | 101.32 | 101.28 | 101.86 |
| Stoi-<br>chiometry             | 20.071 | 20.115 | 20.042 | 20.077 | 20.069 | 19.953 | 19.983 | 19.909 | 20.090 |
| Si                             | 9.728  | 9.317  | 9.836  | 9.345  | 9.525  | 9.747  | 10.275 | 10.811 | 9.779  |
| Ca                             | 2.205  | 2.560  | 2.215  | 2.701  | 2.425  | 2.319  | 1.595  | 1.166  | 2.354  |
| K                              | .032   | .037   | .032   | .021   | .031   | .042   | .099   | .103   | .016   |
| Al                             | 6.216  | 6.634  | 6.057  | 6.537  | 6.397  | 6.200  | 7.009  | 5.220  | 6.043  |
| Fe                             | .074   | .074   | .074   | .059   | .068   | .063   | .042   | .051   | .074   |
| Na                             | 1.817  | 1.493  | 1.787  | 1.415  | 1.622  | 1.583  | 2.208  | 2.558  | 2.133  |
| OR                             | .008   | .009   | .008   | .005   | .008   | .011   | .025   | .027   | .004   |
| An                             | .534   | .626   | .549   | .653   | .594   | .588   | .409   | .305   | .523   |
| Ab                             | .448   | .365   | .443   | .342   | .398   | .401   | .566   | .668   | .473   |

Sill Feldspars

|                                | SB6H2         | SB6H3         | SB6H4         | SB6H5         | SB6H6         | SB6H7         | SB6H8         | SB6H9         |
|--------------------------------|---------------|---------------|---------------|---------------|---------------|---------------|---------------|---------------|
| SiO <sub>2</sub>               | 51.88         | 50.74         | 54.28         | 52.61         | 60.33         | 50.75         | 53.65         | 55.05         |
| CaO                            | 14.49         | 14.57         | 10.24         | 12.68         | 5.75          | 14.80         | 12.20         | 11.20         |
| K <sub>2</sub> O               | 0.11          | 0.04          | 0.17          | 0.11          | 0.61          | 0.05          | 0.04          | 0.20          |
| Al <sub>2</sub> O <sub>3</sub> | 29.58         | 29.66         | 27.03         | 30.78         | 24.63         | 31.17         | 29.86         | 28.67         |
| FeO                            | 0.26          | 0.29          | 4.59          | 0.68          | 0.39          | 0.52          | 0.71          | 0.65          |
| Na <sub>2</sub> O              | 3.77          | 3.95          | 4.73          | 4.13          | 7.61          | 3.25          | 4.60          | 5.30          |
| Total                          | <u>100.10</u> | <u>99.25</u>  | <u>101.05</u> | <u>100.98</u> | <u>99.31</u>  | <u>100.55</u> | <u>101.07</u> | <u>101.07</u> |
| Stoichiometry                  | <u>20.028</u> | <u>20.115</u> | <u>20.059</u> | <u>19.984</u> | <u>19.954</u> | <u>20.005</u> | <u>19.994</u> | <u>20.039</u> |
| Si                             | 9.456         | 9.347         | 9.878         | 9.465         | 10.813        | 9.220         | 9.629         | 9.862         |
| Ca                             | 2.829         | 2.876         | 1.991         | 2.438         | 1.099         | 2.879         | 2.344         | 2.150         |
| K                              | .021          | .005          | .037          | .021          | .137          | .010          | .005          | .042          |
| Al                             | 6.354         | 6.438         | 5.793         | 6.542         | 5.202         | 6.676         | 6.315         | 6.051         |
| Fe                             | .037          | .043          | .694          | .100          | .058          | .074          | .105          | .094          |
| Na                             | 1.332         | 1.405         | 1.666         | 1.436         | 2.646         | 1.146         | 1.596         | 1.840         |
| OR                             | .005          | .001          | .010          | .005          | .035          | .002          | .001          | .010          |
| An                             | .676          | .671          | .539          | .626          | .283          | .713          | .594          | .533          |
| Ab                             | .318          | .328          | .451          | .369          | .682          | .284          | .404          | .456          |

Sill Feldspars

|                                | SB6F1         | SB6F2         | SB6F3         | SB6F4         |
|--------------------------------|---------------|---------------|---------------|---------------|
| SiO <sub>2</sub>               | 51.14         | 53.22         | 50.08         | 52.98         |
| CaO                            | 15.29         | 13.26         | 15.34         | 13.67         |
| K <sub>2</sub> O               | 0.12          | 0.01          | 0.04          | 0.08          |
| Al <sub>2</sub> O <sub>3</sub> | 31.07         | 30.37         | 31.50         | 29.48         |
| FeO                            | 0.60          | 0.77          | 0.64          | 0.41          |
| Na <sub>2</sub> O              | 3.41          | 3.93          | 3.45          | 4.21          |
| Total                          | <u>101.63</u> | <u>101.55</u> | <u>101.06</u> | <u>100.84</u> |
| Stoichiometry                  | <u>20.065</u> | <u>19.938</u> | <u>20.121</u> | <u>20.027</u> |
| Si                             | 9.216         | 9.525         | 9.092         | 9.566         |
| Ca                             | 2.950         | 2.542         | 2.982         | 2.643         |
| K                              | .026          | .000          | .005          | .016          |
| Al                             | 6.593         | 6.401         | 6.737         | 6.271         |
| Fe                             | .090          | .110          | .096          | .058          |
| Na                             | 1.189         | 1.360         | 1.209         | 1.472         |
| OR                             | .006          | .000          | .001          | .004          |
| An                             | .708          | .651          | .711          | .640          |
| Ab                             | .285          | .349          | .288          | .356          |



Sill Feldspars

|                                | SB6D1         | SB6D2         | SB6D3         | SB6D4         | SB6D5         | SB6D6         |
|--------------------------------|---------------|---------------|---------------|---------------|---------------|---------------|
| SiO <sub>2</sub>               | 55.80         | 55.73         | 50.61         | 54.73         | 53.77         | 52.92         |
| CaO                            | 11.02         | 11.23         | 12.95         | 10.98         | 12.59         | 11.06         |
| K <sub>2</sub> O               | 0.33          | 0.22          | 0.04          | 0.11          | 0.07          | 0.15          |
| Al <sub>2</sub> O <sub>3</sub> | 28.50         | 28.66         | 31.55         | 29.64         | 29.79         | 28.45         |
| FeO                            | 0.64          | 0.69          | 0.70          | 0.64          | 0.79          | 0.65          |
| Na <sub>2</sub> O              | 5.51          | 5.63          | 4.01          | 5.31          | 4.48          | 4.86          |
| Total                          | <u>101.80</u> | <u>102.18</u> | <u>99.84</u>  | <u>101.41</u> | <u>101.48</u> | <u>98.09</u>  |
| Stoichiometry                  | <u>20.059</u> | <u>20.086</u> | <u>20.066</u> | <u>20.035</u> | <u>20.002</u> | <u>20.002</u> |
| Si                             | 9.920         | 9.882         | 9.233         | 9.759         | 9.626         | 9.769         |
| Ca                             | 2.098         | 2.133         | 2.528         | 2.098         | 2.412         | 2.183         |
| K                              | .073          | .046          | .005          | .021          | .016          | .032          |
| Al                             | 6.430         | 5.990         | 6.785         | 6.227         | 6.284         | 6.188         |
| Fe                             | .094          | .099          | .102          | .094          | .115          | .097          |
| Na                             | 1.899         | 1.936         | 1.414         | 1.836         | 1.550         | 1.733         |
| OR                             | .018          | .011          | .001          | .006          | .004          | .008          |
| An                             | .516          | .518          | .640          | .530          | .606          | .553          |
| Ab                             | .466          | .470          | .358          | .464          | .390          | .439          |

Sill Feldspars

|                                | SB60H1        | SB60H2        | SB60H3        | SB60F1        | SB60F2        | SB60F4        | SB60F3        | SB60F5        |
|--------------------------------|---------------|---------------|---------------|---------------|---------------|---------------|---------------|---------------|
| SiO <sub>2</sub>               | 48.71         | 49.69         | 51.46         | 52.43         | 49.77         | 54.16         | 57.00         | 52.45         |
| CaO                            | 16.60         | 15.30         | 14.85         | 13.42         | 15.41         | 11.77         | 9.46          | 12.49         |
| K <sub>2</sub> O               | 0.04          | 0.02          | 0.10          | 0.05          | 0.07          | 0.11          | 0.19          | 0.07          |
| Al <sub>2</sub> O <sub>3</sub> | 33.53         | 32.03         | 30.85         | 30.50         | 33.04         | 29.77         | 27.92         | 29.91         |
| FeO                            | 0.65          | 0.49          | 0.48          | 0.33          | 0.52          | 0.42          | 0.47          | 0.34          |
| Na <sub>2</sub> O              | 1.81          | 2.82          | 3.46          | 3.76          | 2.56          | 4.57          | 6.14          | 4.27          |
| Total                          | <u>101.34</u> | <u>100.34</u> | <u>101.20</u> | <u>100.49</u> | <u>101.37</u> | <u>100.79</u> | <u>101.18</u> | <u>99.53</u>  |
| Stoichiometry                  | <u>19.918</u> | <u>19.984</u> | <u>20.020</u> | <u>19.924</u> | <u>19.952</u> | <u>19.916</u> | <u>20.000</u> | <u>19.969</u> |
| Si                             | 8.518         | 9.056         | 9.287         | 9.467         | 8.976         | 9.708         | 10.131        | 9.549         |
| Ca                             | 3.394         | 2.985         | 2.871         | 2.596         | 2.974         | 2.257         | 1.799         | 2.437         |
| K                              | .011          | .000          | .021          | .010          | .010          | .021          | .042          | .016          |
| Al                             | 7.354         | 6.879         | 6.564         | 6.490         | 7.023         | 6.288         | 5.848         | 6.418         |
| Fe                             | .049          | .069          | .069          | .047          | .074          | .058          | .067          | .048          |
| Na                             | .957          | .829          | 1.208         | 1.313         | .894          | 1.583         | 2.113         | 1.501         |
| OR                             | .003          | .000          | .005          | .003          | .003          | .005          | .011          | .004          |
| An                             | .778          | .783          | .700          | .662          | .766          | .585          | .455          | .616          |
| Ab                             | .219          | .217          | .295          | .335          | .231          | .410          | .534          | .380          |

# Sill Feldspars

|                                | SB60F6 | SB60E1 | SB60E2 | SB60E3 |
|--------------------------------|--------|--------|--------|--------|
| SiO <sub>2</sub>               | 52.58  | 57.39  | 50.17  | 49.28  |
| CaO                            | 13.07  | 8.41   | 14.30  | 16.09  |
| K <sub>2</sub> O               | 0.13   | 0.18   | 0.43   | 0.05   |
| Al <sub>2</sub> O <sub>3</sub> | 29.73  | 26.86  | 31.07  | 32.28  |
| FeO                            | 0.47   | 0.35   | 0.51   | 0.30   |
| Na <sub>2</sub> O              | 4.03   | 6.39   | 2.86   | 2.93   |
| Total                          | 100.00 | 99.59  | 99.34  | 100.93 |
| Stoichiometry                  | 19.972 | 19.993 | 19.961 | 20.085 |
| Si                             | 9.552  | 10.325 | 9.226  | 8.958  |
| Ca                             | 2.542  | 1.620  | 2.816  | 3.131  |
| K                              | .026   | .037   | .097   | .010   |
| Al                             | 6.365  | 5.690  | 6.733  | 6.914  |
| Fe                             | .069   | .053   | .075   | .042   |
| Na                             | 1.417  | 2.228  | 1.014  | 1.029  |
| OR                             | .006   | .010   | .025   | .002   |
| An                             | .638   | .416   | .717   | .751   |
| Ab                             | .356   | .573   | .258   | .247   |

CAPE ST. MARY'S DIKE PYROXENES

Samples with relict pyroxenes were only recovered from  
Patricks Cove.

| Sample Number | Analysis Numbers |
|---------------|------------------|
|---------------|------------------|

|       |         |
|-------|---------|
| SB66A | 1 to 7  |
| SB56A | 8 to 19 |

|       | 1     | 2     | 3     | 4     | 5     | 6     | 7     | 8     | 9     | 10    |
|-------|-------|-------|-------|-------|-------|-------|-------|-------|-------|-------|
| SiO2  | 50.07 | 49.46 | 50.69 | 51.91 | 49.66 | 48.21 | 49.16 | 44.95 | 44.44 | 43.91 |
| TiO2  | .64   | 1.04  | .74   | .63   | 1.29  | 1.46  | 1.20  | 3.39  | 3.15  | 3.58  |
| Al2O3 | 2.61  | 3.77  | 2.17  | 2.09  | 3.02  | 4.81  | 3.48  | 7.70  | 7.81  | 8.29  |
| Cr2O3 | .30   | .20   | 0.00  | .20   | 0.00  | .30   | .10   | 0.00  | 0.00  | 0.00  |
| FeO   | 9.08  | 10.09 | 10.90 | 8.93  | 11.34 | 9.79  | 9.79  | 10.07 | 9.62  | 10.68 |
| MnO   | .19   | .21   | .22   | .19   | .20   | .18   | .18   | .16   | .10   | .18   |
| MgO   | 15.59 | 14.24 | 14.14 | 15.65 | 13.23 | 13.46 | 13.48 | 10.65 | 10.89 | 10.16 |
| NiO   | 0.00  | 0.00  | 0.00  | 0.00  | 0.00  | 0.00  | 0.00  | 0.00  | 0.00  | 0.00  |
| CaO   | 19.44 | 19.70 | 20.09 | 19.27 | 20.22 | 20.23 | 21.04 | 22.34 | 22.50 | 21.94 |
| Na2O  | .35   | .45   | .39   | .35   | .53   | .37   | .43   | .59   | .60   | .68   |
| K2O   | .02   | .01   | .01   | 0.00  | .01   | .02   | .01   | 0.00  | .01   | .01   |
| Total | 98.29 | 99.17 | 99.43 | 99.27 | 99.53 | 98.90 | 98.95 | 99.85 | 99.15 | 99.43 |

|       |       |       |       |       |       |       |       |       |       |       |
|-------|-------|-------|-------|-------|-------|-------|-------|-------|-------|-------|
| Si    | 1.898 | 1.869 | 1.917 | 1.939 | 1.884 | 1.832 | 1.869 | 1.712 | 1.704 | 1.686 |
| AlIV  | .102  | .131  | .083  | .061  | .116  | .168  | .131  | .288  | .296  | .314  |
| AlVI  | .015  | .037  | .014  | .031  | .019  | .047  | .025  | .057  | .057  | .061  |
| Ti    | .018  | .030  | .021  | .018  | .037  | .042  | .034  | .097  | .091  | .103  |
| Cr    | .009  | .006  | 0.000 | .006  | 0.000 | .009  | .003  | 0.000 | 0.000 | 0.000 |
| Fe    | .288  | .319  | .345  | .279  | .360  | .311  | .311  | .321  | .308  | .343  |
| Mn    | .006  | .007  | .007  | .006  | .006  | .006  | .006  | .005  | .003  | .006  |
| Mg    | .881  | .802  | .797  | .871  | .748  | .762  | .764  | .605  | .622  | .581  |
| Ni    | 0.000 | 0.000 | 0.000 | 0.000 | 0.000 | 0.000 | 0.000 | 0.000 | 0.000 | 0.000 |
| Ca    | .790  | .798  | .814  | .771  | .822  | .823  | .857  | .912  | .924  | .903  |
| Na    | .026  | .033  | .029  | .025  | .039  | .027  | .032  | .044  | .045  | .051  |
| K     | .001  | .000  | .000  | 0.000 | .000  | .001  | .000  | 0.000 | .000  | .000  |
| Total | 4.034 | 4.031 | 4.028 | 4.007 | 4.031 | 4.029 | 4.033 | 4.040 | 4.051 | 4.049 |

|       |      |      |      |      |      |      |      |      |      |      |
|-------|------|------|------|------|------|------|------|------|------|------|
| Ca    | 40.2 | 41.4 | 41.5 | 40.0 | 42.4 | 43.3 | 44.2 | 49.5 | 49.7 | 49.2 |
| Mg    | 44.8 | 41.7 | 40.6 | 45.2 | 38.6 | 40.1 | 39.4 | 32.8 | 33.5 | 31.7 |
| Fe+Mn | 15.0 | 16.9 | 17.9 | 14.8 | 18.9 | 16.7 | 16.4 | 17.7 | 16.8 | 19.0 |

|       | 11    | 12    | 13    | 14    | 15    | 16    | 17    | 18    | 19    |
|-------|-------|-------|-------|-------|-------|-------|-------|-------|-------|
| SiO2  | 45.61 | 45.95 | 45.04 | 44.79 | 43.70 | 45.59 | 44.89 | 44.78 | 45.54 |
| TiO2  | 3.06  | 2.64  | 2.63  | 3.66  | 3.56  | 2.52  | 2.92  | 3.21  | 3.21  |
| Al2O3 | 7.14  | 6.91  | 7.11  | 7.71  | 8.62  | 6.46  | 8.13  | 7.34  | 7.15  |
| Cr2O3 | 0.00  | 0.00  | 0.00  | 0.00  | 0.00  | 0.00  | 0.00  | 0.00  | 0.00  |
| FeO   | 9.95  | 9.83  | 9.85  | 10.00 | 9.76  | 9.68  | 9.58  | 10.46 | 10.12 |
| MnO   | .11   | .16   | .13   | .14   | .11   | .20   | .11   | .15   | .17   |
| MgO   | 10.57 | 11.28 | 11.24 | 10.11 | 10.31 | 11.06 | 10.87 | 10.70 | 10.38 |
| NiO   | 0.00  | 0.00  | 0.00  | 0.00  | 0.00  | 0.00  | 0.00  | 0.00  | 0.00  |
| CaO   | 22.40 | 21.95 | 22.17 | 21.22 | 22.27 | 22.24 | 22.46 | 21.91 | 21.85 |
| Na2O  | .57   | .64   | .68   | .69   | .70   | .59   | .68   | .64   | .67   |
| K2O   | 0.00  | 0.00  | 0.00  | .02   | 0.00  | .01   | 0.00  | .01   | .01   |
| Total | 99.45 | 99.39 | 98.92 | 98.34 | 99.05 | 98.37 | 99.64 | 99.21 | 99.13 |

|       |       |       |       |       |       |       |       |       |       |
|-------|-------|-------|-------|-------|-------|-------|-------|-------|-------|
| Si    | 1.741 | 1.752 | 1.731 | 1.726 | 1.679 | 1.759 | 1.709 | 1.719 | 1.744 |
| AlIV  | .259  | .248  | .269  | .274  | .321  | .241  | .291  | .281  | .256  |
| AlVI  | .062  | .062  | .053  | .076  | .069  | .052  | .074  | .051  | .066  |
| Ti    | .088  | .076  | .076  | .106  | .103  | .073  | .084  | .093  | .092  |
| Cr    | 0.000 | 0.000 | 0.000 | 0.000 | 0.000 | 0.000 | 0.000 | 0.000 | 0.000 |
| Fe    | .318  | .313  | .317  | .322  | .314  | .312  | .305  | .336  | .324  |
| Mn    | .004  | .005  | .004  | .005  | .004  | .007  | .004  | .005  | .006  |
| Mg    | .601  | .641  | .644  | .581  | .590  | .636  | .617  | .612  | .592  |
| Ni    | 0.000 | 0.000 | 0.000 | 0.000 | 0.000 | 0.000 | 0.000 | 0.000 | 0.000 |
| Ca    | .916  | .897  | .913  | .876  | .917  | .919  | .916  | .901  | .896  |
| Na    | .042  | .047  | .051  | .052  | .052  | .044  | .050  | .048  | .050  |
| K     | 0.000 | 0.000 | 0.000 | .001  | 0.000 | .000  | 0.000 | .000  | .000  |
| Total | 4.031 | 4.041 | 4.057 | 4.019 | 4.049 | 4.044 | 4.050 | 4.046 | 4.028 |

|       |      |      |      |      |      |      |      |      |      |
|-------|------|------|------|------|------|------|------|------|------|
| Ca    | 49.8 | 48.3 | 48.6 | 49.1 | 50.3 | 49.1 | 49.7 | 48.6 | 49.3 |
| Mg    | 32.7 | 34.5 | 34.3 | 32.6 | 32.4 | 33.9 | 33.5 | 33.0 | 32.6 |
| Fe+Mn | 17.5 | 17.2 | 17.1 | 18.3 | 17.4 | 17.0 | 16.8 | 18.4 | 18.1 |

NEW BRUNSWICK PYROXENE ANALYSES

All of the rock samples analyzed are from the Long Reach area.

| Location       | Sample Number | Rock Type              | Analysis Nos. |
|----------------|---------------|------------------------|---------------|
| Browns Flat    | GWD9          | Feldspar Phyric Basalt | 1 to 23       |
|                | GWD8          | Aphyric Basalt         | 24 to 39      |
|                | GWD12         | Aphyric Basalt         | 40 to 53      |
| Greenwich Hill | GWD20         | Aphyric Basalt         | 54 to 67      |
|                | GWD25         | Aphyric Basalt         | 68 to 78      |
|                | GWD26         | Feldspar Phyric Dike   | 79 to 92      |

|       | 1     | 2      | 3     | 4     | 5      | 6      | 7     | 8     | 9     | 10    |
|-------|-------|--------|-------|-------|--------|--------|-------|-------|-------|-------|
| SiO2  | 47.77 | 48.93  | 47.69 | 47.27 | 49.57  | 50.03  | 49.03 | 50.09 | 50.09 | 48.66 |
| TiO2  | 2.60  | 2.13   | 2.77  | 2.13  | 1.88   | 1.98   | 2.30  | 1.16  | 1.92  | 2.45  |
| Al2O3 | 4.38  | 3.18   | 4.23  | 3.15  | 3.11   | 2.34   | 2.77  | 2.66  | 2.85  | 4.12  |
| Cr2O3 | .11   | .10    | .06   | .08   | .04    | .05    | .02   | .04   | .04   | .02   |
| FeO   | 12.35 | 13.99  | 13.58 | 14.18 | 14.83  | 15.50  | 14.44 | 15.86 | 13.52 | 13.41 |
| MnO   | .20   | .22    | .14   | .30   | .37    | .29    | .14   | .43   | .22   | .12   |
| MgO   | 11.42 | 11.59  | 11.68 | 11.73 | 11.86  | 10.88  | 11.54 | 12.61 | 11.65 | 12.11 |
| NiO   | .01   | 0.00   | 0.00  | 0.00  | 0.00   | .05    | 0.00  | .03   | .01   | .04   |
| CaO   | 19.40 | 20.25  | 17.87 | 19.39 | 18.65  | 19.25  | 18.04 | 16.41 | 18.94 | 17.72 |
| Na2O  | .45   | .43    | .29   | .46   | .44    | .42    | .32   | .40   | .41   | .45   |
| K2O   | 0.00  | .05    | .02   | 0.00  | 0.00   | .03    | .05   | 0.00  | 0.00  | 0.00  |
| Total | 98.69 | 100.87 | 98.33 | 98.69 | 100.75 | 100.82 | 98.65 | 99.69 | 99.65 | 99.10 |

|       |       |       |       |       |       |       |       |       |       |       |
|-------|-------|-------|-------|-------|-------|-------|-------|-------|-------|-------|
| Si    | 1.836 | 1.857 | 1.841 | 1.839 | 1.879 | 1.903 | 1.892 | 1.913 | 1.906 | 1.858 |
| Al IV | .164  | .142  | .159  | .144  | .121  | .097  | .108  | .087  | .094  | .142  |
| Al VI | .035  | 0.000 | .034  | 0.000 | .018  | .008  | .018  | .033  | .033  | .043  |
| Ti    | .075  | .061  | .080  | .062  | .054  | .057  | .067  | .033  | .055  | .070  |
| Cr    | .003  | .003  | .002  | .002  | .001  | .002  | .001  | .001  | .001  | .001  |
| Fe    | .397  | .444  | .438  | .461  | .470  | .493  | .466  | .507  | .430  | .428  |
| Mn    | .007  | .007  | .005  | .010  | .012  | .009  | .005  | .014  | .007  | .004  |
| Mg    | .654  | .656  | .672  | .680  | .670  | .617  | .664  | .718  | .661  | .689  |
| Ni    | .000  | 0.000 | 0.000 | 0.000 | 0.000 | .002  | 0.000 | .001  | .000  | .001  |
| Ca    | .799  | .823  | .739  | .808  | .757  | .784  | .746  | .672  | .772  | .725  |
| Na    | .034  | .032  | .022  | .035  | .032  | .031  | .024  | .030  | .030  | .033  |
| K     | 0.000 | .002  | .001  | 0.000 | 0.000 | .001  | .002  | 0.000 | 0.000 | 0.000 |
| Total | 4.004 | 4.027 | 3.993 | 4.043 | 4.014 | 4.003 | 3.991 | 4.008 | 3.990 | 3.995 |

|       |      |      |      |      |      |      |      |      |      |      |
|-------|------|------|------|------|------|------|------|------|------|------|
| Ca    | 43.0 | 42.7 | 39.9 | 41.2 | 39.7 | 41.2 | 39.7 | 35.2 | 41.3 | 39.3 |
| Mg    | 35.2 | 34.0 | 36.2 | 34.7 | 35.1 | 32.4 | 35.3 | 37.6 | 35.3 | 37.3 |
| Fe+Mn | 21.7 | 23.4 | 23.9 | 24.0 | 25.2 | 26.4 | 25.0 | 27.3 | 23.4 | 23.4 |



|       | 11     | 12    | 13    | 14    | 15    | 16     | 17     | 18     | 19     | 20    |
|-------|--------|-------|-------|-------|-------|--------|--------|--------|--------|-------|
| SiO2  | 49.93  | 46.25 | 48.20 | 51.73 | 48.63 | 50.43  | 49.60  | 49.84  | 49.58  | 51.41 |
| TiO2  | 1.91   | 2.64  | 1.55  | 1.00  | 2.21  | 2.38   | 1.93   | 1.74   | 2.11   | .93   |
| Al2O3 | 2.56   | 4.53  | 2.85  | 1.93  | 3.88  | 2.77   | 2.72   | 2.77   | 4.34   | 1.61  |
| Cr2O3 | 0.00   | 0.00  | 0.00  | .07   | 0.00  | 0.00   | .03    | 0.00   | .14    | 0.00  |
| FeO   | 14.74  | 13.71 | 15.48 | 13.38 | 15.59 | 14.51  | 14.43  | 15.05  | 12.11  | 14.73 |
| MnO   | .41    | .16   | .31   | .21   | .34   | .11    | .32    | .20    | .20    | .26   |
| MgO   | 11.90  | 12.00 | 11.03 | 14.25 | 11.77 | 11.32  | 11.94  | 11.72  | 12.74  | 13.53 |
| NiO   | 0.00   | 0.00  | .06   | .01   | .04   | 0.00   | .05    | 0.00   | 0.00   | 0.00  |
| CaO   | 19.37  | 18.54 | 18.62 | 16.23 | 15.54 | 18.49  | 18.97  | 19.12  | 19.73  | 16.22 |
| Na2O  | .35    | .28   | .34   | .21   | .58   | .47    | .46    | .28    | .20    | .29   |
| K2O   | .01    | .03   | 0.00  | 0.00  | .01   | 0.00   | 0.00   | .03    | .03    | 0.00  |
| Total | 101.18 | 98.14 | 98.44 | 99.02 | 98.59 | 100.48 | 100.45 | 100.75 | 101.18 | 98.98 |

|       |       |       |       |       |       |       |       |       |       |       |
|-------|-------|-------|-------|-------|-------|-------|-------|-------|-------|-------|
| Si    | 1.887 | 1.801 | 1.881 | 1.954 | 1.876 | 1.907 | 1.885 | 1.890 | 1.850 | 1.959 |
| Al IV | .113  | .199  | .119  | .044  | .124  | .093  | .115  | .110  | .150  | .041  |
| Al VI | .001  | .008  | .012  | .042  | .052  | .030  | .007  | .014  | .041  | .032  |
| Ti    | .054  | .077  | .045  | .028  | .064  | .068  | .055  | .050  | .059  | .027  |
| Cr    | 0.000 | 0.000 | 0.000 | .002  | 0.000 | 0.000 | .001  | 0.000 | .004  | 0.000 |
| Fe    | .466  | .446  | .505  | .423  | .503  | .459  | .459  | .477  | .378  | .469  |
| Mn    | .013  | .005  | .010  | .007  | .011  | .004  | .010  | .006  | .006  | .008  |
| Mg    | .670  | .696  | .642  | .803  | .677  | .638  | .676  | .663  | .709  | .769  |
| Ni    | 0.000 | 0.000 | .002  | .000  | .001  | 0.000 | .002  | 0.000 | 0.000 | 0.000 |
| Ca    | .784  | .773  | .779  | .658  | .642  | .749  | .772  | .777  | .789  | .662  |
| Na    | .026  | .021  | .026  | .015  | .043  | .034  | .034  | .021  | .014  | .021  |
| K     | .000  | .001  | 0.000 | 0.000 | .000  | 0.000 | 0.000 | .001  | .001  | 0.000 |
| Total | 4.015 | 4.030 | 4.021 | 3.979 | 3.994 | 3.981 | 4.016 | 4.009 | 4.001 | 3.989 |

|       |      |      |      |      |      |      |      |      |      |      |
|-------|------|------|------|------|------|------|------|------|------|------|
| Ca    | 40.6 | 40.3 | 40.2 | 34.8 | 35.0 | 40.5 | 40.3 | 40.4 | 41.9 | 34.7 |
| Mg    | 34.7 | 36.2 | 33.1 | 42.5 | 36.9 | 34.5 | 35.3 | 34.4 | 37.7 | 40.3 |
| Fe+Mn | 24.8 | 23.5 | 26.6 | 22.7 | 28.0 | 25.0 | 24.5 | 25.2 | 20.4 | 25.0 |

|       | 21    | 22     | 23     | 24    | 25    | 26     | 27     | 28     | 29     | 30     |
|-------|-------|--------|--------|-------|-------|--------|--------|--------|--------|--------|
| SiO2  | 48.86 | 51.01  | 47.54  | 52.23 | 52.58 | 52.18  | 53.04  | 52.50  | 51.75  | 52.47  |
| TiO2  | 2.35  | 1.35   | 2.84   | .32   | .30   | .30    | .23    | .21    | .41    | .45    |
| Al2O3 | 3.55  | 2.04   | 4.56   | 3.05  | 1.68  | 2.08   | 2.74   | 2.10   | 2.12   | 2.53   |
| Cr2O3 | .07   | .04    | 0.00   | .29   | .18   | .22    | .73    | .29    | .30    | .44    |
| FeO   | 13.78 | 13.11  | 14.03  | 6.77  | 5.88  | 5.53   | 4.43   | 4.73   | 5.88   | 5.60   |
| MnO   | .20   | .10    | .22    | .16   | .15   | .05    | .04    | .14    | .07    | .10    |
| MgO   | 11.46 | 14.16  | 12.31  | 16.20 | 18.03 | 17.33  | 18.12  | 18.00  | 17.18  | 17.28  |
| NiO   | .01   | .10    | 0.00   | 0.00  | 0.00  | 0.00   | 0.00   | .03    | .01    | 0.00   |
| CaO   | 18.66 | 18.61  | 19.32  | 19.92 | 20.89 | 22.68  | 22.07  | 22.05  | 22.53  | 22.37  |
| Na2O  | .40   | .30    | .21    | .05   | .07   | .17    | .15    | .11    | .10    | .09    |
| K2O   | 0.00  | 0.00   | 0.00   | .08   | 0.00  | .01    | 0.00   | .01    | 0.00   | 0.00   |
| Total | 99.34 | 100.82 | 101.03 | 99.07 | 99.76 | 100.55 | 101.55 | 100.17 | 100.35 | 101.33 |

|       |       |       |       |       |       |       |       |       |       |       |
|-------|-------|-------|-------|-------|-------|-------|-------|-------|-------|-------|
| Si    | 1.870 | 1.911 | 1.799 | 1.934 | 1.934 | 1.912 | 1.909 | 1.920 | 1.904 | 1.906 |
| AlIV  | .130  | .089  | .201  | .066  | .066  | .088  | .091  | .080  | .092  | .094  |
| AlVI  | .030  | .001  | .002  | .067  | .006  | .002  | .026  | .011  | 0.000 | .014  |
| Ti    | .068  | .038  | .081  | .009  | .008  | .008  | .006  | .006  | .011  | .012  |
| Cr    | .002  | .001  | 0.000 | .008  | .005  | .006  | .021  | .008  | .009  | .013  |
| Fe    | .441  | .411  | .444  | .210  | .181  | .169  | .133  | .145  | .181  | .170  |
| Mn    | .006  | .003  | .007  | .005  | .005  | .002  | .001  | .004  | .002  | .003  |
| Mg    | .654  | .791  | .694  | .894  | .988  | .947  | .972  | .981  | .942  | .936  |
| Ni    | .000  | .003  | 0.000 | 0.000 | 0.000 | 0.000 | 0.000 | .001  | .000  | 0.000 |
| Ca    | .765  | .747  | .783  | .790  | .823  | .891  | .851  | .864  | .888  | .871  |
| Na    | .030  | .022  | .015  | .004  | .005  | .012  | .010  | .008  | .007  | .006  |
| K     | 0.000 | 0.000 | 0.000 | .004  | 0.000 | .000  | 0.000 | .000  | 0.000 | 0.000 |
| Total | 3.996 | 4.016 | 4.027 | 3.990 | 4.022 | 4.038 | 4.021 | 4.029 | 4.038 | 4.025 |

|       |      |      |      |      |      |      |      |      |      |      |
|-------|------|------|------|------|------|------|------|------|------|------|
| Ca    | 41.0 | 38.3 | 40.6 | 41.6 | 41.2 | 44.3 | 43.5 | 43.3 | 44.1 | 44.0 |
| Mg    | 35.0 | 40.5 | 36.0 | 47.1 | 49.5 | 47.1 | 49.7 | 49.2 | 46.8 | 47.3 |
| Fe+Mn | 24.0 | 21.2 | 23.4 | 11.3 | 9.3  | 8.5  | 6.9  | 7.5  | 9.1  | 8.7  |

|       | 31     | 32     | 33     | 34     | 35     | 36     | 37     | 38     | 39    | 40     |
|-------|--------|--------|--------|--------|--------|--------|--------|--------|-------|--------|
| SiO2  | 53.57  | 50.46  | 51.18  | 50.42  | 51.54  | 53.02  | 53.46  | 51.28  | 53.28 | 51.98  |
| TiO2  | .42    | .39    | .54    | .61    | .46    | .27    | .19    | .60    | .26   | .41    |
| Al2O3 | 2.50   | 3.29   | 3.76   | 4.16   | 3.18   | 2.58   | 2.43   | 4.11   | 2.09  | 1.69   |
| Cr2O3 | .20    | .34    | .41    | .42    | .52    | .21    | .38    | .27    | .26   | .16    |
| FeO   | 5.50   | 5.89   | 5.97   | 5.99   | 5.43   | 5.73   | 5.06   | 6.42   | 5.22  | 8.37   |
| MnO   | .15    | .09    | .07    | .13    | .07    | .15    | .13    | .10    | .04   | .21    |
| MgO   | 17.53  | 16.98  | 16.79  | 15.28  | 16.76  | 17.94  | 17.60  | 16.02  | 18.05 | 16.96  |
| NiO   | 0.00   | 0.00   | 0.00   | 0.00   | .03    | 0.00   | .04    | .01    | .07   | 0.00   |
| CaO   | 21.50  | 22.95  | 21.55  | 24.36  | 23.41  | 20.53  | 22.03  | 21.31  | 19.35 | 20.57  |
| Na2O  | .05    | .14    | .14    | .09    | .24    | .13    | .05    | .18    | .05   | .11    |
| K2O   | .02    | .02    | 0.00   | 0.00   | .01    | 0.00   | 0.00   | 0.00   | 0.00  | 0.00   |
| Total | 101.44 | 100.55 | 100.41 | 101.46 | 101.65 | 100.56 | 101.37 | 100.30 | 98.67 | 100.46 |

|       |       |       |       |       |       |       |       |       |       |       |
|-------|-------|-------|-------|-------|-------|-------|-------|-------|-------|-------|
| Si    | 1.932 | 1.860 | 1.877 | 1.848 | 1.875 | 1.928 | 1.930 | 1.883 | 1.960 | 1.921 |
| Al IV | .068  | .140  | .123  | .152  | .125  | .072  | .079  | .117  | .040  | .074  |
| Al VI | .038  | .003  | .039  | .028  | .011  | .038  | .033  | .061  | .051  | 0.000 |
| Ti    | .011  | .011  | .013  | .017  | .013  | .007  | .005  | .017  | .007  | .011  |
| Cr    | .006  | .010  | .012  | .012  | .015  | .006  | .011  | .008  | .008  | .005  |
| Fe    | .166  | .182  | .183  | .184  | .165  | .174  | .153  | .197  | .161  | .259  |
| Mn    | .005  | .003  | .002  | .004  | .002  | .005  | .004  | .003  | .001  | .007  |
| Mg    | .942  | .933  | .918  | .835  | .909  | .972  | .947  | .877  | .990  | .934  |
| Ni    | 0.000 | 0.000 | 0.000 | 0.000 | .001  | 0.000 | .001  | .000  | .002  | 0.000 |
| Ca    | .831  | .906  | .847  | .957  | .912  | .800  | .852  | .838  | .763  | .814  |
| Na    | .003  | .010  | .010  | .006  | .017  | .009  | .003  | .013  | .004  | .008  |
| K     | .001  | .001  | 0.000 | 0.000 | .000  | 0.000 | 0.000 | 0.000 | 0.000 | 0.000 |
| Total | 4.003 | 4.058 | 4.026 | 4.042 | 4.046 | 4.011 | 4.010 | 4.014 | 3.985 | 4.032 |

|       |      |      |      |      |      |      |      |      |      |      |
|-------|------|------|------|------|------|------|------|------|------|------|
| Ca    | 42.7 | 44.8 | 43.4 | 48.3 | 45.9 | 41.0 | 43.6 | 43.8 | 39.8 | 40.4 |
| Mg    | 48.5 | 46.1 | 47.1 | 42.2 | 45.7 | 49.8 | 48.4 | 45.8 | 51.7 | 46.4 |
| Fe+Mn | 8.8  | 9.1  | 9.5  | 9.5  | 8.4  | 9.2  | 8.0  | 10.5 | 8.5  | 13.2 |

|       | 41     | 42     | 43     | 44.    | 45.    | 46     | 47     | 48     | 49    | 50     |
|-------|--------|--------|--------|--------|--------|--------|--------|--------|-------|--------|
| SiO2  | 53.34  | 52.86  | 52.73  | 53.70  | 53.72  | 51.80  | 51.13  | 53.53  | 50.64 | 53.59  |
| TiO2  | .22    | .38    | .47    | .50    | .36    | .50    | .43    | .36    | .64   | .43    |
| Al2O3 | 1.83   | 1.86   | 1.68   | 1.76   | 1.87   | 1.92   | 1.91   | 1.82   | 1.43  | 1.72   |
| Cr2O3 | .18    | .23    | .12    | .21    | .25    | .04    | .31    | .26    | 0.00  | .13    |
| FeO   | 8.96   | 8.39   | 8.96   | 8.59   | 8.24   | 10.47  | 7.88   | 7.96   | 12.77 | 8.34   |
| MnO   | .19    | .16    | .21    | .14    | .17    | .18    | .14    | .14    | .30   | .18    |
| MgO   | 17.48  | 16.62  | 16.94  | 16.78  | 16.89  | 17.48  | 16.96  | 16.56  | 15.19 | 16.31  |
| NiO   | .02    | .03    | 0.00   | 0.00   | .09    | 0.00   | 0.00   | .03    | .06   | 0.00   |
| CaO   | 18.64  | 20.42  | 19.90  | 19.34  | 19.45  | 19.33  | 22.01  | 19.54  | 17.94 | 20.39  |
| Na2O  | .27    | .19    | .11    | .17    | .11    | .12    | .13    | .19    | .26   | .15    |
| K2O   | .05    | 0.00   | 0.00   | .05    | .01    | 0.00   | .01    | 0.00   | .09   | 0.00   |
| Total | 101.18 | 101.14 | 101.12 | 101.24 | 101.16 | 101.84 | 100.91 | 100.39 | 99.32 | 101.24 |

|       |       |       |       |       |       |       |       |       |       |       |
|-------|-------|-------|-------|-------|-------|-------|-------|-------|-------|-------|
| Si    | 1.946 | 1.936 | 1.934 | 1.956 | 1.956 | 1.900 | 1.890 | 1.962 | 1.924 | 1.955 |
| Al IV | .054  | .064  | .066  | .044  | .044  | .083  | .083  | .038  | .064  | .045  |
| Al VI | .025  | .016  | .006  | .031  | .036  | 0.000 | 0.000 | .040  | 0.000 | .029  |
| Ti    | .006  | .010  | .013  | .014  | .010  | .014  | .012  | .010  | .018  | .012  |
| Cr    | .005  | .007  | .003  | .006  | .007  | .001  | .009  | .008  | 0.000 | .004  |
| Fe    | .273  | .257  | .275  | .262  | .251  | .321  | .244  | .244  | .406  | .254  |
| Mn    | .006  | .005  | .007  | .004  | .005  | .006  | .004  | .004  | .010  | .006  |
| Mg    | .951  | .907  | .926  | .911  | .916  | .956  | .934  | .905  | .860  | .887  |
| Ni    | .001  | .001  | 0.000 | 0.000 | .003  | 0.000 | 0.000 | .001  | .002  | 0.000 |
| Ca    | .729  | .801  | .782  | .755  | .759  | .760  | .872  | .767  | .730  | .797  |
| Na    | .019  | .013  | .008  | .012  | .008  | .009  | .009  | .013  | .019  | .011  |
| K     | .002  | 0.000 | 0.000 | .002  | .000  | 0.000 | .000  | 0.000 | .004  | 0.000 |
| Total | 4.017 | 4.017 | 4.019 | 3.997 | 3.995 | 4.048 | 4.057 | 3.992 | 4.037 | 3.999 |

|       |      |      |      |      |      |      |      |      |      |      |
|-------|------|------|------|------|------|------|------|------|------|------|
| Ca    | 37.2 | 40.7 | 39.3 | 39.1 | 39.3 | 37.2 | 42.4 | 40.0 | 36.4 | 41.0 |
| Mg    | 48.5 | 46.0 | 46.5 | 47.2 | 47.5 | 46.8 | 45.5 | 47.1 | 42.9 | 45.6 |
| Fe+Mn | 14.3 | 13.3 | 14.1 | 13.8 | 13.3 | 16.0 | 12.1 | 12.9 | 20.7 | 13.4 |

|       | 51     | 52     | 53    | 54    | 55    | 56    | 57    | 58    | 59    | 60    |
|-------|--------|--------|-------|-------|-------|-------|-------|-------|-------|-------|
| SiO2  | 51.64  | 53.17  | 51.91 | 53.43 | 52.20 | 53.32 | 52.90 | 53.64 | 53.21 | 53.02 |
| TiO2  | .38    | .40    | .36   | .34   | .61   | .46   | .43   | .36   | .52   | .39   |
| Al2O3 | 1.85   | 1.72   | 1.79  | 2.17  | 1.97  | 2.12  | 1.95  | 2.09  | .91   | 2.14  |
| Cr2O3 | .27    | .27    | .24   | .43   | 0.00  | .41   | .16   | .34   | 0.00  | .27   |
| FeO   | 9.20   | 8.23   | 7.79  | 7.94  | 11.02 | 7.73  | 8.20  | 7.36  | 19.75 | 7.95  |
| MnO   | .26    | .16    | .16   | .14   | .25   | .14   | .05   | .17   | .39   | .21   |
| MgO   | 17.08  | 16.90  | 17.09 | 16.90 | 16.09 | 17.10 | 16.98 | 16.84 | 20.24 | 16.07 |
| NiO   | .05    | 0.00   | 0.00  | .01   | .01   | .05   | .05   | .04   | 0.00  | 0.00  |
| CaO   | 20.44  | 20.16  | 20.17 | 17.13 | 16.63 | 18.46 | 18.25 | 17.50 | 4.34  | 17.76 |
| Na2O  | .06    | .20    | .27   | .23   | .11   | .13   | .16   | .22   | .05   | .27   |
| K2O   | .04    | 0.00   | .01   | .01   | .03   | 0.00  | .05   | .01   | .08   | 0.00  |
| Total | 101.27 | 101.21 | 99.79 | 98.73 | 98.92 | 99.92 | 99.18 | 98.57 | 99.49 | 98.08 |

|       |       |       |       |       |       |       |       |       |       |       |
|-------|-------|-------|-------|-------|-------|-------|-------|-------|-------|-------|
| Si    | 1.903 | 1.942 | 1.925 | 1.976 | 1.956 | 1.956 | 1.958 | 1.983 | 1.988 | 1.978 |
| Al IV | .080  | .058  | .075  | .024  | .044  | .044  | .042  | .017  | .012  | .022  |
| Al VI | 0.000 | .016  | .003  | .070  | .043  | .047  | .043  | .074  | .028  | .072  |
| Ti    | .011  | .011  | .010  | .009  | .017  | .013  | .012  | .010  | .015  | .011  |
| Cr    | .008  | .008  | .007  | .013  | 0.000 | .012  | .005  | .010  | 0.000 | .008  |
| Fe    | .283  | .251  | .242  | .246  | .345  | .237  | .254  | .228  | .617  | .248  |
| Mn    | .008  | .005  | .005  | .004  | .008  | .004  | .002  | .005  | .012  | .007  |
| Mg    | .938  | .920  | .945  | .931  | .898  | .935  | .937  | .928  | 1.127 | .894  |
| Ni    | .001  | 0.000 | 0.000 | .000  | .000  | .001  | .001  | .001  | 0.000 | 0.000 |
| Ca    | .807  | .789  | .801  | .679  | .667  | .725  | .724  | .693  | .174  | .710  |
| Na    | .004  | .014  | .019  | .016  | .008  | .009  | .011  | .016  | .004  | .020  |
| K     | .002  | 0.000 | .000  | .000  | .001  | 0.000 | .002  | .000  | .004  | 0.000 |
| Total | 4.046 | 4.014 | 4.032 | 3.970 | 3.989 | 3.984 | 3.992 | 3.965 | 3.981 | 3.969 |

|       |      |      |      |      |      |      |      |      |      |      |
|-------|------|------|------|------|------|------|------|------|------|------|
| Ca    | 39.6 | 40.1 | 40.2 | 36.5 | 34.8 | 38.1 | 37.8 | 37.4 | 9.0  | 38.2 |
| Mg    | 46.1 | 46.8 | 47.4 | 50.1 | 46.8 | 49.2 | 48.9 | 50.1 | 58.4 | 48.1 |
| Fe+Mn | 14.3 | 13.0 | 12.4 | 13.4 | 18.4 | 12.7 | 13.3 | 12.6 | 32.6 | 13.7 |

|       | 61    | 62    | 63    | 64    | 65    | 66    | 67    | 68     | 69    | 70     |
|-------|-------|-------|-------|-------|-------|-------|-------|--------|-------|--------|
| SiO2  | 53.09 | 52.22 | 52.80 | 52.98 | 52.67 | 53.25 | 53.00 | 53.14  | 53.41 | 53.67  |
| TiO2  | .45   | .47   | .59   | .46   | .31   | .31   | .69   | .47    | .29   | .46    |
| Al2O3 | 2.18  | 2.10  | 2.08  | 2.16  | 2.14  | 2.16  | 2.05  | 1.84   | 2.28  | 1.95   |
| Cr2O3 | .35   | .46   | .19   | .41   | .43   | .48   | .01   | .13    | .33   | .28    |
| FeO   | 7.72  | 7.83  | 10.82 | 7.62  | 7.82  | 7.74  | 11.08 | 9.56   | 8.10  | 10.55  |
| MnO   | .19   | .16   | .23   | .14   | .11   | .14   | .23   | .18    | .21   | .18    |
| MgO   | 16.32 | 16.94 | 16.18 | 17.11 | 16.97 | 17.16 | 15.48 | 16.56  | 15.62 | 15.68  |
| NiO   | .01   | 0.00  | .09   | .03   | 0.00  | 0.00  | 0.00  | .07    | .04   | 0.00   |
| CaO   | 18.48 | 18.70 | 15.96 | 17.80 | 19.02 | 17.86 | 15.47 | 18.38  | 17.69 | 17.78  |
| Na2O  | .08   | .16   | .16   | .18   | .15   | .13   | .25   | .25    | .30   | .29    |
| K2O   | .01   | .04   | .05   | 0.00  | 0.00  | 0.00  | .04   | 0.00   | 0.00  | 0.00   |
| Total | 98.88 | 99.08 | 99.15 | 98.89 | 99.62 | 99.23 | 98.30 | 100.58 | 98.27 | 100.84 |
| Si    | 1.967 | 1.939 | 1.966 | 1.960 | 1.944 | 1.963 | 1.987 | 1.953  | 1.988 | 1.970  |
| AlIV  | .033  | .061  | .034  | .040  | .056  | .037  | .013  | .047   | .012  | .030   |
| AlVI  | .062  | .031  | .058  | .054  | .037  | .057  | .077  | .033   | .088  | .054   |
| Ti    | .013  | .013  | .017  | .013  | .009  | .009  | .019  | .013   | .008  | .013   |
| Cr    | .010  | .014  | .006  | .012  | .013  | .014  | .000  | .004   | .010  | .008   |
| Fe    | .239  | .243  | .337  | .236  | .241  | .239  | .347  | .294   | .252  | .324   |
| Mn    | .006  | .005  | .007  | .004  | .003  | .004  | .007  | .006   | .007  | .006   |
| Mg    | .901  | .938  | .898  | .943  | .934  | .943  | .865  | .907   | .867  | .858   |
| Ni    | .000  | 0.000 | .003  | .001  | 0.000 | 0.000 | 0.000 | .002   | .001  | 0.000  |
| Ca    | .734  | .744  | .637  | .705  | .752  | .705  | .621  | .724   | .706  | .699   |
| Na    | .006  | .012  | .012  | .013  | .011  | .009  | .018  | .018   | .022  | .021   |
| K     | .000  | .002  | .002  | 0.000 | 0.000 | 0.000 | .002  | 0.000  | 0.000 | 0.000  |
| Total | 3.971 | 4.001 | 3.976 | 3.981 | 4.000 | 3.979 | 3.958 | 4.001  | 3.960 | 3.982  |
| Ca    | 39.0  | 38.6  | 33.9  | 37.3  | 39.0  | 37.3  | 33.8  | 37.5   | 38.5  | 37.1   |
| Mg    | 47.9  | 48.6  | 47.8  | 49.9  | 48.4  | 49.9  | 47.0  | 47.0   | 47.3  | 45.5   |
| Fe+Mn | 13.0  | 12.9  | 18.3  | 12.7  | 12.7  | 12.8  | 19.3  | 15.5   | 14.1  | 17.5   |

|                                | 71    | 72    | 73    | 74     | 75     | 76    | 77    | 78    | 79    | 80    |
|--------------------------------|-------|-------|-------|--------|--------|-------|-------|-------|-------|-------|
| SiO <sub>2</sub>               | 53.56 | 52.95 | 53.14 | 52.69  | 52.23  | 53.42 | 51.59 | 52.69 | 50.23 | 49.39 |
| TiO <sub>2</sub>               | .65   | .40   | .32   | .30    | .38    | .35   | .52   | .43   | 1.79  | 1.63  |
| Al <sub>2</sub> O <sub>3</sub> | 2.14  | 1.83  | 2.22  | 2.02   | 1.75   | 1.69  | 2.53  | 2.22  | 3.95  | 4.40  |
| Cr <sub>2</sub> O <sub>3</sub> | .06   | .22   | .33   | .41    | .29    | .30   | .32   | .27   | .05   | 0.00  |
| FeO                            | 10.52 | 9.14  | 9.33  | 10.30  | 9.14   | 9.17  | 9.61  | 9.32  | 9.61  | 10.80 |
| MnO                            | .17   | .21   | .21   | .07    | .17    | .21   | .19   | .21   | .13   | .13   |
| MgO                            | 15.48 | 16.42 | 16.57 | 15.75  | 16.66  | 15.17 | 15.63 | 16.20 | 13.61 | 13.47 |
| NiO                            | 0.00  | 0.00  | 0.00  | .01    | .03    | 0.00  | 0.00  | 0.00  | .05   | 0.00  |
| CaO                            | 16.07 | 17.72 | 17.06 | 18.11  | 19.30  | 18.93 | 18.00 | 17.24 | 19.92 | 18.41 |
| Na <sub>2</sub> O              | .36   | .10   | .29   | .35    | .12    | .19   | .23   | .36   | .33   | .60   |
| K <sub>2</sub> O               | .11   | .01   | 0.00  | .03    | .02    | .05   | .01   | .01   | 0.00  | 0.00  |
| Total                          | 99.12 | 99.00 | 99.47 | 100.04 | 100.09 | 99.48 | 98.63 | 98.95 | 99.67 | 98.83 |

|       |       |       |       |       |       |       |       |       |       |       |
|-------|-------|-------|-------|-------|-------|-------|-------|-------|-------|-------|
| Si    | 1.989 | 1.969 | 1.964 | 1.954 | 1.935 | 1.983 | 1.937 | 1.961 | 1.880 | 1.869 |
| Al IV | .011  | .031  | .036  | .046  | .065  | .017  | .063  | .039  | .120  | .131  |
| Al VI | .082  | .049  | .061  | .042  | .012  | .057  | .049  | .058  | .054  | .066  |
| Ti    | .018  | .011  | .009  | .008  | .011  | .010  | .015  | .012  | .050  | .046  |
| Cr    | .002  | .006  | .010  | .012  | .008  | .009  | .009  | .008  | .001  | 0.000 |
| Fe    | .327  | .284  | .288  | .319  | .283  | .285  | .302  | .290  | .301  | .342  |
| Mn    | .005  | .007  | .007  | .002  | .005  | .007  | .006  | .007  | .004  | .004  |
| Mg    | .857  | .910  | .913  | .870  | .920  | .839  | .875  | .899  | .759  | .760  |
| Ni    | 0.000 | 0.000 | 0.000 | .000  | .001  | 0.000 | 0.000 | 0.000 | .002  | 0.000 |
| Ca    | .639  | .706  | .676  | .719  | .766  | .753  | .724  | .687  | .799  | .747  |
| Na    | .026  | .007  | .021  | .025  | .009  | .014  | .017  | .026  | .024  | .044  |
| K     | .005  | .000  | 0.000 | .001  | .001  | .002  | .000  | .000  | 0.000 | 0.000 |
| Total | 3.961 | 3.981 | 3.984 | 4.001 | 4.016 | 3.974 | 3.996 | 3.988 | 3.994 | 4.008 |

|       |      |      |      |      |      |      |      |      |      |      |
|-------|------|------|------|------|------|------|------|------|------|------|
| Ca    | 35.0 | 37.0 | 35.9 | 37.6 | 38.8 | 40.0 | 38.0 | 36.5 | 42.9 | 40.3 |
| Mg    | 46.9 | 47.7 | 48.5 | 45.5 | 46.6 | 44.6 | 45.9 | 47.7 | 40.8 | 41.0 |
| Fe+Mn | 18.2 | 15.3 | 15.7 | 16.8 | 14.6 | 15.5 | 16.1 | 15.8 | 16.4 | 18.7 |

|       | 81    | 82     | 83    | 84     | 85    | 86    | 87    | 88    | 89     | 90    |
|-------|-------|--------|-------|--------|-------|-------|-------|-------|--------|-------|
| SiO2  | 48.60 | 49.50  | 50.57 | 50.22  | 48.75 | 48.54 | 47.21 | 53.21 | 51.37  | 52.87 |
| TiO2  | 2.00  | 1.83   | 1.33  | 1.79   | 2.11  | 2.16  | 2.05  | .89   | 1.54   | 1.32  |
| Al2O3 | 4.28  | 4.63   | 4.20  | 4.30   | 4.29  | 3.94  | 4.23  | 2.54  | 4.72   | 1.71  |
| Cr2O3 | .38   | .09    | .60   | .09    | 0.00  | .07   | .10   | .24   | .07    | 0.00  |
| FeO   | 8.47  | 9.30   | 7.87  | 9.84   | 9.92  | 10.03 | 9.86  | 8.39  | 10.23  | 12.96 |
| MnO   | .20   | .18    | .11   | .17    | .16   | .17   | .16   | .13   | .20    | .34   |
| MgO   | 14.58 | 14.70  | 14.98 | 14.52  | 14.02 | 13.89 | 14.52 | 17.58 | 15.40  | 14.34 |
| NiO   | .02   | .03    | .06   | .04    | 0.00  | 0.00  | 0.00  | 0.00  | 0.00   | .05   |
| CaO   | 20.20 | 20.19  | 18.73 | 18.58  | 19.43 | 20.23 | 20.07 | 16.18 | 17.13  | 15.61 |
| Na2O  | .28   | .25    | .43   | .43    | .42   | .39   | .36   | .43   | .43    | .30   |
| K2O   | 0.00  | .05    | 0.00  | .05    | .01   | 0.00  | .04   | .01   | 0.00   | .01   |
| Total | 99.01 | 100.75 | 98.88 | 100.03 | 99.11 | 99.42 | 98.30 | 99.60 | 101.09 | 99.51 |

|       |       |       |       |       |       |       |       |       |       |       |
|-------|-------|-------|-------|-------|-------|-------|-------|-------|-------|-------|
| Si    | 1.832 | 1.835 | 1.887 | 1.869 | 1.842 | 1.836 | 1.807 | 1.951 | 1.880 | 1.979 |
| AlIV  | .168  | .165  | .113  | .131  | .158  | .164  | .191  | .049  | .120  | .021  |
| AlVI  | .023  | .038  | .071  | .057  | .033  | .011  | 0.000 | .061  | .084  | .054  |
| Ti    | .057  | .051  | .037  | .050  | .060  | .061  | .059  | .025  | .042  | .037  |
| Cr    | .011  | .003  | .018  | .003  | 0.000 | .002  | .003  | .007  | .002  | 0.000 |
| Fe    | .267  | .288  | .246  | .306  | .313  | .317  | .306  | .257  | .313  | .406  |
| Mn    | .006  | .006  | .003  | .005  | .005  | .005  | .005  | .004  | .006  | .011  |
| Mg    | .819  | .812  | .833  | .805  | .789  | .783  | .828  | .961  | .840  | .800  |
| Ni    | .001  | .001  | .002  | .001  | 0.000 | 0.000 | 0.000 | 0.000 | 0.000 | .002  |
| Ca    | .816  | .802  | .749  | .741  | .786  | .820  | .823  | .636  | .672  | .626  |
| Na    | .020  | .018  | .031  | .031  | .031  | .029  | .027  | .031  | .031  | .022  |
| K     | 0.000 | .002  | 0.000 | .002  | .000  | 0.000 | .002  | .000  | 0.000 | .000  |
| Total | 4.020 | 4.021 | 3.990 | 4.002 | 4.018 | 4.028 | 4.051 | 3.981 | 3.990 | 3.957 |

|       |      |      |      |      |      |      |      |      |      |      |
|-------|------|------|------|------|------|------|------|------|------|------|
| Ca    | 42.7 | 42.0 | 40.9 | 39.9 | 41.5 | 42.6 | 41.9 | 34.2 | 36.7 | 34.0 |
| Mg    | 42.9 | 42.6 | 45.5 | 43.4 | 41.7 | 40.7 | 42.2 | 51.7 | 45.9 | 43.4 |
| Fe+Mn | 14.3 | 15.4 | 13.6 | 16.8 | 16.8 | 16.8 | 15.9 | 14.1 | 17.4 | 22.6 |



|                                | 91    | 92    |
|--------------------------------|-------|-------|
| SiO <sub>2</sub>               | 46.93 | 48.77 |
| TiO <sub>2</sub>               | 1.21  | 1.56  |
| Al <sub>2</sub> O <sub>3</sub> | 8.45  | 3.64  |
| Cr <sub>2</sub> O <sub>3</sub> | .05   | 0.00  |
| FeO                            | 19.25 | 10.00 |
| MnO                            | .39   | .07   |
| MgO                            | 14.76 | 14.25 |
| NiO                            | .01   | .03   |
| CaO                            | 8.49  | 20.99 |
| Na <sub>2</sub> O              | .09   | .48   |
| K <sub>2</sub> O               | .03   | 0.00  |
| Total                          | 99.66 | 99.79 |

|                  |       |       |
|------------------|-------|-------|
| Si               | 1.779 | 1.841 |
| Al <sup>IV</sup> | .221  | .159  |
| Al <sup>VI</sup> | .156  | .003  |
| Ti               | .034  | .044  |
| Cr               | .001  | 0.000 |
| Fe               | .610  | .316  |
| Mn               | .013  | .002  |
| Mg               | .834  | .802  |
| Ni               | .000  | .001  |
| Ca               | .345  | .849  |
| Na               | .007  | .035  |
| K                | .001  | 0.000 |
| Total            | 4.002 | 4.052 |

|       |      |      |
|-------|------|------|
| Ca    | 19.1 | 43.1 |
| Mg    | 46.3 | 40.7 |
| Fe+Mn | 34.6 | 16.1 |

NOVA SCOTIA (BOURINOT) PYROXENE ANALYSES

Samples for the following pyroxene analyses were provided by K. Cameron and information on the bulk rock chemistry for these samples may be found in Cameron (1980).

| Sample Number | Analysis Numbers |
|---------------|------------------|
| KJC-67        | 1 to 17          |
| KJC-69        | 18 to 38         |
| KJC-65        | 19 to 58         |
| KJC-61        | 59 to 80         |
| KJC-68        | 81 to 96         |

|       | 1     | 2     | 3     | 4     | 5     | 6     | 7     | 8     | 9      | 10    |
|-------|-------|-------|-------|-------|-------|-------|-------|-------|--------|-------|
| SiO2  | 50.84 | 50.56 | 50.71 | 50.88 | 50.05 | 50.54 | 50.17 | 50.56 | 52.41  | 52.50 |
| TiO2  | 1.27  | 1.59  | 2.02  | 1.31  | 1.81  | 1.78  | 1.88  | 2.11  | 1.00   | .90   |
| Al2O3 | 3.39  | 2.47  | 3.05  | 3.27  | 3.14  | 2.75  | 2.86  | 2.36  | 1.64   | 1.66  |
| Cr2O3 | .80   | 0.00  | .10   | .30   | .10   | 0.00  | 0.00  | .10   | .10    | .20   |
| FeO   | 6.54  | 8.54  | 9.15  | 7.46  | 8.73  | 9.11  | 9.24  | 10.61 | 7.80   | 6.97  |
| MnO   | .10   | .21   | .10   | .19   | .20   | .08   | .08   | .05   | .19    | .16   |
| MgO   | 15.30 | 14.70 | 14.60 | 14.84 | 14.30 | 14.21 | 14.38 | 13.49 | 16.28  | 16.25 |
| NiO   | 0.00  | 0.00  | 0.00  | 0.00  | 0.00  | 0.00  | 0.00  | 0.00  | 0.00   | 0.00  |
| CaO   | 20.97 | 20.39 | 18.65 | 20.76 | 19.94 | 19.90 | 20.00 | 19.85 | 21.73  | 20.63 |
| Na2O  | .36   | .13   | .38   | .22   | .33   | .32   | .29   | .45   | .10    | .33   |
| K2O   | .03   | .02   | 0.00  | 0.00  | .05   | .02   | 0.00  | .01   | .04    | .01   |
| Total | 99.62 | 98.64 | 98.78 | 99.24 | 98.65 | 98.72 | 98.90 | 99.59 | 101.37 | 99.63 |

|       |       |       |       |       |       |       |       |       |       |       |
|-------|-------|-------|-------|-------|-------|-------|-------|-------|-------|-------|
| Si    | 1.886 | 1.907 | 1.904 | 1.898 | 1.889 | 1.906 | 1.891 | 1.904 | 1.921 | 1.943 |
| Al IV | .114  | .093  | .096  | .102  | .111  | .094  | .109  | .096  | .071  | .057  |
| Al VI | .034  | .017  | .039  | .042  | .028  | .028  | .018  | .009  | 0.000 | .015  |
| Ti    | .035  | .045  | .057  | .037  | .051  | .050  | .053  | .060  | .028  | .025  |
| Cr    | .023  | 0.000 | .003  | .009  | .003  | 0.000 | 0.000 | .003  | .003  | .006  |
| Fe    | .203  | .269  | .287  | .233  | .276  | .287  | .291  | .334  | .239  | .216  |
| Mn    | .003  | .007  | .003  | .006  | .006  | .003  | .003  | .002  | .006  | .005  |
| Mg    | .846  | .826  | .817  | .825  | .804  | .799  | .808  | .757  | .889  | .896  |
| Ni    | 0.000 | 0.000 | 0.000 | 0.000 | 0.000 | 0.000 | 0.000 | 0.000 | 0.000 | 0.000 |
| Ca    | .834  | .824  | .750  | .830  | .806  | .804  | .808  | .801  | .853  | .818  |
| Na    | .026  | .010  | .028  | .016  | .024  | .023  | .021  | .033  | .007  | .024  |
| K     | .001  | .001  | 0.000 | 0.000 | .002  | .001  | 0.000 | .000  | .002  | .000  |
| Total | 4.006 | 3.998 | 3.984 | 3.997 | 4.002 | 3.995 | 4.002 | 3.999 | 4.019 | 4.005 |

|       |      |      |      |      |      |      |      |      |      |      |
|-------|------|------|------|------|------|------|------|------|------|------|
| Ca    | 44.2 | 42.8 | 40.4 | 43.8 | 42.6 | 42.5 | 42.3 | 42.3 | 42.9 | 42.3 |
| Mg    | 44.9 | 42.9 | 44.0 | 43.6 | 42.5 | 42.2 | 42.3 | 40.0 | 44.7 | 46.3 |
| Fe+Mn | 10.9 | 14.3 | 15.6 | 12.6 | 14.9 | 15.3 | 15.4 | 17.7 | 12.3 | 11.4 |

|       | 11     | 12     | 13    | 14     | 15    | 16     | 17     | 18    | 19     | 20    |
|-------|--------|--------|-------|--------|-------|--------|--------|-------|--------|-------|
| SiO2  | 50.76  | 50.46  | 50.82 | 51.18  | 51.22 | 50.47  | 49.80  | 49.96 | 50.75  | 49.65 |
| TiO2  | 1.66   | 1.46   | 1.43  | 1.82   | .90   | 1.58   | 1.39   | 1.76  | 1.66   | 1.82  |
| Al2O3 | 2.78   | 2.81   | 3.23  | 2.90   | 2.01  | 3.61   | 3.59   | 3.09  | 2.66   | 2.52  |
| Cr2O3 | 0.00   | .30    | .70   | .10    | 0.00  | .80    | .90    | .40   | 0.00   | 0.00  |
| FeO   | 8.36   | 7.43   | 6.62  | 8.64   | 9.05  | 6.77   | 6.80   | 7.20  | 9.41   | 9.31  |
| MnO   | .23    | .11    | .11   | .16    | .21   | .11    | .06    | .13   | .20    | .16   |
| MgO   | 15.09  | 15.13  | 14.89 | 14.79  | 15.26 | 14.77  | 15.02  | 14.80 | 14.32  | 13.94 |
| NiO   | 0.00   | 0.00   | 0.00  | 0.00   | 0.00  | 0.00   | 0.00   | 0.00  | 0.00   | 0.00  |
| CaO   | 21.70  | 22.27  | 20.84 | 21.77  | 20.21 | 22.10  | 22.46  | 21.51 | 20.79  | 20.55 |
| Na2O  | .10    | .38    | .35   | .27    | .35   | .15    | .43    | .36   | .36    | .37   |
| K2O   | 0.00   | .02    | 0.00  | 0.00   | .02   | 0.00   | .03    | .03   | 0.00   | .04   |
| Total | 100.68 | 100.39 | 99.03 | 101.63 | 99.23 | 100.36 | 100.51 | 99.29 | 100.15 | 98.38 |

|       |       |       |       |       |       |       |       |       |       |       |
|-------|-------|-------|-------|-------|-------|-------|-------|-------|-------|-------|
| Si    | 1.881 | 1.874 | 1.896 | 1.880 | 1.923 | 1.866 | 1.848 | 1.872 | 1.895 | 1.890 |
| Al IV | .119  | .123  | .104  | .120  | .077  | .134  | .152  | .128  | .105  | .110  |
| Al VI | .002  | 0.000 | .038  | .006  | .012  | .024  | .005  | .009  | .012  | .003  |
| Ti    | .046  | .041  | .040  | .050  | .025  | .044  | .039  | .050  | .047  | .052  |
| Cr    | 0.000 | .009  | .021  | .003  | 0.000 | .023  | .026  | .012  | 0.000 | 0.000 |
| Fe    | .259  | .231  | .207  | .265  | .284  | .209  | .211  | .226  | .294  | .296  |
| Mn    | .007  | .003  | .003  | .005  | .007  | .003  | .002  | .004  | .006  | .005  |
| Mg    | .833  | .838  | .828  | .810  | .854  | .814  | .831  | .827  | .797  | .791  |
| Ni    | 0.000 | 0.000 | 0.000 | 0.000 | 0.000 | 0.000 | 0.000 | 0.000 | 0.000 | 0.000 |
| Ca    | .861  | .886  | .833  | .857  | .813  | .876  | .893  | .864  | .832  | .838  |
| Na    | .007  | .027  | .025  | .019  | .025  | .011  | .031  | .026  | .026  | .027  |
| K     | 0.000 | .001  | 0.000 | 0.000 | .001  | 0.000 | .001  | .001  | 0.000 | .002  |
| Total | 4.016 | 4.033 | 3.995 | 4.015 | 4.021 | 4.005 | 4.038 | 4.018 | 4.013 | 4.016 |

|       |      |      |      |      |      |      |      |      |      |      |
|-------|------|------|------|------|------|------|------|------|------|------|
| Ca    | 43.9 | 45.3 | 44.5 | 44.2 | 41.5 | 46.0 | 46.1 | 45.0 | 43.1 | 43.4 |
| Mg    | 42.5 | 42.8 | 44.3 | 41.8 | 43.6 | 42.8 | 42.9 | 43.1 | 41.3 | 41.0 |
| Fe+Mn | 13.6 | 12.0 | 11.2 | 14.0 | 14.9 | 11.2 | 11.0 | 12.0 | 15.6 | 15.6 |

|       | 21    | 22     | 23    | 24    | 25    | 26    | 27    | 28    | 29    | 30     |
|-------|-------|--------|-------|-------|-------|-------|-------|-------|-------|--------|
| SiO2  | 49.21 | 51.27  | 49.74 | 50.29 | 51.26 | 51.85 | 48.47 | 49.40 | 49.71 | 50.14  |
| TiO2  | 1.71  | 1.44   | 1.55  | 2.08  | 1.10  | 1.57  | 1.54  | 1.99  | 1.70  | 1.98   |
| Al2O3 | 3.92  | 1.35   | 2.74  | 1.88  | 1.58  | 1.44  | 3.15  | 2.79  | 2.74  | 2.91   |
| Cr2O3 | .60   | 0.00   | 0.00  | 0.00  | .10   | 0.00  | .40   | 0.00  | .10   | .10    |
| FeO   | 7.54  | 10.85  | 8.48  | 12.27 | 7.70  | 10.59 | 7.03  | 8.93  | 8.11  | 8.11   |
| MnO   | .16   | .19    | .20   | .21   | .16   | .20   | .14   | .20   | .16   | .13    |
| MgO   | 14.94 | 14.68  | 14.72 | 12.42 | 16.02 | 14.60 | 15.00 | 14.11 | 15.23 | 14.79  |
| NiO   | 0.00  | 0.00   | 0.00  | 0.00  | 0.00  | 0.00  | 0.00  | 0.00  | 0.00  | 0.00   |
| CaO   | 21.53 | 21.25  | 20.77 | 19.86 | 21.33 | 19.20 | 23.26 | 20.45 | 21.73 | 22.20  |
| Na2O  | .30   | .33    | .37   | .51   | .09   | .28   | .12   | .41   | .41   | .31    |
| K2O   | .03   | .04    | .01   | 0.00  | 0.00  | .09   | 0.00  | .03   | 0.00  | .04    |
| Total | 99.99 | 101.40 | 98.66 | 99.52 | 99.34 | 99.83 | 99.11 | 98.31 | 99.92 | 100.71 |

|       |       |       |       |       |       |       |       |       |       |       |
|-------|-------|-------|-------|-------|-------|-------|-------|-------|-------|-------|
| Si    | 1.837 | 1.907 | 1.883 | 1.913 | 1.917 | 1.941 | 1.833 | 1.879 | 1.861 | 1.862 |
| AlIV  | .163  | .059  | .117  | .084  | .070  | .059  | .140  | .121  | .121  | .127  |
| AlVI  | .010  | 0.000 | .005  | 0.000 | 0.000 | .004  | 0.000 | .004  | 0.000 | 0.000 |
| Ti    | .048  | .040  | .044  | .059  | .031  | .044  | .044  | .057  | .048  | .055  |
| Cr    | .018  | 0.000 | 0.000 | 0.000 | .003  | 0.000 | .012  | 0.000 | .003  | .003  |
| Fe    | .235  | .337  | .268  | .390  | .241  | .332  | .222  | .284  | .254  | .252  |
| Mn    | .005  | .006  | .006  | .007  | .005  | .006  | .004  | .006  | .005  | .004  |
| Mg    | .831  | .814  | .831  | .704  | .893  | .815  | .845  | .800  | .850  | .819  |
| Ni    | 0.000 | 0.000 | 0.000 | 0.000 | 0.000 | 0.000 | 0.000 | 0.000 | 0.000 | 0.000 |
| Ca    | .861  | .847  | .843  | .809  | .854  | .770  | .942  | .834  | .872  | .883  |
| Na    | .022  | .024  | .027  | .038  | .007  | .020  | .009  | .030  | .030  | .022  |
| K     | .001  | .002  | .000  | 0.000 | 0.000 | .004  | 0.000 | .001  | 0.000 | .002  |
| Total | 4.031 | 4.036 | 4.025 | 4.004 | 4.020 | 3.996 | 4.052 | 4.017 | 4.044 | 4.030 |

|       |      |      |      |      |      |      |      |      |      |      |
|-------|------|------|------|------|------|------|------|------|------|------|
| Ca    | 44.6 | 42.3 | 43.2 | 42.4 | 42.9 | 40.1 | 46.8 | 43.3 | 44.0 | 45.1 |
| Mg    | 43.0 | 40.6 | 42.6 | 36.9 | 44.8 | 42.4 | 42.0 | 41.6 | 42.9 | 41.8 |
| Fe+Mn | 12.4 | 17.1 | 14.1 | 20.8 | 12.3 | 17.6 | 11.3 | 15.1 | 13.1 | 13.1 |

|       | 31    | 32    | 33    | 34     | 35     | 36     | 37     | 38    | 39    | 40    |
|-------|-------|-------|-------|--------|--------|--------|--------|-------|-------|-------|
| SiO2  | 49.23 | 49.59 | 52.25 | 51.09  | 51.29  | 51.44  | 50.54  | 52.18 | 50.73 | 49.29 |
| TiO2  | 1.84  | 1.44  | .04   | 1.80   | 1.59   | 1.32   | 1.66   | .95   | 1.67  | 2.30  |
| Al2O3 | 2.91  | 3.07  | 1.57  | 2.36   | 2.55   | 2.88   | 3.47   | 1.71  | 3.20  | 3.26  |
| Cr2O3 | .10   | .30   | .10   | 0.00   | .10    | .20    | .70    | .20   | .10   | .10   |
| FeO   | 8.87  | 7.36  | 8.02  | 11.23  | 8.74   | 7.90   | 7.10   | 7.31  | 8.87  | 9.75  |
| MnO   | .20   | .21   | .16   | .21    | .16    | .18    | .14    | .14   | .16   | .16   |
| MgO   | 14.49 | 14.74 | 16.47 | 13.32  | 15.01  | 14.52  | 15.11  | 16.14 | 14.08 | 13.71 |
| NiO   | 0.00  | 0.00  | 0.00  | 0.00   | 0.00   | 0.00   | 0.00   | 0.00  | 0.00  | 0.00  |
| CaO   | 20.78 | 21.64 | 20.27 | 20.27  | 22.19  | 22.71  | 21.09  | 20.07 | 20.63 | 20.33 |
| Na2O  | .31   | .32   | .27   | .49    | .32    | .34    | .35    | .07   | .38   | .37   |
| K2O   | .01   | .02   | .04   | .04    | .01    | 0.00   | 0.00   | .02   | .01   | .02   |
| Total | 98.74 | 98.69 | 99.21 | 100.85 | 101.96 | 101.49 | 100.22 | 98.79 | 99.88 | 99.30 |

|       |       |       |       |       |       |       |       |       |       |       |
|-------|-------|-------|-------|-------|-------|-------|-------|-------|-------|-------|
| Si    | 1.867 | 1.872 | 1.949 | 1.908 | 1.882 | 1.891 | 1.871 | 1.946 | 1.893 | 1.862 |
| Al IV | .130  | .128  | .051  | .092  | .110  | .109  | .129  | .054  | .107  | .138  |
| Al VI | 0.000 | .009  | .018  | .011  | 0.000 | .015  | .023  | .021  | .034  | .008  |
| Ti    | .052  | .041  | .001  | .051  | .044  | .036  | .046  | .027  | .047  | .065  |
| Cr    | .003  | .009  | .003  | 0.000 | .003  | .006  | .020  | .006  | .003  | .003  |
| Fe    | .281  | .232  | .250  | .351  | .268  | .243  | .220  | .228  | .277  | .308  |
| Mn    | .006  | .007  | .005  | .007  | .005  | .006  | .004  | .004  | .005  | .005  |
| Mg    | .819  | .829  | .916  | .741  | .821  | .795  | .834  | .897  | .783  | .772  |
| Ni    | 0.000 | 0.000 | 0.000 | 0.000 | 0.000 | 0.000 | 0.000 | 0.000 | 0.000 | 0.000 |
| Ca    | .844  | .875  | .810  | .811  | .872  | .894  | .837  | .802  | .825  | .823  |
| Na    | .023  | .023  | .020  | .035  | .023  | .024  | .025  | .005  | .027  | .027  |
| K     | .000  | .001  | .002  | .002  | .000  | 0.000 | 0.000 | .001  | .000  | .001  |
| Total | 4.026 | 4.027 | 4.025 | 4.009 | 4.029 | 4.020 | 4.009 | 3.990 | 4.002 | 4.012 |

|       |      |      |      |      |      |      |      |      |      |      |
|-------|------|------|------|------|------|------|------|------|------|------|
| Ca    | 43.3 | 45.0 | 40.9 | 42.5 | 44.4 | 46.1 | 44.2 | 41.5 | 43.6 | 43.1 |
| Mg    | 42.0 | 42.7 | 46.2 | 38.8 | 41.7 | 41.0 | 44.0 | 46.4 | 41.4 | 40.5 |
| Fe+Mn | 14.7 | 12.3 | 12.9 | 18.7 | 13.9 | 12.8 | 11.8 | 12.0 | 14.9 | 16.4 |

|       | 41     | 42     | 43    | 44    | 45    | 46    | 47     | 48    | 49     | 50    |
|-------|--------|--------|-------|-------|-------|-------|--------|-------|--------|-------|
| SiO2  | 49.88  | 50.24  | 49.01 | 50.08 | 50.17 | 49.90 | 51.71  | 49.21 | 50.28  | 50.13 |
| TiO2  | 2.55   | 2.38   | 2.11  | 1.04  | 2.03  | 2.13  | 1.23   | 2.25  | 1.90   | 1.02  |
| Al2O3 | 2.88   | 3.70   | 4.19  | 3.05  | 3.22  | 3.58  | 1.45   | 2.89  | 3.03   | 3.46  |
| Cr2O3 | 0.00   | .20    | .20   | .10   | .10   | .20   | .10    | 0.00  | .10    | .20   |
| FeO   | 10.14  | 8.28   | 8.75  | 9.30  | 9.26  | 8.89  | 9.57   | 10.21 | 10.07  | 8.59  |
| MnO   | .16    | .14    | .14   | .16   | .16   | .14   | .11    | .23   | .23    | .11   |
| MgO   | 13.27  | 14.10  | 14.29 | 14.23 | 14.30 | 14.25 | 15.47  | 13.66 | 13.65  | 14.13 |
| NiO   | 0.00   | 0.00   | 0.00  | 0.00  | 0.00  | 0.00  | 0.00   | 0.00  | 0.00   | 0.00  |
| CaO   | 21.11  | 20.93  | 20.00 | 20.65 | 18.54 | 19.50 | 21.98  | 20.46 | 21.00  | 21.61 |
| Na2O  | .50    | .32    | .25   | .35   | .43   | .36   | .13    | .38   | .40    | .33   |
| K2O   | 0.00   | 0.00   | .03   | .02   | .02   | .02   | 0.00   | 0.00  | 0.00   | 0.00  |
| Total | 100.52 | 100.31 | 99.00 | 98.99 | 98.23 | 98.98 | 101.84 | 99.33 | 100.69 | 99.61 |

|       |       |       |       |       |       |       |       |       |       |       |
|-------|-------|-------|-------|-------|-------|-------|-------|-------|-------|-------|
| Si    | 1.868 | 1.865 | 1.846 | 1.892 | 1.897 | 1.876 | 1.906 | 1.865 | 1.877 | 1.880 |
| Al IV | .127  | .135  | .154  | .108  | .103  | .124  | .063  | .129  | .123  | .120  |
| Al VI | 0.000 | .027  | .032  | .028  | .040  | .034  | 0.000 | 0.000 | .010  | .033  |
| Ti    | .072  | .066  | .060  | .030  | .058  | .060  | .034  | .064  | .053  | .029  |
| Cr    | 0.000 | .006  | .006  | .003  | .003  | .006  | .003  | 0.000 | .003  | .006  |
| Fe    | .318  | .257  | .276  | .294  | .293  | .279  | .295  | .324  | .314  | .269  |
| Mn    | .005  | .004  | .004  | .005  | .005  | .004  | .003  | .007  | .007  | .003  |
| Mg    | .741  | .780  | .802  | .801  | .806  | .798  | .850  | .772  | .759  | .790  |
| Ni    | 0.000 | 0.000 | 0.000 | 0.000 | 0.000 | 0.000 | 0.000 | 0.000 | 0.000 | 0.000 |
| Ca    | .847  | .832  | .807  | .836  | .751  | .785  | .868  | .831  | .840  | .868  |
| Na    | .036  | .023  | .018  | .026  | .032  | .026  | .009  | .028  | .029  | .024  |
| K     | 0.000 | 0.000 | .001  | .001  | .001  | .001  | 0.000 | 0.000 | 0.000 | 0.000 |
| Total | 4.014 | 3.996 | 4.008 | 4.023 | 3.988 | 3.995 | 4.032 | 4.020 | 4.016 | 4.023 |

|       |      |      |      |      |      |      |      |      |      |      |
|-------|------|------|------|------|------|------|------|------|------|------|
| Ca    | 44.3 | 44.4 | 42.7 | 43.2 | 40.5 | 42.0 | 43.0 | 43.0 | 43.7 | 45.0 |
| Mg    | 38.8 | 41.6 | 42.5 | 41.4 | 43.4 | 42.7 | 42.2 | 39.9 | 39.5 | 40.9 |
| Fe+Mn | 16.9 | 14.0 | 14.8 | 15.4 | 16.1 | 15.2 | 14.8 | 17.1 | 16.7 | 14.1 |

|       | 51     | 52     | 53    | 54    | 55    | 56     | 57     | 58     | 59    | 60    |
|-------|--------|--------|-------|-------|-------|--------|--------|--------|-------|-------|
| SiO2  | 49.97  | 49.36  | 49.58 | 49.87 | 48.10 | 49.12  | 50.43  | 49.51  | 50.46 | 50.08 |
| TiO2  | 2.15   | 2.28   | 1.93  | 2.03  | 2.26  | 2.12   | 1.05   | 2.38   | 1.40  | 1.68  |
| Al2O3 | 3.33   | 3.22   | 3.01  | 3.24  | 3.29  | 3.43   | 3.52   | 3.57   | 1.59  | 3.41  |
| Cr2O3 | .10    | .20    | 0.00  | .10   | 0.00  | .30    | .30    | .10    | .10   | .20   |
| FeO   | 8.94   | 8.75   | 9.54  | 8.71  | 9.90  | 8.71   | 8.78   | 9.47   | 9.87  | 8.04  |
| MnO   | .16    | .20    | .18   | .07   | .18   | .16    | .18    | .18    | .27   | .11   |
| MgO   | 14.31  | 14.11  | 13.97 | 14.54 | 13.57 | 14.39  | 14.36  | 14.02  | 15.66 | 14.41 |
| NiO   | 0.00   | 0.00   | 0.00  | 0.00  | 0.00  | 0.00   | 0.00   | 0.00   | 0.00  | 0.00  |
| CaO   | 22.05  | 22.45  | 20.81 | 20.49 | 21.97 | 21.87  | 21.30  | 21.80  | 18.73 | 20.26 |
| Na2O  | .41    | .47    | .23   | .37   | .42   | .41    | .42    | .18    | .08   | .26   |
| K2O   | .01    | .03    | 0.00  | 0.00  | .02   | .04    | 0.00   | 0.00   | .04   | .04   |
| Total | 101.43 | 101.07 | 99.26 | 99.43 | 99.75 | 100.56 | 100.39 | 101.21 | 98.25 | 98.50 |

|       |       |       |       |       |       |       |       |       |       |       |
|-------|-------|-------|-------|-------|-------|-------|-------|-------|-------|-------|
| Si    | 1.849 | 1.838 | 1.873 | 1.871 | 1.826 | 1.835 | 1.878 | 1.839 | 1.917 | 1.887 |
| AlIV  | .145  | .141  | .127  | .129  | .147  | .151  | .122  | .156  | .071  | .113  |
| AlVI  | 0.000 | 0.000 | .007  | .014  | 0.000 | 0.000 | .032  | 0.000 | 0.000 | .038  |
| Ti    | .060  | .064  | .055  | .057  | .065  | .060  | .029  | .066  | .040  | .048  |
| Cr    | .003  | .006  | 0.000 | .003  | 0.000 | .009  | .009  | .003  | .003  | .006  |
| Fe    | .277  | .272  | .301  | .273  | .314  | .272  | .273  | .294  | .314  | .253  |
| Mn    | .005  | .006  | .006  | .002  | .006  | .005  | .006  | .006  | .009  | .004  |
| Mg    | .789  | .783  | .786  | .813  | .768  | .801  | .797  | .776  | .887  | .809  |
| Ni    | 0.000 | 0.000 | 0.000 | 0.000 | 0.000 | 0.000 | 0.000 | 0.000 | 0.000 | 0.000 |
| Ca    | .874  | .896  | .842  | .823  | .894  | .876  | .850  | .868  | .762  | .818  |
| Na    | .029  | .034  | .017  | .027  | .031  | .030  | .030  | .013  | .006  | .019  |
| K     | .000  | .001  | 0.000 | 0.000 | .001  | .002  | 0.000 | 0.000 | .002  | .002  |
| Total | 4.032 | 4.042 | 4.014 | 4.013 | 4.052 | 4.041 | 4.026 | 4.021 | 4.010 | 3.997 |

|       |      |      |      |      |      |      |      |      |      |      |
|-------|------|------|------|------|------|------|------|------|------|------|
| Ca    | 44.9 | 45.8 | 43.5 | 43.1 | 45.1 | 44.8 | 44.1 | 44.6 | 38.7 | 43.4 |
| Mg    | 40.6 | 40.0 | 40.6 | 42.5 | 38.7 | 41.0 | 41.4 | 39.9 | 45.0 | 43.0 |
| Fe+Mn | 14.5 | 14.2 | 15.9 | 14.4 | 16.2 | 14.2 | 14.5 | 15.4 | 16.3 | 13.6 |



|       | 61    | 62    | 63     | 64    | 65    | 66    | 67    | 68     | 69     | 70     |
|-------|-------|-------|--------|-------|-------|-------|-------|--------|--------|--------|
| SiO2  | 48.85 | 51.85 | 50.65  | 49.18 | 50.35 | 50.12 | 49.79 | 50.03  | 49.52  | 50.44  |
| TiO2  | 1.59  | .08   | 1.63   | 1.76  | 1.31  | 1.00  | 2.49  | 2.11   | 2.36   | 1.76   |
| Al2O3 | 3.78  | 1.94  | 3.50   | 3.02  | 3.01  | 2.41  | 3.14  | 3.57   | 2.95   | 3.14   |
| Cr2O3 | .50   | .40   | .30    | .20   | .10   | 0.00  | .10   | .20    | 0.00   | .10    |
| FeO   | 7.64  | 7.71  | 7.65   | 8.52  | 8.67  | 10.83 | 10.91 | 8.02   | 10.55  | 8.90   |
| MnO   | .16   | .14   | .09    | .11   | .17   | .17   | .20   | .17    | .17    | .18    |
| MgO   | 14.72 | 16.34 | 14.70  | 14.42 | 14.50 | 13.76 | 13.42 | 14.41  | 13.49  | 14.25  |
| NiO   | 0.00  | 0.00  | 0.00   | 0.00  | 0.00  | 0.00  | 0.00  | 0.00   | 0.00   | 0.00   |
| CaO   | 21.52 | 19.64 | 21.24  | 21.90 | 21.50 | 19.45 | 18.94 | 22.18  | 22.34  | 21.99  |
| Na2O  | .36   | .20   | .46    | .31   | .34   | .38   | .34   | .32    | .45    | .46    |
| K2O   | .04   | .05   | .01    | 0.00  | .02   | 0.00  | .01   | 0.00   | .06    | 0.00   |
| Total | 99.23 | 98.35 | 100.23 | 99.42 | 99.97 | 98.12 | 99.34 | 101.01 | 101.92 | 101.22 |

|       |       |       |       |       |       |       |       |       |       |       |
|-------|-------|-------|-------|-------|-------|-------|-------|-------|-------|-------|
| Si    | 1.840 | 1.945 | 1.877 | 1.855 | 1.882 | 1.916 | 1.880 | 1.851 | 1.842 | 1.868 |
| Al IV | .160  | .055  | .123  | .134  | .118  | .084  | .120  | .149  | .129  | .132  |
| Al VI | .008  | .031  | .030  | 0.000 | .015  | .025  | .020  | .006  | 0.000 | .005  |
| Ti    | .045  | .002  | .045  | .050  | .037  | .029  | .071  | .059  | .066  | .049  |
| Cr    | .015  | .012  | .009  | .006  | .003  | 0.000 | .003  | .006  | 0.000 | .003  |
| Fe    | .241  | .242  | .237  | .269  | .271  | .346  | .344  | .248  | .328  | .276  |
| Mn    | .005  | .004  | .003  | .004  | .005  | .006  | .006  | .005  | .005  | .006  |
| Mg    | .827  | .914  | .812  | .811  | .808  | .784  | .755  | .795  | .748  | .786  |
| Ni    | 0.000 | 0.000 | 0.000 | 0.000 | 0.000 | 0.000 | 0.000 | 0.000 | 0.000 | 0.000 |
| Ca    | .869  | .790  | .843  | .885  | .861  | .797  | .766  | .879  | .890  | .872  |
| Na    | .026  | .015  | .033  | .023  | .025  | .028  | .025  | .023  | .032  | .033  |
| K     | .002  | .002  | .000  | 0.000 | .001  | 0.000 | .000  | 0.000 | .003  | 0.000 |
| Total | 4.037 | 4.012 | 4.013 | 4.036 | 4.026 | 4.015 | 3.991 | 4.021 | 4.045 | 4.030 |

|       |      |      |      |      |      |      |      |      |      |      |
|-------|------|------|------|------|------|------|------|------|------|------|
| Ca    | 44.8 | 40.5 | 44.5 | 45.0 | 44.3 | 41.2 | 40.9 | 45.6 | 45.2 | 45.0 |
| Mg    | 42.6 | 46.9 | 42.8 | 41.2 | 41.5 | 40.6 | 40.3 | 41.2 | 37.9 | 40.5 |
| Fe+Mn | 12.7 | 12.6 | 12.7 | 13.8 | 14.2 | 18.2 | 18.7 | 13.2 | 16.9 | 14.5 |

|       | 71    | 72    | 73     | 74    | 75    | 76    | 77    | 78     | 79    | 80     |
|-------|-------|-------|--------|-------|-------|-------|-------|--------|-------|--------|
| SiO2  | 50.72 | 49.02 | 51.93  | 49.20 | 50.26 | 50.02 | 48.92 | 50.98  | 50.13 | 49.76  |
| TiO2  | 1.39  | 2.38  | 1.17   | 1.90  | 1.77  | 1.05  | 2.06  | 2.05   | 1.93  | 2.13   |
| Al2O3 | 3.50  | 3.02  | 1.64   | 3.20  | 3.34  | 3.12  | 3.72  | 2.99   | 3.43  | 2.70   |
| Cr2O3 | .40   | 0.00  | 0.00   | 0.00  | .10   | 0.00  | .10   | .10    | .20   | 0.00   |
| FeO   | 7.51  | 11.43 | 11.00  | 9.59  | 9.89  | 9.34  | 9.80  | 8.91   | 8.76  | 9.90   |
| MnO   | .13   | .21   | .21    | .16   | .14   | .16   | .22   | .20    | .13   | .13    |
| MgO   | 14.86 | 12.79 | 15.02  | 13.89 | 13.92 | 13.79 | 14.05 | 14.50  | 14.50 | 14.06  |
| NiO   | 0.00  | 0.00  | 0.00   | 0.00  | 0.00  | 0.00  | 0.00  | 0.00   | 0.00  | 0.00   |
| CaO   | 19.38 | 19.79 | 20.30  | 21.19 | 20.04 | 20.91 | 20.63 | 21.48  | 20.09 | 21.52  |
| Na2O  | .26   | .50   | .28    | .30   | .35   | .38   | .39   | .34    | .29   | .47    |
| K2O   | .01   | 0.00  | .01    | 0.00  | .03   | 0.00  | .04   | .06    | .01   | 0.00   |
| Total | 98.16 | 99.26 | 101.61 | 99.43 | 99.85 | 98.80 | 99.94 | 101.61 | 99.55 | 100.68 |

|       |       |       |       |       |       |       |       |       |       |       |
|-------|-------|-------|-------|-------|-------|-------|-------|-------|-------|-------|
| Si    | 1.905 | 1.868 | 1.920 | 1.859 | 1.883 | 1.895 | 1.841 | 1.876 | 1.876 | 1.862 |
| AlIV  | .095  | .132  | .071  | .141  | .117  | .105  | .159  | .124  | .124  | .119  |
| AlVI  | .060  | .004  | 0.000 | .002  | .030  | .034  | .006  | .005  | .027  | 0.000 |
| Ti    | .039  | .068  | .033  | .054  | .050  | .030  | .058  | .057  | .054  | .060  |
| Cr    | .012  | 0.000 | 0.000 | 0.000 | .003  | 0.000 | .003  | .003  | .006  | 0.000 |
| Fe    | .236  | .364  | .340  | .303  | .310  | .296  | .308  | .274  | .274  | .310  |
| Mn    | .004  | .007  | .007  | .005  | .004  | .005  | .007  | .006  | .004  | .004  |
| Mg    | .832  | .726  | .828  | .782  | .777  | .779  | .788  | .795  | .809  | .784  |
| Ni    | 0.000 | 0.000 | 0.000 | 0.000 | 0.000 | 0.000 | 0.000 | 0.000 | 0.000 | 0.000 |
| Ca    | .780  | .808  | .804  | .858  | .804  | .849  | .832  | .847  | .806  | .863  |
| Na    | .019  | .037  | .020  | .022  | .025  | .028  | .028  | .024  | .021  | .034  |
| K     | .000  | 0.000 | .000  | 0.000 | .001  | 0.000 | .002  | .003  | .000  | 0.000 |
| Total | 3.982 | 4.014 | 4.022 | 4.026 | 4.006 | 4.020 | 4.032 | 4.015 | 4.002 | 4.036 |

|       |      |      |      |      |      |      |      |      |      |      |
|-------|------|------|------|------|------|------|------|------|------|------|
| Ca    | 42.1 | 42.4 | 40.6 | 44.0 | 42.4 | 44.0 | 43.0 | 44.0 | 42.6 | 44.0 |
| Mg    | 44.9 | 38.1 | 41.8 | 40.2 | 41.0 | 40.4 | 40.7 | 41.4 | 42.7 | 40.0 |
| Fe+Mn | 13.0 | 19.5 | 17.5 | 15.8 | 16.6 | 15.6 | 16.3 | 14.6 | 14.7 | 16.0 |

|       | 81    | 82     | 83     | 84     | 85    | 86    | 87     | 88    | 89     | 90     |
|-------|-------|--------|--------|--------|-------|-------|--------|-------|--------|--------|
| SiO2  | 49.95 | 50.79  | 50.59  | 51.46  | 52.24 | 50.09 | 51.16  | 51.05 | 52.24  | 49.80  |
| TiO2  | 1.79  | 1.43   | 1.72   | 1.59   | 1.21  | 1.02  | 1.80   | 1.48  | 1.01   | 1.80   |
| Al2O3 | 2.95  | 2.81   | 3.34   | 1.48   | 1.48  | 3.40  | 1.57   | 3.18  | 1.52   | 3.02   |
| Cr2O3 | .20   | .10    | .30    | 0.00   | 0.00  | .10   | 0.00   | .20   | .30    | .10    |
| FeO   | 8.09  | 7.96   | 7.64   | 10.26  | 9.09  | 8.83  | 10.34  | 7.15  | 7.64   | 8.41   |
| MnO   | .10   | .20    | .10    | .21    | .08   | .25   | .21    | .18   | .17    | .19    |
| MgO   | 14.79 | 15.23  | 14.89  | 14.64  | 15.43 | 15.06 | 14.16  | 15.05 | 16.28  | 14.88  |
| NiO   | 0.00  | 0.00   | 0.00   | 0.00   | 0.00  | 0.00  | 0.00   | 0.00  | 0.00   | 0.00   |
| CaO   | 20.36 | 22.62  | 22.53  | 21.38  | 19.32 | 20.62 | 21.42  | 21.29 | 20.58  | 22.61  |
| Na2O  | .09   | .28    | .29    | .34    | .23   | .39   | .26    | .25   | .27    | .36    |
| K2O   | 0.00  | .02    | .04    | 0.00   | 0.00  | .01   | .01    | .01   | 0.00   | 0.00   |
| Total | 98.32 | 101.44 | 101.44 | 101.45 | 99.08 | 99.82 | 100.93 | 99.84 | 100.05 | 101.26 |

|       |       |       |       |       |       |       |       |       |       |       |
|-------|-------|-------|-------|-------|-------|-------|-------|-------|-------|-------|
| Si    | 1.887 | 1.871 | 1.861 | 1.909 | 1.953 | 1.874 | 1.907 | 1.893 | 1.933 | 1.848 |
| AlIV  | .113  | .122  | .139  | .065  | .047  | .126  | .069  | .107  | .066  | .132  |
| AlVI  | .018  | 0.000 | .005  | 0.000 | .018  | .024  | 0.000 | .032  | 0.000 | 0.000 |
| Ti    | .051  | .040  | .048  | .044  | .034  | .029  | .050  | .041  | .028  | .050  |
| Cr    | .006  | .003  | .009  | 0.000 | 0.000 | .003  | 0.000 | .004  | .009  | .003  |
| Fe    | .256  | .245  | .235  | .318  | .284  | .276  | .322  | .222  | .236  | .261  |
| Mn    | .003  | .006  | .003  | .007  | .003  | .008  | .007  | .006  | .005  | .006  |
| Mg    | .833  | .836  | .816  | .809  | .860  | .840  | .787  | .832  | .898  | .823  |
| Ni    | 0.000 | 0.000 | 0.000 | 0.000 | 0.000 | 0.000 | 0.000 | 0.000 | 0.000 | 0.000 |
| Ca    | .824  | .893  | .888  | .850  | .774  | .827  | .856  | .846  | .816  | .899  |
| Na    | .007  | .020  | .021  | .024  | .017  | .028  | .019  | .018  | .019  | .026  |
| K     | 0.000 | .001  | .002  | 0.000 | 0.000 | .000  | .000  | .000  | 0.000 | 0.000 |
| Total | 3.997 | 4.037 | 4.026 | 4.027 | 3.989 | 4.035 | 4.017 | 4.003 | 4.011 | 4.047 |

|       |      |      |      |      |      |      |      |      |      |      |
|-------|------|------|------|------|------|------|------|------|------|------|
| Ca    | 43.0 | 45.1 | 45.7 | 42.8 | 40.3 | 42.4 | 43.4 | 44.4 | 41.7 | 45.2 |
| Mg    | 43.5 | 42.2 | 42.0 | 40.8 | 44.8 | 43.1 | 39.9 | 43.7 | 45.9 | 41.4 |
| Fe+Mn | 13.5 | 12.7 | 12.3 | 16.4 | 14.9 | 14.6 | 16.7 | 11.9 | 12.4 | 13.4 |

|       | 91     | 92    | 93     | 94     | 95     | 96     |
|-------|--------|-------|--------|--------|--------|--------|
| SiO2  | 50.13  | 49.33 | 50.14  | 51.03  | 50.75  | 50.54  |
| TiO2  | 1.81   | 2.26  | 1.50   | .89    | 1.70   | 1.67   |
| Al2O3 | 3.44   | 2.87  | 3.17   | 1.78   | 2.82   | 3.59   |
| Cr2O3 | .30    | 0.00  | .10    | .20    | .10    | .50    |
| FeO   | 7.13   | 10.02 | 7.82   | 7.62   | 8.37   | 7.36   |
| MnO   | .13    | .23   | .16    | .20    | .14    | .16    |
| MgO   | 14.89  | 13.62 | 14.94  | 16.36  | 14.89  | 14.95  |
| NiO   | 0.00   | 0.00  | 0.00   | 0.00   | 0.00   | 0.00   |
| CaO   | 22.45  | 20.70 | 21.87  | 23.08  | 22.38  | 20.83  |
| Na2O  | .34    | .42   | .36    | .12    | .33    | .42    |
| K2O   | .02    | .01   | .02    | .05    | 0.00   | .02    |
| Total | 100.71 | 99.47 | 100.08 | 101.36 | 101.48 | 100.08 |

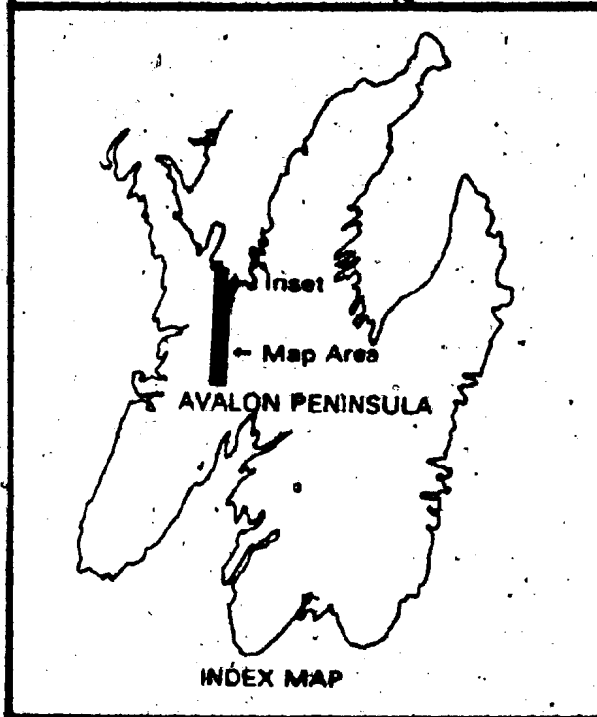
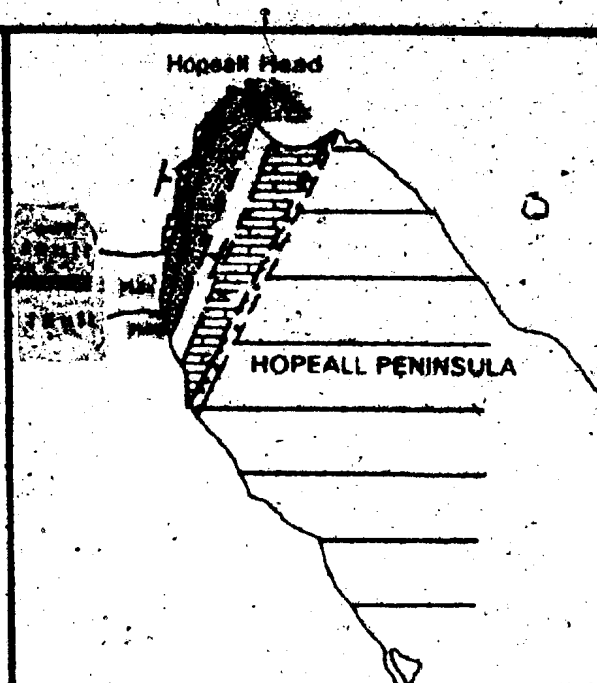
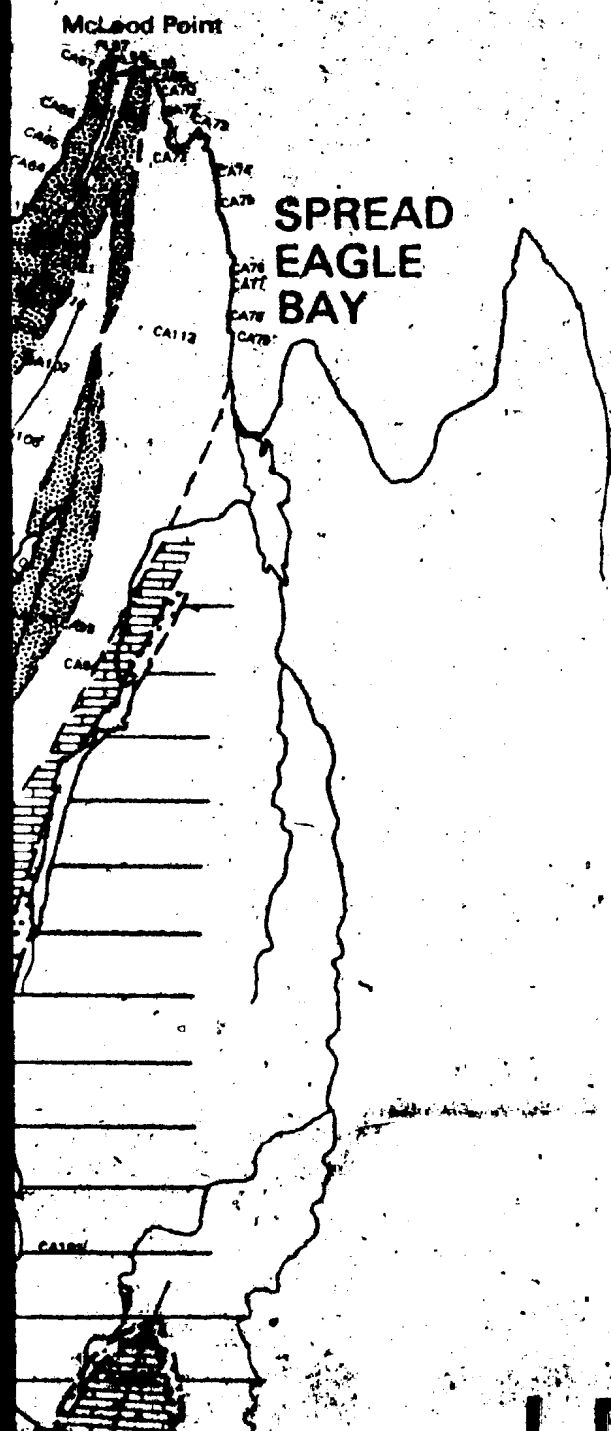
|       |       |       |       |       |       |       |
|-------|-------|-------|-------|-------|-------|-------|
| Si    | 1.856 | 1.866 | 1.869 | 1.883 | 1.871 | 1.874 |
| AlIV  | .144  | .128  | .131  | .077  | .123  | .126  |
| AlVI  | .006  | 0.000 | .008  | 0.000 | 0.000 | .031  |
| Ti    | .050  | .064  | .042  | .025  | .047  | .047  |
| Cr    | .009  | 0.000 | .003  | .006  | .003  | .015  |
| Fe    | .221  | .317  | .244  | .235  | .258  | .228  |
| Mn    | .004  | .007  | .005  | .006  | .004  | .005  |
| Mg    | .822  | .768  | .830  | .900  | .818  | .826  |
| Ni    | 0.000 | 0.000 | 0.000 | 0.000 | 0.000 | 0.000 |
| Ca    | .890  | .839  | .873  | .913  | .884  | .827  |
| Na    | .024  | .031  | .026  | .009  | .024  | .030  |
| K     | .001  | .000  | .001  | .002  | 0.000 | .001  |
| Total | 4.027 | 4.021 | 4.032 | 4.056 | 4.031 | 4.010 |

|       |      |      |      |      |      |      |
|-------|------|------|------|------|------|------|
| Ca    | 46.0 | 43.4 | 44.7 | 44.4 | 45.0 | 43.9 |
| Mg    | 42.4 | 39.8 | 42.5 | 43.8 | 41.6 | 43.8 |
| Fe+Mn | 11.6 | 16.8 | 12.7 | 11.8 | 13.4 | 12.4 |



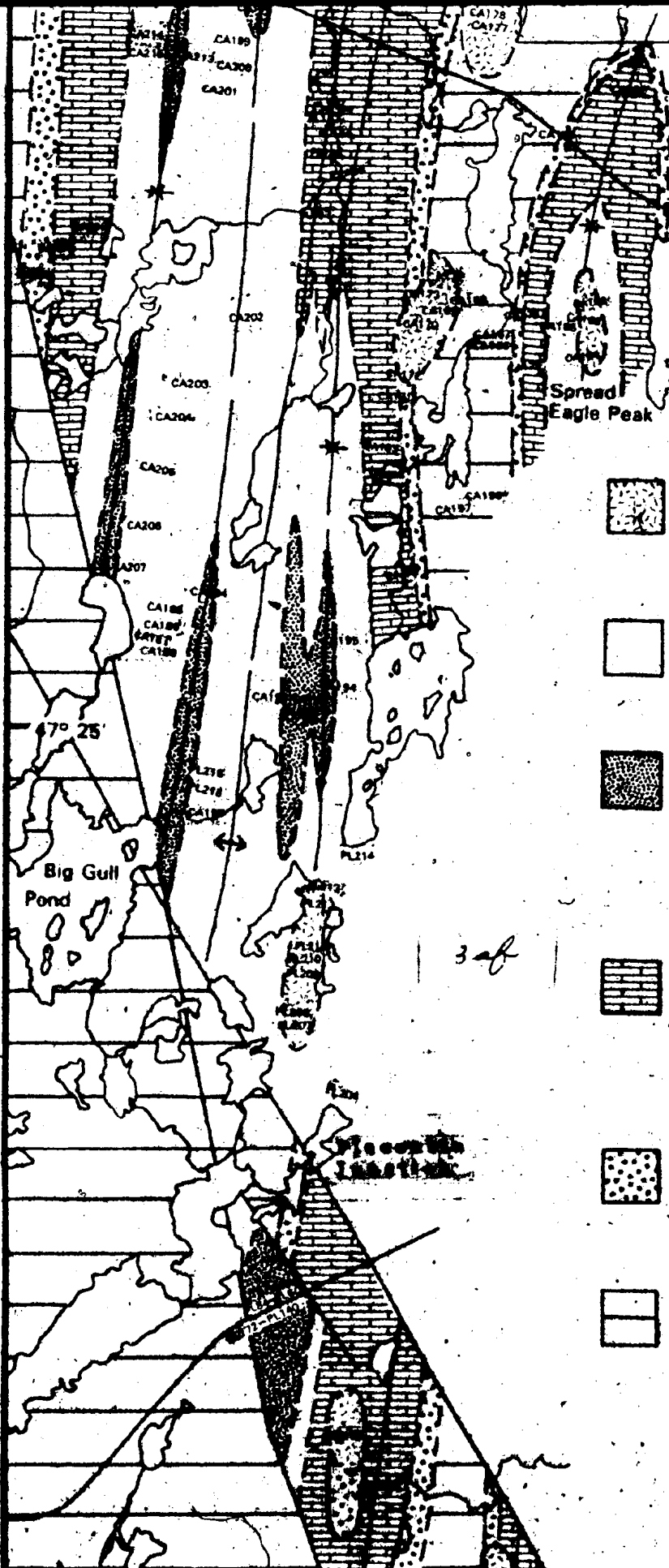
2 of

53° 35'



LEGEND

# LEO



## PRE-FOLDING?

PLUGS: diabase, occasional

## CAMBRIAN

MIDDLE CAMBRIAN  
CHAMBERLAIN S BROOK and  
ATIONS: Black, grey, green  
siltstones with abundant fossils

CHAPEL ARM and HOPEAL  
Pillow lavas and volcaniclast  
Arm M.) and Chamberlain  
Formations, often inseparable

## LOWER CAMBRIAN

BONAVISTA, SMITH POINT,  
siltstones and red limestone

## LOWER CAMBRIAN PROTEROZOIC

RANDOM FORMATION: White  
sandstones.

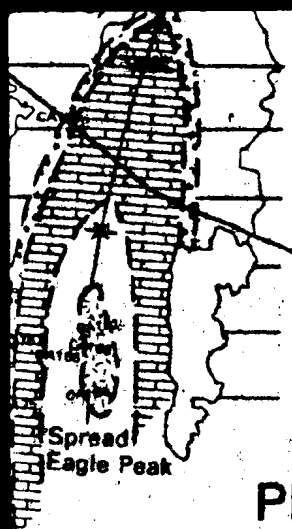
## LATE PROTEROZOIC

MUSGRAVE TOWN GROUP  
sediments.

# SYM

Geological Boundary (defined by...)  
Fault  
Anticline

# LEGEND



| 4 of |

## PRE-FOLDING?



PLUGS: diabase, occasionally with columnar jointing.

## CAMBRIAN

### MIDDLE CAMBRIAN



CHAMBERLAIN'S BROOK and MANUEL'S RIVER FORMATIONS: Black, grey, green and sometimes red shales and siltstones with abundant fossils.



CHAPEL ARM and HOPEALL HEAD VOLCANIC MEMBERS: Pillow lavas and volcanoclastics in the Manuel's River (Chapel Arm M.) and Chamberlain's Brook (Hopeall Head M.) Formations, often inseparable.

## LOWER CAMBRIAN



BONAVISTA, SMITH POINT, and BRIGUS FORMATIONS: Red siltstones and red limestones.

## LOWER CAMBRIAN to LATE PROTEROZOIC



RANDOM FORMATION: White quartzite and green-gray silt-sandstones.

## LATE PROTEROZOIC



MUSGRAVETOWN GROUP: Late proterozoic clastic sediments.

# SYMBOLS

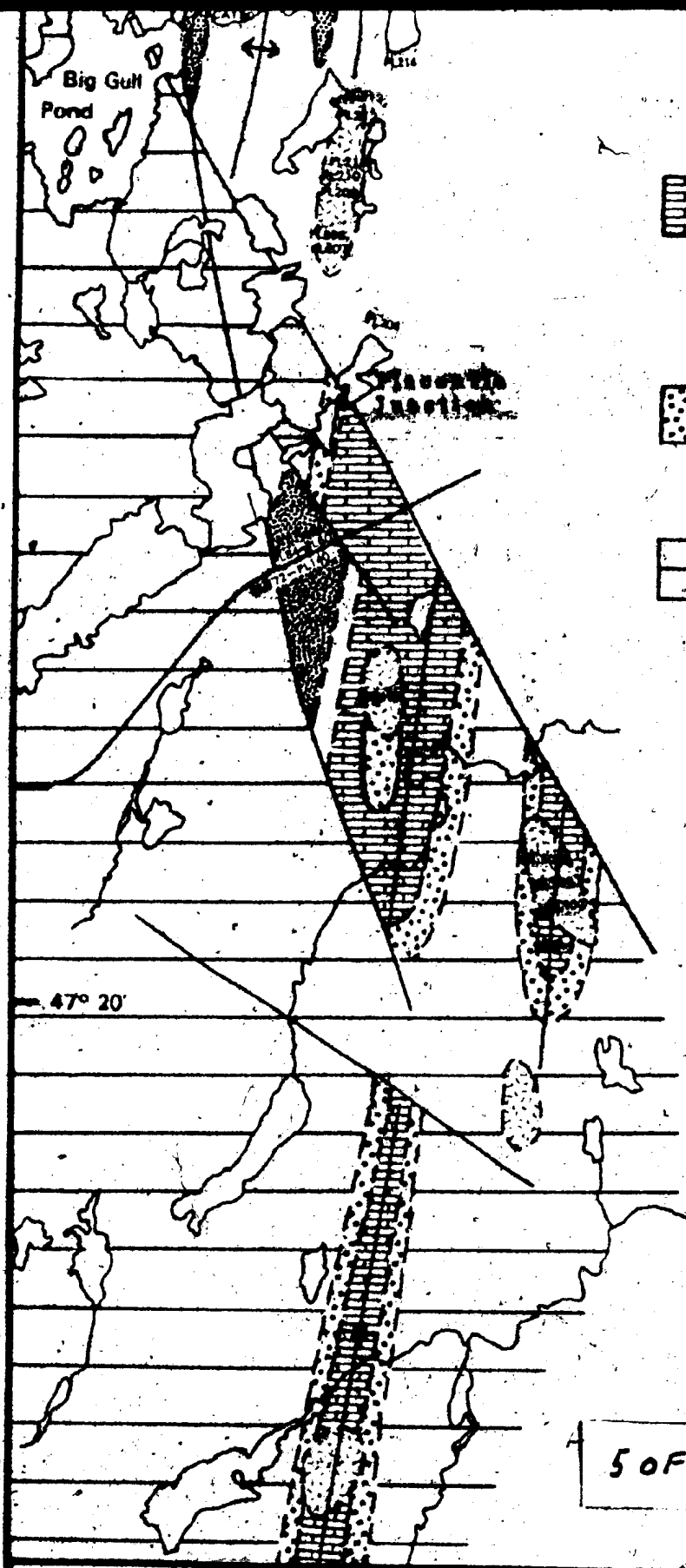
Geological Boundary (defined, inferred) ————

Fault ————

Anticline ————

Syncline ————





Arm M.) and Chamberla  
Formations, often inseparat

## LOWER CAMBRIA

BONAVISTA, SMITH POINT  
siltstones and red limestone

## LOWER CAMBRIA PROTEROZOIC

RANDOM FORMATION: Wh  
sandstones.

## LATE PROTEROZO

MUSGRAVETOWN GROU  
sediments.

SYM

Geological Boundary (define  
Fault

Anticline

Syncline

Roads

Sample Locations

Map by Greenough 1980  
McCartney 1967.

Scale 1:50,000

1 km. 0. 1

5 OF

Arm M.) and Chamberlains Brook (Hopeall Head M.)  
Formations, often inseparable.

## LOWER CAMBRIAN



BONAVISTA, SMITH POINT, and BRIGUS FORMATIONS: Red  
siltstones and red limestones.

## LOWER CAMBRIAN to LATE PROTEROZOIC



RANDOM FORMATION: White quartzite and green-gray silt-  
sandstones.

## LATE PROTEROZOIC



MUSGRAVETOWN GROUP: Late proterozoic clastic  
sediments.

# SYMBOLS

Geological Boundary (defined, inferred) ——— ——— ———

Fault ———

Anticline ———

Syncline ———

Roads ———

Sample Locations

Map by Greenough 1980 with some information from  
McCartney 1967.

Scale 1:50,000

1 km. 0 1 2

646

54° 10'

14

# PLACENTIA BAY

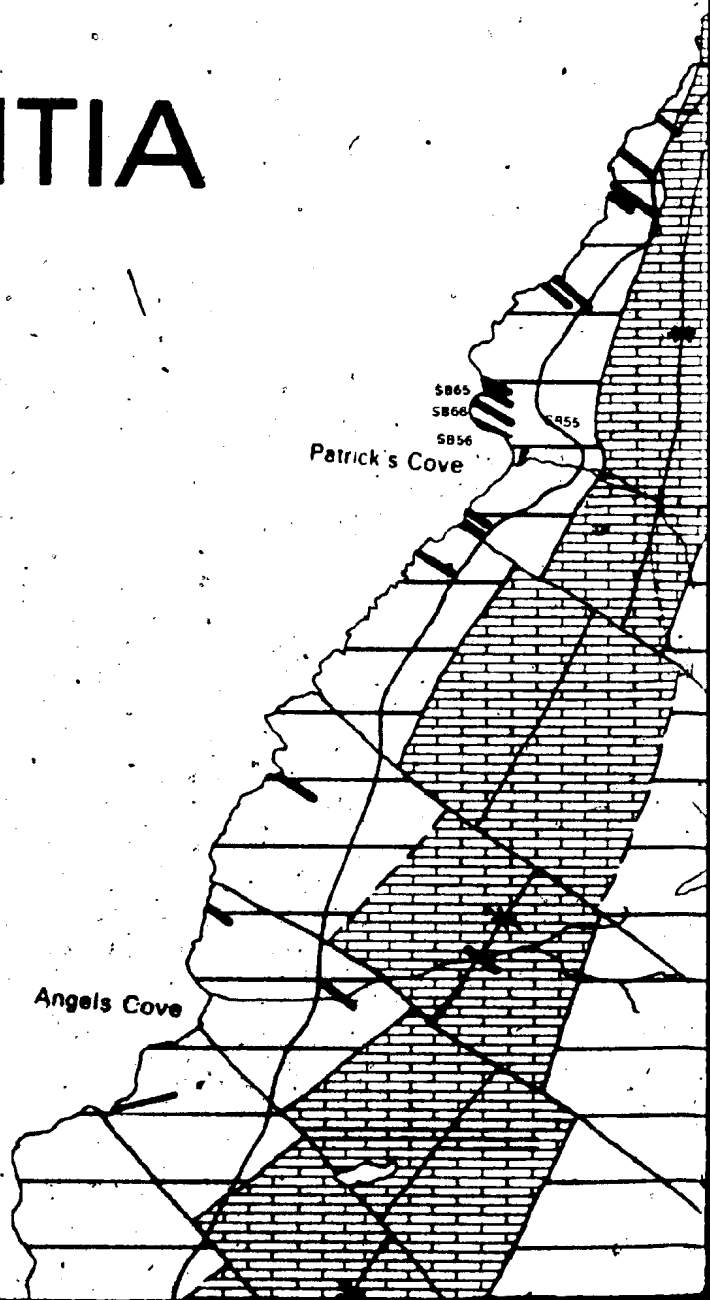
Gooseberry C

S865  
S866  
S856

Patrick's Cove

Angels Cove

47° 00'



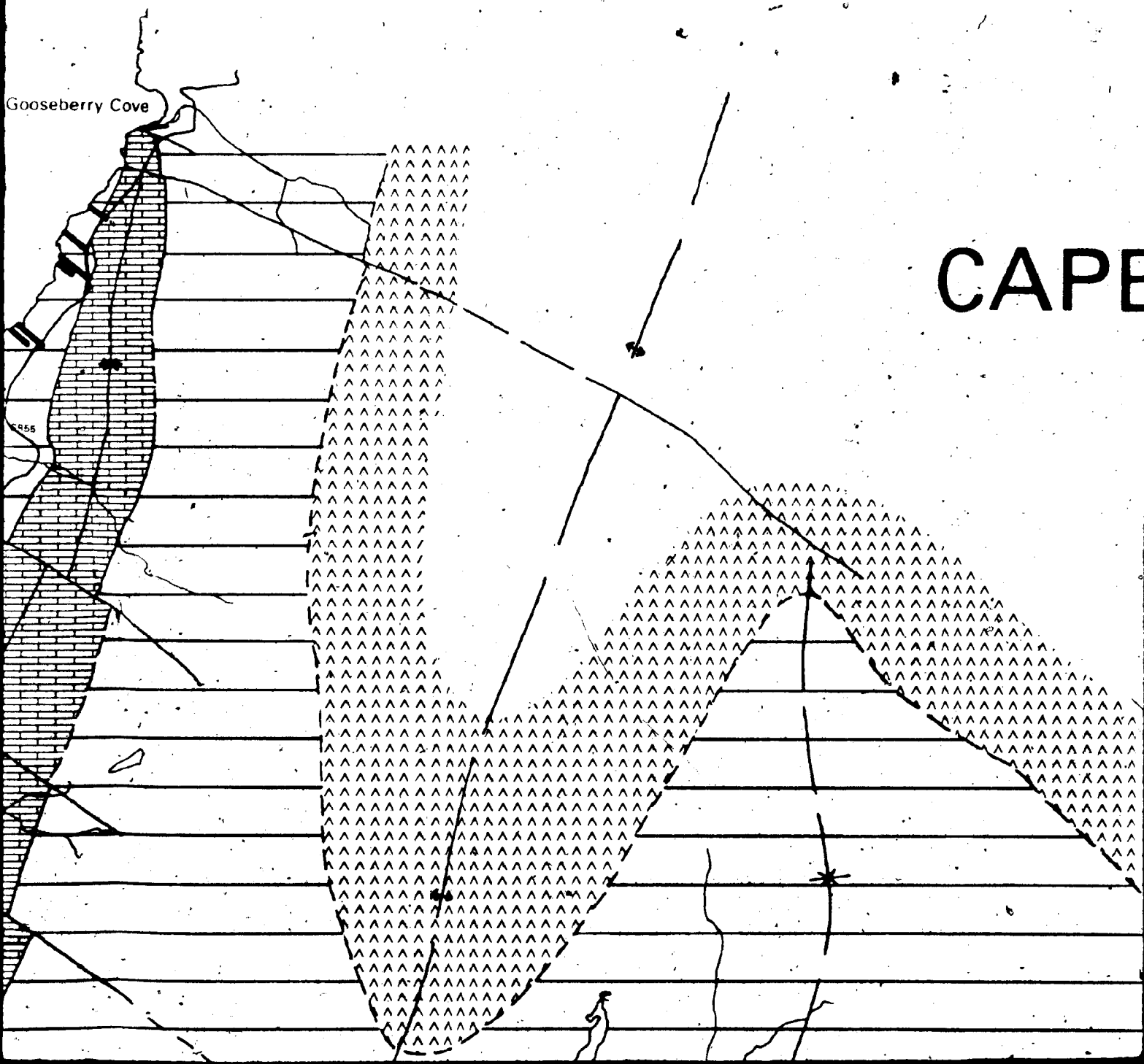
54° 05'

54° 00'

2 OF

Gooseberry Cove

CAPE

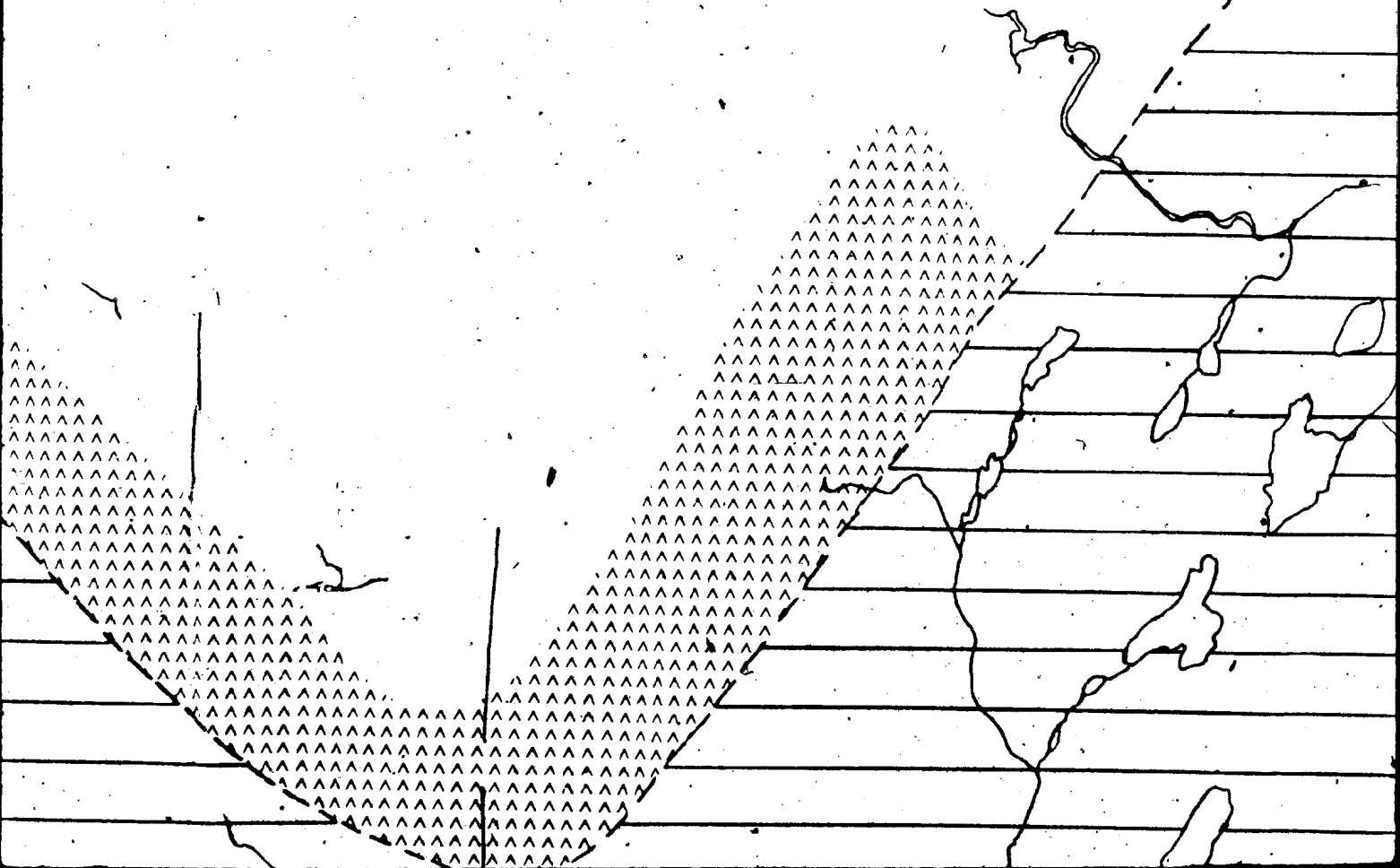


53° 55'

53° 50'

3af

CAPE ST. MARY'S



53° 50'

53° 45'

4 of 1

Dog  
Cove

Cape Dog

Bear Head

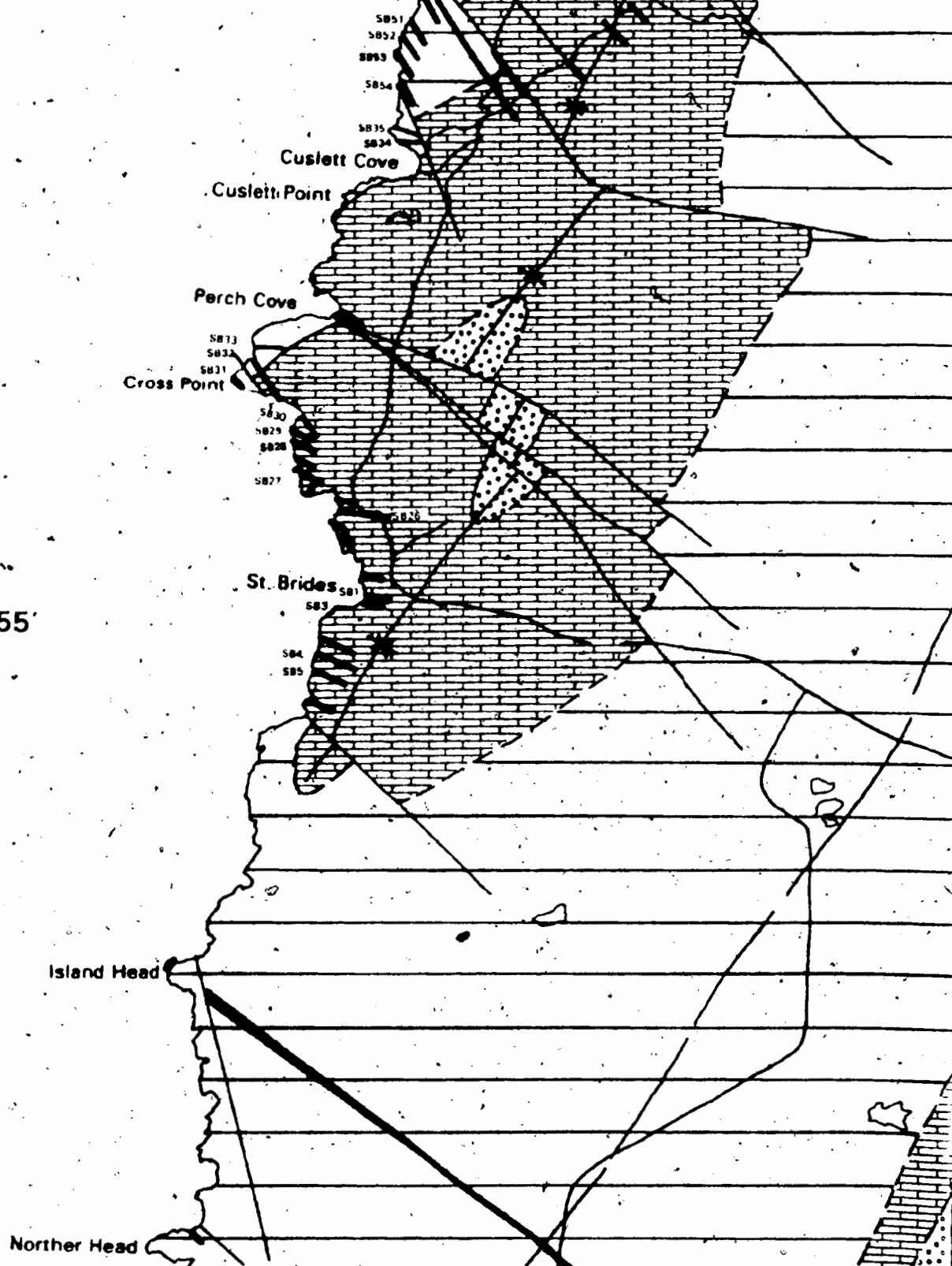
Little Barachois

Wild Cove

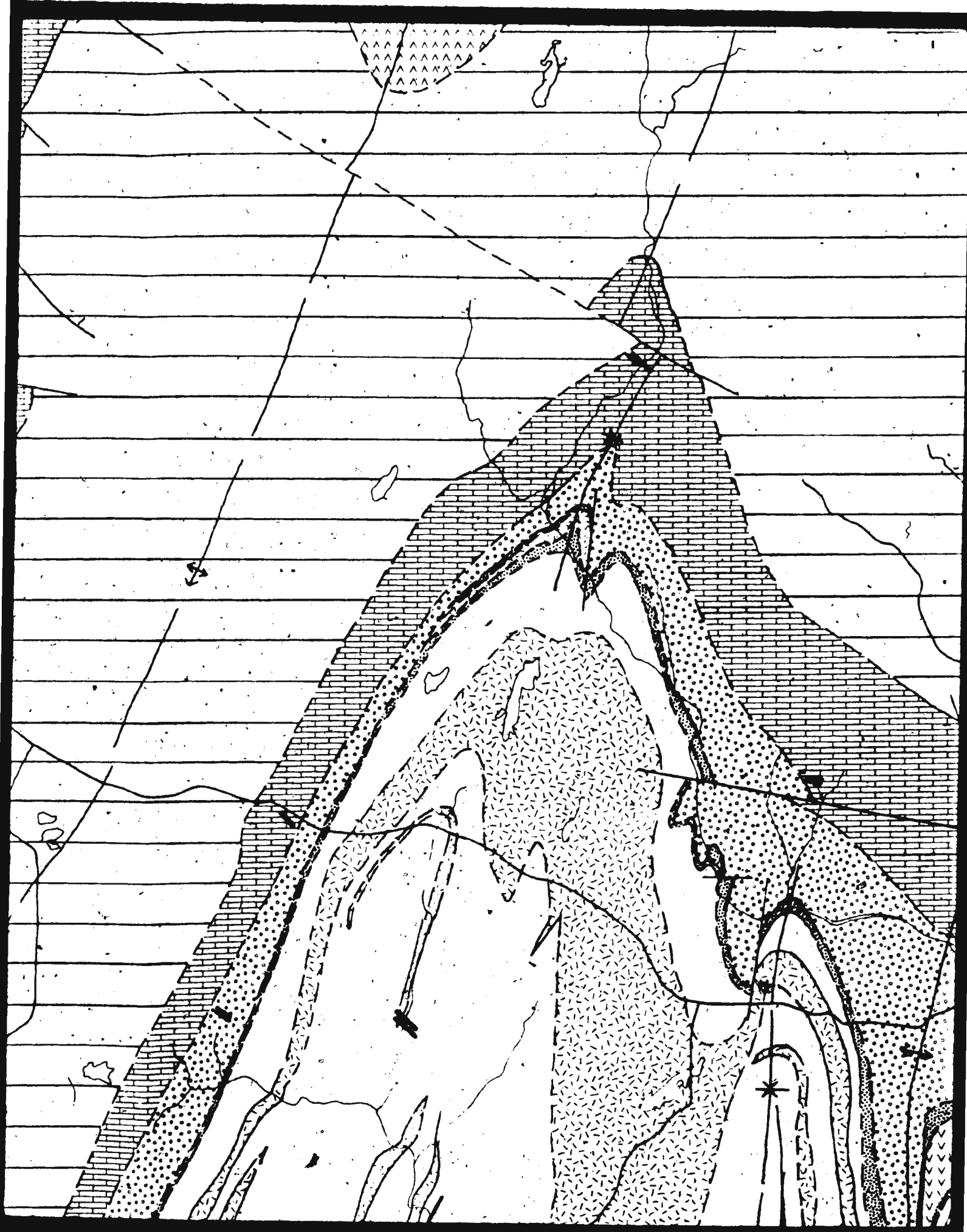
Lansecan Point

LEGEND

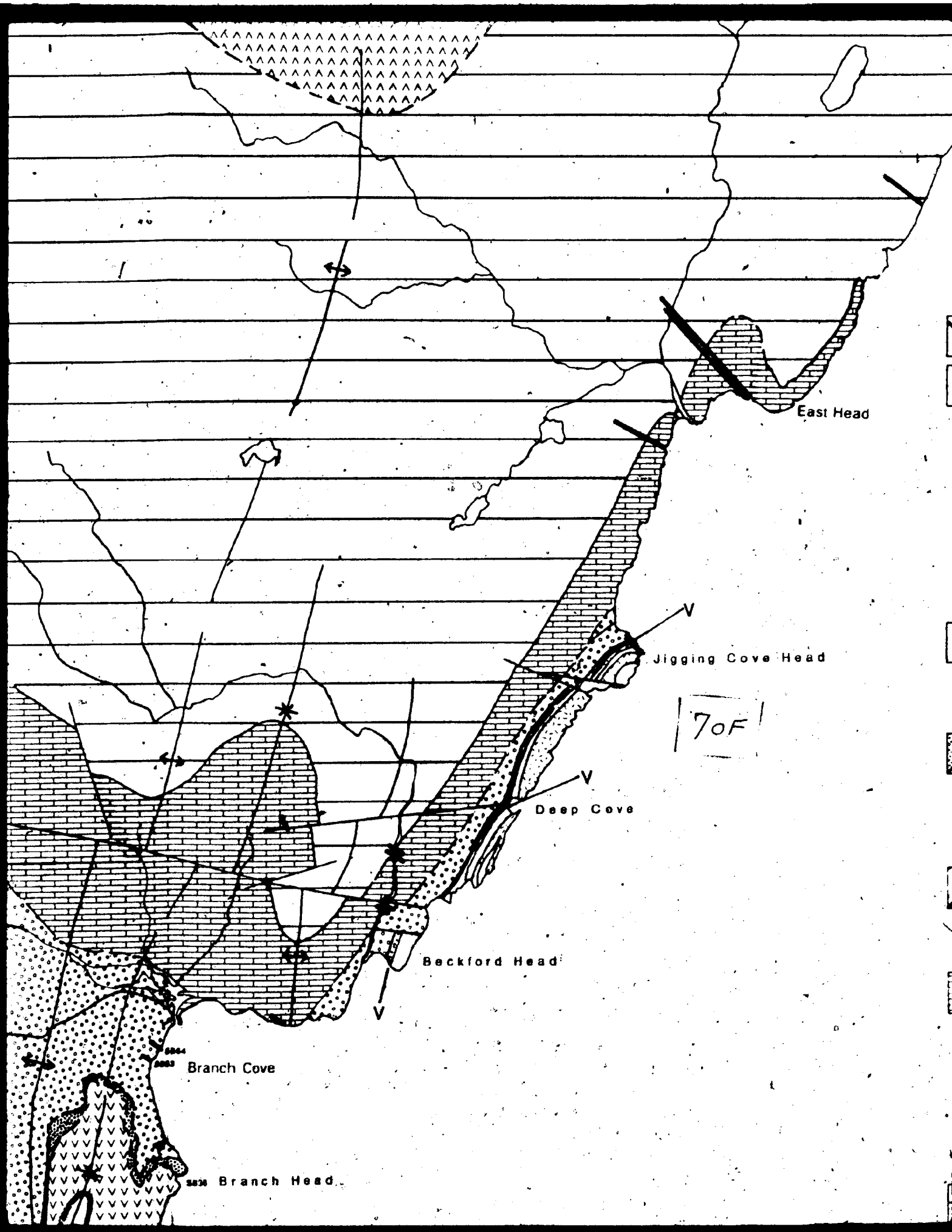
5 of 1

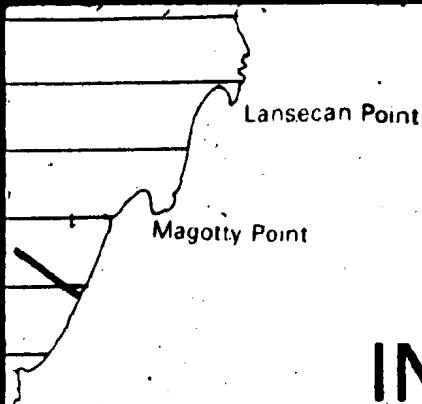


46° 55'









# LEGEND

8 of

## INTRUSIVE

### PRE-FOLDING



DYKES: diabase, often occur as multiple injections.



SILLS: diabase, sometimes show gravity layering.

## SEDIMENTARY & VOLCANIC ROCKS

### LATE MIDDLE to UPPER CAMBRIAN

#### HARCOURT GROUP



GULL COVE and BECKFORD HEAD FORMATIONS: grey green to black siltstones and shales.

### MIDDLE CAMBRIAN



MANUELS RIVER FORMATION: black to dark grey silty shales. V — Hay Cove Volcanic Member.

#### ADEYTON GROUP



CHAMBERLAIN'S BROOK FORMATION: grey and red siltstones and P-Cape Dog pillow lavas and volcaniclastics.

### LOWER CAMBRIAN



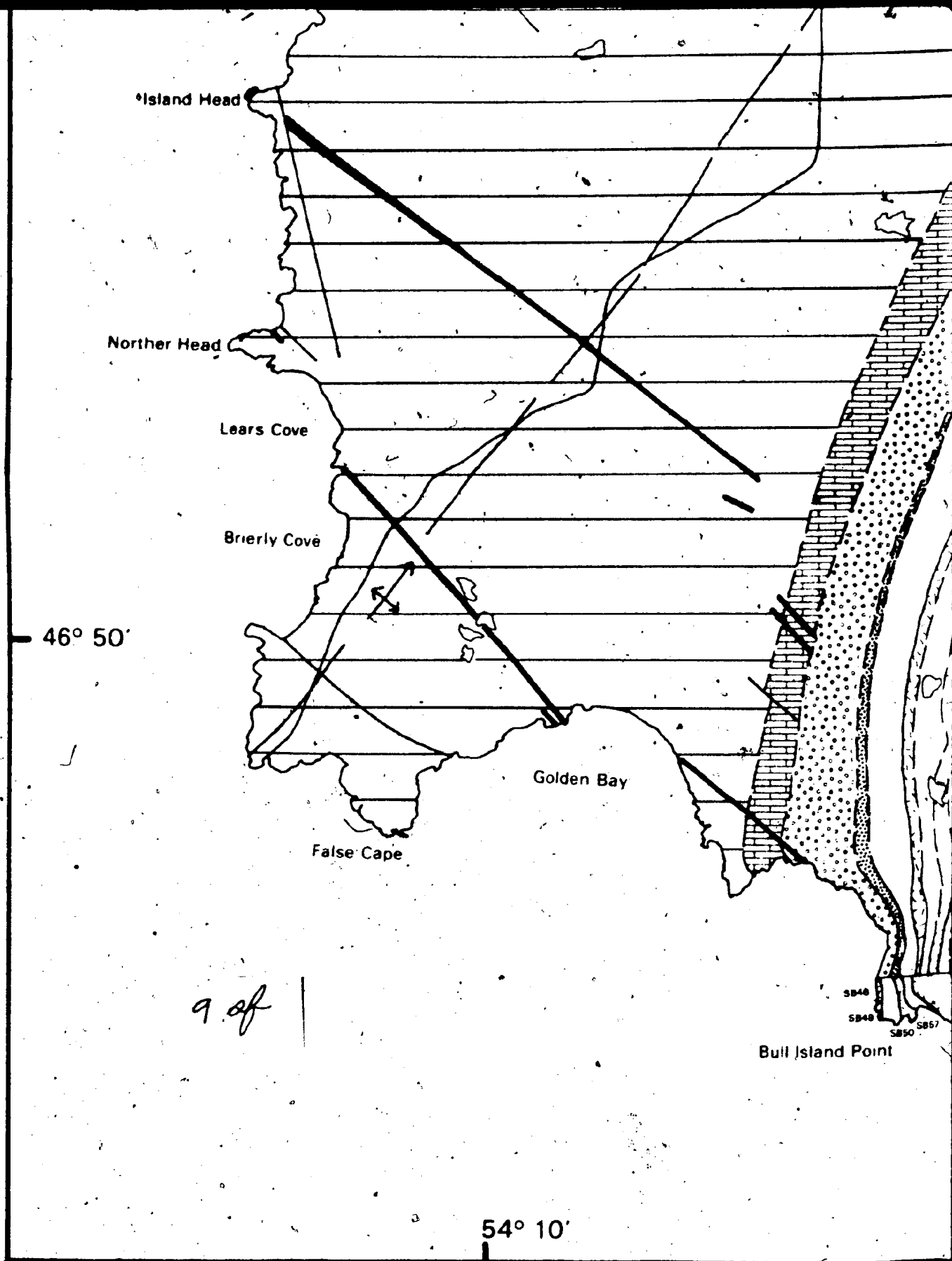
BRIGUS, SMITH POINT, BONAVIDA and RANDOM FORMATIONS: red siltstones, red limestone, red siltstone; and white green and grey silt-sandstones, respectively.

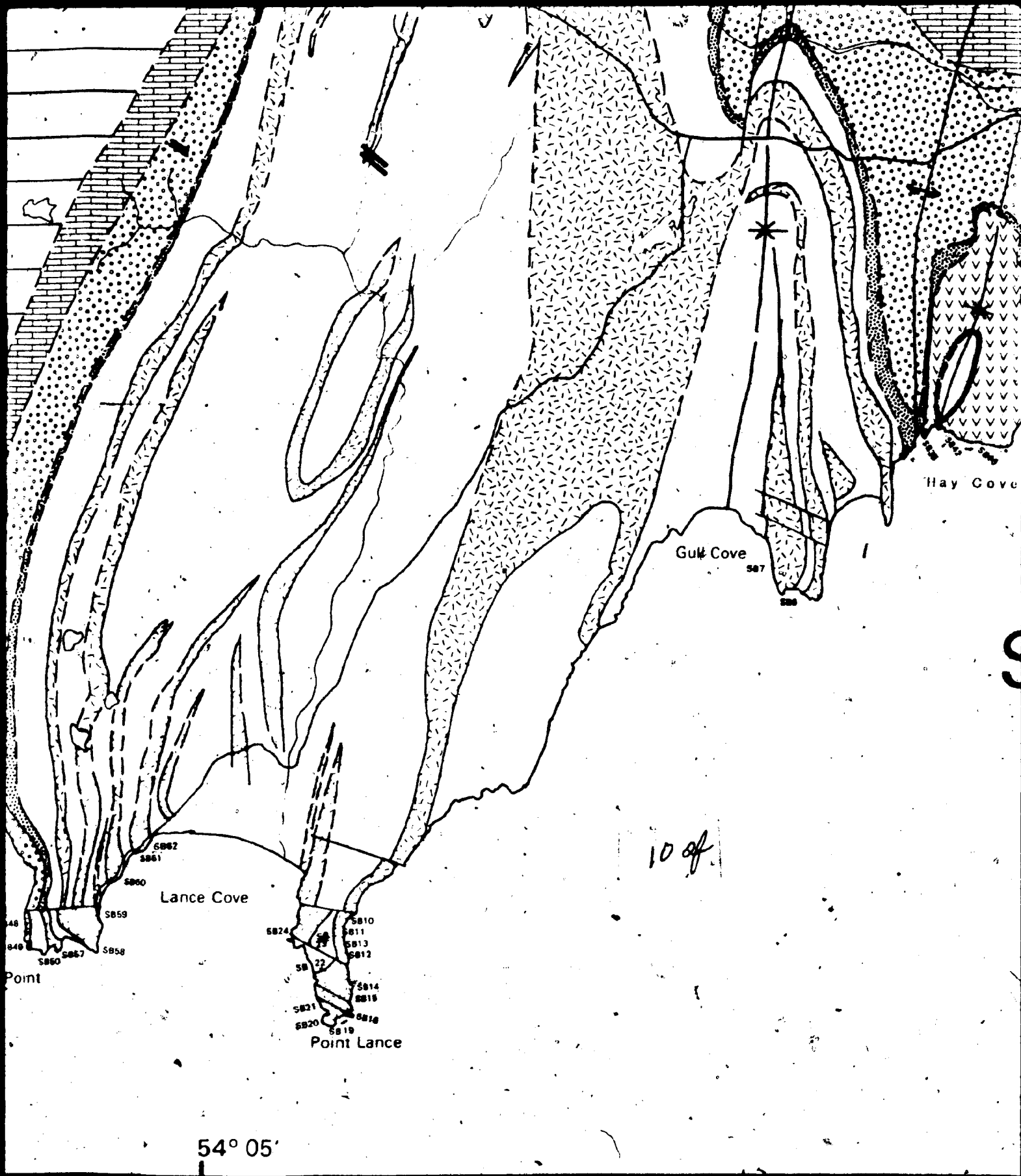
#### MUSGRAVETOWN GROUP

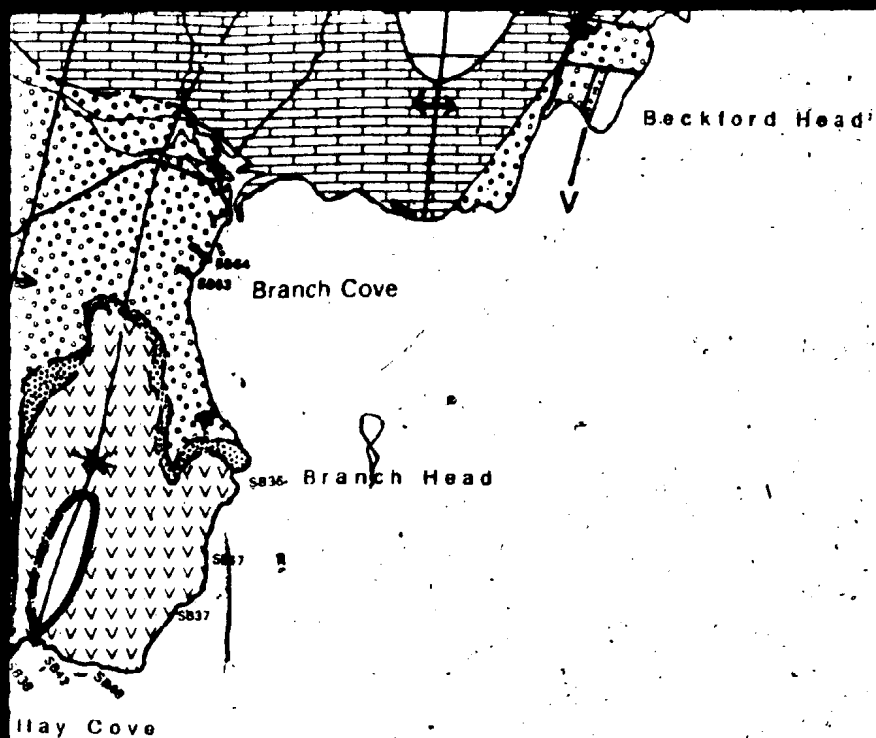
### LATE PROTEROZOIC



BRIERY COVE, LEARS COVE, NORTHERN HEAD and CROSS POINT FORMATIONS: late proterozoic clastic







# ST. MARY'S BAY

11 OF 1

Scale 1:50,000

1 km. 0 1 2 3

siltstones and P-Cape Dog pillow lavas and volcaniclastics.

## LOWER CAMBRIAN



BRIGUS, SMITH POINT, BONAVIDA and RANDOM FORMATIONS: red siltstones, red limestone, red siltstone; and white green and grey silt-sandstones, respectively.

## MUSGRAVETOWN GROUP

## LATE PROTEROZOIC



BRIERY COVE, LEARYS COVE, NORTHERN HEAD and CROSS POINT FORMATIONS: late proterozoic clastic sediments.



BULL ARM FORMATION: basic lavas, breccia, tuff and minor rhyolites.

## SYMBOLS

Geological Boundary, (defined, inferred) \_\_\_\_\_

Fault \_\_\_\_\_

Anticline

Syncline

Roads \_\_\_\_\_

Sample Locations

Map modified after Fletcher 1971

